Polish Academy of Sciences
University of Engineering and Economics in Rzeszów
Lviv Polytechnic National University
University of Life Sciences in Lublin
Faculty of Production Engineering

ECONTECHMOD

AN INTERNATIONAL QUARTERLY JOURNAL ON ECONOMICS IN TECHNOLOGY, NEW TECHNOLOGIES AND MODELLING PROCESSES

Vol. 5, No 3

LUBLIN–RZESZÓW 2016

All the articles are available on the webpage:
http://www.pan-ol.lublin.pl/wydawnictwa/Teka-Motrol.html

ISSN 2084-5715

All the scientific articles received positive evaluations by independent reviewers

Linguistic consultant: *Mikhail Suknov, Orest Grech*
Typeset: *Tetiana Serhiienko, Adam Niezbecki, Vasyl Tomyuk*
Cover design: *Hanna Krasowska-Kołodziej*

Editorial

Editorial Office Address
Polish Academy of Sciences Branch in Lublin
Pałac Czartoryskich, Plac Litewski 2, 20-080 Lublin, Poland
e-mail: eugeniusz.krasowski@up.lublin.pl

Edition 200+16 vol.

Energy management in rural households as a way of optimising accounts in the context of prosumer energy development

Marek Horyński, Jacek Majcher

Dr inż. Marek Horyński, Institute of Computer and Electrical Engineering, Lublin University of Technology,20 - 618 Lublin, Nadbystrzycka 38A, E-mail: m.horynski@pollub.pl, Polska
Dr inż. Jacek Majcher, Institute of Computer and Electrical Engineering, Lublin University of Technology,20 - 618 Lublin, Nadbystrzycka 38A, E-mail: j.majcher@pollub.pl, Polska

Received July 07.2016: accepted November 10.2016

Abstract. In recent years we have seen a gradual increase in demand for electricity due to the increasing number of customers connected to the network and a growing consumer demand for quality energy supply. The article addresses issues related to energy management in rural households and presents the advantages resulting from the emergence of a new type of energy producers, i.e. prosumers.

Key words: energy, management, prosumer.

INTRODUCTION

Energy efficiency is a concept denoting efficient use of energy aimed at reducing its demand. This concept has been appearing ever more often in recent years in laws and directives. One of them is the European Union directive according to which from 2021 all buildings erected within the Union are to be characterised by reduced consumption of electricity, as well as partial use of renewable energy sources. This is due to the dynamic growth in demand for energy, and the increasing cost associated with its use. Such requirements are forcing building designers to come up with new solutions to reduce excessive energy consumption. An answer to these demands is the concept of an intelligent building, equipped with a number of measures restricting electricity consumption, as well as using alternative energy sources [6, 7, 8, 9].

Poland's accession to the European Union on 1 May 2004 meant that in many areas the country had to adapt its laws to EU legislation. This resulted in huge changes in many areas of the economy, which had to begin to operate under the new rules [26].

One of the areas forced by EU policies to undergo deep reforms was agriculture. The common agricultural policy implemented in the Member States forced profound changes in agricultural and food economy. It became an opportunity for Polish farms due to substantial funding [20]. The main instrument supporting rural Poland are direct payments towards agricultural land. This instrument is important to the extent that it affects all persons holding land in excess of the size of 1 hectare. In parallel to this action, there are several other programs supporting Polish rural areas, but targeting narrower sections of society. An example of this can be "Help in starting a business for young farmers" in the framework of the Rural Development Programme.

Not all farmers are happy with the common agricultural policy, indicating its various threats. One such disadvantage is the rise in the prices of the means of production, or the strong competition from agricultural producers from other EU countries. Difficulties in competing are mainly due to the wide dispersion of farms in Poland. According to the Agency for Restructuring and Modernisation of Agriculture, the average size of a farm in Poland is 10.49 hectares, while in some regions this figure is less than 4 hectares (małopolskie) [19]. In turn, the average area of farms in Poland in 2010 was 9.6 ha, while in Germany it was 55.8 ha [5]. With such fragmentation of the Polish farmland, its owners have difficulty obtaining adequate economic balance of their agricultural production and look for other sources of income.

In the future, we risk the depletion of the natural resources of coal, oil, gas and uranium. [4, 5, 11, 12]. Ensuring a country's energy security depends not only on major international contracts, but also on the proper behaviour of citizens. According to the segmentation assumptions of the energy prosumer market, homeowners, farmers, residential communities, building administrators (building energy technology) belong to the first segment of consumers/producers of energy [6, 7, 13, 23, 24].

An important solution for power consumers has in recent years become the possibility of using renewable energy sources (RES) and the construction of passive or energy-plus houses [2, 11, 14, 15, 16, 17, 18]. Renewable energy sources are characterised by features that allow the user to obtain the following benefits [31]:

- local stabilisation of energy,
- lack of transmission and losses connected with it,
- raising awareness and responsibility of producers and consumers of energy and a

sense of mission to protect the environment and create the country's electricity economy,
- contribution to energy saving,
- improving the quality of energy,
- positive impact on the climate and the environment.

So far, a number of solutions exist that enable the use of these advantages as much as possible [10, 27]. In addition to the search for new energy sources it is important how the energy is used. Keeping an 'energy umbrella' over many customers does not seem to be a very economical solution, since not all of them have to use the power source at the same time. It seems that the principle 'supply power only to what you currently use' is the right solution.

In connection with the emergence of a new category of energy consumers, i.e. prosumers, rational energy management in households is becoming increasingly important, with the idea of reselling its potential surpluses. This requires the application of such precision measurement devices in the installation as:
- energy meters (electronic and intelligent)
- monitors of energy consumption

as well as optimisation of tariffs and zones and establishing contractual and connection power. An important component of the electricity economy is also the shaping of appropriate customer attitudes and the proper selection of subscriber profiles and RES installations [8, 21, 22]. Among the new trends and EU regulations related to energy appears the concept of Autonomous Energy Regions AER (sometimes also referred to as Municipal Energy Centres).

POWER GENERATION ON A FARM AS AN EXAMPLE OF ENHANCED ECONOMIC EFFICIENCY

An important factor in maintaining a household in good financial condition is to rationalise its running costs. This principle also applies to rural households, which in the face of ever-smaller production profitability should look for additional revenue. Due to the specific nature of rural households one can indicate the following aspects which may be their distinguishing features:
- Large roof surface area,
- Farm space around the house,
- Unused organic waste.

However, on the expenditure side, apart from the main costs of running the farm, an important part of the overheads is related to energy. To reduce the operating costs, use should be made of the above-mentioned features. In order to successfully compete in the market, farmers specialise in plant or animal production.

A by-product of this production is copious waste that can be used for energy production in biogas plants, obtaining biogas through the processing of organic waste by microorganisms. This gas is produced in digesters specially constructed for this purpose [21]. According to the literature it consists of more than 60% methane and about 30% carbon dioxide; other ingredients may also be present, including hydrogen, nitrogen or hydrogen sulfide [22]. An exemplary diagram of the biogas plant is shown in Figure 1.

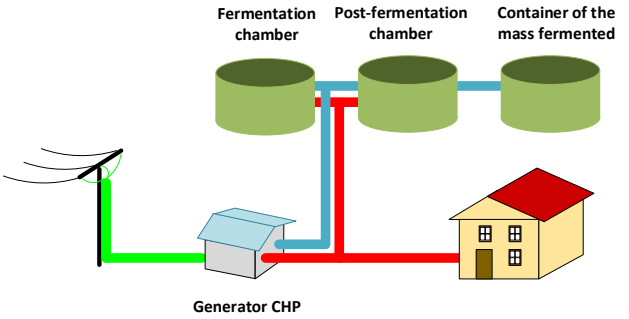

Fig. 1. Outline of a biogas plant [21]

The gas produced in the biogas plant can be used as follows:
- For the production of electricity,
- For the production of heat,
- As a motor fuel [21, 22].

Today, an ever more common solution is cogeneration, involving the simultaneous production of electricity and thermal energy. This is done in CHP (combined heat and power) generators.

Another way to obtain free energy on the farm is to use the sun. Solar energy is converted into electrical energy in photovoltaic cells in the process of photovoltaic conversion. Single cells have little power and are therefore combined in a series or in parallel in order to obtain sufficient power. The energy thus obtained is transferred through an appropriate controller to the battery, which is used for its storage. The role of this device is very important because it allows one to use free energy after sunset [14]. For this energy to power a conventional device, it is converted by an inverter into alternating current of a specified frequency and amplitude. An exemplary flow chart of the photovoltaic cell is shown in Figure 2.

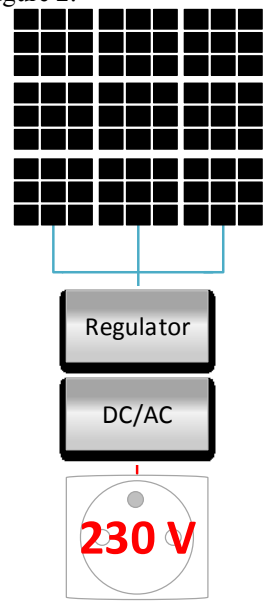

Fig. 2. Diagram of a photovoltaic system

According to the authors [3], PV systems provide from 10% to 100% of the electricity consumed in the

household. When cells provide too much energy it is possible to sell the resulting surplus. In this case, it is necessary to have one inverter, which synchronises the system to the network.

DISTRIBUTED GENERATION IN RURAL AREAS

With the development of modern farms, attention should be paid to the growing demand for electricity. Recipients from rural areas who use the power of professional power stations are placed at the end of the transmission line. Distribution of energy over long distances entails heavy losses, which result in an increase in electricity prices. Such recipients are forced to seek alternative sources to meet the growing demand for energy. Because of a large up-front investment, production of energy from renewable sources without financial support is still less profitable than conventional sources. For this reason, EU member states pursue policies aimed at increasing the attractiveness of renewable energy sources for small farms for economic reasons. In favour of the implementation of this type of distributed generation speaks also the possibility of using raw materials from farms and recycling waste to generate energy.

Renewable sources which work best in agriculture include:

- biomass boilers [21, 22]
- micro biogas plants [2]
- small wind turbines [14, 17]
- solar collectors [15]
- photovoltaic panels [23, 24, 26]
- heat pumps [27].

The use of these methods of energy production can completely or largely eliminate the need to purchase it from large conventional power plants.

Energy demand in rural areas can be divided as follows:

- in order to meet basic needs, such as heating buildings, obtaining hot water and powering electrical appliances and lighting,
- for agricultural purposes, including irrigation, animal husbandry, greenhouse cultivation, drying facilities, etc. [10].

According to the Central Statistical Office, in 2013 heat consumption in agriculture amounted to 1,000 TJ. Electricity consumption in the same areas, exclusively for the purposes of production, irrespective of the needs of households amounted to 1,539 GWh. In turn, the demand for electricity in households, taking into account agriculture, amounted in 2013 to 28442 GWh [4].

Fuel consumption in agriculture in 2013, according to the Central Statistical Office [4], broke up as follows:

- Coal, 1600 thousand tonnes,
- Liquid gas, 50 thousand tonnes,
- Light fuel oil, 80 thousand tonnes,
- Heavy fuel oil, 24 thousand tonnes.

Despite regular reconstruction of the transmission network in rural areas, it is still not adapted to the requirements imposed by modern recipients.

The main problems of the current network include:

- Low voltage parameters,
- Insufficient transformer stations of high and medium voltage,
- Too long power lines, which are vulnerable to overload,
- Peak power per unit farm is 2 kW.

Maximum power which is supplied to households is unable to satisfy the demands of energy-intensive equipment and machinery. Factors hindering the development of large sources of renewable energy in the country, including long distances and poor state of the power grid, may at the same time be an impulse for the development of small distributed systems for individual households [10].

A way out may be the creation of energy-independent households, which together will form Autonomous Energy Regions. An example of regional energy independence is the Kisielice Commune located in the Warmian-Masurian Voivodeship, which is Poland's first energy-independent municipality. Its area is 17,000 ha, and the population is about 6,600. In 2014 it won the ManagEnergy 2014 competition organised by the European Commission.

Achieving the objectives of the use of renewable energy sources started in 2002. The municipality acquires its energy primarily from a wind farm consisting of 27 turbines with a total capacity of 40.5 MW. Since 2014 the production of energy has been supported by a farm biogas plant with a thermal capacity of approx. 1 MW and electrical power of 0.99 MW. Currently, work is under way on the second phase of investments, the aim of which is to build a second wind farm. Six new turbines will be installed with a total capacity of 12 MW. The Kisielice Commune was presented at the conference "Heating and cooling in the European energy transition", held in Brussels in February 2015 [10].

What is also noteworthy is the promotion of energy-saving and energy-independent, autonomous buildings. To achieve a positive energy balance, the building uses many techniques minimising energy loss, and the most important goal is to produce energy from renewable sources. For example, the orientation of the building is designed to maximise the power of natural light. This eliminates the need for indoor lighting during the day and at the same time accumulates heat. Triple-glazed windows that allow more heat entering the building rather than going out. With good insulation of its partitions, the building consumes several times less energy for heating. During the heating season, to heat one square meter of housing one needs 15 kWh. By comparison, the heat demand for conventional building is about 120 kWh/(m²•year). One source of additional energy are solar panels, aesthetically integrated into the façade of the building. In addition, solar technology is accessible, particularly as regards maintenance and repairs.

An important difference between the passive construction and energy-plus standards is that the latter brings the user of the building material benefits arising from the resale of surplus energy produced. In addition, the building is built exclusively from natural construction materials; it could be said that it is one step ahead of the

passive standard due to the positive energy balance [29, 30, 31, 31].

Today, the energy-plus standard can be adapted to buildings with a traditional body, or to modern high-tech buildings. Regardless of its body, a building – to become safe, comfortable and economical – must have a system that manages all subsystems contained within the structure, or an intelligent installation.

The basis of the innovation of energy-plus construction is the technology used in it. After analysing the climatic conditions prevailing in the area where the building is located, and taking into account the economic criterion of the investment, it will be possible to use in such buildings renewable energy sources and building automation systems.

PROSUMER ENERGY ON FARMS – LEGAL ASPECT

Agriculture in Poland brings together 5.4 million electricity consumers in the agricultural sector. The share of agriculture in the national consumption of final energy (5.8%) is more than twice the EU average (2.2%).

In February 2015, after more than three years, work was completed on the law on renewable energy sources. The main objective of the Act is the introduction of new mechanisms to support producers of energy from renewable sources, both small and large. In addition, regulation introduces fixed rates for purchasing electricity produced from renewable energy sources [12, 13, 25, 28].

Investments finalised by the end of 2015 will benefit from support in the form of green certificates, while all investments from January 2016 will be supported in the auction system. In this system, increase in power obtained from renewable sources will be linked with an administrative decision. Responsibility for such a decision will rest with the Council of Ministers, Ministry of the Economy, and the Energy Regulatory Office. They will decide how much electricity from renewable energy sources to contract in a year. Companies remaining in the support system through green certificates can benefit from the support period of 15 years, but not beyond 2035.

The Act implements new definitions of micro- and small installations. A micro-installation of renewable energy has a total capacity of:

- Up to 40 kW for electricity,
- Up to 70 kW for thermal energy.

The definition does not include installations for the production of electricity, heat or cooling from biogas, as well as installations for the production of biogas itself. A small installation differs only in limiting values. For each type of energy they are as follows:

- From 40 kW to 200 kW for electricity,
- From 70 kW to 300 kW for thermal energy.

This definition does not include installations using or generating biogas either.

Production of electricity in micro-installations for one's own use and for sale, in accordance with the provisions of the Act, is not activity of an economic nature. This is a key change in the law, as so far being in business was required in such situations. Consequently, in the case of power generation plants with an installed capacity of up to 40 kW, there is no need to set up a business. The only responsibility of the owner of the micro-system is notifying one's operator about connecting the installation to the network by a certified installer. The Act also introduces a fixed rate of purchase by the network operator of the prosumer electricity produced from renewable energy sources. These rates are varied, and the criterion for determining the rates is the capacity of the installation. In the case of micro-installations with an installed capacity of up to 3 kW, the owner can count on [27, 28]:

- 0.75 zł/kWh for hydro-power,
- 0.75 zł/kWh for wind energy on land,
- 0.75 zł/kWh for solar energy.

Different rates obtain in the case of plants with a capacity of 3-10 kW, and are as follows:

- 0.70 zł/kWh for agricultural biogas,
- 0.55 zł/kWh for biogas from landfills,
- 0,45 zł/kWh for biogas from wastewater treatment plants,
- 0.65 zł/kWh for hydro-power,
- 0.65 zł/kWh for wind energy on land,
- 0.65 zł/kWh for solar energy.

As can be seen, these rates are slightly different. These purchase prices are protected by law for a period of 15 years from the date of delivery of such an installation, or if the total committed capacity exceeds:

- 300 MW for plants with installed capacity of up to 3 kW,
- 500 MW for plants with installed capacity of 3-10 kW.

After this period, the selling price of electricity produced from renewable energy sources will be determined by the Ministry of Economy.

For this reason, it becomes important to develop research methods and tools useful for the development of integrated renewable energy micro-grids. A special role here lies with universities and research centres. The foundation of the Laboratory for Energy Efficient Building Systems is aimed at preparing a base for the later development of micro- and intelligent networks with the participation of RES, by: conducting comprehensive monitoring of energy consumption and the potential of renewable energy sources to users also in rural areas, preparing tools for selection and optimisation of the use of renewable energy technologies in small micro-grids, analyses enabling the design of a comprehensive decision support system for prosumer acting in micro-grids.

ANALYSIS OF THE OPERATION OF AN ENERGY ACTOR DURING DEMAND GROWTH FOR ELECTRICITY

In addition to actively reducing energy consumption by automatic control of lighting, heating and air conditioning and ventilation, it becomes extremely important also to monitor the current consumption. Load management plays a key role in the economic management of electricity. For this purpose, energy actors can be used, e.g. SE/S 3.16.1, which is compatible with KNX/EIB. It allows load management in the master-slave mode, which is used to control the set limit of load by

disconnecting equipment according to its degree of disconnection. This allows one to align the daily power consumption (Fig. 3).

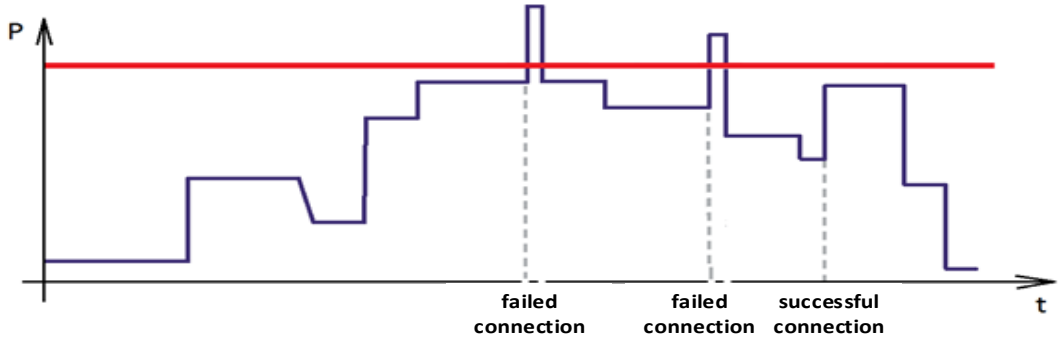

Fig. 3. Sample graph of power consumption by controlling the energy actor

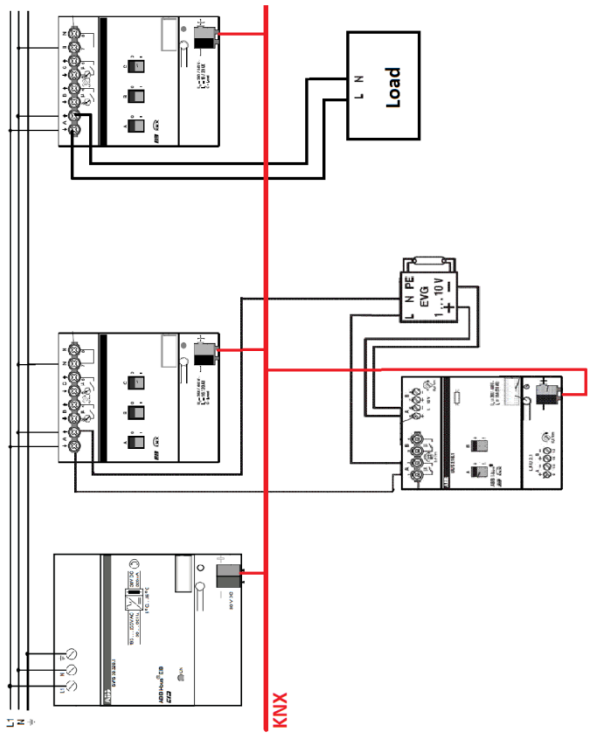

Fig. 4. The circuit diagram for master-slave load control [1]

CONCLUSIONS

According to the decisions taken in the European Union, since 2020 all new buildings will have to be made at least to a standard that ensures their efficiency. The combination of low energy building technologies with the optimal use of renewable energy sources allows for excellent performance parameters of buildings.

The use of energy actors equipped with measurement modules provides a constant source of information about the current energy consumption at home and contributes to increasing the environmental awareness of its inhabitants.

Control of renewable energy sources using the tools offered by the building automation systems, for example. KNX/EIB, will contribute to even greater interest in the subject of prosumer energy.

Autonomous buildings function independently of the external infrastructure. This situation forces the architects and designers to use solutions focused mainly on saving electricity and using some raw materials and waste for reuse.

In the coming years we can expect further development of technologies related to renewable energy sources. This is due to the benefits its use provides for both local communities, increasing the level of energy security, as well as environmental benefits, primarily reducing emissions of carbon dioxide.

REFERENCES

1. ABB catalog of the manufacturer. 2015 (in Polish).
2. **Bańkowski T., Żmijewski K. 2012.** Analysis of the possibility and advisability of introducing of supporting mechanisms in microinstallations gas cogeneration, Institute of them. E. Kwiatkowski, (in Polish).
3. **Dołęga, W. 2013.** Practical aspects of the use of photovoltaic systems in the construction industry. Drives and Controls, 15(6), 92-95, (in Polish).
4. **Central Statistical Office. 2014.** Consumption of fuels and energy carriers in 2013.
5. Farms in Poland against EU farms - the impact of the CAP, ed. Poczty W. Agricultural Census 2010. Central Statistical Office. Warsaw. 2013 (in Polish).
6. **Góra S. 1975.** The economy in the electric power industry. PWN Warszawa, (in Polish).
7. **Horyński M. 2014.** Building automation systems in the revitalization of rural space. Logistyka. 06, 4527-4534, (in Polish).
8. **Horyński M. 2015.** Energy security of the smart home in the rural space. TTS Technology of the Rail Transport. No. 12, 2582-2585. (in Polish).
9. **Horyński M. 2014.** The use of wireless technologies to modernize the electrical systems in buildings agritourism. Motrol. Automotive and energy agriculture . No. 1, Vol. 16, 37-41, (in Polish).
10. Institute for Sustainable Development in cooperation with the Institute for Renewable Energy. 2011: The

Power dissipated, Ed. Foundation Institute for Sustainable Development. (In Polish).
11. **Janowski T., Holuk M. 2011.** The use of Stirling engine in micro home. The work of the Institute of Electrical Engineering, Volume 249, 117-128 (in Polish).
12. **Kacejko P. 2004.** Distributed generation in the power system, Ed. Lublin University of Technology, (in Polish).
13. **Kacejko P. i inni, 2014.** Prosumer - friend, enemy or just a hobbyist? Energy Market, 5, 83-89 (in Polish).
14. **Kapica J. 2014.** Comparison of wind turbine energy production models for rural applications. Teka. Commission of Motorization and Energetics in Agriculture. Vol. 14, No. 3, 37–42.
15. **Kapica J. 2014.** Fuel Cells as Energy Storage for Photovoltaic Energy Sources in Rural Areas. Teka. Commission of Motorization and Energetics in Agriculture. Vol. 14, No. 3, 43–46.
16. **Lytvyn V., Oborska O., Vovnjanka R. 2015.** Approach to decision support Intelligent Systems development based on Ontologies. Econtechmod. An International Quarterly Journal. Vol. 4. No. 4, 29-35.
17. **Medykovskyj M., Kravchyshyn V., Shunevych O. 2015.** Analysis and modelling of load parameters of wind power station. Econtechmod. An International Quarterly Journal. Vol. 04, No. 2, 19–24.
18. **Nęcka K., Trojanowska M. 2014.** Comparative Analysis of the variability of daily Electric power loads. Vol. 14, No. 4, 87–92.
19. The notice of the President of the Agency for Restructuring and Modernization of Agriculture of 21 September 2015 on the size of the average area of agricultural land on a farm in each province and the average area of agricultural land on a farm in the country in 2015, (in Polish).
20. **Poczta W. 2010.** The income situation of farmers in Poland after accession to the EU and its determinants as a condition of development of agriculture. Annual. Agri Sciences. G series 97.3, (in Polish).
21. **Romaniuk W., Łukaszuk M., Karbowy A. 2010.** Potential for development of biogas plants on farms in Poland. Problems of Agricultural Engineering, 18, 129-139. (in Polish).
22. **Rosik-Dulewska Cz. 2006.** Basics of waste management. PWN. Warsaw, 342, (in Polish).
23. **Sarniak M. 2014.** Energy Balance of a Prosument Microinverter On-Grid Photovoltaic System. Teka. Commission of Motorization and Energetics in Agriculture – 2014, Vol. 14, No. 3, 99–102.
24. **Siedliska K. 2014.** Photovoltaics – The Present and the Future. Teka. Commission of Motorization and Energetics in Agriculture. Vol. 14, No. 3, 103–110, (in Polish).
25. **Słupik S. 2014.** Regional and international economy. Prosumer energy and its impact on the electricity market. Scientific Papers of the University of Szczecin. Studies and works Faculty of Economics and Management. No. 37 T.2, 127-136, (in Polish).
26. **Ścibisz M., Pawlak H. 2008.** The use of PLC as an element of control over technological lines in the agri-food industry, Agricultural Engineering, 8 (117), Cracow, 231-236, (in Polish).
27. **Tevyashev A., Nikitenko G., O. Matviyenko. 2015.** Optimal stochastic control of the modes of operation of the sewage pumping station. Econtechmod. An International Quarterly Journal. Vol.4, No.3, 47-55.
28. The Act of 20 February 2015 on renewable energy sources. Journal of the Polish Republic, (in Polish).
29. **Wnuk R. 2007.** Installations in a passive house and energy-saving. Guide to building, (in Polish).
30. **Zaverbny A. 2013.** Peculiarities of development and reforming markets of electric energy as one of the key energy products in the European Union. Econtechmod. An International Quarterly Journal, Vol. 2, No. 1, 69–73.
31. **Zimny J. 2010.** Renewable energy sources in low-energy construction. Issue I, WNT, Warsaw, (in Polish).

The variability of mechanical properties of the kohlrabi stalk parenchyma

Agnieszka Starek[1], Elżbieta Kusińska[2]

[1]Department of Biological Bases of Food and Feed Technologies, University of Life Sciences
Głęboka 28, 20-612 Lublin, Poland
e-mail: agnieszka.starek@up.lublin.pl
[2]Department of Engineering and Food Machinery, University of Life Sciences
Doświadczalna 44, 20-280 Lublin, Poland

Received July 04.2016: accepted July 11.2016

Abstract. The paper presents the results of the impact of kohlrabi parenchyma sampling site on textural properties. Selected texture parameters, i.e. hardness, springinees, cohesiveness and chewiness were determined by the double compression test TPA. The study was conducted on samples taken from well-defined kohlrabi layers (upper layer, middle layer, lower layer) and zones (A, B, C), because the vegetable's structure is heterogeneous. The samples were compressed at the longitudinal and transverse orientation of the fibers relative to the movement of the working tool. The results were statistically analyzed using the program Statistica 8.0. The research has shown that the place of sampling and orientation of the fibers have a significant impact on the value of all the kohlrabi texture parameters.

Key words: kohlrabi, mechanical properties, place of sampling

INTRODUCTION

The most important economic sector of food for our country is fruit and vegetable processing. Poland producing annually about 5-5.5 million tons of vegetables is one of the leading producers in the European Union. This sector is quite innovative for the products (more and more attention is paid to new, tasty varieties or health aspects of vegetables). Quality values of the raw materials supplies are important for the processing enterprises, because they translate directly to the wares quality [4, 17].

However, in order to properly process the raw material it is necessary to precisely determine its mechanical properties. For the determination of mechanical properties of materials using the strength tests, the compression test is commonly used, because it is the closest simulation of biting and chewing. Among the many configurations of trials used in compression tests, the most frequently-mentioned is the compression between parallel plates, i.e. the texture profile analysis test TPA (*Texture Profile Analysis*). The current methods of textural analysis, based on fairly advanced technical research instruments, allow for an objective assessment of the properties of the tested materials [1, 5, 16, 18, 19, 21].

Information about the physical properties of raw materials, despite extensive research in this area, is still of limited value due to the heterogeneity of materials of plant origin. Therefore, the characteristics of the raw material should take into account the geometrical characteristics, surface conditions, moisture, fiber orientation and the procedure of sampling, as well as a precise description of the process parameters. Moreover, a description of the material should contain comprehensive data on the growing conditions, varieties, humidity, state of maturity and pre-treatment [2, 10, 12].

In the publications and studies describing the work of vegetable scientists, only the mechanical properties of potato tubers, roots of sugar beet and carrots have been subjected to extensive studies and investigations [3, 7, 9]. The reports of research on brassica vegetables have occurred sporadically.

Kohlrabi (*Brassica oleracea var. gongylodes* L.) is a variety of cabbage. The edible part is the bulky and thick stalk. Kohlrabi is a very valuable vegetable, with high nutritional value and taste. It is a source of vitamins B, C, K, beta-carotene and minerals (calcium, magnesium, iron and phosphorus). In addition, it contains lutein necessary for the proper functioning of eyes [8, 15]. A separate valuable class of compounds contained in healthy kohlrabi are glucosinolates, whose main role is detoxification [6, 13, 14]. Kohlrabi as a vegetable belongs to the group rarely causing allergies, and so is suitable for administration to children from six months of age. Kohlrabi is especially recommended for diabetics, patients with hypoglycemia and atherosclerosis, due to the slow process of raising blood sugar levels, while having low calorific value [11, 20].

The studies of kohlrabi, in addition to the high cognitive value, are also significant for practical applications.

The aim of the study was to determine the mechanical properties of the kohlrabi parenchyma samples taken from particular places with clearly different structure and compressed along the longitudinal and transverse orientation of the fibers.

MATERIALS AND METHODS

The raw material used for the study was kohlrabi of Kossak variety. The research material was taken from the second day after the date set for the seventh day. The vegetables were stored in a ventilated place at the temperature of 4°C and relative humidity of 95%. The shape of the stalk was similar to round of an average size of 9 ± 0.5 cm.

Due to the different and heterogeneous structure of kohlrabi, the cutting of samples for testing was performed in a specific way.

Figure 1 shows the appearance of the structure of vegetables after cutting a) along the length and b) across the fibers and the place of samples' cutting.

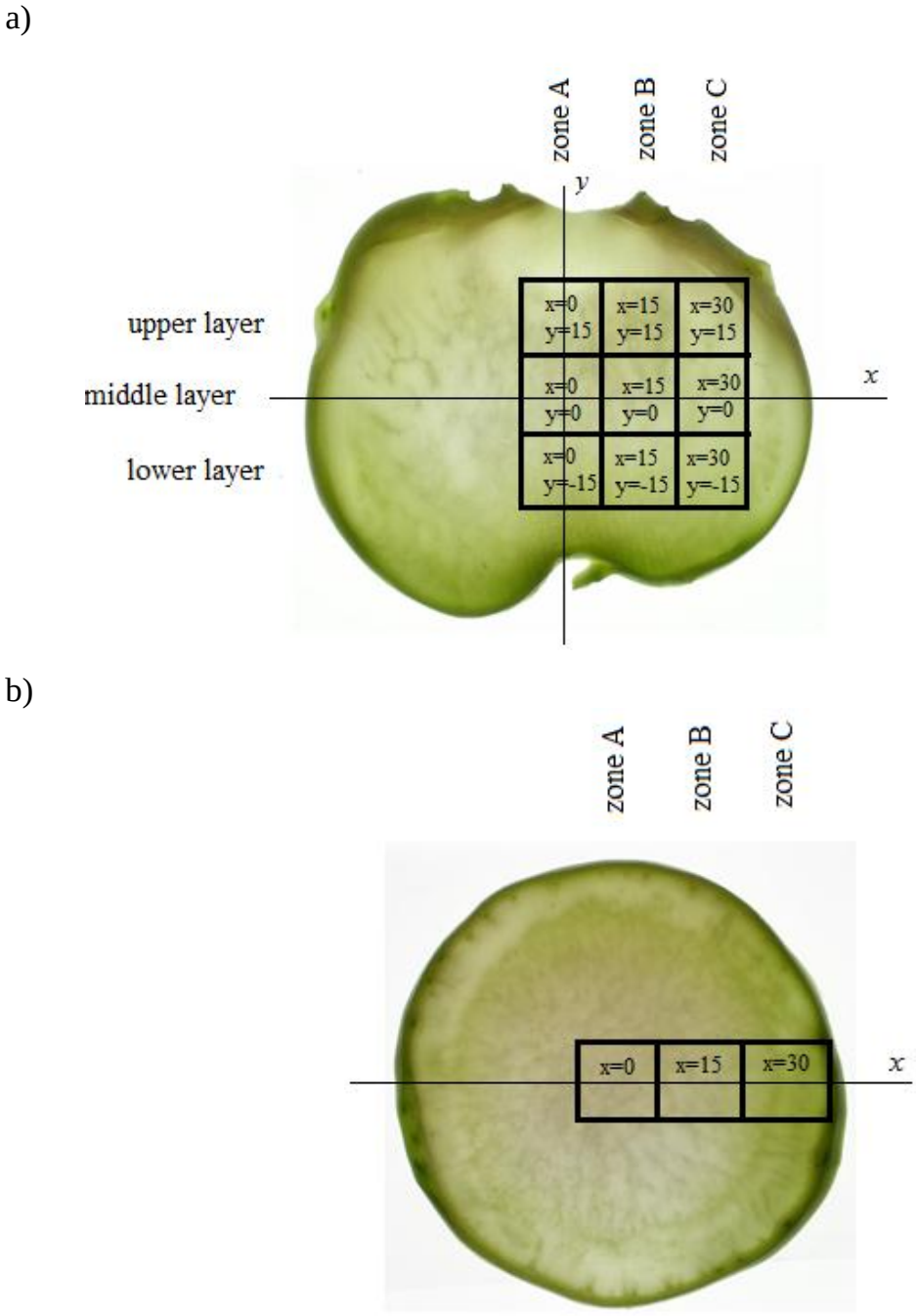

Fig. 1. Structure of kohlrabi tissue after cutting: a) along the length, b) across the fibers

It was assumed that kohlrabi stem is symmetric along the *y*-axis. The figure above shows that the structure of the raw material is heterogeneous. The vegetable has coriaceous fiber layers which are separated by a soft

parenchyma. In the illustrated kohlrabi longitudinal section (Fig. 1a) the high density of fibers in the lower layer and the cross-section is evident, which is illustrated by the radial fiber distribution (Fig. 1b) in the middle of the vegetables and the rind.

The samples were prepared in the following way: each vegetable was partitioned into three layers (upper, middle and lower) with the thickness of 15 mm. Then, from each layer cuboids were cut out with the dimensions of 45x15x15 mm, which were partitioned into three zones A, B and C (15 mm wide). This resulted in the cubes of 15 mm sides. To ensure the accuracy of cutting, the samples were prepared by means of a metal plate with four parallel-spaced knives with 15 mm spaced blades. In order to be able to carry out mathematical statistical analyses, the location of the centers of respective samples was located. The coordinate system *x*-*y* was assumed, which crossed at the point 0. The *y*-axis coincided with the vertical axis of the zone A, the *x*-axis with the horizontal axis of the middle layer. Vertical axis tests were located in the zone B and C of *y*-axis, spaced respectively 15 and 30 mm, and the horizontal axes samples from upper and lower layers were spaced 15 -15 mm from the axis *x*. Coordinates *x* and *y* were related to the middle of cubes.

The double compression test TPA was conducted in the texturometer TA.XT plus Stable Micro Systems, cooperating with a computer having the Texture Exponent 32 software, using the nine samples in the form of cubes with the side length 15 mm of the ten roots at the longitudinal (sample a) and the transverse (sample b) fiber arrangement (Fig. 2).

Each tested specimen was compressed by a 25 mm cylindrical tester up to 50% of its initial height. The test speed was 0,83 mm s^{-1}.

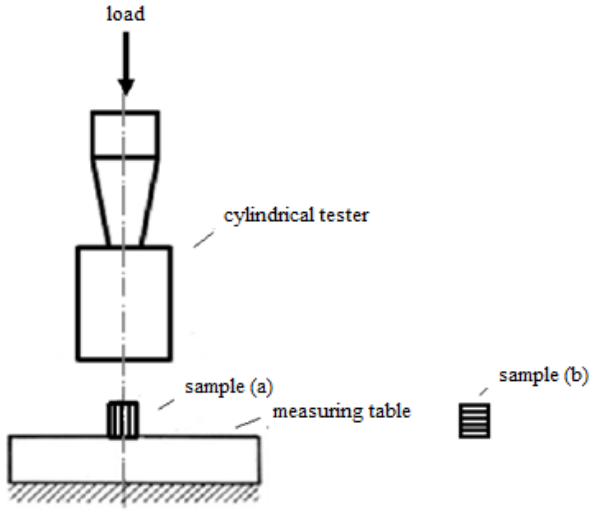

Fig. 2. The layout scheme of TPA testing

The analysis of the measurements in the form of texturograms in two coordinate force deformations allowed to determine the parameters of texture (Fig. 3).

Following the example of part of the research work [9, 12, 18, 21] and the popularity of units used in the processing industry, the following determinants of textures and units were determined:

- hardness *H* (N): first compression maximum force,
- springiness (-): expressed as the material's ability to regain its initial dimensions, which is described as second-to-first deformation ratio *(Spr=L2/L1)*,
- cohesiveness (–): characteristics of product integrity expressed by internal cohesive forces, which is described as deformation work at second-to-first cycle ratio (*Coh=W2/W1*).
- chewiness *Ch* (N): expressed as the force needed to chew a piece of particular food structure to the form which is ready to swallow, which is described as multiplication of hardness, cohesiveness and springiness. The graphic presentation of double compression test is shown in Fig. 3.

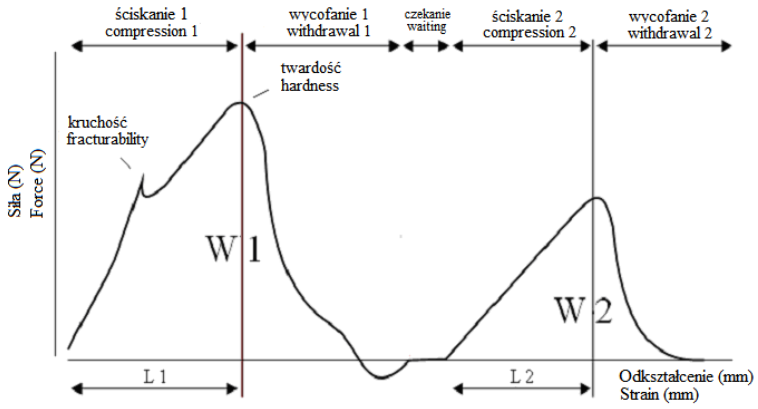

Fig. 3. Example of a graph obtained in the double compression test (TPA)

The results were statistically analyzed using the statistical package Statistica 8.0. In order to investigate the significance of differences between the site and download the various determinants of texture, the multivariate ANOVA test was conducted. Inference was made with the significance level of 0.05. A detailed analysis of medium confidence intervals was made using Tukey's test. Using the regression analysis, equations were derived that describe the texture parameters depending on the place of sampling and arrangement of fibers.

RESULTS AND DISCUSSION

The results of measuring the impact of the kohlrabi parenchyma sampling obtainment place on the determinants of texture are shown in Figures 4 - 7. Various letters included in the average values in the graphs indicate the occurrence of significant differences between them.

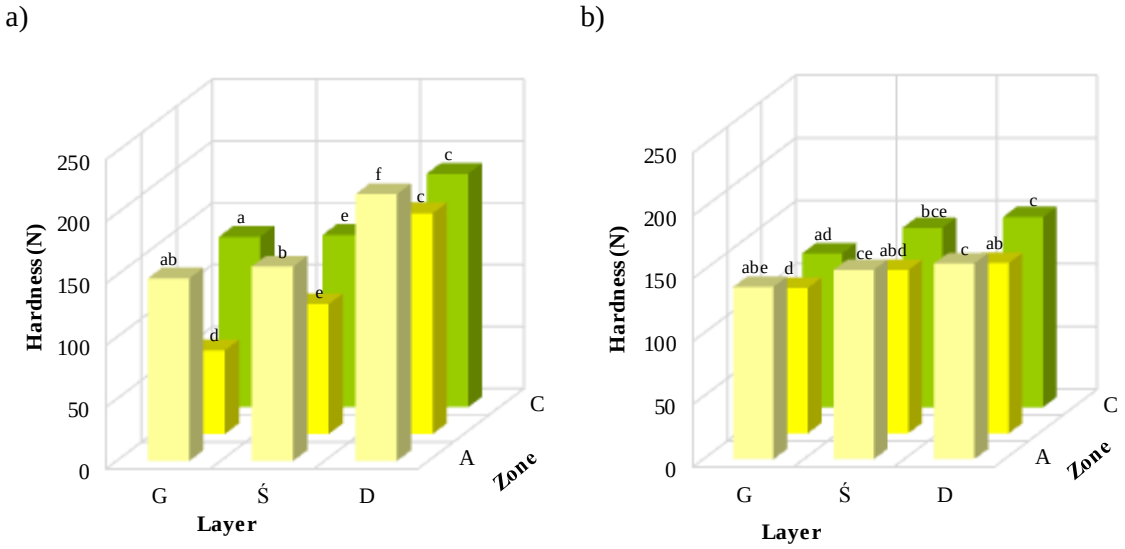

Fig. 4. Dependence of kohlrabi parenchyma hardness on the place of sampling at: a) the longitudinal b) transverse fibers orientation

One of the parameters determined by the compression tests was the kohlrabi parenchyma hardness (Fig. 4). The conducted statistical analysis showed a significant effect of obtainment sites on the hardness of the samples arranged along and across the fibers. The highest hardness was observed in samples taken from the lower layer of parenchyma in the zone A, the maximum value of the determinant was 215.61 N. The hardness of the samples from the upper layer of the zone B was about 68% lower. It was also significantly influenced by the direction of the fibers in the kohlrabi parenchyma (Fig. 5). At the same measurement sites but for the raw material arranged across the fibers it was observed that the differences in the values were much smaller. The largest and lowest values amounted to 155.77 N and 115.66 N. This is due most likely to a different arrangement and the course of the fibers in the kohlrabi parenchyma. The obtained results clearly show that in each case the raw material had the highest hardness in the zone A, which is located in the vegetables core.

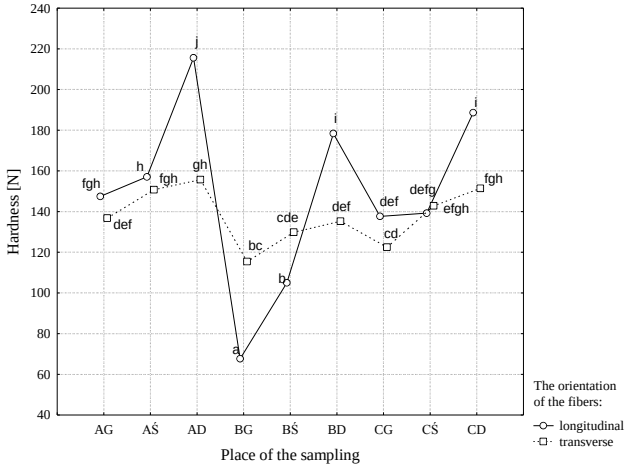

Fig. 5. The Tukey significance of differences between the hardness of the kohlrabi parenchyma samples taken from specific places along the longitudinal and transverse direction of the fibers

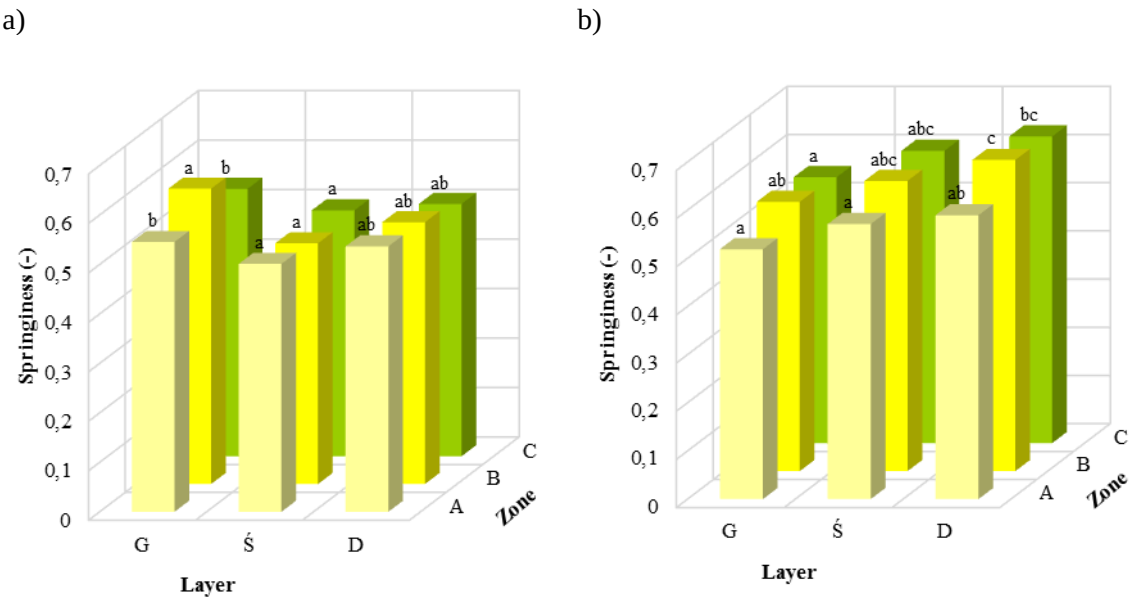

Fig. 6. Dependence of kohlrabi parenchyma springiness on the place of sampling at: a) the longitudinal b) transverse fibers orientation

Another characteristic determined during compression testing was springiness of the material (Fig. 6). The highest value of the parameter was observed in the samples placed along the fibers in the upper kohlrabi layer. The measurement results were as follows: for the samples taken from the core (zone A) the value of springiness amounted to 0.55, zone B - 0.6 and for the material placed the closest to the kohlrabi peel (zone C) - 0.54. Arrangement of parenchyma samples across the fibers caused a reversal of the trend in changes in the springiness of kohlrabi tissue. The values of this parameter for the samples located in the upper layer ranged from 0.57 - 0.58. The highest springiness was observed in transversely arranged samples, obtained from lower layer parenchyma of the vegetables. The values determined for zones A, B and C were, respectively, 0.59, 0.65 and 0.64. Figure 7 shows the average values of springiness of the fibers according to the indication of homogeneous groups ($p \leq 0.05$). The results of calculations indicate that, in most cases, the parameter values do not differ significantly.

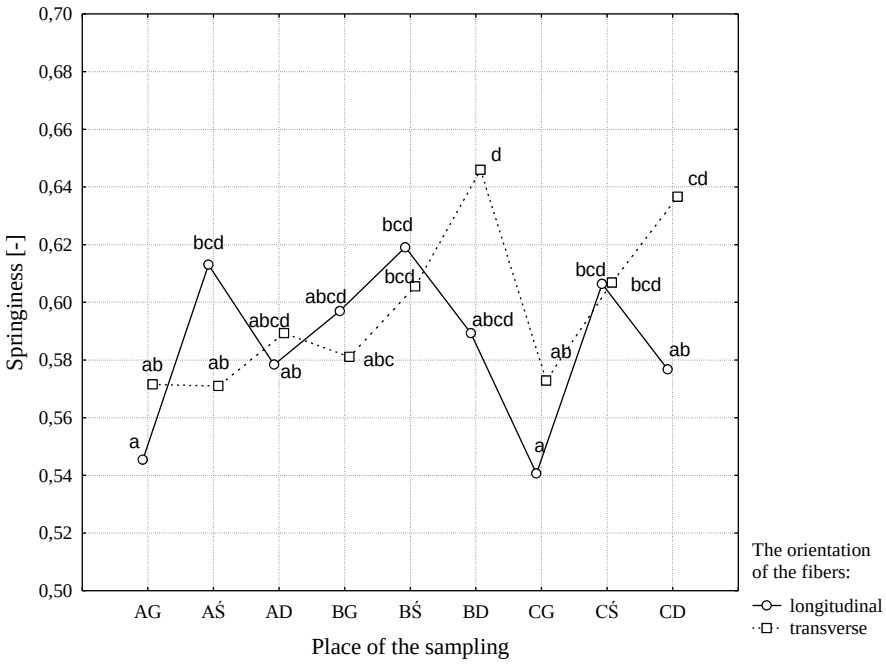

Fig. 7. The Tukey significance of differences between the springiness of the kohlrabi parenchyma samples taken from specific places along the longitudinal and transverse direction of the fibers

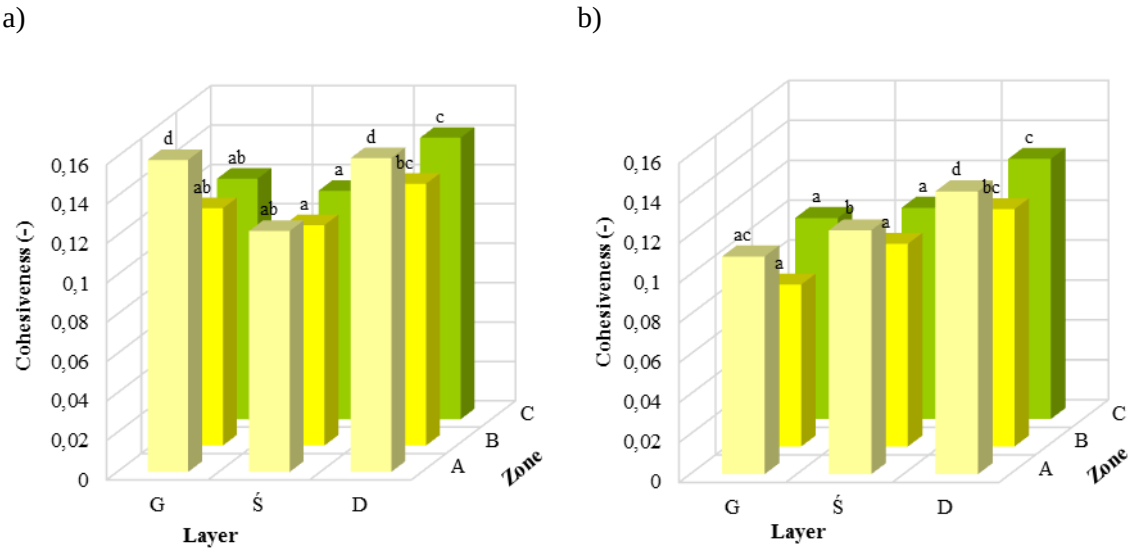

Fig. 8. Dependence of kohlrabi parenchyma cohesiveness on the site of sampling at: a) a longitudinal b) transverse fibers orientation

It was observed that the cohesiveness (Fig. 8) kohlrabi parenchyma was highest for samples coming from the lower layer of the zone A. The value of the determinant of the longitudinal orientation of fibers kohlrabi was 0.16, and the transverse was 11% lower. The lowest value of the properties observed during compression of the parenchyma arranged across the fibers of the upper layer zone B. Cohesiveness of the parenchyma samples taken from this location amounted 0.08. The results shown in Figure 9, which shows the mean values cohesiveness with their associated homogeneous groups ($p \leq 0.05$) indicates that the orientation significantly influence its cohesiveness. The greatest difference in the values observed for the raw tissue taken from upper layer of the zone A. The cohesiveness average value of the parenchyma samples arranged in the longitudinal direction was 0.16 and 0.11 in the transverse direction.

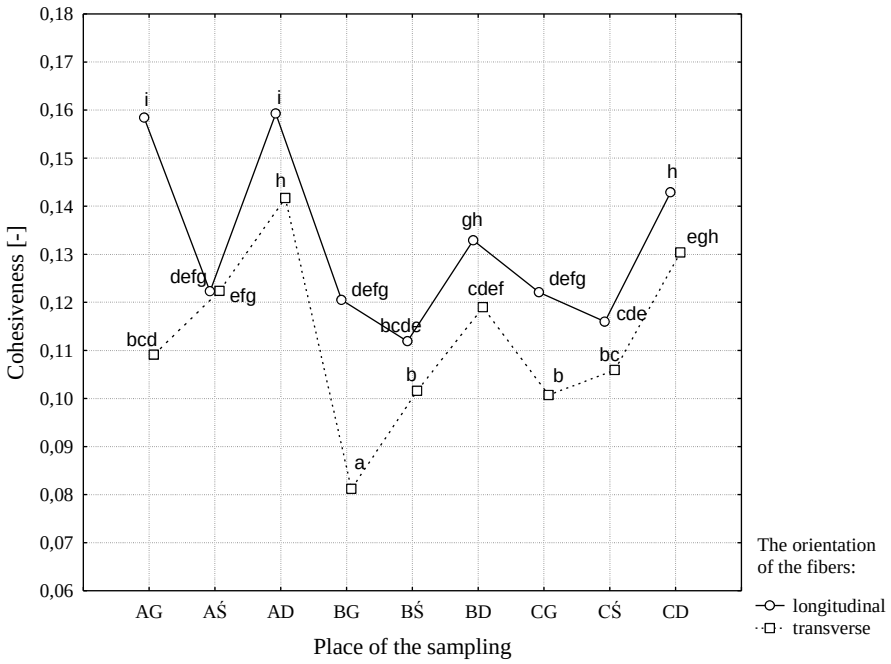

Fig. 9. The Tukey significance of differences between the cohesiveness of the parenchyma kohlrabi samples taken from specific places along the longitudinal and transverse direction of the fibers

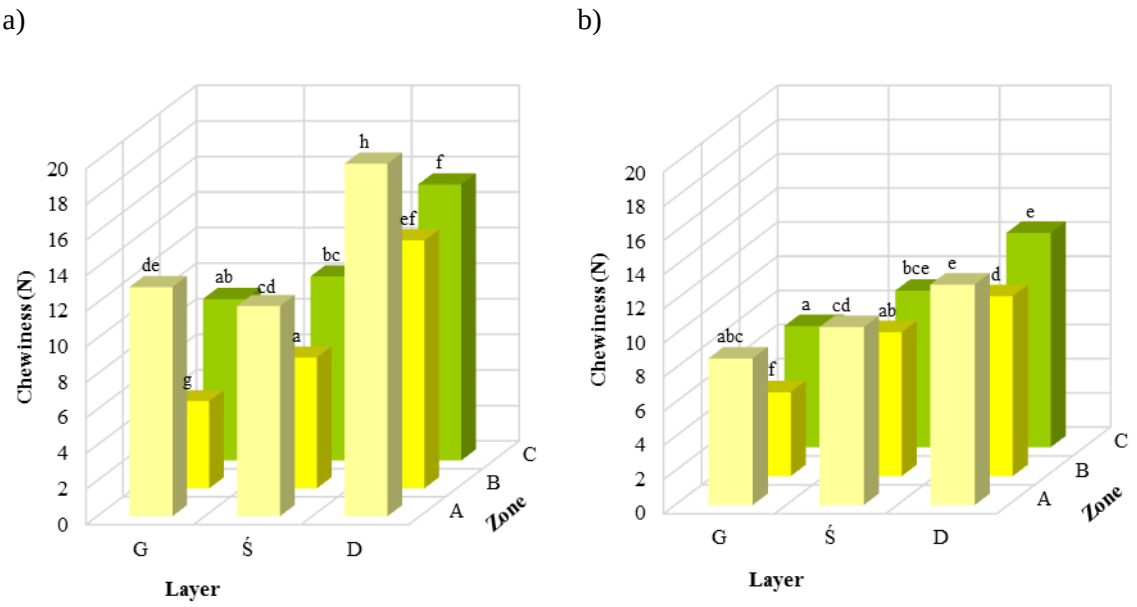

Fig. 10. Dependence of kohlrabi parenchyma chewiness on the place of sampling on: a) the longitudinal b) transverse fibers orientation

The chewiness of kohlrabi parenchyma (Fig. 10) located along fibers showed the highest values for the lower layer in zone A - 19.82 N, and the lowest in the upper layer of the zone B, where the value was 75%. In all the cases, the lowest chewiness was observed for zone B. The lowest value (4.9 N) of the determinant was observed in the upper layer, at the longitudinal orientation of fibers. Using the significance of differences Tukey test the values were calculated for most of the resulting statistically significant differences between kohlrabi tissues arrangement in the longitudinal and transverse orientation (Fig. 11). For the samples of material taken from zone A of the upper layer (sample compression along the fibers) the determinant value was12.88 N, 11.82 N for the middle layer and for the samples from the lowest layer kohlrabi - 19.82 N. At the transverse orientation of the fibers the parameter's values were lower by, respectively, 33%, 12% and 35%.

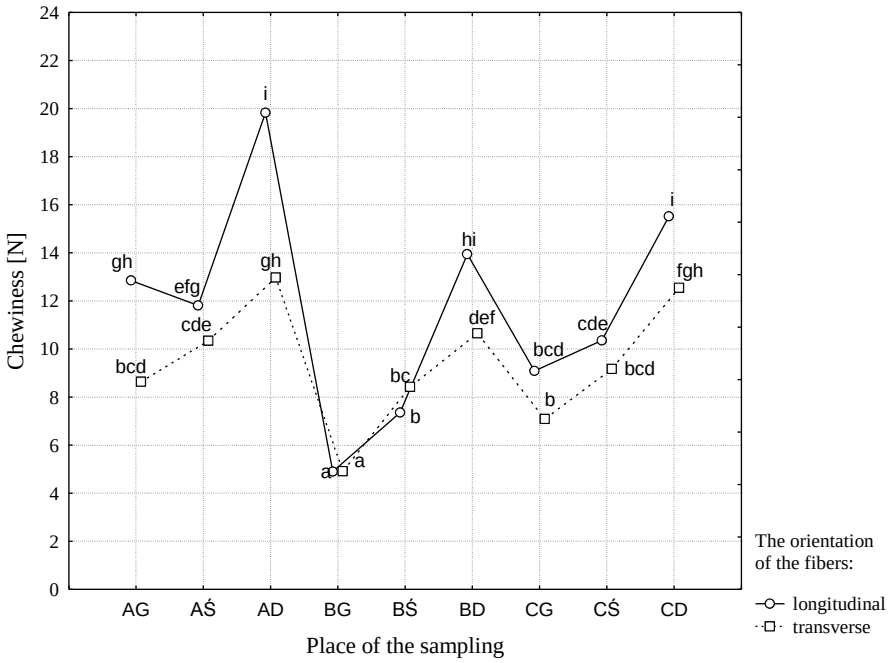

Fig. 11. The Tukey significance of differences between the chewiness of the parenchyma kohlrabi samples taken from specific places at the longitudinal and transverse direction of the fibers

Table 1 shows the regression equation describing the effect of the measurement place on the various texture determinants of kohlrabi parenchyma.

The distance from the *x* and *y* had a significant impact on the value of individual texture determinants.

Table 1. The regression equations and coefficients of determination R^2 describing texture determinants of kohlrabi parenchyma of the longitudinal and transverse fibers orientation depending on the place of sampling

Texture parameters	Fiber laying	Regression equation	Coefficients of determination R^2
Hardness [-]	longitudinal	$H = 0{,}21\,x^2 + 0{,}098\,y^2 - 6{,}918\,x - 2{,}553\,y + 158{,}632$	0,868
	transverse	$H = 0{,}073\,x^2 - 2{,}5\,x - 0{,}754\,y + 147{,}778$	0,592
Springiness [-]	longitudinal	$Spr = -0{,}000183\,y^2 + 0{,}606$	0,725
	transverse	$Spr = -0{,}003\,y + 0{,}573$	0,742
Cohesiveness [-]	longitudinal	$Coh = 0{,}000067\,x^2 + 0{,}0001\,y^2 - 0{,}0027\,x - 0{,}00038\,y + 0{,}1$	0,699
	transverse	$Coh = 0{,}000079\,x^2 - 0{,}003\,x - 0{,}001\,y + 0{,}124$	0,79
Chewiness [N]	longitudinal	$Ch = 0{,}02\,x^2 + 0{,}013\,y^2 - 0{,}707\,x - 0{,}249\,y + 12{,}929$	0,872
	transverse	$Ch = 0{,}01\,x^2 - 0{,}319\,x - 0{,}173\,y + 10{,}648$	0,772

where: *x* - distance measuring point from axis of ordinates [mm], and *y* - distance measuring point from abscissa [mm].

The equations are valid for the values of *x* (in the range of 0 ÷ 30 mm) and *y* (in the range of -15 to 15 mm) and are designated at the level of significance of differences $\alpha \leq 0.05$.

CONCLUSIONS

1. Place of the sampling and orientation of the kohlrabi parenchyma fibers had a significant impact on the value of texture determinants.
2. Hardness and chewiness of kohlrabi parenchyma were the highest in the lower layer and the lowest in the upper layer. In the case of samples compression, higher values of hardness and chewiness were observed at the transversal than the longitudinal fiber section.
3. Kohlrabi cohesiveness showed the lowest value in the zone B and they were higher during the compression od fibers placed in the longitudinal direction than of the transverse ones.
4. Morphological heterogeneity of kohlrabi cause variation of mechanical properties during the compression test.

REFERENCES

1. **Bianchi T., Guerrero L., Gratacós-Cubarsí M., Claret A., Argyris J., Garcia-Mas J., Hortós M., 2016.** Textural properties of different melon *(Cucumis melo L.)* fruit types: Sensory and physical-chemical evaluation. Scientia Horticulturae, 201, 46-56.
2. **Bohdziewicz J., 2006.** Effects of morphological diversification on the mechanical proprieties of brussels sprouts. Agricultural Engineering, 2, 165-173.
3. **Bohdziewicz J., Czachor G., Grzemski P., 2013.** Determination of rheological properties of vegetables and fruit based on work inputs of strain. Agricultural Engineering, 17, 35-42.
4. **Fosińska M., Nowicki A., Czart A., 2015.** Production analysis of chosen vegetable spiecies in Poland and production group 'Daukus' in the years 2011-2014. Infrastructure and Ecology of Rural Areas, III/1, s. 691–699.
5. **Gołacki K., Stankiewicz A., Stropek Z., 2005.** Effect of deformation rate on selected characteristics of viscoelastic plant materials. Acta Agrophysica, 5(3), 645-655.
6. **Gong R., Zhang X., Liu H., Sun Y., Liu B., 2007.** Uptake of cationic dyes from aqueous solution by biosorption onto granular kohlrabi peel. Bioresource Technology, 98, 1319-1323.
7. **Imaizumi T., Tanaka F., Hamanaka D., Sato Y., Uchino T., 2015.** Effects of hot water treatment on electrical properties, cell membrane structure and texture of potato tubers. Journal of Food Engineering, 162, 56-62.
8. **Jałoszyński K., Pasławska M., Surma M., Stępień B., 2013.** Drying kohlrabi with microwave method in the lowered pressure conditions. Agricultural Engineering, 17(4), 91-99.
9. **Kamali E., Farahnaky A., 2015.** Ohmic-Assisted Texture Softening of Cabbage, Turnip, Potato and Radish in Comparison with Microwave and Conventional Heating. Journal of Texture Studies, 46(1), 12-21.
10. **Karathanos V. T., Kanellopoulos N. K., Belessiotis V. G., 1996.** Development of porous structure during air drying of agricultural plant products. Journal of Food Engineering, 29(2), 167-183.
11. **Kunachowicz H., Nadolna I., Przygoda B., Iwanow K., 1998.** Tables of nutritional value of food products. Prace IŻŻ, 85, ISBN 83-200-3112-5, Warszawa.
12. **Kusińska E., Starek A., 2014.** The impact of potato sampling site on selected texture properties. TEKA Commission of Motorization and Energetics in Agriculture, 14(3), 61-66.
13. **Kusznierewicz B., Iori R., Piekarska A., Namieśnik J., Bartoszek A., 2013.** Convenient identification of

desulfoglucosinolates on the basis of mass spectra obtained Turing liquid chromatography-diode array-electrospray ionisation mass spektrometry analysis: Method verification for sprouts of different Brassicaceae species extracts. Journal of Chromatography, 1278, 108-115.

14. **Mousavizadeh S.J., Sedaghathoor S., Khorami H., 2011.** Essential oils as reducing agents of cabbage peroxidase. Scientia Horticulturae, 128, 388-392.
15. **Nurzyński J., Dzida K., Nowak L., 2007.** The effect of different nitrogen fertilization on yielding of kohlrabi and chemical composition in leaves and stems. Rocz. AR w Poznaniu, 383, 583-587.
16. **Stępień B., 2009.** Modification of mechanical and rheological properties of selected vegetables under different drying methods. Wydawnictwo Uniwersytetu Przyrodniczego we Wrocławiu, Wrocław.
17. **Szyperek M., 2015.** Today and tomorrow in processing. Owoce, Warzywa, Kwiaty, 04, 50-51.
18. **Ślaska-Grzywna B., Andrejko D., Kuna-Broniowska I., Sagan A., Blicharz-Kania A., 2013.** Shaping some selected textural properties of pumpkin *(Cucurbita maxima duch.)* by optimized heat treatment. Food. Science. Technology. Quality, 4(89), 195 – 209.
19. **Weber A., Braybrook S., Huflejt M., Mosca G., Routier-Kierzkowska A. L., Smith R. S., 2015.** Measuring the mechanical properties of plant cells by combining micro-indentation with osmotic treatments. Journal of Experimental Botany, 66(11), 3229-3241.
20. **Zalega J., Szostak-Węgierek D., 2013.** Nutrition in cancer prevention. Part I. Plant polyphenols, carotenoids, dietary fiber. Probl. Hig. Epidemiol., 94(1), 41-49.
21. **Zdunek A., Cybulska J., Konopacka D., Rutkowski A., 2010.** New contact acoustic emission detector for texture evaluation of apples. Food Engineering, 99(1), 83-91.

The safety of modern and traditional communication protocols in vehicles

Andrzej Sumorek

Lublin University of Technology, Department of Structural Mechanics
Poland, 20-618 Lublin, Nadbystrzycka 40, e-mail: a.sumorek@pollub.pl

Received July 18.2016: accepted July 25.2016

Abstract. Communication infrastructure of vehicles sub-assemblies has undergone three phases of development. The first phase was initiated by the need to reduce emission levels. The function of vehicle sub-assemblies health monitoring was introduced simultaneously. This phase took place in the 70s and 80s of the 20th century. The second phase was focused on the elimination of redundant sensors and implementation of new functions of the vehicle. This phase has been particularly noticeable since the beginning of the 21st century. At the moment, there are 2 directions of development. On the one hand, the works are being continued in the scope of autonomous movement of vehicle and, on the other hand multimedia solutions are being introduced in order to make the time spent in a vehicle more attractive (multimedia, the Internet, …).

The present study is focused on the mechanisms of protection applied in communication protocols used in vehicles. Furthermore, it contains the classification of communication methods, characteristics of the basic methods of protection incorporated in the described protocols and the practical cases of security breach. Therefore, it is possible to answer the question why it is possible for third persons to interfere into the communication network of a vehicle and to indicate potential methods of protection against the functioning disturbance in such communication networks.

Keywords: Vehicle Communication Protocol, Protocol Safety.

INTRODUCTION

Communication systems of vehicles sub-assemblies have undergone three phases of development. The first phase was initiated by the United States Congress which approved „Clean Air Act" and established Environmental Protection Agency (EPA) in 1970. The principal goal of legislator was to reduce emission levels. As a result of introduction of „Clean Air Act" two new functions have been introduced by motor vehicles manufacturers. On the one hand, the manufacturers commenced to provide motor vehicles with controllers ensuring reduction of emission levels. Simultaneously, they also commenced to install the sockets enabling the diagnostics of vehicle condition in a manner independent on the manufacturer.

The second phase of communication networks development was focused on the elimination of redundant sensors and implementation of new functions. As a result of the elimination of redundant sensors, it was possible to reduce the costs of motor vehicle production. Another effect is the introduction of multiple driver assistance systems e.g. Anti-Lock Braking System (ABS), Electronic Stability Program (ESP) or Acceleration Slip Regulation (ASR). Increased performance of electric and electronic systems (micro-controllers) combined with reduced prices resulted in the introduction of new functions, i.e. temperature measurement in multiple points of vehicle cabin, introduction of several airbags, possibility to adjust the settings of air-conditioning, seats or mirrors by means of pushbuttons.

Currently, 2 directions of development are visible. On the one hand, the works are continued in the scope of autonomous movement of a vehicle and, on the other hand multimedia solutions are introduced in order to make the time spent in a vehicle more attractive (multimedia, the Internet, …). The commonly used parking assistant enables parallel parking without touching the steering wheel. The scope of other driver assistance systems encompasses forward collision warning, lane depth warning, auto steering road edge or pedestrian detection [20]. Less known is the more advanced BMW solution „Remote Valet Parking Assistant" enabling autonomous travel of a parked vehicle to the driver or automatic parking without the driver presence in a motor vehicle [10, 37]. Complete or partial hands-off solutions are applied in Google and Audi motor vehicles. At the time of this writing, autonomous travel of Audi vehicle on highways was equal to almost 1000 km [10]. The travel of autonomous Google motor vehicle has been equal to about 2 million kilometers [18]. Google motor vehicle seems to be the closest to introduction to everyday use. Mr. Stanley from Stanford University, a co-author of the autonomous vehicle, was the first manager of the autonomous vehicle construction project. Stanley vehicle won the first competition for the autonomous vehicle construction arranged by United States Department of Defense (DARPA). The first winner of DARPA competition in the year 2005 and Google motor vehicle in the year 2016 is illustrated in Fig. 1 [28]. As a result of dynamic development, communication networks previously dedicated for various applications are applied in the same motor vehicle.

Fig. 1. The first model (2005) and actual prototype Google motor vehicle (2016) [16, 28]

AUTOMOTIVE NETWORKS AND PROTOCOLS

Before the introduction of data bus communication into a motor vehicle, data exchange was carried out on the basis of simple cable connections between sensors and actuators of the vehicle as well as signaling devices and switches accessible to the driver. Initially, 3 classes of protocols (A, B, and C) were introduced by SAE J1850 standard which were dedicated to various applications between 10 Kbps and 1 Mbps [6, 24, 36]. As early as at the start of the 21st century, the protocols with higher complexity and data baud rate marked as C+, D or Infotaiment began to be used [3, 6, 22, 32, 34]. The structures of every currently manufactured vehicle incorporate simple A class networks (LIN – Local Interconnect Network), as well as D class networks (Medium Oriented System Transport), as illustrated in Fig. 2.

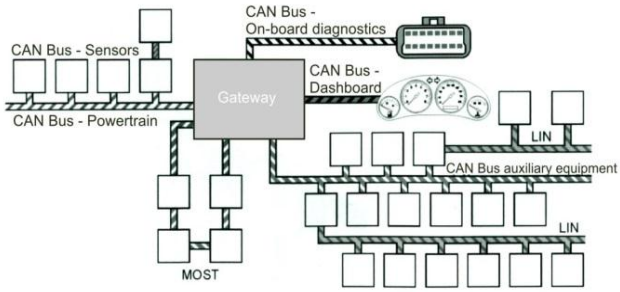

Fig. 2. Conventional communication infrastructure of motor vehicle sub-assemblies [3]

The diagram of communication infrastructure of higher class vehicles is shown in Fig. 3. The diagram illustrates the majority of conventional communication networks from Fig. 2 and additional communication systems. The additional communication systems can be subdivided into two groups. The first group is represented by FlexRay protocol. This group consists of protocols dedicated for automotive sector applications. The representatives of the second group are show in Fig. 3 in the vicinity of Telematics Head Unit (THU). Often, they are solutions associated with typical IT technology i.e. Ethernet network, WLan (Wireless LAN), USB (Universal Serial Bus). This group is supplemented with the solutions enabling the access to mobile telephony networks or to Global Navigation Satellite Systems e.g. GPS (Global Positioning System). Their task is to make vehicle use more comfortable through facilitated vehicle driving (GPS), communication (mobile telephony networks and Bluetooth), multimedia data exchange and entry into motor vehicle from portable devices and the Internet.

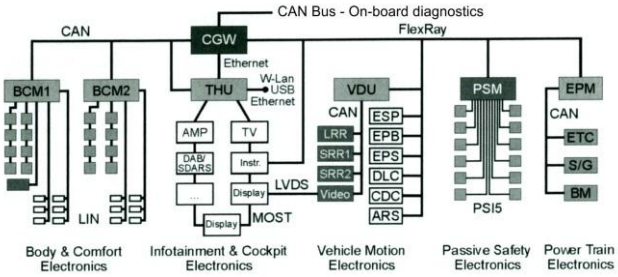

Fig. 3. Example of an advanced communication infrastructure of vehicle sub-assemblies [3]

Elements of communication structures illustrated in Fig. 2 and Fig. 3 are characterized by a high variety of communication methods. A single motor vehicle contains „slow" protocols enabling an exchange of small messages between a precisely defined number of motor vehicle sub-assemblies (e.g. LIN protocol). On the other hand, the multimedia devices can communicate with unknown external multimedia sources (e.g. Wireless LAN) in a fast and wireless mode. The vehicle communication structure integrates the systems dedicated for motor vehicle sub-assemblies control (e.g. FlexRay protocol) and general type systems (e.g. Universal Serial Bus).

The dynamic development in the scope of networks and protocols dedicated for various applications is reflected in the diversified architecture of protocols. Fig. 4 illustrates the basic layer structure based on ISO-OSI model and accompanied by selected structures applied in case of MOST (Medium Oriented System Transport), CAN (Controller Area Network) and Bluetooth protocols. In case of protocols it is not necessary to specify and use all the layers. In case of a protocol serving a single and separated network segment, there are no communication problems between modules regardless the incomplete description of protocol. A diversified structure of many motor vehicles network would require consistency between the protocols, for instance consisting in similar security levels to be ensured in individual layers. Stacks of protocols illustrated in Fig. 4 confirm that various solutions are applied in practice. There are protocols defined in all the 7 layers of ISO-OSI model (e.g. MOST)

as well as protocols defined in only one physical layer (e.g SAE J1850 PWM - Pulse Width Modulation and SAE J1850 VPW - Variable Pulse Width) or in several layers – physical layer and data link (e.g. CAN). Diversified communication methods within a motor vehicle are caused by the absence of any technical guidelines in the scope of communication in the initial period of data bus development; only expected emission levels and types of data accessible by means of diagnostic equipment were determined by the legislator. The current problems result from the necessity to make the product, i.e. a motor vehicle, more attractive and to immediately introduce digital technique solutions which could be unsuitable for motor vehicles. Software errors in "household" computers can be eliminated through corrections of successive program versions but software errors in motor vehicle controllers may lead to collisions and accidents.

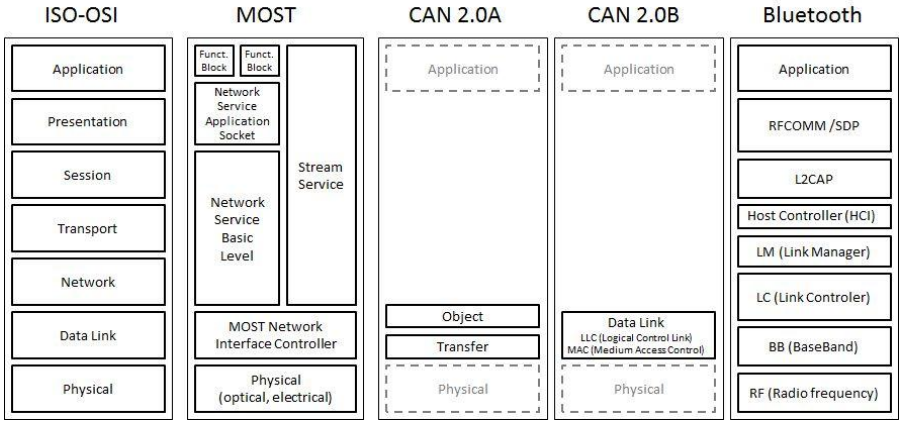

Fig. 4. Layers in the ISO-OSI model and layers in selected communication methods [13, 34]

Examples of communication structures of motor vehicles information network illustrated in Fig. 3 and 4 are associated with more than ten protocols and networks. The characteristics of the 3 selected data buses and protocols representative for networks in A, B and C classes are presented below.

LIN Bus. LIN bus/ protocol (Local Interconnect Network) depending on the baud rate (between 1 and 20 Kbps) can be classified in A or B protocols class. Its first practical implementation took place in 2001. LIN is applied in BCM (Body Control Module) as illustrated in Fig. 3. It is also applied in control and adjustment systems for windows, seats, doors and mirrors [34, 38].

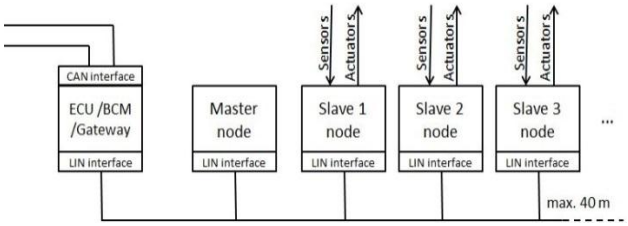

Fig. 5. Single-wire implementation of LIN cluster [23, 32]

LIN bus is operated in single-wire implementation configuration. Maximum 16 nodes can be attached to a single wire bus. The bus should not be longer than 40 meters. Single-wire implementation incorporates a master node and up to 15 slave nodes. Such an arrangement is called cluster (Fig. 5).

The functioning of the whole cluster is based on one or more"schedule tables". A "schedule table" contains the list of successive orders including the time and conditions of their transmission by the master node. Communication of cluster nodes is initiated by the master node in accordance with the "schedule table". The cluster nodes use messages (frames) with the structure shown in Fig 6. The frame is divided into two parts. The first part called the header contains an identifier i.e. a number to which slave node activity is assigned. Responding to the identifier, the slave node may: a) receive and complete the order of master node which is contained in „response" part, b) send data determined by means of the identifier in „response" part to the master node, c) receive the data determined by means of the identifier from another slave node.

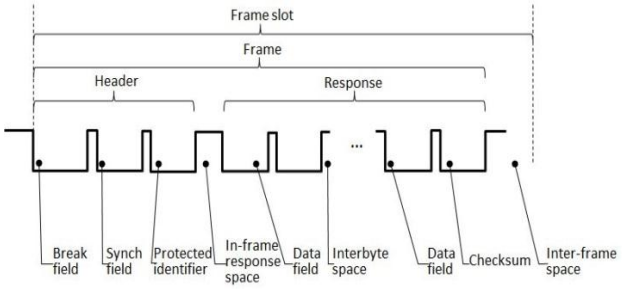

Fig. 6. LIN message frame [23, 34]

Commands of a master node contained in the identifier in the header are secured by means of two additional check bits. Data transmitted to and from a slave node in response are secured by means of an additional byte of checksum. In later protocol versions it is possible to enter an additional bit confirming the correctness of data receipt. There are no advanced mechanisms of data protection in the course of a normal operation of LIN network cluster. In case of identifier or data bytes error detected in the frame, such frame is ignored. In case of lack of declared additional checking procedures, the headers and data with incorrect checksums will not be identified by the cluster. The cluster area does not contain any mechanisms verifying whether the received frame has really originated in the master node. Each node which is

physically connected to the bus line is able to generate messages disturbing the operation of the whole cluster. An external device connected to the diagnostic port is able to generate messages for LIN cluster by means of a gateway. The lack of nodes authentication is one of the reasons of LIN bus use in the systems in which high security level is not required.

CAN Bus. Currently, Controller Area Network shall mean the communication protocol, data bus, communication method. Originally, CAN was developed as the communication protocol. It has been introduced for the first time in the year 1991. CAN protocol specification describes Data Link Layer only (Fig. 4). Due to its common application on the market, multiple CAN specifications occurred in the physical and application layer. Therefore, CAN can be applied as B and C class protocol. Unless significant transmission rate is required, it is possible to use the CAN described in ISO 11898-3. In such case, the bandwidth is lower than 250 Kbps. High Speed CAN described in ISO 11898-2 is used in the systems with the bandwidth reaching 1 Mbps. Additional descriptions introduced by ISO standards mainly relate to the physical layer requirements enabling to achieve the required rate of data exchange [3, 30, 31, 36,38]. On the other hand, CAN has been extended by the description of functioning in the application layer and DeviceNet, CANOpen and CAN Kingdom specifications have been created.

In most cases, CAN bus is built in the form of double-wire implementation (Fig. 7). Linear and star topology is applied. Linear bus topology is commonly used in motor vehicles (Fig. 7). The number of nodes connected to the bus is limited by electric parameters only. The bus is operated in a multi-master mode i.e. the priority of all the nodes is identical. There are no master and slave nodes like in the case of LIN bus. All the nodes can commence transmission at the same time. All the nodes can access the data transmitted by the bus.

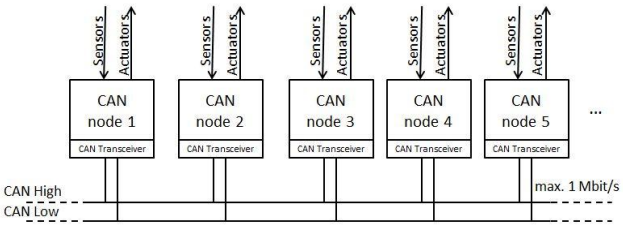

Fig. 7. Double-wire implementation of CAN Bus [13, 32]

Access to data is controlled by arbitration field of CAN message frame (Fig. 8) [33]. In case of simultaneous start of transmission by several nodes, the transmission is continued by the node with greater number of prevailing bites in the arbitration field of CAN message frame. Such a mechanism of the access to CAN bus makes it possible to easily attach new nodes. When entering new messages and new frames, it is only required to avoid collisions with previously used messages.

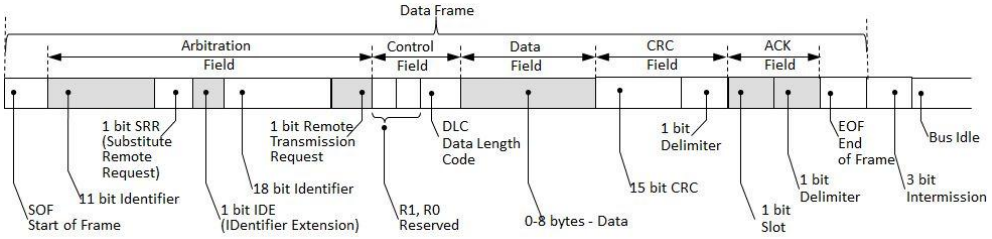

Fig. 8. CAN message frame [3, 31]

There are several mechanisms ensuring security within CAN network. Two methods are used to reduce errors level in the physical layer. Node transceivers are capable to check the bits emitted and present on the bus. In case of non-conformity of the bit emitted and present on the bus, transmission error is detected. In order to avoid bus saturation condition, „bit stuffing" mechanism has been introduced. When five identical bits are transmitted to the bus successively, the sixth bit is automatically transmitted as an opposite bit and automatically eliminated by the receivers. The occurrence of six identical bits despite destuffing will automatically result in the detection of transmission error. Frame structure makes it possible to introduce four additional methods of errors detection (Fig. 8). DLC field indicates the length of data contained in Data Field. CRC field makes it possible to enter checksum consisting of 15 fields for data from Data Field. Inconsistency of sums in the transmitting node and receiving node will result in the transmission of CRC error to the bus. The acknowledging of a bit in ACK field transmitted by the frame recipient will assure the sender that the transmission has been effective. CAN protocol frame has a constant format (equal sizes of fields in the frame). In case of a non-conformity of the bits number with the assumed ones, "frame error" will be generated by any frame recipient.

Presented characteristics of CAN bus and protocol may indicate a high CAN resistance to errors. The estimated number of non-detected errors in relation to the number of bytes transmitted included between 10^{-11} and 10^{-6} [35, 35]. The presented mechanisms do not protect against the introduction of any unknown nodes and additional messages to the bus if the new messages will conform to the required frame format. We could easily imagine that there is a node which will monopolize the bus through continuous transmission of top priority messages.

FlexRay Bus. FlexRay bus is the latest solution dedicated to motor vehicles communication networks which has been applied in practice. The purpose of FlexRay Consortium established in the year 2000 was to develop a solution enabling the communication with a rate higher than in the case of CAN bus and

simultaneously ensuring higher security. The bus is mainly dedicated for the supporting of driving systems and active safety systems [3, 38].

The bus can be operated in point – to point topology, star topology, active star topology and hybrid topology, constituting the combination of 3 preceding topologies. Each node can support 2 communication channels. Depending on the applied interface, data transmission is possible by means of 2 wires or fibre optic link. Each channel supports a bandwidth from 10 Mbps. Therefore it is possible to achieve data exchange rate of 20 Mbps or to have a reserve communication channel. The connection between the nodes should not exceed 24 meters.

The nodes communicate by means of frames with the structure presented in Fig. 9. This structure is similar to CAN protocol frame structure. In this case it is also possible to detect errors at the frame structure level. Frame ID indicates frame location in communication cycle. „Payload length" field contains the information on utility data. The header and data are secured by means of checksums.

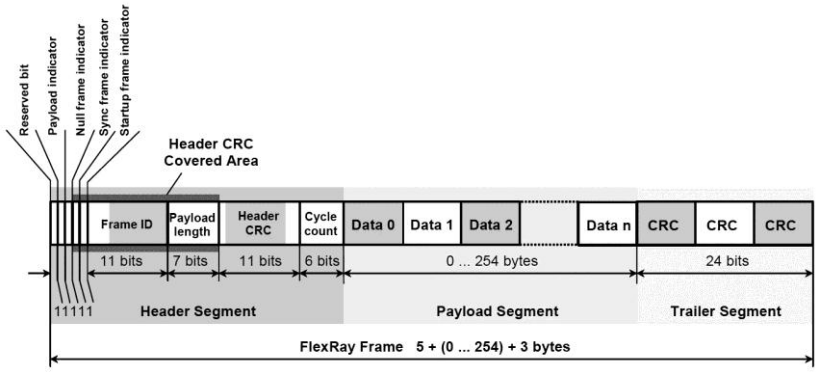

Fig. 9. FlexRay frame format [8]

In case of FlexRay, the control of access to the bus combines the methods applied in LIN and CAN buses. The communication cycle can be subdivided into 4 segments: static, dynamic, symbol window and network idle time. Fig. 10 illustrates a communication cycle without „symbol window". In the static part, the nodes can transmit data in time slots precisely determined for them (like in case of LIN). In the dynamic part, the nodes communicate depending on their priorities (like in case of CAN). This communication method enables a deterministic data transfer, simultaneously ensuring quick support in case of unexpected events.

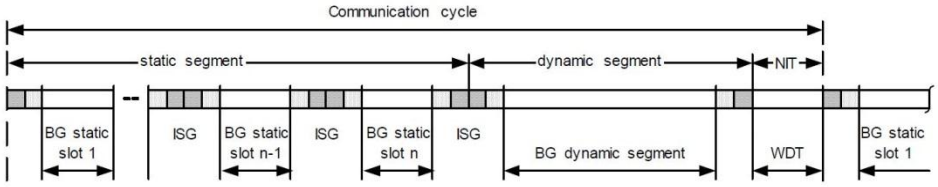

Fig. 10. Bus guardian communication schedule with static and dynamic segment [7]

Bus Guardian module presence in the bus controllers is essential for security assurance [7]. The task of this module is to permit the controller to communicate only in the slots assigned to this controller in communication cycle. Therefore, the possibility of communication disturbance by a single controller on the whole bus is excluded. Additionally, in case of active star topology, it is possible to cut off nodes or network segments generating interfering signals. Owing to these features, FlexRay bus is the fastest and most secure communication bus from among the buses described herein.

PRACTICAL VIOLATION OF SECURITY

The three most common data buses used in motor vehicles and described in the preceding chapter are based on protocols which seem to be resistant to errors to a various degree. The present chapter contains the descriptions of practical experiments consisting in cracking into communication systems in vehicles, descriptions of methods used to disturb the operation of sub-assemblies being the elements of the communication network of a motor vehicle.

Disturbance of motor vehicle functioning by OBD diagnostic port. OBD diagnostic port is an element installed in each manufactured vehicle. Pursuant to ISO 15031-5, diagnostics tester connected to this port can be operated in 9 modes. Most frequently, modes 3 and 4 are most commonly used in vehicle servicing. The modes 3 and 4 consist in reading and deleting permanent defects recorded in the controller. Simultaneously, there are operation modes making it possible to obtain the information on the current parameters of the driving assembly and to take over the control in order to check the correctness of its operation. Additionally, SAE J2534 and ISO 23248 standards define the manner of controllers reprogramming by means of diagnostic protocols [38]. This property is used by a person who wants to disturb

motor vehicle operation. False data frames supplied by means of a diagnostic port are not distinguished from frames generated by the vehicle network nodes. Obviously, there is a problem of physical access to the vehicle in order to make the connection to OBD diagnostic connector. Therefore, malice reprogramming is possible only in the case of the vehicle owner's absence. It is unnecessary to use any special diagnostic tester for reprogramming. It is possible by means of software running on PCs communicating with OBD system by means of RS, USB port, Bluetooth network and WiFi. A potential impact on the functioning of motor vehicle controllers has been reported many times [4, 15, 19]. It was also possible to modify the controllers functioning in the course of a vehicle's motion [19].

Software change by means of multimedia system elements. One of the elements of Medium Oriented System Transport shown in Fig. 2 and Fig. 3 is often used as CD or more frequently DVD player. In order to improve the functionality of players, their manufacturers make it possible to update firmware. A properly prepared CD or DVD disc makes it possible to change the player software without the awareness of user. As in the case of "household" players, in selected models update process is triggered by pressing of indicated combination of buttons or updating is carried out automatically [25, 26]. The compromised player constituting an element of MOST bus is still able to affect the multimedia system elements which are frequently used to establish phone, Internet and Bluetooth connections. Changed software can disturb on-board networks systems if it is permitted by multimedia network gate.

Local and remote breaking into vehicle. Variable coding is applied in the central lock systems of vehicles. Therefore it is impossible to open the motor vehicle by means of a known intercepted code. „Man-in-the-middle" attack carried out by an expert in the scope of IT security proved that all the locks with radio pilots are insufficient protections [9]. Samy Kamkar built RollJam device (Fig. 11). RollJam incorporates three antennas. Two antennas are used to disturb the key fob (remote control) signal and the third antenna intercepts this signal at each button pressing. The first key fob signal is intercepted and recorded but not received by the receiver in the vehicle. When the second signal is transmitted, the first recorded signal opening the locks is transmitted by the device. The second recorded signal can be used for locks opening in future [9, 12]. Remote attack methods are based on Telematic systems of exclusive vehicles. The thief knowing the vehicle data and the manner of owner's verification can establish phone connection with vehicles fleet management centre and enforce the vehicle opening in remote mode. Another method of vehicle protection consists in keyless systems and immobilizers based on RFID technology. Practical tests proved that it is possible to build a device effectively simulating RFID transponder operation. In executed tests, apart from the immobilizer blocking removal from the vehicle, it was possible to make the payments verified by means of the device using RFID transponder [1].

Fig. 11. Universal "remote control" – RollJam (on the left) [11]. Hardware platform for the false GPS transmitter (on the right) [15]

Attack on Bluetooth network. Bluetooth Network support is included in Infotaiment and Cockpit Electronics system (Fig. 3) of each currently manufactured vehicle. The task of Bluetooth interface is to ensure short range wireless communication for personal devices. The present version of standard 1.0 with the bandwidth of 15 Kbps has been upgraded to version 4.2 in December 2014. Multi-functionality of Bluetooth has been reflected in the complex structure of protocols stack illustrated in Fig. 4 and consequently in increased sensitivity to external attacks. The following types of attacks have been reported in the course of Bluetooth development:

- Bluebug – establishing of connections, sending of SMS messages, acquisition of information from the device (e.g. directory) without the user's awareness [29];
- Bluesnarf – acquisition of information e.g. address directory, photos, schedule from a device with Bluetooth interface [14];
- Bluejack – spam transmission / received in the form of visit cards from the devices within radio range after the receipt of properly prepared visit card [29];
- Car whispering – voice interception and sending to car kits or audio devices [14, 27, 29].

The described attacks has been eliminated by later version of protocols in Bluetooth protocols stack, authentication mechanism has been corrected and PIN codes have been made longer. However, it is still possible to listen to a non-encrypted transmission or to record an encrypted transmission in order to decrypt this transmission later. An active Bluetooth interface will be exposed to „Big POLL" attack consisting in continuous responding to POLL packages transmitted by an attacker preventing the devices switchover to low power sleep mode [29].

Attack on satellite navigation system. GPS system considered the first generally accessible navigation system achieved its full functionality in the year 1993. This navigation system facilitates motor vehicle driving performing the role of dynamic chart, facilitates vehicles fleet management and supports the localization of stolen vehicles. Navigation signal disturbance practically makes the vehicle motion impossible. The disturbance of satellite

signal seems to be impossible. In practice, GPS receiver prefers the strongest satellite signal. However, a portable transmitter built in the year 2008, is capable to generate information about erroneous position (Fig. 11) [5, 15]. Such device is not capable to disturb the signal for fast moving car but is capable to affect the determination of the route for a parked autonomous vehicle. The presence of such transmitter sending "own" GPS signal can mislead the systems localizing stolen vehicles. It is hard to determine the behaviour of Web VANET network in case of occurrence of a vehicle with deformed position coordinates [17].

Remote taking control over vehicle. Charlie Millerand Chris Valasek are the leading specialists in the scope of intrusions into voice and data transmission networks of motor vehicles [9]. Initial attempts of such intrusions required cable connection with vehicle network. In case of later attempts it was possible in remote mode. A documented attack was carried out to Jeep vehicle. This vehicle was connected with the Internet via UConnect system. Physical connection of UConnect is possible by means of mobile telephony services provided by Sprint company. On the basis of query directed by means of browser it was possible to localize IP address of motor vehicle in Sprint network. Due to a gap in vehicle software it was possible to change firmware of a chip in the vehicle entertainment system. After chip reprogramming to was possible to complete remote commands and to take the control over a majority of a vehicle's sub-assemblies i.e. steering and breaking system, air – conditioning and central lock [9, 11]. In this case, the attack was possible thanks to erroneous software. Therefore it can be classified as the attack to application layer. Remote attack was possible via the link of Spring mobile telephony and Wi-Fi network. This gap has been eliminated from 1.4 million vehicles through software updating.

CONCLUSIONS

Owing to the solutions reducing emission levels, improving safety and comfort of the driver and passengers, the problems associated with vehicle failures are concentrated on electronic systems as well as data processing and transfer systems. Striving for higher comfort and autonomous vehicle motion will intensify the problems associated with on-board computer systems installed in motor vehicles. On the basis of presented functioning analysis for selected communication buses and documented cases of the influence on data exchange influence in vehicles, the following conclusions can be drawn:

1. Protocols and data buses of motor vehicles are characterized by functionality assumed by their authors. The protocols ensure transmission security and rate in accordance with the corresponding classes. They have not been designed in terms of intentional interferences caused by third persons.

2. Newer communication protocols (e.g. FlaxRay) are provided with mechanisms increasing their reliability and security of use (redundant communication channels, increased bandwidth, bus access control by Bus Guardian module).

3. Dynamic development of automotive industry is the source of potential disturbances in data exchange systems operation. Therefore, several electronic, mechatronic and computer sub-assemblies characterized by diversified complexity levels and diversified resistance to disturbances and intrusions and originating from various manufacturers are integrated in the same vehicle.

4. Increased vulnerability of the whole system to disturbances and intrusions is caused by a mix of solutions from various fields of life (automotive industry, consumer electronics, mobile telephony, IT).

5. In most cases, physical vehicle access is required (ODB port, DVD player, Bluetooth communication activating …) to reduce vehicle use safety.

6. The cases of attacks reducing vehicle user safety, analyzed and presented above, require comprehensive theoretical knowledge and research facilities. Attacks are carried out as multi-phase attempts. There is no hazard of fast popularization of effective attacks to computerized vehicles.

REFERENCES

1. **Bono S.C., Green M., Stubblefield A. Juels A., Rubin A.D., Szydlo M. 2005.** Security Analysis of a Cryptographically-Enabled RFID Device. Proceedings of USENIX Security 2005, USENIX Association.
2. **Bosch R. GmbH. 1991.** CAN Specification. Version 2.0, Stuttgart.
3. **Bosch R. GmbH. 2008.** Data exchange network in vehicles. Wydawnictwa Komunikacji i Łączności, Warszawa (in Polish).
4. **Checkoway S., McCoy D., Kantor B., Anderson D, Shacham H., Savage S., Koscher K., Czeskis A., Roesner F., Kohno T. 2011.** Comprehensive Experimental Analyses of Automotive Attack Surfaces. Report for the National Academy of Sciences Committee on Electronic Vehicle Controls and Unintended Acceleration, http://www.autosec.org/pubs/cars-usenixsec2011.pdf.
5. **Cornell University. 2008.** GPS Navigation Devices Can Be Spoofed, Counter Measures Not Effective In Certain Cases. https://www.sciencedaily.com/releases/2008/09/080922122523.htm (23.09.2008).
6. **Fijalkowski B.T. 2011.** Automotive Mechatronics: Operational and Practical Issues. Volume 1. Springer Science+Business Media B.V.
7. **FlexRay Consortium. 2004.** FlexRay Communications System. Bus Guardian Specification, Version 2.0. www.uni-salzburg.at/fileadmin/multimedia/SRC/docs/teaching/SS08/PS_VS/FlexRayCommunicationSystem.pdf.
8. **FlexRay Consortium. 2010.** FlexRay Communications System. Protocol Specification, Version 3.0.1, svn.ipd.kit.edu/nlrp/public/FlexRay/FlexRay%E2%84%A2%20Protocol%20Specification%20Version%203.0.1.pdf.
9. **Gozdek J. 2015.** Hackers without limits. Chip, 11, 104-108 (in Polish).
10. **Gozdek J. 2015.** The spring novelties. Chip, 4, 20-25 (in Polish).

11. **Greenberg A. 2015.** Hackers Remotely Kill a Jeep on the Highway—With Me in It. Wired, www.wired.com/2015/07/hackers-remotely-kill-jeep-highway, 21.07.2015.
12. **Greenberg A. 2015.** This Hacker's Tiny Device Unlocks Cars And Opens Garages. Wired, www.wired.com/2015/08/hackers-tiny-device-unlocks-cars-opens-garages, 06.08.2015.
13. **Grzemba A. 2008.** MOST - The Automotive Multimedia Network. Frazis Verlag GmbH.
14. **Haataja K., Hyppönen K., Pasanen S., Toivanen P. 2013.** Bluetooth Security Attacks. Comparative Analysis, Attacks, and Countermeasures. Springer Berlin Heidelberg.
15. **Humphreys T.E, Ledvina B.M., Psiaki M.L., O'Hanlon B.W., Kintner P.M. 2008.** Assessing the Spoofing Threat: Development of a Portable GPS Civilian Spoofer. Proceedings of ION GNSS, The Institute of Navigation, Savanna, Georgia, USA.
16. **Jaffe E., 2015.** Google's New Self-Driving Car Is About to Hit the Streets. CityLab, http://www.citylab.com/tech/2015/05/googles-new-self-driving-car-is-about-to-hit-the-streets/393323.
17. **Joe M.M., Ramakrishnan B. 2015.** Review of vehicular ad hoc network communication models including WVANET (Web VANET) model and WVANET future research directions. Wireless Networks. Springer Science+Business Media New York.
18. **Korn J. 2015.** Computer: The Sorcerer's Apprentice. Chip, 9, 108-111 (in Polish).
19. **Koscher K., Czeskis A., Roesner F., Patel S., Kohno T., Checkoway S., McCoy D., Kantor B., Anderson D., Shacham H., Savage S. 2010.** Experimental Security Analysis of a Modern Automobile. Proceedings of IEEE Symposium on Security and Privacy, Oakland, CA, May 16–19, 2010, http://www.autosec.org/pubs/cars-oakland2010.pdf.
20. **Kulas T. 2015.** New methods of security. Chip, 8, 100-101 (in Polish).
21. **Larson U.E., Nilsson D.K. 2008.** Securing vehicles against cyber attacks. Mili and Krings editors, CSIIRW '08, ACM Press.
22. **Leen G., Hefferman D. 2000:** Talking to the car. The Engineneer, http://www.theengineer.co.uk/news/talking-to-the-car/285325.article, 5 October 2000.
23. **LIN Consortium. 2006.** LIN Specification Package Revision 2.1. tge.cmaisonneuve.qc.ca/barbaud/R%C3%A9f%C3%A9rences%20techniques/Bus%20LIN/LIN-Spec_Pac2_1.pdf.
24. **Merkisz J., Mazurek S. 2007.** On-board Diagnostic Systems of Vehicles. Wydawnictwa Komunikacji i Łączności, Warszawa (in Polish).
25. **Panasonic Corporation. 2016.** DMP-BD10 Firmware Download. http://av.jpn.support. panasonic.com/support/global/cs/bd/download/bd10/europe_uk/index.html
26. **Sony Europe. 2016.** Sony Home Audio and Video: Firmware Download. https://www.sony.co.uk/support/en/content/cnt-dwnl/prd-tvhc/sony-rdrhxd-firmware-update-v170/RDR-HXD870
27. **Soppera A., Burbridge T. 2005.** Wireless identification - privacy and security. BT Technology Journal, Vol 23, 4, 54-64.
28. **Stavens D. M. 2011.** Learning to Drive: Perception For Autonomous Cars. Dissertation Submitted to the Department of Computer Science and the Committee on Graduate Studies of Stanford University, http://purl.stanford.edu/pb661px9942.
29. **Stern A. 2013.** Bluetooth Connectivity Threatens Your Security. https://blog.kaspersky.com/bluetooth-security/1637/ (15.04.2013).
30. **Sumorek A. 2010.** Safe Communication Among Vehicle Sub-Assemblies on the Basis of the Embedded Functions of CAN Protocol. Teka (Archives) of the Commission of Motorization and Power Industry in Agriculture, Vol. 10, 432-439.
31. **Sumorek A. 2010.** The Variability of Electrical Parameters of CAN Protocol Signals in Vehicles. Logistyka, 6, 3263-3272 (in Polish).
32. **Sumorek A., Buczaj M. 2011.** The Problems in Fibre Optic Communication in the Communication Systems of Vehicles. Teka (Archives) of the Commission of Motorization and Power Industry in Agriculture, Vol. 11, 363-372.
33. **Sumorek A., Pietrzyk W. 2011.** Controlling of Access of Mechatronic Nodes to the Information Networks of Vehicles. MOTROL - Motorization and Power Industry in Agriculture, Vol. 13, 290-301 (in Polish).
34. **Sumorek A. 2011.** The Variability of Diagnostic, Control and Multimedia Protocols in Vehicles. Logistyka, 3, 2583-2592 (in Polish).
35. **Tran E., Koopman P. (advisor). 1999.** Multi-Bit Error Vulnerabilities in the Controller Area Network Protocol. Carnegie Mellon University, Institute for Complex Engineered Systems, 33. Pittsburgh.
36. **Widerski T., Kędzierski J. 2004.** Automotive information networks (CAN). Auto Moto Serwis, 4, Warszawa, Wydawnictwo Instalator Polski, 38-42 (in Polish).
37. **Wolański R. 2016.** Every car will be able do it in five years. Chip, 3, 106-107 (in Polish).
38. **Zimmermann W., Schmidgall R. 2008:** Bussystems in Automotivetechnology: Protocolls and Standards. Wydawnictwa Komunikacji i Łączności, Warszawa (in Polish).

Problems of searching for failures and interpretation of error codes (DTCs) in modern vehicles

Andrzej Sumorek [1], Marcin Buczaj[2]

[1]Lublin University of Technology, Department of Structural Mechanics, Poland, 20-618 Lublin, Nadbystrzycka 40, e-mail: a.sumorek@pollub.pl
[2]Lublin University of Technology, Institute of Electrical Engineering and Electrotechnologies, Poland, 20-618 Lublin, Nadbystrzycka 38A, e-mail: m.buczaj@pollub.pl

Received July 15.2016: accepted July 19.2016

Abstract. Volkswagen model launched in 1968 is deemed as the first motor vehicle provided with on-board diagnostics functions. However, the introduction of systems for the monitoring of vehicle sub-assemblies contributing to emission levels in all vehicles was enforced by environmental protection requirements. The California Air Resources Board (CARB) introduced the necessity to use the basic functions of on-board diagnostics (OBD) in all the motor vehicles sold in California since 1991.

The article presents the results of practical tests in the scope of on-board diagnostics for "premium" class vehicle. The tests were carried out by means of 4 diagnostic interfaces. Data volume obtained from motor vehicles varied depending on the applied device, although OBD II standards should be introduced in an identical manner by the manufacturers of motor vehicles and diagnostic devices.

Key words: On-board Diagnostics, Diagnostic Trouble Codes DTC.

INTRODUCTION

The introduction of on-board diagnostics systems is necessary due to air quality standards. This case has been expressed in regulation issued by the California Air Resources Board (CARB) introducing the necessity to use the basic functions of on-board diagnostics (OBD) in all the motor vehicles sold in California since 1991 [10]. The beginnings of OBD implementation encountered the problems in the form of non-uniform communication protocols, diversified diagnostic links and diversified interpretation of errors. The use of on-board diagnostics systems compliant with OBD II standard (increased number of monitored parameters, increased number of indicated and recorded data) has been mandatory since 1996. Since 2003 a similar standard, i.e. European On-Board Diagnostics (EOBD), has been mandatory in Europe.

The development of OBD standard commenced in the mid-eighties of the 20th century has additionally resulted in the development of communication networks in motor vehicles. The networks have been transformed from slow diagnostic networks with bandwidths lower than 10 Kbps (e.g. ALDL - Assembly Line Diagnostic Link) into reliable fibre optic solutions with bandwidths close to 150 Mpbs (e.g. MOST – Medium Oriented System Transport) [24, 25]. Simultaneously, data transfer security has been significantly improved [23]. Motor vehicle sub-assemblies have been transformed into mechatronic systems providing access to information about their condition, following the instructions or being reprogrammed. They can also establish the connections between vehicles, often characterized by different security levels [12, 13, 21].

The functions of on-board diagnostics systems are performed on electronic and mechatronic sub-assemblies installed in motor vehicle and connected by numerous communication networks. The manufacturers of sub-assemblies, motor vehicles and diagnostic testers shall ensure the support of non-uniform network environment. As a result of almost 30 years of development in the scope of networks, buses and data buses, there is no universal diagnostic tool which could be used for all types of motor vehicles. This study presents practical problems occurring in course of diagnostic procedures performed by means of diagnostic testers delivered by various manufacturers.

ON-BOARD DIAGNOSTICS

The variety of communication and diagnostics protocols applied in motor vehicles results from the long term evolution of OBD I and OBD II systems. Fig. 1 illustrates selected standards applicable in the scope of vehicle sub-assemblies diagnostics.

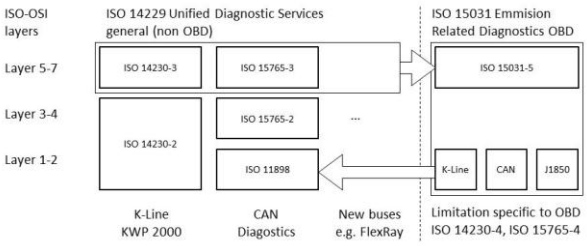

Fig. 1. Selected standards of diagnostic protocols [28]

A failure defined in accordance with OBD II standard will be indicated by means of DTC code consisting of a letter and four digit number e.g. P0484 Cooling Fan Circuit Over Current [19]. DTC codes values use generic and manufacturer-specific codes e.g. C0xxx or C3xxx-generic codes, C1xxx or C2xxx - manufacturer-specific codes (Fig. 2).

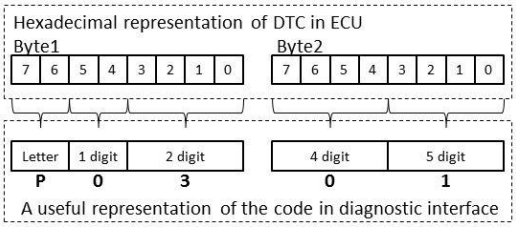

Fig. 2. Hexadecimal and useful representation of DTC error code [28]

Simultaneously, the vehicle manufacturer can define its own codes nonconforming with OBD standard provided that these codes are not colliding with standard requirements. The scientists and service personnel focus their attention not only on DTCs but on algorithm used for execution of repairs and for data acquisition [8, 20].

Wireless solutions are used in communication networks. Originally they have been used for motor vehicles protection (GSM, GPRS, GPS) [6]. Wireless solutions are also frequently used in OBD diagnosis. The connections between measurement interfaces installed in motor vehicle and the computer with testing software by means of Bluetooth and WiFi are standard solutions. The other solution consists in Bluetooth diagnostic communication of fleet motor vehicles when driving through the company gate or in sending messages on vehicle condition by means of GPRS network. Diagnostic data acquisition and processing in computing cloud seems to be the most interesting idea [11, 14]. The vehicle network itself is also regarded as a distributed system [2, 18, 26]. The efforts are still being made in order to find faster and reliable detection methods e.g. based on an additional database [7, 16].

Diagnostic network itself regarded as technical device can be also damaged which will affect the communication of motor vehicle subassemblies and diagnostics. Research works are carried out in the scope of detection of errors in communication networks e.g. by means of fuzzy logic [7, 27].

Problems with detection of trouble and with representation of error code are possible on several levels: tester – vehicle physical connection, a protocol in communication protocols stack, manufacturer – specific error code; method of determination by ECM whether the object status is incorrect.

PRACTICAL TESTS

Upper class vehicle manufactured in 2010 has been used as the object for checking the testers functionality. The vehicle was equipped with Diesel engine with the power of 150 kW (204 HP) and capacity of 3,0 litres. There are two reason of such choice. Firstly, it is the vehicle from premium segment with hybrid type network. Gateway integrates all types of networks from A class networks (Local Interconnect Network), typical B class solutions (Controller Area Network) and fast reliable C class networks (FlexRay) up to multimedia MOST network (Medium Oriented Systems Transport). Another reason of such choice was the period of 5 years elapsed after motor vehicle launch. This period is sufficient for the testers manufacturers to consider motor vehicle support in their devices.

Fig. 3 illustrates the engine compartment of motor vehicle. The engine system has been subjected to three modifications which should be indicated as errors in powertrain system. After disconnection of sensors, the engine was running for more than ten minutes. The errors generated by motor vehicle ECU shall be indicated in OBD diagnostic network because introduced troubles contribute to emission levels. In order to simulate real errors, the following sensors have been disconnected from engine controller:

- turbocharging pressure sensor (A);
- air flow sensor (B),
- air temperature sensor (B),
- intake manifold flap position sensor (C).

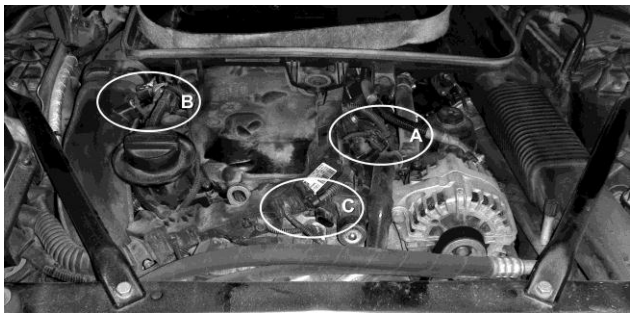

Fig. 3. View of the engine compartment

Practical test 1. X431 tester applied in the tests was manufactured in 2011 i.e. in the same period during which the vehicle under tests was manufactured (Fig. 4). On the basis of information published on websites of its distributors, the tester supports about 50 vehicles makes. Simultaneously, BMW and OBDII / EOBD standards are specified (Fig. 5). The following tester functions are specified: reading of controller version and system, cancelling of errors, reading of current parameters, actuators; systems encoding and programming, programming of keys and immobilizers; cancelling of service inspection; cancelling of crash data airbag.

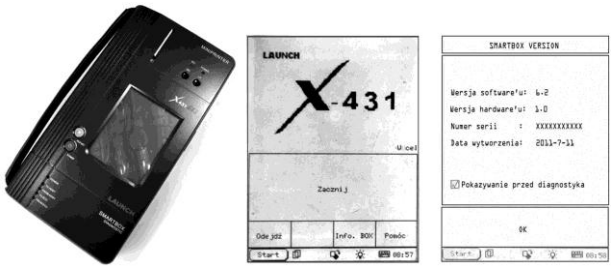

Fig. 4. Launch X431 GX3 tester view with starting screens [15]

In course of tests, it was possible to connect the tester to motor vehicles, to select the brand and controllers

group of vehicle to be tested. Message informing about the lack of communication with the controller was the result of performed tests (Fig. 5). Similar negative result was obtained from general OBD test of motor vehicle. Despite declaration of vehicle manufacturer concerning the presence of vehicle diagnostic network conforming with OBD and despite of tester manufacturer declaration concerning OBD diagnostics support, it was impossible to establish communication between vehicle and tester. Tester communication is possible by means specified contacts of diagnostic socket (socket conforming with SAE 15031-3 standard): 2, 7, 10 and 15. Such configuration allows only the communication by means of protocols conforming with SAE J1850 (contacts 2 and 10) and K data bus (contacts 7 and 15) in accordance with ISO 9141-2 and 14230-4.

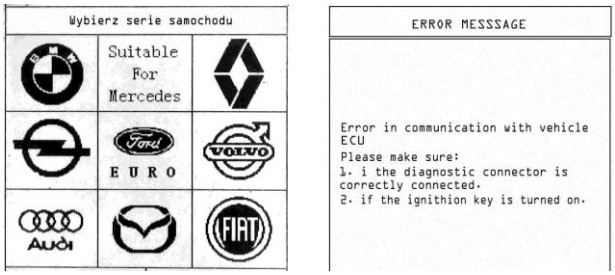

Fig. 5. X432 screens of: choice of car type (on the left); error message (on the right)

Practical test 2. Mobile tester Asian Gold is regarded by many employees working in independent service centres as a reliable device in case of the necessity to carry out the tests of motor vehicles originating from Far East markets. The tester incorporates built – in OBD II diagnostics function and supports the protocols conforming with SAE J1587, KWP-2000, OBD-II (ISO 9141-2 and SAE-J1850) as well as CAN Bus [17]. The device supports more than 40 makes of vehicles. In many cases, the access is possible to service functions accessible to authorized service centres only. The manufacturer ensured access to non-standard service connectors e.g. 20-pin BMW diagnostic conductor, 20-pin PSA diagnostic conductor or 20-pin Ford diagnostic conductor. Tester screens in course of successive steps of vehicle type declaration are presented in Fig. 6.

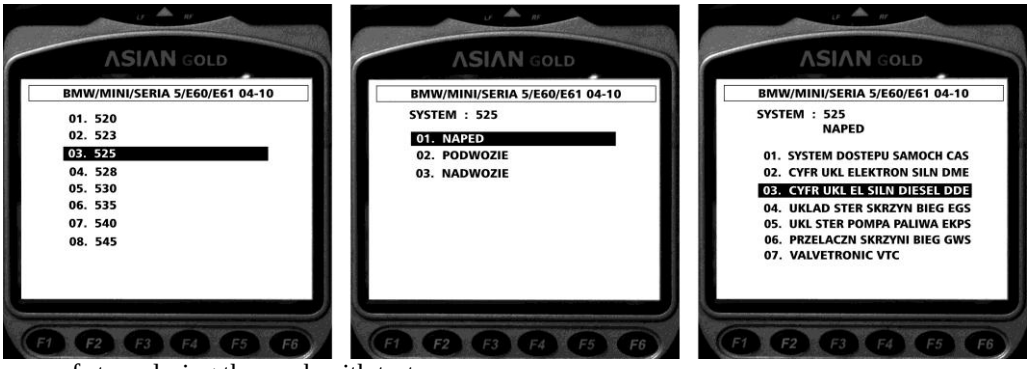

Fig. 6. Sequence of steps during the work with tester

The power supply to the tester was possible from diagnostics connector. The brand of vehicle being tested was present in the database. During next steps, it was possible to declare the type of motor vehicle (525), controllers group (powertrain) and to select diesel engine controller (diesel DDE) (Fig. 6). In connection with the wide range of additional equipment, it was necessary to select the type of conductor connecting the tester with vehicle (Fig. 7) before the commencement of diagnostics. However, the running of diagnostic scanning failed and message informing about the necessity to connect Gateway was displayed (Fig. 7). Similar attempts to establish communication with body and chassis systems were also unsuccessful. Motor vehicle scanning without indicating its type, on the basis of general OBD diagnostics also failed.

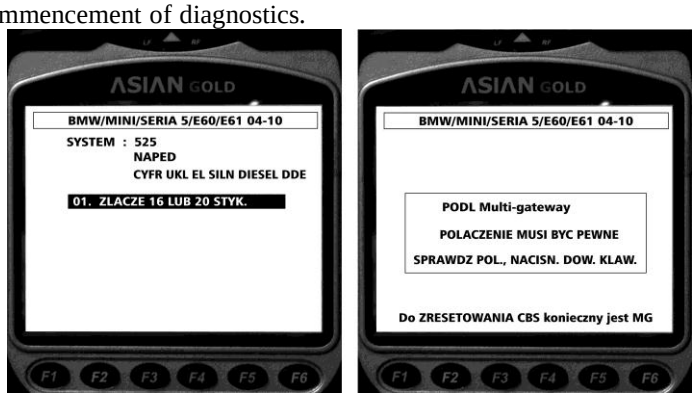

Fig. 7. Tester screens: choice of cable type (on the left), diagnosis effect (on the right)

Practical test 3. Solus Pro diagnostic scanner is characterized by functionality similar to two testers specified previously. Software provides vehicle-specific trouble codes for various vehicle control systems such as engine, transmission, antilock brake system (ABS), selected functional tests and troubleshooting information [22]. The scanner supports diagnostic protocols conforming with OBD-II/EOBD e.g. SAE J1850 (VPW), SAE J1850 (PWM), ISO 9141-2, ISO 14230-4 (KWP 2000), ISO 15765-4 (CAN). In the groups of vehicles service professionals, the device is equated with the tool necessary for servicing American, Japanese and Korean vehicles. A specific scanner feature consists in the use of memory cards dedicated for motor vehicles to be diagnosed. The cards are installed on the diagnostic conductor connector.

In the course of diagnosis, the scanner displayed information about the support of the type of vehicle identical to the type of vehicle connected to scanner. A card corresponding to the type of vehicle connected to scanner was included in the set of memory cards. Unfortunately, as in the previous tests, it was impossible to establish communication with any vehicle controller (Fig. 8).

Fig. 8. Solus Pro tester - communication error

The scanner makes it also possible to carry out diagnostic procedure in a general manner based on OBD diagnostics. It is possible to select communication protocol manually or to use all the built – in protocols automatically (Fig. 9a).

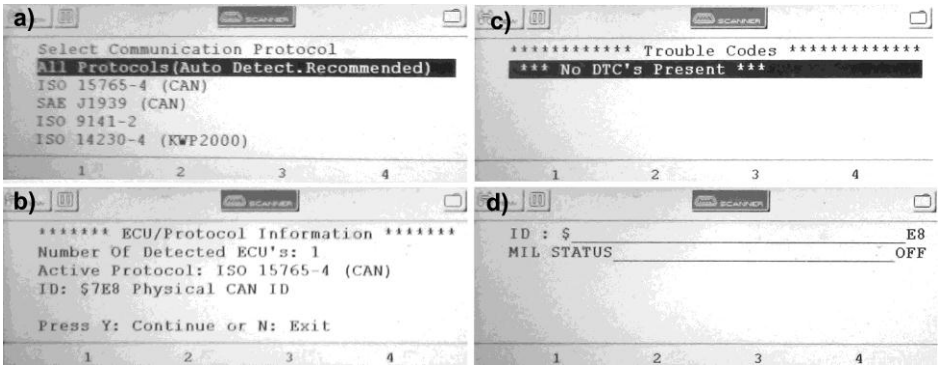

Fig. 9. Screen of tester in ODB mode

As a result of OBD diagnosis in automatic mode it was possible to establish communication between scanner and tester by means of ISO 15765-4 protocol (Fig. 9b). It is a significant progress in comparison with the two previous tests when it was impossible to establish communication with vehicle network. Message on lack of errors (Fig. 9b) was displayed as a result of further diagnosis. This message is non-conforming with real status because the signals from 4 sensors (turbocharging pressure sensor, air flow sensor, air temperature sensor, intake manifold flap position sensor) are not transmitted to the engine controller. Additionally an information has been received about disconnection of MIL (Malfunction Indicator Lamp). This message is non-conforming with real status because MIL lamp on the dashboard indicated errors presence in motor vehicle. In summary, like in the previous tests, it was impossible to establish correct communication with any vehicle controller.

Practical test 4a. Bosch KTS 540 tester with ESI[tronic] software package installed on a PC was used as diagnostic device. KTS 540 is not a stand – alone device but constitutes communication interface with motor vehicle. Diagnosis and signals interpretation is carried out by means of PC in programmed mode.

The diagnostics device incorporates additional multimeter functions. Therefore it is possible to perform voltage measurements up to 200V, current measurements up to 600A (with an additional shunt) and resistance measurements up to 1 M□. Within diagnostics area, the communication is possible by means of the following protocols: ISO 9141-2 (K and L lines), SAE J1850VPW, SAE J1850PWM, CAN ISO 11898, ISO 15765-4 (OBD) (CAN-H and CAN-L lines), CAN Single Wire and CAN Low Speed [4]. KTS 540 diagnostic interface was supported by ESI[tronic] software package 2.0. Its structure consists of modules. The following [Bosch 2013] elements have been used in described case:

- SD – motor vehicle controllers diagnosis module;
- SIS – errors and failures finding module;
- M – repair activities sequence module;
- P – electric diagrams for selected vehicle systems.

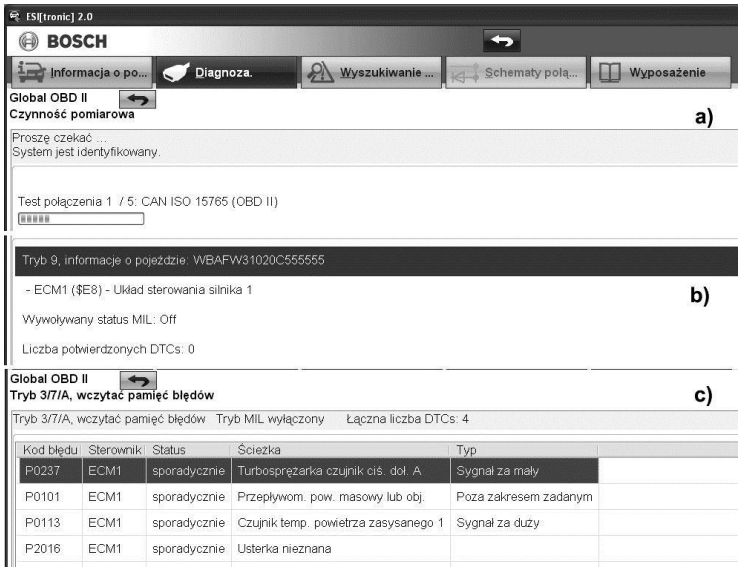

Fig. 10. Printscreens of ESI[tronic] software during diagnosis: a) starting communication; b) general vehicle information; c) list of diagnostic trouble codes

In the course of tests, KTS 540 interface with ESI[tronic] software was operated in two modes. In the first described case, KTS 540 interface with ESI[tronic] software performed typical diagnostic tests conforming with OBD II standard. The effects of tester operation should be identical to the effects of tests performed by means of other testers. Despite procedure followed in case of KTS interface identical to procedure applied for Solus Pro, Asian Gold and X431 interfaces, obtained effect was different:

- communication with ECU engine module has been established correctly. The same protocol (ISO 15765-4) has been effectively used in communication. Its functioning with Solus Pro (Fig. 9b, Fig. 10a) tester was possible in part only;
- reading of MIL control lamp status was incorrect (Fig. 9d, Fig. 10b). This reading made by Solus Pro tester was also incorrect;
- reading of DTC errors number (Fig. 9c, Fig. 10b) was incorrect. The errors number identified by Solus Pro tester was also incorrect;
- despite indicated lack of DTC diagnostic errors they are identified as sporadic errors.

The sporadic errors detected by KTS 540 interface set with ESI[tronic] software 2.0 have been correctly interpreted as (Fig. 10c):

- P0237 - turbo charger boost - sensor A circuit low,
- P0101 - mass or volume air flow circuit range,
- P0113 - intake air temperature sensor 1 circuit high,
- P2016 – unknown trouble. No description introduced at P2016 error code. The trouble corresponding to description „Intake Manifold Runner Position Sensor/Switch Circuit Low” has been correctly interpreted by P2016 value.

Practical test 4b. In the second vehicle testing mode, the type of motor vehicle being tested was directly defined by means of Bosch KTS 540 tester with ESI[tronic] software. The obtained results were marked by means of error codes from out of OBD (Fig. 11). Thanks to indication of vehicle type, it was also possible to display information about other errors occurring in engine system. Spark plugs glowing time control error (not displayed before) has been presented. This error occurred in controlled system in Local Interconnect Network cluster.

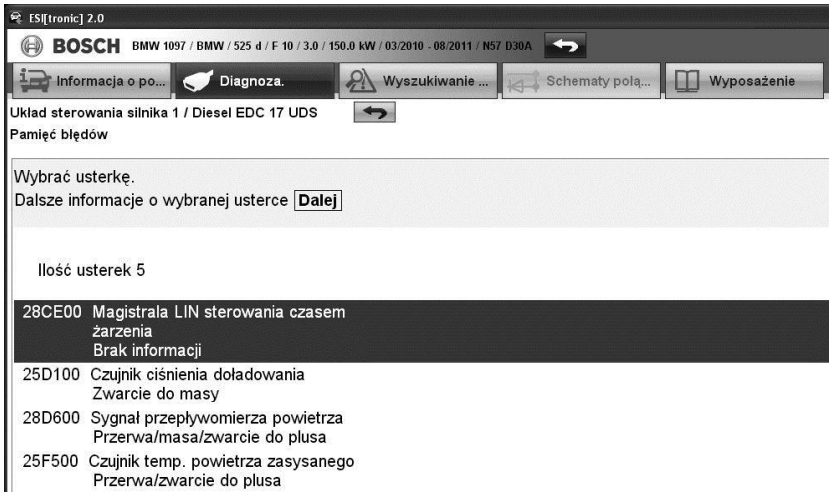

Fig. 11. Final screen of ESI[tronic] software after diagnosis

The appearance of list of errors marked with internal manufacturer's codes was as follows:

- 28CE00 - glow control LIN data bus missing,
- 25D100 = P0237 - turbo charger boost - sensor A circuit low,
- 28D600 = P0101 - mass or volume air flow circuit range,
- 25F500 = P0113 - intake air temperature sensor 1 circuit high,
- 264100 = P2016 - intake manifold runner position sensor/switch circuit low.

After selection of error code field it is possible to commence service procedures. It is possible to familiarize with information about damaged systems, to perform measurement of actual values, to familiarize with typical methods of trouble elimination.

In order to perform measurement of current values associated with P0101 error (28D600), it is possible to directly enter to measurement screen as illustrated in Fig. 12.

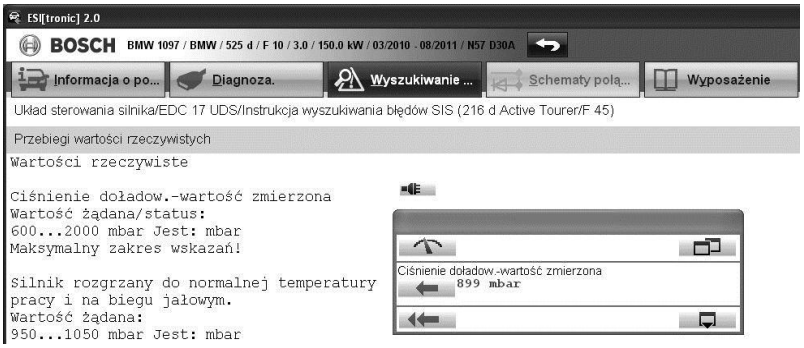

Fig. 12. Measurement of real values connected to DTC P0101

CONCLUSIONS

It is impossible to perform a full and error-free diagnosis in case of currently manufactured vehicles by means of a standard diagnostic tester. Unexpected situations could be faced as a result of tester design as well as vehicle communication network organization. Executed tests demonstrated that potential reasons of diagnosis failure could be as follows:

1. Impossibility of physical connection of the tester – lack of pins in diagnostics plug of the tester which correspond to protocol used for communication with vehicle (practical test 1).
2. Lack of built–in diagnostics protocol conforming with protocol supported by motor vehicle (practical test 2).
3. Manner of DTC errors interpretation by the tester. Sporadic errors can be interpreted as non-existing errors (practical test 3).

Simultaneously, the following conclusions were drawn by the experiments participants in the course of tests:

1. Up–to–date software of the testers makes it possible to access to information and service functions included in the scope of OBD (practical test 4a).
2. Application of „dedicated" software for motor vehicle combined with the use of "standard" tester extends service capabilities beyond OBD standard (practical test 4b).
3. In case of the necessity to access to selected communication networks (e.g. MOST networks in case of BMW make) it is necessary to apply dedicated diagnostic heads /interfaces (e.g. GT1 or OPS head).
4. Currently, the capabilities of Electronic Control Units (ECUs) are much higher than only making diagnostic data available. It was demonstrated in Volkswagen group scandal in 2015. Thanks to the extended capabilities in the scope of engine ECU reprogramming, the values of emission levels were underestimated in the course of stationary tests. This problem occurred in diesel engines with the capacity of 2 litres manufactured in the years 2009–2015 [1, 9].

RREFERENCES

1. **Barrett S.R.H., Speth R.L., Eastham S.D., Dedoussi I.C., Ashok A., Malina R. Keith D.W. 2015.** Impact of the Volkswagen emissions control defeat device on US public health. Environmental Research Letters, 11, 2015, DOI: 10.1088/1748-9326/10/11/114005, pp. 10.
2. **Biteus J., Nyberg M., Frisk E., Åslund J. 2009.** Determining the fault status of a component and its readiness, with a distributed automotive application. Engineering Applications of Artificial Intelligence, vol 22, 3, 363-373.
3. **Bosch R. GmbH. 2008.** Data exchange network in vehicles. Wydawnictwa Komunikacji i Łączności, Warszawa (in Polish).
4. **Bosch R. GmbH. 2010.** Innovative and reliable: Professional electronic control unit diagnosis from Bosch. http://rb-aa.bosch.com/boaa-pl/Product.jsp?prod_id=154&ccat_id =73&language=en-GB&publication=3. January 2016.
5. **Bosch R. GmbH. 2013.** ESI[tronic]-C Vehicle diagnosis and troubleshooting instructions. http://rb-aa.bosch.com/boaa-pl/Category.jsp?ccat_id=119&language=en-GB&publication=4, Germany, January 2016.
6. **Buczaj M. 2011.** The elimination of the human decision factor by the technical medium of the transmission of information signal in control and supervision alarm systems. MOTROL - Motorization

and Power Industry in Agriculture, vol. 13, s. 34-42 (in Polish).
7. **Chen J., Roberts C., Weston P. 2008.** Fault detection and diagnosis for railway track circuits using neuro-fuzzy systems. Control Engineering Practice, vol 16, 5, 585–596.
8. **Chougule R., Rajpathak D., Bandyopadhyay P. 2011.** An integrated framework for effective service and repair in the automotive domain: An application of association mining and case-based-reasoning. Computers in Industry, vol 62, 7, 742-754.
9. **Davenport C., Ewing J. 2015.** VW Is Said to Cheat on Diesel Emissions; U.S. to Order Big Recall. The New York Times, 18 September 2015, ISSN 0362-4331.
10. **Eisinger D.S., Wathern P. 2008.** Policy evolution and clean air: The case of US motor vehicle inspection and maintenance. Transportation Research Part D: Transport and Environment, Vol. 13, 6, 359-368.
11. **Fan S., Yang D., Zhang T., Lian X. 2013.** Distributed Diagnostic Monitoring and Fault Tolerant Control of Vehicle Electrical and Electronic Devices. Proceedings of the FISITA 2012 World Automotive Congress. Vol. 6: Vehicle Electronics, SAE-China, FISITA, Springer Berlin Heidelberg, 221-230.
12. **Förster D., Kargl F., Löhr H. 2016.** PUCA: A pseudonym scheme with strong privacy guarantees for vehicular ad-hoc networks. Ad Hoc Networks, 37, 122–132.
13. **Gorrieri A., Martalò M., Busanelli S., Ferrari G. 2016.** Clustering and sensing with decentralized detection in vehicular ad hoc networks. Ad Hoc Networks, 36, 450–464.
14. **Jhou J.S., Chen S.H. 2014.** The Implementation of OBD-II Vehicle Diagnosis System Integrated with Cloud Computation Technology. Intelligent Data analysis and its Applications, Vol. I, Advances in Intelligent Systems and Computing, Springer International Publishing Switzerland, 413-416.
15. **Launch Tech. 2007.** X-431 User's Manual. http://www.diagtools.lv/soft/X431_ manual _English.pdf, January 2016.
16. **Li Yanqiang, Li Yang, Wang Z., Zhuang R., Li Jainxin. 2013.** Automotive ECUs Fault Diagnosis Modeling Based on the Fault Database. Proceedings of the FISITA 2012 World Automotive Congress. Vol. 6: Vehicle Electronics, SAE-China, FISITA, Springer Berlin Heidelberg, 271-281.
17. **Magneti Marelli. 2012.** Air conditioning, diagnostics, mechanics. Equipment for Magneti Marelli workshops. http://www.edpol.pl/frontend/files/urzadzenia/Katalog-MM-2012.pdf, January 2016 (in Polish).
18. **Murphey, Y. L., Crossman, J. A., Chen, Z., Cardill J. 2003.** Automotive fault diagnosis II: A distributed agent diagnostic system. IEEE Transactions on Vehicular Technology, Vol. 52, 4, 1076-1098.
19. **SAE Standard. 2002.** SAE J1979: E/E Diagnostic Test Modes. Vehicle EE Systems Diagnostics Standards Committee. SAE International.
20. **Saxena A., Wu B., Vachtsevanos G. 2005.** Integrated diagnosis and prognosis architecture for fleet vehicles using dynamic case-based-reasoning. Proceedings of the IEEE Autotestcon. 26-29 Sept. 2005, 96 - 102.
21. **Schaub F., Ma Z., Kargl F. 2009.** Privacy requirements in vehicular communication systems. Proceedings of the International Conference on Computational Science and Engineering, IEEE, 2009, 139–145.
22. **Snap-on Inc. 2012.** Solus Pro User Manual. Ver ZEESC316C Rev. C. https://www1.snapon.com/Files/Diagnostics/UserManuals/SOLUSPROUserManual_ZEESC316C.pdf, January 2016.
23. **Sumorek A. 2010.** Safe Communication Among Vehicle Sub-Assemblies on the Basis of the Embedded Functions of CAN Protocol. Teka (Archives) of the Commission of Motorization and Power Industry in Agriculture, Vol. 10, 432-439.
24. **Sumorek A., Buczaj M. 2011.** The Problems in Fibre Optic Communication in the Communication Systems of Vehicles. Teka (Archives) of the Commission of Motorization and Power Industry in Agriculture, Vol. 11, 363-372.
25. **Sumorek A., Buczaj M. 2012.** New elements in vehicle communication ”Media Oriented Systems Transport” protocol. Teka (Archives) of the Commission of Motorization and Power Industry in Agriculture. Vol. 12, 275-279.
26. **Suwatthikul J. 2010.** Fault detection and diagnosis for in-vehicle networks (chapter). Fault detection, ISBN 978-953-307-037-7, edited by Wei Zhang, 283-306.
27. **Suwatthikul J., McMurran R., Jones R.P. 2011.** In-vehicle network level fault diagnostics using fuzzy inference systems. Applied Soft Computing, vol. 11, 4, 3709-3719.
28. **Zimmermann W., Schmidgall R. 2008.** Bussystems in Automotivetechnology: Protocolls and Standards. Wydawnictwa Komunikacji i Łączności, Warszawa (in Polish).

Assessing the possible use of hulled and naked oat grains as energy source

Renata Tobiasz-Salach, Edyta Pyrek-Bajcar, Dorota Bobrecka-Jamro

University of Rzeszów, e-mail: edyta.pyrek.bajcar@gmail.com
rentobsa@univ.rzeszow.pl

Received June 06.2016: accepted June 20.2016

Abstact. The paper is an analysis of the suitability of oat grains for energy purposes. The comparison covered two types of grain oats, hulled (Krezus variety) and naked (Polar variety), using varied nitrogen fertilization. The calorific value of the grains, including their ash content was determined. The study helped to demonstrate that oat grains exemplified excellent parameters, which advances its use for fuel purposes in power generation. The average calorific value obtained was 18.4 MJ kg^{-1}, while the ash content was 2.28% of dry mass. Although increasing nitrogen fertilization restricted the grain's calorific value, it did not lead to increases in the level of ash content. The Polar variety of naked oats was characterized by better suitability for energy purposes than the Krezus variety of hulled oats. The results obtained support the claim that oat grains can compete with other sources of raw materials for energy purposes.

Key words: biomass, nitrogen fertilization, calorific value, ash content, hulled and naked oat grains

INTRODUCTION

Poland holds large potentials and possibilities for biomass production for energy purposes. This potential may be put to use to meet the EU obligatory Directive of 17 December, 2008, which mandates the attainment of 15% share of renewable energy sources in total energy consumption by 2020 and a 20% threshold by 2030. The percentage share of power from renewable sources in overall energy consumption in 2013 in Poland was 11.3%, with 80.3% of it coming from biomass [7]. The Minister of Economy's regulation of 14 August 2008 defines biomass to be "any solid or liquid substance of plant or animal origin that is biodegradable, derived from products, waste and residues of agricultural and forestry production and allied companies as well as kinds of waste products that are biodegradable including grain cereals that do not meet quality requirements of corn for intervention buying" [5].

The introduction of energy crops cultivation may provide alternative use for degraded and fallowed lands. Such cultivation, however, needs regulations and monitoring as it is capable of impacting on biodiversity and the preservation of potential for food production. The use of agricultural biomass for energy purposes is, to a large extent, antagonistic with farming that has remained the key source of food so far [3, 18].

Farms occupy 16.3 million hectares of land in Poland. The total cultivated land amounts to 10.8 million hectares, with the largest area of 69.9% being taken by cereals [8]. One of the possible uses of cereals is for energy purposes. Oats, in particular, could be a useful source of renewable energy due to its high fat and low ash content. This use of oats is popular in several other countries, including Sweden. Arguments in favour of such raw material include, among other things, its small size, high specific weight, less complicated transport and storage requirements when compared to straw and wood, low soil quality requirements, wide availability of cultivating and harvesting machines, long farming traditions, the introduction of burners for oats, and the possible use of ash as fertilizer in fields. The grain can also be subjected to various technological processes. A positive aspect of this is the country's independence from non-reliance on external energy supply inputs. The only hindrance is psychological, being the result of the high esteem accorded to grains, especially nutritious quality grains. [6, 9, 11, 13, 4, 28].

The objective of the study was to determine and compare the calorific value of two types of oats grains with regards to varying nitrogen fertilization.

The adopted research hypothesis assumes that naked oats is a better-suited type for energy purposes than hulled oats, and that increased nitrogen fertilization will result in different ash content in grains, including its calorific value.

MATERIALS AND METHODS

The research material consisted of two oat varieties namely, the naked variety, Polar and the hulled variety, Croesus [Krezus].

The field trials were conducted at the Teaching and Research Station of the Faculty of Biology and Agriculture of the Rzeszow University in Krasne, near Rzeszow in 2010-2012. It was established in randomized block form with sub-blocks in four replications. The oat grains were sown from 1st to 20th April in the study period. The following rates of nitrogen fertilization were applied during the vegetative period:

— N0 — a plot without nitrogen fertilization 0kg $N \cdot ha^{-1}$ (control);

— N1 — a plot fertilised with 40 kg $N \cdot ha^{-1}$ (post sowing);

— N2 — a plot fertilised with 80 kg·N·ha^{-1}, (post sowing and post emergence with a dose of 40 kg N·ha^{-1} each stage);
— N3 — a plot fertilised with 120 kg N·ha^{-1} (post sowing, post emergence and during propagation phase at a rate of 40 kg N·ha^{-1} each).

The research was carried out on brown soils from loess, composed of mechanical particles of medium soils, belonging to good wheat complex and IIIrd soil class quality. The soil was characterized by a neutral pH ratio (pH $_{KCl}$ of 6.1 – 7.2). The content of digestible components at the 0-25 cm soil layer in mg·kg^{-1} was: phosphorous -138.3; potassium -161.4 and magnesium – 48.2. The microelement content was at a medium level, reaching: B – 1.6; Mn – 149.1; Cu – 4.6; Zn – 8.6 and Fe – 988.3.
Weather conditions during the oats vegetative period are illustrated in Table 1.

Table 1. Weather conditions in Krasne, near Rzeszow in 2010-2012.

Month	Precipitation [mm]				Air temperature [^{0}C]			
	2010	2011	2012	1995-2009	2010	2011	2012	1995-2009
III	22,3	20,0	28,5	32,1	2,7	2,8	4,19	2,7
IV	49,9	50,0	26,1	50,6	8,9	10,3	9,73	8,7
V	177,0	49,2	56,0	80,8	14,3	13,9	14,79	13,9
VI	126,1	88,5	83,6	82,00	17,9	18,1	18,39	17,0
VII	200,2	233,7	53,5	88,2	20,8	18,6	21,34	19,0
VIII	98,6	28,6	56,3	68,8	19,5	19,0	19,04	18,2

Source: authors' own research, according to data from the Meteorological Station in Jasionka, near Rzeszow.

Oats grains were harvested at full maturity with 15% humidity. Study samples were collected for laboratory analysis to determine its calorific value and ash content.

The analysed material was reduced to particle sizes of less than 1 mm using a lab mill, thus obtaining a homogeneous material. Next, 1 gram tablets were derived from the total sample using an automatic tableting machine for a direct analysis of its calorific value. The calorific value was determined using the calorific testing apparatus LECO AC500. The heat of combustion was determined by burning the sample in an oxygenated pressurized container surrounded in water jacket from all sides to ensure the monitoring of heat transfer. A 8 cm long wire was used to ignite the sample. No additional catalysts were applied for the analysis. Measurements of the water temperature was monitored using an electronic thermometer, with the accuracy of 0,0001°C. The heat exchange was continually measured using a measuring gauge. The calorific value of the analysed material was determined based on the amount of heat generated.

The ash content was determined by burning the sample in a muffle furnace at 600 ^{0}C [PN-EN 14775:2010].

The results obtained were statistically analysed using the variation analysis method at the significance level of α= 0.05 . The statistical analysis was conducted using the Statistica 10 software.

RESULTS AND DISCUSSION

Solid biofuels include varied materials such as energy crops, wood, straw and grains. These are primary energy resources, which besides the environmental and economic benefits offer opportunities for agricultural development [17]. Cereal grains, especially oats and maize, are increasingly being used for energy purposes in Poland and globally, especially in Scandinavia and the USA. It is a raw material that is easy to transport, store and the process of feeding the fuel to boiler is easily automated [13, 17, 28]. Most modern heating devices are adequately fitted for biomass combustion. They come with interchangeable burners and grates, hence the heating device can be adapted to burning grains at a very low cost [14, 28]. Such devices are characterized by low exploitation costs, simplicity and rather little time consuming operations. Modern boilers are designed to burn several types of fuels, for example, coal, pellets, grain or oils [14].

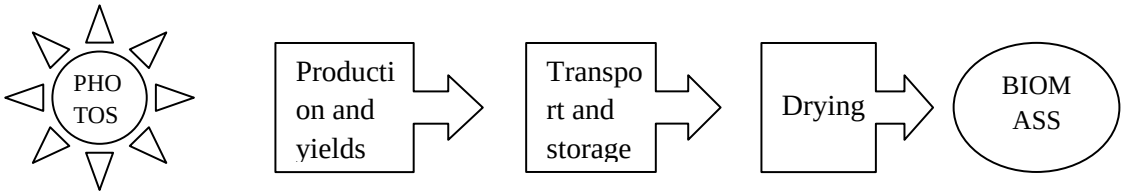

Fig. 1. Flow chart of biomass production
Source: Own calculations, based on Roszkowski 2013

The biomass applied for energy uses could be used for direct burning or further processing. Subjecting the solid biomass to thermochemical, biochemical and thermal processes yields liquid, solid and gaseous fuels. The liquid fuels consist of ethanol, biodiesel, bio-oils and methanol [24]. Oat grains with their low fat content in the

range of 3-6% when compared to rapeseed (about 40%) are not suitable for liquid fuel production but can be used for solid fuels. Biomass has the best conversion efficiency, while the highest direct combustion, which reaches up to 90%, has been associated with bio-gas [23, 26]. The form with the least difficulties (Fig 1) but the most efficient combustion (Table 2) is when grains are used for direct combustion.

Table 2. Efficiency of biomass conversion into energy (the conversion of biomass in a processing plant)

Kind of product	[%]
Biogas (electric energy)	10-15
Esters (biodiesel)	30-40
FC lignocellulose (electric energy)	30-40
FT (fuels, electric energy)	30-50
Gasification (electric energy)	40-50
Ethanol, methanol	40-50
Ethanol of II generation LC	50-60
Biomass pyrolysis	60-70
Combustion (heat)	70-90

Source: de WIT, FAAIJ 2010, Roszkowski 2012, Roszkowski 2013

A key indicator in assessing the energy use of the analysed energy resources was their calorific value [1]. The different types of biomass material are characterized by varying calorific values (Table 3). The lowest, amongst those tested, was shown by meadow hay, whilst the highest was found for beech wood pellets, which was comparable to oat grains in terms of energy value. The difference was in the range of 0,2 MJ kg^{-1}. When compared with the most popular source of energy in Poland, coal, the result can be considered as very satisfying. Low quality coal has a lower calorific value than biomass, including oat grains (Table 3). Oat grains as a biomass material, according to Roszkowski [22, Table3] display high suitability for energy purposes from physical, technical and technological perspectives.

Table 3. Average calorific value for selected energy raw materials

Type of plant materials	Calorific value of the dry state, MJ kg^{-1}
Pelet – beech wood	18,6
Pelet – pine wood	17,7
Wheat straw	16,8
Rye straw	17,1
Maize straw	17,5
Rape straw	17,3
Meadow hay	16,6
Oat grains	18,4
Black coal	14,7-29,3

Source: Own calculations, based on Roszkowski 2012, Bajcar 2014, Niedziółka, Szpryngiel 2014, and Niedziółka 2015

Table 4 illustrates the calorific value of oat grains obtained over the three-year research period, using four levels of nitrogen fertilization for the two varieties of oats. It was observed that the level of nitrogen fertilization resulted in varied levels of calorific values of the grains. High levels of nitrogen fertilization of up to 120 $kg \cdot ha^{-1}$ had negative impacts on the grain's calorific value in each year of the study. Both varieties, namely Krezus (hulled oats) and Polar (naked oats) attained higher values at the lowest levels of fertilization. The observed differences may have arisen from the fact that nitrogen fertilization has a negative impact on fat content but a positive impact on protein content of cereal grains, a fact that has been corroborated in researches by various authors [2, 10, 12, 19].

Table 4. Calorific value of oat grains relative to the nitrogen fertilization and grain variety [MJ kg-1]

Cultivar (I)	Nitrogen Fertilization (II)	2010	2011	2012	2010-2012
Krezus	0	18,608	18,154	18,270	18,381
	40	18,538	17,826	17,793	18,182
	80	18,441	17,884	18,106	18,163
	120	18,425	17,903	18,697	18,164
Polar	0	18,373	18,935	19,091	18,654
	40	18,389	18,770	18,909	18,580
	80	18,749	18,280	18,369	18,514
	120	18,770	17,808	18,639	18,289
$NIR_{\alpha=0,05}$ (I x II)		**r.n.**	**0,362**	**0,412**	**0,071**
Mean					
Krezus		18,503	17,942	18,217	18,223
Polar		18,570	18,448	18,752	18,509
$NIR_{\alpha=0,05}$ (I)		**0,021**	**0,362**	**0,462**	**0,236**
	0	18,491	18,544	18,680	18,518
	40	18,464	18,298	18,351	18,381
	80	18,595	18,082	18,238	18,339
	120	18,598	17,856	18,668	18,227
$NIR_{\alpha=0,05}$ (II)		**0,101**	**0,231**	**0,132**	**0,261**
Total mean		18,537	18,195	18,484	18,366

r. n. – non significant differences; Source: own calculations

Increasing the fat content of grains is most desired, judging from the energy perspective. The combustion of 1 gram of fat releases twice more energy than the combustion of equivalent amount of protein. The naked oat (cv Polar) types are known to contain higher fat content in the grain in comparison to the hulled types [19, 20]. This relativity was confirmed in the studies. The Polar variety that contained more fat in the grain in comparison with the Krezus variety (Table 3) achieved higher calorific value irrespective of the level of nitrogen fertilization. The calorific value of grains from the studied oat varieties, 18,4 MJ kg^{-1} , is indeed a very good result when compared to results obtained from other types of biomass designated for energy purposes. Both pine and beech woods are known to have similar calorific values as oat grains. They can without doubt compete successfully with low quality coal, which additionally contains several harmful pollutants that it emits into the atmosphere. Oat grains are also very competitive when compared to meadow hay whose calorific value is estimated at 14 MJ kg^{-1} from the first swath [27] through to 16.2-16.6 MJ kg^{-1} from the third swath [1, 15, 16].

The grain's ash content also impacts on the calorific value of the raw material (Table 5). The lower the content, the more suitable the raw material is for energy purposes. The ash content of biomass is decisively lower than in traditional fossil fuels, which makes biomass a more attractive energy source [1].

Table 5. Ash content in selected energy raw materials

Type of plant materials	Ash content (% s. m.)
Pelet – beech wood	2,7
Pelet – pine wood	5,6
Wheat straw	7-11
Maize straw	3,7-4
Rape straw	5,0
Meadow hay	5,3-9
Oat grains	2,28
Black coal	8-34

Source: own calculations, based on Roszkowski 2012, Bajcar 2014, Niedziółka, Szpryngiel 2014, and Niedziółka 2015

The combustion of clean biomass releases insignificant quantities of ash (Table 5), that is devoid of harmful substances [17]. Such ash is suitable for use as mineral fertilizer as it contains large amounts of potassium and calcium oxides (lime-potassium fertilizer) [13, 14]. Given the advantageous properties of biomass in terms of ash content, its content in oat grains relative to the level of nitrogen fertilization (Table 6) was also analysed in the studies. The popular opinion is that higher nitrogen fertilization increases the ash content of oat grains [21, 25].

Table 6. Ash content in oat grains [% dry mass]

Cultivar (I)	Nitrogen Fertlization (II)	2010	2011	2012	2010-2012
Krezus	0	2,55	1,36	2,78	2,55
	40	2,57	1,32	2,96	2,57
	80	2,62	1,62	2,86	2,62
	120	2,75	1,72	2,83	2,75
Polar	0	1,86	1,16	2,73	1,86
	40	1,88	1,11	2,93	1,88
	80	1,88	1,22	2,45	1,88
	120	2,11	1,44	3,02	2,11
$NIR_{\alpha=0,05}$ (I x II)		**r. n.**	**0,13**	**r. n.**	**r. n.**
Mean					
Krezus		2,62	1,51	2,62	2,62
Polar		1,93	1,23	1,93	1,93
$NIR_{\alpha=0,05}$ (I)		**0,24**	**0,14**	**0,32**	**0,50**
	0	2,21	1,26	2,76	2,21
	40	2,22	1,21	2,94	2,22
	80	2,25	1,42	2,65	2,25
	120	2,43	1,58	2,93	2,43
$NIR_{\alpha=0,05}$ (II)		**0,19**	**r. n.**	**r.n.**	**r. n**
Total mean		**2,28**	**1,37**	**2,82**	**2,28**

r. n. – non significant difference; Source: own calculations

This claim was not, however, confirmed in the course of these studies (Table 6). Nitrogen fertilization did not result in increased ash content in the grains of oats over the three-year period, except for 2010 with extreme weather conditions, namely huge rainfalls in May and June (Table1). Significant differences amongst the varieties were observed. Due to its content of hulls the Krezus variety was shown to have about 0.7% more dry mass than the Polar variety. The average ash content, however, in both the varieties at different levels of fertilization during the three years amounted to 2.2% dry mass, which from the perspective of calorific value was a very good result.

CONCLUSIONS

1. The calorific value of 18.4 MJ kg^{-1} and average ash content of 2.3% of dry mass obtained for oats is competitive in relation to other energy sources derived from biomass, which confirms its suitability for use in power industries for heating purposes.
2. Higher doses of nitrogen fertilization, namely, 80 and 120 kg $N \cdot ha^{-1}$hampered the calorific value of oats, but had no influence on the ash content of grains.
3. The naked variety of oats, Polar, was characterized by better suitability for heating purposes than the hulled, Krezus, variety. Its grain had a higher calorific value and contained less ash.

REFERENCES

1. **Bajcar M., Czernicka M., Saletnik B., Zagula B., Puchalski Cz., Gorzelany J. 2015**. Assessment of Energy Properties of Plant Biomass Pellets. TEKA. Commission Of Motorization And Energetics In Agriculture
2. **Bartnikowska E., Lange E., Rakowska M. 2000**. Oats grain – an underrated source of nutrients and biologically active substances. Part I. General characteristics of Oats. Proteins, Fats. IHiAR Newsletter. 215, 209-219. (in Polish)
3. **Booth E., Bell J., Mc Govern R ., Hodsman L**. **2007**. Review of the Potential for On Farm Processing of Various Non Food Crop Products National Non Food Crops Centre. 117.
4. **Burczyk H**. **2011.** Suitability of cereal crops for the production of renewable Energy based on experimental results. Problems of Agricultural Engineering. 3/2011. 43-51. (in Polish)
5. **Journal of Laws No. 156, item 969**. **2008.** Regulations for the Minister of Economy of 14 August 2008 concerning detailed scope of responsibilities to obtain and submit for the redemption of certificates of origin, payment of ancillary fees, purchase of electricity and heat from renewable energy sources including the obligation to confirm the data relating to the amount of electricity generated from renewable energy source. (in Polish)
6. **Dzik T., Mięso R. 2005.** Small and micro-scale production and combustion of biomass fuels of plant origin. Monographs, publishing of the School of Conservation and Environmental Engineering W. Goetel Memorial. Kraków. 253. (in Polish)
7. **Central Statistical Office. 2015.** Energy, Warszawa. (in Polish)
8. **Central Statistical Office. 2015.** Land-Use and Cultivable land area, 2015. Warszawa. (in Polish)
9. **Janowicz L. 2006.** Heat from grain. Agroenergetics. 1(15). 39-41. (in Polish)
10. **Jarecki W., Buczek J., Bobrecka-Jamro D. 2013.** Impacts of notrogen fertilization on grain yield of durum wheat (Triticum durum dest.). Fragmenta Agronomica. 30(2). 68-75. (in Polish)
11. **Kaszkowiak E., Kaszkowiak J. 2010.** Energy uses of grains of Oats and Spring Barley. Engineering and Chemical Apparatus. 5/2010. 57-58. (in Polish)
12. **Knapowski T., Kozera W., Majcherczak E., Barczak B. 2010.** Impact of nitrogen and zinc fertilization on the chemical composition and protein yield of grains of spring triticale. Fragmenta Agronomica. 27(4). 45-55. (in Polish)
13. **Kwaśniewski D. 2010.** Production and use of grain oats as a renewable source of energy, Problems of Agricultural Engineering. No. 3/2010. (in Polish)
14. **Nakonieczny P., Kluza P. A., Tatar G., Bródka R. 2014.** Types, characteristics and selected issues in exploiting boilers and furnaces powered with varied types of fuels. Acta Scientarum Polonorum. Technica Agraria 13(1-2). 27-40. (in Polish)
15. **Niedziółka I., Kachel-Jakubowska M., Kraszkiewicz A., Szpryngiel M., Szymanek1 M., Zaklika B. 2015.** Assessment of quality and energy of solid biofuel production. Bulgarian Journal of Agricultural Science. 21 (No 2). 461–466.
16. **Niedziółka I., Szpryngiel M. 2014.** Assessment of energy consumption of pellets and briquettes production in compressing devices. Agricultural Engineering. 2(150). 145-154.
17. **Niedziółka I., Zuchniarz A. 2006.** Energy analysis of selected plant sourced biomass. MOTROL 8A. 232–237. (in Polish)
18. **Petersen J.E. 2007.** Umweltfreundliche Bioenergie production: Analysen und Strategien auf EU-Ebene. Berlin. 10.
19. **Piątkowska E., Witkowicz R., Pisulewska E. 2010.** Major chemical components of selected types of oats. Food. Science. Technology. Quality. 3(70). 88-99. (in Polish)
20. **Pisulewska E., Tobiasz-Salach R., Witkowicz R., Cieślik E., Bobrecka-Jamro R. 2011.** Impact of habitat on the quantity and quality of lipids in selected types of oats. Food. Science. Technology. Quality. 3(76), 66-77. (in Polish)
21. **Podolska G., Maj L., Nita Z. 2006**. Level of grain yield and chemical composition of naked types of dwarf oats in relations to sowing density and nitrogen fertilization. IHAR Bulletin 239. pp. 49-59. (in Polish)
22. **Roszkowski A. 2012.** Biomass and Bioenergy – technological and energy barriers. Problems of Agricultural Engineering. vol. 3(77). 2012 (VII-IX). 79-100. (in Polish)
23. **Roszkowski A. 2013.** Energy from biomass – Energy effectiveness, efficiency and suitability. Part 1.

Problems of Agricultural Engineering. 1(79). 2013 (I-III). 97-124. (in Polish)

24. **Roszkowski A**. **2003.** Prospects of use of biomass as a source of engine fuels, MOTROL 5, 143-151. (in Polish)
25. **Tobiasz-Salach R. 2013.** Effect of nitrogen fertilization on yield and grain quality of oats cultivated in soil and climatic conditions of Podkarpacie Province. Publishing of the University of Rzeszów . pp. 104 (78-79). (in Polish)
26. **de WITT M., FAAIJ A. 2010.** European biomass resource potential and costs. Biomass and Bioenergy. Vol. 34. 188–202.
27. **Terlikowski J. 2012.** Biomass from permanent grasslands as a source of renewable energy. Problems of Agricultural Engineering. vol. 1 (75). 2012 (I-III). 43-49. (in Polish)
28. **Żabiński A., Sadowska U. 2012.** Combustion heat of cereal grains with reduced quality features. Agricultural Engineering. 2(136) T. 1. 353-359. (in Polish).

The impact of heat treatment on the components of plant biomass as exemplified by *Junniperus sabina* and *Picea abies*

Barbara Drygaś[1], Joanna Depciuch[2], Czeslaw Puchalski[1],Grzegorz Zaguła[1]

[1]Department of Bioenergy Technology, Faculty of Biology and Agriculture, University of Rzeszów, Zelwerowicza 4, 35-601 Rzeszów, e-mail: barbara.drygas.ur@gmail.com
[2]Faculty of Biology and Agriculture, Ćwiklińskiej 1, 35-601 Rzeszów

Received July 16.2016: accepted July 18.2016

Abstract. Torrefaction is the process of drying biomass at high temperatures in order to transform it into biofuels with properties and composition resembling carbon. The impact of high temperature breaks the chains of hemicellulose, lignin and cellulose and degrades the biomass to simpler organic compounds. The aim of this publication was to specify the impact of the duration of the heat treatment on the stability of biomass structures such as lignocellulose illustrated with examples of selected species of conifers. The research material consisted of shoot tips of *Junniperus sabina* and *Picea abies*. The material used in the process was air-dried, dried at 150^{o}C and torrefied at temperatures of 200, 250 and 300^{o}C in a LECO camera – TGA 701 apparatus for 30 minutes. Fresh needles and their torrefied products were measured spectroscopically using FTIR Vertex 70v made by Bruker. Microscopic photographs of samples were taken in the scales 10 μm, 20 μm, and 50 μm using the TESCAN VEGA3 scanning electron microscope. The unprocessed plant material did not differ significantly from one another – the FTIR spectra of both plants exhibited the same functional groups. The biomass heat treatment led to significant changes in its chemical composition and topographic changes in the obtained biochars.

Key words: torrefaction, biomass, FTIR spectra, changes, biochars

INTRODUCTION

Torrefaction is the thermal processing of biomass to the form of solid fuel, the so-called biochar [2, 6, 24, 25,]. Torrefaction occurs at temperatures of approximately 200 – 300°C in pressure close to atmospheric and with no access to oxygen [2, 3, 4, 25]. The impact of high temperature leads to the decomposition of polymeric structures and breaking of the biomass fibrous structures as it loses its mechanical resistance [19]. Hemicellulose is the first to decompose [20]. De-carbonated biomass densifies and obtains hydrophobic properties and more favourable energy parameters in comparison with the untreated biomass, e.g. it is more carbonated and has a higher calorific value [2, 18, 8, 28].

The duration of the process and residence of the material in the reactor depends primarily on the conditions of the process and the nature of the input material [1, 5, 11]. Although the concept of torrefaction is not new, there is still much to be done in terms of accurate analyses of the transition process at the level of chemical bonds in the constituent structures of the input material. Therefore, the following publication arises out of the necessity to complete these studies [20]. The research on the process may allow to eliminate the surplus of plant residues from the agricultural sector, whereas the resultant biochar may be used for fertilisers or as fuel (charcoal replacement), which will reduce the use of traditional fertilisers or energy fuels.

The basic components of lignocellulosic biomass are: cellulose, hemicellulose and lignin, which differ significantly from each other in terms of energy efficiency. Cellulose, a structural component of the cell wall of plants, constitutes, depending on the species and type, 40-60 percent of the dry lignocellulosic mass and is a linear polymer of cellobiose (glucose polymer). An important structural component in terms of energy values is hemicellulose constituting 20-40 percent of dry biomass and containing bonded short chains of various carbohydrates; pentoses: xylose, and arabinose, as well as hexoses: galactose, glucose and mannose. Lignin, whose content in the lignocellulose biomass of a plant amounts to 10-15 percent, is a complex polymer built out of phenylpropane and polyphenol derivatives [7, 17, 27]. Hemicellulose decomposes more easily than cellulose [14, 15, 16, 20, 21]. Lignin is a product of the condensation of three phenolic monomers [29]. Lignin decomposition is a complex process mainly due to the numerous carbon C-C and ether bonds [9, 10]. The biomass "resistance" to degradation depends on the relation of lignin to celulose quantities, specific properties of the plant species (molecular organization of cellulose and lignin polymers, presence of sclerenchyma, structure of epidermis, cuticle) [10]. The thermal (pyrolytic) distribution of biomass is a complex process in which the following reactions mutually overlap: dehydration (at approx. 155-200°C), isomerisation, aromatisation, coalification, oxidation (200-280°C) and others [12, 13].

During the thermolysis of biomass, at the stage of torrefaction, biochar is obtained (torrefied products) – a substance with properties similar to charcoal [2, 3, 6].

MATERIAL AND METHODS

The research material consisted of shoot tips of two species of conifers: juniper (*Junniperus sabina*) and spruce (*Picea abies*). The process of high temperature drying was conducted with the use of a thermo-gravimetric TGA 701 analyser made by LECO under pressure close to atmospheric and at temperatures: 150, 200, 250 and 300°C for the period of thirty minutes in nitrogen atmosphere with the purity of 99.99% and flow of 10l/min in eight iterations. The samples for the drying process and torrefaction were collected and prepared in accordance with the following standards: PN-EN 14778:2011 and EN 14780:2011. The surplus amounted to 6g. The process parameters are as follows: 30 minutes of residence time, change time: 8 minutes, total time: 38 minutes.

The spectroscopy measurements of fresh plant shoots tips and torrefied products were performed using FTIR spectroscope (Fourier transform infrared spectroscope) Vertex 70v by Bruker. Each sample was measured in eight iterations, then using the OPUS programme and the "calculate spectrum" function, the spectra were added up and averaged. The number of scans amounted to 32, resolution - 2cm $^{-1}$. The region of the average infrared (400-4000 cm $^{-1}$) - biological materials' function groups vibrate within these regions [26]. ATR (Attenuated Total Reflectance) technique was applied. The amount of particular compounds was determined with the help of the OPUS programme, determining the absorbance value that was assigned to the relevant peak. Microscopic photographs of samples for scale 10 µm, 20 µm, 50 µm were taken using a TESCAN VEGA3 scanning electron microscope.

RESULTS

The jupiter FTIR spectrum exhibits wave numbers corresponding to the vibration of groups typical of chemical compounds such as polysaccharides, nucleic acids and phospholipids, amines, aromatic rings, secondary amides, fats, alcohols and phenols. Drying at 150°C does not cause major chemical changes in the analysed material; the nature of the spectrum is slightly different but the chemical bonds in organic compounds remain unchanged. The increase in temperature to 200°C causes the loss of C-C group characteristic of aromatic rings (wave numbers 1450 and 1500^{-1}). Operating with temperature of 250°C leads to the breaking of C-N bonds (amines), and the raising of temperature to 300°C eliminates vibration for PO^{2-}group (nucleic acids, phospholipids). The FTIR spectra of fresh material from juniper shoot tips and their torrefied products are listed in Figure 1.

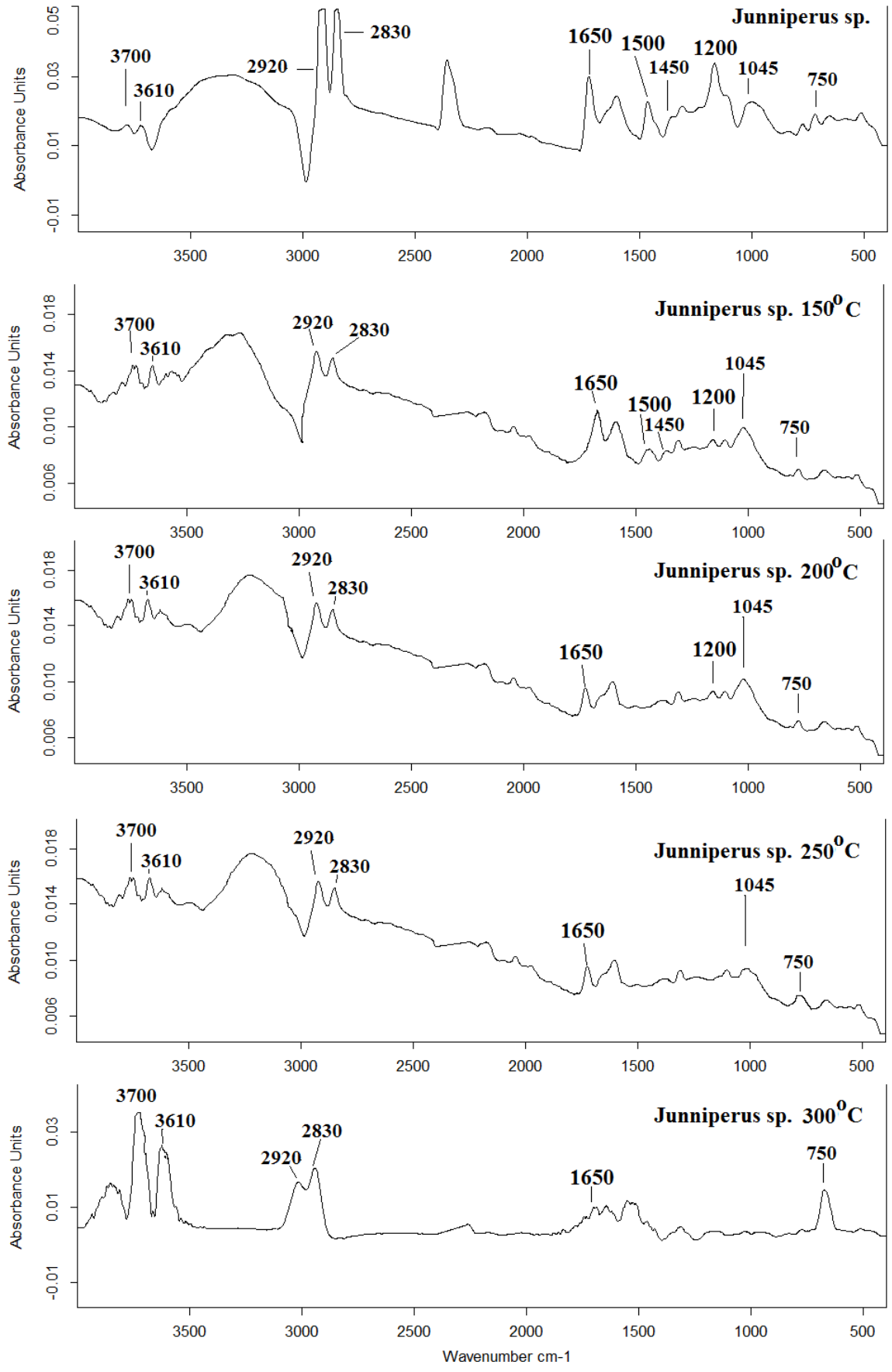

Fig 1. The FTIR spectra of fresh juniper and the products of its torrefaction

Table 1. Types of vibrations for function groups together with the assigned wave number - juniper

No.	Wave number (cm^{-1})	Type of vibration	Fresh needles of juniper	Needles of juniper 300°C
1	750	Vibration of –C=C group (polysaccharides)	PRESENT	PRESENT
2	1045	Symmetrical vibrations for PO^{2-} group (nucleic acids and phospholipids)	PRESENT	**ABSENT**
3	1200	Vibrations of C-N group (amines)	PRESENT	**ABSENT**
4	1370	Vibrations of C-H group (polysaccharides, proteins)	**ABSENT**	**ABSENT**
5	1450	Vibrations of C-C group (aromatic rings)	PRESENT	**ABSENT**
6	1500	Vibrations of C-C (aromatic rings)	PRESENT	**ABSENT**
7	1650	Secondary amide (bending vibrations of N-H group and stretching vibrations of C-N group)	PRESENT	PRESENT
8	2830	Symmetrical vibration of CH_2 group (fats)	PRESENT	PRESENT
9	2920	Asymmetric vibrations of CH_3 group (fats)	PRESENT	PRESENT
10	3610	Vibrations of O-H group (alcohols, phenols)	PRESENT	PRESENT
11	3700	Vibrations of O-H group (alcohols, phenols)	PRESENT	PRESENT

The FTIR spectrum of spruce exhibits wave numbers corresponding to the vibration of groups typical of the following chemical compounds: polysaccharides, nucleic acids and phospholipids, amines, proteins, aromatic rings, secondary amides, fats, alcohols and phenols. Drying at 150°C causes the loss of vibration with the wave number equal to 1200^{-1} corresponding to the vibrations of C-N group (amines). The increase in temperature by further 50°C does not effect in breaking consecutive bonds. Torrefaction at 250°C marks the disintegration of aromatic rings, whereas a complete loss of C-C groups is observed when the temperature increases by 300 °C. At this temperature vibrations responsible for nucleic acids and phospholipids also disappear. FTIR spectra for fresh material from spruce shoot tips and their products of torrefaction are listed in Figure 2.

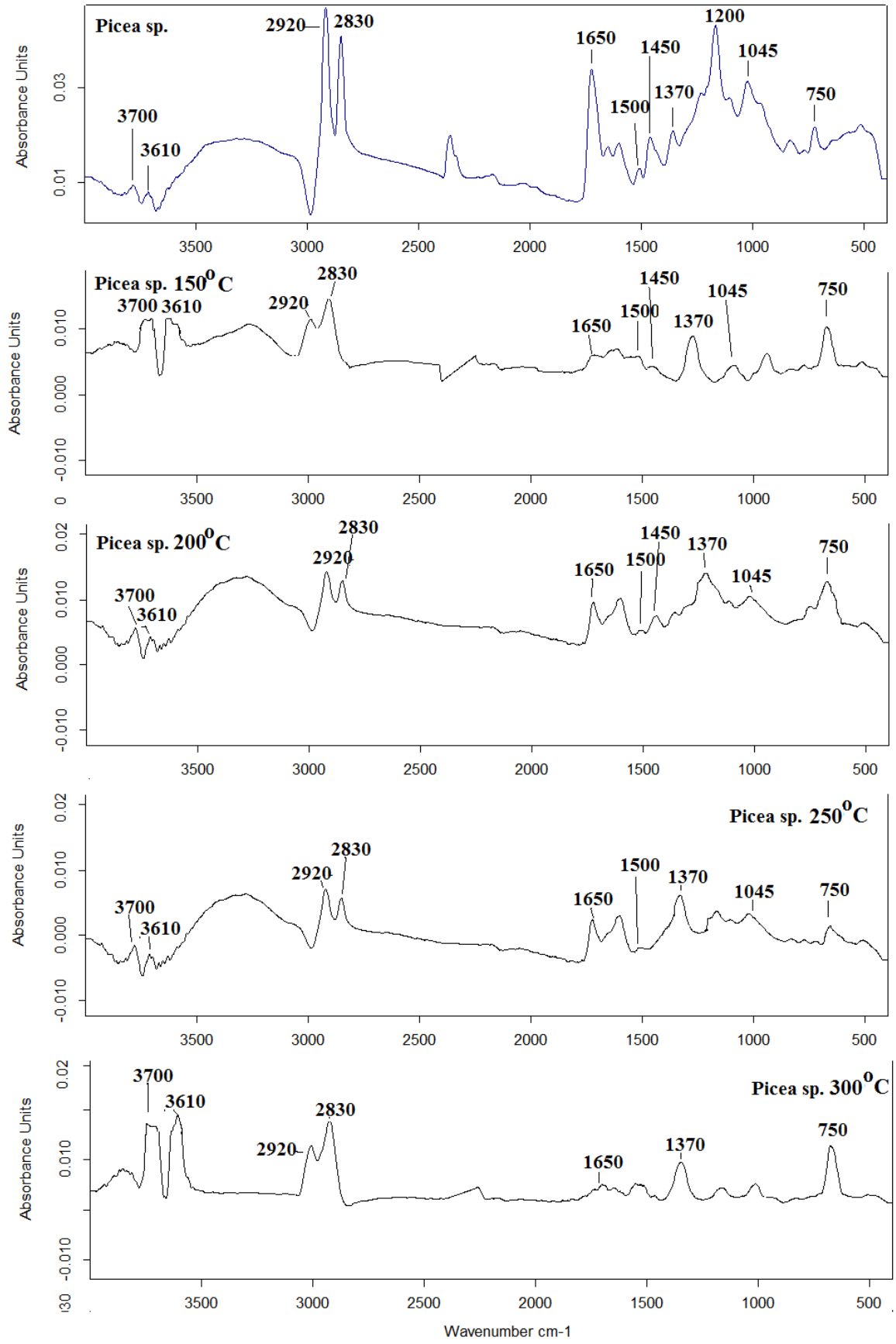

Fig. 2. The FTIR spectra of fresh spruce and the products of its torrefaction

Table 2. Types of vibrations for function groups together with the assigned wave number - spruce.

No.	Wave number (cm^{-1})	Type of vibrations	Fresh needles of spruce	Spruce needles at 300°C
1	750	Vibration of –C=C group (polysaccharides)	PRESENT	PRESENT
2	1045	Symmetrical vibrations for PO^{2-} group (nucleic acids and phospholipids)	PRESENT	PRESENT
3	1200	Vibrations of C-N group (amines)	PRESENT	**ABSENT**
4	1370	Vibrations of C-H group (polysaccharides protein)	PRESENT	PRESENT
5	1450	Vibrations of C-C group (aromatic rings)	PRESENT	**ABSENT**
6	1500	Vibrations of C-C group (aromatic rings)	PRESENT	**ABSENT**
7	1650	Secondary amide (bending vibrations of N-H and stretching vibrations of C-N group)	PRESENT	PRESENT
8	2830	Symmetrical vibrations of CH_2 group (fats)	PRESENT	PRESENT
9	2920	Asymmetric vibrations of CH_3 group (fats)	PRESENT	PRESENT
10	3610	Vibrations of O-H group (alcohols, phenols)	PRESENT	PRESENT
11	3700	Vibrations of O-H group (alcohols, phenols)	PRESENT	PRESENT

The wave number of 750 cm^{-1} corresponds to the vibration of C=C function group characteristic of polysaccharides and present in both plants. The wave number of 1045 cm^{-1} is assigned to the symmetrical vibrations of PO^{2-} group – these are nucleic acids and phospholipids. 1200 represents vibrations of the C-N (amines) group, 1370 represents C-H (polysaccharides protein) group, whereas 1450 and 1500 – are vibrations of C-C group typical of aromatic rings. With 1650 cm^{-1} wave number bending vibrations are observed for N-H and stretching vibrations for C-N (typical of secondary amides) and with 2830 – symmetrical vibrations of CH_2 group and assymetrical vibrations of CH_3 group, typical of fats. Wave numbers 3610 and 3700 correspond to the vibration of O-H group (alcohols and phenols).

Unprocessed needles of spruce contain a greater amount of amines, whereas juniper has a greater amount of lipids. There is a difference in the absence of C-H group (indicating the presence of polysaccharides and proteins) in the spectrum of juniper at wave number equal to 1370 cm^{-1}. Tips of spruce shoots show greater resistance to temperature compared with the material from juniper. The argument is that there is a greater number of function groups typical of fresh needles in the spruce FTIR spectrum than in juniper's after the process of torrefaction. At 150°C only spruce needles exhibited chemical shifts (such as no vibration of amine function groups at 1200 cm^{-1}), however at 200°C and above greater resistance to high temperatures was seen in the needles of spruce. The temperature of 200°C broke function groups originating from the vibration of aromatic rings (1450 cm^{-1}, 1500 cm^{-1}) only in the needles of juniper. A further increase in temperature by 50°C broke amine vibrations (1200 cm^{-1}) in the material from juniper and from that moment on, the observations show that a greater number of juniper's function groups were broken under high temperature than it was in the case of spruce. The torrefaction process at 200°C completely destroyed the aromatic rings in the material from the juniper, while in the case of spruce a complete loss of vibration was observed only at 300°C. The comparison of temperature impact on both materials is shown in Table 1.

Table 3. The juxtaposition of chemical compounds degrading at different temperatures during the process based on the material from the juniper and spruce

Temperature	The elimination of compounds	
	Junniperus sabina	*Picea abies*
150°C	-	amines
200°C	aromatic rings	-
250°C	amines	aromatic rings
300°C	nucleic acids, phospholipids	aromatic rings, nucleic acids, phospholipids

Source: Own design

In addition to chemical shifts, the torrefaction process also brings about topography changes in the processed biomass. In the case of spruce needles high temperature also brought about deep pores with thin boundaries. The surface of needles became more porous. The surface of juniper needles became rougher under high temperature; the smooth structure weakened. The changes were shown in Figures 7 and 8.

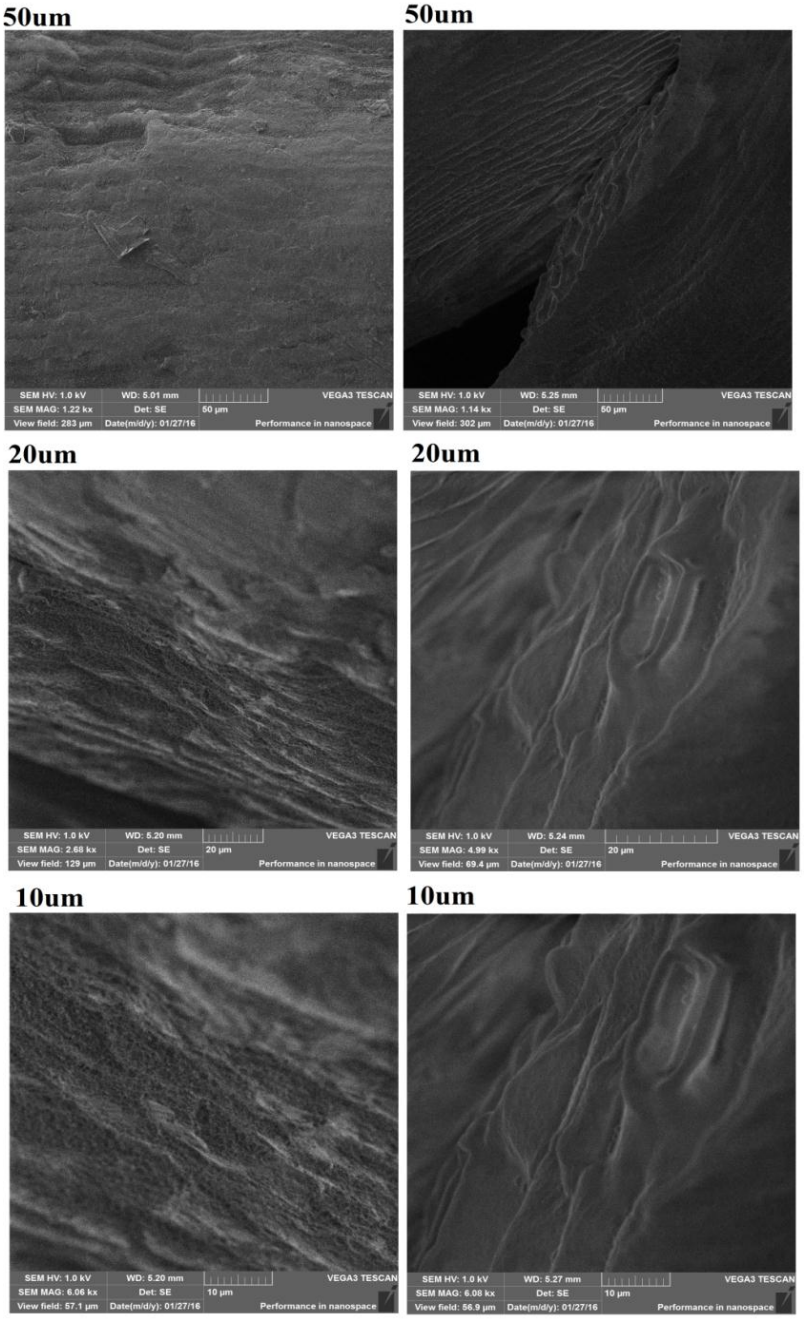

Fig. 7. Torrefied products from juniper needles produced at 300^{o}C – microscopic view at the magnification of 10, 20 and 50 μm.

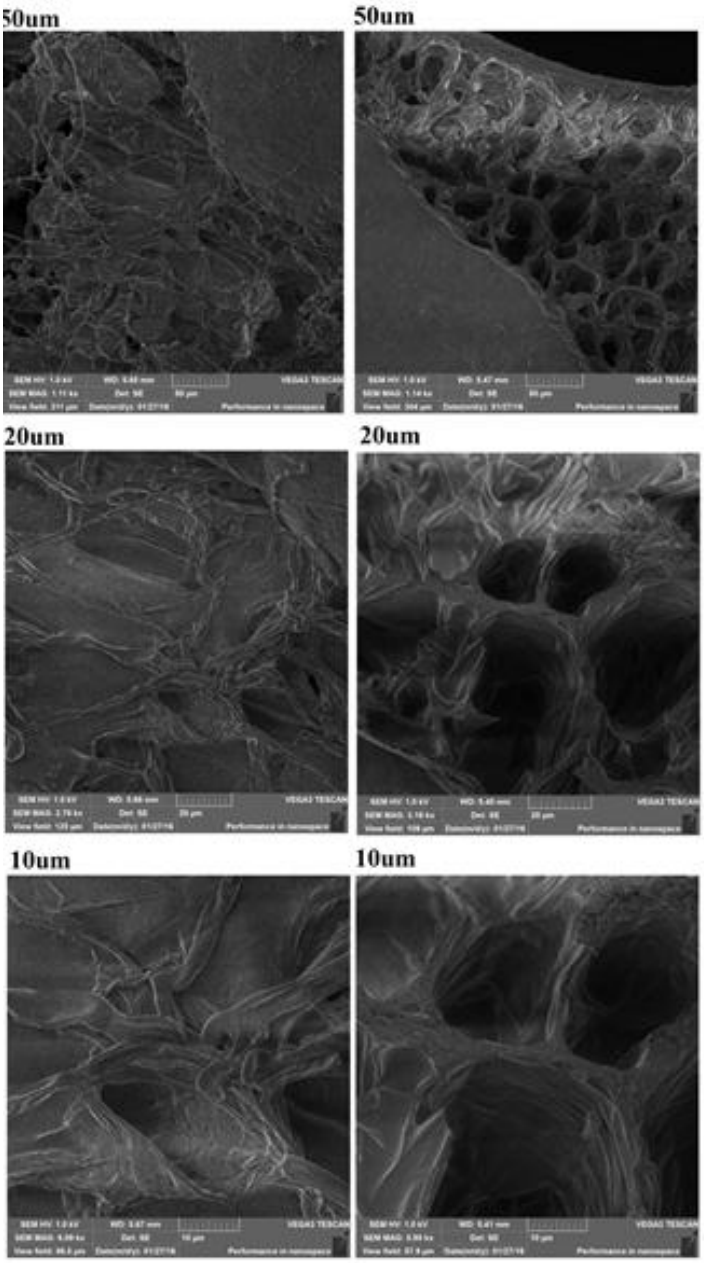

Fig. 8. Torrefied products of spruce needles produced at 300°C –microscopic view at the magnification of 10, 20 and 50 μm

CONCLUSIONS

1. Drying at 150°C does not cause major changes and damage in the analysed plant biomass.
2. Together with the increase in temperature, further bonds in biomass break and simpler organic compounds are created.
3. Various chemical compounds undergo degradation at different temperatures and in juniper the compounds degrade as follows: aromatic rings, amines, nucleic acids, phospholipids. In spruce material the compounds degrade as follows: amines (at a lower temperature), aromatic rings (at higher temperatures), nucleic acids, phospholipids.
4. The type of biomass significantly affects the process of torrefaction and its products.
5. After torrefaction at 300°C the following compounds remain intact: polysaccharides, secondary amines, fats, alcohols and phenols (lignin components).
6. By becoming familiar with the exact mechanism of the torrefaction process, one may obtain products of desirable properties and chemical composition.

REFERENCES

1. **Acharya B., Pradchan R. R., Dutta A., 2015.** Qualitative and kinetic analysis of torrefaction of lignocellulosic biomass using DSC-TGA-FTIR.AIMS. Energy, 3, 4, 760-773.
2. **Bajcar M., Zaguła G., Saletnik B., Puchalski Cz., 2015**. Influence of temperature during torrefaction process on the quality of torrefied products obtained from rapeseed straw and common osier. Teka

Commission of Motorization and Energetics in Agriculture, 15, 4, 7-12.
3. **Bajcar M., Zaguła G., Saletnik B., Puchalski Cz., Czernicka M., Zapałowska A., Zardzewiały M., Rybka S. 2015**. The influence of torrefecation process on the biomass plant energy properties. Productivity and health of the environment, ed. Puchalski Cz., Kaniuczak J., Gajdek G., 89-99. (in Polish)
4. **Bergman P. C. A., Kiel J. H. A. 2005**. Torrefaction for biomass upgrading. ECN publication, Report ECN-RX-05-180.
5. **Binti Saleh S., Hansen B. B., Jensen P. A., Dam-Johansen K., 2013**. Influence of Biomass Chemical Properties on Torrefaction Characteristics. Energy Fuels, 12, 7541-7548.
6. **Czernik S., Bridgwater A. V., 2004**. Overview of applications of biomass fast pyrolysis oil. Energy Fuels, 18, 590-598.
7. **Hamelinck C. N., Hooijdonk G., Faaij A., 2005**. Ethanol from lignocellulosic biomass: techno-economic performance in short-, middle- and long-term. Biomass and Bioenergy, 28, 4, 384-410.
8. **Kazakova N., Petkov V., Mihailov E., 2015**. Modelling of Biomass Pyrolysis. Journal of Chemical Technology and Metallurgy 50, 3, 278-281.
9. **Kristensen J.B., Borjesson J., Bruun M.H., Tjerneld F., Jørgensen H., 2007**. Use of surface active additives in enzymatic hydrolysis of wheat straw lignocellulose. Enzyme and Microbial Technology 40, 888-895.
10. **Lalak J., Kasprzyka A., Murat A., Paprota E. M., Tys J., 2014**. Pretreatment methods of lignocelulosic biomass to improve methane fermentation process (a review). Acta Agrophysica, 21, 1, 51-62. (in Polish)
11. **Lê Thành K., Commandré J-M., Valette J., Volle G., Meyer M., 2015**. Detailed identification and quantification of the condensable species released during torrefaction of lignocellulosic biomasses. Fuel Processing Technology 139, 226-235.
12. **Lewandowski W., Radziemska E., Ryms M., Ostrowski P., 2010**. Modern methods of thermochemical biomass conversion into gas, liquid and solid fuels. Proceedings of ECOpole 4, 2, 453-457. (in Polish)
13. **Lewandowski W., Ryms M., Meler P., 2010**. Termochemical pyrolysis into liquid and gas biofuels as a method of increasing biomass energy conversion efficiency. Nafta-Gaz 8, 675-680. (in Polish)
14. **Li M-F., Chen L-X., Li X., Chen Ch-Z., Lai Y-Ch., Xiao X., Wu Y-Y., 2016**. Evaluation of the structure and fuel properties of lignocelluloses through carbon dioxide torrefaction. Energy Conversion and Management 119, 463-472.
15. **Lv P., Almeida G.,Perré P., 2015**. *TGA-FTIR* Analysis of Torrefaction of Lignocelulosis Components (cellulose, xylan, lignin) in Isothermal Conditions over a Wide Range of Time Durations. Bio-Resources, 10, 3, 4239-4251.
16. **Mafu L. D., Neomagus H.W.J.P. Everson R. C., Carrier M., Strydom Ch. A., Bunt J. R., 2016**. Structural and chemical modifications of typical South African biomasses during torrefaction. Bioresource Technology, 202, 192-197.
17. **Malherbe S., Cloete T. E., 2002**. Lignocellulose biodegradation: Fundamentals and applications. Reviews in Environmental Science & Bio-Technology, 1, 105-114.
18. **Pach M., Zanzi R., Björnbom E., 2002**. Torrefied Biomass a Substitute for Wood and Charcoal (6th Asia-Pacific International Symposium on Combustion and Energy Utilization 20 May 2002 – 22 May 2002, Kuala Lumpur).
19. **Park J., Meng J., H. L. Kwang, Rojas O. J., Park S., 2013**. Transformation of lignocellulosic biomass during torrefaction. Journal of Analytical and Applied Pyrolysis, 100, 199-206.
20. **Peng Y., Wu S., 2010**. The structural and thermal characterictics of wheat straw hemicellulose. Journal of Analytical and Applied Pyrolysis, 88, 134-139.
21. **Piskorz J., Radlein D., Scott D. S., 1986**. On the mechanism of the rapid pyrolysis of cellulose. Journal of Analytical and Applied Pyrolysis, 9, 2, 121-137.
22. PN-EN 14778:2011(U). Solid biofuels – collecting samples. (in Polish)
23. PN-EN 14780:2011(U). Solid biofuels – preparing samples. (in Polish)
24. **Pushkin S. A., Kozlova L. V., Makarov A. A., Grachev A. N., Gorshkova T. A., 2015**. Cell wall components in torrefied softwood and hardwood samples. Journal of Analytical and Applied Pyrolysis, 116, 102-113.
25. **Ratte J., Fardet E., Mateos D., Hery J-S., 2011**. Mathematical modeling of a continuous biomass torrefaction reactor: TORSPYD (TM) column. Biomass and Bioenergy, 35, 8, 3481-3495.
26. **Riberto de Luz B., 2006**. Attenuated total reflectance spectroscopy of plant leaves: a tool for ecological and botanical studies, New Phytologist, 172, 2, 305-318.
27. **Sun Y., Cheng J., 2002**. Hydrolysis of lignocellulosic material for ethanol production: a review. Bioresource Technology, 83, 1-11.
28. **Wilk M., Magdziarz A., Kalemba I., 2015**. Characterisation of renewable fuels torrefaction process with different instrumental techniques. Energy, 87, 259-269.
29. **Zaldivar J., Nielsen J., Olsson L., 2001**. Fuel ethanol production from lignocellulose: a challenge for metabolic engineering and process integration Applying Microbiological Biotechnology, 56, 17-34.

Effects of mineral fertilization and pre-sowing magnetic stimulation on the yield and quality of sugar beet roots

Miłosz Zardzewiały, Bogdan Saletnik, Marcin Bajcar, Grzegorz Zaguła, Maria Czernicka, Czesław Puchalski

Department of Bioenergy Technology, Faculty of Biology and Agriculture, Rzeszów University, Ćwiklińskiej 2D, 35-601 Rzeszów, e-mail: g_zagula@ur.edu.pl

Received July 12.2016: accepted July 18.2016

Abstract. Magnetic field may be applied as a physical factor to improve germination capacity as well as growth and development of plants. In order to investigate the influence of stimulation with magnetic field and fertilization on the yield and quality of sugar beet roots, a field experiment was carried out in 2015 and it was designed to examine three cultivars of sugar beets, two variants of magnetic stimulation applied to seeds: stimulation in the magnetic field of 40 mT, and control conditions (no stimulation), as well as two variants of mineral fertilization: optimal, based on the contents of nutrients in soil, and control conditions (no fertilization). Observation of the plants' growth and development was conducted during the vegetation period. The examined values included yield of roots and leaves, as well as contents of heavy metals, macro- and micro-elements and sugar. The observations carried out during the experiment and following harvest showed that the applied variable factors used in the experiment, i.e. the pre-sowing stimulation with magnetic field as well as properly designed fertilization, positively affect the parameters of the plants germination, growth and development as well as the contents of sugar in the examined sugar beet roots.

Key words: magnetic stimulation, fertilization, sugar beet, yield.

INTRODUCTION

In Polish climate sugar beet is the only feasible raw material for production of sugar. It has been cultivated for over 150 years and during this time there have been numerous developments in both sugar beet culture and breeding which led to refinement and enhancement of the plant. Due to the increasing competition in sugar industry and the decreasing profitability of sugar beet cultivation, growers are forced to reduce costs of production, and to look for ways to increase the yield and to improve technological quality of the crop. The yield and the qualitative characteristics largely depend on the optimal farmland cultivation and rational mineral and organic fertilization [12].

Population growth poses a demand for constant increase in food production. In order to meet people's nutrition-related needs, in terms of both quantity and quality, it is necessary to improve crop yields. Measures of progress in biology mainly include the rate and stability of yield in new cultivars, as well as immunity of plants to diseases and environmental stressors [14]. In recent years there has been growing interest in organic and integrated cultivation methods with focus on sustainable methods of enhancing the quality and health of seeds [8]. High demand for organic produce and the overall increase in the demand for plant material for food manufacturing have led to research into methods enabling production growth [6]. Seeds germination capacity and plant growth are positively impacted by cleaning and selection of seeds for their physical qualities as well as treatment with temperatures, irradiation with light of various wavelengths and intensity as well as treatment with alternating magnetic field [5]. Today we know that the use of magnetic fields with extremely low frequencies positively affects the characteristics of plants as well as processes occurring in them. The observed effects include improved germination capacity, faster development, increased length of seedlings and higher quantity of raw mass [3, 7]. Plants are exposed to the operation of constant, variable, oscillating [11] and pulsed magnetic field [1]. Physical methods are recognized as safe for the environment, therefore they are important from the standpoint of ecological farming [10]. The relevant physical methods may definitely supplement chemical methods, yet they cannot replace them [1]. Earlier studies conducted both in laboratories and at micro-fields have demonstrated positive influence of stimulation with variable magnetic field on germination, growth and yield in selected cereals, pulses, root crops, vegetables and flowering plants [2, 4, 9].

Moreover, the use of fertilizers is of great importance as the basic treatment in agriculture impacting both plants productivity and quality of crops. It is estimated that in the conditions defined by Polish soils and climate, treatments with fertilizers account for 40-50% of crops productivity. At the same time inadequate use of fertilizers decreases the quality of soils by stimulating acidity, disturbing ionic equilibrium of the elements, reducing microbiological activity, introducing harmful

substances/elements and inducing salinity. Fertilization may also lead to eutrophication of surface waters and contamination of ground waters with nitrates and nitrite [Wójcik2014].

MATERIAL AND METHODS

A field experiment carried out in Gać near Przeworsk in 2015 was designed to identify the influence of pre-sowing stimulation of seeds with magnetic field and treatment with mineral fertilizers on the yield of sugar beet and the quality of its roots. The field experiment was established in split-block/split-plot design, in three repetitions. The assessment was carried out for three common sugar beet cultivars, in two variants: seeds magnetically stimulated and seeds without stimulation. Likewise, two variants of fertilization were applied: treatment with and without mineral fertilizers. The factor of fertilization was also used in combination with the factor of pre-sawing stimulation of seeds, which resulted in the total of 4 experimental variants in three block repetitions. The seeds were exposed to magnetic field of 50 mT, generated by air-spaced coil with inner diameter of 11 cm and length of 15 cm, powered from a source of single-phase alternating current. The coreless coil consisted of 13 layers, with 115 turns per each layer (Fig. 1.).

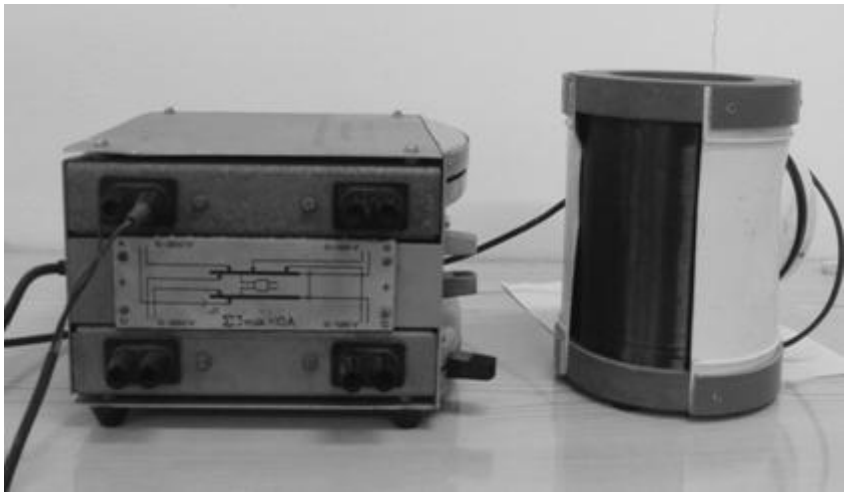

Fig. 1. Station for inducing large slow-changing magnetic field.

Calculations of such coil parameters as: resistance, inductance, reactance, impedance, intensity of current flowing in the coil, and the strength of the magnetic field in the central point of the coil were performed with the use of technical method of computing based on Ampere's law. To facilitate theoretical considerations a special application was developed to enable automatic computing of the required parameters in LabView environment.

Sample calculations for magnetic field induction at the level of 50 mT, at the frequency of 50 Hz are shown in Fig. 2.

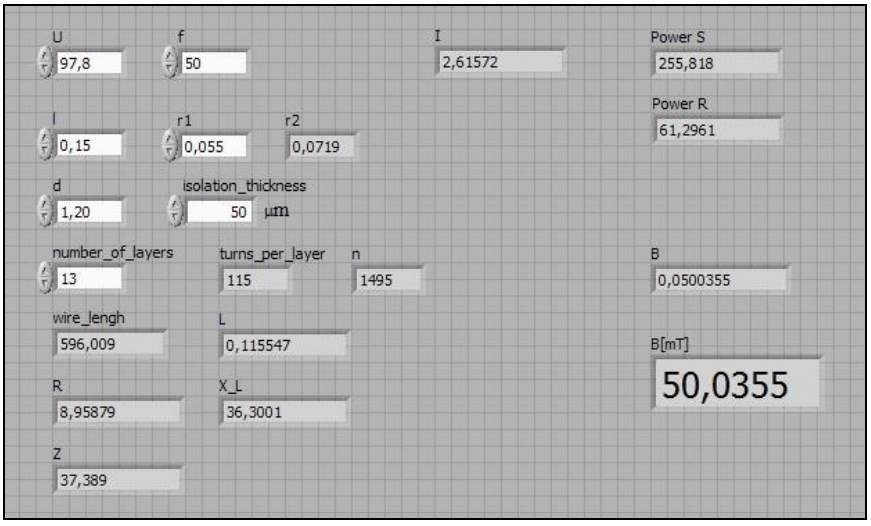

Fig. 2. The system parameters at specific induction of magnetic field

U [V] – voltage on coil clamps; f [Hz] – frequency of the magnetic field; l [m] – coil length; r1 and r2 [m] – internal and external coil radius; d [mm] – coil wire thickness; isolation thickness [µm]; number of layers; turns per layer; n – total number of turns in the coil; total wire length [m]

Duration of exposition was defined as 60 seconds, taking into account temperature coefficient and stimulation was performed each time on the day the seeds were planted:

$$R_T = R_0 (1 + \alpha \cdot \Delta T)$$

where: R_T [Ω] – resistance at temperature T,

R_0 [Ω] – resistance at temperature 0°C

α $[K^{-1}]$ – temperature coefficient of resistance (Table 1).

Table 1. Values of temperature coefficient of resistance for selected materials [13]

Iron	Tungsten	Aluminium	Copper	Silver
$6{,}5 \cdot 10^{-3}$	$4{,}5 \cdot 10^{-3}$	$4{,}4 \cdot 10^{-3}$	$4{,}3 \cdot 10^{-3}$	$4{,}1 \cdot 10^{-3}$

For example, with a change in temperature amounting to 10 K, coil resistance changes by 4.3%, which leads to change in the current strength, at the constant voltage of 100V by approx. 0.1A (nominal current in this case is approx. 2.5A).

Taking that into account, a model of magnetic field distribution around the applied solenoid was drawn (Fig. 3.)

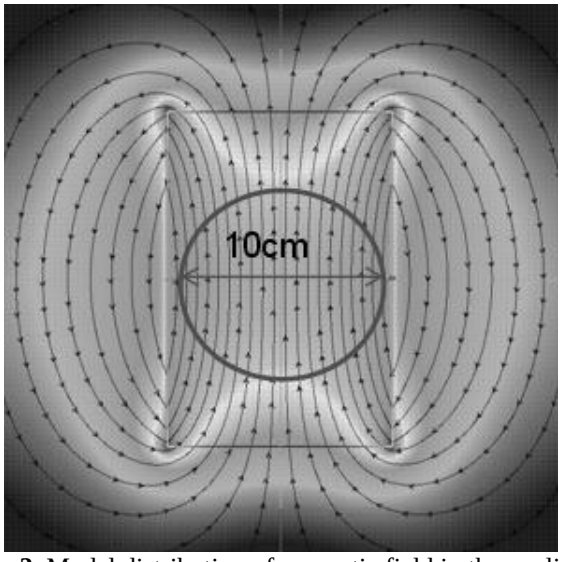

Fig. 3. Model distribution of magnetic field in the applied solenoid

Soil samples were collected in the year preceding the start of the experiment, i.e. in the 4th decade of October 2014. More specifically, 30 single samples were collected from the surface of the field in order to identify the average sample. The single samples were collected with Egner's stick, from the arable layer 0-20 cm, along the diagonals of the field designated for the experiment. The soil samples collected this way were subjected to analyses in Stacja Chemiczno-Rolnicza (Chemical and Agricultural Research Laboratory) in Rzeszów. The assays were performed to identify soil pH, and salinity as well as the contents of nitrogen, phosphorus, potassium, calcium, magnesium and chlorine. The findings were used to elaborate recommendations regarding fertilizer treatments to be used during the field experiment. Then, in November 2014 a specific amount of fertilizers was distributed, in compliance with the recommendations. The field was ploughed before the winter. In spring (late March/early April) 2015, after seedbed preparation, which included application of more fertilizers to meet the guidelines, on 15 April 2015 the field experiment was established in an area of 14 ares. Sugar beets were cultivated in compliance with agricultural technologies. Winter wheat was used as a forecrop.

Observation of the plants' growth and development was conducted during the vegetation period. Harvest was conducted in the 4th decade of October. The yield of roots and leaves was determined. Then samples of roots and leaves were collected from each plot in order to examine chemical composition. The contents of water, ash, carbon, nitrogen and volatile substances were measured with TGA701 Thermogravimetric Analyzer, and concentrations of macroelements were examined with ICP OES iCAP Dual 6500. The contents of sugar were measured with liquid chromatography system Thermo Dionex Ultimate 3000. Additionally calculated, the harvest index reflected the ratio of root yield to the overall yield of leaves and roots.

RESULTS AND DISCUSSION

Field emergence was significantly related to the factors applied during the field experiment. Moreover, variety-specific characteristics and pre-sawing stimulation with magnetic field affected that property in all the examined sugar beet cultivars. Significantly higher field emergence, compared with the other cultivars, was found in cultivar No. III (88.9%). The seeds of Cultivars I and II germinated at the rates of 85.5% and 81.3%. Pre-sowing seeds stimulation with the magnetic field of 50 mT significantly influenced field emergence, on average improving seeds germination capacity by 7.2 %. On the other hand, optimal fertilization was not related to seeds germination capacity, yet later it affected the speed of growth, development and the ultimate crop yield.

Both the yield of roots and the yield of leaves were related to the applied variable factors. The yield of roots on average ranged from 53.9 t/ha for the control sample, for stimulated seeds on average 58.4 t/ha, for the variable factor, i.e. magnetic stimulation and fertilization 62.4 t/ha up to 71.9 t/ha for cultivars treated with optimal fertilization. The applied optimal fertilization improved yield of roots in Cultivar No. I by 15.2 t/ha, Cultivar II by 23.4 t/ha and Cultivar III by 15.5 t/ha compared with the control sample. Combination of the variable factors, i.e. magnetic stimulation and fertilization led to the increase in the mean yield in the investigated cultivars by 8.5 t/ha. Pre-sowing stimulation of seeds improved the yield from roots in each of the examined cultivars. In comparison to the control sample, the increase in the yield of Cultivar

No. I amounted to 3.9 t/ha, Cultivar II – 5.6 t/ha, and Cultivar III – 4.1 t/ha.

The yield of leaves ranged from 33.0 t/ha to 52.8 t/ha. Pre-sowing stimulation, regardless of the cultivar, increased the yield of leaves on average by 6.8 t/ha compared with the control sample. In terms of the yield of leaves, positive response to the stimulation was observed in the cultivars; the yield of leaves in Cultivar I increased by 5.0 t/ha, Cultivar II by 8.3 t/ha and Cultivar III by 7.5 t/ha. The applied variable factors, i.e. optimal fertilization and optimal fertilization combined with magnetic stimulation increased the yield of leaves on average by 16.0 t/ha and 9.9 t/ha, respectively. There was a similar response of all the cultivars to pre-sowing seeds stimulation with magnetic field and optimal fertilization in terms of increased yield of roots and leaves.

Harvest index was used to assess plants productivity, and expressing the relation of utility index to biological yield, it is in the range of 0.57-0.61 and matches the limit values adopted in the available literature.

Table 2. Field emergence, yield of roots and leaves as well as harvest index

Cultivar	Type of applied variable factor	Field emergence [%]	Yield of roots [t·ha^{-1}]	Yield of leaves [t·ha^{-1}]	Harvest index
I	Control	81.5	54.5	35.5	0.61
	Stimulation 50 mT	89.4	58.4	40.5	0.59
	Stimulation 50 mT + optimal fertilization	89.2	62.1	44.0	0.59
	Fertilization	81.7	69.7	51.5	0.58
	Mean	85.5	61.2	42.9	0.59
II	Control	78.0	49.8	33.0	0.60
	Stimulation 50 mT	85.5	55.4	41.3	0.57
	Stimulation 50 mT + optimal fertilization	84.2	60.9	43.5	0.58
	Fertilization	77.5	73.2	49.4	0.60
	Mean	81.3	59.8	41.8	0.58
III	Control	85.0	57.3	37.0	0.61
	Stimulation 50 mT	91.7	61.4	44.5	0.58
	Stimulation 50 mT + optimal fertilization	92.7	64.2	47.9	0.57
	Fertilization	86.0	72.8	52.8	0.58
	Mean	88.9	63.9	45.6	0.59
Mean	Control	81.5	53.9	35.2	0.61
	Stimulation 50 mT	88.7	58.4	42.1	0.58
	Stimulation 50 mT + optimal fertilization	88.7	62.4	45.1	0.58
	Fertilization	81.7	71.9	51.2	0.58

Pre-sowing stimulation of seeds and fertilization resulted in higher accumulation of sugar in the sugar beet roots. Compared to the control sample, sugar contents in the investigated cultivars increased on average by 0.98 % for the sample exposed to magnetic field of 50 mT. The increase in the case of Cultivar I was by 0.91 %, for Cultivar II – 1.03 % and Cultivar III by 1.00 %. The biological yield of sugar was higher as a result of magnetic stimulation. In comparison to the control sample, the variable factor of stimulation led to the mean increase in biological yield of sugar by 1.40 t·ha^{-1}. Taking into account the mean sugar yield, the best result was observed in Cultivar No. III, at the level of 12.64 t of sugar per one hectare. The other applied variable factors, i.e. fertilization combined with magnetic stimulation, and fertilization alone, significantly improved the biological yield of sugar in sugar beet roots. The mean increase in this value in the case of fertilization combined with magnetic stimulation was found at the level of 2.7 t·ha^{-1} in the investigated cultivars of sugar beet, in comparison to the control sample. On the other hand optimal fertilization increased the yield of sugar on average by 5.12 t·ha^{-1} compared with the control sample.

Table 3. Biological yield of sugar, and selected items of chemical composition of sugar beet roots

Cultivar	Type of applied variable factor	Sugar, [%]	Biological yield of sugar, [t·ha^{-1}]	Contents of water, [%]	Soluble ash, [%]
I	Control	19.54	10.65	75.42	0.47
	Stimulation 50 mT	20.45	11.94	77.37	0.63
	Stimulation 50 mT + optimal fertilization	20.60	12.79	77.81	0.53
	Fertilization	21.02	14.65	77.15	0.43
	Mean	20.40	12.51	76.93	0.52
II	Control	17.97	8.95	76.44	0.57
	Stimulation 50 mT	19.00	10.53	76.94	0.68
	Stimulation 50 mT + optimal fertilization	19.67	11.98	77.35	0.63
	Fertilization	21.03	15.39	76.87	0.52
	Mean	19.41	11.71	76.90	0.60
III	Control	18.03	10.33	76.41	0.60
	Stimulation 50 mT	19.03	11.68	77.43	0.61
	Stimulation 50 mT + optimal fertilization	20.67	13.27	77.08	0.62
	Fertilization	20.97	15.27	77.42	0.55
	Mean	19.67	12.64	77.08	0.60
Mean	Control	18.51	9.98	76.09	0.54
	Stimulation 50 mT	19.49	11.38	77.24	0.64
	Stimulation 50 mT + optimal fertilization	20.31	12.68	77.41	0.59
	Fertilization	21.00	15.10	77.14	0.50

Statistical analysis did not show a significant effect of pre-sowing stimulation, fertilization, and combination of these two variable factors in the contents of dry matter and ash. Nonetheless, there is a visible positive impact of the applied variable factors on the contents of water and soluble ash in the roots of the examined cultivars. There was a noticeable tendency for growth in water contents after the variable factors were applied; in the stimulated sample by 1.15 %, for fertilization combined with stimulation by 1.32 % and for fertilization alone by 1.05 % compared to the control. The aforementioned tendency was observed in all the relevant cultivars. Likewise, there was an increase in ash contents following magnetic stimulation (on average by 18.50%) and combined stimulation and fertilization (on average by 9.25%) compared to the control sample. Application of optimal fertilization led to a decrease in ash contents, on average by 7.40%. The above trend was observed in all the three cultivars of sugar beet.

Based on a study on two cultivars of sugar beets, Wójcik [15] showed that pre-sowing stimulation with the value of 75 mT significantly modified the yield of roots, in comparison with the control sample, on average by 6 t/ha. Moreover, she reported that pre-sowing stimulation of seeds led to an increase in the contents of sugar in the roots, on average by 0.65%. It was also demonstrated that pre-sowing exposition to magnetic field resulted in increased field emergence in the investigated cultivars, on average by 6%.

Table 4. Biometric characteristics of the plants at harvest, depending on the cultivar and the applied variable factor

Cultivar	Experimental factors			
	Control sample	Pre-sowing stimulation 50 mT	Pre-sowing stimulation 50 mT + optimal fertilization	Optimal fertilization
Raw mass of root (g)				
I	605	650	688	766
II	544	611	667	811
III	633	677	711	800
mean	594	646	688	792
Raw mass of leaves and petioles (g)				
I	393	448	481	559
II	359	452	473	543
III	405	487	526	576
mean	385	462	493	559

Each of the applied variable factors positively impacted the investigated biometric properties. As a result of magnetic stimulation, the raw mass of roots increased in each of the examined cultivars, on average for all the three cultivars by 52 g. Application of such variable factors as fertilization and fertilization combined with magnetic stimulation produced increase in root mass by 198 g and 94 g, respectively.

In the case of leaf petioles and blades the tendency was the same as in sugar beet roots. The variable factors applied in the experiment produced higher yield of leaves in all the cultivars. Raw mass of leaf petioles and blades of sugar beets ranged from 385 g in the control sample, to as much as 559 g in the sample treated with optimal fertilization. Magnetic stimulation resulted in an increase in leaf mass by 77 g, compared to the control.

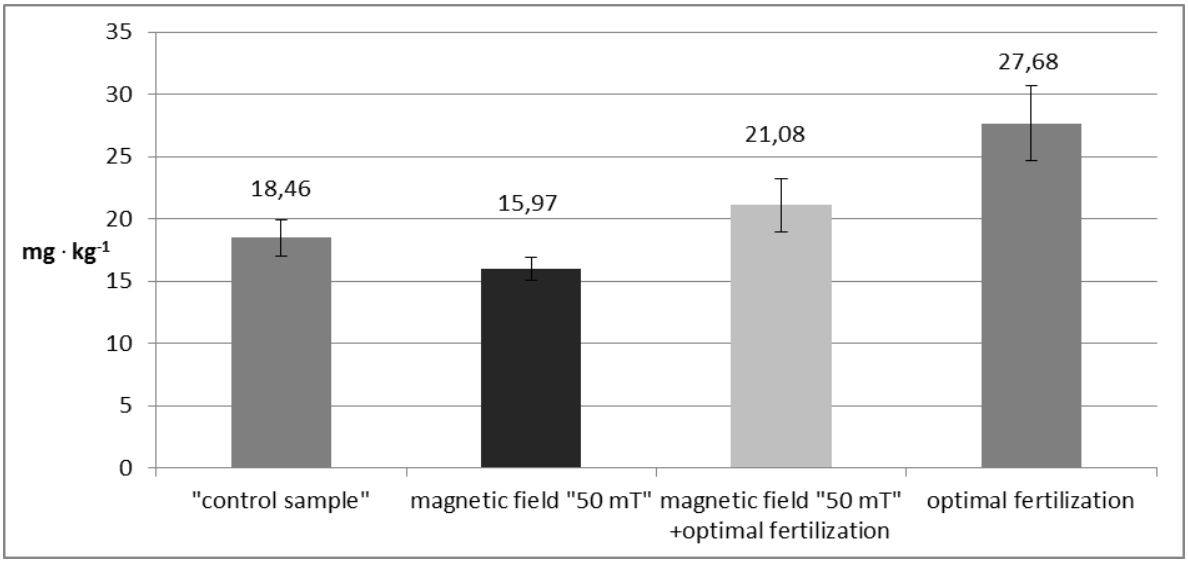

Fig. 4. Mean contents of heavy metals in the roots of the examined sugar beet cultivars

Fig. 4. shows mean total contents of heavy metals, i.e. aluminum, cadmium, chromium, copper, nickel, strontium, titanium, and zinc in raw mass of sugar beet roots, for Cultivars I, II and III. The findings show that magnetic pre-stimulation led to a decrease in the contents of heavy metals in the examined roots by 13.5%, compared with the control. On the other hand there is a visible relationship between the applied optimal fertilization and the increase in heavy metals contained in sugar beet roots of all the cultivars. In all the cases the combined treatment with magnetic field and optimal fertilization resulted in 23.9% reduction in the contents of heavy metals in sugar beet raw mass, in comparison to treatment with a single variable factor of optimal fertilization.

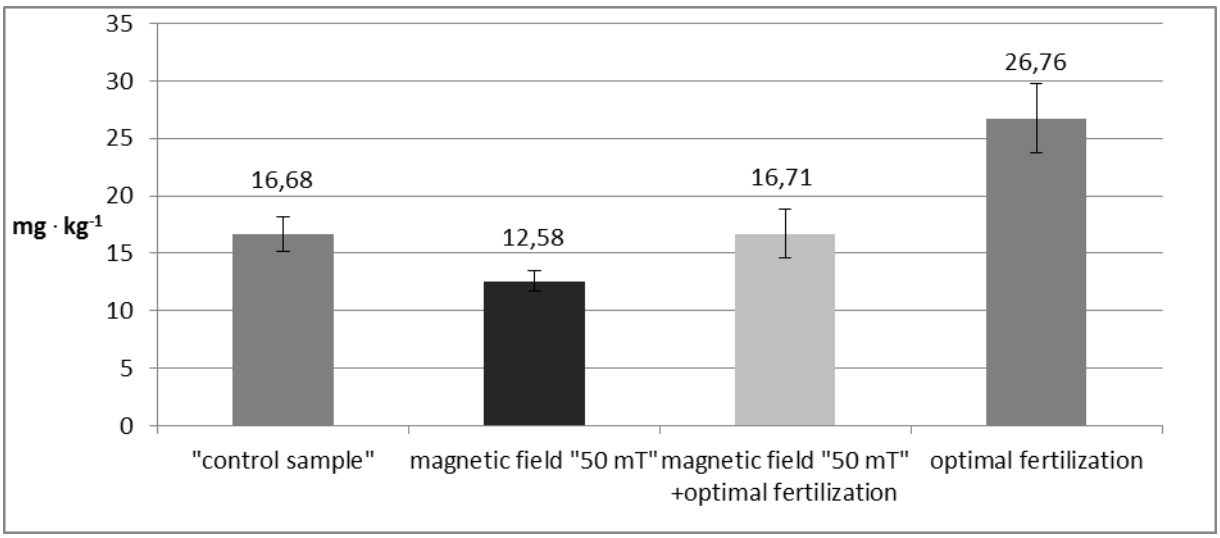

Fig. 5. Mean contents of microelements in roots of the examined sugar beet cultivars

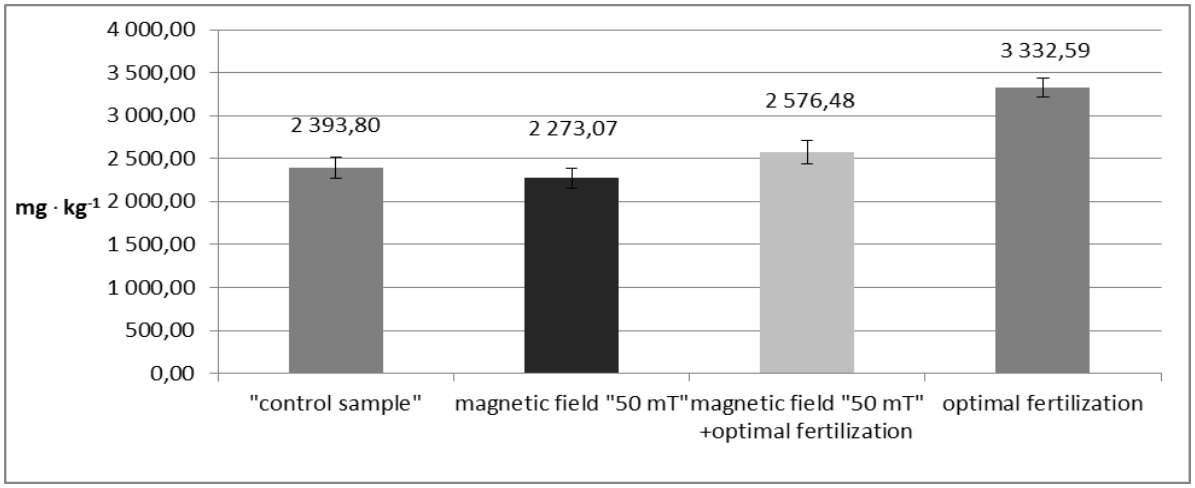

Fig. 6. Mean contents of macroelements in roots of the examined sugar beet cultivars

Figure 5 presents mean contents of microelements, i.e. manganese, molybdenum, selenium, iron and barium in raw mass of sugar beet roots, for Cultivars I, II and III. On the other hand, Fig. 6 shows mean values for macroelements, i.e. calcium, potassium, sodium, magnesium, phosphorus and sulphur, in raw mass of sugar beet roots, in Cultivars I, II and III. Like in the case of heavy metals, for micro- and macroelements there is a visible relationship between the pre-sowing magnetic stimulation and a decrease in the contents of the examined elements in raw mass of the examined cultivars of sugar beet. The use of magnetic field in the examined cultivars on average led to a decrease in the quantity of microelements by 24.6 %, and macroelements by 5.05 % compared with the control samples. On the other hand the applied well-designed fertilization increased the mean contents of microelements by 60.43 % and macroelements by 39.21 % in the examined raw mass of sugar beet roots of all cultivars, compared with the control samples.

CONCLUSIONS

1. The applied optimal mineral fertilization positively influenced the contents of micro- and macroelements, the biological yield of sugar and the yield in all of the examined cultivars of sugar beet, while also increasing the contents of heavy metals in raw mass of beetroots.
2. The applied magnetic field of 50 mT significantly enhanced field emergence of sugar beet, and by synergic effect with yield rates, it improved the contents of sugar and biometric properties.
3. The applied magnetic field, acting alone and in combination with fertilization significantly reduced accumulation of heavy metals in the harvested sugar beet roots.

REFERENCES

1. **Bilalis D., Katsenios N., 2012.** Efthimiadou A., Efthimiadis P., Karkanis A., Pulsed electromagnetic fields effect in oregano rooting and vegetative propagation: A potential new organic method, Acta Agr. Scand. B.-S. P., vol. 62, 1, 94-99.
2. **Bujak K., Frant M., 2009.** Effect of pre-sowing stimulation of seeds with alternating magnetic field on the yields of spring wheat, Acta Agrophysica, 14(1), 19-29.
3. **Cakmak, T., R. Dumlupinar, S. Erdal., 2010.** Acceleration of germination and early growth of wheat and bean seedlings grown under various magnetic field and osmotic conditions. Bioelectromagnetics 31, 120-129.
4. **Camps-Raga B., Gyawali S., Islam N.E., 2009.** Germination rate studies of soybean under static and low-frequently magnetic field, IEEE T. Dielect. El. In., vol. 16, 5, 1317-1321.
5. **Ciupak A., Szczurowska I., Gładyszewska B., Pietruszewski S., 2007.** Impact of laser light and magnetic field stimulation on the process of buckwheat seed germination, Technical Sciences, 10, 1-10.
6. **Domínguez-Pacheco, A., C. Hernández-Aguilar, A. Cruz-Orea, A. Carballo-Carballo, R. Zepeda-Bautista, E. Martínez-Ortíz., 2010.** Semilla de maíz bajo la influencia de irradiación de campos electromagnéticos. Rev. Fitotec. Mex. 33(2), 23-28.
7. **Esitken, A., 2003:** Effect of magnetic fields on yield and growth in strawberry 'Camarosa'. J. Hort. Sci. Biotechnol. 78(2), 145-147.
8. **Janas R., Grzesik M., 2006.** Pro-ecological methods of improving quality of seeds for horticulture, Zesz. Probl. Pos. Nauk Roln., 510, 213- 221.
9. **Kornarzyński K., 2006.** Effects of magnetic and electric field on germination of selected flowering plants. Agr. Eng., 5, 305-312.
10. **Podleśny J., Pietruszewski S., 2007.** The role of magnetic stimulation of seeds in formation of faba bean plants resistance to water deficit in the soil substrate, Acta Agrophysica, 9(2), 449-458
11. **Racuciu M. 2011.** 50 Hz Frequency Magnetic Field Effects on Mitotic Activity in the Maize Root, Rom. J. Phys., t.21, 1, s.53-62.

12. **Rajewski J., Zimny L., Kuc P. 2008.** Effect of various types of conservative cultivation on technological value of sugar beet root. Probl. Inz. Roln., 1, 109–116.
13. **Resnick R. 2001.** Physics, vol.2, PWN publishing house, Warszawa.
14. **Święcicki W. K., Surma M., Koziara W., Skrzypczak G., Szukała J., Bartkowiak-Broda I., Zimny J., Banaszak Z., Marciniak K. 2011.** Advanced technologies in plant production – friendly for people and the environment, Polish Journal of Agronomy, 7, 102–112.
15. **Wójcik S. 2006.** Yields and technological quality of sugar beet roots depending on stimulation of seeds, Agr. Eng., 6, 383-388.

3d design procedure, fem analyses and optimization of the tiller's sprocket

Karol Tucki, Michał Sikora

* Department of Production Management and Engineering, Warsaw University of Life Sciences – SGGW

Received July 02.2016: accepted July 13.2016

Abstract. This article present selected issued of the analysis of the computer modelling of the tiller's sprocket with the Solid Edge ST software. The geometry presented in the article was prepared so that they may be used to perform simulation presenting the influence of the loads generated by the ground work on the distribution and values of the stress forces within the tiller's sprocket - Finished Element Method. The analysis covered the sprockets subjected to the forces of: 200N, 400N, 600N, 800N and 1000N. Geometric models were developed based on the available catalogue materials and the Polish Standard PN+92/R-58051-1. The FEM analyses performed allowed suggesting solutions to optimise the whole geometry in terms of the strengths.

Key words: tiller's sprocket, geometry, modelling, optimization, agriculture

INTRODUCTION

The farms, irrespective of their cultivation area [23], ate equipped with various machinery and tools for plant cultivation and maintenance. The tools used for cultivating the soil and fertilizing it play one of the main roles in farms - they influence the soil quality directly with their specific stricture and purpose [16, 22]. One shall bear in mind that they are classified as the most energy-consuming machines due to the characteristics of their operating conditions and the intensity of their ability to influence the soil quality [8, 17].

They may be used for agrotechnological processes in the farms to obtain and provide both correct and as effective as possible growth of the crops thanks to the additional soil breaking as well as its unification and levelling [3]. What is more, they may affect the soil humidity, as well as disturb or inhibit further growth of weeds. Which tools are used and how they work, as well as the number of procedures performed, depends on various factors requiring previous planning od the agricultural production in a given farm [21]. Planning the above one shall consider the following data: plant kind and variety, their current condition, precrops. An important factor in selecting the procedures comprises the condition of the soil, its type and selecting the appropriate working depth of the tools to be used [4].

It may be noticed within the recent years, that the increasing number of the tools used for agrotechnological processed in the farms are not individual machines by multifunctional aggregates (e.g. tooth harrow and cage rollers). Their main function is to provide the crop cultivated with the best possible growth conditions with the lowest number of machinery passes over the soil cultivated. Multiple machinery passes over the soil cultivated affects it significantly [26]. This is particularly visible when using the multifunctional aggregates, whose weight with the tractor is heavier, hence the influence is more negative [19]. Therefore, despite the fact that cultivation tools are combined into aggregated and despite their advantages, the above-mentioned solutions has also disadvantages, therefore individual tools (not combined into cultivation aggregates) are still common. An example of such action is the use of a tiller, that is perfect for procedures improving the soil quality due to its properties based on its construction and operating principle, but at the expense of its reduced energy consumption compared to other tools.

To consider the aspects of the strength of a tiller's sprocket during its operation in the soil, one may apply the Finite Element Method. However, before this is possible, one shall properly prepar.e the geometry of the elements under analysis

TILLERS

Tillers are one of may tools available used for agrotechnological procedures, previously performed by ploughing as the main procedure aimed at improving the soil quality. What is more, contrary to the ploughing, using the tools for no-tillage cultivation, such as disc cultivators or tillers instead of the ploughs, what positively influences the crop energy and economic efficacy [5].

However, the main objective of the tillers used as the tools in agriculture is to improve the soil condition and quality following the preceding procedure of ploughing, to fertilize the soil better following ploughing and to mix the fertilized with the soil properly. Thanks to its construction, cultivating ensures deeper agitation and aeration of the soil following the preceding ploughing, and the soil itself is broken up and mixed. Using the proper type of the sprocket, tillers may be used for various purposes. A tiller with spring sprocket may for example be used to dig elymus and other weeds in the

plowed ground. What is more, due to its working depth and the strive for cost minimization, agrotechnological procedures with the tillers may be used for stubble cultivation instead of the ploughs. Tiller may also be used before the ploughing itself to destroy the turf and facilitate plough embedding, what may improve the energy efficacy of the ploughing itself.

Also subsoilers may be found on the farm, the so-called heavy tillers composed of rigid chisel components for deep soil agitation. This is performed to destroy the plough pan. The nature of the tool's structure and operation principle results in the working depth of 70 cm.

Tillers used in agriculture are equipped with working units called sprocket. Depending on the type of soil and the conditions in which the tiller is used, three types of sprocket fixed on the tillers are distinguished: spring sprockets, composed of a single spring or supported with an additional soring in its upper part, semi-rigid sprocket and rigid sprocket, with individual protection if the sprocket would hit a rock [1]. The so-called shear pin or spring fuse constitute the protection referred to above [10].

3D modelling of a tiller's sprocket

Computer 3D modelling is an example how the IT development facilitated the production processes [6].

Thanks to the technology, not only the design stage (design philosophy), but also the time necessary to have the final product from the design changed [14, 24, 25].

Solid Edge ST6 software allows preparing a 3D digital prototype of individual components in the *Część* [Part] menu, and then creating the final tool out of multiple individual components in the *Złożenie* [Fitting] menu of the Solid Edge software [7, 20].

The following actions are necessary to perform a 3D model of a tiller's sprocket in the Solid Edge software:

- selecting the main reference plane with the shape drawing (Figure 1) of the tiller's sprocket;
- placing new reference planes on the sprocket drawing with *Normalna do krzywej* [Normal to curve] to create the sprocket model with a specific cross-section (Figure 2);
- using the cross-sections placed on the reference planes (Figure 3) one may move forward from the drawing to the three-dimensional model of the sprocket to be designed with the *Wyciągnięcie po krzywej* [Extrude along the curve];
- having defined the input parameters - the path and the cross-sections - the three-dimensional model of the sprocked is generated (Figure 4).

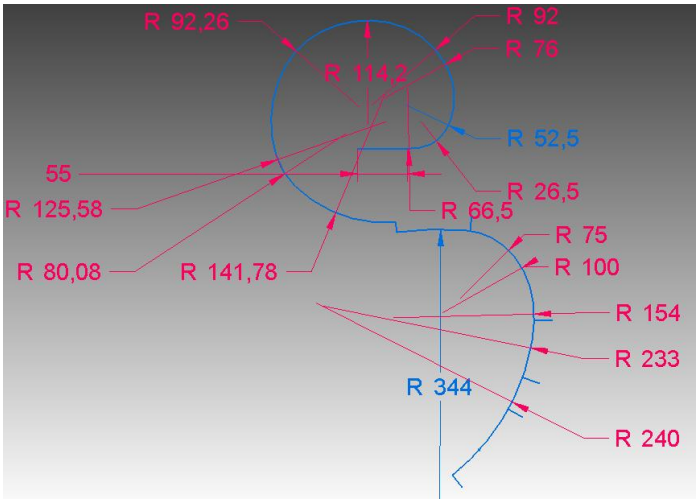

Fig. 1. The drawing with the tiller's sprocket curvature dimensions - 28x11 [Own elaboration]

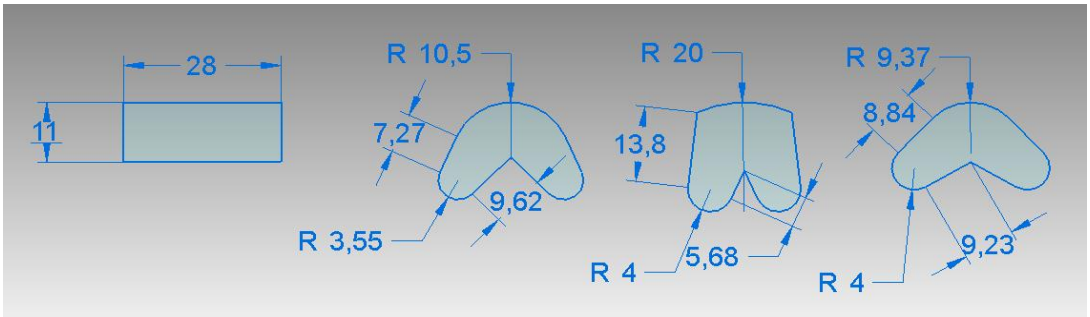

Fig. 2. 28x11 Tiller's sprocket cross-sections [Own elaboration]

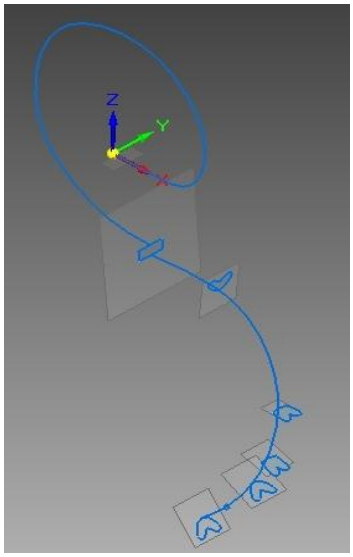

Fig. 3. Drawing together with drawings of the tiller's sprocket cross-section – 28x11 [Own elaboration]

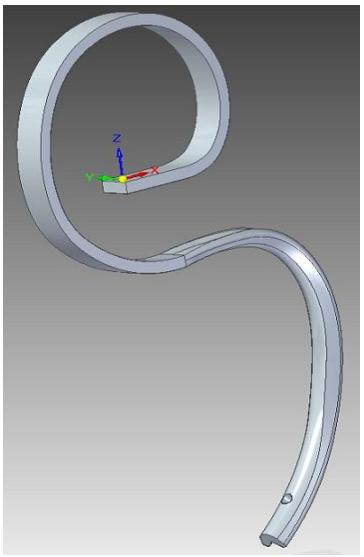

Fig. 4. Three-dimensional model of tiller's sprocket with the function [Own elaboration]

Despite the use of the *Wyciągnij po krzywej* option, two openings were provided - in the top to fix the tiller's sprocket to the frame and on the bottom to fix the tip. Similarly, three other components composing the sprocket under analysis were modelled, namely the tip (Figure 5 and 6) and the bolt with the nut fixing the tip to the sprocket.

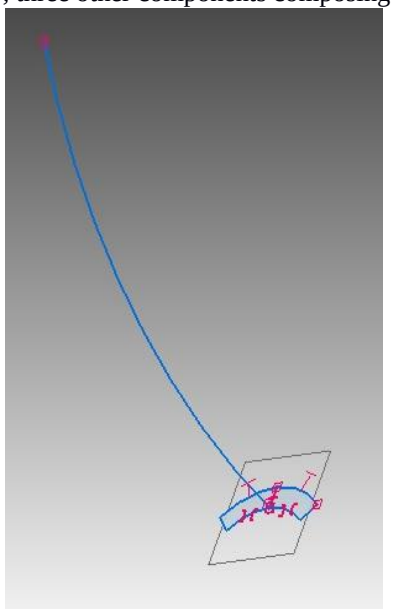

Fig. 5. Drawing of the tip base with the cross-section drawing [Own elaboration]

Fig. 6. Three-dimensional model of the tiller's sprocket tip following the option [Own elaboration]

With all the components of the sprocket, namely the sprocket base, the tip and the bolt with the nut, one may forward to the *Złożenie* menu. There, using the *Biblioteka części* [Parts' library] option one shall select the sprocket base as the first component. It shall be the reference plane in placing thee remaining components The remaining components are transferred similarly as the first component. Then the components are combined together with the option *Składaj* [Fix] on the *Main tools* toolbar and by providing the appropriate relations to the individual components.

When the components are provided with the proper relations, the model so generated (Figure 7) may be saved as a separate file. The default saving format of the Solid Edge software is *.asm, but since the files will be used by other software, such models shall be saved in more multifunctional format of Parasolid *.x_t.

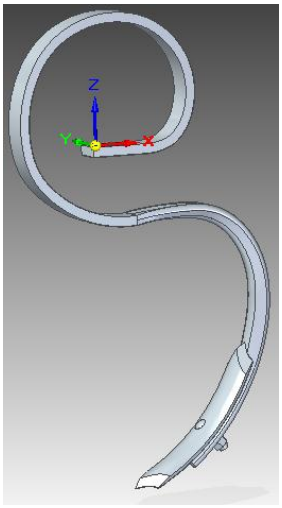

Fig. 7. 28x11 Tiller's sprocket fixing [Own elaboration]

Taking into consideration the soil conditions in which the spring tiller's sprockets work, as well as different soil condition, its different firmness and humidity, one may see different solutions for developing the sprockets. Starting from the sprockets made of single S-shaped steel piece by combining two components - the top and the bottom one, up to spiral (screw) sprockets.

Similarly to the above-mentioned sprocket (28x11), the other spring tiller's sprockets were designed, namely: 60x11 (Figure 8); 32x10 (Figure 9); 45x11 (Figure 10); 45x11 (Figure 11);

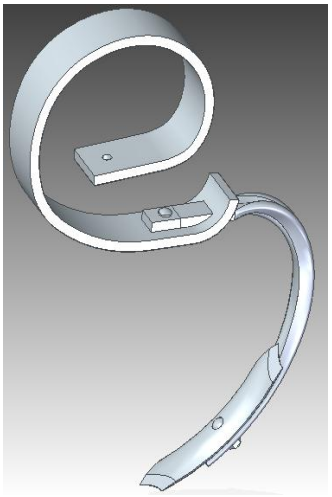

Fig. 8. Three-dimensional model of the tiller's 32x10 sprocket [Own elaboration]

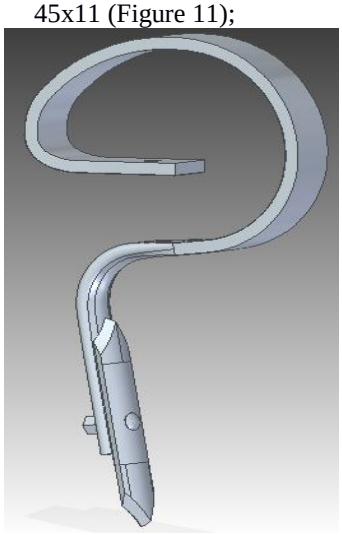

Fig. 9. Spring tiller's sprocket – 60x11 [Own elaboration]

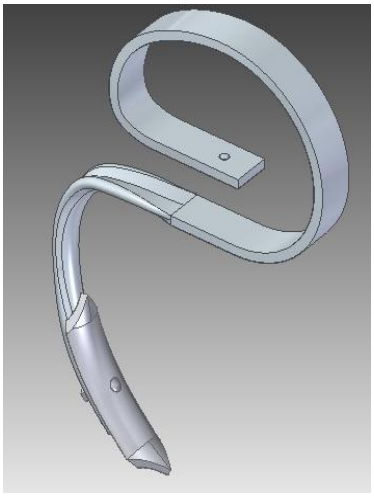

Fig. 10. Spring tiller's sprocket - 45x11 [Own elaboration]

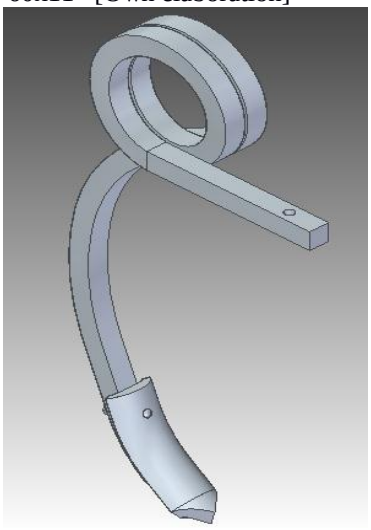

Fig. 11. Spring tiller's sprocket - spiral 35x35 [Own elaboration]

Despite the modern and most complex agricultural machines and tools available, the tillers still play an important role in the crop growing process due to their simplicity, strong influence on the soil and reduced energy consumption. The designing of a tiller's sprocket without the state-of-art professional software facilitating the designer to prepare comprehensive technical documentation together with detailed technical analyses is complicated. The possibility to verify the selected model in 3D, automatic generation of the component layouts and the ability to perform comprehensive strength analyses combined with the user-friendly nature of such state-of-art professional software suggest its quick popularization.

Using the computing numerical codes for computer simulation with the Finite Element Method

Using the state-of-art computer software, the engineers may perform the analyses of computer models described with mathematical equations [20].

The Finite Element Method is one of the basic components used in the computer aided technological calculations. This is one of the partitioning methods, striving for dividing the continuous geometric layouts into components with a limited number of subsections [12]. The method may be applied for both individual parts and highly complex structures. The main assumption of the method described is to divide the continuous geometric layout into the so-called finite components combined in the nodes, resulting in the creation of a discrete geometric model, hence the layout with unlimited number of the degrees of freedom is transformed into a layout with a limited number of the degrees of freedom. When solving various issues such as. e.g. material strength, also the issue of the so-called layout boundary conditions shall be considered.

Five models of the tiller's sprocket varying in terms of their geometric construction were subjected to simulations in the numerical computing software. The analysed tiller's sprockets were made of the spring steel compliant with the Polish Standard PN-74/H-84032 [19], namely the 50S2 low alloy silicon steel [15]. That steel is dedicated for thermal processing purposes. Therefore the assumed flexible material models with the following parameters is typical for the computer models of the sprockets:

- Young's Module E=200 GPa;
- Poisson's coefficient v = 0.3;
- Yield strenth R_e = 1080 MPa;
- Tensile stresses R_m = 1280 MPa.

It was assumed that the soil resistance affecting the tip is directed downwards at 15 degree angle [2]. It is assumed that the average soil resistance is applied to the tip at the height of $h = 0.2a$ (Figure 12), measured from the blade's tip. The value og the resistance components affecting the sprocket with the tip increases with the tool's working depth. The loads applied to the sprockets in the simulation are provided in the table below.

Table 1. Distribution of the forces applied to the tiller's sprocket pursuant to the parameters assumed

200	400	600	800	1000	Load [N]
51.8	103.5	155.3	207.0	258.8	Z component [N]
193.2	386.4	579.5	772.7	965.9	Z component [N]

Own elaboration based on [2]

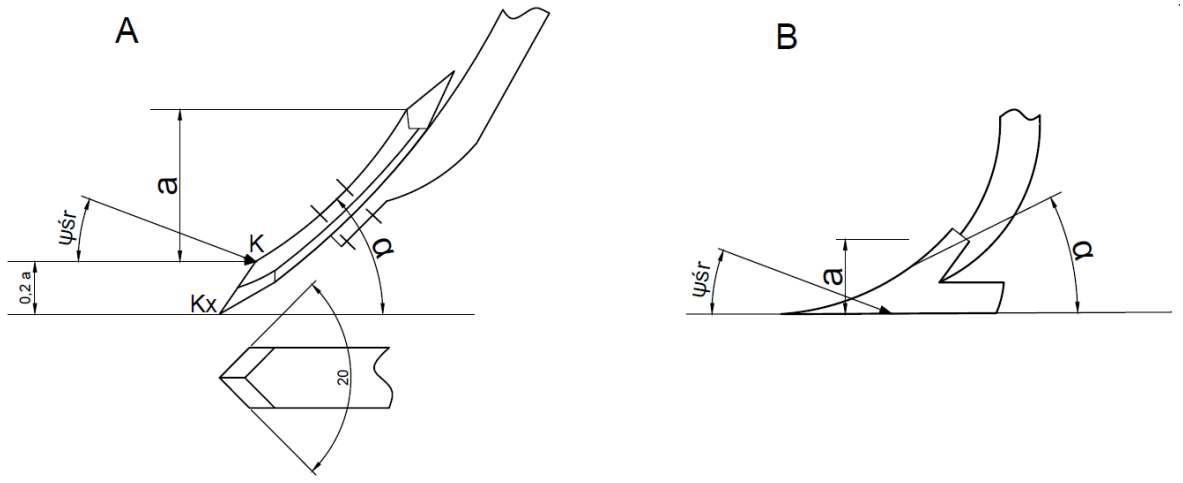

Fig. 12. The interdependence of the resistance of the tiller's sprocket on the working depth: a - sprocket with the tip, b - sprocket with the duckfoot share, K_x – resistance of the sprocket with the tip [2]

With the above information given, one may move forward to the next step, namely applying the structure support conditions simulating its actual operation, namely the border conditions and the load on the structure [9, 13].

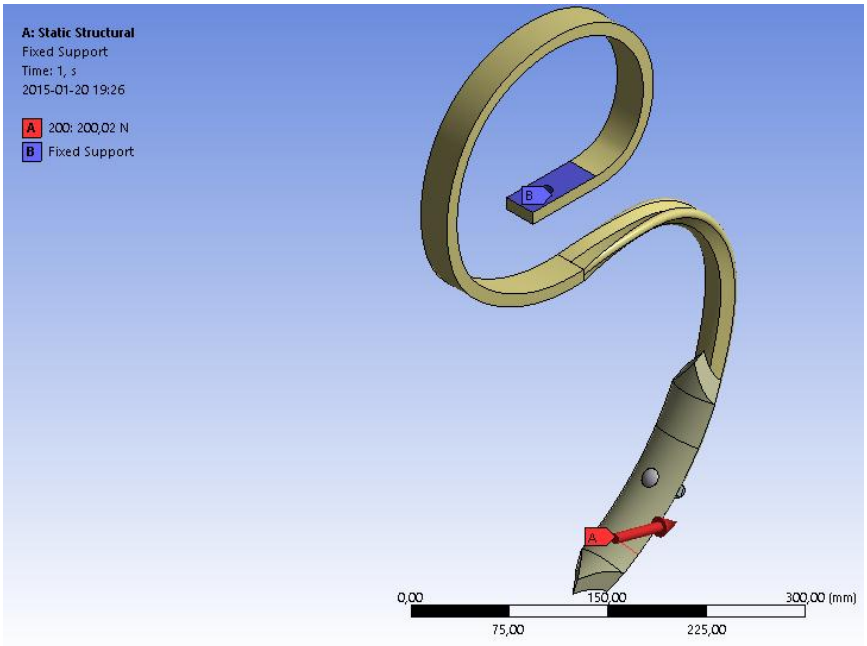

Fig. 13. 28x11 Tiller's sprocket - border conditions. A - model's load, B - model's fixed joint [Own elaboration]

The point B (Fig. 13), the sprocket is fixed to the frame, therefore both translation and rotational degrees of freedom has been eliminated there. In point A, on the other hand, the forces were applied on the sprocket. The above assumptions of the border conditions refers to all the tiller's sprocket models used in this analysis.

The next step in analysing the tiller's sprocket is to generate the finite elements network. To minimise the number of FEM network components, the geometry was divided into smaller areas (Figure 14) with *Virtual Topology* tool; in consequence the model under analysis contained more optimized node and finite element network for analysis. Such action not only reduced the time required to perform the full analysis ordered by the user and the load and fixed joint conditions given by the used, but also reduces the load of computer workstation where the analysis is being performed. Additionally, excessive number of components may affect the simulation result. Therefore the user may optimize the simulation with the above-mentioned actions comprising the use of the *Virtual Topology* tool and selecting the method of generating the finite element network.

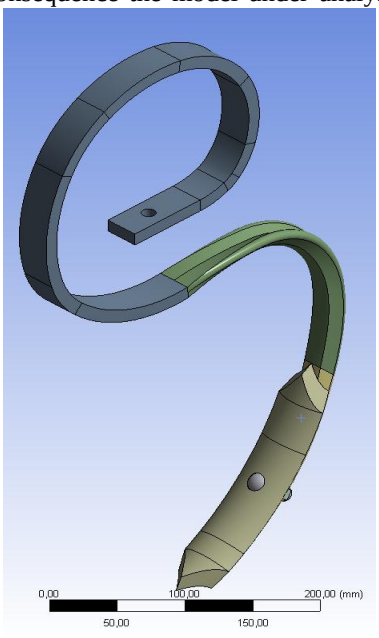

Fig. 14. 28x11 tiller's sprocket following the application of the Virtual Topology tool [Own elaboration]

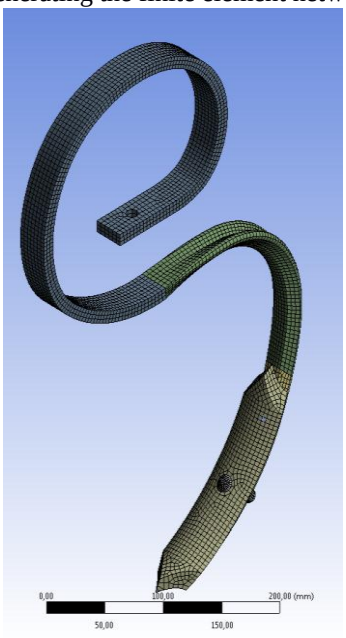

Fig. 15. FEM network of the 28x11 Tiller's sprocket developed manually [Own elaboration]

In result of the previous actions, the finite element network composed mainly of tetrahedrons is generated manually (Figure 15). As a rule, using the FEM network composed of triangles is avoided.

Identical procedure is applied for the remaining tiller's sprockets used in this analysis.

Strength analysis of the tiller's sprockets

Due to the nature of its structure and its operation principle, tillers are subject to large mechanical loads when operating, in particular the tiller's working parts - the sprockets - are mostly subjected to such loads. The sprockets shall therefore be resistant to multiple intense folding. The analysed spring tiller's sprockets vibrate strongly in the soil, therefore the intensity of their influence on the soil is improved. In result the soil id broken up and mixed.

Most frequent damage to the sprocket due to the working conditions is its breaking. Therefore various geometric variants of the sprockets were selected for analysis. This allowed to present the differences between them in the case of the same loads. In the simulation we mostly expected feedback in the following aspects:

- Huber-von Mises' stresses ecting;
- total displacement;
- safety coefficient.

Having entered all the necessary input data and used the FEM network, the figures below (Figures 16-18) present the result of the strength simulations for the tiller's sprockets. The initial load of 200N was applied as assumed previously.

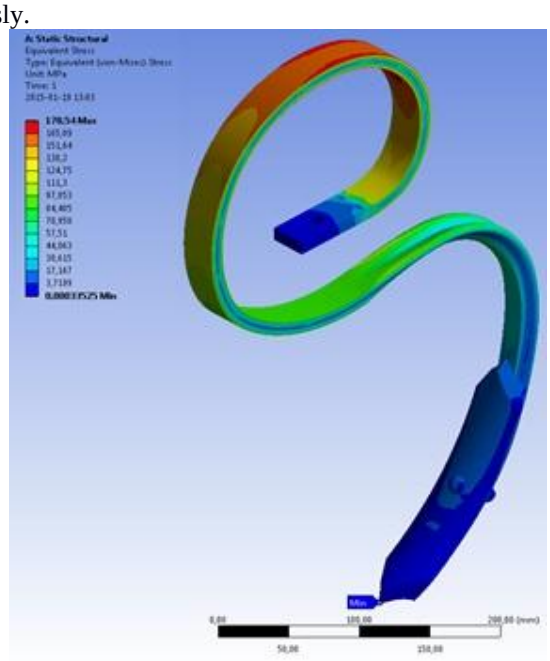

Fig. 16. Huber von Mises' reduced stress; 28x11 tiller's sprocket [Own elaboration]

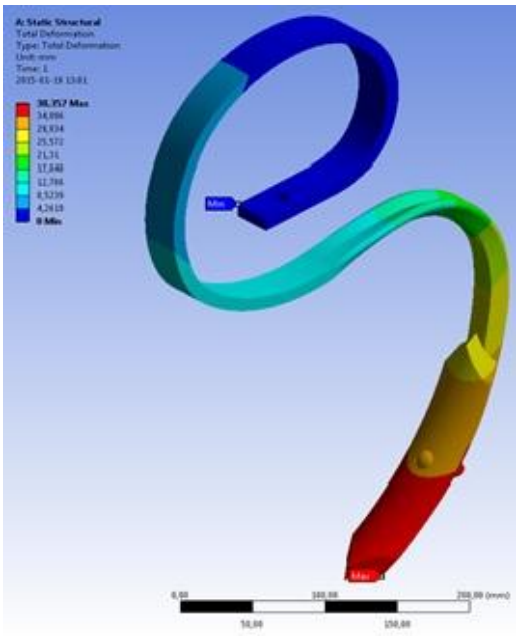

Fig. 17. Total displacement; 28x11 tiller's sprocket [Own elaboration]

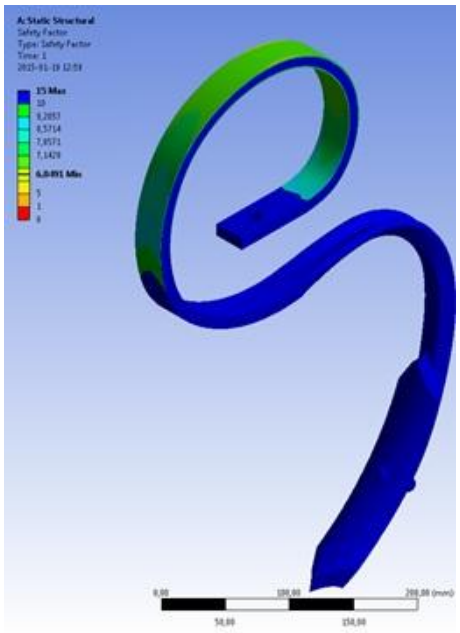

Fig. 18. Safety coefficient; 28x11 tiller's sprocket [Own elaboration]

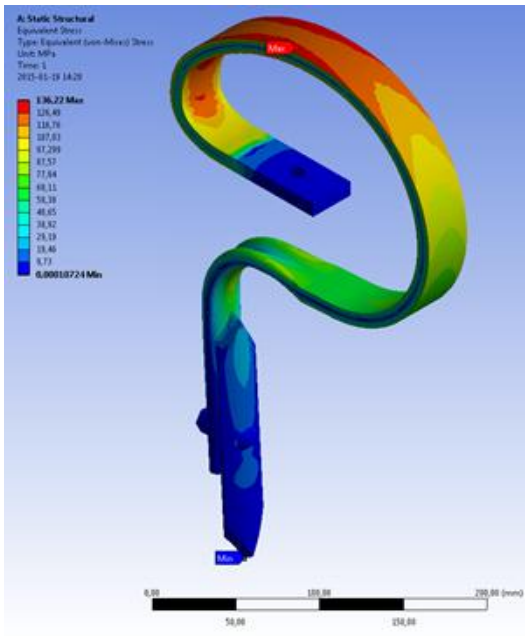

Fig. 19. Huber von Mises' reduced Huber von Mises' stress 32x10 tiller's sprocket [Own elaboration]

With the same load, the results for 32x10 sprocket (Figure 19-21) differ significantly, despite the appearing less flexible structure.

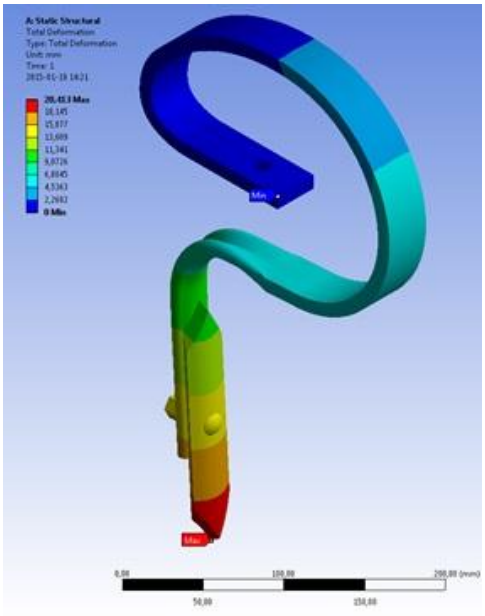

Fig. 20. Total displacement; tiller's sprocket – 32x10 [Own elaboration]

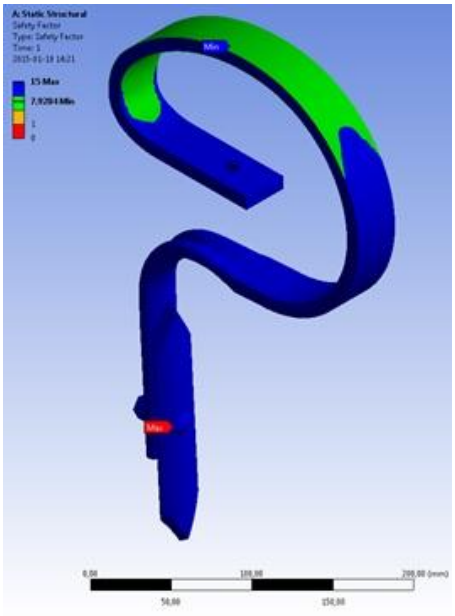

Fig. 21. Safety coefficient; 32x10 tiller's sprocket [Own elaboration]

In view of the above results and the information resulting, the solutions with better strength properties of the whole geometry were sought. Two possible modifications were noted, presented on the figures below.

The first option was to increase the width of the top sprocket's cross-section, which is the place where the largest stresses were present, as presented on the figures (Figure 22-24), meaning that this is the weakest point of the tool. That action significantly reduced the stresses present there, prolonging the life of that sprocket and its usefulness.

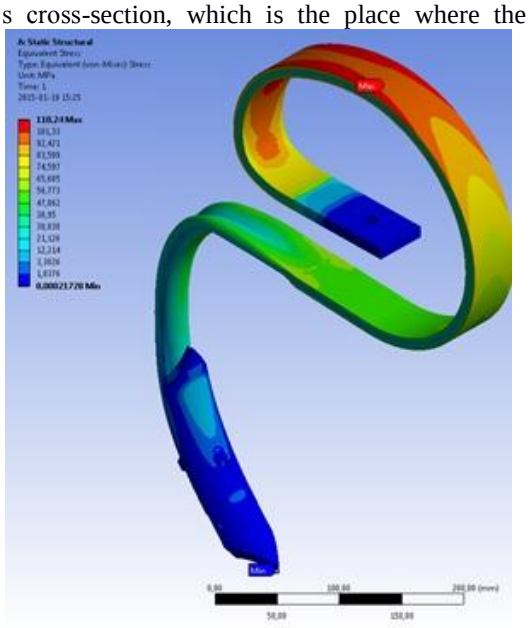

Fig. 22. Huber von Mises' reduced Stress; 45x11 tiller's sprocket [Own elaboration]

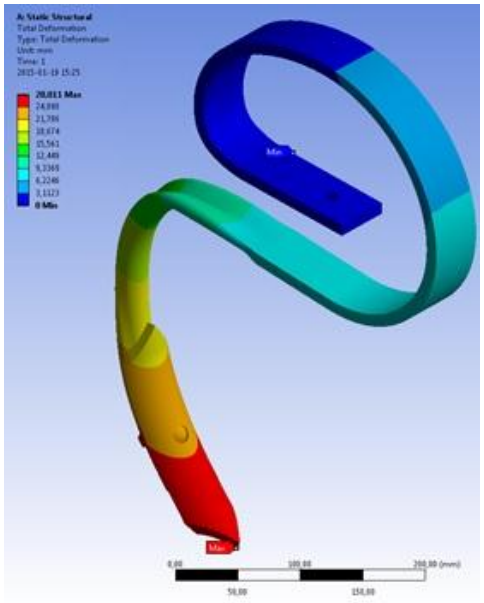

Fig. 23. Total displacement; 45x11 tiller's sprocket [Own elaboration]

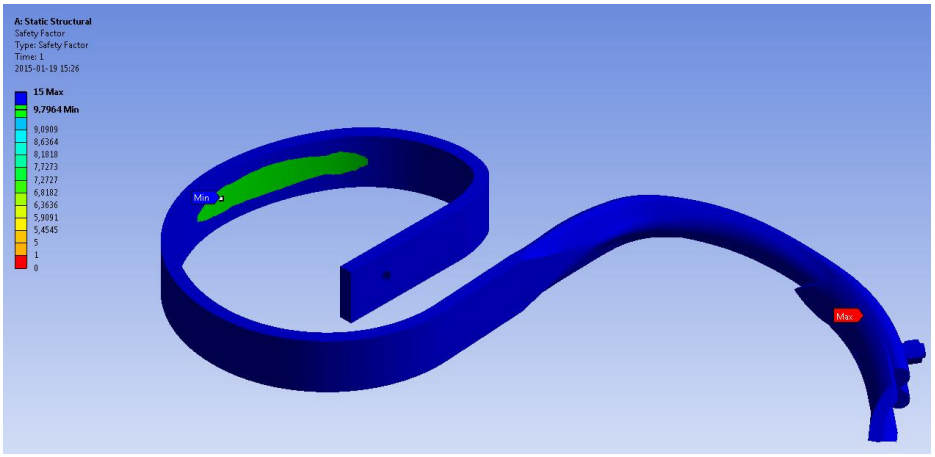

Fig. 24. Safety coefficient; 45x11 tiller's sprocket [Own elaboration]

The other solution noted when searching the solution of that problem, allowing the prolonged tool's life is making the sprocket of two separate components, as presented below (Figure 25-27):

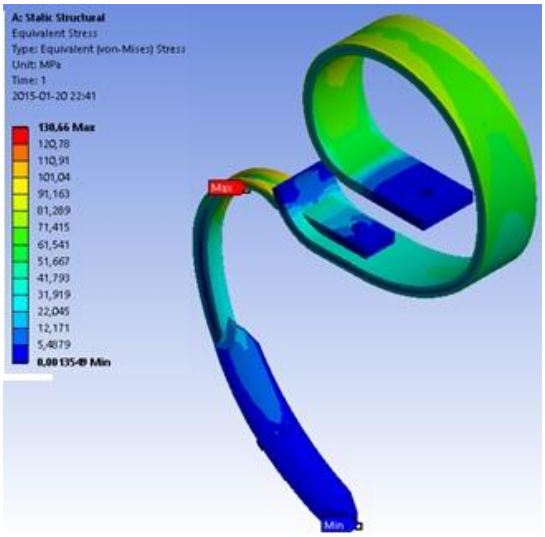

Fig. 25. Huber von Mises' reduced stress; 60(35)x11 tiller's sprocket [Own elaboration]

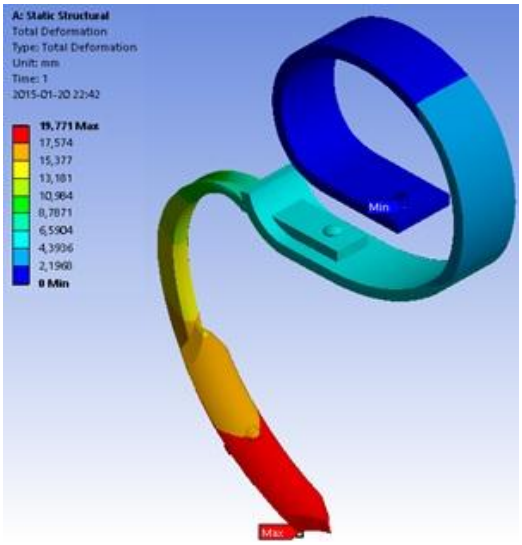

Fig. 26. Total displacement; 60(35)x11 tiller's sprocket [Own elaboration]

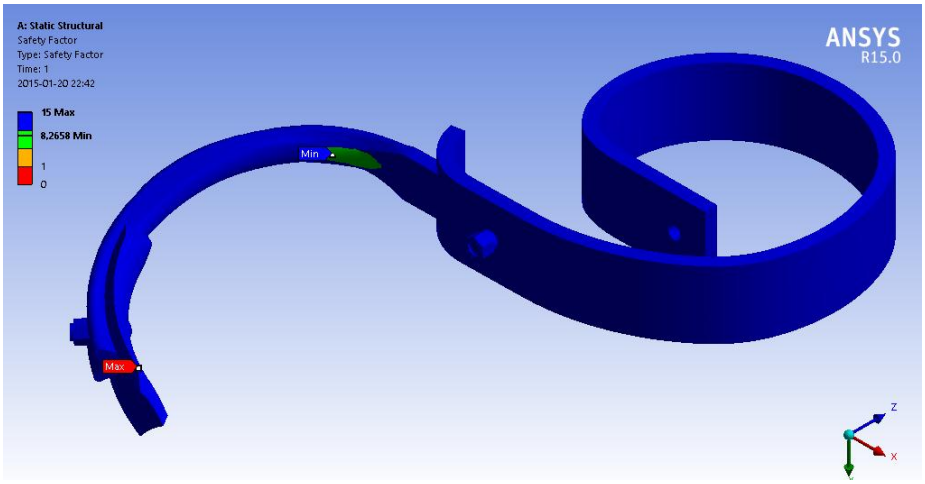

Fig. 27. Safety coefficient; 60(35)x11 tiller's sprocket [Own elaboration]

On the basis of the above illustrations one may pose a hypothesis that the stress id related to the width of the top part of the tiller's sprocket.

Another example of seeking the solution allowing for reducing the stresses applied to the sprocket is the spiral model, presented on the figures below (Figure 28-29):

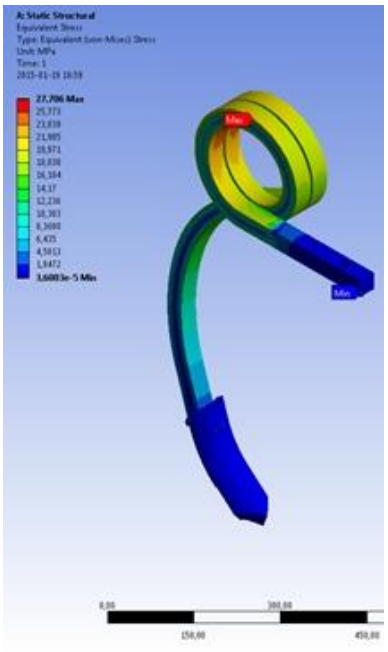

Fig. 28. Huber von Mises' reduced stress; 35x35 tiller's sprocket [Own elaboration]

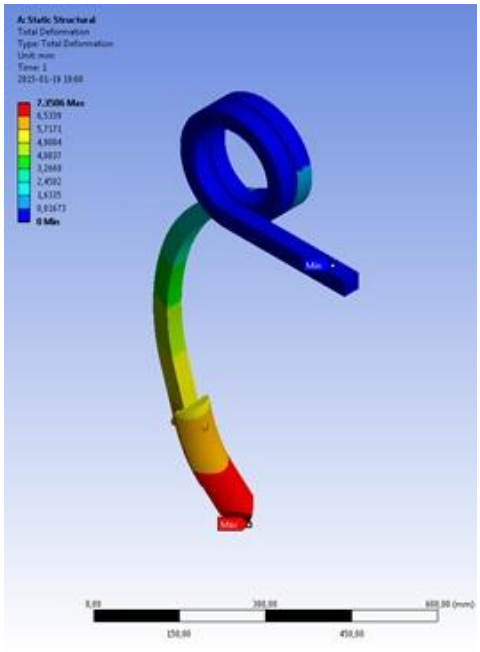

Fig. 29. Total displacement; 35x35 tiller's sprocket [Own elaboration]

The above figures present the distribution of the reduces stresses and the total displacement for the tools loaded with the force of 200N. Below the same models are presented (Figure 30-33), subjected to the force od 800N together with the stress distribution throughout their geometry.

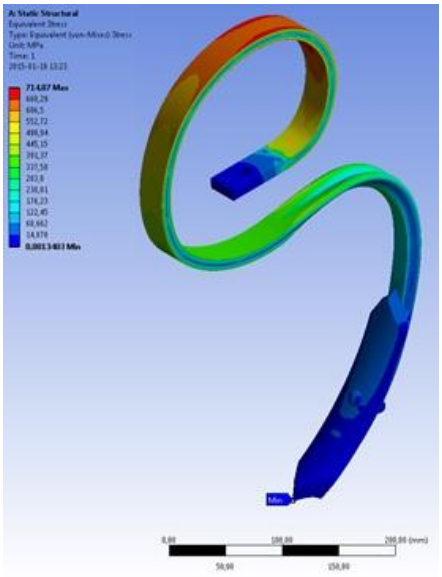

Fig. 30. Huber von Mises' reduced stress; 28x10 tiller's sprocket [Own elaboration]

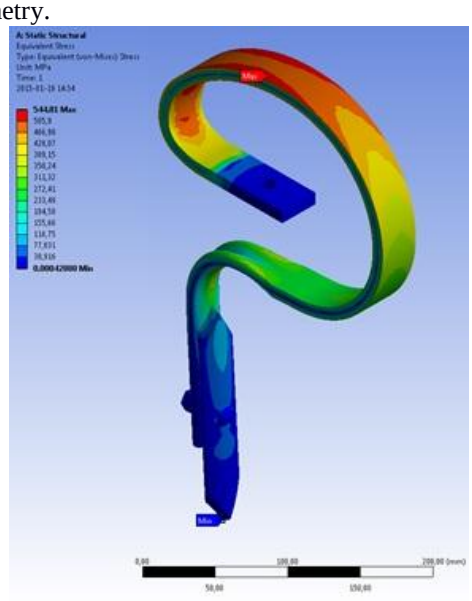

Fig. 31. Huber von Mises' reduced stress; 32x10 tiller's sprocket [Own elaboration]

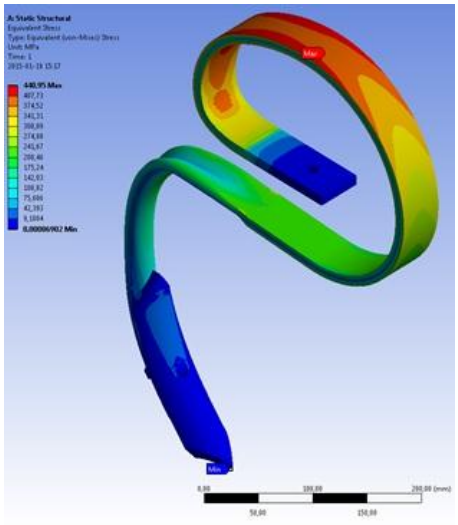

Fig. 32. Huber von Mises' reduced stress; 45x11 tiller's sprocket [Own elaboration]

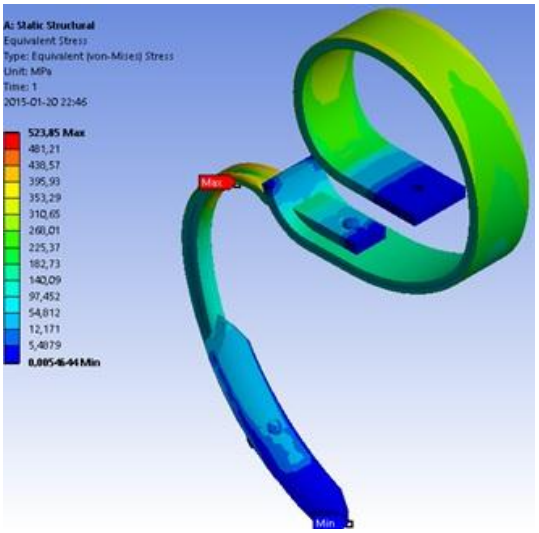

Fig. 33. Huber von Mises' reduced stress; 60(35)x11 tiller's sprocket [Own elaboration]

As presented on the figures above, having applied four times the force to the tool under analysis, one may note that the area of the largest stress is greatly the same, despite large difference in the forces applied.

As stated above, the analysis covered the sprockets subjected to the forces| of: 200N, 400N, 600N, 800N and 1000N. The tables below (Table 2 and 3) present the data on the maximum reduced stresses and total displacements for all the sprockets under the strength analysis:

Table 2. Summary of the maximum Huber von Mises' reduced stresses [Own elaboration]

Sprocket model		200	400	600	800	1000	Force [N]
28x11	MAX	178.54	357.08	535.53	714.07	892.61	Stresses [Mpa]
32x10		136.22	272.44	408.59	544.81	681.03	
45x11		110.24	220.5	330.69	440.95	550.76	
60(35)x11		130.66	261.96	392.89	523.85	654.85	
35x35		27.706	55.413	83.105	110.81	138.52	

Table 3. Summary of the maximum total displacements [Own elaboration]

Sprocket model		200	400	600	800	1000	Force [N]
28x11	MAX	38.36	76.72	115.06	153.42	191.77	Total displacement [mm]
32x10		20.41	40.83	61.23	81.65	102.06	
45x11		28.01	56.03	84.02	112.04	139.94	
60(35)x11		19.77	39.57	59.31	79.08	98.9	
35x35		7.35	14.7	22.05	29.4	36.75	

Despite the fact the the spring tiller's sprocket work at the working depth of up to 8 cm, and the resistance of a single sprocket may reach 55-N [18, 19], the sprockets were subjected to the load of up to 1000N. This suggests

that the machines working in the soil such as the tiller may during their work hit e.g. rocks, and in result the resistance then generated is much higher than the resistance of the soil itself.

CONCLUSIONS

The computer simulations perform allow to present on the early design stage, which parts of the tiller's sprocket are mostly exposed to the largest stress, and hence to the damage to the sprocket as a whole. The data provided above shall launch the process of seeking solutions aimed and eliminating the stresses and reducing their value. The easiest solution allowing improved strength properties of a sprocket is the extension of the sprocket's cross-section in the flat section of the sprocket, where it is fixed to the tiller's frame, or, as in the case of the 60(35)x11 sprocket, assembling the sprocket from two separate components. The obtained results of the analysis additionally allowed to determine, how a given structure may behave in the soil when operating and evaluate the influence of the working depth on the tool.

REFERENCES

1. **Arvidsson J., Hillerstrom O. 2010.** Specific draught, soil fragmentation and straw incorporation for different tine and share types. Soil & Tillage Research. 110(2010), 154–160.
2. **Bernacki H. 1981.** Theory and design of agricultural machinery. Vol. 1. Part I i II. PWRiL. Warsaw.
3. **Buliński J., Gach S., Waszkiewicz Cz. 2009:** Energy and qualitative aspects of the soil passive gears. Problemy Inżynierii Rolniczej, No. 4, 51-58.
4. **Buliński J., Marczuk T. 2008.** Affect of type of agricultural tractormachine outfit on soil compaction in the arable layer, Agricultural Engineering. No. 1 (99), 49-56.
5. **Dobek T. 2005.** Assessment of economics and energy requirement of various technologies of soil preparation for winter rape planting. Agricultural Engineering, No. 3 (63), 133-140.
6. **Kazimierczak G., Pacula B., Budzyński A. 2004**: Solid Edge. Computer-aided design. Helion.
7. **Kęska P. 2013**: SolidWorks 2013. CADvantage, Warsaw.
8. **Kogut Z. 2011b.** Work quality of the disc harrows under differentiated operation conditions. Problemy Inżynierii Rolniczej. No. 3, 53–67.
9. **Konstecki P., Borowiak P. 2007**: The method of measurement of soil pressure exerted on surfaces of the elements working in the soil. Agricultural Engineering. No. 8(96), 119-126.
10. **Kuczewski J., Waszkiewicz Cz., 2007**: Mechanization of agriculture. Machinery and equipment for crop and livestock production. SGGW, Warsaw.
11. Key to Materials. Total Materia. Desktop Edition 2014 – provided by Faculty of Engineering Production SGGW.
12. **Labocha S., Skotny Ł. 2014.** Linear and non-linear FEM analysis. GMSystem.
13. **Lejman K., Owsiak Z., Pieczarka K. 2013.** Effect of the cultivator tines elasticity on the quality and efficiency of clay soils loosening. Agricultural Engineering. 4(147) Vol.1, 179-190.
14. **Lejman K., Szulczewski W. 2007**: Computer aid design of rotary tiller parameters. part ii – knife geometry. Agricultural Engineering. No. 2(90), 143-149.
15. **Łabęcki M., Gościański M., Kapcińska D., Parowski Z. 2007.** Research of the tribology, strength and structure of materials used for the agricultural machines elements working in soil. Journal of Research and Application in Agricultural Engineering. Vol. 52(2), 43-51.
16. **Mieszkalski L. 1991**: Agricultural machinery in diagrams. ART. Olsztyn.
17. **Moitzi G., Haas M., Wagentristl H., Boxberger J., Gronauer A. 2013.** Energy consumption in cultivating and ploughing with traction improvement system and consideration of the rear furrow wheel-load in ploughing. Soil & Tillage Research. 134(2013), 56–60.
18. **Owsiak Z., Lejman K., Wołoszyn M. 2006.** Impact of cutting parameters on the quality and efficiency of soil scarification with cultivator prongs. Agricultural Engineering. No. 4 (79). 45-53.
19. **Patyk R., Kukiełka L. 2009.** Predicting cultivator tine fatigue strength using numerical methods. Agricultural Engineering. No. 9 (118). 181-187.
20. **Pawłowski T., Szczepaniak J., Mielec K., Grzechowiak R. 2006.** Application of modeling, computer simulation and validation method in the new agricultural machine implementation. Agricultural Engineering. No. 2 (77). 51-59.
21. **Piecak A., Ślaska-Grzywna B., Szmigielski M., Koszel T. 2013.** Energy consumption on plant production in the chosen farms. MOTROL. Vol. 15, No. 1, 105–110.
22. **Powałka M., Buliński J. 2014.** Changes in soil density under inÀ uence of tractor wheel pressures. Annals of Warsaw University of Life Sciences – SGGW. Agriculture No 63 (Agricultural and Forest Engineering), 15–22.
23. **Raport GUS. 2012.** Use of the land, sown area and livestock populations in 2012. Warsaw.
24. **Szymczak P. 2012**: Solid Edge ST. Designing synchronous. CAMdivision.
25. **Tucki K., Klimkiewicz M., Piątkowski P. 2015**: Design of digester biogas tank Part 3 3D digester biogas tank model, TEKA, Commission of Motorization and Energetics in Agriculture. Vol. 15, No 1, 89-94.
26. **Zbytek Z., Talarczyk W. 2012**. Ways to limiting the negative impact of tractor aggregates on the soil. Institute of Technology and Life Sciences, Falenty. 4 (78), 57–68.

Influence of biochar and biomass ash applied as soil amendment on germination rate of Virginia mallow seeds (Sida hermaphrodita R.)

Bogdan Saletnik, Marcin Bajcar, Grzegorz Zaguła, Maria Czernicka, Czesław Puchalski

Department of Bioenergy Technology, Faculty of Biology and Agriculture, Rzeszów University, Ćwiklińskiej 2D, 35-601 Rzeszów, e-mail: bogdan.saletnik@urz.pl

Received July 15.2016: accepted July 19.2016

Abstract. The paper presents findings showing the influence of amending soil with biochar and biomass ash on the germination rate of Virginia mallow. Comparative analyses examined the relationship between the applied dosage of the natural fertilizers and the effectiveness of seed germination as well as mass of the plants at the initial stage of growth. The obtained plant material was also examined for the contents of selected macro-elements (phosphorus, potassium and calcium). The study shows that biochar applied as a fertilizer, at specific dosage, may enhance germination rate of Virginia mallow seeds. Addition of biomass ash into the soil, at certain doses, significantly impacts the growth of mass in Virginia fanpetals at the initial stage of development. It has been determined that addition of biochar, or biomass ash or their mixtures into the soil alters the concentration of phosphorus, potassium and calcium in above-ground parts of the plants.

Key words: Virginia mallow, germination rate, biochar, biomass ash, macroelements.

INTRODUCTION

Virginia mallow (Sida hermaphrodita R.), also known as Virginia fanpetals, is a perennial, polycarpic plant native to North America [5]. Virginia mallow may be cultivated in Poland, in all types of soils, including lands which have been set aside and degraded, provided they have sufficient moisture content [22]. The plant develops a strong and deep-seated root system able to penetrate deeper substrate layers, which is a determining factor for the ability to accumulate toxic compounds. Therefore, the plant is widely used in reclamation of polluted areas. Virginia mallow is resistant to various types of soil contaminants, which is an advantage in production of biomass for energy-related purposes in degraded areas [21]. In addition to its application as an energy crop, the plant is also used as a herb, in production of fibre, honey and as a raw material in cellulose and paper production. Virginia mallow plantation can be used for a period ranging from 15 to 20 years, and the yield of the obtained raw mass may be as high as 25t ha^{-1} [22]. Virginia fanpetals reproduce from seeds which are characterized by low germination capacity – they sprout unevenly and at a low rate. Application of seeds conditioning may lead to a higher pace of germination and to increased percentage of the sprouting seedlings [9]. Quality of seeds is a challenge for dynamic and effective development of cultivation of this plant. Seeds obtained in Poland are characterized by the maximum germination capacity in the range of 45 – 70% [6].

Biochars are heavily carbonized materials acquired in the process of pyrolysis, and containing aromatic and aliphatic compounds as well as oxidized carbon compounds [15]. They also contain stable organic carbon, eluted carbon and ash. The mineral fraction of biochars consists of macro- and microelements which may be the source of mineral substances for microorganisms living in soils [17]. Biochar introduced into soil is highly resistant to degradation and decay caused by activity of microorganisms, which affects the stability of their chemical composition. Porous structure is a characteristic feature of pyrolyzates and it determines water absorbability and sorption capacity of soil [1, 3].

Biochar positively affects soil fertility and productivity and may protect plants against disease-causing infections [18]. Introduced into soil, it may lead to an increase in water capacity of the land, and a decrease in soil acidity [12]. Due to its physicochemical properties it may be used in sequestration of carbon in soil, production of fertilizers and in soil reclamation [16]. Biochars also have the capacity to retain and exchange nutritional substances, which results in a better availability of nutrients to plants and improved properties of the soil [10, 16].

By-products of biomass combustion include ash with highly alkaline pH and significant content of macro-elements. The material, treated as waste, may be used as soil amendment, provided that it does not contain pollutants, e.g. heavy metals [13]. Notably, application of biomass ash for purposes related to fertilization is a sustainable method of its neutralization, or utilization [24].

The present study was designed to investigate the relationship between soil treatment with the use of biochar and biomass ash and germination capacity of Virginia mallow seeds.

MATERIAL AND METHODS

The study used biochar and ash obtained from agricultural waste biomass and applied as a natural soil amendment as well as commercially available seeds of Virginia mallow (Sida hermaphrodita R.). The experiment was carried out in planters, each with the volume of 0.5 litre, with the use of MLR-352 phytotron. For this purpose 200g portions of soil were weighed and transferred to 30 planters. In the study we used universal soil based on peat, pH = 6 and salinity up to 1.9 g NaCl/dm^3. The soil contained a starting dose of compound fertilizers NPK (14-16-18): 0.6 kg/m^3. The planters were divided into two groups: the control sample (with no biochar or ash in the substrate), and the experimental sample, and then the same number of seeds were inserted in each planter. 9 variants of fertilization were applied, in three respective repetitions: addition of biochar at the level of 10, 15, 20 g; addition of ash at the level of 10, 15, 20 g and addition of biochar and ash mixture, at the levels of 20 and 10g; 20 and 15g; 20 and 20g, respectively. Throughout the experiment the planters were kept in climatic chamber and the same quantity of demineralized water was used daily in each variant. After 20 days of growth in constant conditions, i.e. temperature of 25°C, air humidity of 90% and stable lighting, the above-ground parts of the plants were collected for further examinations. Percentage of germinating seeds was calculated and then the plants were weighed. The collected plant material was carefully rinsed in demineralized water in order to remove soil residues. Subsequently, the plant samples were subjected to microwave mineralization with condensed nitrogen acid, at elevated pressure, in Teflon vessels in ETHOS ONE microwave digestion system from Milestone. Mineralization of the examined material was performed in three corresponding repetitions. The contents of the selected macro-elements in the samples were determined with the method based on inductively coupled plasma atomic emission spectroscopy (ICP-OES) with the use of iCAP Dual 6500 apparatus from Thermo Scientific. The contents of elements were calculated with the use of calibration curves based on the models of the examined compounds.

Before they were used in the experiment, biochar and biomass ash were evaluated for their pH in KCl and examined in TrueSpec apparatus for the contents of carbon and nitrogen (CHN module) in accordance with PN-EN 15104:2011(U) [26]. The analysis performed with the True Spec apparatus for simultaneous identification of carbon and nitrogen was based on the principles of Dumas Method, which is a method of high-temperature combustion in the presence of oxygen. As a result it was possible to identify the elements in the time which did not exceed 4 minutes. The total contents of phosphorus, potassium, magnesium and calcium as well as heavy metals (Cd, Pb, Ni) in the samples were determined with the use of iCAP Dual 6500 apparatus from Thermo Scientific. Table 1 shows the results of biochar and ash analyses. The contents of cadmium, lead, and nickel in biochar and ash were below the threshold of detectability, defined as 1 μg*g^{-1}.

Table 1. Contents of carbon, nitrogen, phosphorus, magnesium, and pH values for biochar and ash used in the experiment

	pH (KCl)	Carbon	Nitrogen	P	K	Mg	Ca
		%		mg*100g^{-1}			
Biochar	6.59 ± 0.21	74.3 ± 0.20	0.93 ± 0.02	138 ± 2	501 ± 19	128 ± 5	1824 ± 60
Biomass ash	12.89 ± 0.32	1.22 ± 0.02	0.17 ± 0.01	1517 ± 42	7059 ± 16	2720 ± 32	12335 ± 198

The obtained findings were subjected to statistical analysis with the use of Statistica 10 software. Mean values were compared with the use of Duncan's test, at significance level $p = 0.05$, for $n = 3$.

RESULTS AND DISCUSSION

Fig. 1 presents germination rates observed in Virginia mallow seeds in the control sample and depending on the quantity of biochar and biomass ash added into the soil (experimental sample). Germination capacity in the control sample was at the level of 66.7%, and in the examined fertilization variants ranged from 29.2 to 86.1%. Addition of processed plant material (biochar and biomass ash) affected the quantity of sprouting seeds. Biochar added at the quantity of 10 g to 200 g of soil increased germination rate in the seeds by nearly 20%. Higher dosage of biochar as a fertilizing material did not significantly influence seeds germination capacity. Addition of biomass ash as well as biochar and ash mixture did not affect the number of sprouting seeds. Interestingly, when ash was applied to the substrate at the rate of 20 g per 200 g of soil, there was a decrease in germination capacity of the seeds, from 66.7 to 29.2%. Biochar favourably affects soil productivity and is a good source of macro- and microelements. Grzesik et al. [8] argue that effective methods of enhancing seeds in terms of their germination capacity include hydro-conditioning, osmo-conditioning and matri-conditioning. The same authors also report that by providing soil with phosphorus it is possible to enhance seeds germination and growth of sprouting plants, while potassium improves vitality of seeds and protects them against deformations. Uzoma et al. [23] believe that due to its properties, biochar may contribute to increased crop yield.

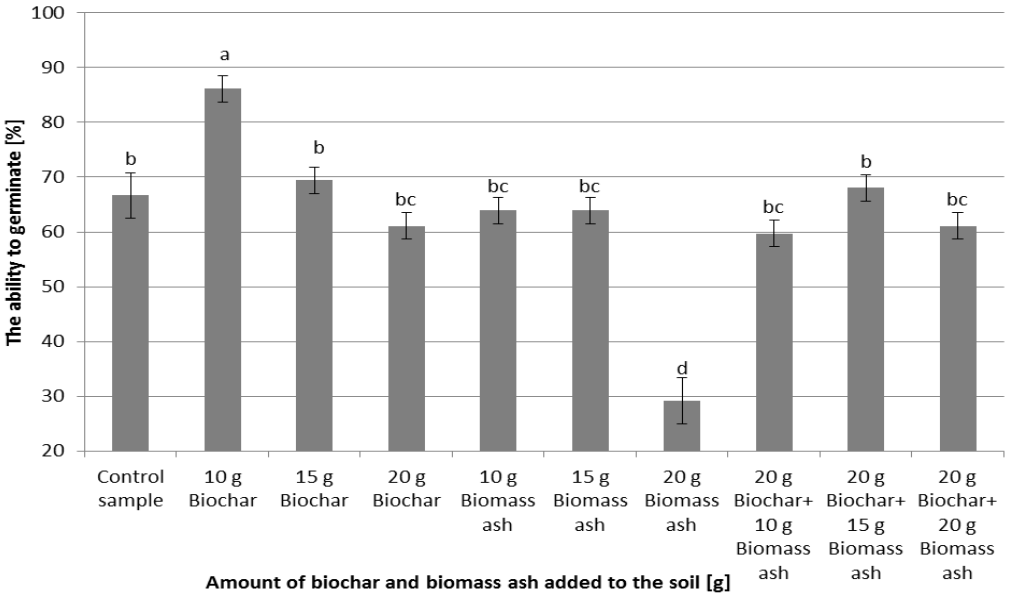

Fig. 1. Germination rates in Virginia mallow seeds in the control sample and depending on the quantity of biochar and biomass ash introduced into the soil. Different letters show statistically significant differences between the mean values (for $p \leq 0.05$).

Fig. 2 presents the effect of adding biochar and biomass ash to soil in the total mass of the plants obtained after the experiment continued for 20 days. The highest values of 9.78; 9.65; 8.26 g were observed in soils previously supplemented with 10 g biochar as well as 10 and 15 g of biomass ash, respectively. Further increase in the quantity of biochar and ash added to the soil led to progressive and significant decrease in the obtained total mass of plants – the lowest value was observed in the case of ash fertilizer applied at the rate of 20 g. The present findings also show that addition of biomass ash at the rates of 10 and 15 g per 200g of soil did not improve seeds germination capacity, yet it led to a significant increase in the mass of the obtained plants, in comparison to the control sample. Piekarczyk et al. [20] have reported that ash acquired from agricultural biomass (barley straw) may be applied as a fertilizer. These authors conducted an experiment whereby they demonstrated that application of biomass ash led to an increase in the soil pH and in its contents of macro- and microelements available to plants. Numerous studies have demonstrated positive effects of applying ash biomass as a soil amendment. For instance, Phongphan and Mosier [19] reported improved yield of rice as a result of treatment with rice hull ash; Ikpe and Powell [11] observed positive change in the yield of millet following addition of ash into the soil.

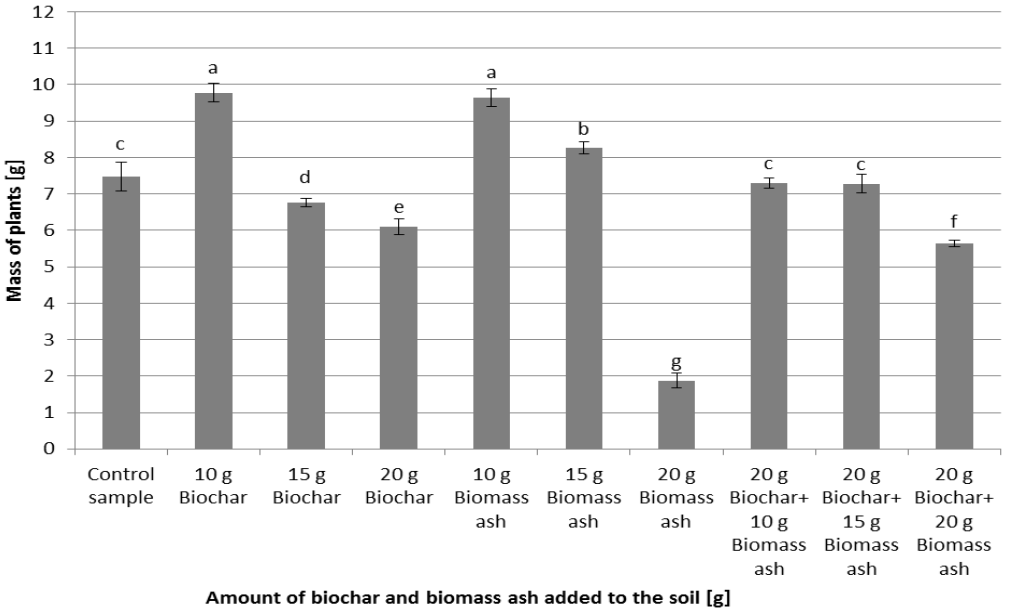

Fig. 2. Total mass of plants in the control sample and depending on the quantity of biochar and biomass ash introduced into the soil, after 20 days of the experiment. Different letters show statistically significant differences between the mean values (for $p \leq 0.05$).

Fig. 3. presents the results showing the total contents of phosphorus and calcium in above- ground parts of Virginia mallow, in the control sample and depending on the quantity of biochar and biomass ash added into the soil, after the experiment continued for 20 days. The maximum values of P and Ca , at the level of 164.4 and 262.9 mg*100g^{-1}, respectively, were identified in the plants which grew in the substrate supplemented with a mixture of biochar and ash (20/10g). The lowest concentrations of phosphorus and calcium, at the levels of 93.9 and 159.9 mg*100g^{-1}, respectively, were observed in the variant where the soil was supplemented with 10 g biochar. The dose of biochar applied at the rate of 10g per 200g of soil, which improved germination capacity of *Sida* seeds, at the same time led to a decrease in the contents of P and Ca in the obtained plants in comparison to the control sample. At the early stage of plant development phosphorus plays an important role as it enables appropriate growth of roots, while calcium plays a structural function and is a universal information carrier [2, 25]. According to Borkowska and Lipiński [4] the contents of chemical elements in biomass depend on genetic determinants which are modified by environmental factors, such as soil property (richness, pH), availability of water as well as by fertilizing.

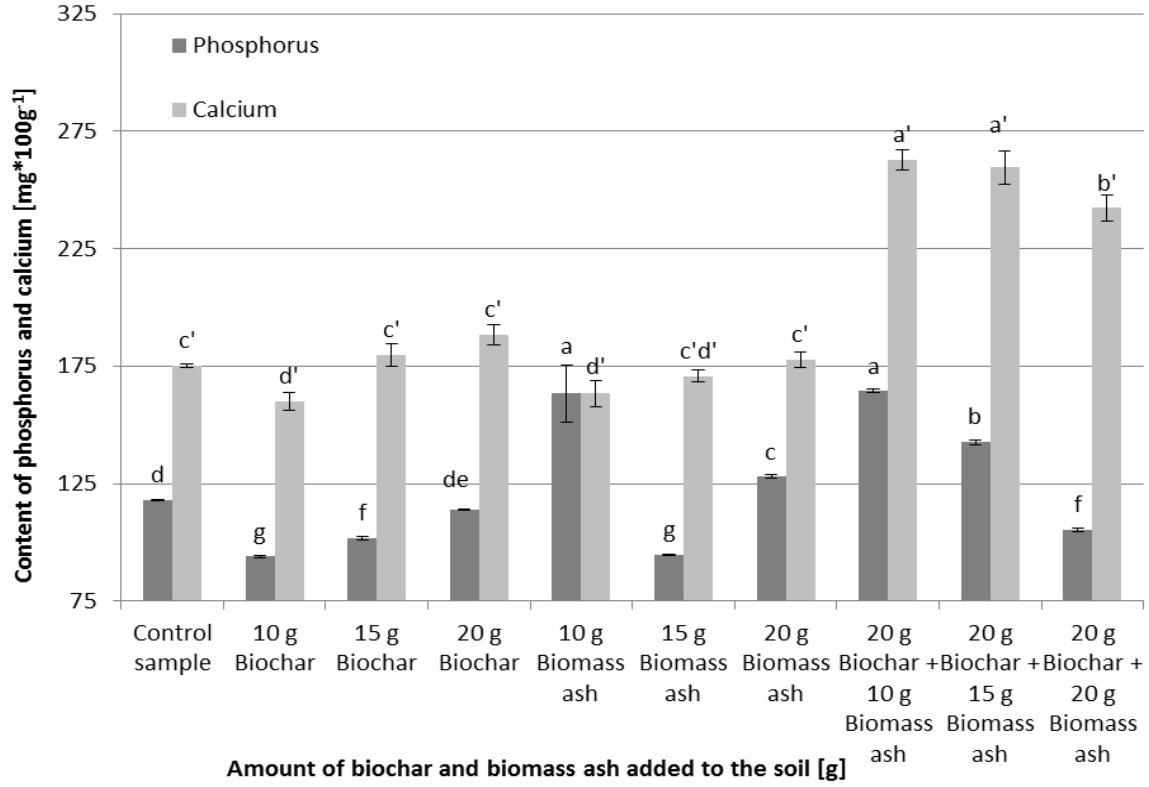

Fig. 3. Total contents of phosphorus and calcium in above-ground parts of Virginia mallow, in the control sample and depending on the quantity of biochar and biomass ash introduced into the soil, after 20 days of the experiment. Different letters show statistically significant differences between the mean values within the group x, x' (for $p \leq 0.05$).

Fig. 4 shows the results for the total contents of potassium in above-ground parts of Virginia mallow plants, in the control sample and depending on the quantity of biochar and biomass ash introduced into the soil, after 20 days of the experiment. The present findings show that the highest contents of potassium –1636.6 mg*100g^{-1} were characteristic for plants obtained in soil substrate amended with a mixture of biochar and ash (20/20g). Treatment of soil with the use of either biochar, or biomass ash or their mixture produced an increase in the contents of potassium in above ground parts of plants, compared to the control sample. Concentration of potassium in plants grew successively with an increase in the dosage of the supplements added to the soil. This chemical element is recognized among the essential nutrients for plants, and together with nitrogen, phosphorus, calcium, magnesium and sulphur it plays a crucial role in plant nutrition, enabling proper growth and development of plants [7]. Potassium is an element which, after nitrogen, is absorbed by plants most rapidly, particularly by young plants with fast growing meristem responsible for development of roots and stalks [14].

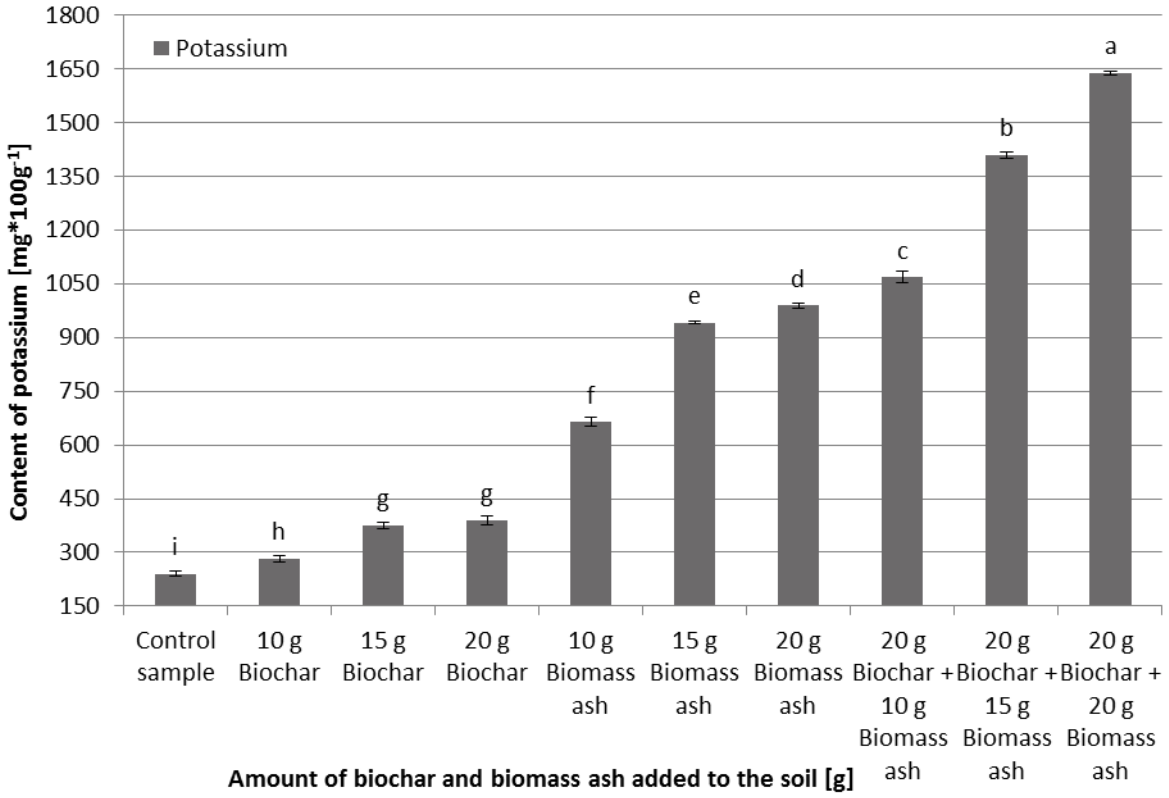

Fig. 4. Total contents of potassium in above-ground parts of Virginia mallow plants, in the control sample and depending on the quantity of biochar and biomass ash introduced into the soil, after 20 days of the experiment. Different letters show statistically significant differences between the mean values (for $p \leq 0.05$).

CONCLUSIONS

1. The present study shows that by supplementing soil with biochar it is possible to increase germination rate in Virginia mallow seeds by up to 20%.
2. It was observed that biomass ash introduced at the rate of 10 and 15 g per 200g of soil led to a significant increase in the mass of the obtained plants at the early stage of their development.
3. It was determined that the optimal dosage of biochar (supplement of 10g biochar per 200g soil), enhancing effectiveness of seeds germination, resulted in reduced contents of phosphorus and calcium in the obtained plants.
4. The findings show that addition of biochar, biomass ash or their mixture into soil leads to increased contents of potassium in above-ground parts of plants

REFERENCES

1. **Atkinson C.J., Fitzgerald J.D., Hipps N.A., 2010:** Potential mechanisms for achieving agricultural benefits from biochar application to temperate soils: review. Plant Soil, 337, 1-18.
2. **Bezak-Mazur E., Stoińska R., 2013:** The importance of phosphorus in the environment- review article. Archives of Waste Management and Environmental Protection, 15, 3.
3. **Bis Z., 2012:** Biochar – return to the past, a chance for the future. Czysta Energia, 6.
4. **Borkowska H., Lipiński W., 2007:** Contents of selected chemical elements in biomass of several species of energy crops. Acta Agrophysica, 10, 287–292.
5. **Borkowska H., Styk B., 2003:** Polish Journal of Environmental Studies Vol. 12, (1): 51.
6. **Doliński R., Kociuba W., Kramek A., 2006:** Influence of short-term hot water treatment, chemical scarification and gibberellic acid on germination of Virginia mallow (Sida hermaphrodita Rusby) seeds. Advances of Agricultural Sciences Problem, 517: 139-147.
7. **Fotyma M., 2000:** Demand of Polish agriculture for soil amendements. Chemik, 3, 64, 66.
8. **Grzesik M., Janas R., Górnik K., Romanowska-Duda Z., 2012:** Biological and physical methods of seed production and processing. Journal of Research and Applications in Agricultural Engineering, 57, 3, 147-152.
9. **Grzesik M., Romanowska-Duda Z. B., 2009:** Technology of hydro-conditioning applied to Virginia mallow (Sida hermaphrodita) seeds from the viewpoint of climate changes. Monograph: Biomass production. Selected problems. Wieś Jutra, ed. A. Skrobacki, chapter 7, 63-69.
10. **Hossain M.K., Strezov V., Chan K.Y., Ziolkowski A., Nelson P.F., 2011:** Influence of pyrolysis temperature on production and nutrient properties of wastewater sludge biochar. Journal of Environmental Management, 92, 223-228.

11. **Ikpe F.N., Powell J.M., 2002:** Nutrient cycling practices and changes in soil properties in the croplivestock farming systems of western Niger Republic of West Africa. Nutr Cycl Agroecosyst 62:37–45.
12. **Karhu K., Mattila T., Bergstrom I., Regina K., 2011:** Biochar addition to agricultural soil increased CH4 uptake and water holding capacity - Results from a short-term pilot field study, Agriculture, Ecosystems and Environment, 140, 309-313.
13. **Kowalczyk-Juśko A., 2009:** Ash of various energy crops. Proceeding of ECOpole, Vol. 3, No. 1, p. 159–164.
14. **Krzywy E., 2000:** Fertilization of soils and plants. Akademia Rolnicza, Szczecin.
15. **Lehman J., 2007:** Bio-energy in the black. Frontiers in Ecology and the Environment, 5(7), 381-387.
16. **Lehman J., Joseph S. (ed)., 2009:** Biochar for Environmental Management: Science and Technology. Earthscan, London.
17. **Lehmann J., Rilling M.C, Thies J., Masiello C.A., Hockaday W.C., Crowley D., 2011:** Biochar effects on soil biota - A review. Soil Biotechnology and Biochemistry, 43, 1812-1836.
18. **Nigussie A., Kissi E., Misganaw M., Ambaw G., 2012:** Effect of biochar application on soil properties and nutrient uptake of lettuces (Lactuca sativa) grown in chromium polluted soils. American- Eurasian Journal of Agricultural and Environmental Sciences, 12(3), 369-376.
19. **Phongpan S., Mosier A.R., 2003:** Impact of organic residue management in nitrogen use efficiency in an annual rice cropping sequence of lowland central Thailand. Nutr Cycl Agroecosyst 66: 233–240.
20. **Piekarczyk M., Kotwica K., Jaskulski D., 2011:** Application of ash from spring barley straw and its effects in the chemical properties of light soils. Fragm. Agron. 28, 91–99.
21. **Romanowska-Duda Z. B., Grzesik M., 2010:** Rational use of sewage sludge and Cyanobacteria in production of Virginia mallow biomass for energy related purposes. 5th International Conference on Renewable Energy, Zakopane, Poland, 23–24 March 2010, 21.
22. **Romanowska-Duda Z., Grzesik M., Pszczółkowski W., Piotrowski K., Pszczółkowska A., 2014:** Educational and environmental functions of the energy crops collection at OŹE technology transfer centre in Konstantynów Łódzki. Acta Innovations, ISSN 2300-5599, no. 13.
23. **Uzoma K.C., Inoue M., Andry H., Fujimaki H., Zahoor A., Nishihara E., 2011:** Effect of cow manure biochar on maize productivity under sandy soil condition. Soil Use Manag., 27, 205–212.
24. **Wacławowicz R., 2011:** Agricultural application of ash from biomass combustion. Seminar. Utilization of by-products of biomass combustion, Warszawa, p. 181–206.
25. **Wińska-Krysiak M., 2006:** Calcium transporting proteins in plants. Acta Agrophysica, 2006, 7(3), 751-762.
26. PN-EN 15104:2011(U). Solid Biofuels - Determination of Total Content of Carbon, Hydrogen and Nitrogen - Instrumental Methods.

Statistical analysis of supply voltage levels for rural customers

Krzysztof Nęcka, Małgorzata Trojanowska

University of Agriculture in Krakow
e-mail: krzysztof.necka@ur.krakow.pl, malgorzata.trojanowska@ur.krakow.pl

Received July 14.2016: accepted July 19.2016

Abstract. In the elaboration, levels of supply voltage at the ends of loaded low-voltage lines were statistically evaluated, describing them using basic statistical measures and examining the frequency distributions. Levels of voltages and time of their occurrence on the background of current regulations were also assessed. It was found out that in spite of the fulfilment of statutory requirements electricity consumers complained about the poor, in their opinion, quality of the voltage.

Key words: low voltage networks, supply voltage quality

INTRODUCTION

Among the parameters characterizing the quality of the electric power supply the value of the supply voltage has the basic impact on the work of electric receivers. Too low voltage level translates to malfunctioning of most electronic devices, deterioration of lighting conditions, problems with the operation of induction motors, heating, etc.

Receivers most sensitive to voltage deviations include a electric light sources. For bulbs changing of this parameter affects, among others, the value of the luminous flux (the relationship of the power of 3.5), efficiency (the relationship in the power of 2), changes in power consumption (the relationship in the power of 1.6), and with the rapid changes can cause flickering lights [1 - 4].

The second group of receivers very sensitive to the value of the supply voltage is IT equipment, including control systems. Lowering of the supply voltage may lead to malfunctions, commonly used to control, microprocessors and uncontrolled interruption of the process and even damage the equipment. Microprocessor systems after return of the voltage to the rated value are unable very often to continue working because of lost or erroneous data, and they must be reprogrammed [5 - 9].

The switchgear is also sensitive on the supply voltage value, in particular contactors and relays, which, when the voltage drops, can switch off the controlled device in an uncontrolled manner [8, 9].

Another group consists of induction motors whose the main parameter, which is the torque, is dependent on the square of the supply voltage. So, reducing the supply voltage by 10% means that torque will be only ~80% of its value occurring at the nominal voltage. With a significant voltage drops may even unplanned stop it. The reduced supply voltage results also in a reduction in engine speed and increasing the value of the input current, which in extreme conditions, through a significant increase in operating temperature, will shorten the life of the winding insulation and the insulation between the sheets of magnetic circuits [3, 8 -11].

The reduction of the supply voltage adversely affects also the performance of the heating units and prolongs its work, thus increasing costs [10, 12, 13].

Fluctuations in voltage supply work negatively not only on the work of receivers, but also on the distribution network, from which they are powered. In power lines voltage variations affect the present in them power losses and voltage drops. In the case of transformers, voltage deviations increases the risk of damage to the insulation and can cause an unfavourable change in the operating point of the transformer, as well as the impact on the increase of losses for the idle state [14 -15].

On the level of voltage in the power network technical characteristics (mainly the length and cross-sections of the line) have decisive influence, in addition to the load by apparent power. It is therefore recommended that the length of low voltage circuits leaded from transformer stations will not exceed 500 m, and in exceptional situations 1000 m. Unfortunately in distribution networks, especially in rural areas, often there are circuits of considerable length and small cross-section wires [16 - 20]. In this situation ensuring the legally required level of the supply voltage is very difficult. Costs of poor power quality, which can be a big, burden for both suppliers and consumers of electricity.

OBJECTIVES

The purpose of the elaboration was to evaluate the statistical levels of voltage at the ends of loaded low-voltage lines. In particular, basic statistical parameters were designated and frequency distributions were analysed for the tested variable. In the elaboration levels of voltages and time of their occurrence on the background of current regulations were also assessed.

TEST METHOD

Studies of the voltage quality were performed on rural areas of the South Poland. They consist of the registration of voltage levels in the three transformer stations selected and at ends of the loaded low-voltage lines leaded out from these stations. Tested transformer stations were columnar stations, equipped with transformers having power ratings from 100 kVA to 160 kVA. Low voltage lines leaded from these stations are made of AL cables (flat) and AsXSn (twist) with a diameter of 25 - 70 mm^2, and their average length is 530 m. In contrast, measurements of supply voltages are limited only to the beginnings and ends of the longest circuits whose length contained in the range of 1550 to 2250 m.

Own studies were conducted in the winter period not less than one week using the network analyser REM-370. This analyser recorded, among others, momentary and averaged 1 and 10-minute supply voltage.

RESEARCH RESULTS

The effective value of the voltage is the main parameter that characterizes the quality of the supply voltage. According to the regulations being in force in Poland, every week 95% of a set of 10-minute averages of effective voltage at the point of delivery of electricity from the low-voltage network must be within the tolerance band of ± 10% of rated voltage [21, 22].

The supply voltage level in the power network is subject to change. These changes may be the nature of the planned (deterministic) or random changes. The first are the result of the voltage adjustment using the transformer, aiming to provide appropriate voltages for receivers, the second - random power flow as a consequence of random changes of the power consumed by receivers. The value of the current flowing in networks is related with the size of the consumed power. The current flowing in the network causes voltage drops. The voltage value supplied the recipient at any time is dependent on the voltage value in the power source and the total voltage drop across all components of the supply network. Lowest supply voltages are present at the ends of circuits, so for the purpose of assessing the quality of power supply voltage measurements are performed in these places.

Figure 1 shows waveforms of changes for the 10-minute effective values of the voltage recorded at the end of the longest circuits leaded out from the tested transformer stations. For purposes of statistical analysis parameters describing these voltages in a systematic way were determined [23], and in particular the calculated measures of association, dispersion, asymmetry and concentration, the size of some of which are presented in Table 1. In addition, Figure 2 shows the frequency distributions of voltage levels at the ends of analysed lines.

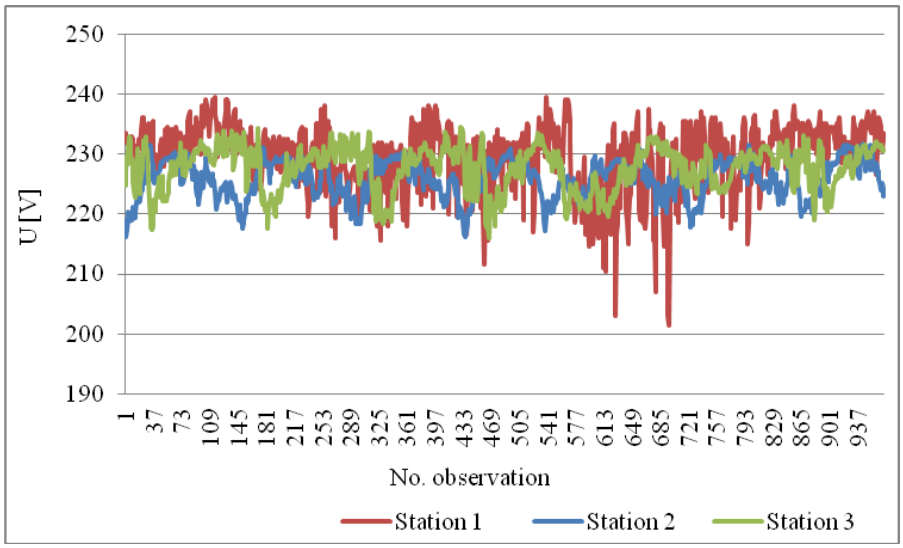

Fig. 1. Waveforms of average 10-minute voltage values at ends of the low-voltage lines

Table 1. Statistical parameters describing average 10-minute supply voltage values at ends of the low-voltage lines

Specification	Parameter			
	U_a [V]	V [%]	A	K
Station 1	235.88	64.78	-0.15	-0.68
Station 2	234.42	58.87	- 0.15	-0.67
Station 3	237.80	59.95	-0.16	-0.24

where: U_a - average value, V - coefficient of variation, A - skewness, K - kurtosis

Histograms shown in Figure 2 illustrate the qualitative properties of the actual distribution of voltage levels at the end of low-voltage lines, taking into account the adjustment of voltages using the transformer, and the asymmetry of the phase currents and voltage drops in the low-voltage lines. Voltage drops in low-voltage lines

causes the asymmetry of distribution of voltage levels at the end of the line. As is apparent from Figure 2 and Table 1 this is the negative asymmetry. Distributions for the negative asymmetry are less researched than those with the positive asymmetry, however, in the analysis of voltage levels at the end of low-voltage lines the distribution of the right-hand skewness can be obtained through a simple linear transformation [24].

Having regard to the distributions shown in Figure 2 that the normal distribution is the best suited for the description of information on the change of the voltage at the ends of low-voltage lines, the distribution of the analysed variable gets closer to normal when moving from the ends to the beginnings of low-voltage lines.

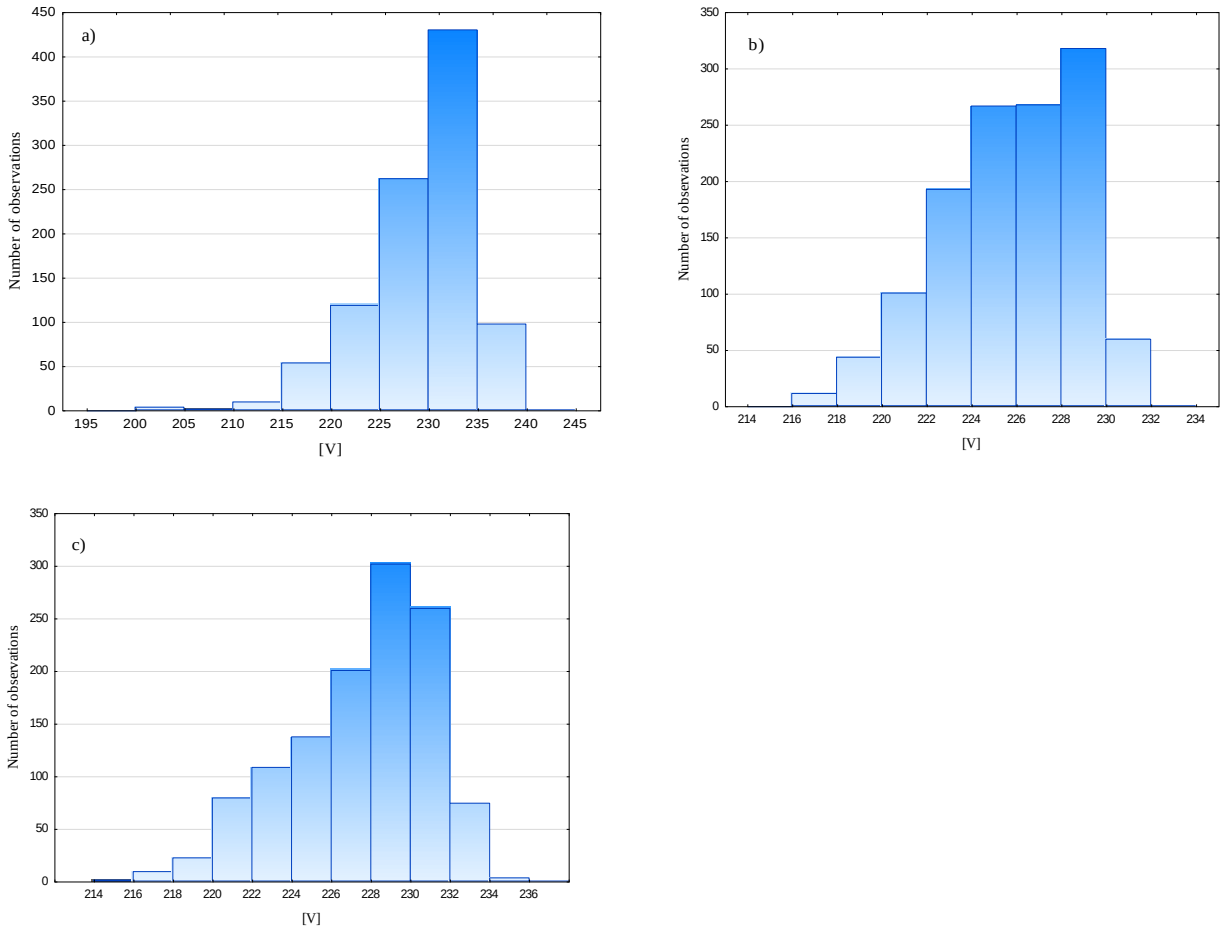

Fig. 2. The frequency distribution of voltage levels at ends of the low-voltage line leaded out from transformer stations: a) 1, b) 2, c) 3

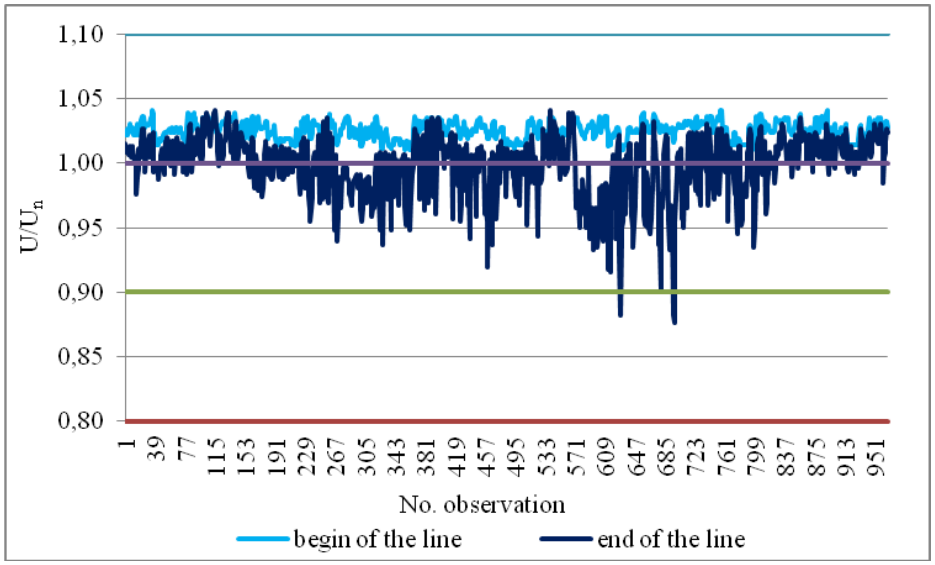

Fig. 3. Waveforms of average 10-minute voltage values at the begin and end of the longest low-voltage line; where: U_n - nominal voltage

For the analysis of the quality of the power voltage the knowledge not only waveform at the end, but also at the beginning of the circuit is needed. Figure 3 shows such waveforms for the line having the worst voltage conditions. From Figure 3 it shows that the recipients exceeded the lower allowable voltage range. However, it also can be seen that the exceedances could not might be for the suitable adjustment of the voltage under the load using transformers.

The evaluation of the voltage quality in terms of its effective values at the point of supply of the electricity (Table 2) were carried out separately for each phase of the tested circuits, taking into account also, according to current requirements, time in which the voltage is within the specified range.

Table 2. The statistics of average 10-minutes voltage values at ends of the low-voltage line in measuring periods

Specification	Parameter	Voltage [V]		
		L1	L2	L3
Station 1	Minimum (95% of week)	214.0	219.0	221.0
	Maximum (95% of week)	237.0	236.0	238.0
	Minimum (100% of week)	186.0	201.5	206.0
	Maximum (100% of week)	244.0	239.5	243.0
Station 2	Minimum (95% of week)	216.7	207.1	228.2
	Maximum (95% of week)	229.1	227.5	239.5
	Minimum (100% of week)	210.1	197.2	220.3
	Maximum (100% of week)	232.1	234.9	244.9
Station 3	Minimum (95% of week)	217.8	213.6	224.6
	Maximum (95% of week)	233.4	231.6	239.9
	Minimum (100% of week)	203.4	205.4	212.0
	Maximum (100% of week)	240.0	235.2	244.3

As can be seen from the Table 2 requirements for voltage levels at receiving points of the electricity and time of their occurrence are met. Despite that electricity consumers have complained about the poor quality of power supply and the associated nuisance and incurred losses. This is because the majority of the currently operated electricity receivers is apparently sensitive to even short-term reduction of the supply voltage exceeding the limits by law. So it seems that being in force in the assessment of the quality of electricity, a 10-minute period of voltage averaging is too long.

In power quality analysers commonly available on the market one minute is the shortest possible averaging time. The Table 3 compares the results of the voltage measurement at the end of the longest low-voltage line at various averaging. Taking into account the average 1-minute supply voltage it can be seen that the number of registered exceedances of the allowable voltage range in the L2 phase is over 100 times higher than for 10-minute averaging.

Table 3. Number of observations exceeding by ± 10% the nominal supply voltage at the end of the longest line leaded out from the station 2, depending on the measurement averaging time

Phase	For supply voltage value	Number of observations
L1	average 10-minute	0
	average 1-minute	6
L2	average 10-minute	57
	average 1-minute	600
L3	average 10-minute	0
	average 1-minute	0

Customer complaints on the poor quality of power, despite the fulfilment of statutory requirements, however, should encourage distribution companies to take measures to improve the voltage conditions of their clients. The modernization of the network which consists of increasing cross-section of power cables, leading the additional track or shorter circuit by mounting a transformer station is the typical way to solve problems of voltage drops [25, 26]. Commercially available voltage adjusters of the low-voltage network can be also used [27,

28]. The latter solution is much cheaper than actions of modernizing of the network. Since the voltage adjustment by means of these devices is carried out independently for each phase, voltage adjusters symetrise simultaneously the distribution of phase voltages.

CONCLUSIONS

Distributions of voltage levels at ends of loaded low-voltage lines is characterized by negative asymmetry, and for the description of this variable, from well-studied theoretical distributions, the normal distribution is best suited. The distribution of supply voltage levels for receivers gets closer to normal when moving from the end of the line to buses of the transformer station.

The fulfilment of statutory requirements in relation to the effective values of the voltage at the point of delivery of electricity from the low-voltage network is not the same with the satisfactory, perceived by receivers, quality of the voltage. Most electric receivers currently in use is in fact sensitive to even short-term reduction of the voltage exceeding 10% of the nominal value. So it seems that being in force in the assessment of the quality of electricity, a 10-minute period of voltage averaging is too long.

This Research was financed by the Ministry of Science and Higher Education of the Republic of Poland

REFERENCES

1. **Strzałka-Gołuszka K., Strzałka J. 2010.** Power quality and its influence on the work of electrical receivers. Krakow: Bulletin of the Polish Electricians Association, No. 182-183, Pp. 39-65. (in Polish)
2. **Goshko M. 2015.** Investigation of contemporary illuminants characteristics the led lamps example. Econtechmod, No. 4, Pp. 65-70.
3. **Markiewicz H., Klajn A. 2001.** Influence of changes of the parameters determining the power quality on the receivers' work. Wroclaw: Publishing House of the Polish Center of Copper Promotion, No. 02/03, Pp. 3-20. (in Polish)
4. **Kowalski Z. 2007.** Power quality. Lodz: Publishing House of the Lodz University of Technology. (in Polish)
5. **Bednarek K. 2006.** Electromagnetic compatibility – the standard and legal problems. Computer applications in electrical engineering (ed. R. Nawrowski). Poznan: ALWERS Press, Pp. 89-105.
6. **Ciszewski T., Olczykowski Z. 2005.** Quality and safety power of servers. Radom: Elektryka, No. 1. (in Polish)
7. **ukasik Z., Ciszewski T., Olczykowski Z. 2007.** Influence of power quality on the stability of computer systems. Zakopane: XI International Conference "Computer support systems science, industry and transport", Pp. 509-514. (in Polish)
8. **Hanzelka Z. 2009.** Power quality. Vademecum of an electrician (ed. J. Strojny), Warszawa: COSiW SEP Library, Pp. 629-653.(in Polish)
9. **anzelka Z., Firlit A. 2013.** Poor quality of electricity supply threat to the proper operation of industrial receivers. Skawina: IV Conference Producers of Electricity and Heat. (in Polish)
10. **Hanzelka Z. 2004.** Electric power quality in a rural environment – analysis of selected cases. Jachranka: II National Conference "Electrical power in rural areas", Pp. 22-28. (in Polish)
11. **usiał E. 2004.** Power quality assessment in industrial systems. Jurata: Scientific Conference "Automation, measurement, disruptions", Pp. 103-122. (in Polish)
12. **Bielecki S. 2007.** Power quality on the energy market. Przegląd Elektrotechniczny, No. 7/8, Pp. 68-72. (in Polish)
13. **Pawlęga A. 2003.** The problems of power quality in places of its delivery to individual customers. Przegląd Elektrotechniczny, No. 11, Pp. 805-810. (in Polish)
14. **Bocheński B. 2006.** Influence of voltage distortion on loadability of power transformers. Przegląd Elektrotechniczny, No. 1k, Pp. 28-31. (in Polish)
15. **Hołdyński G., Skibko Z. 2010.** Problems connected with operation of power transformers supplying nonlinear loads. Wiadomości Elektrotechniczne, No. 5, Pp. 32-35. (in Polish)
16. **Kulczycki J., Niewiedział E., Niewiedział R. 2009.** Selected problems of rural networks' development. INPE - Monthly of the Polish Electricians Association, No. 122-123, Pp. 75-85. (in Polish)
17. **Niewiedział E., Niewiedział R. 2012.** Needs for development and modernization of electrical power network in the country lands. Wiadomości Elektrotechniczne, No. 8, Pp. 3-10. (in Polish)
18. **Strożek K. 2009.** Current needs of rural power networks' renewal and upgrading. Poznan: PTPiREE Press. (in Polish)
19. **Trojanowska M. 2009.** Statistical evaluation of the quality of medium and low voltage networks on rural areas. Problemy Inżynierii Rolniczej, No. 4, Pp. 21-28. (in Polish)
20. **Trojanowska M., Nęcka K. 2007.** Analysis of power supply voltage quality in rural farms. Agricultural Engineering, No. 7, Pp. 221-227. (in Polish)
21. Regulation of the Minister of Economy on the detailed conditions for the functioning of the energy system. Journal of Laws from 2007, No. 93, item 623. (in Polish)
22. PN-EN 50160. 2002. Parameters of supply voltage in public distribution networks. (in Polish)
23. Statistical methods of data analysis (ed. W. Ostasiewicz). 1999. Wroclaw: Publishing House of the University of Economic. (in Polish)
24. **Popczyk J. 1991.** Probabilistic models applied to power networks. Warszawa: WN-T Press. (in Polish)
25. **Marzecki J. 2007.** Strategy of LV and MV power networks' development. Energetyka, No. 5, Pp. 326-337. (in Polish)
26. Distribution power networks (ed. S. Kujszczyk). 2004. Warszawa: Publishing House of the Warsaw University of Technology. (in Polish)
27. **Ozorowski M. 2014.** Elimination of voltage drops at the ends of LV lines. Energia Elektryczna, No. 2, Pp. 23-25. (in Polish)
28. **Ozorowski M. 2014.** Voltage control at the ends of loaded LV lines. Wiadomości Elektrotechniczne, No. 9, Pp. 132-135. (in Polish)

A computational scheme for decentralized time-optimal resource allocation in a sequence of projects of activities under constrained resource

Anna Stankiewicz

Faculty of Production Engineering, University of Life Sciences in Lublin, Poland
e-mail: anna.m.stankiewicz@gmail.com

Received July 14.2016: accepted July 19.2016

Abstract. We consider a sequence of projects of independent activities; each project composed of activities available for realization at the same time. It is assumed that the activities are continuous dynamical systems whose dynamics depend continuously on the allotted amounts of the resource, and the initial and terminal states are fixed. The problem is to allocate a renewable, continuously divisible resource (e.g., power, fuel flow, money per time unit, approximate manpower) to the activities in order to minimize the performance time of the sequence of projects under the assumption that the allowable level of the total usage of the resource is constant. Although the solution to this problem is known in the literature, nevertheless there is a lack of effective computational algorithms for the time-optimal resource allocation, especially in the case of really large projects. In this paper a decentralized two-level control scheme using the time-decomposition is proposed to find the time-optimal resource allocation in a sequence of projects. The price mechanism is applied to coordinate the lower level tasks of the optimal resource allocation in the successive time intervals determined by the moments at which the successive projects are available for realization. Necessary and sufficient conditions to ensure the determination of the optimal resource allocation according to the method proposed are stated. The problems connected with the numerical realization of the scheme are discussed and the resulting computer algorithm is outlined.
Key words: project of activities, resource allocation, time-optimal control, dynamical system, decentralized control

INTRODUCTION

The concept of the control of a project of activities was introduced by Burkov [4] and Lerner and Tejman [20] as a special approach to resource allocation in PERT networks. Its distinctive feature is that the activities are continuous dynamical systems relating at any time the performance speeds of the activities to the allotted amounts of a resource, and that the initial and terminal states are fixed. By optimal control of a project of activities we shall mean an assignment of constrained resources to activities such that to minimize a performance index of the whole project, e.g. time or cost. The approach naturally employs the fact that every activity is characterized by an amount of work to be performed with controllable rate which depends on the amount of resource. Two resource categories can be distinguished from the viewpoint of resource divisibility: discrete (i.e., discretely divisible) and continuous (i.e., continuously divisible) ones [2,9,14]. Examples of discrete resources include: machines, tools, workers. The most typical continuous resources are: power, energy, liquids and money.

There exist an intensive and ever-increasing literature dealing with various aspects of resource allocation control and scheduling of multi-project of activities [1,2,9,13-15,25-28] and its applications in different areas (see, for example, [2,16,21,24]). During a last four decades a variety of different algorithms for resource allocation and project scheduling have been proposed. The results were obtained for general cases, where all the models relating performance speeds of activities to resource amounts were arbitrary continuous increasing functions [4,9,11,12,14,26], as well as for multi-projects of activities described by specific concave and convex functions [9,11,12,26,27], and even for a special case of simple linear with respect to the resource amount models [10,15,18,19]. The project duration optimization [9,11,12,19,26], minimizing inventory, backlog and production related costs over a production horizon [17], minimizing maximum lateness or just-in-time [13] criteria were used as the objective functions. Optimal resource allocation policies were proposed both for singly [9,11,12] and for doubly constrained resources [9,18]. The most typical renewable continuous resource, which is power, is also, most often, doubly constrained, since its consumption, i.e. energy, is also limited. For the survey of the problems of resource allocation among activieties which can be processed using resources of various categories and types see [1,2,28]. Further explanations, theory and examples on control of project of activities can be fund in [21,25], see also [9,11,12].

The paper deals with a class of time-optimal resource allocation problems in which the total usage of renewable and continuously divisible resource is constrained at every time of the project performance.

A sequence of projects is considered, each project composed of activities which are available for realization at the same time. This assumption, essential for the idea of the time-decomposition applied, seems to be a realistic assumption in most real processes. No specific assumptions concerning the models of activities, like linearity, convexity or concavity are made here. The problem is to find an admissible control minimizing the performance time of the sequence of projects under the assumption that the allowable level of the total usage of the resource is constant during the projects duration. This problem has been solved in [12], where necessary and sufficient optimality conditions are stated in terms of the performance time and the existence of the optimal control is proved. However, the solution concept proposed in [12] leads to the reduction of the primary dynamic optimization problem to some static programming task, the computational complexity of this task grows, in general, faster than the dimension of the problem, i.e., the number of activities and the number of the moments at which the successive projects are available for realization. The paper discusses hierarchical decentralized method for solving this class of optimal resource allocation problems.

TIME-OPTIMAL CONTROL OF A SEQUENCE OF PROJECTS

We consider a sequence of k projects of independent activities (this means that no precedence relations exists among them), each project composed of activities available for realization at the same time, described by the equations:

$$\left.\begin{array}{ll} \dot{x}_{ri}(t) = f_{ri}\big(u_{ri}(t)\big), & t \geq 0 \\ x_{ri}(t) = 0, & t \leq t_r \end{array}\right\} i = 1, \dots, n_r, r = 1, \dots, k, \tag{1}$$

where: $x_{ri}(t)$ and $u_{ri}(t)$ are, respectively, the state of the i-th activity in the r-th project and the amount of resource allotted to this activity at the time t. Here t_r is the specified, fixed time at which the r-th project is available for realization, $t_{r+1} \geq t_r$, where $t_1 = 0$, and n_r is the number of activities in the r-th project, $r = 1, \dots, k$. We also assume that for any $i = 1, \dots, n_r$ and $r = 1, \dots, k$ the functions $f_{ri}: \mathcal{R}_+ \to \mathcal{R}_+$ describing the speed (i.e., the rate of activity performance):

$$v_{ri}(t) = \dot{x}_{ri}(t) = f_{ri}\big(u_{ri}(t)\big)$$

are continuous, increasing and such that $f_{ri}(0) = 0$, $\mathcal{R}_+$ is the set of nonnegative real numbers. The assumption means that the greater the assigned resource $u_{ri}(t)$ is, the higher is the speed $v_{ri}(t)$ of execution of the activity.

We say that the activity (r, i) is completed if its state has attained a given terminal state $w_{ri} > 0$. We also assume that the amount of a renewable and continously divisible resource, e.g. power or budget available per time unit for management, is constant and equal to N for any time $t \geq 0$. By the performance time T of a sequence of projects we mean the time at which all the activities are completed, i.e.:

$$T = min\{\tau > t_k : x_{ri}(\tau) = w_{ri}, i = 1, \dots, n_r, r = 1, \dots, k\}.$$

We introduce, for convenience, the following vector notation:

$$\boldsymbol{x}_r = [x_{r1} \quad \dots \quad x_{rn_r}]^T, \quad \boldsymbol{x} = [\boldsymbol{x}_1^T \quad \dots \quad \boldsymbol{x}_k^T]^T,$$
$$\boldsymbol{u}_r = [u_{r1} \quad \dots \quad u_{rn_r}]^T, \quad \boldsymbol{u} = [\boldsymbol{u}_1^T \quad \dots \quad \boldsymbol{u}_k^T]^T.$$

The vectors $\boldsymbol{v}_r$ and $\boldsymbol{v}$ of speeds of the r-th project activities and all activities, respectively, as well as the vectors of final states $\boldsymbol{w}_r$ and $\boldsymbol{w}$ are defined by analogy. The vector-functions $\boldsymbol{f}_r(\boldsymbol{u}_r)$ and $\boldsymbol{f}(\boldsymbol{u})$ are defined as follows:

$$\boldsymbol{f}_r(\boldsymbol{u}_r) = \big[f_{r1}(u_{r1}) \quad \dots \quad f_{rn_r}\big(u_{rn_r}\big)\big]^T,$$
$$\boldsymbol{f}(\boldsymbol{u}) = [\boldsymbol{f}_1(\boldsymbol{u}_1)^T \quad \dots \quad \boldsymbol{f}_k(\boldsymbol{u}_k)^T]^T.$$

Define for the successive time intervals determined by the times t_r, $r = 1, \dots, k$, the sets od admissible values of resource allocation:

$$\boldsymbol{U}^r = \big\{\boldsymbol{u} \in \mathcal{R}_+^n : \boldsymbol{u}_s = 0,\ s \geq r+1, \textstyle\sum_{s=1}^{r}\sum_{i=1}^{n_s} u_{si} \leq N\big\},$$

where:

$$n = \textstyle\sum_{r=1}^{k} n_k$$

is the number of all activities. The sets of feasible performing speeds of operations within the r-th time interval will be denoted by:

$$\boldsymbol{V}^r = \{\boldsymbol{v} \in \mathcal{R}_+^n : \boldsymbol{v} = \boldsymbol{f}(\boldsymbol{u}),\ \boldsymbol{u} \in \boldsymbol{U}^r\}.$$

Note, that $\boldsymbol{U}^r$ and $\boldsymbol{V}^r$ are compact subsets of $\mathcal{R}^n$. The following condition is satisfied:

$$\boldsymbol{v}^{r,1} \in \boldsymbol{V}^r,\ \mathbb{0}_n \leq \boldsymbol{v}^{r,2} \leq \boldsymbol{v}^{r,1} \implies \boldsymbol{v}^{r,2} \in \boldsymbol{V}^r, \tag{2}$$

here $\mathbb{0}_n$ is zero vector of dimension n. The resource allocation (control):

$$\boldsymbol{u}(t) = [\boldsymbol{u}_1^T(t) \quad \dots \quad \boldsymbol{u}_k^T(t)]^T,$$

where:

$$\boldsymbol{u}_r(t) = [u_{r1}(t) \quad \dots \quad u_{rn_r}(t)]^T$$

and the functions:

$$u_{r1}: [0, T] \to \mathcal{R}_+ \text{ for } i = 1, \dots, n_r, r = 1, \dots, k,$$

is said to be admissible for the sequence of projects, if the following conditions are satisfied:

(*i*) $\boldsymbol{u}(t) \in \boldsymbol{U}^r$ for $t_r \leq t < t_{r+1},\ r = 1, \dots, k,$ where $t_{k+1} = \infty$,

(*ii*) $\boldsymbol{u}(t)$ is piecewise continuous function,

(*iii*) $\int_0^T \boldsymbol{f}\big(\boldsymbol{u}(t)\big) = \boldsymbol{w}$.

The problem is to find an admissible control $\boldsymbol{u}(t)$ for which all the projects are completed as soon as possible, i.e. a control minimizing the performance time T of the sequence of projects.

OPTIMALITY CONDITIONS

In the paper [12] a solution to the above problem is presented, based on the notion of the set of reachable states. This approach leads to the reduction of the primary dynamic optimization problem to the static programming task. The following result follows immediately from [12; Theorem 2].

Theorem 1. T^* is the minimum performance time if and only if T^* and $\boldsymbol{v}^{1*}, \dots, \boldsymbol{v}^{k*}$ are the solutions of the following optimization task:

$$T \to min \tag{3}$$

subject to:

$$\begin{aligned} \boldsymbol{w} &= \tau_1 \boldsymbol{v}^1 + \cdots + \tau_{k-1}\boldsymbol{v}^{k-1} + (T - t_k)\boldsymbol{v}^k, \\ \boldsymbol{v}^r &\in conv(\boldsymbol{V}^r), r = 1, \dots, k, \end{aligned} \tag{4}$$

where: $conv(\boldsymbol{V}^r)$ is the convex hull of $\boldsymbol{V}^r$ (the smallest convex set containing $\boldsymbol{V}^r$, i.e., the set of all convex combinations of points in $\boldsymbol{V}^r$) and $\tau_r = t_{r+1} - t_r$ for $r = 1, \dots, k-1$.

The problem (3), (4) is static convex programming task. However, the above task can be solved by using standard convex numerical optimization techniques [3], the computational complexity of this problem grows, in general, faster than the dimension of the problem, i.e., the number of activities and the number of the time moments t_r at which the successive projects are available for realization. Thus, in order to reduce the computational and storage requirements the following two-level scheme is proposed. Taking into account the successive time-intervals structure of both the original dynamic optimal resource allocation problem [12] as well as the static optimization task (3), (4), the time-decomposition approach is applied.

DECENTRALIZED TWO-LEVEL SCHEME FOR RESOURCE ALLOCATION

Note first, that for any positive constant ρ the optimization problem (3), (4) is equivalent to the minimization of the modified strictly convex index:

$$T + \rho T^2 \to min \tag{5}$$

subject to the constraints (4). By introducing a vector of prices $\boldsymbol{\lambda} \in \mathcal{R}^n$, we can define the Lagrangian for the optimization task (5), (4):

$$\begin{aligned} L(T, \boldsymbol{v}^1, \dots, \boldsymbol{v}^k, \boldsymbol{\lambda}) = T + \rho T^2 + \langle \boldsymbol{\lambda}, \boldsymbol{w} - \tau_1 \boldsymbol{v}^1 + \cdots \\ -\tau_{k-1}\boldsymbol{v}^{k-1} - (T - t_k)\boldsymbol{v}^k \rangle, \end{aligned} \tag{6}$$

where: ρ is some positive constant and $\langle \cdot, \cdot \rangle$ denotes the inner product. Notice that $L(T, \boldsymbol{v}^1, \dots, \boldsymbol{v}^k, \boldsymbol{\lambda})$ is continous with respect to all arguments and can be expressed as:

$$\begin{aligned} L(T, \boldsymbol{v}^1, \dots, \boldsymbol{v}^k, \boldsymbol{\lambda}) = \textstyle\sum_{r=1}^{k-1} \tau_r L_r(\boldsymbol{v}^r, \boldsymbol{\lambda}) + \\ L_k(T, \boldsymbol{v}^k, \boldsymbol{\lambda}) + \langle \boldsymbol{\lambda}, \boldsymbol{w} \rangle, \end{aligned} \tag{7}$$

where for $r = 1, \dots, k-1$ the local Lagrangians are equal:

$$L_r(\boldsymbol{v}^r, \boldsymbol{\lambda}) = -\langle \boldsymbol{\lambda}, \boldsymbol{v}^r \rangle, \tag{8}$$

while for the last time interval we have:

$$L_k(T, \boldsymbol{v}^k, \boldsymbol{\lambda}) = T + \rho T^2 - (T - t_k)\langle \boldsymbol{\lambda}, \boldsymbol{v}^k \rangle. \tag{9}$$

Consider the following two-level scheme.

Infimal Problem (IP). Given $\boldsymbol{\lambda} \in \mathcal{R}^n$, for $r = 1, \dots, k-1$ find the performance speed vectors $\hat{\boldsymbol{v}}^r(\boldsymbol{\lambda})$ such that:

$$L_r(\hat{\boldsymbol{v}}^r(\boldsymbol{\lambda}), \boldsymbol{\lambda}) = min_{\boldsymbol{v}^r \in conv(\boldsymbol{V}^r)} L_r(\boldsymbol{v}^r, \boldsymbol{\lambda}), \tag{10}$$

and the pair $\left(\hat{\boldsymbol{v}}^k(\boldsymbol{\lambda}), \hat{T}(\boldsymbol{\lambda})\right)$ such that:

$$L_k\left(\hat{T}(\boldsymbol{\lambda}), \hat{\boldsymbol{v}}^k(\boldsymbol{\lambda}), \boldsymbol{\lambda}\right) = min_{T, \boldsymbol{v}^k \in conv(\boldsymbol{V}^k)} L_k(T, \boldsymbol{v}^k, \boldsymbol{\lambda}). \tag{11}$$

By virtue of the compactness of the sets $conv(\boldsymbol{V}^r)$ and the continouity of the Lagrangians $L_r(\boldsymbol{v}^r, \boldsymbol{\lambda})$ with respect to $\boldsymbol{v}^r$, the solutions of (10) exist for any $\boldsymbol{\lambda} \in \mathcal{R}^n$, $r = 1, \dots, k-1$, on the basis of the well-known Weierstrass's theorem which asserts the existence of continuous function extrema on compact sets [29; Theorem 7.1]. Compactness of $conv(\boldsymbol{V}^k)$ together with the strict conxexity of the continous local Lagrangian $L_k(T, \boldsymbol{v}^k, \boldsymbol{\lambda})$ with respect to T implies the existence of (11) solution. If the solution of (10) with respect to $\boldsymbol{v}^r$ is not unique, take any:

$$\hat{\boldsymbol{v}}^r(\boldsymbol{\lambda}) \in \hat{\boldsymbol{V}}^r(\boldsymbol{\lambda}),$$

$\hat{\boldsymbol{V}}^r(\boldsymbol{\lambda})$ being the set of speed vectors minimizing $L_r(\boldsymbol{v}^r, \boldsymbol{\lambda})$ on $conv(\boldsymbol{V}^r)$, $r = 1, \dots, k-1$. Similarly, if the solution to (11) is not unique take any $\hat{\boldsymbol{v}}^k(\boldsymbol{\lambda}) \in \hat{\boldsymbol{V}}^k(\boldsymbol{\lambda})$ minimizing $L_k(T, \boldsymbol{v}^k, \boldsymbol{\lambda})$. For given $\hat{\boldsymbol{v}}^k(\boldsymbol{\lambda})$ locally optimal $\hat{T}(\boldsymbol{\lambda})$ is unique due to $L_k(T, \boldsymbol{v}^k, \boldsymbol{\lambda})$ strict convexity with respect to T – for details see the next section.

Coordination Problem (CP). Find $\hat{\boldsymbol{\lambda}} \in \mathcal{R}^n$ such that:

$$L_D\left(\hat{\boldsymbol{\lambda}}\right) = max_{\boldsymbol{\lambda} \in \mathcal{R}^n} L_D(\boldsymbol{\lambda}), \tag{12}$$

where the dual function $L_D(\boldsymbol{\lambda})$ is defined as follows:

$$L_D(\boldsymbol{\lambda}) = L\left(\hat{T}(\boldsymbol{\lambda}), \hat{\boldsymbol{v}}^1(\boldsymbol{\lambda}), \dots, \hat{\boldsymbol{v}}^k(\boldsymbol{\lambda}), \boldsymbol{\lambda}\right), \tag{13}$$

and take $\hat{\boldsymbol{v}}^r = \hat{\boldsymbol{v}}^r\left(\hat{\boldsymbol{\lambda}}\right)$, $r = 1, \dots, k$ as the vectors of the optimal performance speeds of the activities in the successive time intervals.

PROPERTIES OF IP AND CP

Let us consider first the IP tasks (10). Since $\mathbb{O}_n \in conv(\boldsymbol{V}^r)$, taking into account (8) we see that for any $r = 1, \dots, k-1$ the solutions of (10) are such that:

$$L_r(\widehat{\boldsymbol{v}}^r(\boldsymbol{\lambda}), \boldsymbol{\lambda}) = -\max_{\boldsymbol{v}^r \in conv(\boldsymbol{V}^r)} \langle \boldsymbol{\lambda}, \boldsymbol{v}^r \rangle \leq 0. \quad (14)$$

Consider an arbitrary $\boldsymbol{\lambda} \in \mathcal{R}^n$. It is obvious that for any positive constant α we have:

$$L_r(\widehat{\boldsymbol{v}}^r(\alpha\boldsymbol{\lambda}), \alpha\boldsymbol{\lambda}) = -\alpha \max_{\boldsymbol{v}^r \in conv(\boldsymbol{V}^r)} \langle \boldsymbol{\lambda}, \boldsymbol{v}^r \rangle = \alpha L_r(\widehat{\boldsymbol{v}}^r(\boldsymbol{\lambda}), \boldsymbol{\lambda}).$$

Since the compact set $conv(\boldsymbol{V}^r) \cap \mathcal{R}^{p_r}$ is an absorbing set for the subspace $\mathcal{R}_+^{p_r}$, taking into account property (2) it is easily seen that the solutions of (10) are such that:

$$\widehat{\boldsymbol{v}}^r(\boldsymbol{\lambda}) \in bd[conv(\boldsymbol{V}^r)],$$

where $bd[conv(\boldsymbol{V}^r)]$ is boundary of the set $conv(\boldsymbol{V}^r)$. Here:

$$p_r = \sum_{s=1}^{r} n_s$$

is the number of operations accessible for realization in the r-th time interval, $p_k = n$.

Let us consider now the last IP task (11). According to the parametric approach of successive optimization [7] applied to (11) the following equivalence holds:

$$L_k\big(\hat{T}(\boldsymbol{\lambda}), \widehat{\boldsymbol{v}}^k(\boldsymbol{\lambda}), \boldsymbol{\lambda}\big) = \min_{\boldsymbol{v}^k \in conv(\boldsymbol{V}^k)} [\min_T L_k(T, \boldsymbol{v}^k, \boldsymbol{\lambda})]. \quad (15)$$

The unique solution of the internal optimization task of the right-hand side of (15) is given by:

$$T = \frac{1}{2\rho}[\langle \boldsymbol{\lambda}, \boldsymbol{v}^k \rangle - 1].$$

Whence, the external task of the right-hand side of (15) takes the form:

$$\min_{\boldsymbol{v}^k \in conv(\boldsymbol{V}^k)} \bar{L}_k(\boldsymbol{v}^k, \boldsymbol{\lambda}), \quad (16)$$

with the function $\bar{L}_k(\boldsymbol{v}^k, \boldsymbol{\lambda})$ defined by:

$$\bar{L}_k(\boldsymbol{v}^k, \boldsymbol{\lambda}) = -\frac{1}{4\rho}[\langle \boldsymbol{\lambda}, \boldsymbol{v}^k \rangle]^2 + \left(\frac{1}{2\rho} + t_k\right)\langle \boldsymbol{\lambda}, \boldsymbol{v}^k \rangle - \frac{1}{4\rho}. \quad (17)$$

Let $\boldsymbol{\lambda} \neq \mathbb{O}_n$ and $\overline{\boldsymbol{v}}^k(\boldsymbol{\lambda}) \in conv(\boldsymbol{V}^k)$ and $\overline{\overline{\boldsymbol{v}}}^k(\boldsymbol{\lambda}) \in conv(\boldsymbol{V}^k)$ be such that:

$$\min_{\boldsymbol{v}^k \in conv(\boldsymbol{V}^k)} \langle \boldsymbol{\lambda}, \boldsymbol{v}^k \rangle = \langle \boldsymbol{\lambda}, \overline{\boldsymbol{v}}^k(\boldsymbol{\lambda}) \rangle, \quad (18)$$

$$\max_{\boldsymbol{v}^k \in conv(\boldsymbol{V}^k)} \langle \boldsymbol{\lambda}, \boldsymbol{v}^k \rangle = \langle \boldsymbol{\lambda}, \overline{\overline{\boldsymbol{v}}}^k(\boldsymbol{\lambda}) \rangle. \quad (19)$$

Taking into account the properties of the square function (17) of (variable) $\langle \boldsymbol{\lambda}, \boldsymbol{v}^k \rangle$ in (16), as easily check that, the solution $\widehat{\boldsymbol{v}}^k(\boldsymbol{\lambda})$ of (16) for $\boldsymbol{\lambda} \neq \mathbb{O}_n$ is given by:

$$\widehat{\boldsymbol{v}}^k(\boldsymbol{\lambda}) = \begin{cases} \overline{\boldsymbol{v}}^k(\boldsymbol{\lambda}) & \eta\langle \boldsymbol{\lambda}, \overline{\boldsymbol{v}}^k(\boldsymbol{\lambda}) \rangle - [\langle \boldsymbol{\lambda}, \overline{\boldsymbol{v}}^k(\boldsymbol{\lambda}) \rangle]^2 < \eta\langle \boldsymbol{\lambda}, \overline{\overline{\boldsymbol{v}}}^k(\boldsymbol{\lambda}) \rangle - [\langle \boldsymbol{\lambda}, \overline{\overline{\boldsymbol{v}}}^k(\boldsymbol{\lambda}) \rangle]^2 \\ \overline{\boldsymbol{v}}^k(\boldsymbol{\lambda}) \text{ or } \overline{\overline{\boldsymbol{v}}}^k(\boldsymbol{\lambda}) & \eta\langle \boldsymbol{\lambda}, \overline{\boldsymbol{v}}^k(\boldsymbol{\lambda}) \rangle - [\langle \boldsymbol{\lambda}, \overline{\boldsymbol{v}}^k(\boldsymbol{\lambda}) \rangle]^2 = \eta\langle \boldsymbol{\lambda}, \overline{\overline{\boldsymbol{v}}}^k(\boldsymbol{\lambda}) \rangle - [\langle \boldsymbol{\lambda}, \overline{\overline{\boldsymbol{v}}}^k(\boldsymbol{\lambda}) \rangle]^2 \\ \overline{\overline{\boldsymbol{v}}}^k(\boldsymbol{\lambda}) & \text{otherwise} \end{cases},$$

where: $\eta = 2 + 4\rho t_k$. Note, that since for any $\boldsymbol{\lambda} \neq \mathbb{O}_n$ at least one of inner products $\langle \boldsymbol{\lambda}, \overline{\overline{\boldsymbol{v}}}^k(\boldsymbol{\lambda}) \rangle$ and $\langle \boldsymbol{\lambda}, \overline{\boldsymbol{v}}^k(\boldsymbol{\lambda}) \rangle$ differs from zero, i.e.:

$$\langle \boldsymbol{\lambda}, \overline{\overline{\boldsymbol{v}}}^k(\boldsymbol{\lambda}) \rangle - \langle \boldsymbol{\lambda}, \overline{\boldsymbol{v}}^k(\boldsymbol{\lambda}) \rangle > 0,$$

the inequality related to $\overline{\boldsymbol{v}}^k(\boldsymbol{\lambda})$ in the curly brackets in the above formula is equivalent to $\varphi(\boldsymbol{\lambda}) < \eta$, where:

$$\varphi(\boldsymbol{\lambda}) = \langle \boldsymbol{\lambda}, \overline{\overline{\boldsymbol{v}}}^k(\boldsymbol{\lambda}) \rangle + \langle \boldsymbol{\lambda}, \overline{\boldsymbol{v}}^k(\boldsymbol{\lambda}) \rangle.$$

Thus $\widehat{\boldsymbol{v}}^k(\boldsymbol{\lambda})$ solving (16) for $\boldsymbol{\lambda} \neq \mathbb{O}_n$ can be rewritten in compact form as follows:

$$\widehat{\boldsymbol{v}}^k(\boldsymbol{\lambda}) = \begin{cases} \overline{\boldsymbol{v}}^k(\boldsymbol{\lambda}) & \varphi(\boldsymbol{\lambda}) < \eta \\ \overline{\boldsymbol{v}}^k(\boldsymbol{\lambda}) \text{ or } \overline{\overline{\boldsymbol{v}}}^k(\boldsymbol{\lambda}) & \varphi(\boldsymbol{\lambda}) = \eta \\ \overline{\overline{\boldsymbol{v}}}^k(\boldsymbol{\lambda}) & \text{otherwise} \end{cases}. \quad (20)$$

Thus, the optimum:

$$L_k\big(\hat{T}(\boldsymbol{\lambda}), \widehat{\boldsymbol{v}}^k(\boldsymbol{\lambda}), \boldsymbol{\lambda}\big) = \min\{\bar{L}_k(\overline{\boldsymbol{v}}^k(\boldsymbol{\lambda}), \boldsymbol{\lambda}), \bar{L}_k(\overline{\overline{\boldsymbol{v}}}^k(\boldsymbol{\lambda}), \boldsymbol{\lambda})\}, \quad (21)$$

can be rewritten in the compact form as:

$$L_k\big(\hat{T}(\boldsymbol{\lambda}), \widehat{\boldsymbol{v}}^k(\boldsymbol{\lambda}), \boldsymbol{\lambda}\big) = -\frac{1}{4\rho}[\langle \boldsymbol{\lambda}, \widehat{\boldsymbol{v}}^k(\boldsymbol{\lambda}) \rangle]^2 + \left(\frac{1}{2\rho} + t_k\right)\langle \boldsymbol{\lambda}, \widehat{\boldsymbol{v}}^k(\boldsymbol{\lambda}) \rangle - \frac{1}{4\rho}, \quad (22)$$

with $\widehat{\boldsymbol{v}}^k(\boldsymbol{\lambda})$ given by (20). Since $\overline{\boldsymbol{v}}^k(\boldsymbol{\lambda})$ and $\overline{\overline{\boldsymbol{v}}}^k(\boldsymbol{\lambda})$ are boundary points of the set $conv(\boldsymbol{V}^k)$, we also have:

$$\widehat{\boldsymbol{v}}^k(\boldsymbol{\lambda}) \in bd[conv(\boldsymbol{V}^k)].$$

Let $\mathbb{O}_n \neq \boldsymbol{\lambda} \in \mathcal{R}^n$. It is obvious, due to affine with respect to $\boldsymbol{\lambda}$ form of the inner product in (18) and (19), that for any positive constant α we have:

$$\overline{\boldsymbol{v}}^k(\alpha\boldsymbol{\lambda}) = \overline{\boldsymbol{v}}^k(\boldsymbol{\lambda}) \text{ and } \overline{\overline{\boldsymbol{v}}}^k(\alpha\boldsymbol{\lambda}) = \overline{\overline{\boldsymbol{v}}}^k(\boldsymbol{\lambda}).$$

Whence, if $\varphi(\boldsymbol{\lambda}) > \eta$, then for any α such that $\alpha > \eta/\varphi(\boldsymbol{\lambda})$, thus in particular for any $\alpha \geq 1$, we have $\widehat{\boldsymbol{v}}^k(\alpha\boldsymbol{\lambda}) = \overline{\overline{\boldsymbol{v}}}^k(\boldsymbol{\lambda})$, and for any $\alpha < \eta/\varphi(\boldsymbol{\lambda})$, we have $\widehat{\boldsymbol{v}}^k(\alpha\boldsymbol{\lambda}) = \overline{\boldsymbol{v}}^k(\boldsymbol{\lambda})$. When $\varphi(\boldsymbol{\lambda}) < \eta$, for any α such that $\alpha < \eta/\varphi(\boldsymbol{\lambda})$, we have $\widehat{\boldsymbol{v}}^k(\alpha\boldsymbol{\lambda}) = \overline{\boldsymbol{v}}^k(\boldsymbol{\lambda})$ and for any α such that $\alpha > \eta/\varphi(\boldsymbol{\lambda})$, we have $\widehat{\boldsymbol{v}}^k(\alpha\boldsymbol{\lambda}) = \overline{\overline{\boldsymbol{v}}}^k(\boldsymbol{\lambda})$. In both cases for $\alpha = \eta/\varphi(\boldsymbol{\lambda})$ each of $\overline{\boldsymbol{v}}^k(\boldsymbol{\lambda})$ and $\overline{\overline{\boldsymbol{v}}}^k(\boldsymbol{\lambda})$ can be chosen. When $\varphi(\boldsymbol{\lambda}) = \eta$, i.e., both $\overline{\boldsymbol{v}}^k(\boldsymbol{\lambda})$ and $\overline{\overline{\boldsymbol{v}}}^k(\boldsymbol{\lambda})$ are

locally optimal for $\boldsymbol{\lambda}$, for $\alpha\boldsymbol{\lambda}$ we have $\widehat{\boldsymbol{v}}^k(\alpha\boldsymbol{\lambda}) = \overline{\boldsymbol{v}}^k(\boldsymbol{\lambda})$ for $\alpha < 1$, and $\widehat{\boldsymbol{v}}^k(\alpha\boldsymbol{\lambda}) = \overline{\overline{\boldsymbol{v}}}^k(\boldsymbol{\lambda})$ for $\alpha > 1$. The above results in:

$$\widehat{\boldsymbol{v}}^k(\alpha\boldsymbol{\lambda}) = \begin{cases} \overline{\boldsymbol{v}}^k(\boldsymbol{\lambda}) = \widehat{\boldsymbol{v}}^k(\boldsymbol{\lambda}) & \varphi(\boldsymbol{\lambda}) < \eta,\ \alpha < \eta/\varphi(\boldsymbol{\lambda}) \\ \overline{\overline{\boldsymbol{v}}}^k(\boldsymbol{\lambda}) & \varphi(\boldsymbol{\lambda}) < \eta,\ \alpha > \eta/\varphi(\boldsymbol{\lambda}) \\ \overline{\overline{\boldsymbol{v}}}^k(\boldsymbol{\lambda}) = \widehat{\boldsymbol{v}}^k(\boldsymbol{\lambda}) & \varphi(\boldsymbol{\lambda}) > \eta,\ \alpha > \eta/\varphi(\boldsymbol{\lambda}) \\ \overline{\boldsymbol{v}}^k(\boldsymbol{\lambda}) & \varphi(\boldsymbol{\lambda}) > \eta,\ \alpha < \eta/\varphi(\boldsymbol{\lambda}) \\ \overline{\boldsymbol{v}}^k(\boldsymbol{\lambda}) \text{ or } \overline{\overline{\boldsymbol{v}}}^k(\boldsymbol{\lambda}) & \alpha = \eta/\varphi(\boldsymbol{\lambda}) \\ \overline{\boldsymbol{v}}^k(\boldsymbol{\lambda}) & \varphi(\boldsymbol{\lambda}) = \eta,\ \alpha < 1 \\ \overline{\overline{\boldsymbol{v}}}^k(\boldsymbol{\lambda}) & \varphi(\boldsymbol{\lambda}) = \eta,\ \alpha > 1 \end{cases}. \quad (23)$$

Then, we get the following result.

Proposition 1. Let $\boldsymbol{\lambda} \in \mathcal{R}^n$ and $\boldsymbol{\lambda} \neq \mathbb{O}_n$. The solutions of IP tasks are such that:

(i) $\widehat{\boldsymbol{v}}^r(\boldsymbol{\lambda}) \in bd[conv(\boldsymbol{V}^r)]$ for $r = 1, \dots, k$,

(ii) $\widehat{\boldsymbol{v}}^r(\alpha\boldsymbol{\lambda}) = \widehat{\boldsymbol{v}}^r(\boldsymbol{\lambda})$ for any $\alpha > 0, r = 1, \dots, k-1$,

(iii) $\widehat{\boldsymbol{v}}^k(\alpha\boldsymbol{\lambda})$ is given by (23) for any $\alpha > 0$.

From (7), (10), (11) and (13) as a straightforward conclusion we see that IP tasks can expressed in compact form as:

$$\min_{\substack{T, \boldsymbol{v}^r \in conv(\boldsymbol{V}^r), \\ r=1,\dots,k}} L(T, \boldsymbol{v}^1, \dots, \boldsymbol{v}^k, \boldsymbol{\lambda}) = L_D(\boldsymbol{\lambda}),$$

whence the equivalent sum-form of the dual function follows:

$$L_D(\boldsymbol{\lambda}) = \sum_{r=1}^{k-1} \tau_r L_r(\widehat{\boldsymbol{v}}^r(\boldsymbol{\lambda}), \boldsymbol{\lambda}) + L_k\big(\hat{T}(\boldsymbol{\lambda}), \widehat{\boldsymbol{v}}^k(\boldsymbol{\lambda}), \boldsymbol{\lambda}\big) + \langle \boldsymbol{\lambda}, \boldsymbol{w} \rangle. \quad (24)$$

Since the local Lagrangians (8) are continuous with respect to all arguments, from the compactness of $conv(\boldsymbol{V}^r)$ using the known results concerning the continuity of minimum of continuous functions on compact sets [29; Theorem 7.2] we conclude that the functions $L_r(\widehat{\boldsymbol{v}}^r(\boldsymbol{\lambda}), \boldsymbol{\lambda})$ defined by (10) are continuous on $\mathcal{R}^n$, $r = 1, \dots, k-1$. In view of the same result the right hand size of (18) and (19) are continuous functions of $\boldsymbol{\lambda}$, whence the continuity of $L_k\big(\hat{T}(\boldsymbol{\lambda}), \widehat{\boldsymbol{v}}^k(\boldsymbol{\lambda}), \boldsymbol{\lambda}\big)$ defined by (22), (23) follows. Thus the continuity of $L_D(\boldsymbol{\lambda})$ is resolved. Dual function $L_D(\boldsymbol{\lambda})$ as minimum of the weighted sum (24) of local Lagrangians plus affine component $\langle \boldsymbol{\lambda}, \boldsymbol{w} \rangle$ is concave function, for details see proof of Theorem 2.16 in [7]. The next result is valid

Proposition 2. The dual function $L_D(\boldsymbol{\lambda})$ (13) is continuous concave function in the space $\mathcal{R}^n$.

Having already proved that the dual function is continuous on the space $\mathcal{R}^n$, we wish to show that the solution to the CP there exists. The proof is based on the observation that the maximization of the continuous dual function on $\mathcal{R}^n$ can be restricted to some compact ball $\boldsymbol{\mathcal{B}}(\mathbb{O}_n, \alpha_{max}) \subset \mathcal{R}^n$, the radius α_{max} is defined by (27) and (28) below.

Note that on the basis of (24), (14) and (22) for $\boldsymbol{\lambda} = \mathbb{O}_n$ we have $L_D(\mathbb{O}_n) = -1/4\rho$. Let us consider an arbitrary $\mathbb{O}_n \neq \boldsymbol{\lambda} \in \mathcal{R}^n$. Since, in view of (14), each term in the first sum of (24) is non-positive, taking into account (22) we have:

$$L_D(\boldsymbol{\lambda}) \leq L_k\big(\hat{T}(\boldsymbol{\lambda}), \widehat{\boldsymbol{v}}^k(\boldsymbol{\lambda}), \boldsymbol{\lambda}\big) + \langle \boldsymbol{\lambda}, \boldsymbol{w} \rangle. \quad (25)$$

Obviously, for any $\boldsymbol{\lambda} \neq \mathbb{O}_n$ at least one of the inner products $\langle \boldsymbol{\lambda}, \overline{\overline{\boldsymbol{v}}}^k(\boldsymbol{\lambda}) \rangle$ and $\langle \boldsymbol{\lambda}, \overline{\boldsymbol{v}}^k(\boldsymbol{\lambda}) \rangle$ differs from zero. Without the loss of generality we assume that $\langle \boldsymbol{\lambda}, \overline{\overline{\boldsymbol{v}}}^k(\boldsymbol{\lambda}) \rangle > 0$. In view of (20), this means that $\varphi(\boldsymbol{\lambda}) \geq \eta$, i.e., $\eta/\varphi(\boldsymbol{\lambda}) \leq 1$. Due to (21):

$$L_k\big(\hat{T}(\boldsymbol{\lambda}), \widehat{\boldsymbol{v}}^k(\boldsymbol{\lambda}), \boldsymbol{\lambda}\big) \leq \bar{L}_k(\overline{\overline{\boldsymbol{v}}}^k(\boldsymbol{\lambda}), \boldsymbol{\lambda}),$$

which, in view of (25) and (17), yield:

$$L_D(\boldsymbol{\lambda}) \leq -\frac{1}{4\rho}[\langle \boldsymbol{\lambda}, \overline{\overline{\boldsymbol{v}}}^k(\boldsymbol{\lambda}) \rangle]^2 + \left(\frac{1}{2\rho} + t_k\right)\langle \boldsymbol{\lambda}, \overline{\overline{\boldsymbol{v}}}^k(\boldsymbol{\lambda}) \rangle + -\frac{1}{4\rho} + \langle \boldsymbol{\lambda}, \boldsymbol{w} \rangle. \quad (26)$$

Let us now prove that for any $\boldsymbol{\lambda} \in \boldsymbol{\mathcal{A}}(\mathbb{O}_n, \varepsilon, 1)$, where $\boldsymbol{\mathcal{A}}(\mathbb{O}_n, \varepsilon, 1)$ is closed annulus in $\mathcal{R}^n$, i.e., a region bounded by two concentric circles of radiuses equal ε and 1:

$$\boldsymbol{\mathcal{A}}(\mathbb{O}_n, \varepsilon, 1) = \{\boldsymbol{\lambda} \in \mathcal{R}^n : \varepsilon \leq \langle \boldsymbol{\lambda}, \boldsymbol{\lambda} \rangle \leq 1\},$$

there exists a positive coefficient $\alpha_0(\boldsymbol{\lambda})$ such that for any $\alpha > \alpha_0(\boldsymbol{\lambda})$ the inequality:

$$L_D(\alpha\boldsymbol{\lambda}) < L_D(\mathbb{O}_n)$$

holds. Let:

$$\alpha_0(\boldsymbol{\lambda}) = max\left\{1, \frac{(2+4\rho t_k)\langle \boldsymbol{\lambda}, \overline{\overline{\boldsymbol{v}}}^k(\boldsymbol{\lambda}) \rangle + 4\rho\|\boldsymbol{\lambda}\|\|\boldsymbol{w}\|}{[\langle \boldsymbol{\lambda}, \overline{\overline{\boldsymbol{v}}}^k(\boldsymbol{\lambda}) \rangle]^2}\right\}, \quad (27)$$

where: $\|\cdot\|$ denotes the Euclidean norm in $\mathcal{R}^n$. For any $\alpha > \alpha_0(\boldsymbol{\lambda})$ we have, in particular, that:

$$\alpha[\langle \boldsymbol{\lambda}, \overline{\overline{\boldsymbol{v}}}^k(\boldsymbol{\lambda}) \rangle]^2 > (2 + 4\rho t_k)\langle \boldsymbol{\lambda}, \overline{\overline{\boldsymbol{v}}}^k(\boldsymbol{\lambda}) \rangle + 4\rho\|\boldsymbol{\lambda}\|\|\boldsymbol{w}\|,$$

and the inequality:

$$\alpha > 1 > \eta/\varphi(\boldsymbol{\lambda}) \text{ or } \eta/\varphi(\boldsymbol{\lambda}) = 1 < \alpha$$

from the third and seventh rows of (23), respectively, is satisfied. Thus, taking into account Proposition 1 (iii), the Schwarz inequality and (26) it is easy to check that:

$$L_D(\alpha\boldsymbol{\lambda}) \leq -\alpha^2\frac{1}{4\rho}[\langle \boldsymbol{\lambda}, \overline{\overline{\boldsymbol{v}}}^k(\boldsymbol{\lambda}) \rangle]^2 + \alpha\left(\frac{1}{2\rho} + t_k\right)\langle \boldsymbol{\lambda}, \overline{\overline{\boldsymbol{v}}}^k(\boldsymbol{\lambda}) \rangle - \frac{1}{4\rho} + \alpha\langle \boldsymbol{\lambda}, \boldsymbol{w} \rangle < -\frac{1}{4\rho}.$$

The assumed positivity of $\langle \boldsymbol{\lambda}, \overline{\overline{\boldsymbol{v}}}^k(\boldsymbol{\lambda}) \rangle$ combined with its continuity and compactness of the set $\boldsymbol{\mathcal{A}}(\mathbb{O}_n, \varepsilon, 1)$ implies that there exists:

$$\alpha_{max} = max_{\boldsymbol{\lambda} \in \boldsymbol{\mathcal{A}}(\mathbb{O}_n, \varepsilon, 1)} \, \alpha_0(\boldsymbol{\lambda}) > 1. \qquad (28)$$

From the above it follows that for any $\boldsymbol{\lambda}$ such that $\|\boldsymbol{\lambda}\| > \alpha_{max}$, we have:

$$L_D(\alpha \boldsymbol{\lambda}) < L_D(\mathbb{O}_n).$$

Thus the dual function maximization in (12) can be restricted to closed ball $\boldsymbol{\mathcal{B}}(\mathbb{O}_n, \alpha_{max})$ of radius α_{max}, i.e., the equivalence hols:

$$L_D(\hat{\boldsymbol{\lambda}}) = max_{\boldsymbol{\lambda} \in \mathcal{R}^n} \, L_D(\boldsymbol{\lambda}) = max_{\boldsymbol{\lambda} \in \boldsymbol{\mathcal{B}}(\mathbb{O}_n, \alpha_{max})} \, L_D(\boldsymbol{\lambda}), \qquad (29)$$

and the existence of $\hat{\boldsymbol{\lambda}}$ is guaranteed by continuity of $L_D(\boldsymbol{\lambda})$. Thus, we proved the next result.

Theorem 2. The solution $\hat{\boldsymbol{\lambda}}$ of the CP (12) there exists.

APPLICABILITY OF THE SCHEME

By a simple reasoning it is obvious that the scheme is applicable to the time-optimal control of the sequence of projects, i.e. ensures the determination of the optimal resource allocation, if and only if for every $\hat{\boldsymbol{\lambda}}$ being the solution of the dual problem (12):

$$\left(\hat{T}(\hat{\boldsymbol{\lambda}}), \hat{\boldsymbol{v}}^1(\hat{\boldsymbol{\lambda}}), \dots, \hat{\boldsymbol{v}}^k(\hat{\boldsymbol{\lambda}})\right)$$

is the solution to the original optimization task (5), (4), i.e., $\left(\hat{\boldsymbol{v}}^1(\hat{\boldsymbol{\lambda}}), \dots, \hat{\boldsymbol{v}}^k(\hat{\boldsymbol{\lambda}})\right)$ is the vector of the optimal performance speeds of the activities in the successive time intervals. It is well known that if the saddle point of the Lagrangian $L(T, \boldsymbol{v}^1, \dots, \boldsymbol{v}^k, \boldsymbol{\lambda})$ (6) there exists, then the dual approach can be successfully applied to solve (5), (4). If the solutions of IP tasks (10) and (11) are unique for any $\boldsymbol{\lambda} \in \mathcal{R}^n$, then the existence of a saddle point of the Lagrangian follows immediately from [8; Theorem 1, (ii) and (iii)]. Thus, the following theorem is valid.

Theorem 3. If the solutions of the IP tasks (10) and (11) are unique for any $\boldsymbol{\lambda} \in \mathcal{R}^n$, then the two-level scheme is applicable to the problem of time-optimal control of a sequence of projects of activities.

The uniqueness of IP solutions is guaranteed for any $\boldsymbol{\lambda} \in \mathcal{R}^n$, for example, if the sets $conv(\boldsymbol{V}^r)$, $r = 1, \dots, k$, are strictly convex, so for example when the functions f_{ri} in (1) are strictly concave [9,11,28], see also [12]. Note, hat in view of (29) the uniqueness requirement from Theorem 3 can be restricted to $\boldsymbol{\lambda} \in \boldsymbol{\mathcal{B}}(\mathbb{O}_n, \alpha_{max})$.Using [7; Lemmas 2.9 and 2.10] we can state for the case less restrictive than the uniqueness requirement from Theorem 3, the following condition.

Theorem 4. If the set $\boldsymbol{\Omega}(\hat{\boldsymbol{\lambda}})$, where:

$$\boldsymbol{\Omega}(\boldsymbol{\lambda}) = \left\{\boldsymbol{\omega}(\boldsymbol{\lambda}) = \sum_{r=1}^{k-1} \tau_r \hat{\boldsymbol{v}}^r(\boldsymbol{\lambda}) + \left(\hat{T}(\boldsymbol{\lambda}) - t_k\right)\hat{\boldsymbol{v}}^k(\boldsymbol{\lambda}) : \hat{\boldsymbol{v}}^r(\boldsymbol{\lambda}) \in \hat{\boldsymbol{V}}^r(\boldsymbol{\lambda})\right\},$$

consists of a single point for any $\hat{\boldsymbol{\lambda}}$ being the solution to CP task (12), then the scheme is applicable to optimal resource allocation problem.

Notice, that the last result requires only the uniqueness of the state vector $\hat{\boldsymbol{\omega}} = \boldsymbol{\omega}(\hat{\boldsymbol{\lambda}})$ achieved for the performance speeds $\hat{\boldsymbol{v}}^r(\hat{\boldsymbol{\lambda}})$, and the uniqueness of the vectors $\hat{\boldsymbol{v}}^r(\hat{\boldsymbol{\lambda}})$ is not required here. Thus, the optimal resource allocation does not have to be unique, if only the vector $\hat{\boldsymbol{\omega}}$ of final states is uniquely determined. Also, the uniqueness of the dual problem solution is not necessary. Note finally, that the applicability of the scheme requires, after all, the existence of a sadle point of the Lagrangian (6). However, this is the crucial necessary applicability condition for most decentralized schemes, c.f., [7,8].

COMPUTATION OF THE OPTIMAL RESOURCE ALLOCATION

Assume that the applicability conditions are satisfied and the two-level scheme results in:

$$\left(\hat{T}, \hat{\boldsymbol{v}}^1, \dots, \hat{\boldsymbol{v}}^k\right),$$

where: $\hat{T} = \hat{T}(\hat{\boldsymbol{\lambda}})$ and $\hat{\boldsymbol{v}}^r = \hat{\boldsymbol{v}}^r(\hat{\boldsymbol{\lambda}})$ for $r = 1, \dots, k$. Note, that in view of Proposition 1 by the known Caratheodory's theorem, which asserts that any boundary point of the convex hull of compact set in $\mathcal{R}^n$ is a convex combination of its extreme points, the vectors $\hat{\boldsymbol{v}}^r$ can be expressed as:

$$\hat{\boldsymbol{v}}^r = \sum_{s=1}^{p_r} \alpha_r^s \, \hat{\boldsymbol{v}}^{r,s}, \qquad (30)$$

where: $\hat{\boldsymbol{v}}^{r,s} \in \boldsymbol{V}^r$ for $s = 1, \dots, p_r$, and the nonnegative constants α_s^r are such that $\sum_{s=1}^{p_r} \alpha_r^s = 1$ for $r = 1, \dots, k$.

Let us introduce the vector function:

$$\hat{\boldsymbol{u}}(t) = \begin{cases} \hat{\boldsymbol{u}}^{r,s} & t_r + \tau_r^{s-1} \le t < t_r + \tau_r^s, \; s = 1, \dots, p_r, r = 1, \dots, k \\ \hat{\boldsymbol{u}}^{k,n} & t = \hat{T} \end{cases}, \qquad (31)$$

where $\widehat{\boldsymbol{u}}^{r,s} \geq \mathbb{O}_n$ are such that:

$$\widehat{\boldsymbol{v}}^{r,s} = \boldsymbol{f}(\widehat{\boldsymbol{u}}^{r,s})$$

and

$$\tau_r^s = \sum_{q=1}^{s} \alpha_r^q \, \tau_r \text{ for } s = 1, \dots, p_r, \; r = 1, \dots, k-1,$$

and for the last time interval:

$$\tau_k^s = \sum_{q=1}^{s} \alpha_k^q \left(\hat{T} - \, t_k\right), \; s = 1, \dots, n,$$

with $\tau_r^0 = 0$, $r = 1, \dots, k$. If the activities models f_{ri} are strictly increasing, then:

$$\widehat{\boldsymbol{u}}^{r,s} = \boldsymbol{f}^{-1}(\widehat{\boldsymbol{v}}^{r,s}),$$

where $\boldsymbol{f}^{-1}$ denotes the inverse function. By virtue of (30) and the definitions of the sets $\boldsymbol{V}^k$ and $\boldsymbol{U}^k$, the conditions (*i*), (*ii*) are satisfied for $\widehat{\boldsymbol{u}}(t)$ in (31), in view of (4) the given terminal state $\boldsymbol{w}$ is reached, thus $\widehat{\boldsymbol{u}}(t)$ (31) is admissible resource allocation (control), and in view of Theorems 1 and 3 or 4 its optimality is guaranteed. The control (31) is generally not unique in the set of time-optimal resource allocations. In view of the above, there is at least one piecewise constant time-optimal resource allocation with at most $\sum_{r=1}^{k} p_r - 1$ discontinuity points.

COMPUTATIONAL ALGORITHM

The computations should be arranged hierarchically in two-level structure, i.e., in each iteration of the maximization procedure of CP level the whole optimization procedures for solving IP independent tasks must be realized (see, Fig. 1).

Step 1: Determine in the following two-level computations the optimal speeds $(\widehat{\boldsymbol{v}}^1, \dots, \widehat{\boldsymbol{v}}^k)$ in the successive time intervals, $r = 1, \dots, k$, and the optimal performance time $\hat{T}$.

Step 1.0: Choose the initial point $\boldsymbol{\lambda}^o$ for numerical procedure applied to solve the coordination problem (12).

Step 1.1: Let $\boldsymbol{\lambda}^m$ be the m-th iterate in the numerical maximization procedure chosen to solve (12). For $\boldsymbol{\lambda} = \boldsymbol{\lambda}^m$ solve $k-1$ independent local resource allocation tasks (10) and the task (11) according to the chosen numerical optimization procedures and determine the performance speeds $\widehat{\boldsymbol{v}}^r(\boldsymbol{\lambda}^m)$, $r = 1, \dots, k-1$, and $\left(\hat{T}(\boldsymbol{\lambda}^m), \widehat{\boldsymbol{v}}^k(\boldsymbol{\lambda}^m)\right)$.

Step 1.2: Using $\widehat{\boldsymbol{v}}^r(\boldsymbol{\lambda}^m)$, $r = 1, \dots, k$ and $\hat{T}(\boldsymbol{\lambda}^m)$ compute, according to the numerical procedure selected to solve CP (12), the new vector of prices $\boldsymbol{\lambda}^{m+1}$ which is the next approximation of $\hat{\boldsymbol{\lambda}}$. If for $\boldsymbol{\lambda}^{m+1}$ the stopping rule of the chosen maximization scheme is satisfied, e.g.:

$$\|\boldsymbol{\lambda}^{m+1} - \boldsymbol{\lambda}^m\| \leq \varepsilon_1$$

or

$$|L_D(\boldsymbol{\lambda}^{m+1}) - L_D(\boldsymbol{\lambda}^m)| \leq \varepsilon_2,$$

where ε_1 and ε_2 are preselected small positives, put:

$$\widehat{\boldsymbol{v}}^r = \widehat{\boldsymbol{v}}^r(\boldsymbol{\lambda}^m), \; r = 1, \dots, k$$

as the vectors of the optimal performance speeds and:

$$\hat{T} = \hat{T}(\boldsymbol{\lambda}^m)$$

as the optimal performance time of the multi–project and go to step 2. Otherwise return to step 1.1 and continue the computations for $\boldsymbol{\lambda} = \boldsymbol{\lambda}^{m+1}$.

Step 2: Compute the vector of the optimal control $\widehat{\boldsymbol{u}}(t)$ according to (31).

Remark 1. It is known that too large Lagrangian functions may be a drawback when applying numerical optimization, since large Lagrangians cannot completely prevent the constraint from violation. This disadvantage is overcome in the scheme. The equivalence (29) implies that CP can be replaced by dual function maximization with the constrain:

$$\boldsymbol{\lambda} \in \boldsymbol{\mathcal{B}}(\mathbb{O}_n, \alpha_{max})$$

imposed. However, the numerical studies suggest that it is unnecessary in most cases.

Remark 2. The appealing feature of the scheme is that only the values of local Lagrangians $L_r(\widehat{\boldsymbol{v}}^r(\boldsymbol{\lambda}^m), \boldsymbol{\lambda}^m)$ and $L_k\left(\hat{T}(\boldsymbol{\lambda}^m), \widehat{\boldsymbol{v}}^k(\boldsymbol{\lambda}^m), \boldsymbol{\lambda}^m\right)$, not the IP solutions $\widehat{\boldsymbol{v}}^r(\boldsymbol{\lambda}^m)$ and $\hat{T}(\boldsymbol{\lambda}^m)$, are used for $\boldsymbol{\lambda}^m$ in successive iterations of the numerical procedure solving CP (see Fig. 1).

Remark 3. In view of Proposition 1, the vectors resulting from the IP tasks in each iteration of numerical procedure solving CP are such that:

$$\widetilde{\boldsymbol{v}}^r = \widehat{\boldsymbol{v}}^r(\boldsymbol{\lambda}^m) \in bd[conv(\boldsymbol{V}^r)].$$

Thus $\widetilde{\boldsymbol{v}}^r$ can be expressed as a convex combination of the form (30). Hence the respective control $\widetilde{\boldsymbol{u}}^r(t)$ of the form (31) exists and can be treated as an approximate solution of the overall problem.

Remark 4. Since $L_D(\boldsymbol{\lambda})$ is continuous concave function on $\mathcal{R}^n$ (Proposition 2), known sub-gradient methods of non-differentiable optimization [3,6] may be implemented for constrained maximization task (12). Also (10) and (11) (equivalently (18) or (19)) are convex optimization tasks and can be solved by using standard convex programming methods [3].

Both in centralized (global) resource allocation by direct T minimization in (3) (or equivalently in (5)) subject to constraints (4) and in decentralized computations of the scheme, there are two types of constraints. The inequality constraints:

$$0 \leq \alpha_r^s \leq 1 \text{ and } \hat{v}_{ri}^{r,s} \geq 0,$$

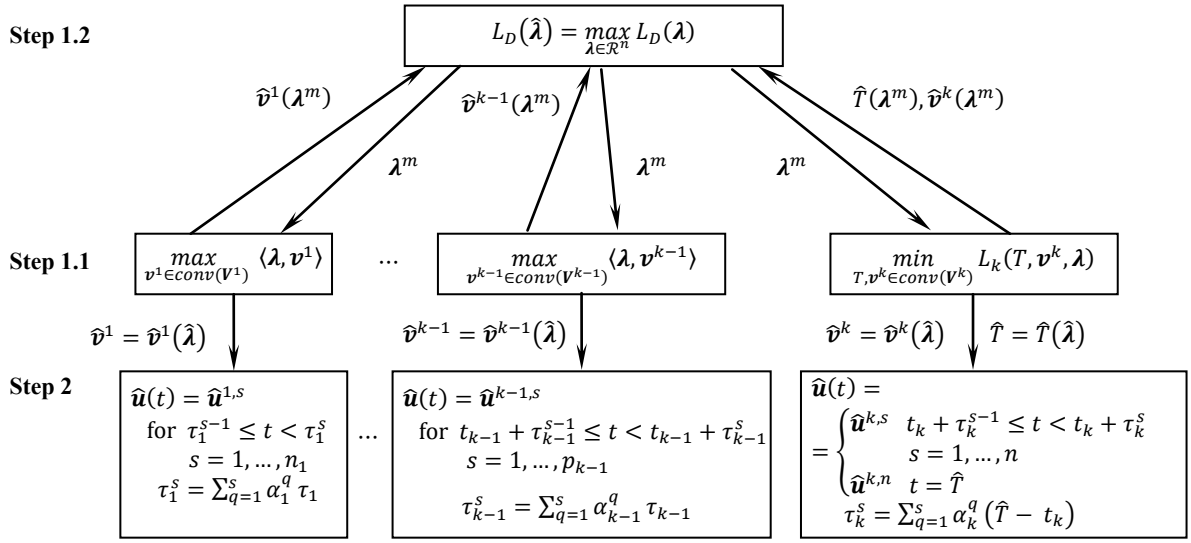

Fig. 1. Two-level decentralized procedure for optimal resource allocation

which are imposed on every α_r^s and $\hat{v}_{ri}^{r,s}$, $i = 1, \dots, n_r$, $s = 1, \dots, p_r$, $r = 1, \dots, k$ in the convex combination representation (30) of $\hat{\boldsymbol{v}}^r$. The set of equality constraints is composed of convex combination coefficients sum:

$$\sum_{s=1}^{p_r+1} \alpha_r^s = 1$$

and the total resource usage constraints imposed on any $\hat{\boldsymbol{v}}^{r,s}$ in (30). If the functions f_{ri} are strictly increasing, i.e. f_{ri}^{-1} exists for each operation, then in view of Proposition 1 the last constraints take the form:

$$\sum_{q=1}^r \sum_{i=1}^{n_q} f_{qi}^{-1}(\hat{v}_{qi}^{r,s}) = N, \; s = 1, \dots, p_r, r = 1, \dots, k.$$

In the case of centralized resource allocation by direct T minimization the total number of constraints (inequality and equality) is equal to:

$$CN = \sum_{r=1}^{k-1}[1 + 3p_r + p_r^2] + 1 + 4n + n^2,$$

while the number of optimization variables:

$$DV = 1 + \sum_{r=1}^{k-1}[2p_r + p_r^2] + 2n + n^2.$$

For decentralized scheme the number of constraints for IP (10):

$$CN_r = 1 + 3p_r + p_r^2, r = 1, \dots, k-1,$$

and for the last local task (11) is:

$$CN_k = 1 + 3n + n^2.$$

The respective numbers of optimization variables are as follows:

Table 1. The numbers of optimization variables and constraints (inequalities and equalities together) in global and decentralized approaches; the meanings of symbols are explained in the text

Each project composed of $n_r = 2$ operations				
k	2	4	6	8
DV	33	161	449	961
CN	44	192	508	1056
DV_r	8,25	8,24,48,81	8,24,48,80,120,169	8,24,48,80,120,168,224,289
CN_r	11,29	11,29,55,89	11,29,55,89,131,181	11,29,55,89,131,181,239,305
Each project composed of $n_r = 4$ operations				
k	2	4	6	8
DV	105	561	1625	3553
CN	126	620	1738	3736
DV_r	24,81	24,80,168,289	24,80,168,288,440,625	24,80,168,288,440,624,840,1089
CN_r	29,89	29,89,181,305	29,89,181,305,461,649	29,89,181,305,461,649,869,1121

$$DV_r = 2p_r + p_r^2 \text{ for } r = 1, \dots, k-1$$

and

$$DV_k = 1 + 2n + n^2.$$

To compare the computations for decentralized and global approaches the numbers of optimization variables and constraints are summarized in Table 1 and visualized in Fig. 2 and 3 for a few exemplary sequences of projects data. In Fig. 2 and 3 the average numbers of both the optimization variables and constraints for decentralized approach are given. The sequences of $2-8$ projects, each project set composed of 2,4,6 activities, were included in the experiment. One can observe from Table 1 and Fig. 2,3, that the mean numbers of the optimization variables and constraints are evidently reduced for decentralized approach in comparison to the primary global optimization task.

FINAL REMARKS

Efficient time-decomposition algorithm for finding globally optimal resource allocation is proposed and discussed. The Lagrangian based time-decomposition approach is applied. It allows the global solution to be found in decentralized manner. The convexification technique is combined with the price coordination in order to guarantee its applicability. The necessary and sufficient applicability conditions are derived and analyzed. Taking into account the specific properties of IP and CP tasks it is proved that the scheme is applicable to time-optimal resource allocation even if the solutions of lower level and coordination tasks are not unique. The applicability conditions suggest that the scheme can be successfully applied to find the optimal resource allocation for a wide class of activity models, including, in particular the commonly used in project modelling practice models being concave with respect to the resource amount. The considerable decrease on the mean numbers of both the optimization variables and constraints are reported for the scheme. An alternative approach of local optimization of a sequence of project is proposed in [11], according to which the choice of the optimal control is made at every moments t_r of the successive project appearance for all the activities actually at performance and the final states of activities that are equal to given terminal states minus the states so far reached. However, for control determined by this algorithm the performance time is, in general, greater than the globally optimal performance time determined by two-level scheme. A considerable range of technical and economic applications should be pointed out. The main fields are the following: the allocation of working power of building concern among enterprises in the course of building (cf., [9]), the allocation of a financial outlay among projects under constrained intensity of investing [1,2,5,6,9,23], the allocation of a common primary memory among independent tasks appearing at different times in a multiprocessor systems (cf., [1,21,24,27]), can be also applied in decision support intelligent systems [22], where different resources with constrained consumption must be optimized.

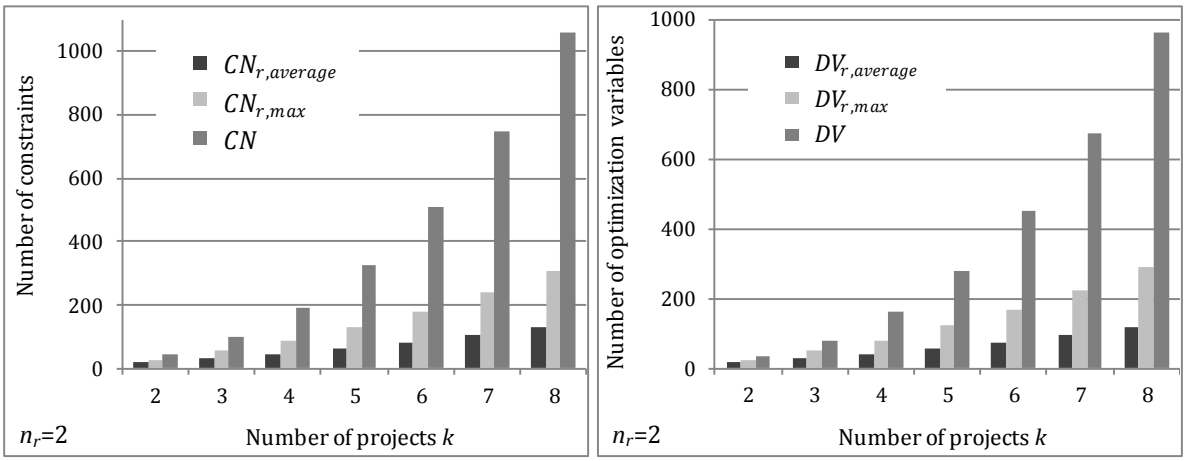

Fig. 2. The numbers of optimization constraints and variables in global and decentralized approach; $CN_{r,max}$, $DV_{r,max}$ and $CN_{r,average}$, $DV_{r,average}$ – maximal and average numbers of constraints and decision variables for IP tasks, CN and DV – the total numbers of constraints and optimization variables for global approach, number of project activities $n_r = 2$

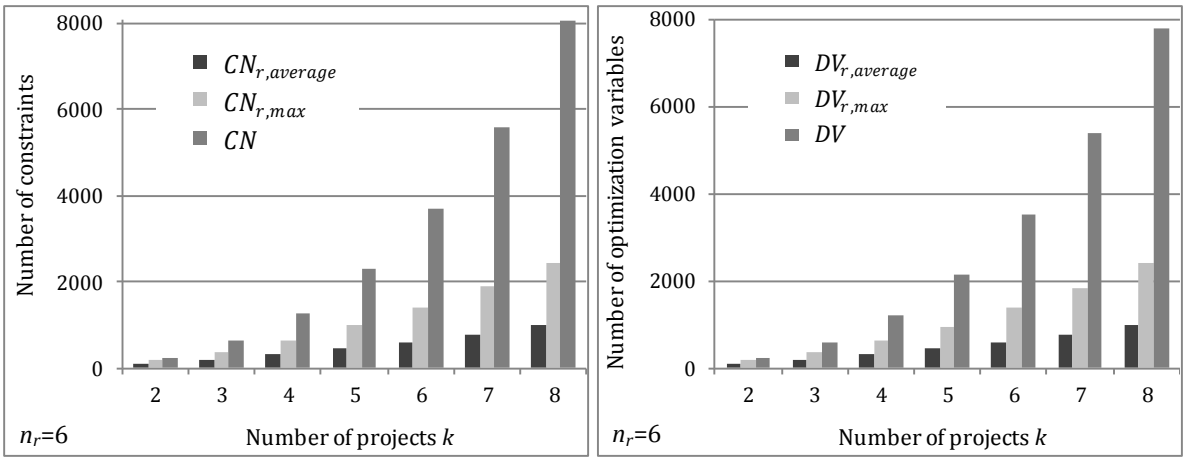

Fig. 3. The numbers of optimization constraints CN, $CN_{r,max}$, $CN_{r,average}$ and variables DV, $DV_{r,max}$, $DV_{r,average}$ in global and decentralized approaches, number of project activities $n_r = 6$

REFERENCES

1. **Błażewicz J., Ecker K.H., Pesh E., Schmidt G., Węglarz J. (Eds) 2010.** Scheduling Computer and Manufacturing Processes. Springer-Verlag, Berlin, Heidelberg, New York.
2. **Błażewicz J., Ecker K.H., Pesh E., Schmidt G., Węglarz J. (Eds) 2007.** Handbook on Scheduling: From Theory to Applications. Springer-Verlag, Berlin, Heidelberg, New York.
3. **Boyd S., Vandenberghe L. 2004.** Convex Optimization. Cambridge University Press, Cambridge, New York, Melbourne, Madrid, Cape Town, Singapore, São Paolo, Delhi.
4. **Burkov V.N. 1966.** Resources distribution as a problem of time optimality. Avtomatika i Telemekhanika, Vol. 27, No. 7, 119–129 (in Russian).
5. **Burkov V.N. 1996.** Economical mechanisms of production management. Moscow, 32.
6. **Dem'yanov V.F., Vasil'ev L.V. 2012.** Nondifferentiable Optimization. Springer, New York.
7. **Findeisen W., Bailey F.N., Brdyś M., Malinowski K., Tatjewski P., Woźniak A. 1980.** Control and Coordination in Hierarchical Systems. Wiley, New York.
8. **Hasiewicz Z., Stankiewicz A. 1985.** On Applicability of Interaction Balance Method to Global Identification of Interconnected Steady-State Systems. IEEE Transactions on Automatic Control, Vol. 31, No. 1, 77–80.
9. **Janiak A. 1991.** Exact and approximate algorithm of job sequencing and resource allocation in discrete manufacturing processes. Wyd. Politechniki Wrocławskiej, Wrocław (in Polish).
10. **Janiak A., Portmann M-C. 1998**. Genetic algorithm for the permutation flow-shop scheduling problem with linear models of operations. Annals of Operations Research, Vol. 83, 95–114.
11. **Janiak A., Stankiewicz A. 1983.** The equivalence of local and global time-optimal control of a complex of operations. International Journal of Control, Vol. 38, No. 6, 1149–1165.
12. **Janiak A., Stankiewicz A. 1988.** On Time-Optimal Control of a Sequence of Projects of Activities under Time-Variable Resource. IEEE Transactions on Automatic Control, Vol. 33, No. 3, 313–316.
13. **Józefowska J. 2007.** Just-in-time scheduling. Models and Algorithms for Computer and Manufacturing Systems. Springer, Berlin, Heidelberg, New York.
14. **Józefowska J., Węglarz J. 1998.** On a methodology for discrete-continuous scheduling problems. European Journal of Operational Research, Vol. 107, No. 2, 338–353.
15. **Kis, T. 2006.** RCPS with variable intensity activities and feeding precedence constraints. In: International Series in Operations Research and Management Science. (Vol. 92, pp. 105–129). Springer New York LLC.
16. **Klein R. 2000.** Scheduling of Resource–Constrained Projects. Kluwer Academic Publishers, Boston, London.
17. **Kogan K. 2006.** Optimal scheduling of parallel machines with constrained resources. European Journal of Operational Research, Vol. 170, 771–787.
18. **Kogan K., Khmelnitsky E. 1998.** Tracking Demands in Optimal Control of Managerial Systems with Continuously-divisible, Doubly Constrained Resources. Journal of Global Optimization, Vol. 13, 43–59.
19. **Leachman R.C., Dincerler, A., Kim S. 1990.** Resource-constrained scheduling of projects with variable-intensity activities. IIE Transactions, Vol. 22, No. 1, 31–39.
20. **Lerner A.Ya., Tejman A.I. 1969.** On Optimal Resourees Allocation, Proc. 4-th Congress of the International Federation of Automatic Control, Warszawa 16-21 June 1969. Technical Session No. 35, Wyd. NOT, Warszawa, pp. 3–20.
21. **Leung J.Y-T. 2004.** Handbook of Scheduling: Algorithms, Models, and Performance Analysis. Chapman & Hall/CRC Computer and Information Science Series. CRC Press.
22. **Lytvyn V., Oborska O., Vovnjanka R. 2015.** Approach to decision support intelligent systems development based on ontologies. ECONTECHMOD, Vol. 4. No. 4, 29–35.

23. **Petrovich J.M., Novakivskii I.I. 2012.** Modern concept of a model design of an organizational system of enterprise management. ECONTECHMOD, Vol. 1, No. 4, 41–48.
24. **Schwindt Ch. 2006.** Resource Allocation in Project Management. Springer Science & Business Media, Heidelberg, New York, London.
25. **Słowiński R., Weglarz J. 2013.** Advances in Project Scheduling. Studies in Production and Engineering Economics. Elsevier.
26. **Węglarz J. 1976.** Time-optimal control of resource allocation in a complex of operations framework. IEEE Transactions on Systems, Man, and Cybernet. Vol. 6, No. 11, 783–788.
27. **Weglarz J. 1980.** Multiprocessor scheduling with memory allocation–A deterministic approach. IEEE Transactions on Computers., Vol. 29, 703–709,
28. **Węglarz J., Józefowska J., Mika M., Waligóra G. 2011.** Project scheduling with finite or infinite number of activity processing modes–A survey. European Journal of Operational Research, Vol. 208, 177–205.
29. **Zangwill W.I. 1969.** Nonlinear Programming; a Unified Approach. Prentice-Hall, Englewood Cliffs, New Jersey, USA.

Dual model for classic transportation problem as a tool for dynamizing management in a logistics company

Jacek Wawrzosek, Szymon Ignaciuk

Department of Applied Mathematics and Computer Science, Faculty of Production Engineering, University of Life Sciences in Lublin, Poland
Głeboka 28, PL 20 612 Lublin, Poland
e-mail: jacek.wawrzosek@up.lublin.pl, szymon.ignaciuk@up.lublin.pl

Received August 12.2016: accepted September 01.2016

Abstract. This paper presents and, for the first time, widely interprets the dual model for the classic model of the transportation problem. Moreover, potential possibilities connected with the use of ambiguities of the obtained solutions to the dual problem have been shown. It has been pointed out how these capabilities can be applied to a flexible financial policy of a logistics company.

Key words: transport logistics, transport model, primary and dual problems, cost, revenue

INTRODUCTION

The process of turning inside out is mainly related to tailoring and it is used in altering a garment by turning the fabric inside out. It allows the owner of the garment to obtain additional benefits existing within the fabric of the clothing. This concept has its counterpart in problems of linear programming (*LP*) in the form of a pair of primary and dual problems. Both of these issues also have their economic sources. F.L. Hitchcock [9] formulated the transportation problem, and G. Stigler [25] distinguished the mathematical problem of diet related directly to the war and food rationing. J. von Neumann was familiar with the duality principle as early as in 1947, but directly after G. Dantzig [2] formulated the general *LP* problem covering transport and diet, von Neumann proposed his duality theorem pertaining to the *LP* problem. Later, Dantzig [3] introduced the simplex algorithm for *LP*. Since then, different methods of operational research have been widely developed, including the problem of algorithmization of *LP* [8, 12, 23, 24, 31].

Each primary model of the linear programming problem has a corresponding dual model. Creating a dual model consists of:

1. converting a maximization problem into one of minimization or vice-versa,
2. creating *decision variables* (*DecVar_D*) for the *dual* model in a number equal to the number of the *limiting conditions* (*LC_P*) of the original *primary* model,
3. transposition of the matrix $\boldsymbol{A}$ of the *limiting conditions*,
4. exchanging the roles between the parameters $\boldsymbol{b}$ of the right sides *of the limiting conditions* (*LC_P*) and the coefficients $\boldsymbol{c}$ of the *objective function* (*OF_P*),
5. the appropriate change in the relations between the left and right side of the *limiting conditions*,
6. proper modification of the *boundary conditions* (*BC*).

Strict rules formulating the principles of creating the dual problem are known in the literature [4, 5, 8, 13, 18]. The simplex method, in addition to determining the optimal solution for the original problem, also allows specifying a solution to the dual problem. Following the creator of the dual problem for the issues concerning the *linear programming*, it should be noted that the aforementioned operations, originating from optimization problems of the revenues generated from production, lead to the dual problem model, where the competition intends to buy the company for the cheapest price possible. At the same time, maximizing the revenues from the selection range of production is replaced by the minimization of the purchase costs of the means of production from the manufacturer [7, 14, 30]. Hence, the dual problem has found its permanent place in planning business activities. It manifests itself through the use of dual models for developing the business plans with post-optimization methods and is intended to provide stability to a business venture when

changing the planned parameters describing the situation of the enterprise and its environment.

Started in 1947 by J. von Neumann, the process of using the dual models in various technical and economic problems leads to increasingly more precise description of encountered problems, thus contributing to the development and dynamization of various business activities. So far, the dual problem solution serves mainly the post-optimization procedure, i.e. the analysis of modification of the primary model [21, 22, 28, 29]. However, the dual model itself is not generally subject to a deeper study and no conclusions are drawn from its full analysis.

Instability of parameters of the transportation model corresponds to the dynamic economic conditions and the difficulties of strictly defining them [1, 15], to the changes which result from the introduction of innovative solutions in the enterprise [11], the highly variable political and legal environment [17, 27]. Moreover, MacKenzie, et al. [16], Schrijver [20], Sab [19] and Glaeser [6] point to the sensitivity of the transport systems for natural disasters, military operations and terrorist threats.

The ambiguity of the solution of the dual model to the classic transportation problem has neither been properly studied yet, nor included in the literature, and its exhaustive interpretation has not been presented. This is despite the permanent place of the transportation models in solving economic issues. This paper attempts to provide a possibly broad interpretation of the economic advantages inherent to this ambiguity. It is presented in the following example. This dual model is the basis for a problem that has not been discussed here, namely the *post-optimization* resulting from changes in the parameters of the primary model. Post-optimization problems for the transport models are not fully studied, and some recent results in this area can be found in studies [10, 26, 27, 28, 29].

MATERIAL AND METHODS – A MATHEMATICAL MODEL OF THE CLASSIC TRANSPORTATION PROBLEM

I The primary problem: Company *A* mediates transport between two warehouses: M_1 and M_2 and three stores: S_1, S_2, S_3. The quantity of goods in the warehouses is 40 and 60 tonnes, respectively. The stores' requirements are 35, 35 and 30 tonnes, respectively. *The established unit costs* of transport borne by the logistics company *A* in €/tonne are presented in Table 1 below.

Table 1. The unit transport costs c_{ij} between warehouses M_i and stores S_j

c_{ij}	S_1	S_2	S_3
M_1	7.3	8.2	6.5
M_2	8	6.9	7.4

The problem consists in establishing the transport plan, i.e., ***which transport routes should be taken to minimize the total transport costs***?

Since the total supply is equal to the total demand, the classic ***primary ZZT1 model*** was applied to the balanced transportation problem in the following form:

$$\boldsymbol{A}=\begin{bmatrix}1&1&1&0&0&0\\0&0&0&1&1&1\\1&0&0&1&0&0\\0&1&0&0&1&0\\0&0&1&0&0&1\end{bmatrix},\qquad \boldsymbol{b}=\begin{bmatrix}40[t]\\60[t]\\35[t]\\35[t]\\30[t]\end{bmatrix},\qquad \boldsymbol{c}=\begin{bmatrix}7.3[€/t]\\8.2[€/t]\\6.5[€/t]\\8.0[€/t]\\6.9[€/t]\\7.4[€/t]\end{bmatrix},\quad \boldsymbol{x}=\begin{bmatrix}x_{1,1}\\x_{1,2}\\x_{1,3}\\x_{2,1}\\x_{2,2}\\x_{2,3}\end{bmatrix},$$

DecVar_P (*the decision variables in the primary model*): $x_{i,j}$ - stock quantity [*t*] transported from the *i*-th warehouse to the *j*-th shop store $i \in \{1,2\}$, $j \in \{1,2,3\}$,

OF_P:	$f_P(\boldsymbol{x}) = \boldsymbol{c}' \cdot \boldsymbol{x} \rightarrow min$	*the objective function in the primary model,*
LC_P:	$\boldsymbol{A} \cdot \boldsymbol{x} = \boldsymbol{b}$,	*the limiting conditions in the primary model,*
BC_P:	$x_{i,j} \geq 0$; i=1,2; j=1,2,3	*the boundary conditions in the primary model.*

The limiting conditions are to ensure the implementation of the supply and demand. Note, that for $\boldsymbol{w}' = [w_i]'_{i\in\{1,\dots5\}} = [1; 1; -1; -1; -1]$ we have $\boldsymbol{w}' \cdot \boldsymbol{A} = \boldsymbol{0}$. Hence, we get *the balance condition* of total supply and total demand in the form of $\boldsymbol{w}' \cdot \boldsymbol{b} = 0$. The only vectors orthogonal towards $\boldsymbol{A}$ in the form of $s \cdot \boldsymbol{w}$, where $s \in R\backslash\{0\}$ are the *balancing vectors* which describe the linear dependence of the ranks of the matrix A. The existence of the vector $\boldsymbol{w}$ causes the rank of the matrix $\boldsymbol{A}$ of the size (5×6) to equal 4, i.e. *the number of warehouses* (2) plus *the number of stores* (3) minus 1.

II The dual problem: The logistic company *A* decided to support the transport from the warehouses M_1 and M_2 to the stores S_1, S_2, S_3. It was established that from the warehouses M_1 and M_2 40 and 60 tonnes, respectively, would be transported. And to the stores S_1, S_2, S_3, 35, 35 and 30 tonnes, respectively, would be delivered. It is known that the *unit revenue* [€/t] from the transport of 1 tonne of goods on a specified route *does not exceed* the values contained in Table 1. The problem is, then,

what revenues should the company A generate while receiving goods from different warehouses, and what revenues should it generate while providing for each store to <u>maximize the total revenue</u>?

The dual model for ZZT1 is the following:

DecVar_D (*the decision variables in the dual model*): y_i - revenue (loss) per unit [€/*t*] obtained for: the acceptance of one tonne of goods from the *i*-th warehouse for $i \in \{1,2\}$; or at the delivery of one tonne of goods to the (*i*-2)-th stores for $i \in \{3,4,5\}$; $\boldsymbol{y} = [y_i]_{i\in\{1,\dots,5\}}$,

OF_D:	$f_D(\boldsymbol{y}) = \boldsymbol{b}' \cdot \boldsymbol{y} \rightarrow max$	*the objective function in the dual model,*
LC_D:	$\boldsymbol{A}' \cdot \boldsymbol{y} \leq \boldsymbol{c}$,	*the limiting conditions in the dual model,*
BC_D:	$y_i \in R$; i=1,… ,5	*the boundary conditions in the dual model.*

Since *the limiting conditions* are to ensure the return of the unit transport costs on the routes where the cargo transport will take place, we have the following equations in *LC_D* [21].

In the primary problem, the minimization of the total costs of transport is associated with the needs of senders and recipients. In the dual model it is represented by a logistics company's pursuit to obtain the maximum revenue from the transport services. What can be observed here is the opposite convergence to the common optimum of total costs and revenues amounting to [€]709.50. While creating this dual model, we can note that it is necessary to change the way of indexation of the *decision variables* in the dual problem from double to single. Consequently, the transport organisation in a transport company is divided into inbound transport (with the corresponding indexes from 1 to 2) and outbound transport (with the corresponding indexes from 3 to 5). In the dual model, the direct routes connecting senders and recipients disappear. The company performs any potential transhipment procedures in their own facilities.

RESULTS AND DISCUSSION

Ambiguity of the dual problem solution. Despite the fact that the *objective function* value amounting to [€]709.50 is common for the primary and dual problems, in this case the unambiguous, integer, non-negative solution to the primary problem in the form of the vector $\boldsymbol{x}^{*\prime} = \left[x^*_{1,1};\ x^*_{1,2};\ x^*_{1,3};\ x^*_{2,1};\ x^*_{2,2};\ x^*_{2,3}\right] =$ $[10;\ 0;\ 30;\ 25;\ 35;\ 0]$ is accompanied by the one-dimensional space *J* of real solutions to the dual problem. The manner of its representation is not unambiguous either. For example, it may be the following:

$$\tilde{\boldsymbol{y}}^*_t = \tilde{\boldsymbol{y}}^* + t \cdot \left(\tilde{\boldsymbol{y}}^* - \tilde{\tilde{\boldsymbol{y}}}^*\right),$$

where
$\tilde{\boldsymbol{y}}^{*\prime} = [\tilde{y}^*_1;\ \tilde{y}^*_2;\ \tilde{y}^*_3;\ \tilde{y}^*_4;\ \tilde{y}^*_5] = [7.3;\ 8.0;\ 0;\ -1.1;\ -0.8]$,
$\tilde{\tilde{\boldsymbol{y}}}^{*\prime} = [\tilde{\tilde{y}}^*_1;\ \tilde{\tilde{y}}^*_2;\ \tilde{\tilde{y}}^*_3;\ \tilde{\tilde{y}}^*_4;\ \tilde{\tilde{y}}^*_5] = [6.2;\ 6.9;\ 1.1;\ 0;\ 0.3]$,
$t \in R$. Hence, alternatively, the space *J* can be also formulated as

$$\boldsymbol{y}^*_s = \tilde{\boldsymbol{y}}^* + s \cdot \boldsymbol{w} = \tilde{\boldsymbol{y}}^*_{1.1\cdot t}$$

where $\boldsymbol{w}$ is a pre-defined *balancing vector* of the classic transportation problem, and $R \ni s = 1.1 \cdot t$ (cf. Fig. 1). Note that for each $s \in R$ the ambiguity of the solution of the dual problem stems from the orthogonality of the balancing vector $\boldsymbol{w}$ against the matrix $\boldsymbol{A}$ and the vector $\boldsymbol{b}$ because:

$$\begin{aligned} f_D(\boldsymbol{y}^*_s) &= \boldsymbol{b}' \cdot \boldsymbol{y}^*_s = \boldsymbol{b}' \cdot (\tilde{\boldsymbol{y}}^* + s \cdot \boldsymbol{w}) \\ &= \boldsymbol{b}' \cdot \tilde{\boldsymbol{y}}^* + s \cdot (\boldsymbol{w}' \cdot \boldsymbol{b})' = \boldsymbol{b}' \cdot \tilde{\boldsymbol{y}}^* \\ &= 709.50[€] \end{aligned}$$

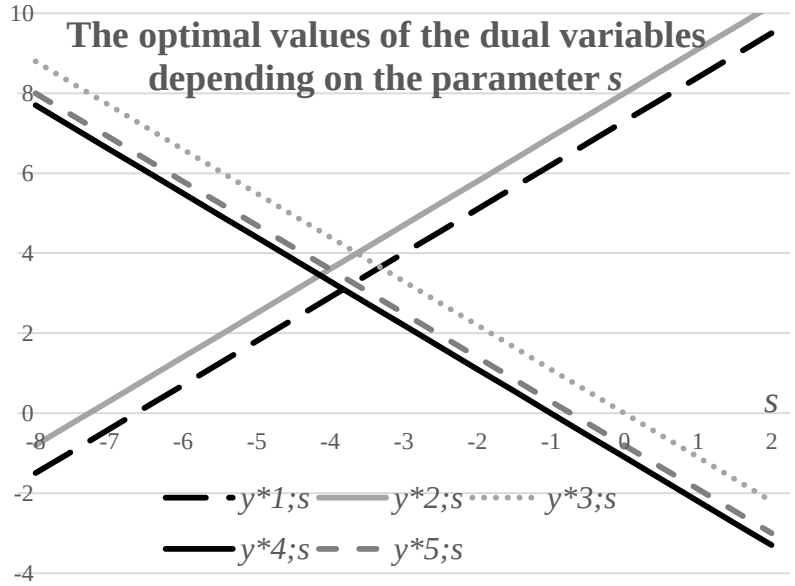

Fig. 1. The optimal values of the dual variables depending on the parameter s

Interpretation of *the limiting conditions of the* dual problem. Interestingly, *LC*1_*D* means that the revenue obtained from the inbound transport of the goods from warehouse 1 integrated with the separate revenue from the outbound transport to store 1 cannot exceed 7.3[€/t] which is the previously established unit cost of transport of 1 [*t*] of cargo on this route. The other *limiting conditions* must be interpreted similarly. Since the values of y_i are not limited by the *boundary conditions*, y_i^* can be shaped freely so that $\boldsymbol{y}^*$ belong to the space *J*. At the same time, it is observed that this surprising limitlessness in *boundary conditions* results also in the possibility of negative dual values of *decision variables*, however, it has its economic justification presented below.

An exemplary solution of the dual problem: 1) $\boldsymbol{y}^*_{-2.2}{}' = [5.1; 5.8; 2.2; 1.1; 1.4]$ for s = -2.2 is interpreted as achieving positive revenues from all inbound and outbound transport procedures; 2) For $s \in [-4.55; -3.65]$ all counterparties provide the company with quite similar inbound and outbound transport revenues (see Fig. 1); 3) For $\widetilde{\widetilde{\boldsymbol{y}}}^* = \boldsymbol{y}^*_{-1.1} = [6.2; 6.9; 1.1; 0; 0.3]'$ distribution to store 2 does not yield revenue; 4) For $\widetilde{\boldsymbol{y}}^* = \boldsymbol{y}^*_0 = [7.3;\ 8.0;\ 0;\ -1.1;\ -0.8]'$ distribution to store 1 does not yield any revenue and outbound transport to stores 2 and 3 yields losses balanced by the increased revenue obtained only from the delivery from warehouses 1 and 2. For $\widetilde{\boldsymbol{y}}^*$, the revenue of the logistics company is shaped only by the revenue obtained from warehouses. This means that the total transport costs are shifted onto only some of the participants in the goods' circulation. Distribution to stores 2 and 3 is associated with losses on the part of the logistics company.

The unit costs of transport estimated in the primary problem do not indicate business entities that are actually supposed to participate in these costs. The fourth selected sample vector $\widetilde{\boldsymbol{y}}^*$ breaks down the logistics company's counterparties into revenue-generating, loss-generating and neutral entities. Fig. 1 enables reading other sample values of the optimal dual variables according to the parameter *s*.

One should notice that zeros for the *i*-th vector coordinate of the optimal dual prices $\boldsymbol{y}_s^* = [y_{1;s}^*;\ y_{2;s}^*;\ y_{3;s}^*;\ y_{4;s}^*;\ y_{5;s}^*]'$ appear when $s = w_i \cdot (-\tilde{y}_i^*)$, as illustrated in the 3rd column of Table 2. And the return of inequalities in column 2 and 4 of Table 2 results from the signs of the coordinates of the vector $\boldsymbol{w}$ and is presented in Fig.1. For the logistics company, the $w_i \cdot (-\tilde{y}_i^*)$ values of the parameter s have the interpretations of transition moments of the *i*-th counterparty from the role of a revenue-generating participant to a loss-generating one (or vice-versa). They allow for creation of the so-called *dual price matrix* with their interpretation relating to changes in the right sides of the *limiting conditions* in *the sensitivity analysis* of the primary problem [29].

Table 2. The values of the parameter s changing the character of the optimal dual variables

s	$y^*_{i;s}<0$	$y^*_{i;s}=0$	$y^*_{i;s}>0$
$y^*_{1;s}$	s<-7.3	-7.3	s>-7.3
$y^*_{2;s}$	s<-8	-8	s>-8
$y^*_{3;s}$	s>0	0	s<0
$y^*_{4;s}$	s>-1.1	-1.1	s<-1.1
$y^*_{5;s}$	s>-0.8	-0.8	s<-0.8

Table 3. The differences between the vector $\boldsymbol{y}_s^*$ coordinates of the dual prices

$y^*_{i;s} - y^*_{j;s}$	$y^*_{1;s}$	$y^*_{2;s}$	$y^*_{3;s}$	$y^*_{4;s}$	$y^*_{5;s}$
$y^*_{1;s}$	0	-0.7	7.3+2s	8.4+2s	8.1+2s
$y^*_{2;s}$	0.7	0	8+2s	9.1+2s	8.8+2s
$y^*_{3;s}$	-7.3-2s	-8-2s	0	1.1	0.8
$y^*_{4;s}$	-8.4-2s	-9.1-2s	-1.1	0	-0.3
$y^*_{5;s}$	-8.1-2s	-8.8-2s	-0.8	0.3	0

In terms of $s \in (-7.3; -1.1)$ all counterparties create positive revenues for the logistics company. It might also be interesting for the analyst to see the differences between the revenues from individual counterparties. In comparison of counterparties from one group (of either only warehouses or only stores), they are fixed, while in comparison of counterparties in different groups, the 2*s* component appears (Table 3).

The capability to freely shape these three groups of counterparties within the space *J* allows the logistics company to conduct a fairly flexible financial policy. This means that it is possible to shift the transport costs to selected entities only, while introducing special offers for other participants of the distribution system. An example of such logistics economy can be a non-profit collection of recyclable materials, such as waste paper, clothing, debris and metals, from which profits are obtained only from recipients of these materials. When the waste inbound transport costs are not matched by relevant revenue from their recipients, they must be balanced and even surpassed in the form of a fixed fee charged on individual property managers with the possible subsidization from the city or municipality budget or other external funding.

The freedom to shape the financial policy, which is reflected by the dual variable values $\boldsymbol{y}_s^*$, is deduced from the arbitrariness of the parameter $s \in R$ and is presented in Fig. 1. It enables a competitive behaviour on the market. In a clash with smaller, local companies, a company that operates in many areas of the market may periodically flexibly shape its financial relations and take over areas of smaller, less flexible business entities. Therefore, businesses can take over a particular area of the market by offering special offers or buying goods at

higher prices and deploying clever economy. One of the tools used for this purpose is the use of exclusivity clauses to acquire particular goods. Each business entity must be aware of the fact that the described seemingly favourable substitution of single revenue is also one of the key factors threatening the attractiveness and stability of each sector of economy. Any business entity which aggressively applies the principle of substitutability of revenue is seen as the one who impairs the market stability and might face a massive and effective retaliation of even seemingly insignificant entities. This model indicates that it is the current transport process where the possibilities for running a flexible financial policy occur, and they do not necessarily require expenditures from previously accumulated funds or loans drawn to this end.

Order of examination of the primary and dual models. It is usually assumed that it is mainly the primary model that is created, while the dual model is used optionally to accelerate the primary or secondary optimization procedure resulting from a change in some of the model's parameters or to draw simple post-optimization conclusions based on sensitivity analysis [10, 26]. But in this case, other surprising conclusions come to mind. The above examples demonstrate the need for simultaneous analysis of both models. And, for the classic transportation problem that is specifically discussed in this paper, even a need for prior consideration of the dual model is recognised. It can be described as follows.

First, the logistics company determines for itself the actual transport costs on individual routes. By complementing them with e.g. a diverse percentage margin that generates the profit, the amounts of unit revenues from individual routes, in this case 6, are achieved. The amounts planned in such manner are on the right side of *the limiting conditions* of the dual problem and they constitute a starting point for linear programming in the dual model. As a result, by finding space *J* of the solutions to the dual problem, the logistics company forms the above-described policy towards its counterparties. After the conclusion of relevant agreements with them, it proceeds to the solution of the so-called primary problem, as a result of which it finds an optimal route for the distribution of goods. Finally, it performs the transport of goods.

If the primary model describes the relationship repeated cyclically and, at the same time, there are changes in the parameters of this model, a need for post-optimizing associated with the use of the dual model also occurs. In total, this indicates a need for interchangeable application of both models (primary and dual) in the entire cycle of management of a logistics company.

Alternative versions of unit revenues. The need to use both the primary and dual model is thus apparent. This leads to several effects: first, the determination of the right sides of *the limiting conditions* of the dual problem gives a logistic company a point of reference as to the possibility (expressed by the space *J*). As it is evident in the above dependency and Figure 1, upon designation of any solution of the dual problem e.g. $\tilde{\boldsymbol{y}}^*$**,** an analyst adjusting the parameter s sees the alternative versions of the vector of unit revenue (loss) $\boldsymbol{y}_s^*$ achieved from individual counterparties, from which they choose a version that is the most convenient and possible to implement. While choosing versions that are possible to implement, they should note that the parameter s multiplies the vector $\boldsymbol{w} = [1; 1; -1; -1; -1]'$ consisting of ones and minus ones. This means that all versions of the solutions proposed by the space *J* are the result of simultaneous increase or decrease of the initial $\tilde{\boldsymbol{y}}^*$ revenue (loss) in the two opposing groups of counterparties (namely warehouses and stores) by values equal to $\pm \Delta s$. And so the unit increase of revenue (loss) [€/*t*] in each of the two warehouses is balanced by the unit increase of loss (revenue) [€/*t*] in each of the three stores. This remark indicates the easiness with which the logistics company's decision-maker, making arrangements with counterparties, finds the final implemented value of the solution to the dual problem. The finally designated $\boldsymbol{y}_s^*$ solution divides the counterparties into three groups described above, and its value determines the level of revenue (loss) negotiated with the counterparties by the logistics company. Thus, it seems that using the original model to determine transportation routes is only an additional problem an analyst of a logistics company must face.

CONCLUSIONS

1. The lasting and prominent place that the classic transportation model takes, requires also to be complemented through full development of its dual problem interpretation, including post-optimization problems.
2. This paper shows that in the transportation processes, it is justified and necessary to use both models: the primary and the dual one.
3. The dual model allows a logistics company to undertake the planned operations of the flexible policy in relation to both business partners and local competitors.
4. Flexible policy of the logistics company requires a relation between the revenues or losses, expressed by the space *J* of the optimal solutions to the dual model. It allows to fulfil the pre-determined *limiting conditions*.
5. Both economic benefits and risks associated with the principle of subsidiarity of the revenue have been indicated.

REFERENCES

1. **Busłowski A. 2000.** Stability of optimal solution of linear programming problem. University of Białystok, (in Polish).
2. **Dantzig, G.B. 1949.** Programming in a Linear Structure, Report of the September 9, 1948 meeting in Madison, Econometrica 17, 73–74.

3. **Dantzig, G.B. 1951.** Application of the Simplex Method to the Transportation Problem, in T.C. Koopmans (ed.), Activity Analysis of Production and Allocation, John Wiley & Sons, New York, 359–373.
4. **Dantzig G.B., Thapa M.N. 1997.** Linear programming. 1. Introduction. Springer. New York, Berlin, Heidelberg.
5. **Dantzig G.B., Thapa M.N. 2003.** Linear programming. 2. Theory and extensions. Springer. New York, Berlin, Heidelberg.
6. **Glaeser E. L., Shapiro J. M. 2002.** Cities And Warfare: The Impact Of Terrorism On Urban Form. Journal of Urban Economics, v51(2,Mar), 205-224.
7. **Goryl A., Walkosz A. 2016.** Elements of the Operational Research. Linear programming. Cracow University of Economics https.//e-uczelnia.uek.krakow.pl/pluginfile.php/96978/mod_folder/content/0/ProgLin.pdf?forcedownload = 1_(in Polish).
8. **Guzik B. 2009.** Introduction to Operational Research, University of Economy, Poznań (in Polish).
9. **Hitchcock F.L. 1941** The distribution of a product from several sources to numerous localities, Journal of Mathematics and Physics 20, 224–230.
10. **Ignaciuk Sz., Wawrzosek J., Piekarski W., Baryła-Paśnik, M. 2014.** Economic aspects of functioning of a biomass distribution network. Logistyka (Pozn.), Vol. 6 in appendix CD ROM No. 1, 62-68.
11. **Julien P-A., Andriambeloson E., Ramangalahy C. 2004.** Networks, weak signals and technological innovations among SMEs in the land-based transportation equipment sector. Entrepreneurship & Regional Development: An International Journal, Volume 16, Issue 4.
12. **Karmarkar N. 1984.** A new polynomial-time algorithm for linear programming. Combinatorica, 4, 373 - 395.
13. **Kolman B., Beck R. E. 1995**. Elementary Linear Programming with Applications, *Computer science and scientific computing*, Gulf Professional Publishing, Academic Press.
14. **Kukuła K. (ed.) 2007.** Operational research in the examples and tasks, collective work, 5th edition, revised and expanded, PWN, Warsaw (in Polish).
15. **Liu S.-T. 2003.** The total cost bounds of the transportation problem with varying demand and supply, Omega-International Journal of Management Science 31, 247 – 251.
16. **MacKenzie C. A., Barker K., Santos J. R. 2014**. Modeling a severe supply chain disruption and post-disaster decision making with application to the Japanese earthquake and tsunami, IIE Transactions, Vol. 46, Iss. 12, http.//www.tandfonline.com/doi/full/10.1080/0740817X.2013.876241
17. **Radebaugh L. H., Sullivan D. P., Daniels J. D. 2015.** International business: Environments and operations. Pearson Education.
18. **Reeb J. E., Leavengood S. 2000.** Operations Research. Using Duality and Sensitivity Analysis to Interpret Linear Programming Solutions, Oregon State University, https.//catalog. extension.oregonstate.edu/em8744.
19. **Sab R. 2014.** Economic Impact of Selected Conflicts in the Middle East: What Can We Learn from the Past?. International Monetary Fund, Working Paper No. 14/100.
20. **Schrijver A. 2016.** On the history of the transportation and maximum flow problems. The Netherlands, and Department of Mathematics, University of Amsterdam http.//homepages. cwi.nl/~lex/files/histtrpclean.pdf
21. **Sikora W. 2005.** Post-optimization analysis in a closed transport task, Scientific Journals, Poznań University of Economics, 62, 199-214 (in Polish).
22. **Sikora W. (ed.) 2008.** Operational research, collective work, PWE, Warsaw 2008 (in Polish).
23. **Smoluk A. 2008.** About the perspective, duality and equilibrium, Statistical Review, Volume 55, no. 2, 5-14 (in Polish).
24. **Smoluk A. 2009.** About the principle of duality in linear programming, Econometrics, 26, 160-169 (in Polish).
25. **Stigler G. 1945.** The Cost of Subsistence. Journal of Farm Economics, 27(2), 303-314. http.//www.jstor.org/stable/1231810 .
26. **Wawrzosek J., Ignaciuk Sz. 2013.** Optimum balancing of the transportation problem as a postoptimization problem regulating the structure of the supply and demand parameters, Episteme (Krak.) No 21(1), 539-550, (in Polish).
27. **Wawrzosek J., Ignaciuk Sz. 2014.** Characteristics of the functioning of agricultural products transportation networks. Teka Komis. Mot. Energ. Rol._Pol. Akad. Nauk., Oddz. Lubl. 2014 T. 14 No 3, 135-140.
28. **Wawrzosek J., Ignaciuk Sz. 2015.** Use f of extended sensitivity reports of linear programming in emergency medicinal services issues. Logistyka (Pozn.) 2015 Vol. 4 in appendix CD ROM No. 2 - Part 5, 8473-8481 (in Polish) .
29. **Wawrzosek J., Ignaciuk Sz. 2016.** Optimization and postoptimization at linear dependence of constraints. Part 3 Matrix of dual prices in a balanced transportation problem. (unpublished).
30. **Woźniak A. 2011.** Operational Research in Logistics and Production Management part. I. Ed. P.W.S.Z. Nowy Sącz (in Polish).
31. **Ye X, Han SP, Lin A. 2010.** A note on the connection between the primal-dual and the A* algorithm. Int. J. Operations Research and Information Systems, 1(1), 73–85.

On the mathematical modelling and optimization of foil consumption for cylindrical bale wrapping

Anna Stankiewicz, *Andrzej A. Stępniewski*, *Janusz Nowak*

Faculty of Production Engineering, University of Life Sciences in Lublin, Poland
e-mail: anna.m.stankiewicz@gmail.com

Received July 14.2016: accepted July 19.2016

Abstract. Aspects of mathematical modelling of wrapping round (i.e. cylindrical) bale related to the optimization of foil consumption are considered for individual bales of agricultural materials wrapped in plastic foil. The article details the mathematical description of bale wrapping, while also identifying both some solved problems and a few open ones, which can be solved to optimize the foil consumption. Mechanical properties of the sealing foil characterized by its Poisson ratio, arbitrary foil and bale size dimensions and overlapping width of subsequent wrapped foil strips were taken into account. After providing a basic understanding of how the foil is consumed in the course of wrapping process, the mathematical model for determining the number of entire foil wrappings is determined. Next the results of mathematical analysis are used for optimization purposes. The foil consumption per unit of the bale volume index is used as a measure of foil expenditure. Two problems of foil consumption optimization are stated and solved. The formulas for computing the optimal foil width and optimal bale size dimensions are derived and estimations of the solution errors are given. Computational results are presented and analyzed for exemplary bale silage.

Key words: baled silage, cylindrical bale, mathematical model, stretch foil consumption, optimization

INTRODUCTION

For over six decades the research and analysis of bale silages has been an area of research within different fields, including biology [1,2], chemistry and biochemistry [1,4,15,19], physics [1], agronomy [2,16] and engineering [16,18,20,21]. Since its origin in the 1950s the subject of baled silage technique has grown into an area with applications in several branches of agriculture, the number of academics working on it and patents in the area has been increasing over the years. A comprehensive review of the studies on the technique of bale silage conservation of agricultural materials can be found in [1,3,14], and for further research [4,10,17]. Studies concerning the usage of plastic foil to bale wrapping, especially the seal integrity and storage quality depending on different features have been carried out since 1990s, e.g., [1,2,3,6,8,12,19]. The study of foil usage has been extensive, with conceptual bases supported by empirical data, but generally, despite a few papers, limited to [6,7,11,13] and other papers of the same authors, there is still a lack of investigations concerning the mathematical description of the foil consumption aspects. Financial expenditures on the purchase of stretch foil constitute a high percentage in the total costs of this technology of silage production [14]. The effect of bale size dimensions and the number of foil layers as well as the value of the overlap of the adjacent strips of the foil on the foil consumption has been taken into account for round and square bales in [7,11]. In our previous paper [17] a direct analytical formula to compute the final number of wrappings necessary to guarantee the required number of foil layers under the assumed standard of wrapping as a function of initial width of foil, its Poisson's ratio and unit deformation of the foil, bale diameter as well as the overlap ratio, was given for the first time. The computer program which contains a graphical module for visualization of geometry of the distribution of subsequent foil strips and the arrangement of foil layer in a bale cross-section has also been presented in [17]. The length and surface area of foil taken from the roll and used for wrapping the bale were determined and its dependence of foil width was examined for two geometrically different ways of wrapping with overlaps equal to 50% and 75% foil width. As a result of the simulation, in [17] some remarks concerning the foil consumption have been formulated. The present study supports a mathematical model proposed in the preceding paper [17], that is, a more detailed analysis is made.

The aim of this paper is to present in a unified way the mathematical model which can be used for foil consumption optimization. First, we describe the idea of the model of foil consumption based on the estimation of the number of wrappings. After providing a basic understanding of how the foil is consumed in the course of wrapping process, the formulas for determining the entire number of foil wrappings and the distance between the edge, from which the wrapping begins, and the opposite edge of the final (applied for the final wrapping)

foil strip (presented briefly in [17]) are derived here and analyzed in detail. The mechanical properties of the foil described by the Poisson ratio as well as the foil and bale dimensions are taken into account. As a result, the mathematical model for exact estimation of the foil consumption for cylindrical bale silages is derived, which provides a basis for the optimization. A simple computational algorithm is described. Next, the foil consumption is discussed based on pole to volume ratio. Two problems of the optimal foil and bale dimensions design are stated and discussed. The solution of the problem of optimal choice of the foil width is given. In the second problem a fixed volume of bale silage must be optimally wrapped by stretch foil. The optimal bale dimensions are sought out. For this problem only suboptimal solution is derived since only an approximate estimation of the foil consumption is used as a quality index for this task. The examples of how the model proposed may be used in the optimal choice of foil and bale size parameters are given. The considerations are confined to the widely practiced method of individual wrapping of separate cylindrical bales [3,14], for illustration see Fig. 1 in [17]. In all the examples it was assumed that the bale is to be protected by at least four layers of foil, cf. [12,19]. The model did not describe the relation between the number of basic foil layers, the number of bale rotations and the overlap ratio. Besides, the article initially presents some open problems in the optimization of foil consumption.

MATHEMATICAL MODEL – PRELIMINARIES

Before describing the mathematical models that are aimed at estimating and optimization of the foil consumption, this article provides some insight into the problems that need to be addressed to achieve the assumed standard of bale silage wrapping. More details on how this standard is understood are provided below.

From the definition of Poisson's ratio v_f we have the following formula [17, Eq. (1)]:

$$b_{fr} = b_f\left(1 - v_f\varepsilon_{lf}\right), \tag{1}$$

which for a given width of unstretched foil b_f and unit deformation ε_{lf} allows to compute foil width after stretching b_{fr}. As in the previous paper [17] we assume that the geometry of movements (the bale's rotation speed and the baler rotation speed) are taken so that the subsequent strips of foil overlap one another creating the overlap $k_f b_{fr}$, where k_f is dimensionless relative ratio determining the width of the contact between adjacent foil strips. This means that all foil strips both overlap and are equally overlapped by successive strips. Symmetry of the bale is assumed, thickness of the foil is ignored here (on typical foil and bale dimensions see e.g., [11,13,19]). It is also assumed that the number n_b of bale rotations around its axis is selected so as to ensure for taken overlap factor k_f the assumed principal (i.e. minimal on the whole bale surface) number of foil layers. In the examples four layers are established. This means that the basic number of entire wrappings i_b obtained directly for n_b rotations of the bale is the largest integer such that the following inequality is satisfied:

$$i_b b_{fr}\left(1 - k_f\right) \le \pi D_b n_b, \tag{2}$$

where: D_b is the outer bale diameter. Thus:

$$i_b = \left\lfloor \frac{\pi D_b n_b}{b_{fr}(1-k_f)} \right\rfloor, \tag{3}$$

where: $\lfloor x \rfloor$ denotes the largest integer not greater than x (floor function [9]). To simplify the notation the expression under floor function brackets in (3) we denote as:

$$i_o = \frac{\pi D_b n_b}{b_{fr}(1-k_f)}. \tag{4}$$

Obviously, the ratio i_o does not have to be (and usually is not) an integer. It provides the upper estimate of the basic integer number of wrappings i_b, since $i_b = \lfloor i_o \rfloor \le i_o$.

The last applied strip of foil creates an overlap $k_f b_{fr}$ on a preceding strip, while the 'distance' between the edge determining the beginning of wrapping and the opposite edge of the foil strip applied during the first wrapping is equal to:

$$z_o = b_{fr}\left[1 + (i_b - 1)\left(1 - k_f\right)\right] - \pi D_b n_b. \tag{5}$$

Note, that in the special case of half rotation of the bale ($n_b = \frac{1}{2}$) 'distance' z_o is identical to the overlap of the last applied foil strip on a first foil strip applied in the previous layer.

We assume that the bale is wrapped correctly, when the last applied strip of foil overlaps the preceding strip with overlap $k_f b_{fr}$ and 'overlaps' the first applied foil strip with the overlap not smaller than $k_f b_{fr}$. Thus, the assumed standard of wrapping is guaranteed directly for n_b rotations whenever $z_o \ge k_f b_{fr}$. If this condition is not satisfied, the additional bale rotation is necessary. To determine when it is necessary three complementary cases:

(*i*) $i_b = \lfloor i_o \rfloor = i_o$,
(*ii*) $i_b = \lfloor i_o \rfloor \ne i_o$ and $z_0 > 0$,
(*iii*) $i_b = \lfloor i_o \rfloor \ne i_o$ and $z_0 \le 0$

must be analysed separately. The analysis ensure more deep insight into the foil expenditure. To illustrate the analysis, the example is given.

Example 1. The following parameters are taken: bale diameter $D_b = 1{,}2\ [m]$, width of unstretched foil $b_f = 0{,}6\ [m]$, Poisson's ratio of foil $v_f = 0{,}34\ [-]$ and unit deformation of foil $\varepsilon_{lf} = 0{,}7\ [-]$, which are assumed to be the same for all the examples and figures. The cross-sections of the bales with indicated geometry of the distribution of overlapping foil strips in exemplary (*i*)-(*iii*) cases is presented in Fig. 1–3; the respective numerical data are summarized in Table 1. The 'overlap' z_o (5) as well as the overlaps $k_f b_{fr}$ and the strips of stretched foil

of width b_{fr} are shown in the figures. For detailed illustration of the successive foil strips and layers distribution see Fig. 4 in the previous paper [17].

Table 1. The numerical data for Example 1

case	(*i*)	(*ii*)	(*iii*)
overlap k_f $[-]$	0,2147	0,6	0,2
bale rotations n_b	2	1	2
number of foil layers	4	4	4
ratio i_o (4)	21	20,6141	20,6141
overlap z_o (5) $[m]$	0,098161	0,162	−0,1332
overlap $k_f b_{fr}$ $[m]$	0,098161	0,2743	0,0914

CASE ANALYSIS

Let us consider in detail the (*i*)–(*iii*) cases defined above. Note, that in view of (3) and (4) the equation (5) can be rewritten in an equivalent form as:

$$z_o = b_{fr}\big[(\lfloor i_o \rfloor - i_o)\big(1 - k_f\big) + k_f\big]. \tag{6}$$

Case (*i*). If $\lfloor i_o \rfloor = i_o$, then from (6) it follows that the distance $z_o = k_f b_{fr}$ is equal to the assumed overlap – see Fig. 1 which illustrates the cross-section of a well-wrapped bale. Additional bale rotation is not needed.

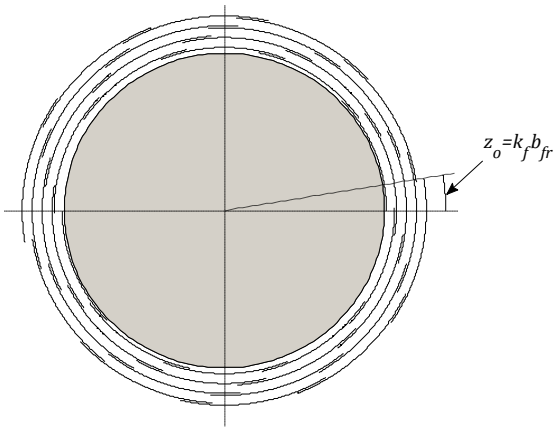

Fig. 1. Distribution of the foil layers and illustration of the 'overlap' z_o – case (*i*)

Case (*ii*). Now $i_o \neq \lfloor i_o \rfloor$. If the distance $z_o > 0$, then based on (6) we have (see Fig. 2):

$$z_o = b_{fr}\big[(\lfloor i_o \rfloor - i_o)\big(1 - k_f\big) + k_f\big] < k_f b_{fr}. \tag{7}$$

The above means that the last foil strip do not make a 'full' overlap on the first strip of the foil. Then, in order to ensure bale wrapping in accordance with the assumed standard, the basic number of wrappings i_b achieved for n_b bale rotations is not sufficient – at least one more wrapping is required. When one additional strip of the foil is applied, the distance z_o is replaced by the final (corrected) one given by:

$$z_f = z_o + \big(1 - k_f\big)b_{fr}, \tag{8}$$

which, in view of (6), is equal to:

$$z_f = b_{fr}\big[(\lfloor i_o \rfloor - i_o)\big(1 - k_f\big) + 1\big]. \tag{9}$$

Since $(1 + \lfloor i_o \rfloor - i_o)\big(1 - k_f\big) > 0$, the following inequality holds:

$$(\lfloor i_o \rfloor - i_o)\big(1 - k_f\big) + 1 > k_f,$$

and then, in view on equation (9), we immediately obtain:

$$z_f > k_f b_{fr}. \tag{10}$$

This means that, by adding to i_b one additional wrapping, we guarantee the final 'overlap' z_f larger than the assumed value $k_f b_{fr}$. Thus, the final number of foil wrappings $i_f = i_b + 1 = \lfloor i_o \rfloor + 1$. Fig. 2 (and Fig. 3 for the next case) show how the adding (to i_b wrappings) of one additional strip of the foil affects the final bale wrapping with the final 'overlap' z_f.

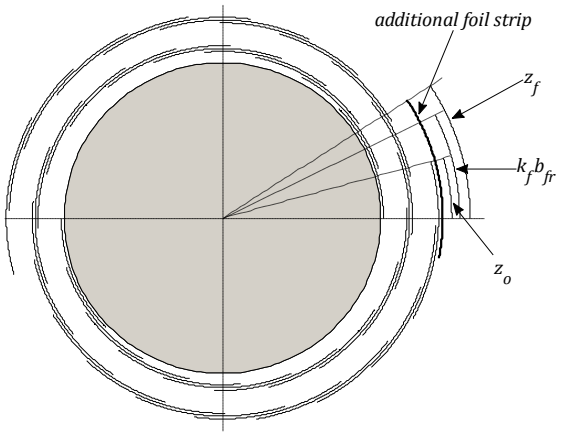

Fig. 2. Distribution of the foil layers and illustration of the 'overlaps' z_o, $k_f b_{fr}$ and z_f – case (*ii*)

Case (*iii*). Now, we will analyse the case when $\lfloor i_o \rfloor \neq i_o$ and the 'distance' z_o is non-positive – see Fig. 3. It is easy to check that if $z_o \leq 0$, then, based on equation (6), we obtain:

$$i_o - \lfloor i_o \rfloor \geq \frac{k_f}{1-k_f}.$$

This particularly means that:

$$1 > \frac{k_f}{1-k_f}, \tag{11}$$

and whence $k_f < 0{,}5$. If $i_o \neq \lfloor i_o \rfloor$, then:

$$\big(1 - k_f\big) > \big(1 - k_f\big)(i_o - \lfloor i_o \rfloor)$$

and the next inequality is also valid:

$$1 - 2k_f > \big(1 - k_f\big)(i_o - \lfloor i_o \rfloor) - k_f.$$

In consequence, the following inequality holds (compare equation (7)):

$$b_{fr} - 2k_f b_{fr} > -b_{fr}\left[\left(1-k_f\right)(\lfloor i_o \rfloor - i_o) + k_f\right] = -z_o. \quad (12)$$

In the case when $z_o \leq 0$, inequality (12) means that the distance $|z_o| = -z_o$ is lower than foil width b_{fr} reduced by double the width of overlap $k_f b_{fr}$. Thus, also in this case in order to guarantee bale wrapping conforming with the assumed standard, it is required to increase the basic number of bale wrappings i_b. Let us apply one additional strip of the foil. As a result, the corrected value z_f of the distance z_o is given by formula (8) and, in view of inequality (12), is such that:

$$z_f > k_f b_{fr}, \quad (13)$$

so it is acceptable. It is easy to check that in view of (8) and the right hand side equality of (12), the final 'overlap' z_f is given by the formula (9).

Note, that in the special case when $z_o = 0$, by adding one additional wrapping, in view of equation (8), we obtain the final 'overlap' of the width:

$$z_f = \left(1-k_f\right)b_{fr}.$$

Since in the case considered the inequality (11) holds, the estimation $z_f > k_f b_{fr}$ is valid, i.e., this overlap is also greater than assumed.

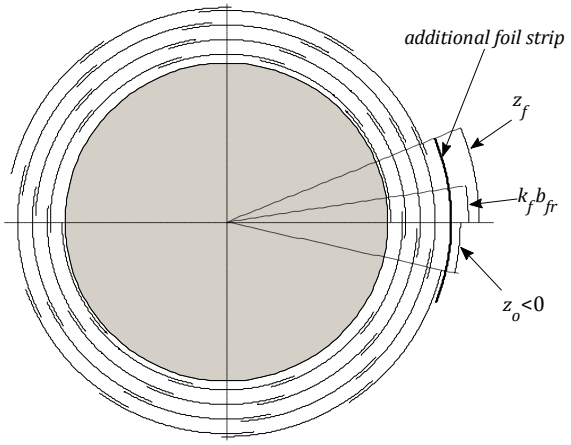

Fig. 3. Distribution of the foil layers and illustration of the 'overlaps' z_o, $k_f b_{fr}$ and z_f – case (*iii*)

NUMBER OF FOIL WRAPPINGS

In view of the above analysis only, in the case (*i*) no additional bale rotation is needed and $i_f = i_b = \lfloor i_o \rfloor$, while in (*ii*) and (*iii*) cases one additional foil strip must be added to achieve the assumed wrapping standard and the final number of wrappings $i_f = i_b + 1 = \lfloor i_o \rfloor + 1$. Thus, the final number of entire wrappings i_f is uniquely determined by the general formula:

$$i_f = \lceil i_o \rceil = \left\lceil \frac{\pi D_b n_b}{b_{fr}\left(1-k_f\right)} \right\rceil = \left\lceil \frac{\pi D_b n_b}{b_f\left(1-\nu_f \varepsilon_{lf}\right)\left(1-k_f\right)} \right\rceil, \quad (14)$$

where: $\lceil i_o \rceil$ is the smallest integer not lower than i_o (ceiling function [9]). The final 'overlap' z_f is given by the general, common to the (*i*)–(*iii*) cases, formula:

$$z_f = b_{fr}\left[\left(i_f - i_o\right)\left(1-k_f\right) + k_f\right], \quad (15)$$

which results directly from (9) and (14). In the case of integer i_o the last overlap is equal to $k_f b_{fr}$, while in the opposite case in view of inequalities (10) and (13) the estimation $z_f > k_f b_{fr}$ holds.

While n_b bale rotations around its axis the bale rotation angle is equal to $2\pi n_b$. During an additional bale rotation in (*ii*) and (*iii*) cases, additional rotation angle equal to $2\frac{\left(1-k_f\right)b_{fr}}{D_b}$ is made. Thus, the final bale rotation angle around its axis is given by the formula:

$$\alpha_f = \begin{cases} 2\pi n_b & if\ \lfloor i_o \rfloor = i_o \\ 2\left(\pi n_b + \frac{\left(1-k_f\right)b_{fr}}{D_b}\right) & if\ \lfloor i_o \rfloor \neq i_o \end{cases}. \quad (16)$$

The ratio i_o (4) not only makes possible determining the total number of wrappings that satisfy the assumed standard of bale wrapping, as characterised by formula (14), but is also significant to design of algorithm for bale wrapping computations, as it allows to easily determine the initial 'distance' z_0 (6) as well as the final 'distance' z_f (9) and the angle α_f (16). This ratio and z_f yields also useful upper estimates of the increase of foil consumption, if compared with the optimal foil consumption – see formulas (25), (26) and (37) below.

Example 2. For the bale silage from Example 1 the dependence of the final number of wrappings i_f (14) on the width of unstretched foil b_f is illustrated in Fig. 4 for overlaps $k_f = \frac{1}{4}, \frac{1}{3}, \frac{1}{2}, \frac{3}{4}$, for which the bale rotation numbers, equal to, respectively, $n_b = 2,2,1,\frac{1}{2}$, are taken in order to guarantee at least four layers of the foil. For b_f variability the interval $0{,}35 \div 0{,}75\ [m]$ is chosen, cf. [11,13]. For the overlaps $k_f = 0{,}5$ and $k_f = 0{,}75$ the graphs in Fig. 4 are identical. It is not surprising, since for these overlaps $\frac{n_b}{1-k_f} = 2$ (see (14)). Only two, one or half rotations of the bale are required to wrap the bale, where 14 to 43 foil strips are wrapped.

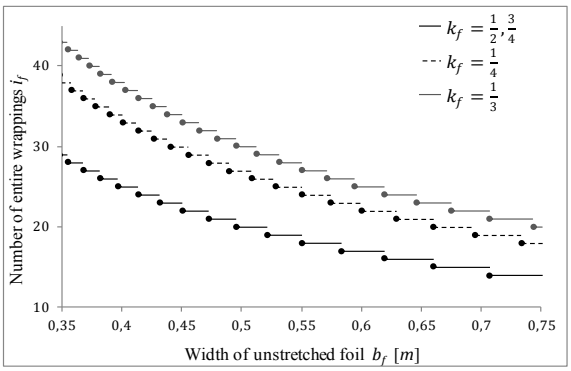

Fig. 4. The final number of wrappings i_f as a function of the width of unstretched foil b_f; the solid dot indicates the value of the function i_f in discontinuity point

FOIL CONSUMPTION

Symmetry of the bale is assumed, thereby the length of stretched foil L_{fr} wrapped over the bale is equal to:

$$L_{fr} = 2i_f(D_b + H_b), \tag{17}$$

here: H_b is bale height, whereas the length of wrapped foil L_f taken from the roll is given by:

$$L_f = \frac{L_{fr}}{\varepsilon_{lf}+1} = \frac{2i_f(D_b+H_b)}{\varepsilon_{lf}+1}. \tag{18}$$

Thus, the surface area of foil taken from the roll is equal to $S_f = L_f b_f$, and can be expressed in form resulting directly from (17) and (18) as:

$$S_f = \frac{2i_f(D_b+H_b)}{\varepsilon_{lf}+1} b_f, \tag{19}$$

where: i_f is given by right hand side of (14). The dependence of the surface area S_f on the foil width b_f for fixed bale dimensions has been studied in the previous paper, see [17, Fig. 3].

A useful measure of the foil consumption is the surface area to volume of silage ratio S_f/V_b [11], here V_b is volume of the bale, which for cylindrical bale is given by:

$$FC = \frac{S_f}{V_b} = \frac{4S_f}{\pi D_b^2 H_b}. \tag{20}$$

Allowing the above, the following scheme can be applied to compute the number of wrappings i_f that guarantees the assumed wrapping standard and to evaluate its effectiveness.

1. Compute i_o according to formula (4), where b_{fr} is given by (1).
2. If i_o is integer, then take $i_f = i_o$; the last 'overlap' is equal to $z_f = b_{fr}k_f$.
3. If $i_o \neq \lceil i_o \rceil$ then take $i_f = \lceil i_o \rceil$ (compare (14)). The last 'overlap' z_f is given by the formula (15).
4. Determine the indices L_f, S_f and FC using the formulas (18), (19) and (20), respectively.

OPTIMIZATION

In view of (19) the FC index depends on the number of foil wrappings i_f according to:

$$FC = \frac{8i_f(D_b+H_b)b_f}{\pi D_b^2 H_b(\varepsilon_{lf}+1)}, \tag{21}$$

and including the formula (14) can be rewritten as:

$$FC = \frac{8(D_b+H_b)b_f}{\pi D_b^2 H_b(\varepsilon_{lf}+1)} \left\lceil \frac{\pi D_b n_b}{b_f(1-v_f\varepsilon_{lf})(1-k_f)} \right\rceil. \tag{22}$$

This formula indicates the dependence of the quality index FC on both the mechanical parameters ε_{lf} and v_f of the foil, the overlap ratio k_f, the number of bale rotations n_b and the bale and foil size dimensions D_b, H_b and b_f.

We assume that the overlap k_f and the number n_b of bale rotations around bale axis are adopted in such a way that the pre-assumed principal number of foil layers is guaranteed and that the parameters ε_{lf}, v_f are given. Thus, only the bale dimensions H_b, D_b and the width of the foil b_f are decision variables.

OPTIMAL CHOICE OF FOIL WIDTH

Assume the bale diameter D_b is given. The index FC (22) is piecewise increasing function of the width of foil b_f in the intervals determined by discontinuity points $b_{f,int}$ such that:

$$\frac{\pi D_b n_b}{b_{f,int}(1-v_f\varepsilon_{lf})(1-k_f)} = \left\lceil \frac{\pi D_b n_b}{b_{f,int}(1-v_f\varepsilon_{lf})(1-k_f)} \right\rceil, \tag{23}$$

i.e., the expression under ceiling function brackets in (23) is integer. In discontinuity points $b_{f,int}$ the lower semi-continuous function $FC(b_f)$ is right–continuous; the notation $FC(b_f)$ indicates the dependence of the function FC given by (22) on the foil width b_f. The course of $FC(b_f)$ index is illustrated in Fig. 5 for the exemplary bale silage considered in Examples 1 and 2; bale height $H_b = 1{,}2\ [m]$, the other parameters as in Example 2.

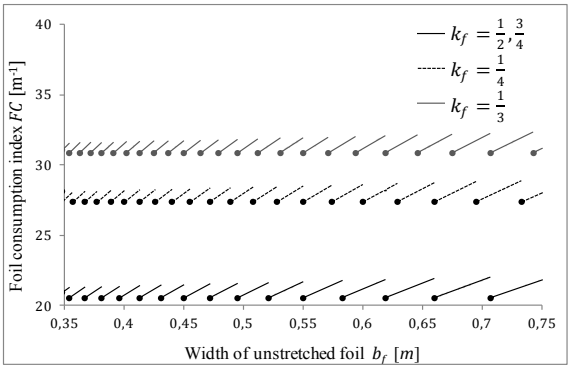

Fig. 5. The foil consumption index $FC(b_f)$ as a function of the width of unstretched foil b_f

On the basis of (22) in discontinuity points $b_{f,int}$ we have:

$$FC(b_{f,int}) = \frac{8n_b(D_b+H_b)}{D_b H_b(\varepsilon_{lf}+1)(1-v_f\varepsilon_{lf})(1-k_f)}. \tag{24}$$

Due to the right-continuity of $FC(b_f)$ at discontinuity points, $FC(b_{f,int})$ given by (24) is the minimal value of FC index with respect to b_f, see Fig. 5. Then, the solution of the problem of foil width design optimal in the sense of FC index there exists and is not unique. Every $b_{f,int}$ defined by the equation (23) is global minimum of the function $FC(b_f)$. The optimal foil consumption $FC(b_{f,int})$ is given by the right hand side of (24) and is $b_{f,int}$ independent. The last has been signalized in the previous paper [17], where the results of numerical

simulations are presented and discussed. Note, that for any optimal solution $b_{f,int}$ the ratio i_o (4) is integer. It is not surprising, since for the previously analyzed case (*i*) of integer i_o no additional foil–consuming wrapping is needed.

The optimal foil consumption is never achieved if (23) is not satisfied. Other than $b_{f,int}$ foil width means a larger than the optimal $FC(b_{f,int})$ foil consumption. From (21), (15), (1), (4) and (24) it follows that:

$$FC(b_f) - FC(b_{f,int}) = FC(b_{f,int})\frac{(z_f - k_f b_{fr})}{\pi n_b D_b}. \quad (25)$$

Thus, the increase of foil expenditure is the greater, the greater is the surplus of the last 'overlap' z_f higher than the assumed value $k_f b_{fr}$. The maximum growth of the foil consumption index is characterized by the following estimation of the relative error:

$$\frac{FC(b_f) - FC(b_{f,int})}{FC(b_{f,int})} \leq \frac{1}{i_o - 1}, \quad (26)$$

which can be derived using (22) and (14), where the ratio i_o (4) decreases with increasing foil width b_f. Thus the increase in foil consumption may accompany the foil width increase (cf. Fig. 5). The estimation (26) means that the bigger is the number of foil wrappings, the lower is the maximum growth of the foil consumption. This confirms the results of rough foil consumption analysis from [11] and [17]. In the exemplary bale silage considered here, the maximum value of the relative error defined by the left hand side of (26) changes from 3,57% to 7,14% for $k_f = \frac{1}{2}, \frac{3}{4}$ and from 2,38% to 4,55% for $k_f = \frac{1}{3}$. Also Fig. 5 shows the described relations. Note also, that in the case when the exact solution $b_{f,int}$ of (23) is practically unrealizable, the foil width should be rounded up to the least practically acceptable value.

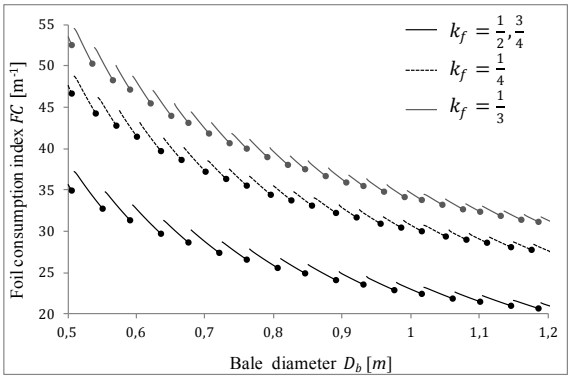

Fig. 6. The foil consumption index $FC(D_b)$ as a function of bale diameter D_b for four values of the overlap k_f; $b_f = 0{,}35\ [m]$.

OPTIMAL DESIGN OF BALE DIMENSIONS

The quality index FC (22) is monotonically decreasing function of the bale height H_b. Simultaneously FC (22) is lower semi-continuous function of the bale diameter D_b, which is decreasing function of D_b in the intervals determined by discontinuity points $D_{b,int}$ such that the argument of ceiling function in (22) is integer, see Fig. 6. Thus FC index cannot be directly applied to foil consumption optimization with respect to D_b and H_b. Additional constraints must be added. Here the bale volume will be fixed.

The ceiling function makes the FC index (22) hard to analyze. One standard method to simplify the analysis is to consider the lower estimation of the rational expression (function) in $\lceil\cdot\rceil$ brackets given by $\lceil x \rceil \geq x$ rather than the exact expression. This approach leads to approximate value of foil consumption index:

$$FC_l = \frac{8(D_b + H_b)n_b}{D_b H_b(\varepsilon_{lf}+1)(1-\nu_f\varepsilon_{lf})(1-k_f)}, \quad (27)$$

which does not depend on the foil width b_f. Note, that the use of only approximate foil consumption index is congruent with the studies presented in [11].

Let us consider the following optimization task. The bale volume $V_b = V_{b0}$ is given. Find geometrical parameters D_b and H_b of the bale guarantying the volume V_{b0} such that the foil consumption index FC takes minimal value. Thus D_b and H_b are such that:

$$V_{b0} = \frac{\pi D_b^2 H_b}{4}. \quad (28)$$

Whence:

$$H_b = \frac{4V_{b0}}{\pi D_b^2} \quad (29)$$

and the approximate foil consumption index FC_l (27) for given fixed V_{b0} denoted as $FC_{V,l}(D_b)$ is a function of the bale diameter D_b described in view of (27) by:

$$FC_{V,l}(D_b) = \frac{2\pi n_b}{V_{b0}(\varepsilon_{lf}+1)(1-\nu_f\varepsilon_{lf})(1-k_f)}\left(D_b^2 + \frac{4V_{b0}}{\pi D_b}\right). \quad (30)$$

Index $FC_{V,l}(D_b)$ is strictly convex function of D_b, thus the bale diameter $\widehat{D}_b$ minimizing index $FC_{V,l}(D_b)$ is uniquely defined by the stationary point condition. Since:

$$\frac{dFC_{V,l}(D_b)}{dD_b} = \frac{4\pi n_b}{V_{b0}(\varepsilon_{lf}+1)(1-\nu_f\varepsilon_{lf})(1-k_f)}\left(D_b - \frac{2V_{b0}}{\pi D_b^2}\right),$$

we immediately obtain:

$$\widehat{D}_b = \sqrt[3]{\frac{2V_{b0}}{\pi}}, \quad (31)$$

and hence the respective bale height is, in view of (29), given by:

$$\widehat{H}_b = 2\sqrt[3]{\frac{2V_{b0}}{\pi}} = 2\widehat{D}_b. \quad (32)$$

Note, that the optimal bale dimensions do not depend on foil width as well as on its mechanical properties and the overlap ratio k_f. The equation (32) means that if the assumed bale volume V_{b0} changes, both bale dimensions changes proportionally. The optimal index:

$$FC_{V,l}(\widehat{D}_b) = \frac{12n_b}{\sqrt[3]{\frac{2V_{b0}}{\pi}}(\varepsilon_{lf}+1)(1-\nu_f\varepsilon_{lf})(1-k_f)} \quad (33)$$

depends on the mechanical parameters of foil and on the overlap ratio k_f, but is b_f independ. Note however, that the bale diameter $\widehat{D}_b$ (31) and high $\widehat{H}_b$ (32) optimal in the sense of $FC_{V,l}(D_b)$ index are, generally, only suboptimal solutions of the original foil consumption minimization problem. Denote by $FC_V(D_b)$ the original non-continuous FC (22) index for fixed bale volume V_{b0}. On the basis of (22) and (29) we have:

$$FC_V(D_b) = \frac{2(\pi D_b^3+4V_{b0})b_f}{\pi D_b^2 V_{b0}(\varepsilon_{lf}+1)}\left\lceil\frac{\pi D_b n_b}{b_f(1-\nu_f\varepsilon_{lf})(1-k_f)}\right\rceil, \quad (34)$$

and let D_b^* be the optimal bale diameter minimizing directly $FC_V(D_b)$ index. The following inequalities hold:

$$FC_{V,l}(\widehat{D}_b) \le FC_{V,l}(D_b^*) \le FC_V(D_b^*) \le FC_V(\widehat{D}_b). \quad (35)$$

Whence we have useful estimation of the suboptimal solution $\widehat{D}_b$ error:

$$0 \le FC_V(\widehat{D}_b) - FC_V(D_b^*) \le FC_V(\widehat{D}_b) - FC_{V,l}(\widehat{D}_b) \quad (36)$$

Since in view of (15) and (4) the last 'overlap' for bale diameter $\widehat{D}_b$ (31) is given by:

$$\hat{z}_f = b_{fr}\left[\left(\left\lceil\frac{\pi\widehat{D}_b n_b}{b_{fr}(1-k_f)}\right\rceil - \frac{\pi\widehat{D}_b n_b}{b_{fr}(1-k_f)}\right)(1-k_f)+k_f\right],$$

taking into account (34), (1), (32) and (30) the right hand side of inequality (36) – upper error estimate – can be rewritten as:

$$FC_V(\widehat{D}_b) - FC_{V,l}(\widehat{D}_b) = \frac{12}{\sqrt[3]{4\pi V_{b0}^2}(\varepsilon_{lf}+1)(1-\nu_f\varepsilon_{lf})(1-k_f)}(\hat{z}_f - k_f b_{fr}). \quad (37)$$

Thus, the greater is the surplus of the overlap $\hat{z}_f$ above $k_f b_{fr}$, the greater is the upper bound of the errors $FC_V(\widehat{D}_b) - FC_V(D_b^*)$. In the particular case of integer $\frac{\pi\widehat{D}_b n_b}{b_{fr}(1-k_f)}$, from (36) and (37) it follows that:

$$FC_V(D_b^*) = FC_{V,l}(\widehat{D}_b) = FC_V(\widehat{D}_b).$$

In view of the uniqueness of minimum $\widehat{D}_b$ and the relation:

$$FC_{V,l}(D_b) \le FC_V(D_b)$$

between the indices, we conclude that $\widehat{D}_b$ is the solution of the original (in the sense of $FC_V(D_b)$ index) bale dimensions optimal design problem, i.e., $\widehat{D}_b = D_b^*$. The course of the relative error:

$$RERR = \frac{FC_V(\widehat{D}_b) - FC_{V,l}(\widehat{D}_b)}{FC_{V,l}(\widehat{D}_b)} \cdot 100\% \quad (38)$$

as a function of b_f for the bale silage from Examples 1 and 2 for three values of the overlap k_f is illustrated in Fig. 7, and as a function of the bale volume V_{b0}, in Fig. 8.

The next example examines the effectiveness of the suboptimal approach applied.

Example 3. Let us consider again the bale silage from previous examples. Assume $k_f = \frac{1}{2}$. The suboptimal bale dimensions computed according to (31) and (32), the optimal bale dimensions D_b^* and H_b^* and the respective values of the original $FC_V(D_b)$ and approximate $FC_{V,l}(D_b)$ indices as well as the suboptimal solution error:

$$ERR = \frac{FC_V(\widehat{D}_b) - FC_V(D_b^*)}{FC_V(D_b^*)} 100\% \quad (39)$$

are summarized in Table 2 for a few values of the foil width b_f and bale volume V_{b0}.

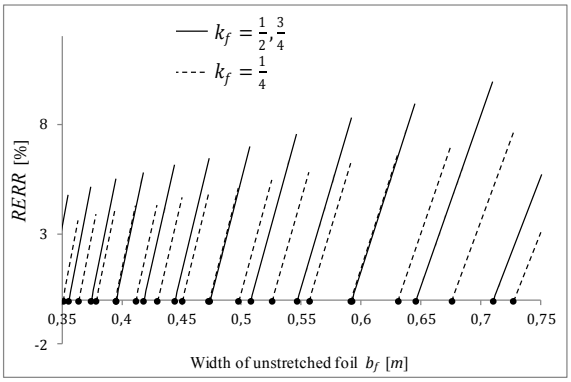

Fig. 7. The relative error $RERR$ (38) as a function of b_f; $V_{b0} = 1\ [m^3]$

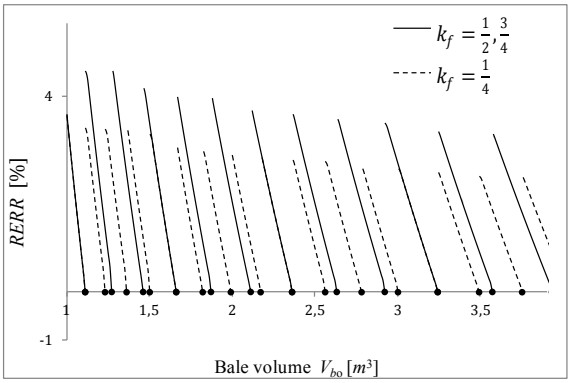

Fig. 8. The relative error $RERR$ (38) as a function of bale volume V_{b0}; $b_f = 0{,}35\ [m]$

Table 2. The optimal D_b^*, H_b^* and suboptimal $\widehat{D}_b$, $\widehat{H}_b$ bale silage parameters and the respective values of foil consumption indices $FC_V(D_b)$, $FC_{V,l}(D_b)$ and the errors ERR (39) for the overlap $k_f = \frac{1}{2}$

$\widehat{D}_b\ [m]$	$\widehat{H}_b\ [m]$	$D_b^*\ [m]$	$H_b^*\ [m]$	$FC_V(\widehat{D}_b)\ [m^{-1}]$	$FC_V(D_b^*)[m^{-1}]$	ERR [%]
$b_f = 0{,}35\ [m], V_{b0} = 1\ [m^3]$						
0,86025	1,7205	0,84893	1,7667	22,316	21,5405	3,599
$b_f = 0{,}5\ [m], V_{b0} = 1\ [m^3]$						
0,86025	1,7205	0,84893	1,7667	22,7714	21,5405	5,714
$b_f = 0{,}75\ [m], V_{b0} = 1\ [m^3]$						
0,86025	1,7205	0,81861	1,89999	22,7714	21,5889	5,477
$b_f = 0{,}75\ [m], V_{b0} = 2\ [m^3]$						
1,08385	2,1677	1,09148	2,13749	17,21412	17,09459	0,699
$b_f = 0{,}75\ [m], V_{b0} = 2{,}5\ [m^3]$						
1,16754	2,33509	1,18244	2,27662	16,0709	15,87099	1,259
$b_f = 0{,}75\ [m], V_{b0} = 3\ [m^3]$						
1,24070	2,4814	1,27339	2,3556	15,3263	14,94296	2,565
$b_f = 0{,}75\ [m], V_{b0} = 3{,}5\ [m^3]$						
1,30612	2,61224	1,27339	2,7482	14,8173	14,1939	4,392
$b_f = 0{,}75\ [m], V_{b0} = 4\ [m^3]$						
1,36557	2,73114	1,36435	2,73599	14,4589	13,5673	6,572

Note finally, that the common practice of the bale having a bale diameter length, i.e. $\breve{H}_b = \breve{D}_b$, where in view of (28):

$$\breve{H}_b = \breve{D}_b = \sqrt[3]{\frac{4V_{b0}}{\pi}},$$

results in 5,827% deterioration of the value of approximate index $FC_{V,l}$ compared with $FC_{V,l}(\widehat{D}_b)$ (33) knowing that:

$$\frac{FC_{V,l}(\breve{D}_b)}{FC_{V,l}(\bar{D}_b)} = \frac{4}{3\sqrt[3]{2}}.$$

The above is a consequence, among others, of irrational multiple overlapping segments on the bale cylinder top and bottom, where there are 2–4 times more foil layers than on the bale lateral surface. For a detailed analysis and illustration of the adverse effect see [11; especially Fig. 4].

FINAL REMARKS

The mathematical model describing both the number of foil wrappings and foil consumption has been presented and analyzed. A special attention has been paid on the aspects of bale wrapping modelling that influence the foil consumption. The proposed model of foil consumption is useful to study and optimize the effect of foil width and bale dimensions as well as Poisson ratio and the overlap ratio. The mathematical formulas and advices are given concerning the optimal choice of foil and bale size dimensions. If the foil width can be chosen freely from continuous set (interval), then not unique, in a general, solution of foil consumption optimization task is given by formula (23). However, if the foil width must be chosen from discrete set, then the foil consumption optimization task is integer programming task which must be solved by applying special methods [5]. Also, exact solution of the bale dimensions optimal design problem needs specialized methods, which take into account the properties of ceiling and floor functions. The overlap ratio k_f related to the basic assumed number of foil layers will be considered as decision variable in a forthcoming paper concerning foil consumption optimization. Such a choice of the overlap ratio and the foil and bale dimensions that the uniform distribution of the foil layers on the bale lateral surface is achieved together with the minimal foil consumption is the next open direction of research.

Note finally, that the FC index (20) is from the optimization point of view equivalent to foil consumption per unit of the mass of forage index [11]:

$$FC_m = \frac{FC}{\gamma},$$

where: γ is bulk density of forage in kg/m^3.

REFERENCES

1. **Baldasano J.M., Gassó S., Pérez C. 2003.** Environmental performance review and cost analysis of MSW landfilling by baling-wrapping technology versus conventional system. Waste Managemen, Vol. 23, 795–806.

2. **Borreani G., Tabacco E. 2010.** Use of new plastic stretch films with enhanced oxygen impermeability to wrap baled alfalfa silage. Transactions of the ASABE, Vol. 53, No. 2, 635–641.
3. **Buxton D.R., Muck R.E., Harrison J.H. 2003.** Silage Science and Technology. Agronomy Series Monograph No. 42, American Society of Agronomy, Inc., Crop Science Society of America, Inc., Soil Science Society of America, Madison (WI), USA.
4. **Coblentz W.K., Coffey K.P., Chow E.A. 2016**. Storage characteristics, nutritive value, and fermentation characteristics of alfalfa packaged in large-round bales and wrapped in stretch film after extended time delays. J. Dairy Sci., Vol. 99, No. 5, 3497–3511.
5. **Conforti M., Cornuejols G., and Zambelli G. 2014.** Integer Programming. Vol. 271 of Graduate Texts in Mathematics. Springer, Heidelberg, New York, London.
6. **Demaldé R. 1996:** Fasciatura delle rotoballe per l'insilamento dei foraggi. Macchine e Motori Agricoli, 5, 16–22.
7. **Gach S., Piotrowska E., Skonieczny I. 2010.** Foil consumption in wrapping of the single green forage bales. Annals of Warsaw University of Life Sciences – SGGW, Agriculture. No 56 (Agricultural and Forest Engineering) 2010: 13–19
8. **Gaillard F. 1990.** L'ensilage en balles rondes sous film étirable. Fourrages, Vol. 123, 289–304.
9. **Graham R.L., Knuth D.E., Patashnik O. 1989**. Concrete mathematics: a foundation for computer science. Addison-Wesley PUBLISHING COMPANY, Reading, Massachusetts Menlo Park, California New York.
10. **Han K.J., McCormick M.E., Blouin D.C. 2014.** Bale Location Effects on Nutritive Value and Fermentation Characteristics of Annual Ryegrass Bale Stored in In-Line Wrapping Silage. Asian-Australasian Journal of Animal Sciences Vol. 27, No. 9, 1276–1284.
11. **Ivanovs S., Gach S., Skonieczny I., Adamovičs A. 2013.** Impact of the parameters of round and square haylage bales on the consumption of the sealing film for individual and in-line wrapping. Agronomy Research, Vol. 11, No. 1, 53–60.
12. **Keles G., O'Kiely P., Lenehan J.J., Forristal P.D. 2009.** Conservation characteristics of baled grass silages differing in duration of wilting, bale density and number of layers of plastic stretch-film. Irish Journal of Agricultural and Food Research, 48, 21–34.
13. **Korpysz K., Gach S. 2011.** Properties of the stretch film used for green foodder bales wrapping vs. quality of the silage. Journal of Research and Applications in Agricultural Engineering, Vol. 56, No. 1, 76–81 (in Polish).
14. **Nowak J. 1997.** Analysis and evaluation of the round bale silage production. Lublin: AR Publishing House (in Polish).
15. **Nucera D.M., Grassi M.A., Morra P., Piano S., Tabacco E., Borreani G. 2016.** Detection, identification, and typing of Listeria species from baled silages fed to dairy cows. Journal of Dairy Science, doi:10.3168/jds.2016–10928.
16. **Schmitz A., Moss C.B. 2015**. Mechanized Agriculture: Machine Adoption, Farm Size, and Labor Displacement. AgBioForum, Vol. 18, No. 3, 278–296.
17. **Stępniewski A., Nowak J., Stankiewicz A. 2016.** Analytical model of foil consumption for cylindrical bale wrapping. ECONTECHMOD. Vol. 5, No. 2, 78–82.
18. **Syrotyuk V.M., Nischenko I.O., Zdobytskyy A.J. 2012.** Determining the deformation of the polimer tape in the process of wrapping. MOTROL Commission of Motorization and Energetics in Agriculture. Vol. 14, No 4, 44–47 (in Ukrainian).
19. **Tabacco E., Bisaglia C., Revello-Chion A., Borreani G. 2013.** Assessing the effect of securing bales with either polyethylene film or netting on the fermentation profiles, fungal load, and plastic consumption in baled silage of grass-legume mixtures. Applied Engineering in Agriculture, Vol. 29, No. 5, 795–804.
20. **Zdobytskyy A. 2015.** Mathematical modeling and research results of the strainedly state of polymer tape in the sealing tape rolls. ECONTECHMOD. Vol. 4, No. 4, 49–54,
21. **Zhortuylov O., Kalym K., Kassymbayev B., Karaivanov D. 2013.** Analysis of Haylage Round Bale Wrapper Operating Mechanism. Life Science Journal, Vol. 10, 349–352.

Impact of the wedge angle on the specific cutting energy of black radish during the exploitation of guillotine knife

Agnieszka Starek[1], Elżbieta Kusińska[2]

[1]Department of Biological Bases of Food and Feed Technologies, University of Life Sciences Głęboka 28, 20-612 Lublin, Poland
e-mail: agnieszka.starek@up.lublin.pl
[2]Department of Engineering and Food Machinery, University of Life Sciences Doświadczalna 44, 20-280 Lublin, Poland

Received July 14.2016: accepted July 19.2016

Abstract. The paper presents the influence of cutting conditions of black radish guillotine knife on specific cutting energy value. The tests were carried out using the texture meter: Texture Analyser TA.XTplus Stable Micro Systems. The structure of the black radish is heterogeneous and, therefore, in order to study the specific cutting energy of black radish its parenchyma was taken from a few specific places. The samples were cut with a longitudinal and transverse orientation of the fibers relative to movement of the working tool. The cutting process was carried at the knives wedge angles: 2.5°; 5°; 7.5°; 10°; 12.5°; 15°, the knives moved at the speed of 0.83 $mm \cdot s^{-1}$. The results were statistically analyzed using the program Statistica 8.0. The statistical analysis showed the impact of the place of sampling, direction of fibers in the black radish parenchyma samples and knife wedge angle on the specific cutting energy. The black radish parenchyma samples obtained from the core of the top layer showed the highest specific energy of cutting. Furthermore, the specific cutting energy showed higher value when the orientation of fibers was in the transverse direction rather than longitudinal. The highest value of the specific cutting energy was obtained for the cutting knife wedge angle of 15°, and the lowest for the knife with $\beta = 2.5°$ wedge angle.

Key words: cutting, specific cutting energy, knife wedge angle, place of sampling, the orientation of fibers

INTRODUCTION

The shredding is a process commonly used in the food industry. During the processing of fruit and vegetables a very common method of shredding is cutting, which aims at the obtainment of the product of desired shape and size. This is because of organoleptic, technological and performance requirements. A greater degree of fragmentation is required in vegetables for salads or juices, but smaller for the heat treatment [7, 8, 10].

The factors that have a significant impact on the process of raw materials cutting are primarily related to their mechanical properties, among others, morphology of plant and the individual characteristics of the variety, time and storage conditions [2, 4, 13, 15, 20].

Another group of factors are construction and exploitation parameters of shredding machines. The process of cuts depends on the configuration and shape of knife or knives, material supplying unit and operating parameters. The mechanism designed to crush has to be adapted to the characteristic properties and dimensions of the raw material [3, 9, 16, 21].

Shredding is an energy intensive process, and it creates the need to conduct research on the impact of various factors on energy consumption during the cutting of plant products. By the optimal selection of knife wedge angle, the specific cutting energy can be significantly reduced. Knife wedge angle should be chosen in such a way that during the cutting process the quality of the raw material is maintained. Too small knife wedge angle may lead to its rapid blunt and uncontrolled loss of the upper edge of the material being cut, while too large knife angle causes excessive area of cutting surface and the formation of large amounts of waste. The resulting shreds are often difficult to remove [1, 5, 11, 12, 17, 18, 19, 22, 23, 24, 25].

Despite many studies, there are still problems with the optimization of the cutting process of plant materials and operating conditions of cutting elements, because the plant materials are characterized by heterogeneity, anisotropy and they belong to diversified categories.

In recent years Poland has increased the consumption of black radish because of its high nutritional value and taste [6, 14], however, in the existing literature there are no reports of cutting and processing this vegetable for food purposes.

The aim of the study was to evaluate the influence of the place of sampling, direction of fibers in the black radish parenchyma sample as well as the knife wedge angle on the specific cutting energy.

MATERIAL AND METHODS

The raw material used for the study was the black radish variety Murzynka. The research material was taken

from the second day after the date set for the seventh day. Vegetables stored in a ventilated room at the temperature of 4°C and relative moisture of 95%. Due to the different anisotropic structure of vegetables, the test samples were taken in a specific way. Figure 1 shows the appearance of black radish structure after cutting: a) longitudinally, b) transversely and indicates the place of sampling.

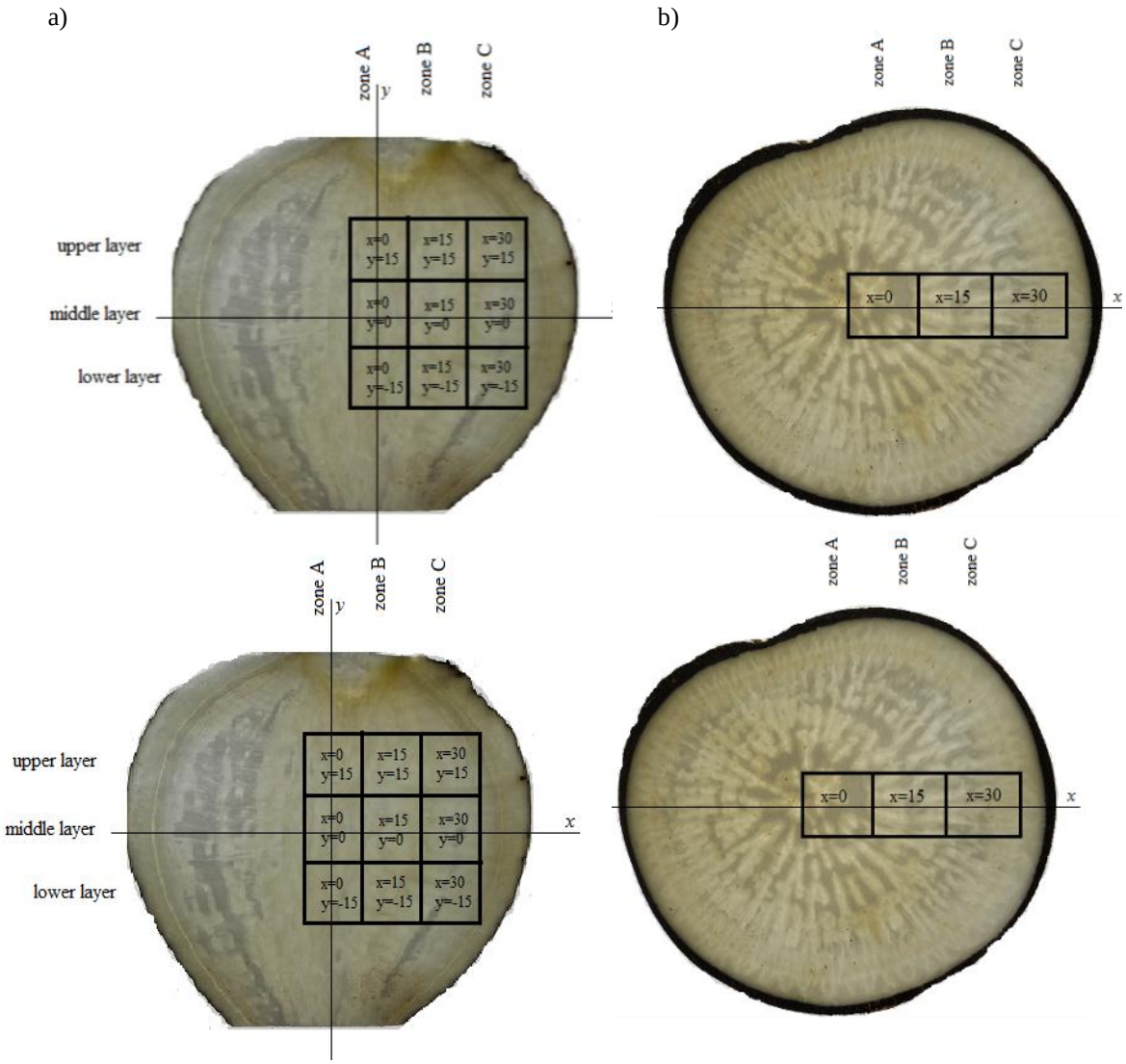

Fig. 1. The structure of black radish parenchyma and place of sampling after cutting: a) longitudinally, b) transversely to the fibers

Samples were prepared in the following way: each vegetable was partitioned into three layers (upper, middle and lower) with the thickness of 15 mm. Then, from each layer cuboids were cut out, sized 45x15x15 mm, which were partitioned into three zones A, B and C (15 mm wide). This resulted in cubes of 15 mm sides. To ensure the accuracy of cutting the samples were prepared on the metal template with four parallel-spaced knives with blades spaced 15 mm. Samples were cut by the knives of texture meter arranging them longitudinally and transversely to the fibers located in parenchyma and to the direction of the knife wedge.

In order to be able to carry out mathematical statistical analysis, the locations of the respective sample centers were determineded. Coordinate system *x*-*y* was assumed, which crossed at the point 0. The *y*-axis coincided with the vertical axis of the zone A, the *x*-axis with the horizontal axis of the middle layer. Vertical axis tests located in zone B and C spaced were the *y*-axis, respectively 15 and 30 mm, and the horizontal axes samples with upper and lower layers were spaced at 15 - 15 mm from the axis *x*. Coordinates *x* and *y* applied were related to the middle of cubes.

It was assumed that the black radish root was symmetric relative to the *y*-axis. Figure 1 shows that the structure of the raw material is heterogeneous. In the illustrated longitudinal section of the black radish (Fig. 1a) it is evident that there is a high fiber density in the top layer and the cross-section, which illustrates the radial distribution of fibers (Fig. 1b), in the middle of the vegetables.

The process of cutting the black radish was conducted on the texture meter Texture Analyser TA.XTplus Stable Micro Systems cooperating with the computer having software Texture Exponent 32. The machines used a starter, which included a set of replaceable knifes with holder for their attachment and the

guide (Fig. 2). The cutting samples were laid longitudinally to the fibers (sample A) and transversely to the fibers (sample b).

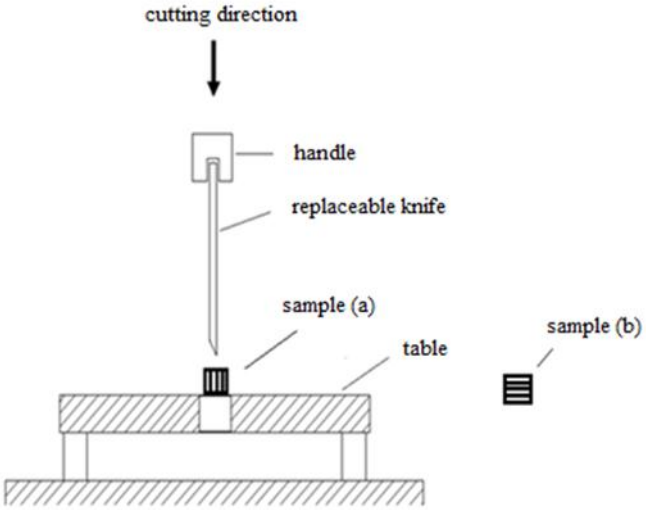

Fig. 2. Scheme of equipment for cutting

In the study straight guillotine knives were used made of steel NC6 with the following knife wedge angles: 2.5°; 5°; 7.5°; 10°, 12.5° and 15°. The angle of the knife was equal to 0°, and the cutting speed was 0.83 mm·s^{-1}.

As a result of the measurement graphs were obtained showing the relationship between the force and displacement of the cutting knife, which defined the maximum value of the cutting force and, using the formula (1), the specific cutting energy was calculated, defined as the labor required to cut the specific area of the material:

$$Ej = \frac{L}{A} \tag{1}$$

where: Ej – specific cutting energy [J·m^{-2}], L – work of cutting [J], A – surface area of the sample [m^2].

The studies were performed in ten replicates (for each sample position and the knife).

The results were statistically analyzed using the statistical package Statistica 8.0. In order to examine the significance of differences between the place of sampling and specific cutting energy, multivariate analysis of variance ANOVA was carried out. Inference was made with the significance level of 0.05. Detailed analysis of medium confidence intervals were made using Tukey's test. Using the regression analysis derived equations that describe the specific cutting energy depending on the place of sampling for the knives of various wedge angles on both directions of the fibers.

RESULTS AND DISCUSSION

Depending on the results of specific cutting energy, samples of the black radish parenchyma taken from specific locations, cut along and across the fibers, at the knives wedge angles 2.5°, 5°, 7.5°, 10°, 12.5° and 15° are presented in the form of graphs in Figures 3, 5, 7, 9 and 11. The different points included in the average values of the graphs indicate the presence of significant differences among them.

a) b)

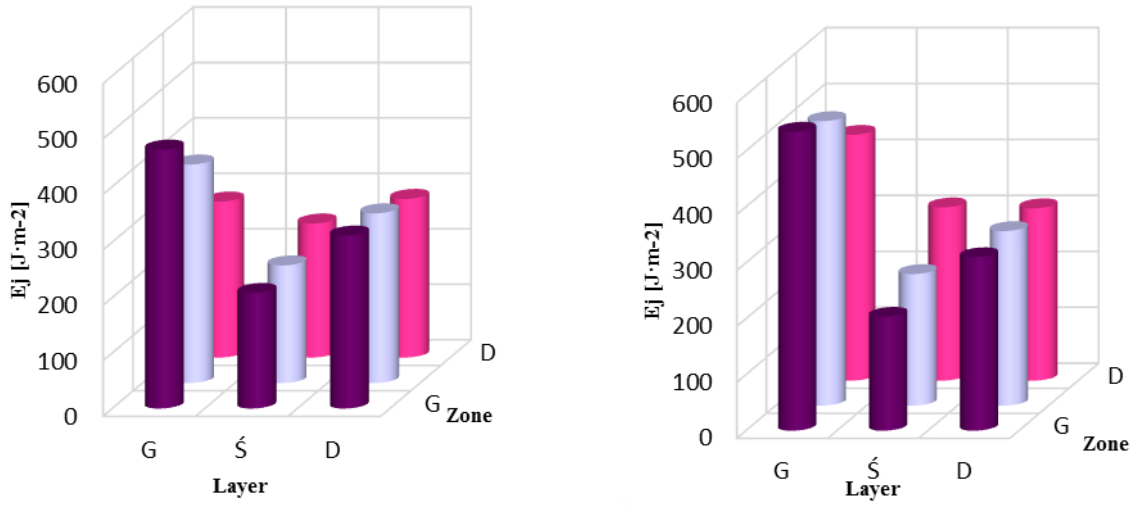

Fig. 3. Dependence of specific cutting energy of the black radish parenchyma at knife wedge angle β = 2.5° on the place of sampling at a) longitudinal b) transverse fibers orientation

Figure 3 contains the average of specific cutting energy samples taken from the parenchyma of black radish, cut with the knife at the wedge angle β = 2.5°. Most of energy for cutting the parenchyma samples from the upper layer was used by black radish fibers arranged transversely. The average value of specific cutting energy for zone A was 500.61 J·m^{-2}, zone B-495.37 J m^{-2} and zone C-467.61 J m^{-2}. The lowest value of the specific cutting energy for samples of black radish arranged longitudinally and transversely was observed in the middle layer zone A. The determined values were, respectively: 208.25 J·m^{-2} and 289.66 J·m^{-2}. Based on the Tukey test of the significance of differences, a significant effect was shown of the place of sampling and fibers orientation (Fig. 4).

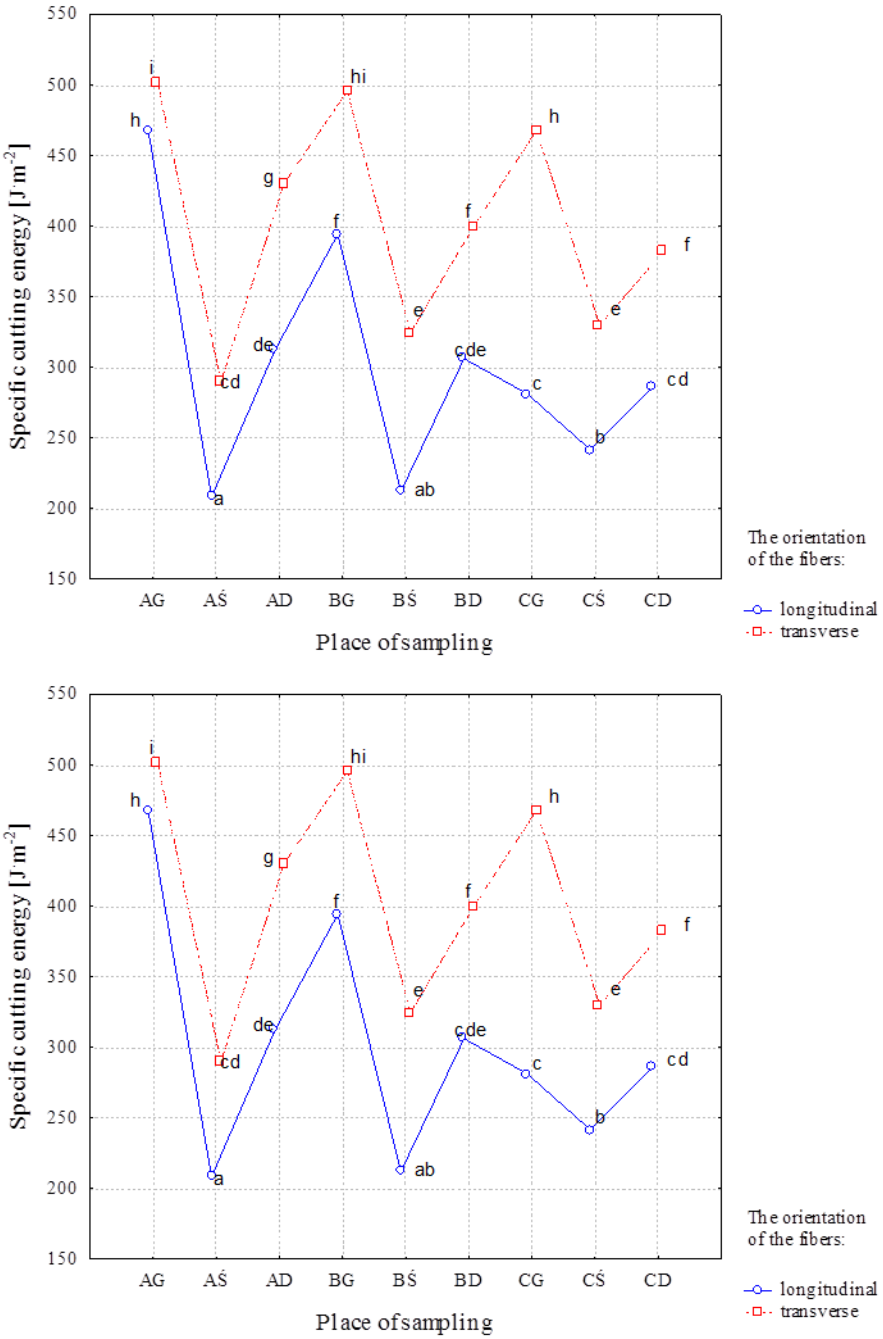

Fig. 4. The significance of differences Tukey test: specific cutting energy at knife wedge angle 2,5° for samples of black radish parenchyma taken from specific places along the longitudinal and transverse direction of fibers

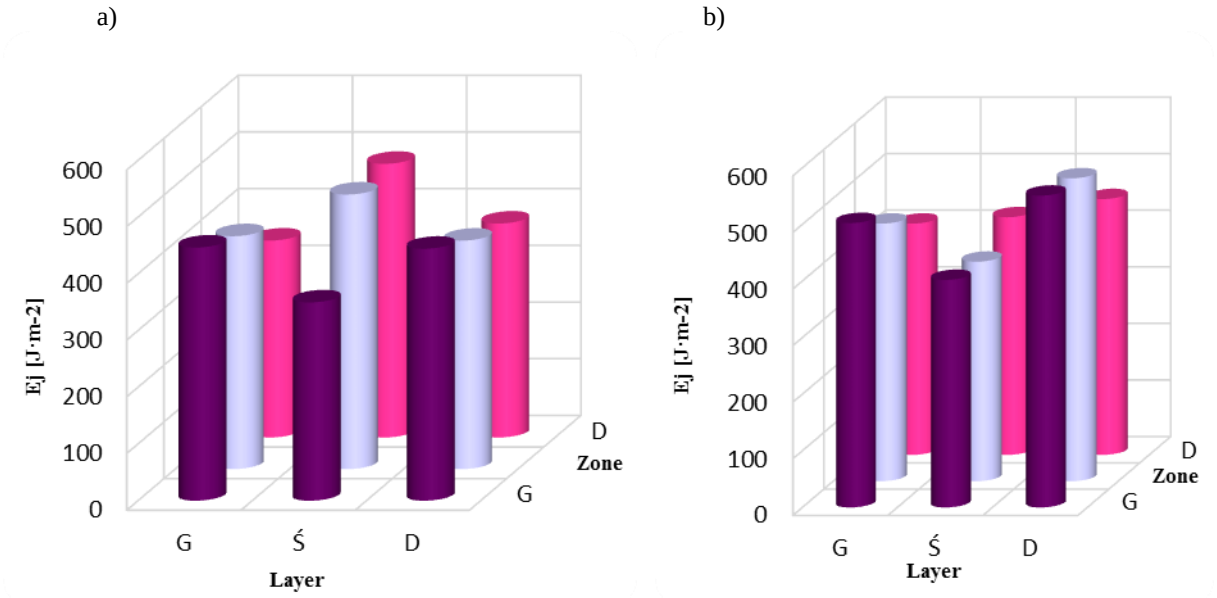

Fig. 5. Dependence of specific cutting energy of the black radish parenchyma at knife wedge angle $\beta = 5^o$ on the place of sampling at a) longitudinal b) transverse fibers orientation

Based on the results obtained during the cutting of the tissue of the root of black radish knife wedge angle $\beta = 5°$ (Fig. 5), it was observed that the average of specific cutting energy are in the numerical interval from 347.33 to 492.06 $J \cdot m^{-2}$ for parenchyma samples a longitudinal orientation of the fibers, and from 387.8 to 550.96 $J \cdot m^{-2}$, the transverse orientation of the parenchyma fibers. The greatest value of the specific cutting energy samples of black radish arranged along the fibers observed in the middle layer zone C, and tissue arranged when cutting across the fibers in the lower layer zone A.

Comparison of average values of specific cutting energy of samples of black radish of the longitudinal and transverse orientation of the fibers of indication groups of uniformity is shown in Figure 6. The different points are included in the average values give rise to a significant difference between them.

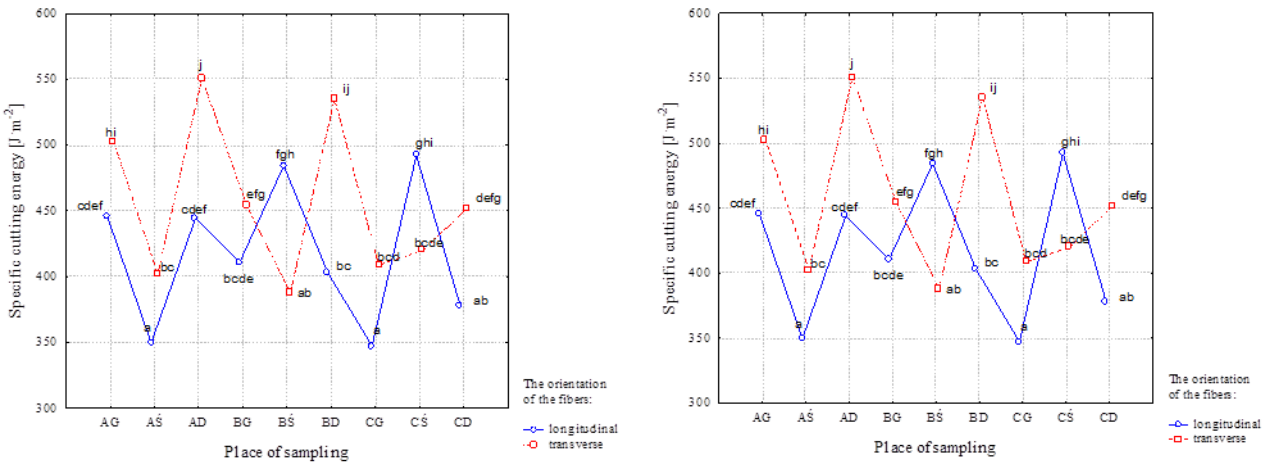

Fig. 6. The significance of differences Tukey test: specific cutting energy at knife wedge angle 5^o for samples of black radish parenchyma taken from specific places at the longitudinal and transverse direction of fibers

In the test of cutting the black radish parenchyma by knife wedge angle $\beta = 7{,}5^o$ when the sample was placed across the fibers (Fig. 7a), the highest specific cutting energy value was observed for the sample taken from the upper layer zone A - 608.99 $J \cdot m^{-2}$. With the longitudinal orientation of the fibers (Fig. 7b), the specific cutting energy of black radish parenchyma taken from the same place was by 19.55% higher. The lowest specific cutting energy was observed for the middle layer zone A cut across the fibers (416.22 $J \cdot m^{-2}$).

Comparison of mean values for both the aspects of black radish parenchyma samples indicating the uniformity of the groups is shown in Figure 8.

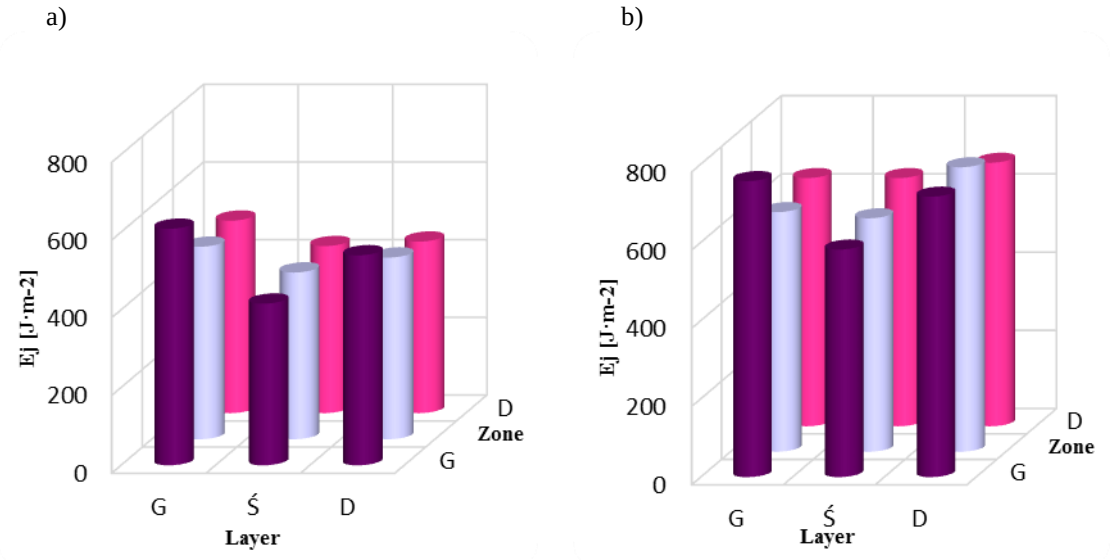

Fig. 7. Dependence of specific cutting energy of the black radish parenchyma at knife wedge angle $\beta = 7.5^{o}$ on the place of sampling at a) longitudinal b) transverse fibers orientation

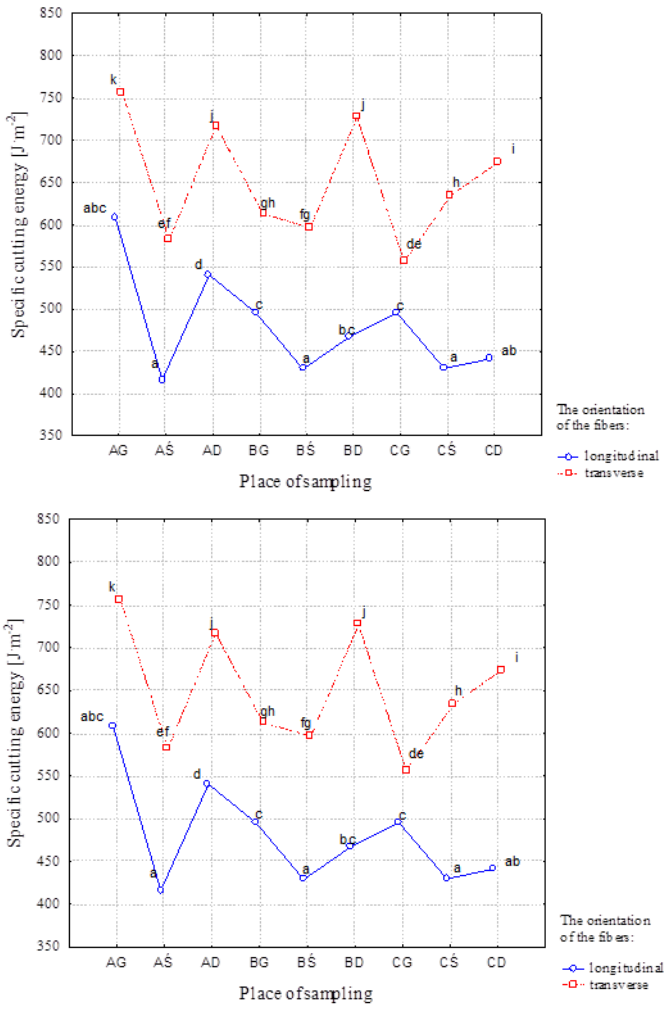

Fig. 8. The significance of differences Tukey test: specific cutting energy at knife wedge angle 7.5^{o} for samples of black radish parenchyma taken from specific places at the longitudinal and transverse direction of fibers

Based on the results of cutting the root tissue at knife wedge angle $\beta = 10°$ (Fig. 9 and 10), it was observed that the average specific cutting energy values were in the numerical interval from 463 to 564.16 $J \cdot m^{-2}$ for samples with longitudinal orientation of the fibers, and from 532.52 to 739.11 $J \cdot m^{-2}$ for the transverse orientation of the parenchyma fibers. The highest value of the specific cutting energy of black radish samples located along and across the fibers was observed in the upper layer of the zone A.

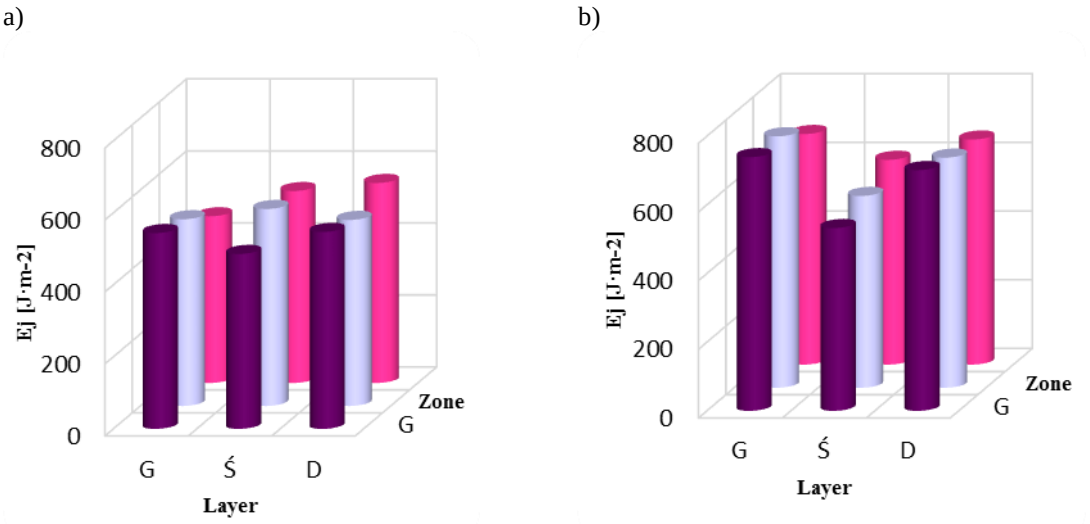

Fig. 9. Dependence of specific cutting energy of the black radish parenchyma at knife wedge angle $\beta = 10^{o}$ on the place of sampling at: a) longitudinal b) transverse fibers orientation

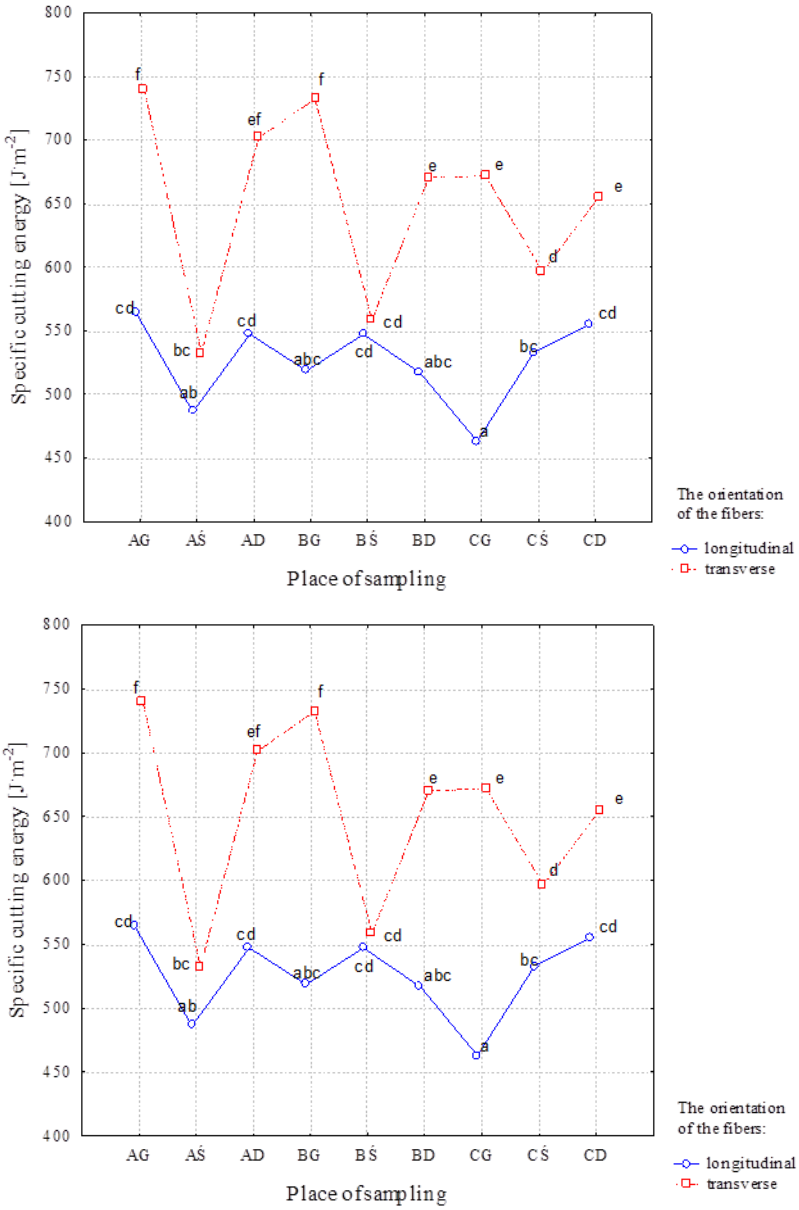

Fig. 10. The significance of differences Tukey test: specific cutting energy at knife wedge angle 10^{o} for samples of black radish parenchyma taken from specific places at the longitudinal and transverse direction of fibers

For black radish parenchyma of the longitudinal orientation of the fibers cut by a knife wedge angle β = 12,5° observed the lowest values of specific cutting energy for the middle layer (Fig. 11). Based on the test the significance of differences Tukey (Fig. 12), there was no significant difference between the specific cutting energy samples of black radish taken from this place. The average value of the specific cutting energy for the zone A was 556.09 J·m^{-2}, zone B 554.45 J·m^{-2} and zone C 588.35 J·m^{-2}. The greatest value of the specific cutting energy observed at the transverse orientation of the fibers parenchyma samples taken from the black radish tissue upper layer zone A (851.58 J·m^{-2}). For the same measuring place, but a sample located along the fiber, this value was about 7.24% lower.

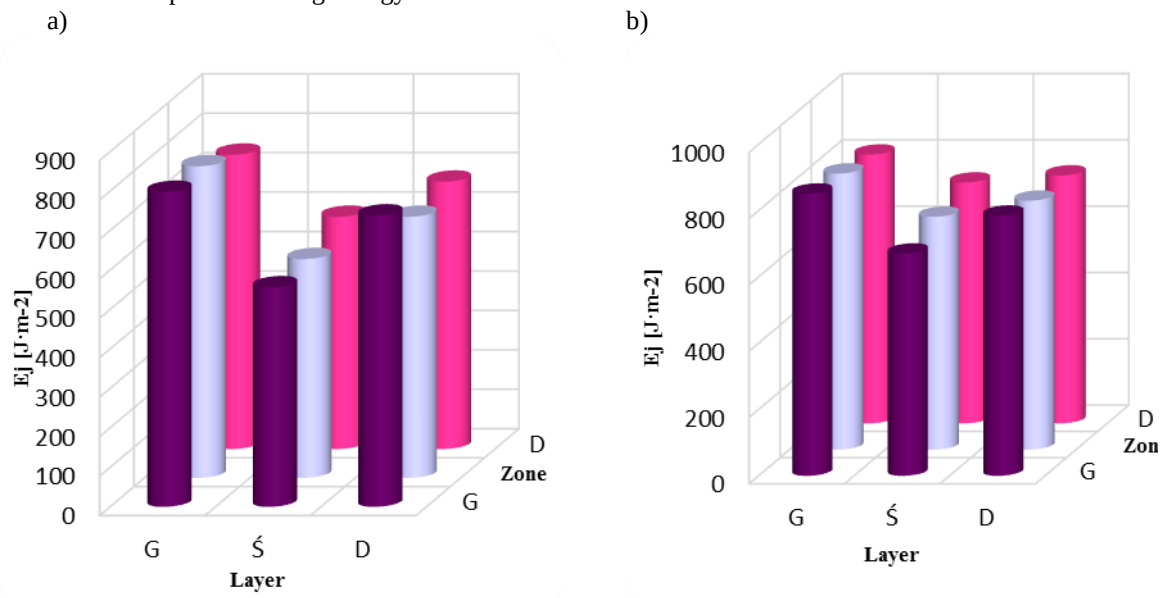

Fig. 11. Dependence of specific cutting energy of the black radish parenchyma at knife wedge angle β = 12.5° on the place of sampling at: a) a longitudinal b) transverse fibers orientation

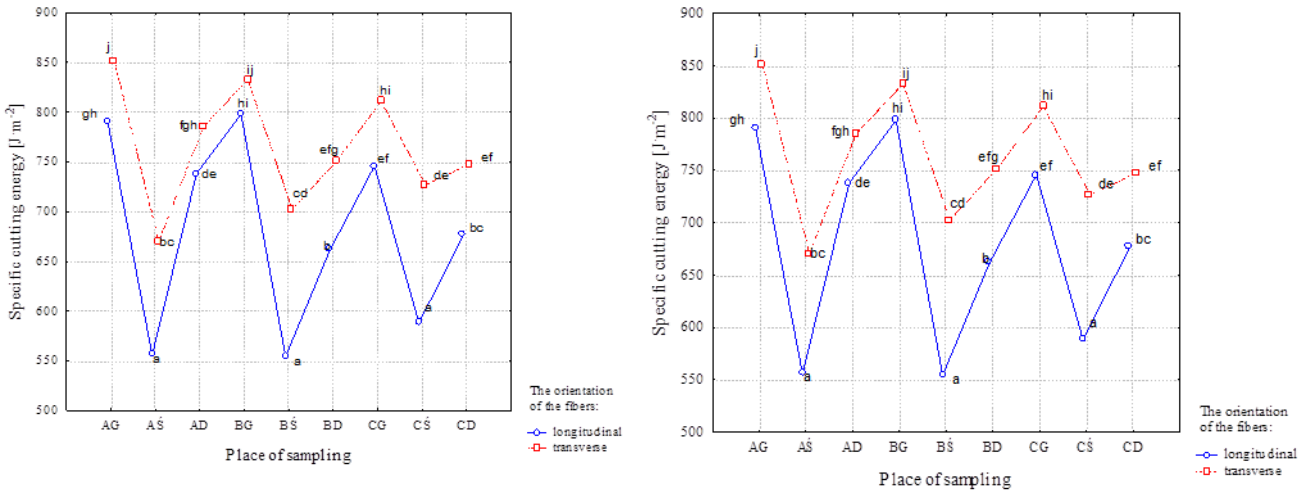

Fig. 12. The significance of differences Tukey test: specific cutting energy at knife wedge angle 12,5° for samples of black radish parenchyma taken from specific places at the longitudinal and transverse direction of fibers

Analyzing the data in the graphs 13a, 13b and 14, it can be concluded that the highest specific cutting energy value was obtained for samples of black radish taken from its core (zone A). The highest specific cutting energy was required to cut the sample arranged transversely and taken from the top layer of the material (1033.43 J·m^{-2}). Its value when placed at longitudinal fibers was by about 182.33 J·m^{-2} lower. Based on the Tukey test of the significance of differences a significant effect was shown of the place of sampling, as well as of the orientation of fibers (Fig. 14).

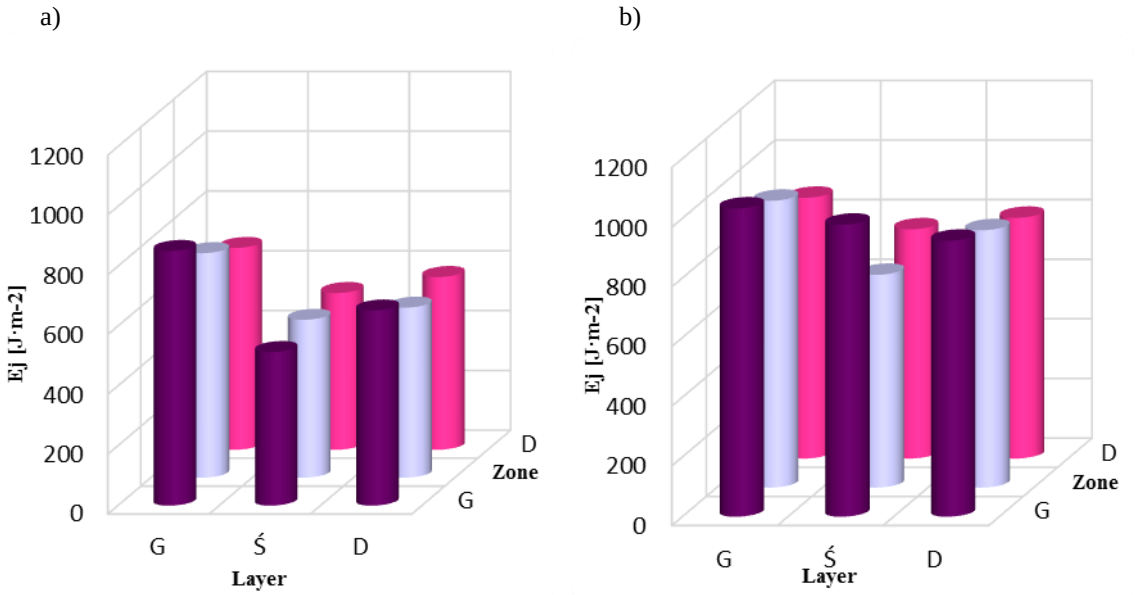

Fig. 13. Dependence of specific cutting energy of the black radish parenchyma at knife wedge angle $\beta = 15^{o}$ on the place of sampling at: a) longitudinal b) transverse fibers orientation

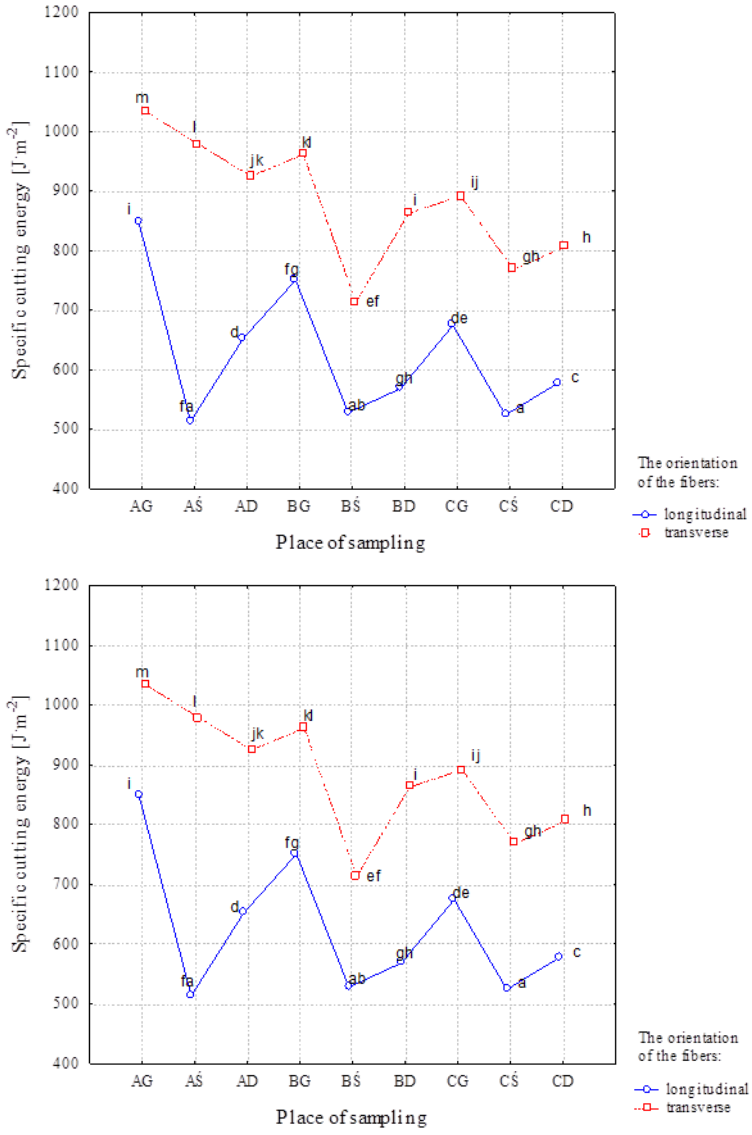

Fig. 14. The significance of differences Tukey test: specific cutting energy at knife wedge angle 15^{o} for samples of black radish parenchyma taken from specific places at the longitudinal and transverse direction of fibers

Table 1 presents the regression equation of specific cutting energy of the black radish parenchyma cut with guillotine knifes at various wedge angles in both the orientations of fibers depending on the place of sampling.

Location of samples, i.e. the distance from the *x*- and *y*-axis had a significant impact on the value of specific cutting energy.

Table 1. The regression equations and coefficients of determination R^2 describing the specific cutting energy of black radish parenchyma for the longitudinal and transverse orientation of fibers, knives wedge angles from 5° to 15° depending on the place of sampling

Knife wedge angle [°]	Fiber orientation	Regression equation	Coefficients of determination R^2
2,5	longitu	$Ej = 0{,}535y^2 - 1{,}976x + 2{,}647y + 250{,}271$	0,729
	transve	$Ej = 0{,}583y^2 + 2{,}808y + 314{,}58$	0,919
5,0	longitu	$Ej = -0{,}15y^2 + 436{,}046$	0,418
	transve	$Ej = 0{,}359y^2 - 1{,}945x - 1{,}909y + 432{,}414$	0,769
7,5	longitu	$Ej = 0{,}37y^2 - 2{,}21x + 1{,}668y + 458{,}269$	0,696
	transve	$Ej = 0{,}309y^2 - 2{,}125x - 2{,}141y + 636{,}298$	0,508
10,0	longitu	$Ej = -0{,}82y^2 + 528{,}916$	0,457
	transve	$Ej = 0{,}589y^2$+1,289y+562,552	0,821
12,5	longitu	$Ej = 0{,}751y^2 + 2{,}848y + 566{,}295$	0,878
	transve	$Ej = 0{,}43y^2 + 2{,}348y + 699{,}934$	0,852
15,0	longitu	$Ej = 0{,}67y^2 - 2{,}677x + 5{,}311y + 561{,}83$	0,855
	transve	$Ej = 0{,}244x^2 + 0{,}415y^2 + 3{,}248y + 916{,}898$	0,828

where: *x* - distance of the point from the axis of ordinates [mm], and *y* - distance of the point from the abscissa [mm].

The equations are valid for the values of *x* (in the range of 0 ÷ 30 mm) and *y* (in the range of -15 to 15 mm) and are designated at the level of significance of differences $\alpha \leq 0.05$.

CONCLUSIONS

1. The knife wedge angle significantly affects the specific cutting energy of black radish.
2. The knife angle increase from 2.5° to 15° caused an increase of specific cutting energy of black radish from 347 to 851 $J \cdot m^{-2}$ (at the longitudinal orientation of fibers), and from 388 to 1033 $J \cdot m^{-2}$ (at the transverse orientation of fibers).
3. When cutting black radish tissue, the highest average value of specific cutting energy was obtained for the parenchyma sample from the upper layer (zone A), and the lowest from the zone C (upper layer).
4. At the transverse direction of the black radish parenchyma fiber the value of the specific cutting energy was significantly higher than at the longitudinal.
5. It is advisable to undertake research on cutting materials of plant origin with particular reference to their structural features, as these materials are characterized by anisotropy, which significantly affects the cutting process.

REFERENCES

1. **Grzemski P., 2013.** Determination of rheological properties of vegetables and fruit based on work inputs of strain. Agricultural Engineering, 17(4), 35-42.
2. **Bohdziewicz J., Czachor G., 2010.** The impact of load on deformation progress for ball-shaped vegetables. Agricultural Engineering, 1(119), 85-91.
3. **Del Aguila J.S., Sasaki F.F., Heiffig L.S., Ortega E.M.M., Jacomino A.P., Kluge R.A., 2006.** Fresh-cut radish using different cut types and storage temperatures. Postharvest Biology and Technology, 40(2), 149-154.
4. **Derossi A., De Pilli T., La Penna M.P., Severini C., 2011.** pH reduction and vegetable tissue structure changes of zucchini slices during pulsed vacuum acidification. LWT-Food Science and Technology, 44(9), 1901-1907.
5. **Dróżdż B., 2010.** Energy analysis in oilseed processing industry. TEKA Commission of Motorization and Energetics in Agriculture, 10, 47-58.
6. **Francisco M., Velasco P., Moreno D.A., García-Viguera C., Cartea M.E., 2010.** Cooking methods of Brassica rapa affect the preservation of glucosinolates, phenolics and vitamin C. Food Research International, 43(5), 1455-1463.
7. **Goyeneche R., Agüero M.V., Roura S., Di Scala K., 2014.** Application of citric acid and mild heat shock to minimally processed sliced radish: Color evaluation. Postharvest Biology and Technology, 93, 106-113.
8. **Góral D., Kluza F., 2009.** Cutting test application to general assessment of vegetable texture changes caused by freezing. Journal of Food Engineering, 95(2), 346-351.
9. **Kowalik K., Sykut B., Marczak H., Opielak M., 2013.** A method of evaluating energy consumption of the cutting process based on the example of hard cheese. Maintenance and Reliability, 15(3), 241–244.

10. **Kusińska E., Starek A., 2014.** Assessment of variability of the maximum cutting force in relation to the beetroot pulp structure. Agricultural Engineering, 1(149), 91-100.
11. **Kusińska E., Starek A., 2012.** Effect of knife wedge angle on the force and work of cutting peppers. TEKA. Commission of Motorization and Energetics in Agriculture, 12, 127-130.
12. **Leong S.Y., Richter L.K., Knorr D., Oey I., 2014.** Feasibility of using pulsed electric field processing to inactivate enzymes and reduce the cutting force of carrot *(Daucus carota* var. *Nantes)*. Innovative Food Science and Emerging Technologies, 26, 159-167.
13. **Li Z., Li P., Liu J., 2011**. Physical and mechanical properties of tomato fruits as related to robot's harvesting. Journal of Food Engineering, 103(2), 170-178.
14. **Lipecki J., Libik A., 2003.** Niektóre składniki warzyw i owoców o wysokiej wartości biologicznej. Folia Horticulturae. Suplement, 1, 16-22.
15. **Nadulski R., Strzałkowska K., Skwarcz J., 2010.** Impact of the knife sharpening angle on the course of cutting selected root vegetables. Agricultural Engineering, 7(125), 161-166.
16. **Nadulski R., Zawiślak K., Panasiewicz M., Skwarcz J., Starek A., 2013.** Characteristics of cutting resistance of selected plant materials of different morphological. Chemical Engineering and Equipment, 52(3), 208-209.
17. **Opielak M., Komsta H., 2000.** Directions of development the grinding equipment for the food industry. Zeszyty Naukowe Politechniki Opolskiej, 61, 167-173.
18. **Schneider Y., Zahn S., Rohm H., 2008.** Power requirements of the high-frequency generator in ultrasonic cutting of foods. Journal of Food Engineering, 86(1), 61-67.
19. **Schneider Y., Zahn S., Schindler C., Rohm H., 2009.** Ultrasonic excitation affect friction interactions between food materials and cutting tools. Ultrasonic, 49, 588-593.
20. **Ślaska-Grzywna B., 2008.** The impact of celery heat treatment parameters on cutting force. Agricultural Engineering, 6, 175-180.
21. **Velchev S., Kolev I., Ivanov K., Gechevski S., 2014.** Empirical models for specific energy consumption and optimization of cutting parameters for minimizing energy consumption during turning. Journal of Cleaner Production, 80, 139-149.
22. **Vreugdenhil D., Xu X., Jung C.S., van Lammeren A.A., Ewing E.E., 1999.** Initial anatomical changes associated with tuber formation on single-node potato (*Solanum tuberosum* L.) cuttings: A re-evaluation. Annals of Botany, 84(5), 675-680.
23. **Xia Q., Wu W.C., Tian K., Jia Y.Y., Wu X., Guan Z., Tian X.J., 2015.** Effects of different cutting traits on bud emergence and early growth of the Chinese vegetable Toona sinensis. Scientia Horticulturae, 190, 137-143.
24. **Yan J., Li L., 2013.** Multi-objective optimization of milling parameters–the trade-offs between energy, production rate and cutting quality. Journal of Cleaner Production, 52, 462-471.
25. **Zastempowski M., Bochat A., 2011.** The study of energy consumption cut plant material. Chemical Engineering and Equipment, 50(3), 91-92.

A unified model of a spinning disc centrifugal spreader

W. Przystupa, M. Kostrzewa, M. Murmyło

University of Life Sciences in Lublin, Faculty of Production Engineering
Głęboka 28, 20-612 Lublin, Poland
e-mail: wojciech.przystupa@up.lublin.pl

Received July 14.2016: accepted July 19.2016

Abstract. A mathematical model was built of the motion of fertilizer particles on the spinning disc and in the air. The Langevin's stochastic differential equation was applied to describe the random disturbances affecting fertilizer particles moving on the disc spreader. The verification of experimental results showed good agreement with the simulation results obtained from the stochastic model. Our results bring new cognitive value in the field of process modeling of mineral fertilizers spreading with disc spreaders and can be used to improve the existing spreaders as well as to design new ones.

Key words: spinning disc, centrifugal fertilizer spreader, Langevin equation

INTRODUCTION

An analysis of the literature on the subject shows that currently only a few issues associated with the process of spreading granular fertilizers with disc spreaders have been explained. Experimental studies have focused on analyzing the motion of fertilizer particles along the spreading disc, and their purpose has been to specify the velocity and angle of fertilizer particles leaving the disc [26,27,28]. Few publications refer to operation and testing investigations and are of a fragmentary nature [9, 11, 29, 30]. Theoretical studies focus mainly on an analysis of the motion of fertilizer particles on the rotating disc [4, 10, 25]. Differences between computer simulation results and the corresponding results from experimental studies are a consequence of deficiencies in the applied mathematical models describing the behaviour of fertilizer particles during spreading. This is due to oversimplification at the stage of formulating mathematical dependencies describing the process of spreading fertilizers with disc spreaders. Among the most frequent assumptions found in the literature on the subject [3, 6, 8, 14] simplifying the mathematical description of the motion of fertilizer particles along the spreading disc is the ignoring of the interactions between the fertilizer particles and the deflections of particles from the rotating disc and blades. The simulation of the motion of the fertilizer mass along the spreader disc is limited to the description of the motion of individual particles and adding together their trajectories using the superposition method. The discrete elements method (DEM) is used to describe the motion of fertilizer particles on the spreading disc, with attempts to include the interactions between them, but with no reference to the structural and operational parameters of the spreading systems [21, 22, 23, 24]. In the case of modelling of the motion of fertilizer particles in the air, the particles are assumed to have a spherical shape, while not taking into account their rotational motion around their own axis and collisions in the air. Literature analysis [4, 5, 6, 14] shows that most authors claim that the most differences between the actual behaviour of fertilizer particles and the assumed model of the process occur during their motion on the rotating disc. Examples of differences between the fertilizer mass distribution obtained during computer simulations and experimental results can be found in investigation results presented in the discussed study [14]. According to the authors of the said study, this is also due to the exclusion of interactions between fertilizer particles moving along the disc. Without an appropriate adjustment of input data it is not possible to obtain simulation results consistent with the experimental data.

The objective of the study was to develop a mathematical model of spreading mineral fertilizers with centrifugal spreaders that includes random shocks to which fertilizer particles moving along the disc are subjected. During the creation of a stochastic model it was assumed that the shape of fertilizer particles is spherical, and that they are uniform in shape, size and density, and also that the interactions between fertilizer particles moving along the spreader disc can be described with the use of stochastic forces [18,19].

THE EQUATION FOR THE MOTION OF FERTILISER PARTICLE ON THE DISC

Figure 1 presents the distribution of forces acting on a fertilizer particle moving along the rotating disc blade of the spreader moving with angle velocity ω.

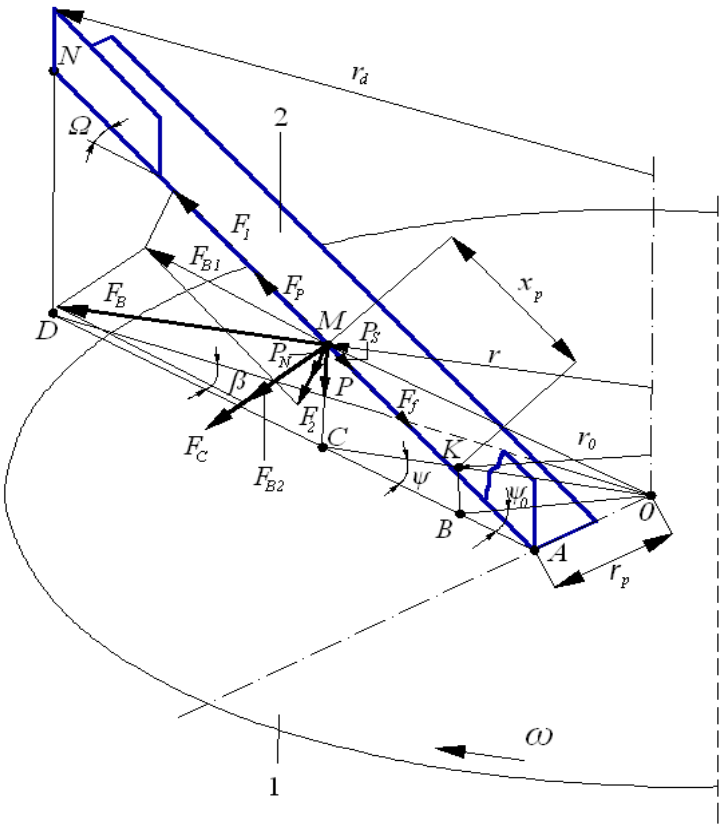

Fig. 1. Distribution of forces acting on the fertilizer particle motion along the vane of spreader disc: 1 – disc, 2 – vane, r – radial coordinate of particle fertilizer, r_d – disc radius, r_p – distance between the vane and axis of disc rotation, r_0 – the feed radius, F_P – inertial force, F_f – friction force, F_C – Coriolis force, F_B – centrifugal force, F_{B1} – component of the force F_B, F_{B2} – normal component of the force F_B, F_1 – tangential component of the force F_{B1}, F_2 – normal component of the force F_{B1}, P – gravity force, P_N – normal component of gravity force, P_S – tangential component of gravity force, β – angle between the vane and disc radius, Ψ – angle between the vane and radius r , Ψ_0 – angle between the vane and radius r_0 , ω – angular velocity of the disc, Ω – angle between the vane and horizontal plane

In the analysed case the blade is inclined towards the horizontal plane at angle Ω and deviates from the disc's radius at angle β. The following forces act on the fertilizer particle located on the disc at distance r from the rotation axis (point M) [1, 2, 7]:

– centrifugal force:

$$F_B = m\omega^2 r\,, \tag{1}$$

–Coriolis force:

$$F_C = 2m\omega\cos\Omega\frac{dx_p}{dt}\,, \tag{2}$$

– gravity force:

$$P = mg\,, \tag{3}$$

– friction force:

$$F_f = \mu_d\left(P_N + F_2\right) + \mu_v\left(F_C + F_{B2}\right), \tag{4}$$

where:

g – gravitational acceleration [m·s^{-2}],

μ_d – friction coefficient for particle-disc interaction [-],

μ_v – friction coefficient for particle-vane interaction [-].

From the equilibrium condition of the forces acting on the fertilizer particle at point M (Fig. 1) it is possible to obtain the following equation for the resultant force F_P acting on the fertilizer particle:

$$F_P = F_1 - P_S - F_f\,, \tag{5}$$

where:

$$F_P = m\frac{d^2x_p}{dt^2}\,, \tag{6}$$

$$F_1 = F_{B1}\cos\Omega\,, \tag{7}$$

$$F_2 = F_{B1}\sin\Omega\,, \tag{8}$$

$$P_S = P\sin\Omega\,, \tag{9}$$

$$P_N = P\cos\Omega\,, \tag{10}$$

$$F_{B1} = F_B\cos\psi\,, \tag{11}$$

$$F_{B2} = F_B\sin\psi\,. \tag{12}$$

Substituting equs (1-4) and (6-12) in equ (5), the equation of motion of the particle on the disc for straight vane (equ (13)) becomes:

$$\frac{d^2x_p}{dt^2} + 2\mu_v\omega\cos\Omega\frac{dx_p}{dt} - r\omega^2\cos\psi\left(\cos\Omega - \mu_d\sin\Omega\right) + \mu_v r\omega^2\sin\psi + g\left(\sin\Omega + \mu_d\cos\Omega\right) = 0. \tag{13}$$

As equation (13) contains two variables, r and $x_{p,}$ determining the location of the fertilizer particle on the disc, the equation was converted as follows:

$$\frac{d^2r}{dt^2} + C_a\left(\frac{dr}{dt}\right)^2 + C_b\frac{dr}{dt} + C_c r + C_d = 0\,, \tag{14}$$

where the coefficients C_a, C_b, C_c and C_d are defined as follows:

$$C_a = -\frac{r_p^2}{r\left(r^2 - r_p^2\right)}, \tag{15}$$

$$C_b = 2\mu_v\omega\cos\Omega\,, \tag{16}$$

$$C_c = \left(\mu_d\sin\Omega\cos\psi - \cos\Omega\cos\psi + \mu_v\sin\psi\right)\cos\Omega\,\omega^2\sqrt{1-\left(\frac{r_p}{r}\right)^2}\,, \tag{17}$$

$$C_d = \left(\sin\Omega + \mu_d\cos\Omega\right)\cos\Omega\,g\sqrt{1-\left(\frac{r_p}{r}\right)^2}\,. \tag{18}$$

The model of the motion of the fertilizer particle on the spreader disc described in equation (14) is a deterministic model. Applying this model always leads to identical solutions with fixed initial conditions. In real conditions fertilizer particles moving along the spreader disc are subjected to random shocks, which the model does not take into consideration. Fertilizer particles moving in a stream interact with one another, which, at the stage of the particles' motion on the disc, causes changes to their velocity and directions of leaving the disc.

In mechanics, stochastic differential equations are used for the description of random shocks to which physical systems are subjected. An example of a stochastic differential equation very frequently used to describe physical systems subjected to random shocks is the Langevin equation.

The Langevin differential equation describing the motion of fertilizer particles on the rotating spreader disc can be expressed as follows:

$$\frac{d^2r}{dt^2} + C_a\left(\frac{dr}{dt}\right)^2 + C_b\frac{dr}{dt} + C_c r + C_d = \sigma_F\xi(t)\,, \tag{19}$$

where:

ξ(t) – the stochastic Langevin force,

σ_F – the intensity of stochastic forces.

The Langevin force occurring in equation (19) has the following properties:

$$\xi(t) = 0\,, \tag{20}$$

$$\xi(t)\xi(t_0 = 2\delta(t - t_0)\,, \tag{21}$$

where: $\delta(t\text{-}t_0)$ is the Dirac function defined in the following way:

$$\delta(t - t_0) = \begin{cases} 0 & for \quad t \neq t_0\,. \\ +\infty & for \quad t = t_0 \end{cases} \tag{22}$$

This study contains a numerical solution of the non-linear equation (14) via the Runge-Kutta method of the fourth order [17], and the stochastic equation (19) via the Runge-Kutta method of the fourth order for stochastic equations [12] with the following initial and boundary conditions:

$$\begin{aligned} &t = 0: \quad r = r_0\,, \quad \varphi = \varphi_i\,, \quad \frac{dr}{dt} = 0\,, \\ &t = t_k: \quad r = r_d\,, \quad \varphi = \varphi_i + \varphi_u\,, \quad \frac{dr}{dt} = V_R\,. \end{aligned} \tag{23}$$

Figure 2 presents the trajectory of a fertilizer particle moving on the rotating disc of the spreader at angle velocity ω. In the simulation model, the coordinates of point K of feeding the fertilizer particle to the disc (φ_i, r_0) are generated on a random basis.

The solution of the deterministic (14) or stochastic (19) equation makes it possible to determine the horizontal component V_R of the fertilizer particle's radial velocity at time $t = t_k$ of the particle's leaving the spreader disc, where t_k is the time at which the particle moved from r_0 to r_d.

Determining the trajectory of the fertilizer particle's motion in the air requires calculating initial velocity V_0 in the air, angle α_0 between the horizontal plane and the direction of initial velocity $V_{0,}$ and angle θ of the fertilizer particle's leaving the disc. Figures 2 and 3 present the distribution of initial velocity V_0 of the fertilizer particle at the end of the blade.

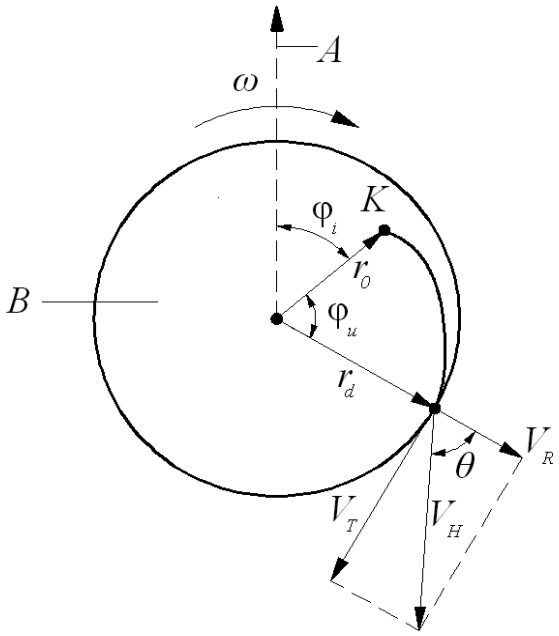

Fig. 2. Trajectory of the fertilizer particle on disc: A – travel direction, B – disc, V_H – horizontal component of the outlet angle of fertilizer particle from disc, V_T – tangential component of V_H velocity, V_R – radial component of V_H velocity, θ – outlet angle of fertilizer particle from disc, ω – angular velocity of the disc, r_d – disc radius, r_0 – the feed radius, φ_i – angle of the initial particle position on disc, φ_u – angle of the particle position on disc

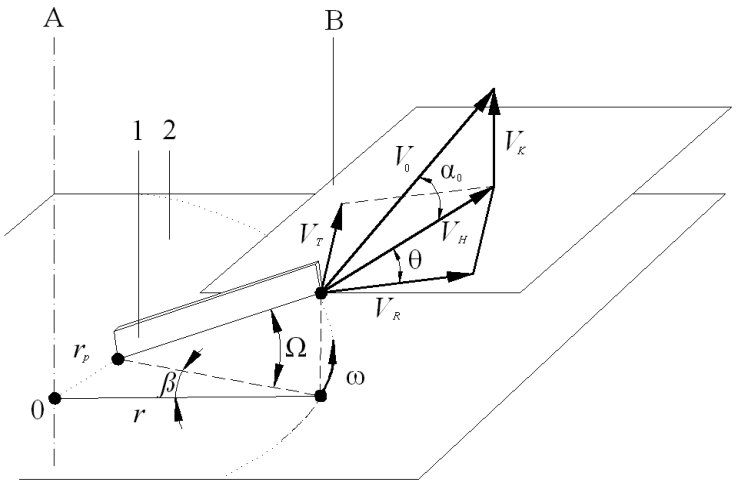

Fig. 3. Distribution of the velocity of fertilizer particle at the edge of vane: 1 – disc, 2 – vane, A – axis of disc rotation, B – horizontal plane, Ω – angle between the vane and horizontal plane, r – radial coordinate of particle fertilizer, ω – angular velocity of the disc, r_p – distance between the vane and axis of disc rotation, θ – outlet angle of fertilizer particle from vane, V_H – horizontal component of outlet velocity of fertilizer particle from disc, V_T – tangential component of V_H velocity, V_R – radial component of V_H velocity, V_K – vertical component of outlet velocity of fertilizer particle from disc, V_0 – outlet velocity of fertilizer particle from disc, α_0 – the initial vertical angle of the particle in the air

The initial velocity V_0 of the fertilizer particle in the air is (Fig. 3):

$$V_0 = \sqrt{V_H^2 + V_K^2}\,. \tag{24}$$

In order to determine the value of angle θ, the value of the component of tangent V_T of the velocity of the fertilizer particle on the horizontal plane must be calculated first (Fig. 3).

$$V_T = \omega r_d - V_R \frac{r_p}{\sqrt{r_d^2 - r_p^2}}\,. \tag{25}$$

Knowing the values of velocity components V_R and V_T from expression (26), it is possible to calculate angle θ of the fertilizer particle's leaving the disc ($r = r_d$):

$$tg\theta = \frac{V_T}{V_R}. \quad (26)$$

Inserting expression (25) into equation (26) yields the value of angle θ of the fertilizer particle's leaving the disc:

$$\theta = arctg\left[\frac{\omega r_d\sqrt{r_d^2 - r_p^2} - V_R r_p}{V_R\sqrt{r_d^2 - r_p^2}}\right]. \quad (27)$$

Knowing the value of velocity V_R and angle θ of the fertilizer particle's leaving the disc, it is possible to calculate the velocity of the particle relative to blade V_{XP} at the time of leaving the disc:

$$V_{XP} = \frac{V_R}{\cos\Omega\cos\beta}. \quad (28)$$

and the horizontal component V_H and the vertical component V_K of initial velocity V_0 of the fertilizer particle in the air:

$$V_H = \frac{V_R}{\cos\theta}, \quad (29)$$

$$V_K = V_{XP}\sin\Omega = \frac{V_R}{\cos\beta}tg\Omega. \quad (30)$$

The initial value of the angle of inclination α_0 of the initial velocity vector V_0 of the fertilizer particle in the air relative to the horizontal plane can be determined through the following expression (Fig. 3):

$$tg\alpha_0 = \frac{V_K}{V_H}. \quad 31)$$

Inserting dependencies (29) and (30) into equation (31) yields the following expression for the value of angle α_0:

$$\alpha_0 = arctg\left[\frac{\cos\theta}{\cos\beta}tg\Omega\right]. \quad (32)$$

In the simulation model, angles α_0 and θ and initial velocity V_0 of the fertilizer particle in the air are determined through equations (32), (27) and (24). Knowing these values, the trajectory of motion of the fertilizer particle in in the air and the place of its falling on the ground can be determined.

THE EQUATION FOR THE MOTION OF A FERTILISER PARTICLE IN THE AIR

At the moment of leaving the blade, the velocity value of the fertilizer particle velocity is V_0. In the case of a conical disc ($\Omega \neq 0$), the velocity vector V_0 forms angle α_0 with the horizontal plane. A fertilizer particle moving in the air is influenced by the gravitational force, air-resistance force and lift force. Because the density of fertilizer particles is considerably higher than air density, in the equation for the particle's motion in the air, the air resistance force was ignored. General equations of the motion of fertilizer particles in the air are as follows [14, 16]:

$$\frac{d^2x_{pp}}{dt^2} = -\frac{1}{2}C_D\frac{\rho_a}{\rho_p}\frac{S_p}{V_P}\frac{dx_{pp}}{dt}\sqrt{\left(\frac{dx_{pp}}{dt}\right)^2 + \left(\frac{dz_{pp}}{dt}\right)^2}, \quad (33)$$

$$\frac{d^2z_{pp}}{dt^2} = -g - \frac{1}{2}C_D\frac{\rho_a}{\rho_p}\frac{S_P}{V_P}\frac{dz_{pp}}{dt}\sqrt{\left(\frac{dx_{pp}}{dt}\right)^2 + \left(\frac{dz_{pp}}{dt}\right)^2}, \quad (34)$$

where:

C_D – air resistance coefficient [-],
S_p – resistance surface of the particle [m^2],
V_p – volume of the particle [m^3],
ρ_a – density of the air [$kg \cdot m^{-3}$],
ρ_p – density of the particle [$kg \cdot m^{-3}$].

Solving the system of differential equations (33) and (34) with initial and boundary conditions (35), it is possible to determine distance x_k between the point of the fertilizer particle's leaving the spreading disc and the place of its falling on the ground (point M, Fig. 4).

$$t = 0: \quad x_{pp} = 0 \quad z_{pp} = h; \quad \frac{dx_{pp}}{dt} = V_H; \quad \frac{dz_{pp}}{dt} = V_K,$$
$$t = t_k: \quad x_{pp} = x_k; \quad z_{pp} = 0, \quad (35)$$

where: horizontal component V_H and vertical component V_K of the resultant velocity V_0 are as follows:

$$V_H = V_0\cos\alpha_0, \quad (36)$$

$$V_K = V_0\sin\alpha_0. \quad (37)$$

Another important step in the presented simulation model is determining the coordinates (x_{tot}, y_{tot}) of the place of the fertilizer particle's falling on the ground in the coordinate system related to the spreader discs. Let us assume that at initial time $t = 0$ the fertilizer particle is on the spreader disc at point K at distance r_0 from the centre of the disc (Fig. 4).

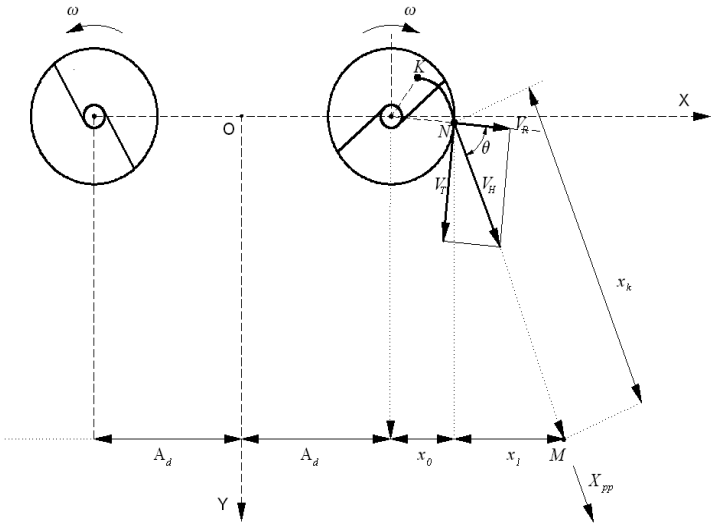

Fig. 4. Position of the fertilizer particle on field: $2A_d$ – distance between two disc centers, V_H – horizontal component of outlet velocity of fertilizer particle from disc, V_R – radial component of V_H velocity, V_T – tangential component of V_H velocity, x_k – distance between the disc edge and the place (M point) of drop, ω – angular velocity of disc, θ – outlet angle of fertilizer particle from disc

At time t_k during the particle's motion from r_0 to r_d the spreader disc will turn by angle $\varphi_u = \omega t_k$ (Fig. 2). Knowing angle θ of the fertilizer particle's leaving the spreader disc and angles φ_i and φ_u, it is possible to determine angles θ_1 and θ_2 :

$$\begin{aligned} \theta_1 &= \varphi_i + \varphi_u + \theta \,, \\ \theta_2 &= \varphi_i + \varphi_u \,, \end{aligned} \tag{38}$$

and later the coordinates of the location of the fertilizer particle on the edge of the disc (x_0, y_0) and distances x_1 and y_1 :

$$x_0 = r_d \sin\theta_2 \,, \qquad x_1 = x_k \sin\theta_1 \,, \tag{39}$$

$$y_0 = -r_d \cos\theta_2 \,, \qquad y_1 = -x_k \cos\theta_1 \,.$$

The coordinates x_{tot} and y_{tot} of the location of the fertilizer particle on the ground can be obtained via the following equations:

$$\begin{aligned} x_{tot} &= x_0 + x_1 + A_d \,, \\ y_{tot} &= y_0 + y_1 \,. \end{aligned} \tag{40}$$

RESULTS

In order to verify the mathematical model of spreading mineral fertilizers with centrifugal spreaders, the results of the investigation performed by the author of this study were used, carried out on an experimental site based on the author's own design. Urea from the current batch manufactured by the Zakłady Azotowe Puławy SA was used for the investigation.

The developed mathematical model of the description of spreading mineral fertilizers with centrifugal spreaders, which includes the impact of random shocks occurring as a result of interactions between fertilizer pellets in a stream, were subjected to validation consisting of the evaluation of the degree of consistency between the values specified on the basis of the model with the actual values obtained on site. This procedure was applied for significant reasons, as the results presented by other authors [11, 15, 29, 30] are not accompanied by documented conditions of measurements (physical properties of the fertilizers, structural and operational parameters of the spreading systems, external conditions, etc.). Furthermore, most of the results of the testing investigations of spreaders are presented in graphic form, which makes it impossible to recreate their actual values [11, 29, 30].

In order to carry out a validation of the compared models, the distribution of the fertilizer mass along the width of the spreading strip was used. One of the commonly used and recommended methods for the evaluation of the conformity of the simulation results with the results of the experimental investigations is regression analysis for a linear model [13].

Figures 5-6 present charts of the actual placement of the fertilizer mass in measurement boxes for urea in comparison to the mass calculated via the deterministic and stochastic models. For both models a strong positive correlation was found between the experimental values of fertilizer mass in the measurement boxes and the values calculated with the use of the models. However, it should be mentioned that the regression coefficient (the slope of the straight line) value is significantly different from zero and amounts to 0.9647 for the equation determining the dependence between the actual distribution of the urea mass and that calculated with the stochastic model. The provided value differs slightly from the value of the coefficient in a perfect situation where the simulation results are consistent with the experimental results. However, it should be emphasized that the mentioned coefficient, in comparison with the one based on the data from the deterministic model, is much lower and amounts to 0.9083. In turn, considering constant values in the regression equations, it can be concluded that they are significantly different (9.0257 and 55.034). In the case of the equation based on the simulation results of the deterministic model, the value is quite substantial and demonstrates the lack of concentration of points along line 1:1 on the plane of interest to the researcher.

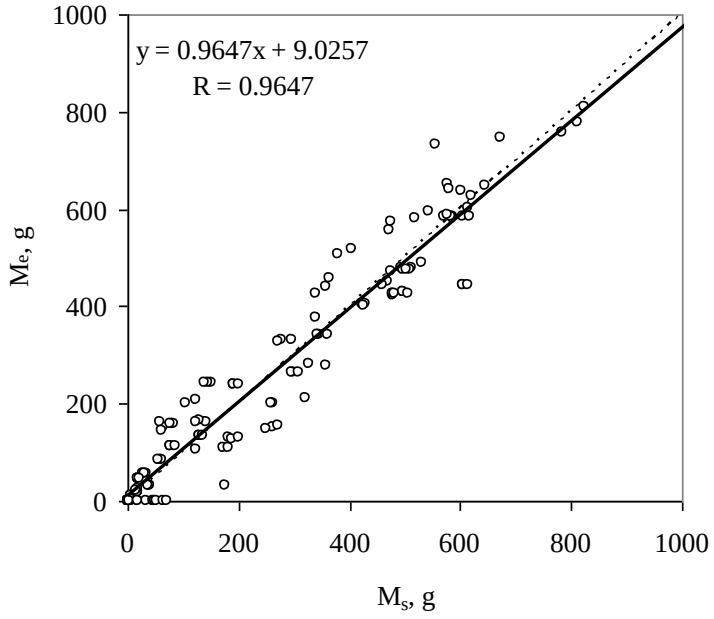

Fig. 5. Regression of real mass of urea in the measuring container (M_e) in relation to mass obtained from stochastic model (M_s); the dashed line represents the ratio of 1:1

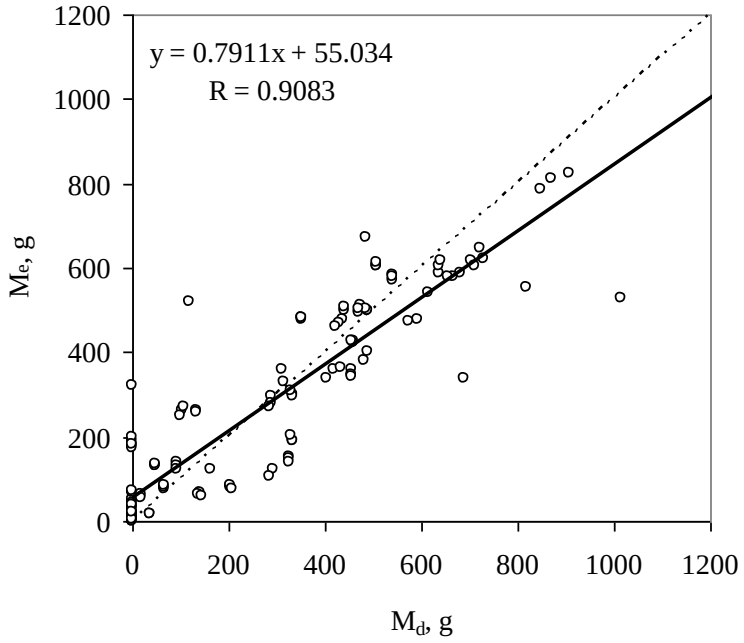

Fig. 6. Regression of real mass of urea in the measuring container (M_e) in relation to mass obtained from deterministic model (M_d); the dashed line represents the ratio of 1:1

CONCLUSIONS

The model for spreading mineral fertilizers developed within the study based on the Langevin stochastic equation describes the mutual interactions between fertilizer particles during their motion along the disc. It also facilitates simulation tests of the transverse distribution of fertilizer mass depending on the physical properties of the fertilizers and the structural and operational parameters of the spreading systems. The developed procedure for simulation calculations, consisting of mutually connected models of the motion of fertilizer particles along the spreader disc and in the air, can be used for designing centrifugal spreading systems and selecting structural and operational parameters depending on the physical properties of fertilizers. The analysis of the regression dependencies of the fertilizer mass actual distribution and of those calculated on the basis of the stochastic and deterministic models showed that the stochastic model developed in this study more accurately described the process of spreading fertilizers with centrifugal spreading systems. This was confirmed by the R^2 coefficient of determination values for the analysed fertilizer.

REFERENCES

1. **Adamčuk V.V. 2003.** Theoretical investigation of the motion of the fertilizer particle on disc spreader. Tractors and farm machinery, 12: 28-31.
2. **Adamčuk V.V. 2004.** Fertilizer application with centrifugal fertilizer spreader. Tractors and farm machinery, 7: 31-33.
3. **Davis J.B., Rice C.E. 1974.** Predicting fertilizer distribution by a centrifugal distributor using CSMP, a simulation language. Transactions of the ASAE, 17(6): 1091-1093.
4. **Dintwa E., Van Liedekerke P., Olieslagers R., Tijskens E., Ramon H. 2004**. Model for simulation of particle flow on a centrifugal fertilizer spreader. Biosystems Engineering, 87(4): 407-415.
5. **Dintwa E., Tijskens E., Olieslagers R., Baerdemaeker J., Ramon H. 2004.** Calibration of a spinning disc spreader simulation model for accurate site-specific fertilizer application. Biosystems Engineering, 88(1): 49-62.
6. **Griffis C.L., Ritter D.W., Matthews E.J. 1983.** Simulation of rotary spreader distribution patterns. Transactions of the ASAE, 26(1): 33-37.
7. **Hofstee J.W., Speelman L., Scheufler B. 1999.** Fertilizer Distributors. CIGR Handbook of Agricultural Engineering. Vol. III, Plant Production Engineering. St. Joseph, MI: ASAE. pp. 240-268.
8. **Jedwabiński Z. 1977.** Optimization of working parameters of the centrifugal fertilizer spreader.Farm machinery and tractors, 11: 6-10.
9. **Kacprzak P. 2008.** Influence of technical-exploitation parameters of the centrifugal fertilizer spreader to the quality of fertilizer spreading. Phd. SGGW. Warszawa.
10. **Kamiński E. 1983.** Analysis of fertilizer spreader granules movement on spreading disc. IBMER. Warszawa.
11. **Kamiński J.R. 1999.** Method of estimation of the influence of parameters of scattering shields on the effectiveness of spreading. Phd. IBMER. Warszawa.
12. **Kloeden P.E., Platen E., Schurz H. 2003.** Numerical solution of SDE through computer experiments. Springer Verlag, Berlin.
13. **Mądry W., Zieliński W., Rozbicki J., Wyszyński Z. 1999.** Calibration and validation of crop simulation model perfomance. Annals of Agriculture Sciences, A114(1-2): 25-40.
14. **Olieslagers R., Ramon H., Baerdemaeker J. 1996.** Calculation of fertilizer distribution patterns from a spinning disc spreader by means of a simulation model. Journal Agricultural Engineering Research, 63(2): 137-152.
15. **Parkin S., Basford B., Miller P. 2005.** Spreading accuracy of solid urea fertilizers. Report for Defra Project NT2610.
16. **Pitt R.E., Farmer G.S., Walker L.P. 1982.** Approximating equations for rotary distributor spread patterns. Transactions of the ASAE, 25(6): 1544-1552.
17. **Press W.A., Teukolsky S.A., Vetterling W.T., Flannery B.P. 1992.** Numerical Recipes in Fortran. Cambridge University Press, Cambridge.
18. **Przystupa W. 2005.** Simutation of the motion of the fertilizer particles on disc spreader. Agricultural Engineering, 14: 301-308.
19. **Przystupa W. 2006.** Mathematical model of the motion of the fertilizer particle after leaving disc spreader. Agricultural Engineering, 6: 177-184.
20. **Van Kampen N.G. 1990.** Stochastic Processes in Physics and Chemistry. PWN. Warszawa.
21. **Van Liedekerke P., Piron E., Vangeyte J., Villette S., Ramon H., Tijskens E. 2008.** Recent results of experimentation and DEM modeling of centrifugal fertilizer spreading. Granular Matter, 10: 247-255.
22. **Van Liedekerke P., Tijskens E., Dintwa E., Anthonis J., Ramon H. 2006.** A discrete element model for simulation of a spinning disc fertilizer spreader I. Single particle simulations. Powder Technology, 170(2): 71-85.
23. **Van Liedekerke P., Tijskens E., Dintwa E., Rioual F., Vangeyte J., Ramon H. 2008**. DEM simulations of the particle flow on centrifugal fertilizer spreader. Powder Technology, 190(3): 348-360.
24. **Van Liedekerke P., Tijskens E., Ramon H. 2009.** Discrete element simulations of the influence of fertilizer physical properties on the spread pattern from spinning disc spreaders. Biosystems Engineering, 102(4): 392-405.
25. **Villette S., Cointault F., Piron E., Chopinet B. 2005.** Centrifugal spreading: an analytical model for the motion of fertilizer particles on a spinning disc. Biosystems Engineering, 92(2): 157-164.
26. **Villette S., Cointault F., Piron E., Chopinet B. 2008.** Centrifugal spreading of fertiliser: deducing three-dimensional velocities from horizontal outlet angles using computer vision. Biosystems Engineering, 99(4): 496-507.
27. **Villette S., Cointault F., Zwaenepoel P., Martin R., Chopinet B., Paindavoine M. 2006.** Centrifugal spreading: Extracting 3D outlet of velocity and flow distribution from motion blurred images. 2nd International Symposium on Centrifugal Fertilizer Spreading, 24-25 September. Montoldre. France.
28. **Villette S., Gée C., Piron E., Martin R., Miclet D., Paindavoine M. 2010.** Centrifugal fertiliser spreading: velocity and mass flow distribution measurement by image processing. AgEng 2010: International Conference on Agricultural Engineering. Clermont Ferrand. France.
29. **Yildirim Y. 2006.** Effect of vane number on distribution uniformity in single-disc rotary fertilizer spreaders. Applied Engineering in Agriculture, 22(5): 659-663.
30. **Yildirim Y. 2006.** Effect of cone angle revolution velocity of disc on fertilizer distribution uniformity in single-disc rotary fertilizer spreaders. Journal of Applied Sciences, 6(14): 2875-2881.

A method of making up a clinic schedule with use of a finite-state automaton

R. Tkachenko, O. Kovalyshyn

National University "Lviv Polytechnic"; email: kovalyshynoleh@gmail.com

Received July 14.2016: accepted July 19.2016

Abstract. The article investigates the problems of scheduling methods for making up the schedules for medical care institutions, with a view to further optimization the conditions and improvement the patient care.

It is noted that a key step in the operation of medical institutions is the scheduling stage process. Depending on the specifics of a particular institution, work plans take different forms, mostly turning into a timetable.

It is established that there are a number of scheduling methods, ranging from manual planning and mathematical programming with limitations, ending with the use of artificial intelligence. Most methods consist of two or more stages and initially require the construction of the very schedule that satisfies the strict limitations of the institution functioning. At a later stage the scheduling optimization of one or more criteria is regarded.

The types of finite-state automata are analyzed and, with their use, developed a method for constructing the supporting schedules for clinics. An algorithm of finite-state machines for clinic schedule construction is established.

Key words: clinic, schedule, schedule construction, abstract automaton, finite-state automaton.

FORMULATION OF THE PROBLEM

The functioning of hospitals and quality of patient care largely depends on the schedule of their work.

Scheduling of clinics functioning is an extremely time-consuming process that takes into account a number of constraints and factors: availability of a qualified physician; a sequence plan of a patient's line therapy; adequate medical equipment at the time of treatment; the need for specialized facilities for the procedures etc.

Schedules can be called the best with the conditions of full realization of the domain restrictions, effective use of available resources, taking into account the wishes of the clinic staff and patients, compliance with the established treatment plan. [14]

If the assembly does not include the full requirements for rehabilitation plans or limits are not satisfied, the quality of treatment is reduced, which in turn significantly affects the quality of medicine itself. On the other hand, with the above restrictions it is desirable to meet the wishes of patients [1].

Taking into account the fact that most Ukrainian clinics scheduling is made by hand, due to the extreme complexity with taking into account the restrictions, attention should be given to automatization with compiling the process.

ANALYSIS OF RECENT RESEARCHES AND PUBLICATIONS

The task of a schedule building is regarded not only as a process that realizes the distribution function of certain procedures at the time. The optimal schedule will provide the maximum benefit from the efficient use of available resources in the clinic, increase the quantity and quality of treatment, the level of satisfaction of employees and patients [18].

The task of schedule compiling and optimization is classified as NP-complete [2, 3]. To solve the problems of this category the approximate methods are used that allow to make suboptimal schedule [4, 5] including:

- The method of simulated annealing,
- Graph coloring method;
- The method of genetic algorithm.

Most methods in one form or another require the correct initial (reference) sample [10, 12, 16]. Its generation is often done randomly that can not be executed in this situation, taking into account the set of binding constraints imposed by the subject area [19].

On the other hand, the set of constraints is a deterministic, the set of operations required to create the schedule and their order are defined.

Accordingly, it is possible to develop a mechanism that will meet the basic restrictions and will make it possible to build the sample.

MAIN MATERIAL PRESENTATION

The process of a schedule construction it is advisable to represent as an abstract machine - abstraction used to describe the way of change of the object state based on the achieved status and information received from outside [6, 7].

The general scheme of the machine can be interpreted as a "black box" [8.15], which provides transformation of input data vector to output vector (Figure 1):

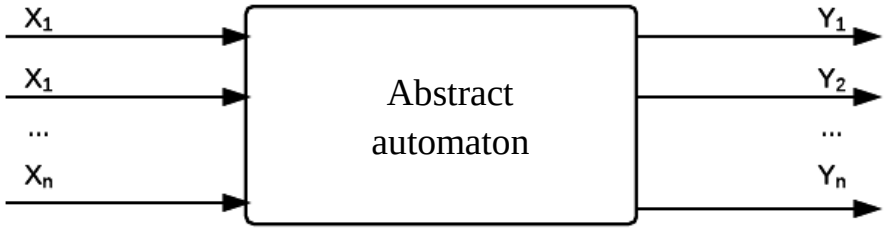

Fig.1. The general scheme of the abstract automaton

Mathematical model of the device can be described as follows [9]:

$$A = (X, Y, S, f_y, f_s, S_0), \quad (1)$$

where X – the set of the automaton input data;
Y – the set of the automaton output data;
S – the set of the allowable states of the machine;
f_y – function of the automaton outputs;
f_s – function of the automaton transitions from one state to another;
S_0 – initial state of the machine.

For the purpose of the automata classification a number of features are considered such as: certainty of the transition function and function of outputs, unambiguous set of functions, stability of conditions, finite sets of input, output data and state [6,17]:

- *by certainty of the characteristic features* automaton of clinic scheduling is defined, whereas all $(s_i, x_k) \in X \times S$, where $s_i \in S, x_k \in X$, that is the characteristic functions are defined for all pairs of input data and possible states.
- *by unambiguous of the transition function* the automaton is deterministic because under some input $x_k \in X$ the machine can move only in one state $s_j \in S$. Conversion mechanism is fully defined, probability of transition is impossible.
- *by the stability of states* the machine is stable, when under the influence of some input $x_k \in X$ there took place a transition into a state $s_j \in S$, then exit from it and the transition to another state is possible only when receiving another input signal $x_z \in X, x_z \neq x_k$.
- *by finitude of states, input and output sets*, the automaton is finite, since the sets *X, Y, S* are finite: $|X| \neq \infty, |Y| \neq \infty, |S| \neq \infty$.

Basic for constructing finite, determined, definite, stable automata are two models - Mealy and Moore machines [11,13].

Specifying the base model, Mealy machine can be supplemented with the following ratios:

$$s(t+1) = f_s(x(t), s(t)),$$
$$y(t) = f_y(x(t), s(t)), \quad (2)$$

where: *s (t + 1)* - the next state, which the automaton will transit in;
f_s – function of the automaton transition to the next state;
x (t) – the current value of the input signal;
s (t) – the current state of the machine;
y (t) – value of the automaton output;
f_y – function of the automaton output.

From the equations (2) we can notice that in the case of Mealy automaton the arguments of characteristic functions are the current value of the input signal and the current status.

Moore machine can be defined as follows:

$$s(t+1) = fs(x(t+1), s(t)),$$
$$y(t) = fy(s(t)) \quad (3)$$

where: *s (t + 1)* - the next state, which the automaton will transit in;
f_s – function of the automaton transition to the next state;
x (t) - the current value of the input signal;
s (t) – the current state of the machine;
y (t) - value of the automaton output;
f_y – function of the automaton output.

From relations (3) it follows that the output signal of the automaton is uniquely determined by its current state and does not depend on the vector components of the input signals [20].

Due to the specific area subject it can be argued that the result of the machine will depend on the type of the procedure, which it will receive at the entrance for inclusion. In its turn, inclusion of the procedures to the schedule will depend on their characteristics and on the current state of the schedule. In this regard, for the construction of the clinic finite automaton it is appropriate to use the Mealy model. Based on its basic principles, we have proposed a method that allows to ultimately develop a schedule of clinics.

Verbally, the process of the automaton work of the clinic schedule can be set as a sequence of the following steps:

Step 1. Achieve a set of procedures for the schedule construction.

Step 2. Selection of the procedures obtained in *step 1* for inclusion in the next schedule. The procedure selection process provides a consistent set of analysis in terms of satisfying the set criteria.

Step 3. Search for the available financial support and free personnel of the clinic for the completion of the procedure selected in *step 2*.

Step 4. Search for available time periods for carrying out the procedure based on the results obtained in *step 3*.

Step 5. Analysis of the possible options for allocation the procedure in the schedule based on data obtained during the *steps 3-4*, and test performance of the limits of the subject area.

Step 6. Direct inclusion of the procedure into the schedule and go back to *step 2*.

For the automaton the set of input data X consists of a set of treatments, from which it is necessary to schedule. The set of output data Y is the resulting set of procedures that make up a schedule and are defined by the algorithm of the automaton functioning. Block diagram of the algorithm for constructing the clinic schedule, which involves the proposed steps 1.6 is shown in Fig. 2.

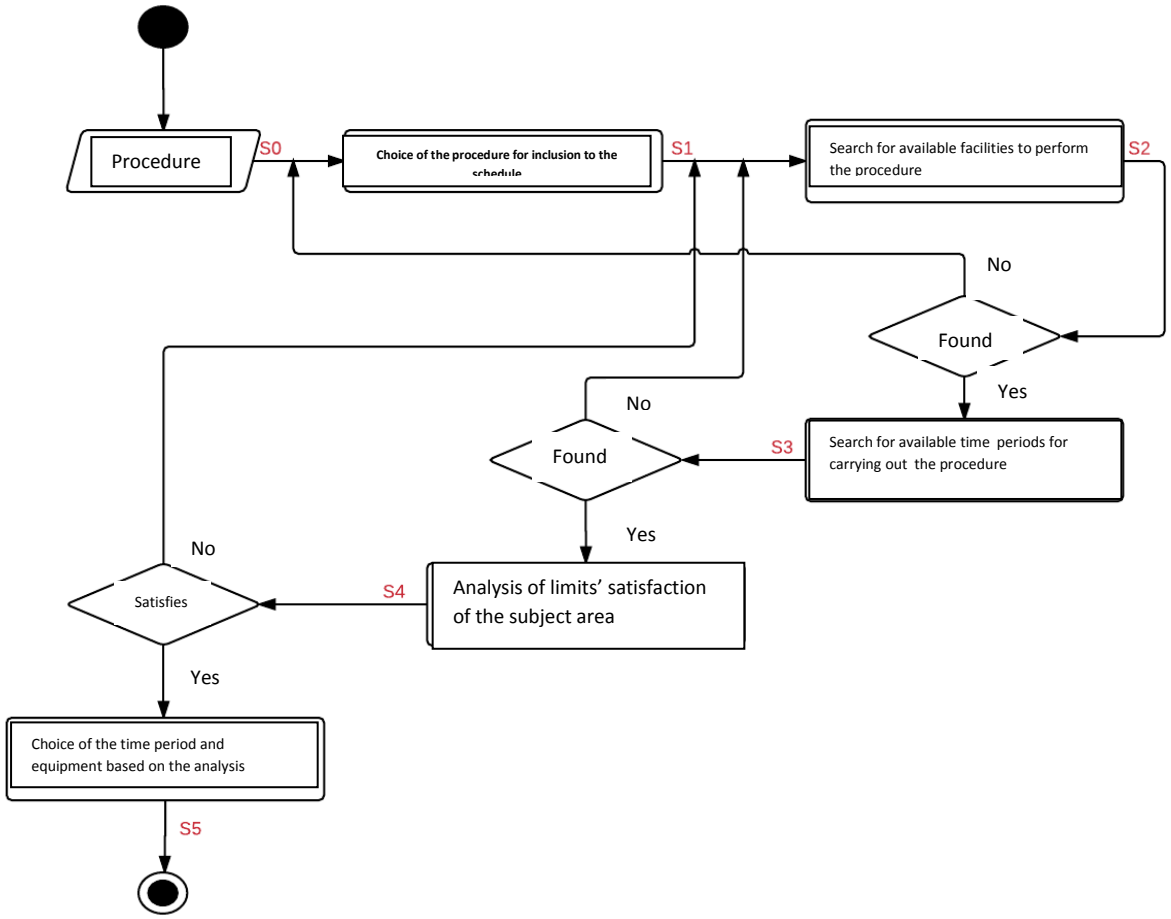

Fig.2. Block diagram of the algorithm for constructing the clinics schedule

According to the flowchart, the set of states contains six elements and has the form $S = \{S_0, S_1, S_2, S_3, S_4, S_5\}$). At the beginning of its work the machine receives the input data and proceeds to its original state (S_0). The next step is the selection of treatments available and a transition to a state S_1. After that the automaton analyzes the equipment for the procedure, free staff etc. In case if the necessary equipment is available machine goes into S_2. With information from the previous step, the analysis of time intervals is being carried out when all the necessary equipment and medical staff are available S_3. For each found time frame the constraints satisfaction analysis of the subject area is being conducted. If successful the machine goes into S_4. Being found, the period and equipment are chosen eagerly to meet the restrictions of the subject area, then record the procedure to schedule and inclusion it in the initial set of data (transition to state S_5).

The transition conditions are boolean functions (as partial satisfaction is unacceptable restriction of the subject area, etc.) which are determined separately for each state.

CONCLUSIONS

1. The study establishes that one of the possible measures to improve the efficiency of hospitals, service quality and level of patients 'satisfaction is an effective use of their work schedule.

2. In order to develop and optimize the clinic scheduling we performed the basic model - Mealy machine, which allows most accurately take into account the specificy of the subject area and the whole ammount of necessary treatments.

3. The presented method of reference schedule of medical treatment institutions in the form of finite automaton allow take into account all the necessary set of treatments, limited time periods for their implementation, necessary equipment and facilities, all of which contributes to the effective formation of a clinic schedule.

REFERENCES

1. **Epifanov V.A., Epifanov A.V., 2014.** Rehabilitation in neurology. GEOTAR Media, 416.
2. **Brouwer V., 1987.** Introduction to the theory of finite automata,. Brouwer, Radio and Communications, 392.
3. **Burdyuk V.Y., Shkurba V.V., 1971.** Theory of schedules. Objectives and methods of solutions. Cybernetics, 1 , 89-102.
4. **Gafarov E.R., Lazarev A.A., 2006.** Proof of NP-hardness particular case of the problem of minimizing the total delay for one device. Izvestiya AN: Theory and management systems, 3, 120-128.
5. **Gary M. Johnson D., 1982.** Computers and Intractability. Mir, 416 p.
6. **Gill A., 1966.** Introduction to the theory of finite automata. Nauka, 272.
7. **Lazarev A.A., Kvaratskhelia A.G., Gafarov E.R., 2007.** Algorithms for solving NP-hard problems of minimization of summarized delay for one device. Reports of the Academy of Sciences 412(6), 739-742.
8. **Karpov Y.G., 2002.** Automata Theory: Textbook for Universities, 224.
9. **Korotkova M.A., 2008.** The mathematical theory of automata: a manual for schools, 116.
10. **Coffman E.G., 1984.** The theory of schedules and computers, 335.
11. **Melikhov A.N., 1971.** Directed graphs and finite state machines, 416.
12. **Sidorin A.B., 2009.** Automation methods of scheduling sessions Part 2: Heuristic optimization methods. News VSTU 12 (60), 120-123.
13. **Hopcroft J., Motvani R. Ullman G., 2002.** Introduction to Automata Theory, Languages and Computing, 527.
14. **Shkurba V.V., Podchasova T.P., Pshichuk A.N. Tur L.P., 1966.** Tasks of scheduling and methods of their solution, Naukova Dumka, 154.
15. **Baptiste Ph., Le Pape C., Nuijten W., 2001.** Constraint-based scheduling: applying constraint programming to scheduling problems, Academic Publishers,198.
16. **Brooks G.N., White C.R., 1965.** An algorithm for finding optimal or near – optimal solutions to the production scheduling problem 16(1), 34 – 40.
17. **Caroll J., Long D., 1989.** Theory of Finite Automata, New Jersey: Prentice Hall, 145.
18. **Rinnooy Kan A.H.G., Lageweg B.J., Lenstra J.K., 1975.** Minimizing total cost in one machine scheduling. Operations Research, 23, 908–927.
19. **Thompson J., Dowsland K., 1996.** Variants of simulated annealing for the examination timetabling problem. Annals of Operational Research, 63, 195.
20. **Tsmots I., Medykovskyy M., 2016.** Skorokhoda A., Teslyuk T., Design of intelligent component of hierarchical control system. ECONTECHMOD. AN INTERNATIONAL QUARTERLY 5(2), 3-10
21. **Kordiyak D., Shakhovska N., 2016.** Analytical review of medical mobile diagnostic systems, ECONTECHMOD. AN INTERNATIONAL QUARTERLY 5(2), 11-16
22. **Melnykova N., Marikutsa U., 2016.** Specifics personalized approach in the analysis of medical information. ECONTECHMOD. AN INTERNATIONAL QUARTERLY 5(1), 113-120.

Price formation of mechanized services for households

V. Lypchuk[1], H. Vyslobodska[2]

[1]Prof. Kielce University of Technology 25-314 Kielce, Aleja Tysiąclecia PP 7, www.tu.kielce.pl e-mail: wlipczuk@ukr.net
[2]Lviv National Agrarian University, e-mail: vyslgal@i.ua

Received July 14.2016: accepted July 19.2016

Abstract. The article deals with the practical aspects of the prices formation of the mechanized services for households. On the basis of the questionnaire data the analysis of changes in prices and production costs of the main types of mechanized services consumed by households in the process of agricultural activity was conducted, the attitudes and motives of service providers for the formation of prices were studied and their validity was assessed.

Key words: households, mechanized services, services price, services market, consumers of mechanized services.

INTRODUCTION

Ukrainian villages have preserved their traditions, most farmers have their own, mostly small-sized households, where agricultural production is carried out, which is mainly used for personal needs of the households. Recently, however, there have been certain transformational changes in households that manifest itself in their consolidation, reduction of size and enhancement of participation in agricultural markets. According to statistics in 2014, the households produced 43.6% of the gross agricultural output [1].

The technological process of agricultural production, regardless of its ownership, legal status of the producer and production volumes, needs to attract agricultural services that are an indispensable part of the production process in agriculture. Among the main services that form the production cost, the employment of household members, and even determine the existence of the household are the mechanized services. The transition from the traditional rural way of land cultivation to the mechanized one updates the significance of pricing for mechanized services for the population, which determines the possibility of managing the households and, ultimately, forms the living standards of rural residents.

In order to determine the level and validity of prices for the mechanized services the direct survey of managers and specialists of agricultural enterprises, farms and individual households, owners and entrepreneurs operating in the market of agricultural production services in Busk, Brody and Zolochiv districts of Lviv region has been conducted.

THE ANALYSIS OF RECENT RESEARCHES AND PUBLICATIONS

Services belong to a sector which recently has developed dynamically, that's why constant attention is paid to their theoretical and practical grounding. In this context, the works by Kotler [2] V.Malchenko [3] R. Mahler [4] R. Norman [5], C. Lavlock [6] T. Hill [7], P . Zavyalova [8] and others are worth mentioning. However, most of their research focus on the market in general, the emphasis is laid on the issues of marketing and management services, the employment in this area. Instead, the issue of the development of the market of agricultural services, in particular the mechanized services for households are practically absent in the domestic economy. There are no studies concerning the price formation for mechanized services, because of the lack and unreliability of relevant information.

OBJECTIVES

This research aims to study the characteristic features, the level of regularities and determinants of prices formation for the mechanized services for households.

THE MAIN RESULTS OF THE RESEARCH

The process of agricultural production, no matter who the manufacturer is consists of clearly defined technological processes. One of them is the use in the process of production agricultural mechanized services.

Households kept by population are the households engaged in agricultural activities both to provide self-sufficiency and to produce marketable agricultural products [9].

Activities of households with agricultural production must be effective enormously the effectiveness of such activities, compared to the performance of these services manually [10].

Organizational and technological progress greatly increased the use of the mechanized agricultural services as a special type of services, without which agricultural production is impossible. For the process of production they are as important as material resources.

The production services should meet two basic criteria:

1) Participation in the production of other wealth;

2) Transfer of its value to the cost of manufactured products.

According to the way of providing the production services in agriculture are divided into services provided by hand and mechanized services.

Mechanization of production processes in agricultural production is aimed at improving the productivity and quality of work, reduction of employment in production, improvement of culture and attractiveness of agricultural workers through introduction of machines, equipment and so on. It diversifies the types of mechanized production services in agriculture, particularly in households (Table 1.).

Table 1. Production Agricultural Services *

Group of services	**Production services included in the group**
I. The main cultivation.	1. Ploughing 2. Disking 3. Peeling stubble 4. Chiseling 5. Subsurface cultivation
II. Pre-tillage and sowing (planting)	1. The harrowing; 2. Seed treatment; 3. Cultivation; 4. Shipping and delivery of fertilizers; 5. Sowing (planting); 6. Compacting of crops.
III. Care of crops	1. The use of herbicides and pesticides; 2. Row cultivation; 3. Reclamation and land drainage etc.
IV. Harvesting and preparation of primary production for sale.	1. Harvesting; 2. Digging potatoes; 3. Collection of other cultures; 4. Transportation of products from the field; 5. Drying grain; 6. The collection and processing of by-products (straw, tops etc.).

* Source: formed on the basis of [11; 12]

Suppliers of the mechanized agricultural production services for households are agricultural enterprises, the farms, individual entrepreneurs. Actually, anyone who has the necessary equipment and skills can provide the mechanized production services.

Households can independently support themselves with production services, involve them from the outside, or even provide such services to other entities. In order to carry out such activities farms must have in their use the agricultural machinery and have appropriate skills to operate it. Recently, the number of means owned by the households has grown (see Table 2). Technical park of the households has increased. In particular, in Lviv region only during 2012-2014 years the number of tractors increased by 7550 units, and combine harvesters by 27 units. Such a sharp increase in the number of tractors is explained not so much by the purchase, but rather by introduction of registration system of the available technical means.

Table 2. Availability of agricultural machinery in households of Lviv region (at year-end; units)

	Year			2014 to 2012, %
	2012	2013	2014	
Tractors	113221	119021	120771	110,5
Combines harvester	1553	1547	1580	105,0

* Source: formed on the basis of [13]

Even such a significant number of means doesn't allow the households to perform the work independently, because tractors are only available in every agricultural household. That's why there is an urgent need to obtain the required mechanized services from the outside

No doubt, each recipient of the mechanized services tends to get it the cheapest, while each service provider tends to realize it the most expensive. If the first person is interested in saving money and reducing the cost of agricultural products produced, the main aim of the second one is profit. To find a compromise between them is quite difficult and not always because of the supply and demand, as evidenced by the dynamics of prices for basic agricultural mechanized services in the region (Table 3, Figure 1).

Table 3. Average selling prices of agricultural mechanized services for households UAH / are *

Kind of services	2012	2013	2014	2014 to 2012, %
Ploughing	11,89	14,91	16,00	134,6
Cultivation	8,62	11,00	13,50	156,6
Disking	8,69	11,09	13,04	150,1
Interrow tillage	5,95	7,93	9,00	151,3
Mechanized planting of grain crops	9,30	11,60	13,00	139,8
Planting of potatoes	7,18	9,40	10,02	139,6
Harvesting of grain crops	12,20	14,27	16,00	131,1
Mowing of grass	7,00	9,06	11,04	157,7
Mechanized digging of potatoes	6,91	8,91	9,53	137,9
Spraying	5,55	7,30	8,60	155,0
Application of organic fertilizers	5,71	7,35	8,40	147,1
Application of mineral fertilizers	5,54	7,08	8,15	147,1
Transport services, km	5,69	9,33	11,00	193,3

* Source: own elaboration based on the processed questionnaires

The data in Table 3 indicate a rapid increase in prices of agricultural mechanized services in 2014 compared with previous years. The largest price increases was observed in transportation services (93.3%), mowing grass (57.7%), cultivation (56.6%), inter-row tillage (51.3%) and disking (50.1%). It is worth emphasizing particularly high prices in 2013. And it happened during the period of a stable exchange rate, and therefore during the period of stable prices for material resources and labour costs.

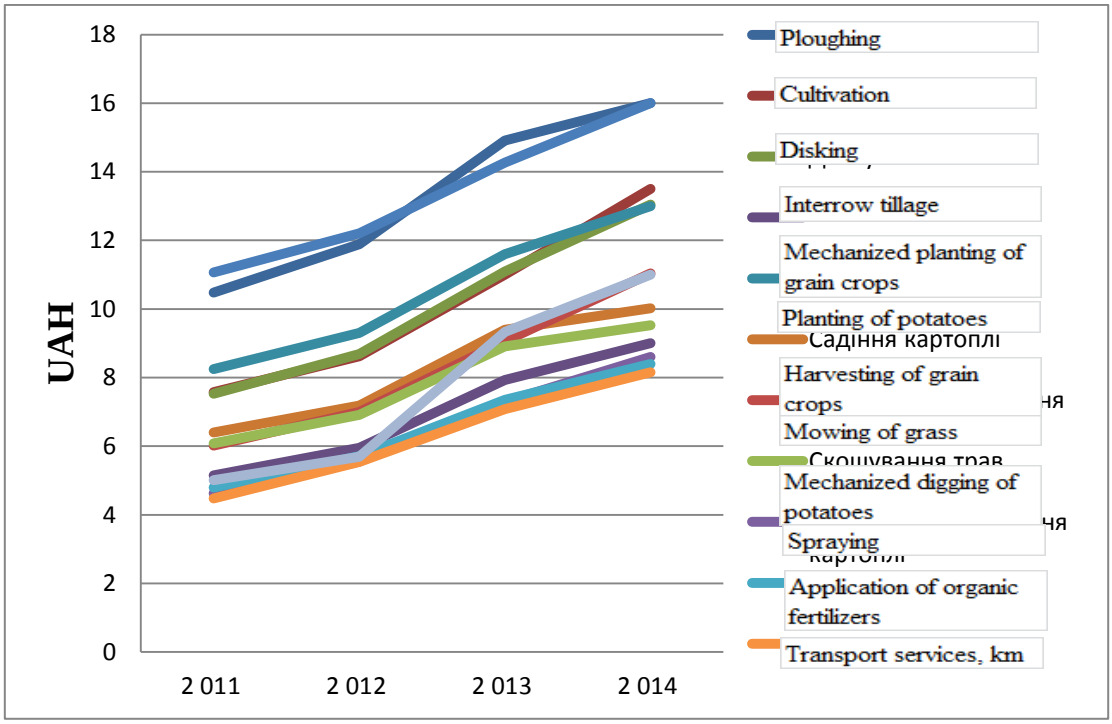

Fig. 1. Dynamics in prices change for mechanized services to the public *

* Source: formed on the basis of the survey conducted

Sufficiently clear are differences in the prices for various mechanized services. The most expensive services are plowing and combine harvesting of grains, the cheapest ones are applying of mineral and organic fertilizers and spraying. With sufficient probability we can state that there are higher prices for services which have greater demand among households, despite operating costs incurred for mechanized works.

The problem of prices for the mechanized services has two aspects: the formal aspect and marketing one. Formal prices for mechanized services are prices contingencies that each entity establishes independently without outside interference, but it takes into account the existing formal legal requirements. Marketing approach takes into consideration the value of service to its recipient, the perception of service quality and competition in the market. Certainly, the price can be measured as economical dimension (the result of the calculation) and as psychological dimension (compromise between the provider of services and the recipient of services).

It is generally accepted in marketing to consider three principles of pricing. They are based on demand, cost and competition. [14]. According to these principles various methods and techniques of pricing are offered. Operating costs are the main pricing factors. This can mainly be explained by an increase in prices for basic mechanized services (Table 4.).

Table 4. The average cost of providing mechanized agricultural production services 1 are *

Kind of services	2012	2013	2014	2014 to 2012, %
Ploughing	10,24	13,13	14,02	136,9
Cultivation	7,71	9,80	10,98	142,4
Disking	7,88	9,90	11,00	139,6
Interrow tillage	4,87	6,52	7,46	153,2
Mechanized planting of grain crops	8,30	10,35	11,10	133,7
Planting of potatoes	6,33	8,38	9,01	142,3
Harvesting of grain crops	10,56	12,80	14,13	133,8
Mowing of grass	6,15	7,85	9,74	158,4
Mechanized digging of potatoes	5,87	7,71	8,16	139,0
Spraying	4,92	6,51	7,64	155,3
Application of organic fertilizers	4,95	6,38	7,57	152,9
Application of mineral fertilizers	4,75	6,07	7,43	156,4
Transport services, km	4,96	8,36	9,79	197,4

* Source: author's own development on the basis of the processed questionnaires

As seen from Table 4, in the period of 2012-2014 there was a significant increase in the cost of providing mechanized production services to the public. The greatest increase was in the cost of transport services at 97.4%, mowing grass - 58.4% fertilization - at 56.4% and herbicide spraying fields - 55.3%. Such growth is due primarily to the rising cost of fuel, fertilizers and crop protection products.

In this context, it is important to explore the changing of profitability of providing mechanized services (Table 5) to assess the validity of the established prices.

Table 5. Dynamics of profitability of providing mechanized services for private households*

Kind of services	The profit on 1 are, UAH			Profitability, %		
	2012	2013	2014	2012	2013	2014
Ploughing	1,65	1,78	1,92	116,1	113,6	113,6
Cultivation	0,91	1,20	1,39	111,8	112,2	111,5
Disking	0,81	1,19	1,99	110,3	112,0	118,0
Interrow tillage	1,08	1,41	1,56	122,2	121,6	121,0
Mechanized planting of grain crops	1,00	1,25	1,43	112,0	112,1	112,4
Planting of potatoes	0,85	1,02	1,02	113,4	112,2	111,3
Harvesting of grain crops	1,64	1,47	1,24	115,5	111,5	108,4
Mowing of grass	0,85	1,21	1,08	113,8	115,4	110,8
Mechanized digging of potatoes	1,04	1,20	1,12	117,7	115,6	113,3
Spraying	0,63	0,79	0,91	112,8	112,1	111,8
Application of organic fertilizers	0,76	0,97	1,22	115,4	115,2	117,0
Application of mineral fertilizers	0,79	1,01	0,94	116,6	116,6	113,0
Transport services, km	0,73	0,97	1,02	114,7	111,6	110,2

* Source: formed on the basis of our own research

As seen from Table 5, activities to provide mechanized agricultural services to the population is profitable for all kinds of these services. The level of profitability varies in the range of 10-22%. The highest level of profitability in the service of mechanized soil cultivation, the other services are almost equal efficiency. On average exercise plowing 1 hectare of land will bring 192 UAH profits.

Validity of prices increase for mechanized services involves consideration of the main factors of its formation (Table 6). These data have not been a high correlation between the price and the services provided.

Table 6. Dynamics of prices for individual mechanized services and factors of its formation,% of 2012 *

Indicator	Year			to 2012p., %	
	2012	2013	2014	2013	2014
Average price[1] , UAH/ 1 are: - Ploughing	11,89	14,91	16,00	125,4	134,6
- Cultivation	8,62	11,00	13,50	127,6	156,6
- Mechanized planting of grain crops	9,30	11,60	13,00	124,7	139,8
- Planting of potatoes	7,18	9,40	10,02	130,9	139,6
- Harvesting of grain crops	12,20	14,27	16,00	117,0	131,1
- Mechanized digging of potatoes	6,91	8,91	9,53	128,9	137,9
- Interrow tillage	5,95	7,93	9,00	133,3	151,3
- Spraying	5,54	7,08	8,15	127,8	147,1
- Application of mineral fertilizers	5,54	7,08	8,15	127,8	147,1
Average cost [2], UAH/ 1 are: - Ploughing	10,24	13,13	14,02	128,2	136,9
- Cultivation	7,71	9,80	10,98	127,1	142,4
- Mechanized planting of grain crops	8,30	10,35	11,10	124,7	133,7
- Planting of potatoes	6,33	8,38	9,01	132,4	142,3
- Harvesting of grain crops	10,56	12,80	14,13	121,2	133,8
- Mechanized digging of potatoes	5,87	7,71	8,16	131,3	139,0
- Interrow tillage	4,87	6,52	7,46	133,9	153,2
- Spraying	4,92	6,51	7,64	132,3	155,3
- Application of mineral fertilizers	4,75	6,07	7,43	127,8	156,4
Inflation index [3]	99,8	100,5	124,9	0,7	+25,1п.
The price of diesel fuel [4], UAH / liter	10,24	11,12	16,87	108,6	164,7
Minimum wages [5], UAH	1 073,00	1147,00	1218,00	106,9	113,5
The average selling price [6], UAH / tonne - grain crops	1545,80	1297,20	1801,40	83,9	116,5
- potatoes	1138,50	1856,60	2173,60	163,1	190,9
- sugar beets	426,80	397,80	494,20	93,2	115,8
- vegetables	1924,20	1856,60	2514,30	96,5	130,7

* Source: Calculated on the basis of: 1; 2data derived from the survey, 3, 5 - [15] 4 - [16] 6 - [17].

The main factors that led to a rapid increase in the cost of production of mechanized services, most suppliers of mechanized services for households include: inflation, rising cost of fuel, rise in machinery and spare parts to it, the price of the service at the same level as that of other suppliers (tab. 7).

Table 7. Grounding of prices rise for mechanized services,% *

Factor	Service providers				
	Farm enterprises	Limited liability company	Private agricultural companies	Householders	Others
Inflation	27,4	29,9	12,9	8,7	19,4
Growth of cost fuel	51,9	49,2	56,7	63,3	59,7
Price increase of appliances	8,3	11,8	15,4	2,1	9,5
Establishing the price as other providers	12,4	9,1	15,0	25,9	11,4
In total	100,0	100,0	100,0	100,0	100,0

* Source: formed on the basis of our own research

It is clear that, according to service providers the most important factor in the rising cost of mechanized production services is the rising cost of fuel. Thus, in 2014 compared to 2011 the cost of diesel fuel increased by 72.7% and gasoline A-95 at 65.6%. [18].

The data in Table 7 show that every year there is a rise in prices for mechanical services for households, this is primarily due to increased costs incurred during their implementation. The rising of costs are attracting the mechanized services leads to increased cost of finished agricultural products. The cost of mechanized services is growing under the influence of inflation in the country and the rising cost of fuel.

The overall growth in prices for mechanized services, in addition to the above mentioned is largely due to weak technical support of agriculture, lack of competition in the market mechanized services, limited public access to different types of services, including the mechanized ones. To some extent, this problem could be solved by creating rural service cooperatives.

So, the decision of the household to get mechanized services are particularly important for its successful development, survival in the competitive market, successful adaptation to environmental changes [19].

Making the decision to choose the source of providing the needs for agricultural production services the agricultural household must assess:

1. The need for agricultural production services;

2. Analyze its own possibilities of the need, cost and quality of services:

3. Examine the environment and identify the alternative ways of obtaining (providing the need) agricultural production services with regard to price, quality, accessibility (territorial distance) and timeliness (according to the technological requirements).

CONCLUSIONS

The growth of volume of mechanized services in householders has been provoked by transformation in agriculture. These changes were accompanied by a simultaneous increase in their prices, which is not sufficient substantiated. Mechanized services providers include to the main pricing factors mechanized services increase in the cost fuel and machines, inflationary processes, establishing the price like other sellers of services and so on. However, it is their subjective opinion, rather justification dictates of prices.

The significant differentiation of the prices on different mechanized services weakly correlates with their cost price and in greater extent depends from the importance of certain types of services, the ability to perform the work manually and its volume. So, the price on mechanized services in aggregate with the timing and quality of its provision should become the basis for making decisions about choosing ways to receive it.

REFERENCES

1. **AG:** Agriculture of Ukraine 2014. Available online at: < http://www.ukrstat.gov.ua/druk/publicat /kat_u/publ7_u.htm
2. **Kotler F. 2007.** Fundamentals of marketing: Brief course. Moskow: Vyliams, 656. (in Russian).
3. **Morhulets O. B. 2012.** Management in the service sector. Kyiv: Center of educational literature, 384. (in Ukrainian).
4. **Vorachek H. O. 2002**. The state of theory of services marketing. Journal of Problems of theory and practice of management. Vol. 1, 99-103. (in Russian).
5. **Service Management. 2001.** Strategy and Leadership in Service Business, 3rd Edition. Richard Normann. 256.
6. **Lavlok K. 2005.** Services marketing : staff, technologies, strategies. Moskow: Vyliams, 1008. (in Russian).
7. **Markova V. D. 1996.** The services marketing. Moskow: Finance and Statistics, 126. (in Russian).
8. **Zavjalov P. S. and Demydov V. E. 1991.** The formula for success. Marketing, International relations. Moscow. Russia. n.2, 416. (in Russian).
9. **SSSU:** State Statistics Service of Ukraine**.** Available online at: < https://ukrstat.org/uk/metod_polog/metod_doc/2008/165/metod.htm
10. **Smolinskyy V., Smolinska S., Homka Z. 2014.** Innovative approaches towards the analysis of the dependence of production efficiency on the parameters of agricultural enterprises land use. Journal on Economics in technology, new technologies and modeling processes (ECONTECHMOD) Vol. III. Nr 4, 39-43. (in Poland).
11. **Ruzhytskyj M.A., Riabets V.I., Kijashko V.M. and other. 2010.** Operation of machines and equipment: Tutorial. Kyiv: The agrarian education, 617. (in Ukrainian).
12. **CEAT:** Classification of Economic Activities Types. Available online at: < http://sfs.gov.ua/dovidniki--reestri--perelik/pereliki-/128651.html
13. **Statistical Bulletin. 2014**. The presence of tractors, agricultural machines and energy capacities in the Lviv region. Lviv: State Office of Statistics in the Lviv region, 31. (in Ukrainian).
14. **Lypchuk V. V. 2007.** Marketing**.** Lviv: Novyi Svit, 288. (in Ukrainian).
15. **MFU:** Financial Portal of Ministry of Finance of Ukraine. Available online at: < http://index.minfin.com.ua/index/infl/
16. **MFU:** The official website of the Ministry of Finance of Ukraine. Available online at: < http://www.me.gov.ua/?lang=uk-UA;
17. **DSU:** Department of Statistics Ukraine. Available online at: < http://www.ukrstat.gov.ua/
18. The official website of the Ministry of Economic Development and Trade of Ukraine Available online at: < http://www.me.gov.ua/?lang=uk-UA
19. **Vysochina, M. 2014**. The innovative approach to the study of decision-making in the context of the specific character of a product of managerial work. Journal on Economics in technology, new technologies and modeling processes (ECONTECHMOD) Vol. 3. Nr 2, 87-92. (in Poland).
20. **Kischak I., Havrysh V. and Kulik A. 2011**. The elements of provide agricultural enterprises of technical means for production. Journal of Motorization and power industry in agriculture (MOTROL). Vol. 13B, 153-159. (in Ukrainian).

Construction of integral equations describing limit equilibrium of cylindrical shell with a longitudinal crack under time-varying load

M. Makhorkin[1,2], M. Nykolyshyn[2]

[1]Lviv National Agrarian University; e-mail: mahorkin@ukr.net
[2]Pidstryhach Institute for Applied Problems of Mechanics and Mathematics National Academy of Sciences of Ukraine

Received July 14.2016: accepted July 19.2016

Abstract. The problem on limit equilibrium of a closed infinite cylindrical shell with a longitudinal crack under the action of time-varying load by the exponential law has been considered. According to presented conditions the expressions for the field of the stress-free deformations along the crack are presented in the form $f^0_{\beta\beta} = f^*_{\beta\beta} e^{\gamma\tau}$ $f = \{\varepsilon, \kappa\}$, where ε^*_{ij}, κ^*_{ij} $(i, j = \alpha, \beta)$ are time-independent; τ is time; γ is a stable factor of dimension [s^{-1}], and the system of equilibrium equations in displacements is written as [5, 6, 12]: $L_{k1}u + L_{k2}v + L_{k3}w - R^2 c_\tau^{-2} \ddot{\cdot}$ $(k = 1,2,3)$, where: L_{km} $(m = 1,2,3)$ are the operators presented in [7, 11]; $g_1 = u$; $g_2 = v$; $g_3 = w$; q_i^{0*} are the right parts of equations which are calculated by the expressions presented in [7, 11.], considering the form of strain field; $c_\tau^2 = E\rho^{-1}(1-\nu^2)^2$.

Using the operator method, the method described in [13], the solution of the system is written as:

$$f(\alpha,\tau) = R\sum_{j=2}^{3}\left(L^*_{jf}\varphi_j + P^*_{jf}\psi_j\right)e^{\gamma\tau} \quad \left(f = \{u, v, w\}\right),$$

where: $L^*_{kl} = L_{kl} + L^{**}_{kl}$, $P^*_{kl} = P_{kl} + P^{**}_{kl}$ $(l = u, v, w)$; L_{kl}, P_{kl} are the operators identical to those given in [7] for the case of static load, and L^{**}_{kl}, P^{**}_{kl} are the operators that take into account the dependence of load on time. Using the same transformations that in the case of static load [7, 11], the key functions φ_j, ψ_j are determined, and the clarification of the shell's stress-state is reduced to solving the system of singular integral equations (SIE). Its general form is similar to the same system constructed for static load [7], and the kernels of SIE have the form $K_{ij} = K^0_{ij} + K^*_{ij} + K^{**}_{ij}$, where K^0_{ij} is a singular part, $K^*_{ij} + K^{**}_{ij}$ is a regular part in which the component K^{**}_{ij}. takes into account the time dependence of load; K^0_{ij}, K^*_{ij} are described by the expressions similar to the same given in [7].

Key words: cylindrical shell, crack, exponential time dependence, varying load, system of singular integral equations.

INTRODUCTION

In aircraft and rocket manufacture, chemical engineering, atomic power, industrial engineering etc. structural elements of shell type are used extensively. Estimation of reliability of structures and systems, which contain stress concentrators (pointed technological cuts, defects such as cracks or inclusions) is based largely on the analysis of stress-strain state in their vicinity. Since the most common defect that leads to destruction, is a pointed crack, the questions relating to the study of their appearance and development at various loads attract attention, and the study of stresses and strains in the vicinity of the ends of the cracks by using experimental and theoretical methods is described in numerous scientific works (see review [4-8])

ANALYSIS OF RECENT RESHERCHES AND PUBLICATIONS

Comprehensive enough overview of the theories and methods of solving the stress-strain state for different kinds of shells with cracks is presented in the monographies [3, 7, 11-13] and in the articles [1, 2, 5, 6, 8-10]. The results were obtained mainly by the boundary integral equations method for an isotropic and anisotropic, homogeneous and piecewise-homogeneous shell under stationary load [4, 7, 9, 10,].

As demonstrated the analysis of scientific literature, modern mathematical apparatus enables the construction of adequate mathematical models for arbitrary loading. Despite this, relatively little researches concern the problem of shells with cracks under the action of time-varying load. The list of publications regarding this problem can be found in the survey of scientific works presented in the articles [2, 5, 14-20]. Some studies of elastic vibrations of cylindrical shells with longitudinal cracks are given in the works [17, 19, 20], and some dynamic problems for cylindrical shells are considered in the articles [9, 10, 14, 19].

OBJECTIVE

The objective of this work is to construct a system of singular integral equations, which will allow to determine the stress state in the vicinity of the ends of a longitudinal cut in a closed cylindrical shell under the action of time-

varying load.

THE MAIN RESULTS OF THE RESEARCH

A closed infinite cylindrical shell with a through longitudinal cut of the length $2l$ is considered (origin of the coordinate system we will choose in the middle of the cut) Fig. 1. Assume that the shell is under the action of surface load which exponentially varies in time.

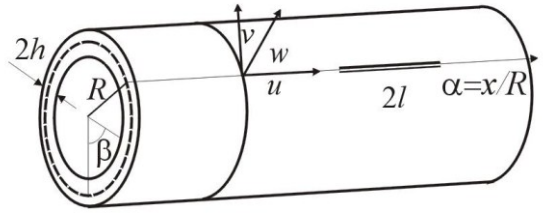

Fig. 1. Scheme cylindrical shell

Under these conditions the field of stress-free deformations [7, 11], the incompatibility of which causes the jumps of displacements and angles of rotation along the cut, will read:

$$\begin{aligned}
&\varepsilon^0_{\beta\beta} = \varepsilon^*_{\beta\beta} e^{\gamma\tau} = R^{-1}\left[v(\alpha,\tau)\right]\delta(\beta),\\
&\varepsilon^0_{\alpha\beta} = \varepsilon^*_{\alpha\beta} e^{\gamma\tau} = R^{-1}\left[u(\alpha,\tau)\right]\delta(\alpha),\\
&\kappa^0_{\beta\beta} = \kappa^*_{\beta\beta} e^{\gamma\tau} = -R^{-1}\times\\
&\quad\times\left\{\left[\theta_\beta(\alpha,\tau)\right]\delta(\beta) - R^{-2}\left[w(\alpha,\tau)\right]\partial_\beta\delta(\beta)\right\},\\
&\kappa^0_{\alpha\beta} = \kappa^*_{\alpha\beta} e^{\gamma\tau} = -R^{-2}\partial_\alpha\left[w(\alpha,\tau)\right]\delta(\beta),\\
&\varepsilon^0_{\alpha\alpha} = \kappa^0_{\alpha\alpha} = 0,
\end{aligned} \tag{1}$$

where: ε^*_{ij}, κ^*_{ij} $(i,j=\alpha,\beta)$ depend on the coordinates;

$$\begin{aligned}
&\left[u(\alpha,\tau)\right] = \left[u^*(\alpha)\right]e^{\gamma\tau},\quad \left[v(\alpha)\right] = \left[v^*(\alpha)\right]e^{\gamma\tau},\\
&\left[w(\alpha,\tau)\right] = \left[w^*(\alpha)\right]e^{\gamma\tau},\quad \left[\theta_\beta(\alpha)\right] = \left[\theta^*_\beta(\alpha)\right]e^{\gamma\tau},
\end{aligned} \tag{2}$$

are the jumps of displacements and angles of rotation; τ is time; γ is a stable factor of dimension [s^{-1}]; $\delta(\beta)$ is Dirac delta-function; $\partial^n_j = \dfrac{\partial^n}{\partial j^n}$ $(n=1,2,3,...)$, $j=\alpha,\beta,\tau$.

Conditions on the crack faces [7] in a general form are written as

$$\begin{aligned}
&N_2^+(\alpha,0,\tau) = N_2^-(\alpha,0,\tau) = f_1(\alpha,\tau),\\
&S^+(\alpha,0,\tau) = S^-(\alpha,0,\tau) = f_2(\alpha,\tau),\\
&M_2^+(\alpha,0,\tau) = M_2^-(\alpha,0,\tau) = f_3(\alpha,\tau),\\
&Q_2^{+*}(\alpha,0,\tau) = Q_2^{-*}(\alpha,0,\tau) = f_4(\alpha,\tau).
\end{aligned} \tag{3}$$

Here:

$$\begin{aligned}
&f_1(\alpha,\tau) = N_2^1(\alpha,+0,\tau) - N_2^0(\alpha,+0,\tau),\\
&f_2(\alpha,\tau) = S^1(\alpha,+0,\tau) - S^0(\alpha,+0,\tau),\\
&f_3(\alpha,\tau) = M_2^1(\alpha,+0,\tau) - M_2^0(\alpha,+0,\tau),\\
&f_4(\alpha,\tau) = Q_2^{*1}(\alpha,+0,\tau) - Q_2^{*0}(\alpha,+0,\tau),
\end{aligned} \tag{4}$$

where: N_2^0, S^0, Q_2^{*0}, M_2^0 is a normal, shear, generalized intersecting effort and bending moment in the shell without a crack, respectively, N_2^1, S^1, Q_2^{*1}, M_2^1 are the same efforts applied to the faces of a real crack.

Taking into consideration that the external loads are time varying by exponential law, corresponding efforts can be represented as:

$$\begin{aligned}
&N_2^i(\alpha,\beta,\tau) = N_2^{i*}(\alpha,\beta)e^{\gamma\tau},\\
&S^i(\alpha,\beta,\tau) = S^{i*}(\alpha,\beta)e^{\gamma\tau},\\
&M_2^i(\alpha,\beta,\tau) = M_2^{i*}(\alpha,\beta)e^{\gamma\tau},\\
&Q_2^{*i}(\alpha,\beta,\tau) = Q_2^{**i}(\alpha,\beta)e^{\gamma\tau},\quad (i=0,1),
\end{aligned} \tag{5}$$

and functions $f_j\left(j=\overline{1,4}\right)$ take the form

$$f_j(\alpha,\tau) = f_j^*(\alpha)e^{\gamma\tau}\left(j=\overline{1,4}\right), \tag{6}$$

where $f_j^*(\alpha,\tau)$ is obtained by replacing in expressions (4) the efforts N_2^i, S^i, M_2^i, Q_2^{*i} by the values N_2^{i*}, S^{i*}, M_2^{i*}, Q_2^{**i}.

The system of equilibrium equations according to [7, 12, 13] has the form

$$L_{k1}u + L_{k2}v + L_{k3}w - R^2 c_\tau^{-2}\ddot{\ldots} \quad (k=1,2,3). \tag{7}$$

Here: $L_{11} = \partial^2_\alpha + 0{,}5\nu_-^{-1}\partial^2_\beta$, $L_{12} = L_{21} = 0{,}5\nu_+^{-1}\partial_\alpha\partial_\beta$,

$L_{13} = L_{31} = \nu\partial_\alpha$, $L_{22} = 0{,}5\nu_-^{-1}\partial^2_\alpha + \partial^2_\beta + c_1^2\left[2\nu_-^{-1}\partial^2_\alpha + \partial^2_\beta\right]$,

$L_{23} = L_{32} = \partial_\beta - c_1^2\left[(2-\nu)\partial^2_\alpha\partial_\beta + \partial^3_\beta\right]$,

$L_{33} = 1 + c_1^2\nabla^2\nabla^2$, $q_1^{0*} = R\left(\nu\partial_\alpha\varepsilon^0_{\beta\beta} + 0{,}5\nu_-^{-1}\partial_\beta\varepsilon^0_{\alpha\beta}\right)$

$q_3^{0*} = R\varepsilon^0_{\beta\beta} - \dfrac{h^2}{3}\left[\nu\partial^2_\alpha\kappa^0_{\beta\beta} + 2\nu_-^{-1}\partial_\alpha\partial_\beta\kappa^0_{\alpha\beta} + \partial^2_\alpha\kappa^0_{\beta\beta}\right]$,

$q_2^{0*} = R\left(\partial_\beta\varepsilon^0_{\beta\beta} + 0{,}5\nu_-^{-1}\partial_\alpha\varepsilon^0_{\alpha\beta}\right) +$

$+\dfrac{h^2}{3}\left[\partial_\beta\kappa^0_{\beta\beta} + 2\nu_-^{-1}\partial_\alpha\kappa^0_{\alpha\beta}\right]$,

$\nabla^2 = \partial^2_\alpha + \partial^2_\beta$, $\partial^n_j\partial^k_l = \dfrac{\partial^{n+k}}{\partial j\partial l}$ $c_\tau^2 = E\rho^{-1}(1-\nu^2)^2$,

$\left(j,l=\alpha,\beta;\ n,k=1,2,3,...\right)$, $c_1^2 = \dfrac{h^2}{3R^2}$, $\nu_\pm = (1\pm\nu)^{-1}$,

E is Young's modulus, ρ is the density of material.

Applying for solution of system (7) the operator method [12, 13], we present the solution of differential equations system by key functions φ_j, ψ_j $(j=1,2)$ as:

$$\begin{aligned}
&u(\alpha,\tau) = u^*(\alpha)e^{\gamma\tau} = R\sum_{j=2}^{3}\left(L^*_{ju}\varphi_j + P^*_{ju}\psi_j\right)e^{\gamma\tau},\\
&v(\alpha,\tau) = v^*(\alpha)e^{\gamma\tau} = R\sum_{j=2}^{3}\left(L^*_{jv}\varphi_j + P^*_{jv}\psi_j\right)e^{\gamma\tau},\\
&w(\alpha,\tau) = w^*(\alpha)e^{\gamma\tau} = R\sum_{j=2}^{3}\left(L^*_{jw}\varphi_j + P^*_{jw}\psi_j\right)e^{\gamma\tau}.
\end{aligned} \tag{8}$$

Here: $L^*_{kl} = L_{kl} + L^{**}_{kl}$, $P^*_{kl} = P_{kl} + P^{**}_{kl}$ $(l=u,v,w)$, (9)

where: L_{kl}, P_{kl} are the operators identical to given in [7] for the case of static load, and L^{**}_{kl}, P^{**}_{kl} are the operators which are caused by dependence of the load on time and have the following form:

$$\begin{aligned}
L^{**}_{2u} = \gamma_1^2\Big[&4\nu\partial^3_\alpha - 2\nu_-^2\left(\partial^5_\alpha + \partial_\alpha\partial^4_\beta + 2\partial^3_\alpha\partial^2_\beta - \partial_\alpha\partial^3_\beta\right) +\\
&+ c_1^{-2}\left(\nu\partial^3_\alpha - \partial_\alpha\partial^2_\beta\right)\Big] - \gamma_1^4 2\nu c_1^{-2}\nu_+\partial_\alpha,
\end{aligned}$$

$$L_{3u}^{**}=\gamma_1^2\left[\partial_\beta^3-\partial_\beta^5-2\partial_\alpha^2\partial_\beta^3-\partial_\alpha^4\partial_\beta+\right.$$
$$\left.+c_1^{-2}\left(\partial_\beta^3-\partial_\beta-\nu\partial_\alpha^2\partial_\beta\right)\right]-\gamma_1^4c_1^{-2}\partial_\beta,$$
$$P_{u2}^{**}=-\gamma_1^2\nu_-^{-1}\left[2\nu^2\partial_\alpha^3+(1+3\nu)\partial_\alpha\partial_\beta^2\right],$$
$$P_{u3}^{**}=-2\gamma_1^2(1+3\nu)\partial_\alpha^2\partial_\beta,\ \gamma_1=R^2\gamma^2c_\tau^{-2},$$
$$L_{3v}^{**}=\gamma_1^2\left[c_1^{-2}\left(\partial_\alpha^3-\partial_\alpha-\nu\partial_\alpha\partial_\beta^2\right)-\partial_\alpha^2-\right.$$
$$\left.-\partial_\alpha\partial_\beta^4-2\partial_\alpha^3\partial_\beta^2\right]-\gamma_1^4c_1^{-2}\partial_\alpha,$$
$$P_{2v}^{**}=-\gamma_1^2\nu_-^{-1}\left[\partial_\alpha^2\partial_\beta-2\nu_-\partial_\beta-(1+\nu)\nu_-\partial_\beta^3-\right.$$
$$\left.-c_1^2\,2\nu_-^{-1}\partial_\alpha^4\partial_\beta\right]-\gamma_1^4\,2\nu_-\partial_\beta,$$
$$P_{3v}^{**}=\gamma_1^4\,4\left[\partial_\alpha^3-\partial_\alpha-2(1+\nu)\partial_\alpha\partial_\beta^2-\right.$$
$$\left.-c_1^2\left(\partial_\alpha^5+\nu\partial_\alpha^3\partial_\beta^2\right)\right]-4\gamma_1^4\partial_\alpha,$$
$$L_{2w}=\partial_\beta^6+\partial_\beta^4+4\partial_\alpha^2\partial_\beta^4+4\partial_\alpha^2\partial_\beta^2+$$
$$+(4-\nu^2)\partial_\alpha^4\partial_\beta^2+c1^{-2}\nu_-^{-1}\nu_+^{-1}\partial_\alpha^4,$$
$$L_{2w}^{**}=\gamma_1^4\,2c_1^{-2}\nu_--\gamma_1^2\left[2(2-\nu)\nu_-\partial_\alpha^2\partial_\beta^2+\right.$$
$$\left.+c_1^{-2}\left(\partial_\beta^2+(3+2\nu)\partial_\alpha^2\right)\right],$$
$$L_{3w}^{**}=\gamma_1^2\left[\partial_\alpha\partial_\beta^2+(2-\nu)\partial_\alpha^3\partial_\beta-c_1^{-2}(1+\nu)\partial_\alpha\partial_\beta\right],$$
$$P_{2w}^{**}=\gamma_1^2(1-\nu)^{-1}\left[(3-\nu)\left(\partial_\beta^4+\nu\partial_\alpha^4+(1+\nu)\partial_\alpha^2\partial_\beta^2\right)+\right.$$
$$\left.+2\partial_\beta^2\right]-\gamma_1^4\,2(1-\nu)\left(\partial_\beta^2+\nu\partial_\alpha^2\right),$$
$$P_{3w}^{**}=\gamma_1^2\left[4\partial_\alpha\partial_\beta^2+2(3-\nu)\left(\partial_\alpha\partial_\beta^3+\partial_\alpha^3\partial_\beta\right)\right]-4\gamma_1^4\partial_\alpha\partial_\beta.$$

Functions φ_j, ψ_j have to satisfy the equations:

$$D\varphi_2=\varepsilon_{22}^*,\ D\varphi_3=\varepsilon_{12}^*,\ D\psi_2=R\kappa_{22}^*,\ D\psi_3=R\kappa_{12}^*, \quad (10)$$

where the operator D has the form

$$D=D^0+D^*+D^{**}. \quad (11)$$

Here D^0 and D^* are the operators that are identical to the same given in [7, 11] for the case of static load, and D^{**} is the operator caused by dependence of load on time:

$$D^0=\nabla^2\nabla^2\nabla^2\nabla^2,$$
$$D^*=\left(8-2\nu^2\right)\partial_\alpha^4\partial_\beta^2+8\partial_\alpha^2\partial_\beta^4+2\partial_\beta^6+$$
$$+\frac{1-\nu^2}{c_1^2}\partial_\alpha^4+4\partial_\alpha^2\partial_\beta^2+\partial_\beta^4,$$
$$D^{**}=2\gamma_1^6\nu_-c_1^{-2}+2\gamma_1^4(1-\nu)^{-1}c_1^{-2}\times$$
$$\times\left\{\left(8-2\nu^2\right)\partial_\alpha^4\partial_\beta^2+c_1^2\left[\nabla^2\nabla^2-\partial_\beta^2-2\nu_-^{-1}\partial_\alpha^2\right]\right\}+$$
$$+\gamma_1^2\left\{c_1^{-2}\left[\nabla^2\nabla^2-\partial_\beta^2-(3+2\nu)\partial_\alpha^2\right]+\right.$$
$$+2\nu_-\left[0{,}5(\nu-3)\nabla^2\nabla^2\nabla^2-0{,}5(3+\nu)\partial_\beta^4+\right.$$
$$\left.+2\nu_-^{-1}\left(\partial_\alpha^4-\partial_\beta^2\right)-\left(2-\nu^2\right)\partial_\alpha^2\partial_\beta^2\right]-$$
$$\left.-2c_1^2\left[2\nu_-^{-1}\partial_\alpha^6+\nu_-^{-1}\nu_+^{-1}\partial_\alpha^4\partial_\beta^2\right]\right\}. \quad (12)$$

Solution of equations (10) we present in the form of a convolution integral:

$$\Psi'=\int_{-\infty}^{\infty}\Phi(\alpha,\beta,\xi,\theta)\vartheta^*(\xi)\,d\xi, \quad (13)$$

where: $\Psi'=\{\varphi_2,\varphi_3,\psi_2,\psi_3\}$; $\vartheta^*(\xi)=\{\varepsilon_{22},\varepsilon_{12},\kappa_{22},\kappa_{12}\}$; $\Phi(\alpha,\beta,\xi,\theta)$ is a fundamental solution (Green's function) for infinitely long cylindrical shell –

$$\Phi(\alpha,\beta,\xi,\theta)=\frac{1}{\pi}\sum_{n=0}^{\infty}\left(1-\frac{\delta_{0n}}{2}\right)\Phi_n(\alpha,\xi)\cos\left[n(\beta-\theta)\right], \quad (14)$$

where: $\delta_{0n}=\{1, if\ n=0;\ 0\ \ if\ n\neq 0\}$ is Kronecker delta.

Considering the presentations(1), (8), we obtain the following expression for desired functions:

$$\varphi_2(\alpha,\beta)=\frac{1}{\pi R}\sum_{n=0}^{\infty}\left\{\left(1-\frac{\delta_{0n}}{2}\right)\cos n\beta\times\right.$$
$$\left.\times\int_{-\alpha_0}^{\alpha_0}\left[v^*(\xi)\right]\Phi_n(\xi-\alpha)\,d\xi\right\},$$
$$\varphi_3(\alpha,\beta)=\frac{1}{\pi R}\sum_{n=0}^{\infty}\left\{\left(1-\frac{\delta_{0n}}{2}\right)\cos n\beta\times\right.$$
$$\left.\times\int_{-\alpha_0}^{\alpha_0}\left[u^*(\xi)\right]\Phi_n(\xi-\alpha)\,d\xi\right\}, \quad (15)$$
$$\psi_2(\alpha,\beta)=-\frac{1}{\pi R}\sum_{n=0}^{\infty}\left\{\left(1-\frac{\delta_{0n}}{2}\right)\cos n\beta\times\right.$$
$$\left.\times\int_{-\alpha_0}^{\alpha_0}\left[\theta^*(\xi)\right]\Phi_n(\xi-\alpha)\,d\xi\right\}+$$
$$+\frac{1}{\pi R}\sum_{n=0}^{\infty}\left(1-\frac{\delta_{0n}}{2}\right)n\sin n\beta\int_{-\alpha_0}^{\alpha_0}\left[w^*(\xi)\right]\Phi_n(\xi-\alpha)\,d\xi,$$
$$\psi_3(\alpha,\beta)=\frac{1}{\pi R}\sum_{n=0}^{\infty}\left\{\left(1-\frac{\delta_{0n}}{2}\right)\cos n\beta\times\right.$$
$$\left.\times\int_{-\alpha_0}^{\alpha_0}\left[w^*(\xi)\right]\frac{d\Phi_n(\xi-\alpha)}{d\alpha}\,d\xi\right\}.$$

Function $\Phi_n(\xi-\alpha)$ is determined by the expression that is similar to that presented in the work [7]:

$$\Phi_n(z)=\frac{1}{X_n}\sum_{j=1}^{2}\left\{\frac{e^{-a_{jn}|z|}}{q_{jn}\left(a_{jn}^2+b_{jn}^2\right)}\times\right.$$
$$\times\left[\left(b_{jn}C_{in}-a_{jn}B_{jn}\right)\cos b_{jn}z+\right.$$
$$\left.\left.+\left(a_{jn}C_{in}-b_{jn}B_{jn}\right)\sin b_{jn}|z|\right]\right\},\ n\geq 1, \quad (16)$$
$$\Phi_0(z)=\left(A_{10}\cos b_{10}z+B_{10}\sin b_{10}|z|\right)e^{-a_{10}|z|}+$$
$$+A_{20}e^{-a_{20}|z|}+B_{20}e^{-b_{20}|z|},$$

where: $X_n=2\left(C_{1n}^2+B_{1n}^2\right)$, $C_{1n}=\left(p_{2n}^--p_{1n}^-\right)^2+q_{2n}^2-q_{1n}^2$,

$C_{2n}=\left(p_{1n}^--p_{2n}^-\right)^2+q_{1n}^2-q_{2n}^2$ $\qquad B_{1n}=2\left(p_{2n}^--p_{1n}^-\right)q_{1n}$,

$B_{2n}=2\left(p_{1n}^--p_{2n}^-\right)q_{2n}$, $p_{jn}^{\pm}=a_{jn}^2\pm b_{jn}^2$, $q_{jn}=2a_{jn}b_{jn}$,

$$A_{10}=\frac{5a_{10}^4+\left(a_{20}^2+b_{20}^2\right)\left(b_{10}^2+b_{20}^2\right)-a_{10}^2\left(3p_{20}^++10b_{10}^2\right)}{4a_{10}p_{10}^+r_1s_1},$$

$$B_{10}=\frac{5b_{10}^4+\left(a_{10}^2-a_{20}^2\right)\left(a_{10}^2+b_{20}^2\right)-b_{10}^2\left(3p_{20}^+-10a_{10}^2\right)}{4b_{10}p_{10}^+r_1s_1},$$

$A_{20}=-\left(2a_{20}p_{20}^-r_1\right)^{-1}$, $\qquad r_1=4a_{20}^2b_{10}^2+\left(a_{10}^2+b_{10}^2-a_{20}\right)$,

$B_{20}=\left(2b_{20}p_{20}^-s_1\right)^{-1}$, $\ s_1=4b_{20}^2b_{10}^2+\left(p_{10}^+-b_{10}\right)$.

The values b_{jn} and a_{jn} are the real and imaginary

parts of the roots $y_{1,2,3,4}=\pm\left(b_{1n}\pm ia_{1n}\right)$, $y_{5,6,7,8}=\pm\left(b_{2n}\pm ia_{2n}\right)$ of the characteristic equation

$$y^8-A_6y^6+A_4y^4-A_2y^2+A_0=0, \qquad (17)$$

$$A_0=n^4\left(n^2-1\right)^2+\gamma_1^2c_1^{-2}\left(n^2+n^4\right)+$$
$$+\nu_-\left[2\gamma_1^6c_1^{-2}+\gamma_1^4\left(n^2(3-\nu)c_1^{-2}+2n^4\right)\right],$$
$$A_2=4n^2(n^2-1)^2+\gamma_1^4\nu_-\left[c_1^{-2}(3-\nu)+4n^2\right]+$$
$$+\gamma_1^2\left[n^2 2c_1^{-2}+3n^4(3-\nu)\nu_-\right],$$
$$A_4=6n^4+\left(c_1^2\nu_-\nu_+\right)^{-1}+2\gamma_1^4\nu_-+$$
$$+\gamma_1^2\left[c_1^{-2}+n^2 3\left(3-\nu\right)\nu_-\right],$$
$$A_6=4n^2+\gamma_1^2(3-\nu)\nu_-.,$$

Note that in contrast to the static case, considered in [7], equation (17) if $n=0$ and $n=1$ does not have multiple roots. Studies have shown that if $n=1$, characteristic equation (17) has eight complex roots, and if $n=0$ there are four complex and four purely imaginary roots that we denote so: $y_{1,2,3,4}=\pm b_{10}\pm ia_{10}$, $y_{5,6}=\pm ib_{20}$, $y_{7,8}=\pm ia_{20}$. Thus the general form of expression for key function if $n=0$ will be different from the expression in the case of static load and if $n=1$ will be described by the first of expressions (16).

In order to derive singularities of the key functions (15) on the line of the cut we present them as

$$\varphi_j(\alpha,\beta)=\varphi_j^0(\alpha,\beta)+\varphi_j^*(\alpha,\beta),$$
$$\psi_j(\alpha,\beta)=\psi_j^0(\alpha,\beta)+\psi_j^*(\alpha,\beta), \qquad (18)$$

where: $\varphi_j^*(\alpha,\beta)=\varphi_j(\alpha,\beta)-\varphi_j^0(\alpha,\beta)$, $\psi_j^*(\alpha,\beta)=\psi_j(\alpha,\beta)-\psi_j^0(\alpha,\beta)$.

Functions $\varphi_j^0(\alpha,\beta)$, $\psi_j^0(\alpha,\beta)$ satisfy the following equation:

$D^0\varphi_2^0=\varepsilon_{22}^*$, $D^0\varphi_3^0=\varepsilon_{12}^*$, $D^0\psi_2^0=R\kappa_{22}^*$, $D^0\psi_3^0=R\kappa_{12}^*$, and their determination is described in detail in [7, 11, 13].

Substitute the expressions (18) into (15) and integrate them (15) by parts, and as a result we rewrite them in the form:

$$\varphi_2(\alpha,\beta)=\frac{1}{\pi R}\sum_{n=0}^{\infty}\left(1-\frac{\delta_{0n}}{2}\right)\cos n\beta\times$$
$$\times\int_{-\alpha_0}^{\alpha_0}\left[v^{*\prime}(\xi)\right]\left[\Psi_n^0(\xi-\alpha)+\Psi_n^*(\xi-\alpha)\right]d\xi,$$
$$\varphi_3(\alpha,\beta)=\frac{1}{\pi R}\sum_{n=0}^{\infty}\left(1-\frac{\delta_{0n}}{2}\right)\cos n\beta\times$$
$$\times\int_{-\alpha_0}^{\alpha_0}\left[u^{*\prime}(\xi)\right]\left[\Psi_n^0(\xi-\alpha)+\Psi_n^*(\xi-\alpha)\right]d\xi,$$
$$\psi_2(\alpha,\beta)=-\frac{1}{\pi R}\sum_{n=0}^{\infty}\left(1-\frac{\delta_{0n}}{2}\right)\cos n\beta\times$$
$$\times\int_{-\alpha_0}^{\alpha_0}\left[\theta^{*\prime}(\xi)\right]\left[\Psi_n^0(\xi-\alpha)+\Psi_n^*(\xi-\alpha)\right]d\xi+$$
$$+\frac{1}{\pi R}\sum_{n=0}^{\infty}\left(1-\frac{\delta_{0n}}{2}\right)n\sin n\beta\times$$
$$\times\int_{-\alpha_0}^{\alpha_0}\left[w^{*\prime}(\xi)\right]\left[\Psi_n^0(\xi-\alpha)+\Psi_n^*(\xi-\alpha)\right]d\xi, \qquad (19)$$
$$\psi_3(\alpha,\beta)=-\frac{1}{\pi R}\sum_{n=0}^{\infty}\left(1-\frac{\delta_{0n}}{2}\right)\cos n\beta\times$$
$$\times\int_{-\alpha_0}^{\alpha_0}\left[w^{*\prime}(\xi)\right]\left[\Psi_n^0(\xi-\alpha)+\Psi_n^*(\xi-\alpha)\right]d\xi,$$

where

$$\Psi_n(z)=\frac{1}{X_n}\sum_{j=1}^{2}\left\{e^{-a_{jn}|z|}\left[C_{jn}^0\cos b_{jn}z\,\mathrm{sgn}\,z+\right.\right.$$
$$\left.\left.+B_{jn}^0\sin b_{jn}z\right]-C_{jn}^0\,\mathrm{sgn}\,z\right\},$$
$$\Psi_0(z)=\frac{A_{10}a_{10}-B_{10}b_{10}}{a_{10}^2+b_{10}^2}\mathrm{sgn}\,z+\left(\frac{A_{10}b_{10}-B_{10}a_{10}}{a_{10}^2+b_{10}^2}\sin b_{10}z-\right.$$
$$\left.-\frac{B_{10}b_{10}-A_{10}a_{10}}{a_{10}^2+b_{10}^2}\cos b_{10}z\,\mathrm{sgn}\,z\right)\mathrm{e}^{-a_{10}|z|}+$$
$$+\left(A_{20}\frac{1-e^{-a_{20}|z|}}{a_{20}}+B_{20}\frac{1-e^{-b_{20}|z|}}{b_{20}}\right)\mathrm{sgn}\,z,$$
$$C_{jn}^0=\frac{q_{jn}C_{jn}-p_{jn}B_{jn}}{q_{jn}\left(a_{jn}^2+b_{jn}^2\right)},\ B_{jn}^0=\frac{p_{jn}C_{jn}+q_{jn}B_{jn}}{q_{jn}\left(a_{jn}^2+b_{jn}^2\right)},$$
$$\Psi_k^0(z)=\frac{1}{96k^8}e^{-k|z|}\left[k^3z^3+9k^2z^2\,\mathrm{sgn}\,z+\right.$$
$$\left.+33kz+48\,\mathrm{sgn}\,z\right]-\frac{1}{2k^8}\mathrm{sgn}\,z,\quad (k=1,2,...).$$

The expressions for the keys functions (15), (19) contain the uknown jumps of displacements and of angles of rotation (2). For their determination we use the boundary conditions (3).

The efforts and moments in the shell are determined by the known formulas [7], which, considering the presentations (1), (8) we write:

$$N_1=N_1^*e^{\gamma t}=D_0\left[\left(1-\nu^2\right)R\right]^{-1}\times$$
$$\times\left(\partial_\alpha u^*+\nu\left(\partial_\beta v^*+w^*\right)-\nu R\varepsilon_{22}^*\right)e^{\gamma t},$$
$$N_2=N_2^*e^{\gamma t}=D_0\left[\left(1-\nu^2\right)R\right]^{-1}\times$$
$$\times\left(\partial_\beta v^*+w^*+\nu\partial_\alpha u^*-R\varepsilon_{22}^*\right)e^{\gamma t},$$
$$M_1=M_1^*e^{\gamma t}=-D_0c^2\times$$
$$\times\left[\partial_\alpha^2w^*+\nu\left(\partial_\beta^2w^*-\partial_\beta v^*\right)+\nu R^2\kappa_{22}^*\right]e^{\gamma t}, \qquad (20)$$
$$M_2=M_2^*e^{\gamma t}=-D_0c^2\times$$
$$\times\left(\partial_\beta^2w^*-\partial_\beta v^*+\nu\partial_\alpha^2w^*+R^2\kappa_{22}^*\right),$$
$$S=S^*e^{\gamma t}=Eh\left[\left(1+\nu\right)R\right]^{-1}\times$$
$$\times\left(\partial_\beta u^*+\partial_\alpha v^*-R\varepsilon_{12}^*\right)e^{\gamma t},$$
$$H=H^*e^{\gamma t}=-D_0c^2\left(1-\nu\right)\times$$
$$\times\left[\partial_\alpha\left(\partial_\beta w^*-v^*\right)+R^2\kappa_{12}^*\right]e^{\gamma t}.$$

In the case of the shell loading symmetric about the crack the shell loading, conditions (3), considering (4) - (6) are simplified and take the form:

$$N_2^{*+}(\alpha,0)=N_2^{*-}(\alpha,0)=f_1^*(\alpha),$$
$$M_2^{*+}(\alpha,0)=M_2^{*-}(\alpha,0)=f_3^*(\alpha). \tag{21}$$

Using in the expressions (20) the presentation (8) we obtain

$$N_2^*=C_{N\varphi}\varphi_2+D_{N\varphi}\varphi_3+C_{N\psi}\psi_2+D_{N\psi}\psi_3,$$
$$M_2^*=C_{M\varphi}\varphi_2+D_{M\varphi}\varphi_3+C_{M\psi}\psi_2+D_{M\psi}\psi_3. \tag{22}$$

Here

$$C_{N\varphi}=D_0\left\langle -\partial_\alpha^4\nabla^2\nabla^2-2\gamma_1^6c_1^{-2}\nu_-^2\nu_+^1+\right.$$
$$+\nu_-\nu_+\gamma_1^4\left\{c_1^{-2}\left[\partial_\beta^2+(3+2\nu)\partial_\alpha^2\right]-2\nu_-\nabla^2\nabla^2\right\}+$$
$$+\gamma_1^2\left\{\nu_-\nu_+\left[\partial_\beta^6+(7+4\nu)\partial_\alpha^4\partial_\beta^2+(5+2\nu)\partial_\alpha^2\partial_\beta^4+\right.\right.$$
$$\left.\left.+(3+2\nu)\partial_\alpha^6\right]-c_1^{-2}\partial_\alpha^4\right\}\Big\rangle,$$
$$D_{N\varphi}=D_0\left[\partial_\alpha^3\partial_\beta\nabla^2\nabla^2-\gamma_1^4c_1^{-2}\nu_-\partial_\alpha\partial_\beta+\right.$$
$$\left.+\gamma_1^2\left(c_1^{-2}\partial_\alpha^3\partial_\beta-\nu_-\partial_\alpha\partial_\beta\nabla^2\nabla^2-\nu_+\partial_\alpha\partial_\beta^3\right)\right],$$
$$C_{N\psi}=D_0\left[c_1^2\nu_+\nu_-^{-1}\partial_\alpha^4\partial_\beta^2P_3-\gamma_1^42\nu_-^2\nu_+\left(2\partial_\beta^2+\nu\partial_\alpha^2\right)-\right.$$
$$\left.-\gamma_1^2\nu_-\nu_+2c_1^2(1-\nu)\partial_\alpha^4\partial_\beta^2\right],$$
$$D_{N\psi}=D_0\left[2c_1^2\nu_+\partial_\alpha^3\partial_\beta P_3P_1-8\gamma_1^4\nu_-\nu_+\partial_\alpha\partial_\beta-\right.$$
$$\left.-\gamma_1^24c_1^2\nu_-\nu_+\partial_\alpha^3\partial_\beta P_1\right],$$
$$C_{M\varphi}=D_0R\left\{c_1^2\nu_-^{-1}\nu_+\partial_\alpha^4\partial_\beta^2P_3-2\gamma_1^4\nu_-^2\nu_+\left(2\partial_\beta^2+\nu\partial_\alpha^2\right)+\right.$$
$$\left.+\gamma_1^2\nu_+\nu_-\left[-2c_1^2(1-\nu)\partial_\alpha^4\partial_\beta^2\right]\right\},$$
$$C_{M\psi}=D_0R\left\langle -\partial_\alpha^4-2\gamma_1^6\nu_-^2\nu_+-c_1^2\nu_+\left[2\partial_\alpha^2\partial_\beta^6+\nu_+^{-1}\partial_\alpha^8+\right.\right.$$
$$+2(2+\nu)\partial_\alpha^6\partial_\beta^2+(5+\nu)\partial_\alpha^4\partial_\beta^4\Big]-$$
$$-\gamma_1^4\nu_-\nu_+\left\{2c_1^2\left(2\partial_\alpha^2\partial_\beta^2+\partial_\alpha^4\right)\right\}+\gamma_1^2\nu_-\nu_+\times$$
$$\left.\times\left\{c_1^2(3-\nu)\left[2\partial_\alpha^2\partial_\beta^4+\nu_+^{-1}\partial_\alpha^6+(3+\nu)\partial_\alpha^4\partial_\beta^2\right]\right\},$$
$$D_{M\varphi}=D_0R\left\{c_1^2\nu_-^{-1}\nu_+\partial_\alpha^5\partial_\beta P_5-\gamma_1^4\nu_-\nu_+\partial_\alpha\partial_\beta-\right.$$
$$\left.-\gamma_1^2\nu_-\nu_+\left[c_1^2(1-\nu)^2\partial_\alpha^5\partial_\beta\right]\right\},$$
$$D_{M\psi}=2c_1^2D_0R\nu_+\left\langle\nu_-^{-1}\left[\partial_\alpha\partial_\beta^7+(1+2\nu)\partial_\alpha^5\partial_\beta^3\right.\right.$$
$$+\nu\partial_\alpha^7\partial_\beta+(2+\nu)\partial_\alpha^3\partial_\beta^5\Big]+2\gamma_1^4\partial_\alpha\partial_\beta P_2-$$
$$\left.-\gamma_1^2(3-\nu)\left[\partial_\alpha\partial_\beta^5+\nu\partial_\alpha^5\partial_\beta+(1+\nu)\partial_\alpha^3\partial_\beta^3\right]\right\rangle,$$
$$P_1=\partial_\alpha^2+\nu\partial_\beta^2,\qquad P_2=\partial_\beta^2+\nu\partial_\alpha^2,\qquad P_3=(2+\nu)\partial_\alpha^2+\partial_\beta^2,$$
$$P_4=(2+\nu)\partial_\beta^2+\partial_\alpha^2,\qquad P_4=\partial_\alpha^2-\nu\partial_\beta^2,\qquad P_5=\partial_\beta^2-\nu\partial_\alpha^2$$
$$\nu_\pm=(1\pm\nu)^{-1}.$$

Substituting (21) in the presentation (22), considering (19), we obtain a system of two integral equations

$$\int_{-\alpha_0}^{\alpha_0}\left[F_1(\xi)K_{11}(\xi-\alpha)+F_3(\xi)K_{13}(\xi-\alpha)\right]d\xi=f_1^*(\alpha),$$
$$\int_{-\alpha_0}^{\alpha_0}\left[F_1(\xi)K_{31}(\xi-\alpha)+F_3(\xi)K_{33}(\xi-\alpha)\right]d\xi=f_3^*(\alpha), \tag{23}$$

where: $F_1(\xi)=\frac{1}{R}\left[\nu'(\xi)\right]$, $F_3(\xi)=-\left[\theta_2'(\xi)\right]$,

$f_1^*(\alpha)=\frac{\pi}{D_0}f_1(\alpha)$, $f_3^*(\xi)=\frac{\pi}{D_0R}f_3(\alpha)$.

The kernels of integral equations system can be presented in the form:

$$K_{11}=a_{11}\operatorname{cth}\frac{z}{2}+\sum_{n=0}^{\infty}\left\langle\left(1-\frac{\delta_{0n}}{2}\right)\frac{\operatorname{sgn}z}{X_n}\times\right.$$
$$\left.\times\sum_{m=1}^{2}\sum_{l=0}^{3}\gamma_1^{2l}A_{mn}^{(l)}\sum_{i=0}^{2}A_{mn}^{(il)}\omega_i-a_{11}K_n^0\right\rangle \tag{24}$$

$A_{mn}^{(3)}=-2A_{mn}^{(2)}$, $A_{mn}^{(2)}=c_1^{-2}a_{nm}^{(1)}$, $A_{mn}^{(1)}=(1-\nu)a_{nm}^{(1)}$,

$A_{nm}^{(02)}=a_{mn}^{(3)}A_{nm}^{(03)}$, $A_{nm}^{(00)}=0$, $A_{nm}^{(0)}=1$, $A_{nm}^{(01)}=-n^6A_{nm}^{(03)}$,

$A_{mn}^{(03)}=B_{mn}p_{mn}-C_{mn}q_{mn}$, $A_{mn}^{(13)}=-\left(C_{mn}p_{mn}+B_{mn}q_{mn}\right)$,

$A_{nm}^{(12)}=-B_{mn}a_{mn}^{(2)}+2c_1^2p_{mn}^+E_{1n}+a_{mn}^{(3)}A_{mn}^{(23)}$,

$A_{nm}^{(11)}=a_{mn}^{(6)}c_1^{-2}E_{1n}-a_{mn}^{(5)}B_{1n}-a_{mn}^{(4)}r_{mn}^{(1)}+n^6A_{mn}^{(23)}$,

$A_{nm}^{(10)}=\left(q_{mn}\right)^{-1}\left((n^4+t_{mn})E_{mn}-2n^2r_{mn}^{(1)}-s_{mn}H_{mn}\right)$,

$a_{nm}^{(1)}=\nu_-^2\nu_+\left(q_{mn}p_{mn}^+\right)^{-1}$, $a_{mn}^{(2)}=(3+4c_1^2n^2-\nu-2\nu^2)p_{mn}^+$,

$a_{mn}^{(3)}=n^2(\nu_-^{-1}+2c_1^2n^2)$, $a_{mn}^{(4)}=(3+2\nu)p_{mn}^+$,

$a_{mn}^{(5)}=n^4(5+2\nu)p_{mn}^+$, $p_{mn}^+=a_{mn}^2-b_{mn}^2$,

$a_{mn}^{(6)}=\left[\left(\nu_-\nu_+\right)^{-1}+c_1^2n^2\left(7+4\nu\right)\right]p_{mn}^+$,

$r_{mn}^{(1)}=\left(s_{mn}C_{mn}+t_{mn}B_{mn}\right)$, $t_{mn}=\left(p_{mn}^-\right)^2-q_{mn}^2$, $\omega_0=1$,

$\omega_1=e^{-a_{mn}|z|}\cos b_{mn}z$, $\omega_2=e^{-a_{mn}|z|}\sin b_{mn}z$,

$E_{mn}=p_{mn}^-B_{mn}+q_{mn}C_{mn}$, $H_{mn}=q_{mn}B_{mn}-p_{mn}^-C_{mn}$,

$A_{mn}=\left(b_{mn}^2-3a_{mn}^2\right)b_{mn}C_{mn}-\left(a_{mn}^2-3b_{mn}^2\right)a_{mn}B_{mn}$,

$s_{mn}=2p_{mn}^-q_{mn}$, $a_{11}=\frac{1}{8}$, $K_0^0(z)=\frac{1}{z}$, $K_i^0=\frac{2^{2i}B_{(2i)}z^{2i-1}}{(2i)!}$,

$D_{mn}=\left(a_{mn}^2-3b_{mn}^2\right)a_{mn}C_{mn}-\left(b_{mn}^2-3a_{mn}^2\right)b_{mn}B_{mn}$; $B_{(2i)}$ are Bernoulli's numbers; the presentations for $A_{mn}^{(2l)}$ are obtained from the expressions for $A_{mn}^{(1l)}$, formally replacing them E_{mn}, H_{mn}, B_{mn}, C_{mn} by H_{mn}, $-E_{mn}$, $-C_{mn}$, B_{mn}.

The expressions for the kernels K_{33} and $K_{31}=K_{31}$ are obtained by formal replacement in the presentation (24) the coefficients a_{11}, $A_{mn}^{(l)}$, $A_{mn}^{(il)}$ by a_{33}, $C_{mn}^{(l)}$, $C_{mn}^{(il)}$ and a_{31}, $B_{mn}^{(l)}$, $B_{mn}^{(il)}$, respectively.

Here: $a_{13}=-\frac{(1-\nu)(3+\nu)c_1^2}{64(1+\nu)}$, $a_{33}=\frac{c_1^2(3+\nu)}{8(1+\nu)}$,

$$C_{mn}^{(10)}=\nu_+\left(q_{mn}\right)^{-1}\left\{E_{mn}\left[(1+\nu)\left(1+c_1^2t_{mn}\right)+c_1^2n^4\left(5+\nu\right)\right]-\right.$$
$$-2c_1^2n^2\left(2+\nu\right)s_{mn}C_{mn}-c_1^2\nu_+^{-1}s_{mn}H_{mn}-$$
$$\left.-c_1^2\left[2n^6+2n^2\left(2+\nu\right)t_{mn}\right]B_{mn}\right\},$$

$C_{mn}^{(0)}=1$, $C_{mn}^{(00)}=0$, $C_{mn}^{(3)}=2\nu_-^2\left(p_{mn}^+\right)^{-1}$, $C_{mn}^{(03)}=C_{mn}^{(13)}$,

$C_{mn}^{(13)}=-C_{mn}+B_{mn}p_{mn}\left(q_{mn}\right)^{-1}$, $C_{mn}^{(2)}=c_1^2$, $C_{mn}^{(02)}=0$,

$C_{mn}^{(12)}=n^2(3+\nu)E_{mn}-C_{mn}\nu_+^{-1}s_{mn}-B_{mn}\left[2n^4+\nu_+^{-1}t_{mn}\right]$,

$C_{mn}^{(1)}=(3-\nu)c_1^2\nu_-\nu_+\left(q_{mn}\right)^{-1}$, $B_{mn}^{(00)}=0$, $C_{mn}^{(01)}=0$,

$C_{mn}^{(11)}=2\left[-2n^2B_{mn}+\left(1+\nu\right)E_{mn}\right]\nu_-\nu_+\left(q_{mn}\right)^{-1}$,

$B_{mn}^{(0)}=c_1^2\nu_-^{-1}\nu_+\left(q_{mn}\right)^{-1}$, $B_{mn}^{(1)}=-2c_1^2n^2\nu_+^{-1}\left(q_{mn}\right)^{-1}$,

$$B_{mn}^{(02)} = 0, \qquad B_{mn}^{(12)} = E_{mn}; \qquad B_{mn}^{(2)} = \nu_-^2 \nu_+,$$

$$B_{mn}^{(10)} = -n^4 E_{mn} + n^2(2+\nu) C_{mn} s_{mn} + n^2(2+\nu) B_{mn} t_{mn},$$

$$B_{mn}^{(03)} = B_{mn}^{(13)} - 2\nu \left(q_{mn}\right)^{-1} B_{mn},$$

$$B_{mn}^{(13)} = \left(p_{mn}^{+} q_{mn}\right)^{-1} \left(4n^2 q_{mn} C_{mn} - 4n^2 p_{mn} B_{mn} + 2\nu p_{mn}^{+} B_{mn}\right),$$

To obtain the coefficients $B_{mn}^{(2l)}$, $C_{mn}^{(2l)}$ it is necessary in the expressions for $B_{mn}^{(1l)}$, $C_{mn}^{(1l)}$ to replace E_{mn}, H_{mn}, B_{mn}, C_{mn} by H_{mn}, $-E_{mn}$, $-C_{mn}$, B_{mn}.

If you put in(24) $\gamma_1 = 0$, then the system(23) will take the form given in [7, 11] for static loading. In this case, at numerical studies one should take into account that the equation (17) if $n = 0$ in the case of technical theory of shells and if $n = 0$, $n = 1$ in the case of the general moment theory will have multiple roots.

CONCLUSIONS

1. We have written explicitly the singular integral equation system for cylindrical shell with longitudinal cracks under the action of time-varying load. Reliability of obtained expressions is confirmed by coincidence with known presentations obtained in the case of static load [7].
2. It is shown that taking into account the time changes of the load does not affect the order of singularity of SIE.
3. The obteined system of integral equations by replacing $u = \frac{\xi}{\alpha_0}$, $s = \frac{\alpha}{\alpha_0}$ results in the SIE system with the kernel of Cauchy type that allows one to make a numerical study of the stress-strain state in the vicinity of the crack, and particularly to study the dynamic behavior of the dynamic intensity factors of effort and moments by the standard methods.
4. The algorithm of numerical solution of the resulting system is constructed.

REFERENCES

1. **Dovbnya K. M., Hordienko M. M. 2010** A study of the strength of an elastoplastic orthotropic shell of arbitrary curvature with a surface crack. Journal of Mathematical Sciences, Vol.170 (6), 687-694.
2. **Goldenweiser A. L., Kaplunov Yu. D. 1998**. Dynamic boundary layer in problems of vibration of shells, Mech. Solids. 23, 146-158.
3. **Goldenweiser A. L. 1961.** Theory of Thin Elastic Shells. Int. Ser. of Monograph in Aeronautics and Astronautics, Pergamon Press, N.Y. 512.
4. **Guz A., Guz I., Menshykov O., Menshikov V. 2011**. Stress-intensity factors for materials with interface cracks under harmonic loading. International Applied Mechanics. Vol. 46. No. 10, 1093-1100.
5. **Kit H., Kushnir R., Mykhas'kiv V., Nykolyshyn M. 2011**. Methods for the determination of static and dynamic stresses in bodies with subsurface cracks. Materials Science. Vol. 47. Issue 2, 177-178.
6. **Kushnir R. M., Nykolyshyn M. M. 2003.** "Stressed state and limiting equilibrium of piecewise homogeneous cylindrical shells with cracks," Mat. Met. Fiz.-Mekh. Polya, 46, No. 1, 60–74. (in Ukrainian).
7. **Kushnir R. M., Nykolyshyn M. M., Osadchuk V. A. 2003.** Elastic and Elastoplastic Limiting State of Shells with Defects [in Ukrainian], Spolom, Lviv, 318. (in Ukrainian).
8. **Kushnir R.M. 2001** Determination of the Limit Equilibrium of a Piecewise–Homogeneous Cylindrical Shell with Longitudinal Crack. Journal of Mathematical Sciences. Vol. 107(1), 3671–3679.
9. **Mirzaei M. 2008.** On amplification of stress waves in cylindrical tubes under internal dynamic pressures. International Journal of Mechanical Sciences. 50 (8), 1292-1303.
10. **Mirzaei M., Karimi R. 2006.** Crack growth analysis for a cylindrical shell under dynamic loading. ASME 2006 Pressure Vessels and Piping/ICPVT-11 Conference, 591-597
11. **Osadchuk, V.A. (1985).** Stress-Strain State and Limit Equilibrium of Shellwith Cuts. Naukova dumka, Kiev, 224 (in Russian).
12. **Pidstrigach Ya.S., Yarema S. Ya. 1961.** Thermal Stresses in Shells, Ukrainian Academy of Sciences Press. Kiev, 212. (in Ukrainian).
13. **Podstrigach Ya.S., Shvetz R.N., 1978**. Thermoelasticity of Thin Shells. Kiev, Naukova Dumka, 344. (in Russian).
14. **Pothula S.G. 2009.** Dynamic response of composite cylindrical shells under external impulsive loads. MSc thesis. University of Akron, 71.
15. **Pukach P. Kuzio I., Nytrebych Z. 2013.** Influence of some speed parameters on the dynamics of nonlinear flexural vibrations of a drill column. Econtechmod : an international quarterly journal on economics in technology, new technologies and modelling processes. Vol. 2, No. 4, 61-66.
16. **Pukach P., Sokhan P., Stolyarchuk R. 2016.** Investigation of mathematical models for vibrations of one dimensional environments with considering nonlinear resistance forces. Econtechmod : an international quarterly journal on economics in technology, new technologies and modelling processes. Vol. 5. No. 1., 97–102.
17. **Roytman A., Titova O. 2002**. Analitical approach to determining dynamic characteristics of a cylinder shell with closing cracks. Journal of Sound and Vibration. 254(2), 379-386.
18. **Savruk M. P. 2003.** New method for the solution of dynamic problems of the theory of elasticity and fracture mechanics. Mat. Sc., 39, No. 4, 465–471.
19. **Titova O.A., Lanko V.P. 2012.** Analysis of the elastic vibrations of cylindrical shells with longidutional cracks. Collection of scientific works "Visnyk of Zaporizhzhya National University. Physical and mathematical Sciences". №1, 161-166. (in Ukrainian).
20. **Zhu X., Li T.Y., Zhao Y., Yan J. 2007.** Vibrational power flow analysis of thin cylindrical shell with a circumferential surface crack. Journal of Sound and Vibration. Vol. 302. Iss. 1–2. No. 17, 332–349.

Theoretical studies of the ellipsoidal-shaped particles' behaviourin the channel of pneumo-electric separator bumping into its walls

S. Kovalyshyn, V. Dadak

Lviv National Agrarian University; e-mail: dadakv@i.ua

Received July 14.2016: accepted July 19.2016

Abstract. It is widely known that during the post-harvest handling of a number of crops pneumatic separators are often used. It is proved that in order to improve separation process by using an air flow becomes possible through the use in the separation channels an electric field of corona discharge as additional working body. The electric field makes an additional force effect on the particles of the separated mixture. Since the seeds of cultivated plants and weeds belong to different species, their electrical properties interact with the working bodies of pneumatic separators in different ways that enables quality improvement of seed mixtures separation.

We consider the ellipsoidal particles' behaviour under the influence of gravity, electric power and air flow in pneumo-electric separator channel taking into account their bumping into the walls. We also worked out the differential equations that reflect the mathematical model of the particles under the totality of these forces. This model describes the movement of particles in the pneumo-electric separator channel and allows at any time to calculate the coordinates of trajectories. Based on their analysis we can explore the influence of the controlled process parameters on the pneumo-electric separation and determine their optimal parameters under which the separation of the investigated seed mixtures is the most effective and the components of which are of ellipsoid shape.

Key words: seed mixture, ellipsoidal-shaped particle, pneumo-electric separator, vertical channel, mathematical model, adjustable settings.

FORMULATION OF THE PROBLEM

Among the existing seed purifying machines used in the post-harvest handling of hard-to-divide seed mixtures, a considerable place is given to pneumatic separators where seed cleaning is carried out by aerodynamic properties of the mixture components. [1, 8, 9, 16].

However, the existing hardware, in which a division is carried out in the air stream, do not provide a quality separation of seed mixtures and many impurities of weeds, especially those which are hard-to-divide, disabled ones (no germs) and dead seeds of culture plants[2,4,7]. The main reason for this is the similarity in the basic physical and mechanical properties, especially aerodynamics of the separating components of the mixtures [15]. Consequently, it is impossible to ensure their effective separation. Under these conditions we need to use an additional force action on the separating components, which can be ensured by an electric field in a vertical channel.

The electric field in this case acts as an additional operating working body. Since the seeds of cultivated plants and weeds belong to different species, their electrical properties interact with the working bodies of pneumatic separators in different ways that enables quality improvement of seed mixtures separation.

ANALYSIS OF RECENT RESEARCHES AND PUBLICATIONS

Theoretical studies widely covered the issue of pneumatic separation [5, 6,7,8]. They are dedicated to the definition of critical speed ratios of floating and windage components of seed mixtures [19,20,21], calculations of air flow [12,13], substantiation of fan settings creating them [14], definition of structural shapes and geometric dimensions of pneumatic channels[17] and so on.

It was also examined the interaction force of seed mixtures particles with air flow, its impact on the trajectory, whereby the possibility of separation by their aerodynamic properties is set [10]. Power interaction takes into account the cumulative effect on the particles of gravity and air flow.

To improve the process of pneumatic separation we may use in separating channels an electric field as an additional working body [6,18]. Under such conditions the seed particles will be influenced by electric power. This study [5] theoretically describes the orientation of the ellipsoidal particles in the channel of pneumo-electric separator influenced by the additional factor of power - the electric field. However, the mathematical description of the behavior of these particles reflects the ideal case - movement without mutual collisions and bruises to the walls of the channel. In reality the ellipsoidal particles of separated components of mixtures are often in contact with each other, and more - with the walls of the channel, which requires more detailed theoretical studies designed to more accurately reflect the process of pneumo-electric separation in a vertical channel.

SETTING OBJECTIVES

The aim of the researches was to increase the efficiency of separation of hard-to-divide seed mixtures in a pneumo-electric separator, the components of which are of ellipsoidal shape, according to mathematical modeling of movement in a vertical channel in view of their bumping into the walls.

MAIN PART

Being fed from the bunker into the pneumo-electric channel much of the seeds hit its walls and contact with them for some time *t*. The hit significantly impacts on the trajectory of the seed mixtures components and, consequently, the quality of separation. It is therefore advisable to consider the behavior of the seed in the channel for the actions of its electric and gravitational forces and bind it to a system of coordinates that is represented in Fig. 1. The beginning of the fixed coordinate system *xoy* we allocate in the place where the seed is supplied from the bunker into the channel.

We introduce the auxiliary coordinate system:

x_2Cy_2 - moving forward together with the center of mass of the particle;

x_1Cy_1 - tightly bounded with the particle;

x_c, y_c - variable coordinates of the center of mass of the particle.

Oy axis is directed along the channel's wall, on which the seed hits during its movement in the air stream.

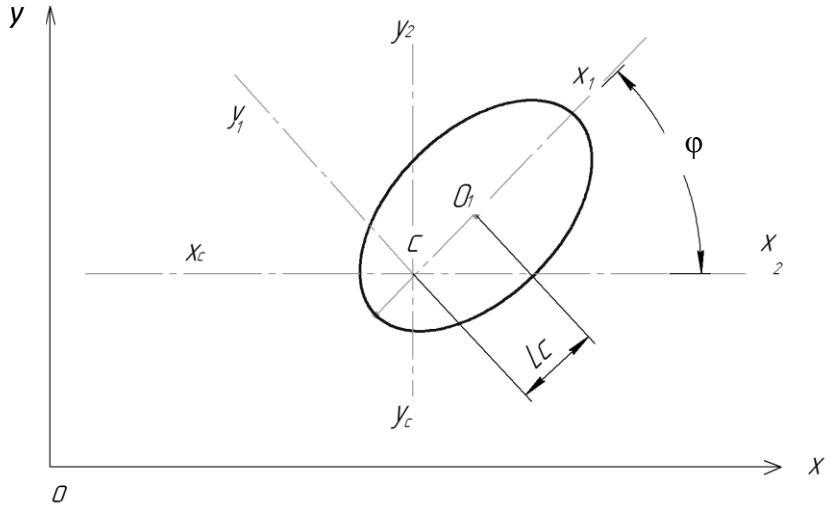

Fig. 1. Position of the ellipsoid-shaped particle relatively to the coordinate systems when it strikes the wall of the pneumatic separation channel

Under these conditions, the equation of an ellipse, which limits the seed in the plane *xoy*, in the coordinate system *xcy* could be written as follows:

$$\frac{(x_1 - l_c)^2}{b^2} = \frac{y_1^2}{a^2} = 1 \ . \qquad (1)$$

The relationship between the coordinates can be expressed as follows:

$$\begin{aligned} x_1 &= x_2 \cos\varphi + y_2 \sin\varphi; \\ y_1 &= y_2 \cos\varphi - x_2 \sin\varphi; \\ x_2 &= x - x_c\,;\ y_2 = y - y_c. \end{aligned} \qquad (2)$$

Taking into account (1.2) we define the relationship between the coordinates of the points of an ellipse and various coordinate systems:

$$\begin{aligned} x_1 &= (x - x_c)\cos\varphi + (y - y_c)\sin\varphi; \\ y_1 &= (y - y_c)\cos\varphi - (x - x_c)\sin\varphi. \end{aligned} \qquad (3)$$

Substituting equation (3) in the formula (1), we obtain the equation of an ellipse in a fixed coordinate system:

$$\frac{\left((x - x_c)\cos\varphi + (y - y_c)\sin\varphi - L_c\right)^2}{b^2} + \frac{\left((y - y_c)\cos\varphi - (x - x_c)\sin\varphi\right)^2}{a^2} = 1 \qquad (4)$$

In equation (4) coordinates of the center of mass of the particle $x_c\,(t)$, $y_c\,(t)$ and the angle of rotation $\varphi\,(t)$ are functions of time.

We reduce equation (4) to the quadratic equation:

$$A = (y - y_c)^2 - 2B(y - y_c) + C = 0, \qquad (5)$$

where:

$$A = \frac{\sin^2\varphi}{b^2} + \frac{\cos^2\varphi}{a^2}\ ;$$

$$B = \frac{(x - x_c)\cos\varphi\sin\varphi}{a^2} + \frac{(L_c - (x - x_c)\cos\varphi)\sin\varphi}{b^2} \qquad (6)$$

$$C = \frac{((x - x_c)\cos\varphi - L_c)^2}{b^2} + \frac{(x - x_c)^2 \sin\varphi^2}{a^2} - 1$$

From equation (6) we find the coordinate y:

$$y = y_c + \frac{B \pm \sqrt{D}}{A} . \quad (7)$$

A seed does not contact with the wall of the channel at $x = 0$. Under this condition discriminant $D < 0$. In the case where $D = 0$, we obtain the equation for determining the point of time $t=t_1$, in which the seed is hit against the wall of the channel. Then the formula (7) defines the ordinate point of contact:

$$y_k = y_c(t_1) + \frac{B(t_1)}{A(t_1)} . \quad (8)$$

Solving differential equations of motion of a particle in the channel of pneumo-electric separator we received kinematic characteristics that describe its position and velocity of the center of mass, angular speed at the moment of impact:

$$x_{c0} = x_c(t_1);\ y_{c0} = y_c(t_1);\ \varphi_0 = \varphi(t_1);$$
$$v_{cx0} = v_{cx}(t_1);\ v_{cy0} = v_{cy}(t_1);$$
$$\omega_0 = \frac{d\varphi}{dt}\Big|_{t=t_1} . \quad (9)$$

Projections of speed point of contact for seed on the axes equal:

$$V_{kx} = v_{cx0} - w_0 (y_k - y_{c0});$$
$$V_{ky} = v_{cy0} - w_0 x_{c0} , \quad (10)$$

where: v_{cx0}, v_{cy0} - projection of center of mass speed of a particle at the moment of impact; ω_0 - angular velocity.

At the moment of impact the coordinates of center of mass and the angle of rotation are constant, and the speed of center of mass and the angular velocity change and take some values v_{cx1}, v_{cy1} and w_1.

Taking into account the theorem of momentum of mechanical systems at impact, we can write:

$$m\ (v_{cx1} - v_{cx0}) = S_x^{sh};$$
$$m\ (v_{cy1} - v_{cy0}) = S_y^{sh};$$
$$I\ (w_1 - w_0) = -S_x^{sh}\ (y_k - y_{c0}) - S_y^{sh} x_c, \quad (11)$$

where: S_x^{sh}, S_y^{sh} - projection external shock pulse;

v_{cx1}, v_{cy1} - projection of center of mass velocity after impact; w_1 - angular velocity after impact.

Note that:

$$S_y^{sh} = f S_x^{sh}, \quad (12)$$

where: f - coefficient of sliding friction of seed against the wall of the channel.

Let us define the projection of speed point of contact of seed V_{kx1} after hitting axle O_x:

$$V_{kx1} = -K v_{kx} = -K_1(v_{cx0} - w_0 (y_k - y_{c0})), \quad (13)$$

where: K_1 - coefficient of restitution after impact.

The left side of (1.13) equation will be represented as:

$$V_{kx1} = v_{cx1} - w_1 (y_k - y_c). \quad (14)$$

Taking into account (14), the equation (13) will be as follows:

$$V_{cx1} - w_1(y_k - y_c) = K_1(v_{cx0} - w_0 (y_k - y_c)). \quad (15)$$

Exclude from equations (1.11) and (1.12) S_x^{sh} and S_y^{sh}:

$$V_{cy} - V_{cy0} = f(v_{cx1} - v_{cx0}); \quad (1.16)$$
$$I = (w_1 - w_0) = -m((v_{cx1} - v_{cx0})(y_k - y_c) + f x_c).$$

The solution of equations (15) and (16) are values of projections of speed of center of mass and the angular velocity of seed after strike:

$$w_1 = \frac{Iw_0 = mV_{cx0}d + mdK_1V_{kx}}{I + md(y_k - y_c)} ; \quad (1.17)$$
$$V_{cx1} = \frac{(Iw_0 + m \cdot V_{x0}d)(y_k - y_c) - IK_1V_{kx}}{I + md(y_k - y_c)} ;$$
$$V_{cy1} = V_{cy0} + f(v_{cx1} - v_{cx0}).$$

where: $d = y_k - y_c + f x_c$.

The values of the coordinates of the center of mass, rotation angle and speed of the particles are the initial conditions in the integration of differential equations that describe its plane-parallel motion in separation channel in condition of its strike into the wall:

$$\begin{cases} m\dfrac{d^2x_c}{dt^2} = -F_e - K\dfrac{dx_c}{dt}A_2; \\ m\dfrac{d^2y_c}{dt^2} = -mg + K(V_i - \dfrac{dy_c}{dt})A_m; \\ I\dfrac{d^2\varphi}{dt^2} = K(V_i - \dfrac{dy_c}{dt})A_1L_c\cos\varphi - F_eL_e\sin\varphi - \\ -\dfrac{d\varphi}{dt}\cdot K \cdot H + K\dfrac{dx_c}{dt}A_2L_c\sin\varphi, \end{cases} \quad (1.18)$$

where:

$$H = 2a\int_{-b+L_c}^{b+L_c} y^2\sqrt{1 - \frac{(y - L_c)^2}{b^2}} ;$$
$$dy = \frac{\pi ab}{4}(4L_c^2 + b^2)\cdot$$

The system of differential equations (18) is being integrated till the moment of time $t_2 > t_1$, in which the condition $D = 0$ is true again and the next srike of the

seed against the wall of the channel will take place, or it reaches the lowest point of the channel ($y_c = 0$).

If the weight of an ellipsoid-shaped particles, by which a number of crop seeds are simulated, is smaller than the resultant of forces of the air flow, their movement is described by the differential equations (19):

$$\begin{cases} m\dfrac{d^2x_c}{dt^2} = -F_e - K\dfrac{dx_c}{dt}A_2; \\ m\dfrac{d^2y_c}{dt^2} = -mg + K(V_n - \dfrac{dy_c}{dt})A_m; \\ I\dfrac{d^2\varphi}{dt^2} = K(V_n - \dfrac{dy_c}{dt})A_1L_c\cos\varphi - F_eL_e\sin\varphi - \\ -\dfrac{d\varphi}{dt}\cdot K\cdot H + K\dfrac{dx_c}{dt}A_2L_c\sin\varphi, \end{cases} \quad (19)$$

where: $A_1 = A_m$.

A_2 – the plane projection of midlength section on axle *ox*:

$$\int_0^b y^2\sqrt{1-\frac{y^2}{b^2}} = b^3\frac{\pi}{16}.$$

The system of differential equations (19) was solved by the numerical method of Runge-Kutta under such initial conditions:

$$t = 0; X_c = 0; Y_c = 0; \varphi = 0; \frac{d\varphi}{dt} = 0;$$

$$\frac{dX_c}{dt} = 0; \frac{dy_c}{dt} = 0.$$

The system of differential equations (19) presents a mathematical model of a particle's behavior of seed mixtures of ellipsoid form in a channel of pneumo-electric separator under the aggregate action of forces: gravity, electrostatic field and air flow in conditions of its strike into its wall. Its solution allows you to find the coordinates of the center of mass as a function of time, and the angle of rotation of a particle around a center of mass to any point in time.

If this seed is moving up then the integration of the equations (19) should be continued until it reaches a certain value y_{max} which is set in advance. The formulas that describe the process of impact remain unchanged.

CONCLUSIONS

1. Due to the counting of the total effect on ellipsoidal-shaped seed of gravitational force, electric power and air flow we obtained the differential equations that reflect the mathematical model of its traffic in the channel of pneumo-electric separator, taking also into account the the strike into the wall of the separation channel.

2. The worked out mathematical model of seed mixture particles components' behaviour takes into account the strike into the walls of the separation channel and allows at any time to calculate the coordinates of the trajectory on the basis of the analysis of which we can decide about the possibility of their separation in a vertical pneumo-electric channel.

3. On the basis of theoretical researches we can simulate the movement of ellipsoidal-shaped particles in the channel of pneumo-electric separator, to investigate the impact on its adjustable parameters and optimize their values in which the separation of seed mixtures is the most effective.

REFERENCES

1. **Abduyev M.,** 2007. Substantiation of separator parameters with inclined air channel to separate grain mixtures. Author. Dis. PhD degree. Nauka, Kharkiv, 22 p. (Ukraine)
2. **Buhaiov V. D. 2012.** Modern technologies of perennial grasses seeds' production. / V.D. Buhaiov, S. F. Antoniv // Posibnyk ukrainskoho hliboroba. – pp. 156-161.
3. **Kravchenko V. A. 2007.** Vegetables. Open and close soil. / V.A. Kravchenko // Nasinnytstvo.– № 6. p. 22-23.
4. **Druncha V. M. 2010.** Basic conceptual development position of seed preparation technology. / V. M. Druncha, B. D. Cudendorziev, S. Pavlov. // Hranenie I pererabotka zerna. –: № 5 - (131) – p. 36-38.
5. **Ukrainian State Standards.** Seeds of plant species: vegetables, hippocastanaceae, fodder and intoxicating-aromatic. Varietal and sowing quality. Technical standard: DSTU 7160.
6. **Bereka O. 2012.** Ionization processes in grain under strong electric fields / O.Bereka, S. Usenko // Econtechmod : an international quarterly journal on economics in technology, new technologies and modelling processes. - Lublin ; Rzeszow, - Volum 1, nomber 1. - p. 17-20.
7. **Baryshev M.G. 2002.** The impact of electromagnetic fields on biochemical processes in plant seeds / M.G. Baryshev, G.I. Kasyanov // Proceedings of the universities. Food technology. - № 6. - p. 21-23.
8. **Chyzhykov A.G. 2001.** Status of mechanization and prospects of development of postharvest handling and storage of grain and seeds. Dostizheniya nauki i tehniki APK. 2001. no. 11, p. 17-20.
9. **Bakum M.V., Olshansky V.P., Krekot M., 2009.** Investigation of the particles in quazihorizontal channel of pneumatic separators. Journal of Kharkov National Technical University of Agriculture n.a.Petro Vasilenko, 132, p. 7 (Ukraine)
10. **Yermak V., 2003.** Substantiation of sunflower separation method in air flow: Author. Dis. for PhD degree. Lugansk, p. 21. (Ukraine)
11. **Kovalyshyn S. Y. 2013.** Pneumo-electric separator for seeds. Vcheni Lviv. Agr. University: Catalogue of innovations. vol. XIII. Lviv. 2013. pp. 48.
12. **Nishchenco I. O., Shvets O. P., 2009.** The investigation of the movement trajectory of seed mixture particles of the globe-shape form along the

movable in the electric field of the friction flat. DSAU, Magazine, Special edition № 2-09. Dnipropetrovsk 2009. – p. 256-259.

13. **Petrenko M.M., Onopa V.A., Kyslun O.A., Onopa V.V., 2009.** Studies of trajectory of impurities in the air stream. Collection of Science. Pr., Kirovograd National Technical University, 2, p.5. (Ukraine)
14. **Turov AK., Mezenov A.A., Pshenov E.A., 2013.** Modelling of air flow velocity field in pneumoscrew .channel. Technology in agriculture, 2, p. 36-40. (Russia)
15. **Kovalyshyn S.J. 2013.** Use of the electro-separation method for improvement of the utility value of winter rapeseeds. // S.J. Kovalyshyn, O.P. Shvets, S. Grundas, and J. Tys // Int. Agrophysics –T. 27, – p. 491-494.
16. **Kovalyshyn S.J. 2014.** Separation efficiency enhancement of forage perennial grasses' seeds. / S. J. Kovalyshyn, V.O. Dadak // Visnyk Harkivskoho nacionalnoho tehnichnoho universytetu im. Petra Vasylenka: Tehnichni systemy i tehnologii tvarynnyctva. – Vol. 144. 225-232.
17. **Dadak V.O. 2013.** Improving of pneumo-separator for small seeded crops. Mechanizaciya ta elektryfikacya silskogo gospodarstwa. Mizhvidomchyy temetychnyy zbirnyk. vol. 97, 2013. pp. 495-501.
18. **Tarasenko A.P., Orbinsky V.I., Gievsky A.M., Sudneev A.A., 2009.** Improving the design of the channel of the second aspiration: Technology in agriculture, 2, pp 29-31. (Russia)
19. **Voytyuk D.G., Yatsun S.S., Dovzhyk M.Y., 2008.** Agricultural Machinery: basic theory and calculation: teach. guidances. for students. University. Sumy: University Book, 543 p. (Ukraine)
20. **Yermak V.P., Bogdanov Y.V., Ilchenko A.A. 2011.** Research of rational airflow velocity on the surface of the body of aerodynamic separator: Journal of Kharkov National Technical University of Agriculture n.a. Petro Vasilenko, 108, p. 108-111. (Ukraine)
21. **Zaika P.M., 2006.** Theory of agricultural machinery. Cleaning and sorting of seeds. Kharkiv, 408 p. (Ukraine)
22. **Kovalyshyn S.J. 2014.** Ways of improvement of post-harvest prepation of small seeded cultivated plants / S.J. Kovalyshyn, V. O. Dadak, V.V. Sokolyk // Motrol: Motorization and power industry in agriculture. – Lublin: Commision of motorization and power industry in agriculture. – Vol. 16D. p.38-44.
23. **Bartneev I.M. 2013.** Technologies perfection and means of mechanization of reforestation. / Drepaliuk M.V., Kizakov V.I. // M.: Flinta, 208.
24. **Bereka O.** Time of exposure to grain processing disinfection in strong electric fields / O.Bereka, S. Usenko // Econtechmod : an international quarterly journal on economics in technology, new technologies and modelling processes. - Lublin ; Rzeszow, 2013. - Volum 2, nomber 2. - p. 27-30.
25. **Batluk V.** Mathematical model for motion of weighted parts in curled flow / V. Batluk, M. Basov, V. Klymets // Econtechmod : an international quarterly journal on economics in technology, new technologies and modelling processes. - Lublin ; Rzeszow, 2013. - Volum 2, nomber 3. - p. 17-24.

Comparative research of efficiency of photovoltaic power systems

Serhiy Syrotyuk[1], Valery Syrotyuk[1], Volodymyr Halchak[1], Andriy Tokmyna[1], Andrzej Chochowski[2], Stanisław Sosnowski[3]

[1]Lviv National Agricultural University
St. Vladimir the Great, 1, Dublyany, Ukraine. E-mail: ssyr@ukr.net
[2]Warsaw University of Life Sciences
St. Nowoursynowska. 166, Warsaw, Poland, e-mail: andrzej.chochowski@sggw.pl
[3]University of Rzeszow, Faculty of Biology and Agriculture Ćwiklińskiej 1a, 35-601 Rzeszow

Received July 14.2016: accepted July 19.2016

Abstract. The article gives results of the development of the system of monitoring for photovoltaic power installations with different configuration to study the factors, increasing their productivity.

Differentiation of impact, made by the components of different structure of photovoltaic power installations is made by application of three independent controlled channels of energy extraction from photovoltaic panels: fixed focused, with application of solar tracker and with application of solar tracker, having flat mirror concentrators.

To secure originality of the record of the electric energy, produced by photovoltaic panels, we have developed unit of control for discharging current of battery banks in each channel. It supports equal level of their charge. Amount of the produced electric energy in each channel is estimated by the value of discharge. Control and measuring system is made on the base of virtual devices with hardware unit of input/output of NI USB-6009 type, produced by National Instruments Company, with software LabVIEW. In the research, software code of the system of monitoring and front panel of operator have been developed. The work provides photos of the developed experimental stand.

Key words: photovoltaic power system, efficiency of photovoltaic power systems, the system of monitoring, control unit, laboratory stand, the solar-tracking installations, flat mirror concentrators.

FORMULATION OF THE PROBLEM

Considering a high cost price of electric energy, produced by solar photovoltaic power stations, intensive scientific research is carried out, focused on increase of their efficiency. Productivity of photovoltaic panels is influenced by incident direction of sun beams on the receiving surface, level of shading, character of radiation (direct or scattered radiation), panel temperature, factor of beams concentration, etc. Among the mentioned factors, the greatest impact is made by incident direction of sun beams on the receiving surface. Optimal angle of incidence can be secured by application of sun-tracking installations.

Efficiency of solar power systems can be considerably higher if using combined production of thermal and electric energy. However, production of electric energy, as the energy of the highest quality, is the main direction. To increase electric productivity, different systems of pointing of photovoltaic power panels to the Sun and increase of the factor of beams concentration are usually developed. To make functional and cost analysis of the systems, which differ in their structural configuration, it is a necessity to make experimental comparative estimation of them. In the research, special attention is paid to correctness of methods of the experiment conduction, considering peculiarities of operation of a photovoltaic panel in the electric system under different ways of electric energy extraction. It is particularly true for self-contained utility systems, operating for electrochemical storage.

Application of any technical means to increase productivity of photovoltaic panels by means of orientation according to the Sun is usually complicated and expensive.

Leading companies and scientific organizations carry out scientific experimental research in the direction of optimization of construction and operating regimes of sun-tracking installations [1, 4, 6, 10, 12, 13, 15-17]. Resupply of the solar-tracking installations with means of solar radiation concentration is a separate direction of the research [2, 3, 7-9, 11, 14].

Argumentation of the optimal level of concentration is not of less importance in relation to application of concentration means, because excess value of it can cause feedback effect, fall of productivity because of excessive heating of photovoltaic panels, depending on their type.

The analyzed works [7-11, 14-17] present theoretical and practical application of mainly network solar-tracking photovoltaic power systems, including the ones, using flat mirror concentrators. However, they do not provide information as to differentiation of contribution of separate elements of photovoltaic power installation to the

increase of its electric productivity. The fact causes difficulties to make functional and cost analysis of them. Besides, not much attention is paid to investigation of impact of seasonal and weather variations of solar radiation on electric productivity.

MATERIALS AND METHODS

For operation of self-contained photovoltaic power systems, it is important to consider the manner of the produced energy extraction, and their comparative estimation requires optimal conditions for energy extraction.

In such systems, it is necessary to secure maximum reception of the energy, produced by a photovoltaic panel and support the recommended regimes of batteries charge. In the systems of comparative estimation of efficiency, it is necessary to secure a charge regime with maximum possible current, which corresponds to maximum productivity of the photovoltaic panel, and, maintaining stable voltage of battery, prevent recharge by automatic outfeed of energy from it.

Object of the research is made by comparative electric productivity of a fixed sun-tracking photovoltaic power system, equipped with flat mirror concentrator of photovoltaic panels.

Subject of the research is to study how configuration of structural scheme of photovoltaic power installation influences its productivity, differentiation of contribution of its components and regime parameters of photovoltaic power installations.

Some technical conditions should be supplied for efficient fulfillment of the task to secure maximum extraction of energy from photovoltaic panel by battery bank. In particular, battery bank should have the overall capacity and level of charge, securing available maximal charged current, which corresponds to the nominal current of completely illuminated photovoltaic panels. To supply correspondence of energy extraction from different systems, it is necessary to provide the same voltage at battery banks. It can be achieved by automatic adjustment of load by a unit of control over discharge of discharging currents with the currents of battery banks charge.

The function to control optimal regimes of battery banks charge is performed by serial MPPT controllers.

RESULTS AND DISCUSSION

Structural scheme of the system of monitoring for photovoltaic power installations with different configuration includes the elements, which are demonstrated at fig. 1.

Optimization of load of photovoltaic panels with different configuration is supported maintaining the set level of charge of separate battery banks, regardless of their productivity. Degree of charge is maintained, regulating discharging current by pulse-width method with tracking system. Its scheme is presented at fig 2.

Fig. 3 gives general view of the developed board of three-channel unit of control for battery banks discharge.

To complete databases of the monitoring for operation of photovoltaic power systems with different configuration under conditions of seasonal, daily and climatic no uniformity of sun radiation, we used the system of virtual devices with hardware unit of input/output of NI USB-6009 type, produced by National Instruments Company, with software LabVIEW. The software LabVIEW widely used to study problems of solar photovoltaic systems [18], and many other systems [19, 20]. Software code of the monitoring system is presented at fig. 4, and front panel of the operator - at fig. 5.

General view of hardware part of laboratory stand is demonstrated at fig. 6 and 7.

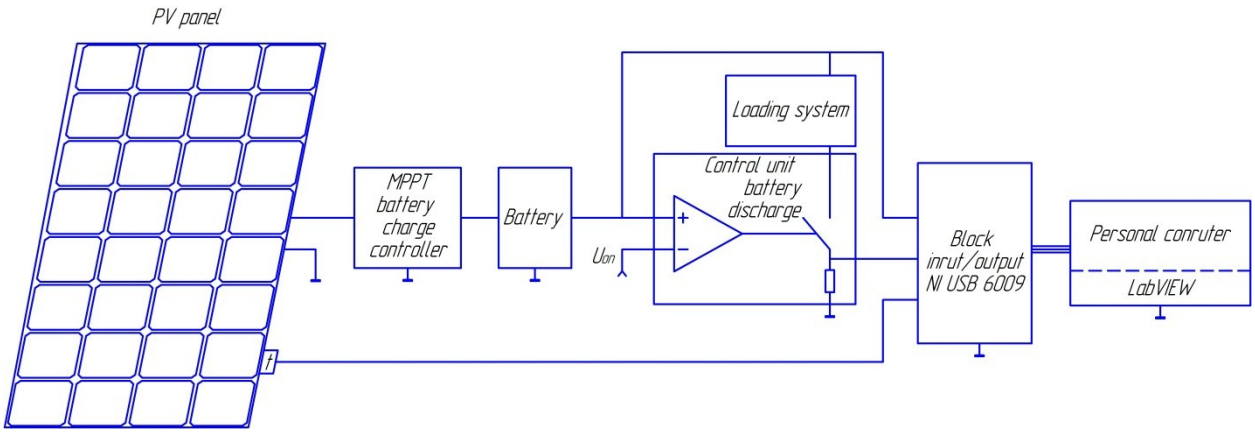

Fig. 1. Structural scheme of the system of monitoring for photovoltaic power installations with different configuration (on the example of one of the channel of a fixed photovoltaic panel)

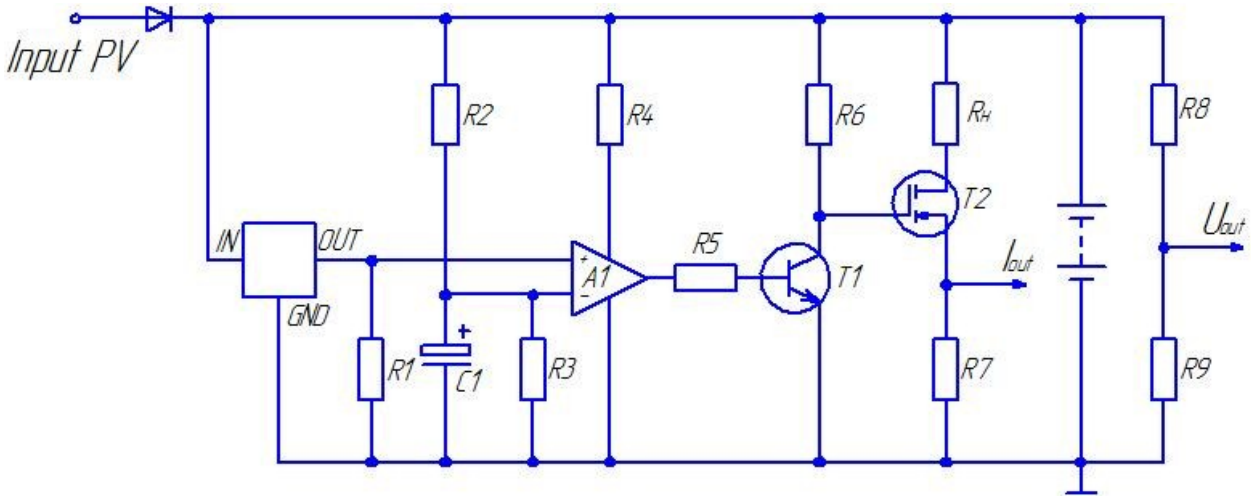

Fig. 2. Electric principal scheme of one channel of control unit, managing discharge of battery bank

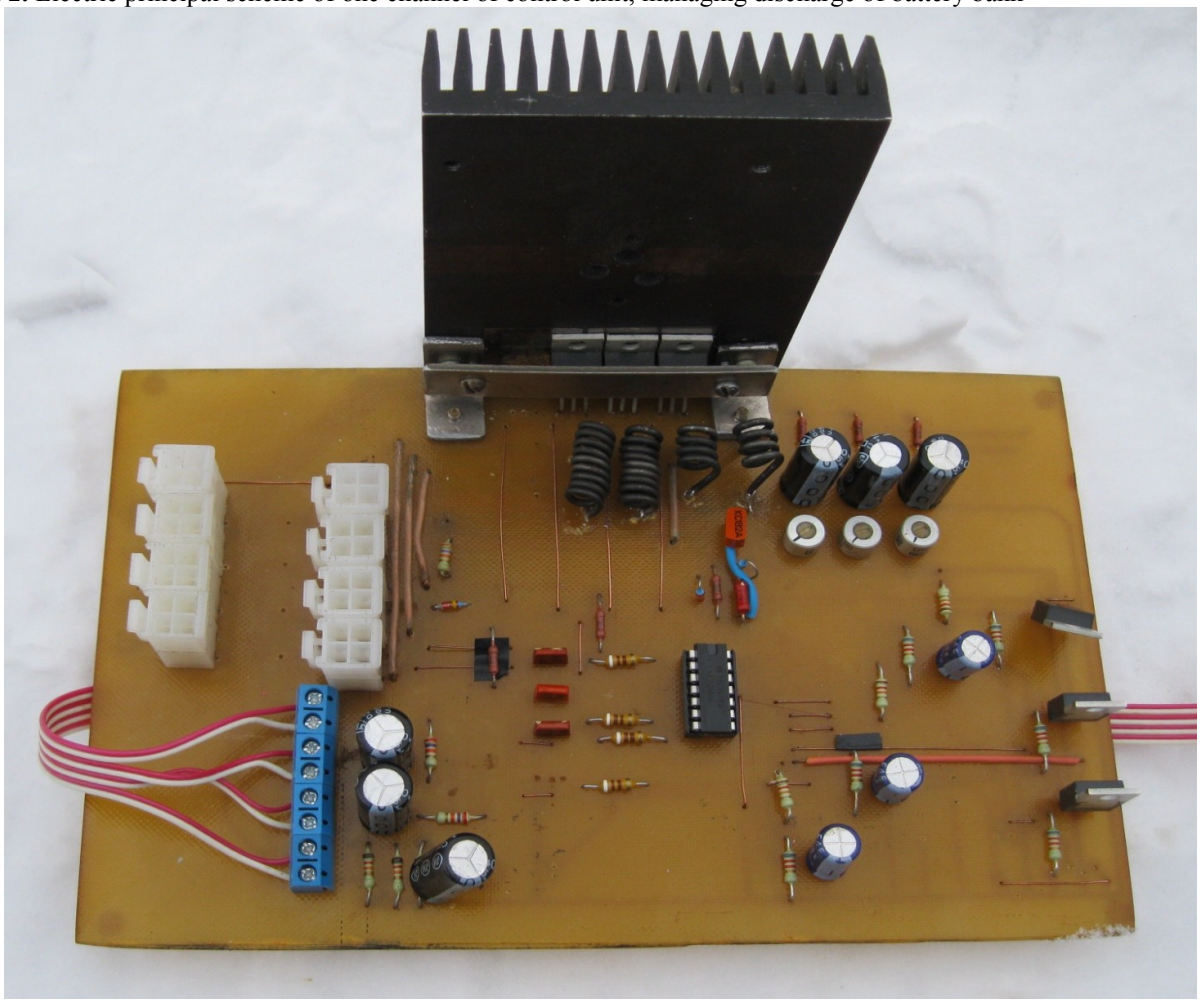

Fig. 3. General view of the board of three-channel unit of control for battery banks discharge

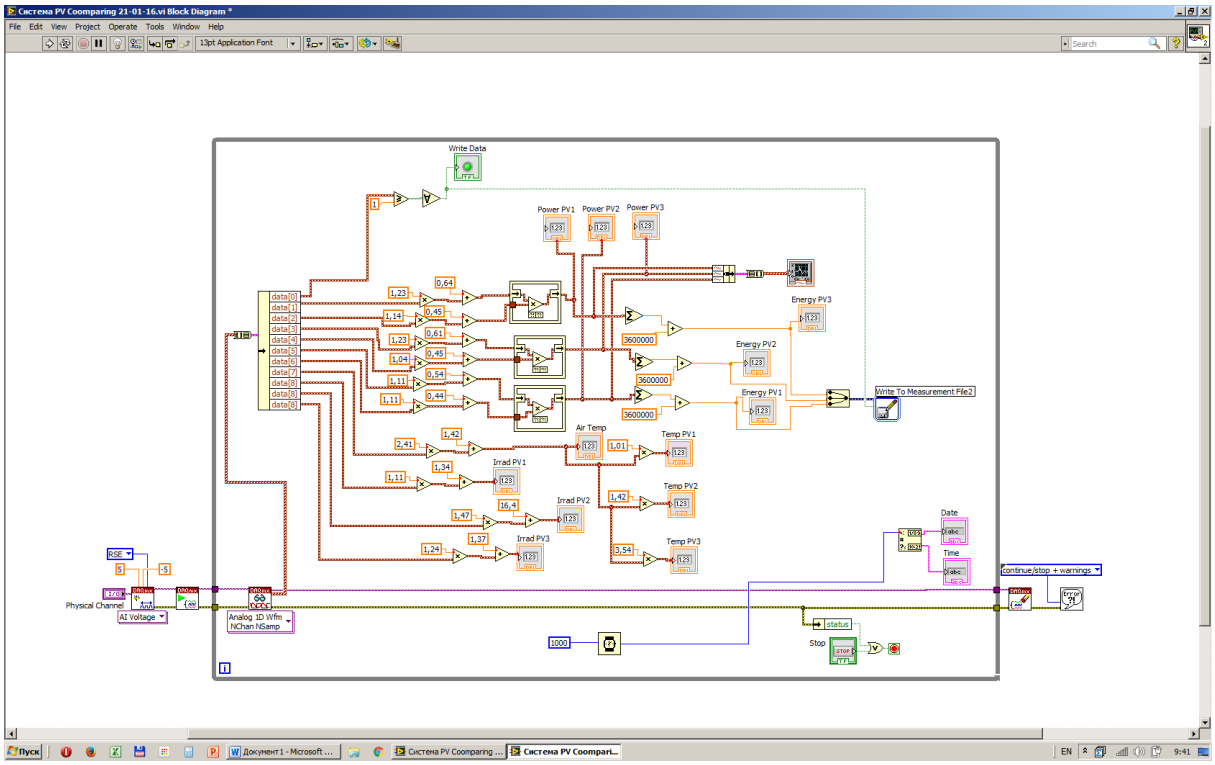

Fig. 4. Software code (block diagram) of the system of monitoring for photovoltaic panels

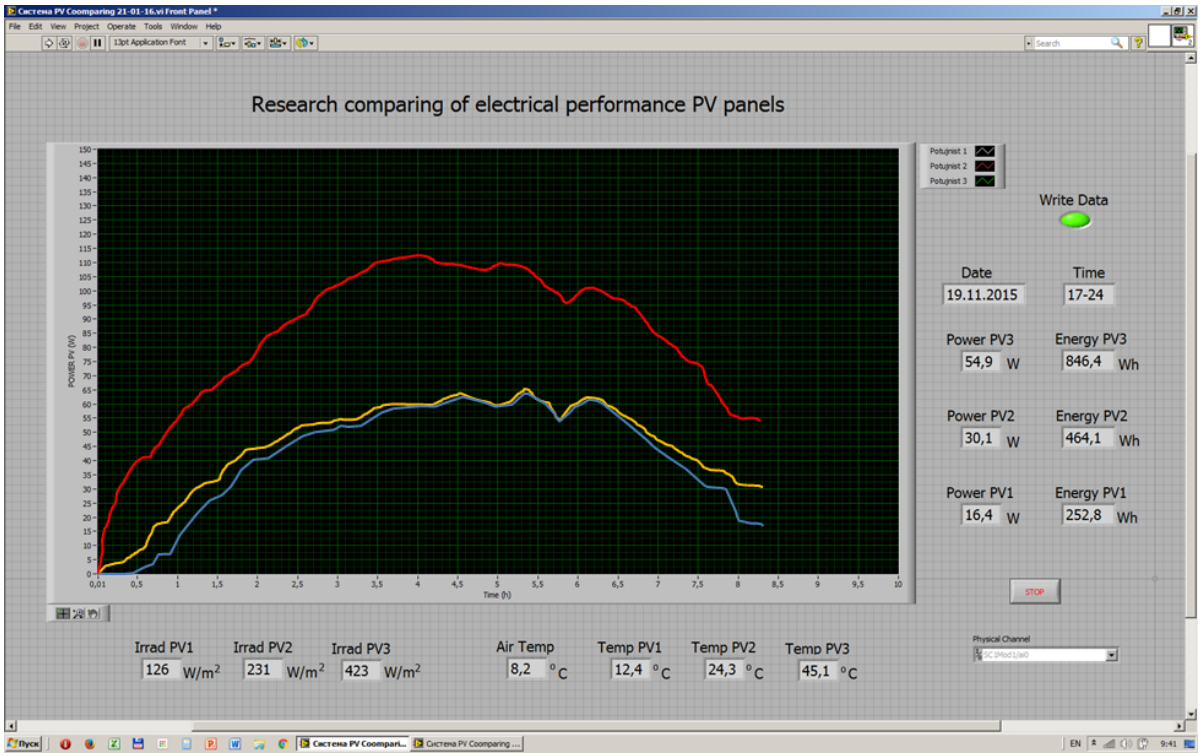

Fig. 5. Panel of operator (front panel) of the system of monitoring for photovoltaic panels

Fig. 6. Photo of experimental installation

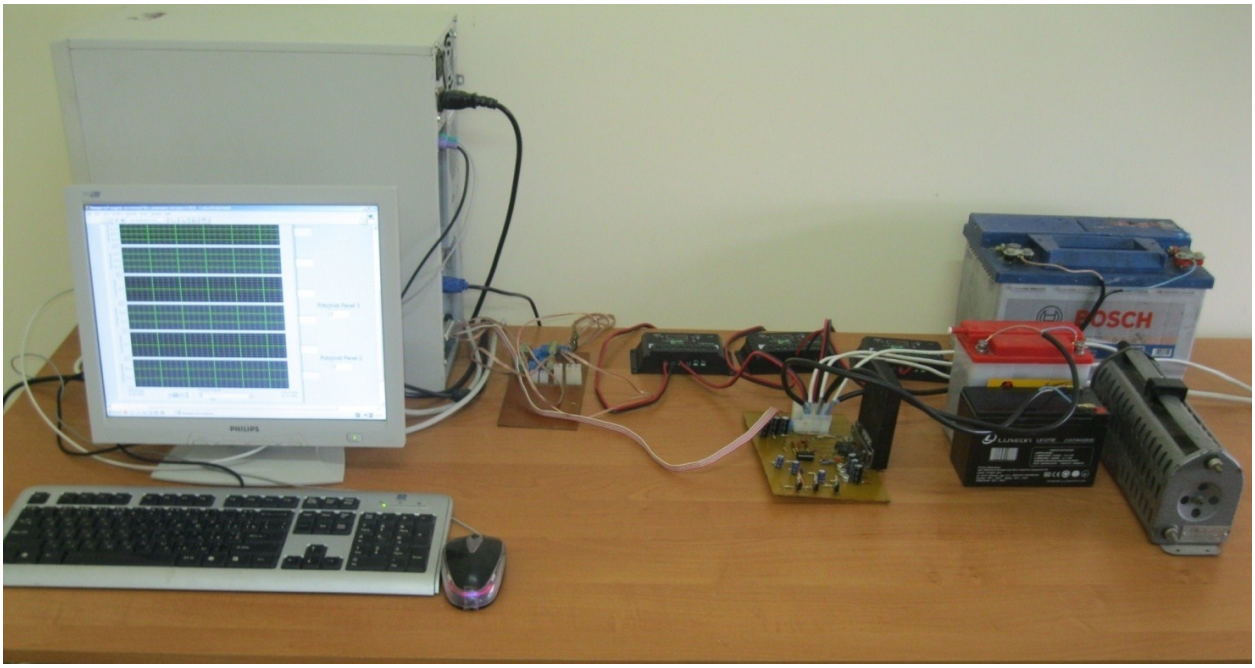

Fig. 7. Measuring part of experimental stand

CONCLUSIONS

1. The developed methods of comparative research on efficiency of photovoltaic power systems with different structural configuration, as well as hardware and software to support the efficiency provide correct methodological basis for experimental researches. It is impossible to apply pulse-width method to regulate charge of battery banks, because in a pause period, a share of electric energy, which is possibly produced by photovoltaic panels, is lost. Thus, it is proposed to adapt operating regime of a separate photovoltaic panel to a battery bank with application of pulse-width unit of control for battery bank discharge to secure reception of all produced energy by the battery.

2. The work proposes methods and hardware for comparative estimation of operating efficiency of photovoltaic power systems with different structure in continuous regime of long-term running, which enable determination of average annual efficiency with consideration of different weather and local conditions.

REFERENCES

1. **Dzhelayni A.T., Nemikhin YU.Ye., Shcheklein S.Ye. 2015.** Research of performance the photovoltaic installation at low-power in Yekaterinburg climatic conditions. Materialy II Vserossiyskoy nauchnoy konferentsii s mezhdunarodnym uchastiyem "Energo- i resursoeffektivnost' maloetazhnykh zhilykh zdaniy". 24-26 marta 2015 goda, Novosibirsk. 203-207.
2. **Halchak V.P., Syrotyuk S.V., Chubay V.YU., Musíy R.Y. 2015.** Substantiation of parameters of the spherical mirror concentrator of solar energy. Netraditsíyní í ponovlyuvaní dzherela yenergíÍ yak alternativní pervinnim dzherelam yenergíÍ v regíoní: Materíali vos'moÍ Mízhnarodnoǐ naukovo-praktichnoǐ konferentsíÍ (Lvív, 2-3 kvítnya 2015): Zb. nauk. prats'. – Lvív: LvDTSNÍÍ. 155–157.
3. **Halchak V., Syrotyuk S., Tatomyr A., Kuznitskiy I. 2014.** Efficiency of increase of power of photo-electric module by flat mirror concentrator. Vísnik Lvívskogo NAU: Agroínzhenerní doslídzhennya. –№18. 294–301.
4. **Boyarchuk V., Syrotyuk V., Syrotyuk S., Halchak V., Boltyanskiy B. 2013.** Development of experimental model for the study of the effectiveness of solar tracking devices. Vísnik Lvívskogo NAU: Agroínzhenerní doslídzhennya. – №17, 2013. 286–293.
5. **Boyarchuk V., Syrotyuk V., Syrotyuk S., Vorobkevich V., Halchak V., Mikhalyuk M. 2011.** A concordance of parameters of storage battery is with the parameters of electric generator of WEU in the conditions of changeability of wind stream. Motrol. Motorization and power industry in agriculture. Volume 13 D. – Lublin. 217–222.
6. **Boyarchuk V., Halchak V., Syrotyuk V., Syrotyuk S., Vorobkevich V., Dzindra Í., Olm M. 2008.** Increasing of electrical performance of photovoltaic solar panels. Vísnik Lvívskogo NAU: Agroínzhenerní doslídzhennya. – № 12. – Том 2. 507–511.
7. **Sviridov K. N., Anisimova S. S., Shadrin V. I., Murashev V. M. 2005.** The solar power module for converting electromagnetic radiation from a remote source of light radiation. Patent of the Russian Federation RU2301379. Available online at: http://www.ntpo.com/izobreteniya-rossiyskoy-federacii/elektroenergetika/alternativnye-istochniki-energii/solnechnaya-energetika/16015-gelioenergeticheskiy-modul-dlya-preobrazovaniya-elektromagnitnogo-izlucheniya-ot-udalennogo-istochnika-svetovogo-izlucheniya.html.
8. **Anisimova S. S., Morozov V. M., Shadrin V. I. 2004.** The solar power module for converting the received electromagnetic radiation and its orientation system. Patent of the Russian Federation RU2270964. Available online at: http://www.ntpo.com/izobreteniya-rossiyskoy-federacii/elektroenergetika/alternativnye-istochniki-energii/solnechnaya-energetika/16145-gelioenergeticheskij-modul-dlya-preobrazovaniya-prinimaemogo-elektromagnitnogo-izlucheniya-i-sistema-ego-orientacii.html.
9. **Poulek V. 1998.** New bifacial solar trackers and tracking concentrators. Solar energy materials and solar cells · february 1998. Available online at: http://www.researchgate.net/publication/242229741_NEW_BIFACIAL_SOLAR_TRACKERS_AND_TRACKING_CONCENTRATORS.
10. **Poulek V., Libra M. 2000.** A very simple solar tracker for space and terrestrial applications. Sol. Energy Mater. Sol. Cells 60, 99-103. Available online at: https://www.researchgate.net/publication/248519921_Libra_M_A_very_simple_solar_tracker_for_space_and_terrestrial_applications_Sol_Energy_Mater_Sol_Cells_60_99-103?enrichId=rgreq-26093c62-35a9-4297-afe7-204dbf2b5c14&enrichSource=Y292ZXJQYWdlOzI0ODUxOTkyMTtBUzoxMTI2NTgxMTYyNTU3NDRAMTQwMzg3MTE5NjY4OQ%3D%3D&el=1_x_2.
11. **Libra M. 2011.** Standard fixed PV panels and Ridge concentrator annual energy [kWh] gain measurement and comparison. // Prague, March. Available online at: http://www.solar-trackers.com/prilohy/Standard%20fixed%20PV%20panels%20and%20Ridge%20concentrator%20annual%20ene..pdf.
12. http://www.electroschematics.com/8019/diy-solar-tracker-system/.
13. http://www.mtmscientific.com/solartracker.html.
14. **Noel León, Héctor García, Carlos Ramírez. 2014.** Semi-passive Solar Tracking Concentrator. Energy Procedia**.** Volume 57. 275–284. 2013 ISES Solar World Congress. Available online at: http://www.sciencedirect.com/science/article/pii/S1876610214013 99X
15. http://www.solar-trackers.com/.
16. Trekery dlya stezhennya za Sontsem. [Electronic resource]. Available online at: http://raytrade.com.ua/ua/blog/45-trekery-dla-sterzennia-za-soncem (Date of request 14.01.2016). – Title from the screen.
17. https://www.lorentz.de/en/products/solar-tracking-systems/etatrack.html.
18. **Sarniak M. 2012.** The application of labview software for the control of a model of a tracking photovoltaic system. Teka. Commission of motorization and energetics in agriculture – 2012, Vol. 12, No. 1, 237–241.
19. **Tłaczała W. 2005.** LabVIEWTM – zintegrowane środowisko programowe, cz. II. Przegląd Elektrotechniczny 2, 15–20.
20. **Buczaj M., Buczaj A. 2012.** The use of labview environment for the building of the grain Dust control system in grain mill. Econtechmod. an international quarterly journal – 2012, Vol. 1, No. 1, 21–26.

Status and trends of agricultural enterprises in Ukraine in terms of market agricultural machinery

T. Vlasenko, V. Vlasovets

Kharkiv Petro Vasylenko National Technical University of Agriculture Kharkiv Petro Vasylenko National Technical University of Agriculture, e-mail: tvlasenko15@gmail.com

Received July 14.2016: accepted July 19.2016

Abstract. The problems of land use and functioning of agricultural machinery and their impact on the development of agricultural enterprises in Ukraine were considered. The measures to improve the efficiency of land use were proposed. The necessity of diversification of domestic agricultural enterprises for sustainable development of the agricultural sector was justified.

Key words: agricultural machinery, size of enterprises, farms, land resources, agricultural technologies.

INTRODUCTION

Providing the population with basic food in sufficient quantity and quality required for food security is inextricably linked to issues of effective use of modern technologies and highly productive agricultural machinery in agricultural enterprises. But the current state of agricultural machinery that is in use in agricultural enterprises is unsatisfactory. To accelerate the development of technical capacity we have to carry out some drastic steps in restructuring the national market system of agricultural machinery.

ANALYSIS OF RECENT RESEARCHES AND PUBLICATIONS

The functioning of the global system of food security is directly related to the efficiency of more than 570 million farms, including farms [1, 2], using different machinery and technology [3-5]. Most of the farms according to the World Bank [6] are placed in countries with low (36%) or below average income (47%). In countries with average incomes are 13% of enterprises, and a high - 4% [7-9]. Numerous sources [10-16] indicate that the average size of farms and the distribution of agricultural land in the world is not constant and varies according to the level of the countries' development. Thus, according to the assessment [17] small farms (of less than 2 hectares) owned approximately 75% of agricultural land in the world. Medium size enterprises decrease in most countries with low and below-average income levels [18]. At the same time, the size of farms increases for countries with high and middle income and in almost all countries with high level of income. Despite the tendency to increase the area of agricultural land that is in use of one farm in high-income countries, data on the optimal size of farms is controversial. For example for the USA, the average size of farms reaches 177 hectares. At the same time, a number of states are characterized by the overwhelming presence of small farms with an area of 50 hectares, and for some it is increased to 1500 hectares. Data on the optimal size of agricultural enterprises in Ukraine is also controversial [19, 20].

According to studies [22, 23], the optimal area of farm land using traditional methods of cultivation which provides the greatest efficiency due to economic zones in Ukraine make: for forest-steppe 3,5-6 thousand hectares, Steppe 6-8 thousand hectares and Polesie - 2 -4 thousand hectares. This area was also mainly a characteristic for 1990 to collective farms and state farms. For the vast proportion of modern agricultural enterprises of Ukraine optimum area usage is much lower [23]. Thus, some scholars believe [24, 25] that the optimal size is an area of 350-400 hectares of agricultural land. At the same time it is believed that the most efficient use of tractor fleet is for size that reaches 350-1000 hectares of farmland. [26] However, the following recommendations are made without regard to ownership and the dynamics of its change [27]. There is also no analysis made for trends to ensure the farms equipment, including tractors and harvesters, which are an indicator of the efficiency of farms.

Thus, issues related to the definition of optimal land use areas and the main components of logistic support of agricultural enterprises require in-depth research.

The purpose of the research is to assess the status and trends of land use and functioning of agricultural machinery and their impact on the development of agricultural enterprises in Ukraine, development of practical recommendations for their improvement.

MAIN RESULTS

According to the State Agency of Land Resources of Ukraine, rapport 2015, of 60.35 million ha territory of Ukraine - 41.5 million ha (68.77%) are agricultural. They include 32.5 million hectares of arable land (half of them are black), 2.4 million ha of grasslands and 5.4 million ha of pastures. After a rapid reduction in the mid-90s beginning from 2010 agricultural land is gradually increasing and approaching the level of 1990.

The main trend in the restructuring of agricultural land in Ukraine is a redistribution of areas classified as fallow, perennial plants, hayfields and pastures upward arable land (Fig. 1).

Out from 41.5 million hectares of agricultural land, 30.8 million hectares are privately owned by 6,920,000 Ukrainians (such as land parcels, shares), the state owns about 10.7 million hectares, communal property makes 0.4 million hectares.

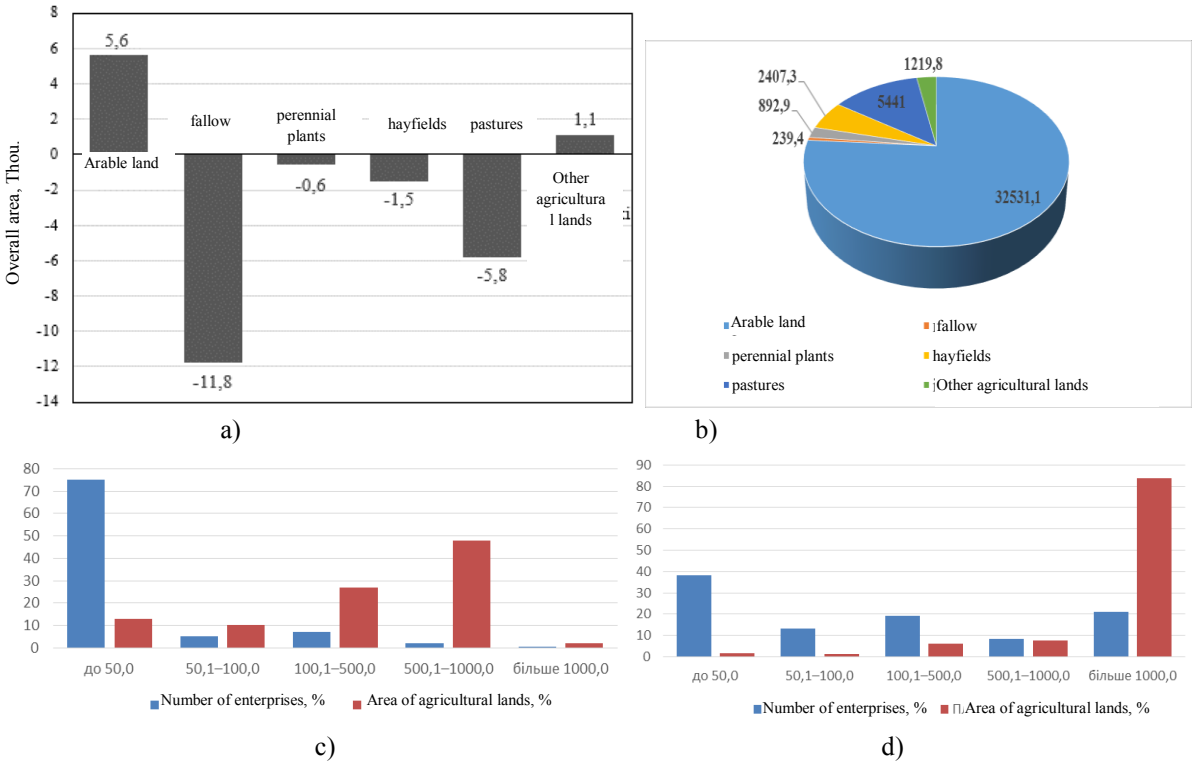

Fig. 1. Redistribution (a) and structure of agricultural land (b) and land resources of Ukraine for 2014 compared to 2013 and distribution of agricultural enterprises (c) and land area (ha) in high-yield countries like USA, Denmark, Germany and Ukraine (d). *Source*: State Agency of Land Resources of Ukraine, World Bank data and the Statistical Yearbook of Ukraine

Ukraine has a moratorium on the sale of agricultural land. Agricultural producers carry out their activities mainly on leased land, particularly at 84.5% (17.4 million ha) of agricultural land. Land owners are mostly retired people due to high migration of the working age population in the city. Today the land is usually leased for 4-10 years, while the maximum rental period reaches 49 years. The rates of land rents range from 296 UAH per 1 hectare per year to 1327 UAH (an average of Ukraine UAH 727.6.). However, a large proportion of rental payments in Ukraine, according AGRICISTRADE are made in natural form.

The area of land owned or used by agricultural enterprises decreased by 23,903.9 thousand ha (39.6%), while slightly increased their size. The area of land that is actually used by citizens, by contrast increased by 14,881.6 thousand ha (24.7%); area of land owned or used by institutions, organizations, industry and other enterprises has remained almost unchanged as in 01/01/2015 p. was 2309.8 thousand ha, which is 28.0 thousand ha less than as it was in 01.01.1995. Land area of forestry enterprises increased by 1666.0 thousand ha (2.8%); reserve land area increased by 7421.8 thousand ha (12.3%) and make 10,775.7 thousand hectares. The rest of the land - 863.7 thousand ha is owned or used by other land users, this area is almost unchanged compared with 1994.

At the beginning of independence of Ukraine large state farms and collective ownership dominated. Number of farms and auxiliary enterprises was small, but eventually formed various forms of agricultural business. So during the 1992-2014 number of farms has increased in 3 times, the area of farmland per 1 farm - in 7.2 times, and the area of arable land - 7.7 times. The greatest intensity of growth for farms in 1992-1995 was related to the adoption of the Law of Ukraine "On peasant (farmer) households» №2009-XII from 20.12.1991. Such a rapid dynamics (20-30 households per month) was due the possibility of obtaining free of charge up to 50 hectares of arable land and 100 hectares of agricultural land to create farms. After reaching the maximum number of farms in 2002-2003 their number gradually began to decline (by 12% compared to 2014) due to the consolidation and increase of agricultural land (44%).

One of the trends of the last period is the reduction of arable land consisting of farmland from 2012 to 2014 to 7%.

Comparison of the number of farms and land area (Fig. 2a), which are in use, revealed the following. In the high-yield countries (USA, Germany, Denmark, etc.) the main share (up to75%) are small farms with a size of 50 hectares of farmland. This allows the countries to create a significant number of jobs. However, the main area of agricultural land (48%) owned farms with an average size of 500-1,000 hectares. These farms provide up to 75% of GDP in developed of the countries. In Ukraine, a large proportion of farms has an area of over 1,000 hectares. The need to have such large areas to provide the appropriate level of production indicates a lower efficiency of land use than in developed countries. This is especially due to the low availability of agricultural technologies and problems of farms with modern equipment. The structure of existing agricultural enterprises of Ukraine by types of business entity in 2014 and the level of provision of agricultural machinery are shown in Fig. 2.

The level of provision of farms by machinery is inadequate. Annually no more than 2% of the existing fleet is updated. It should also be noted that about 80-85% of equipment in farms is located outside the depreciation and economically reasonable working life (over 50% of tractors and combines are older than 20 years), so they can not ensure effective use of modern technology and farming, they are energy intensive compared to new ones. At the same time in Ukraine were developed a large number of technologies and materials that can significantly extend the life of the used vehicles [27, 28].

In the period 2010-2015. Tended to reduce the number of tractors and combines in agricultural enterprises, due to the substantial decline in purchases of new technology medium and large farms (Fig. 3) and the failure of the old.

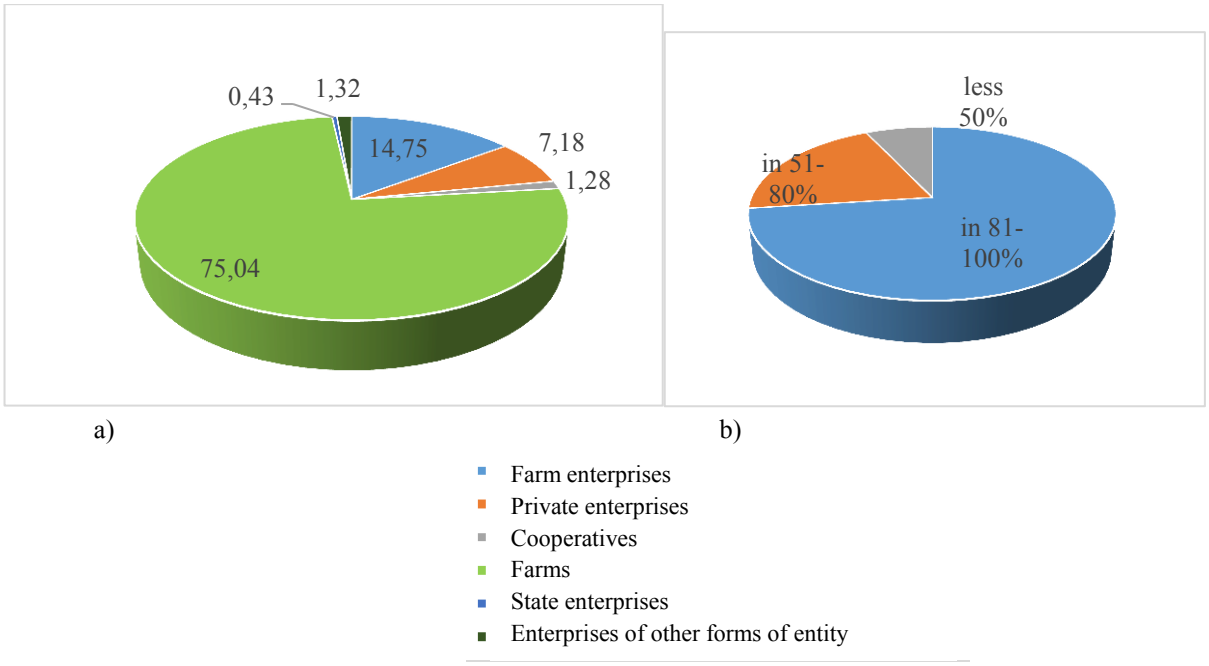

Fig. 2. Structure of existing agricultural enterprises of Ukraine by types of business entity (a) and the level of provision of agricultural machinery (b). *Source*: Based on Agravery.com

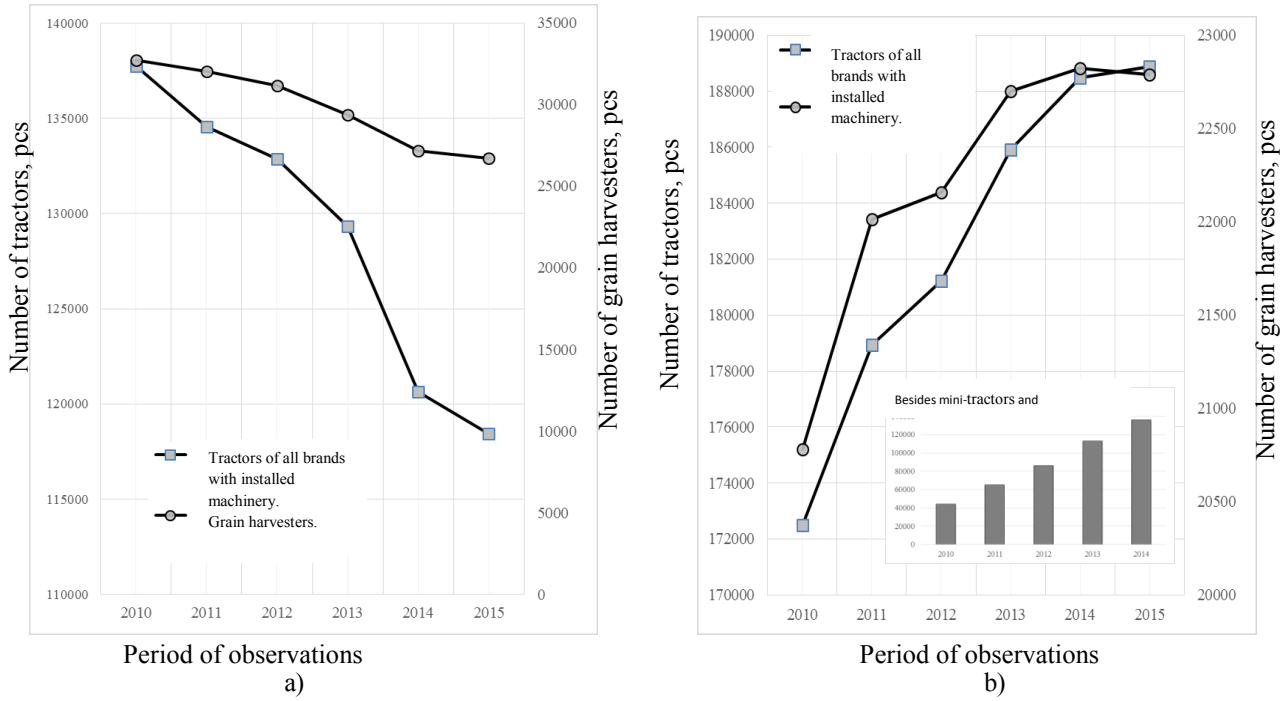

Fig. 3. Availability of tractors and combine harvesters in agricultural enterprises (a) and households (b)

In households we marked the upward trend in increasing the number of vehicles in the period mainly due to its purchase on the secondary market (5% of tractors and combines 3%).

There has been intense market development of tractors and motor blocks used in households. During 2010-2014 it increased up to 58%.

Assessment of tractors and combines' presence in the context of legal forms of entities revealed the following (Fig. 4).

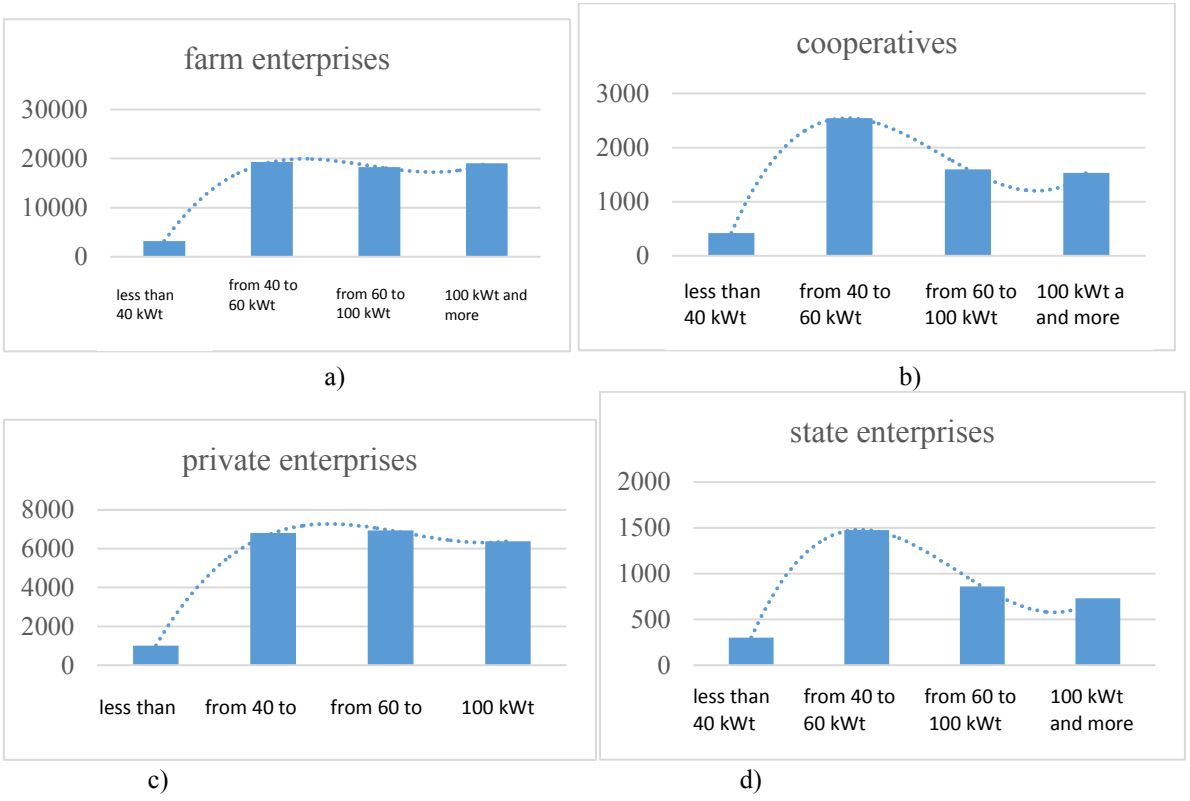

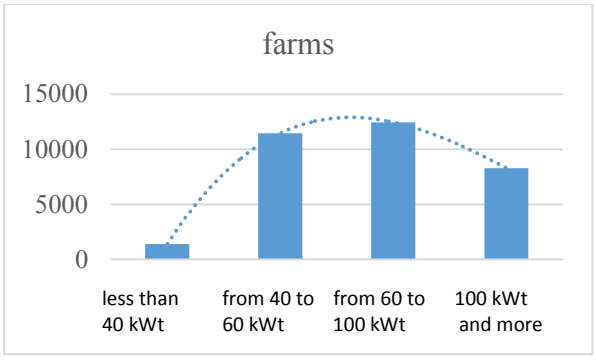

e)

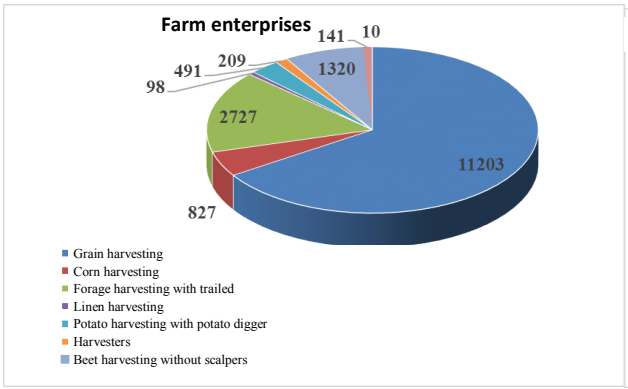

f)

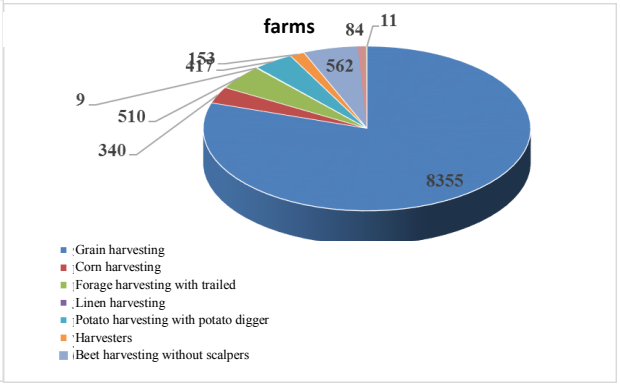

g)

Fig. 4. The presence of machinary in agricultural enterprises by types of business entity in 2014: a-d - tractors of different power; f-g - harvesters

Source: Availability of agricultural machinery and power capacities in agriculture in 2014. Statistical Bulletin.

Farms are characterized by use of medium power tractors of 40-60 kWt and 60-100 kWt. This is due to the fact that the size of the areas that are in cultivation is insignificant 20-1000 ha. Farm enterprises, with larger area of cultivation, are characterized with the presence of tractors with a capacity over 100 kWt. State enterprises and cooperatives owning a small proportion of tractors mainly of low power - 40-60 kWt. A large proportion of combines, which is 75-80%, are grain harvesters.

Ukraine after independence reduced the production of tractors almost in 50 times and currently upgrading their fleet is possible by competitive domestic production technology and imports. However, after the actual collapse of public support programs for budget allocations for the development of domestic engineering for agriculture in 2010, most of the tractors were exported abroad (Fig. 5). In recent years, there was a significant redistribution of the market. So, compared to 2011, exports to Russia in 2016 decreased by 65%. At the same time a redistribution of technology shipped to Kazakhstan took place and it changed toward the development of new markets - Italy, Poland and Egypt.

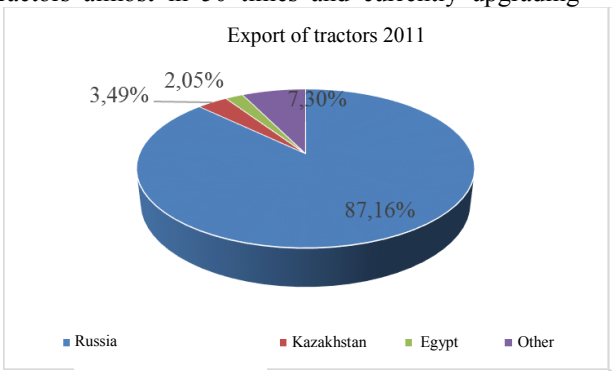

a)

b)

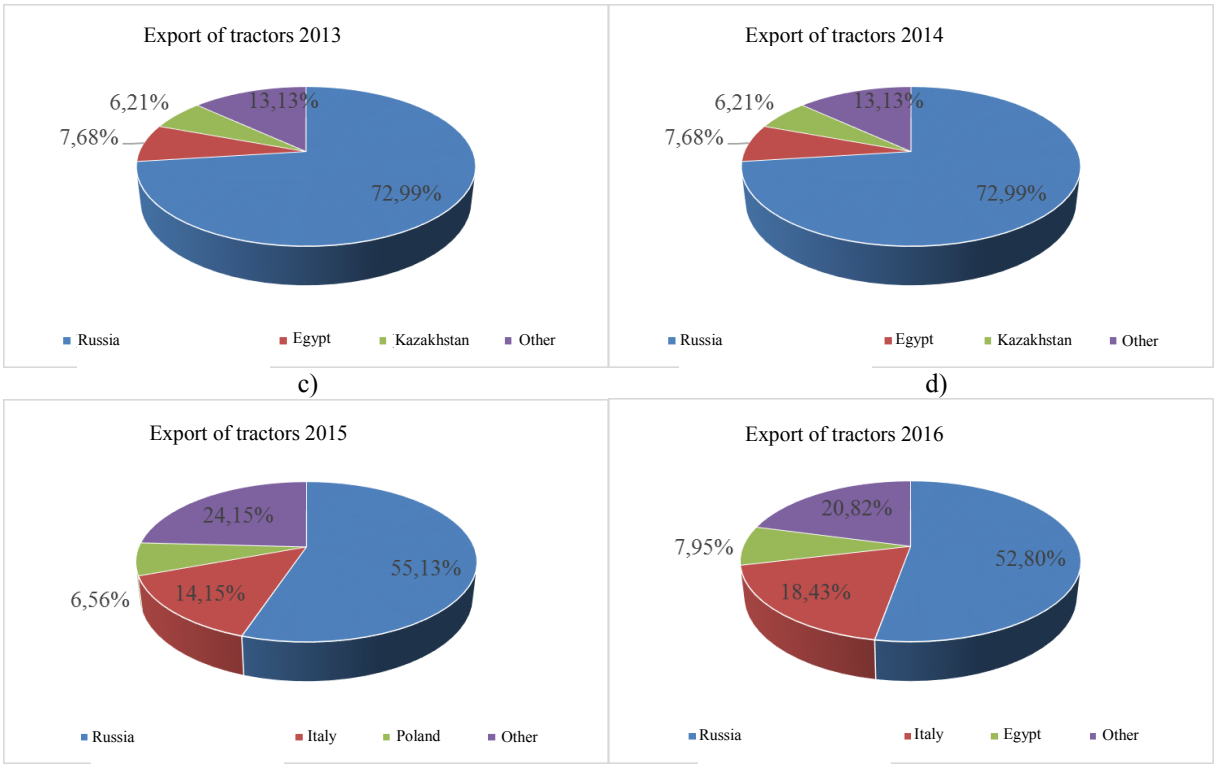

Fig. 5. Exports of tractors of domestic production for 2011-2016. *Source*: According to the State Fiscal Service of Ukraine. Data for 2016 were taken in the first quarter of this year

The devaluation of the national currency, lack of support (including changing the tax code and the abolition of the special VAT regime) and high cost of credit resources in Ukraine in recent years has led to a significant reduction in imports of new technology (Fig. 6) and the reallocation of priorities towards cheaper counterparts - machinery from Belarus and one that was in use. Note that importing countries today do not have the predominant influence (Fig. 7), which was in early 2000. In 2011 the Belarusian tractor plant products ranked first for sales to Ukraine (about 25%). However, during the 2012-2014 the share of tractors decreased to 15,42-18,16%, due mainly to the purchase by farms more powerful tractors with power more than 100 kWt. Number of purchased by farms of Ukraine new tractors and the amount of money spent by their groups of power is shown in Figure 8.

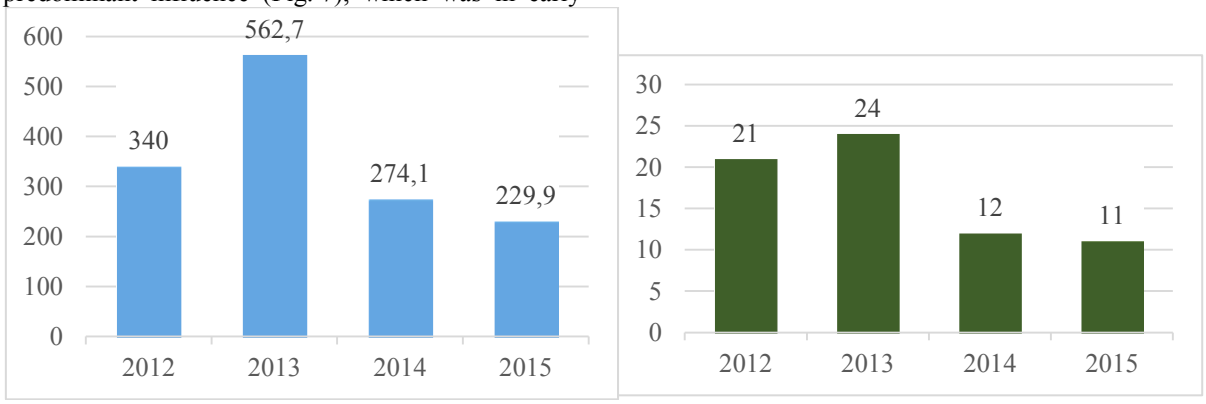

Fig. 6. Number of new (a) and used (b) tractors that were imported to Ukraine, million USD

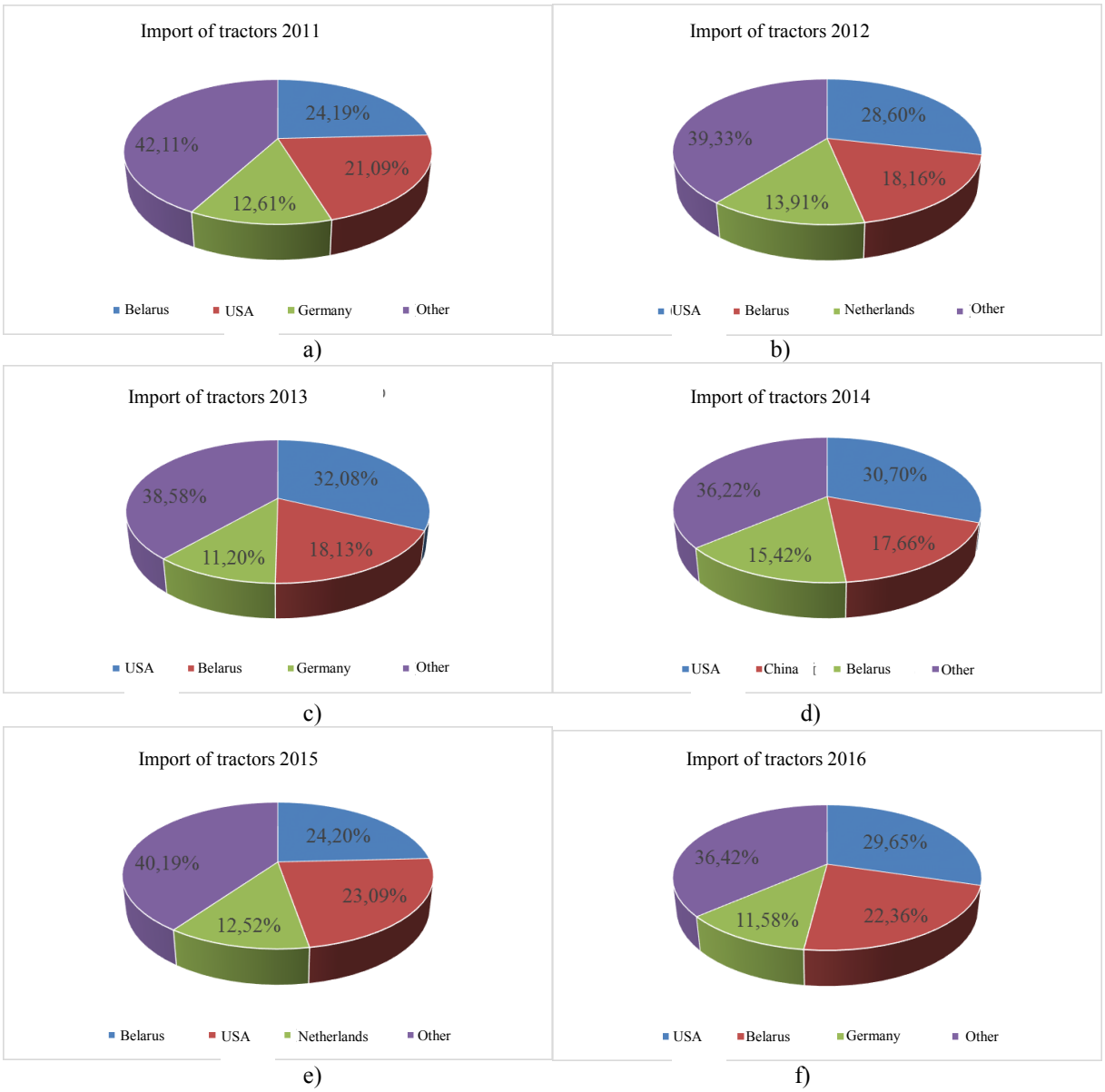

Fig. 7. Import of tractors for 2011-2016. *Source*: According to the State Fiscal Service of Ukraine. Data for 2016 were taken in the first quarter of this year

Production of utility tractors John Deere, CNH (Case, New Holland), AGCO (Fendt, Massey Ferguson, Challenger) come mainly from the USA (83.857 mln USD in 2014), the Netherlands (23.128 mln USD in 2014) and Germany (27.550 mln USD in 2014). At the same time we build up supplies of tractors for small enterprises from China (48.345 mln USD in 2014). However, the crisis has led to pent-up demand on the part of farmers to buy new powerful technology products and increased the share of Belarusian and domestic tractor factories in Ukraine (Fig. 9).

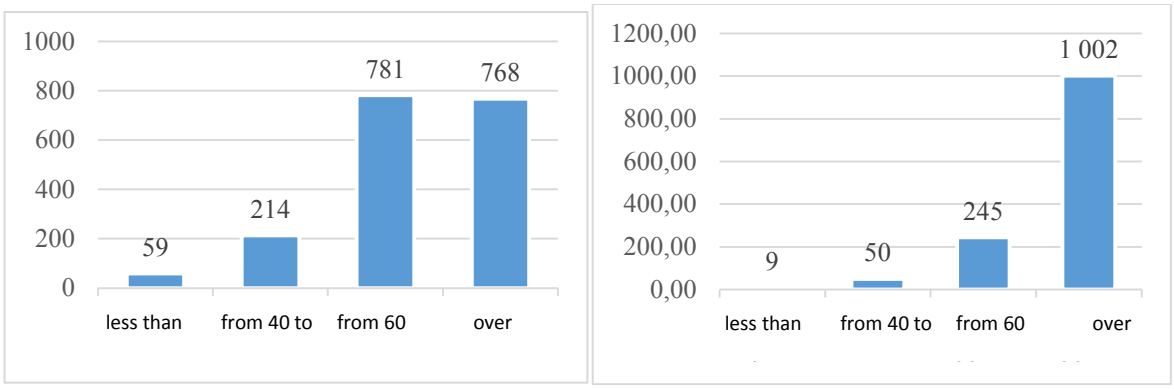

a) b)

Fig. 8. Number of purchased tractors (a) the amount of money spent (b) by groups of power. *Source*: According to the State Statistics Service of Ukraine

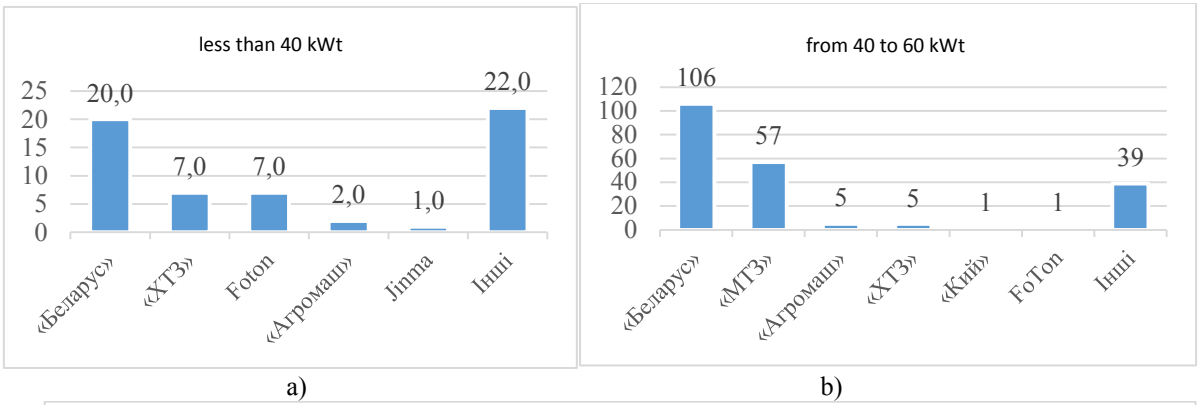

a) b)

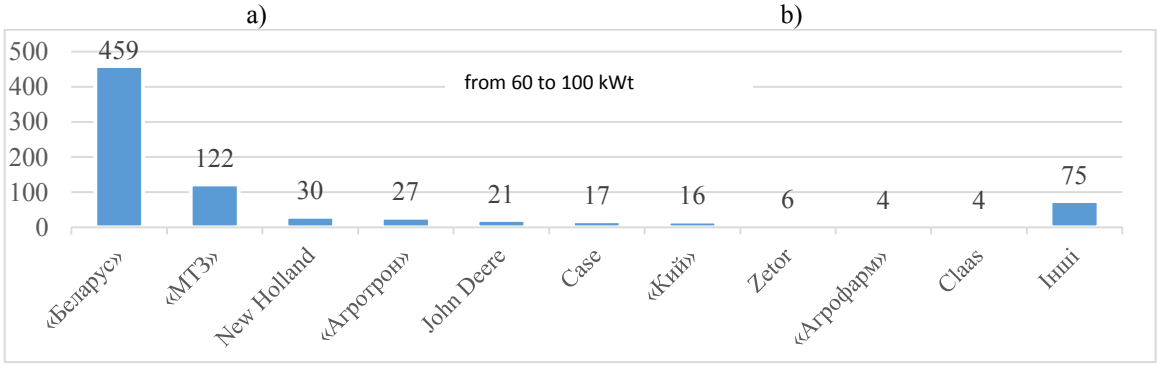

c)

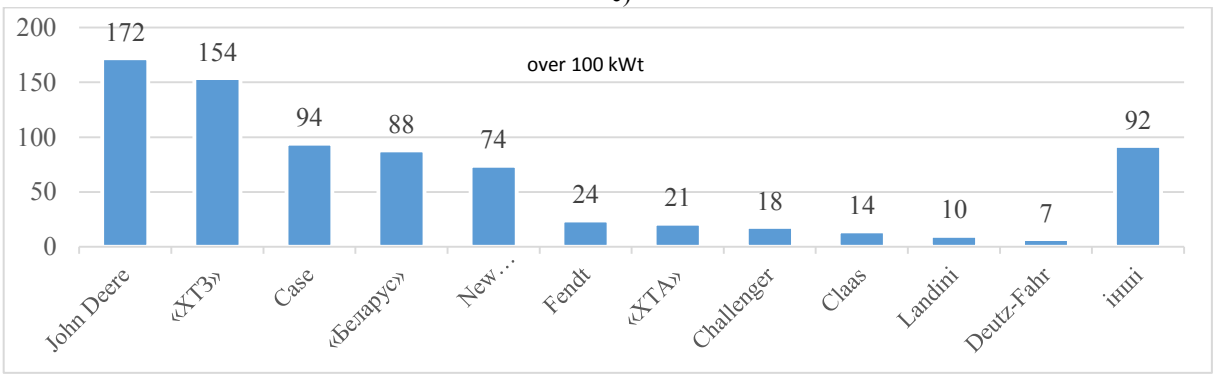

d)

Fig. 9. The brand composition of the purchased by agricultural enterprises agricultural machinery in 2014 by power: a - less than 40 kWt; b - 40-60 kWt; c - 60-100 kWt; d – more than 100 kWt. *Source*: According to the State Statistics Service of Ukraine

Among the combine harvesters there are the most popular brands - John Deere (29%), Case (16%), Claas (14%) Tucano (11%) and the Lexion (9%). The share of these brands in the segment of combine harvesters is over 50%.

The largest suppliers of combine harvesters for the period 2011-2015 were Germany, USA, Belgium, Poland (Figure 11).

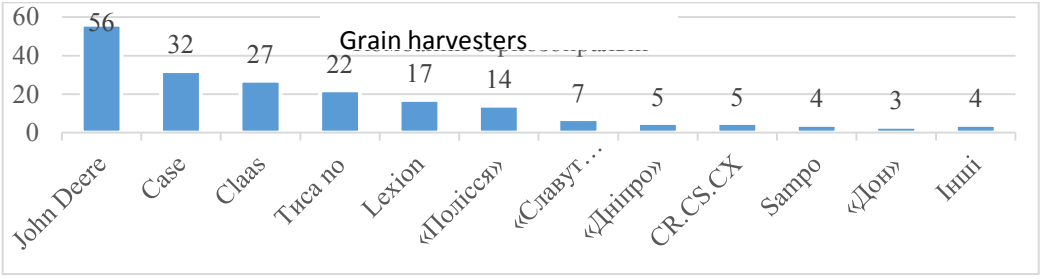

Fig. 10. Number grain harvesters purchased by agricultural enterprises in Ukraine in 2014. *Source*: According to the State Statistics Service of Ukraine.

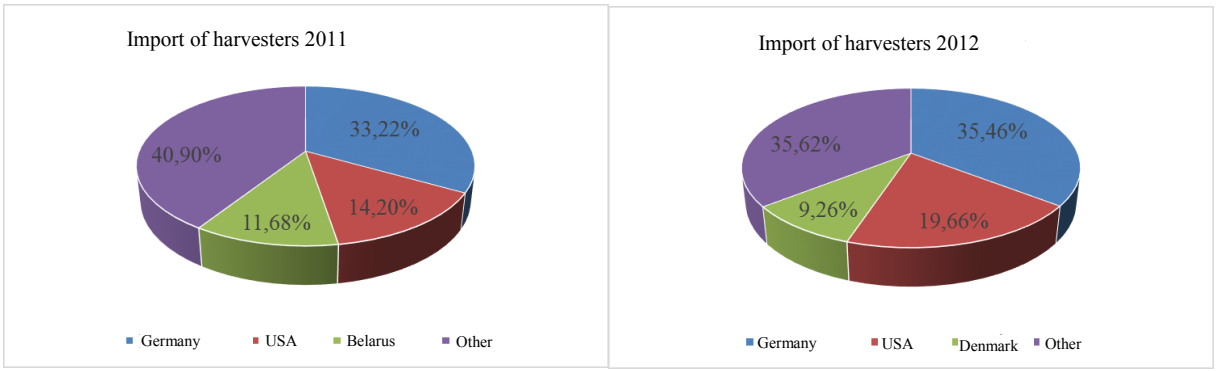

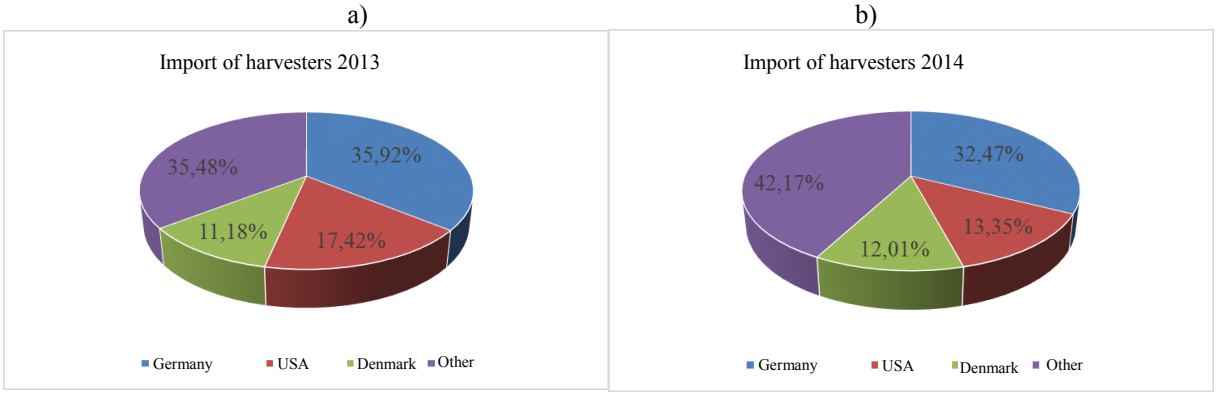

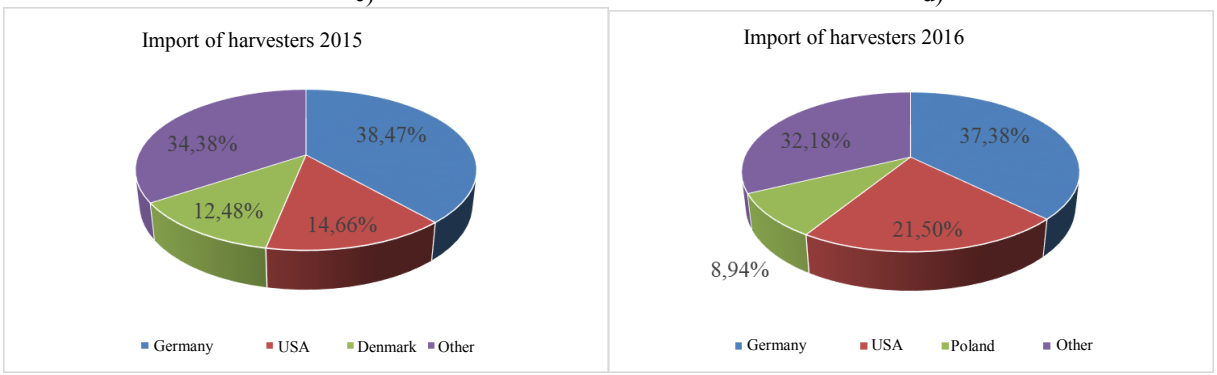

Fig. 11. Import of harvesters to Ukraine for 2011-2016. *Source*: According to the State Fiscal Service of Ukraine. Data for 2016 were taken in the first quarter of the year

Market of imported equipment in 2015 decreased almost threefold compared to 2014. At the same time import of equipment that was in use declined by only 20%. Used equipment for Ukraine comes mostly from North America and the EU. In fig. 12 we represented the largest grounds for the sale of used equipment.

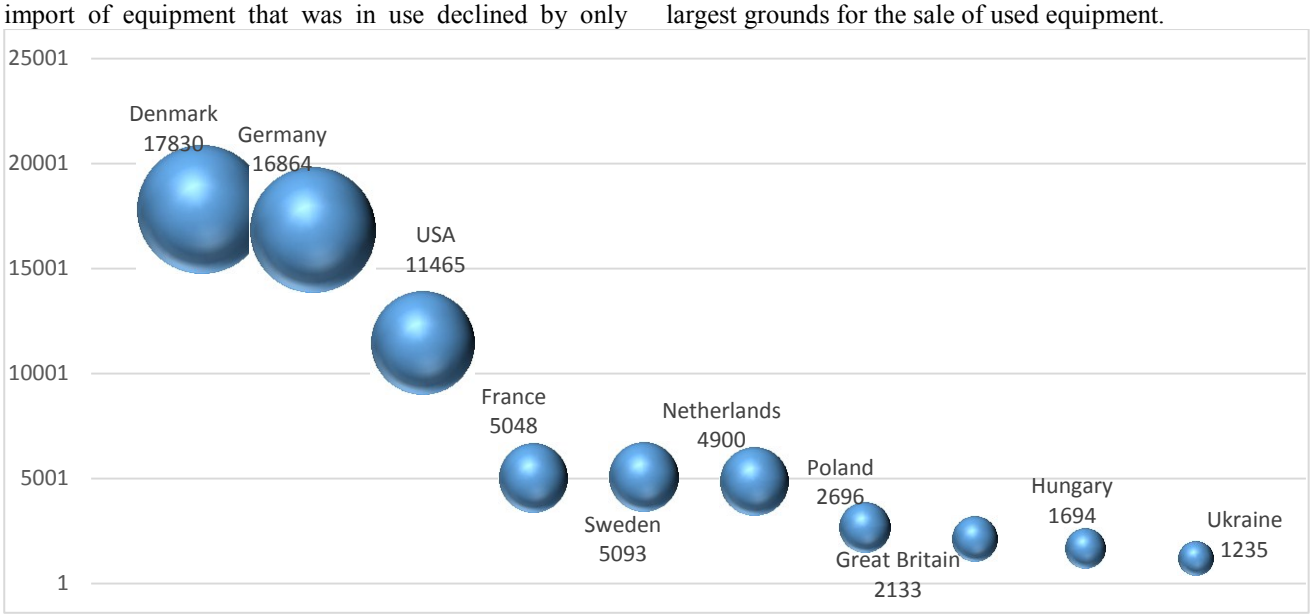

Fig. 12. Size of the grounds for sale of used vehicles imported to Ukraine in 2016
Source: According www.mascus.com.ua.

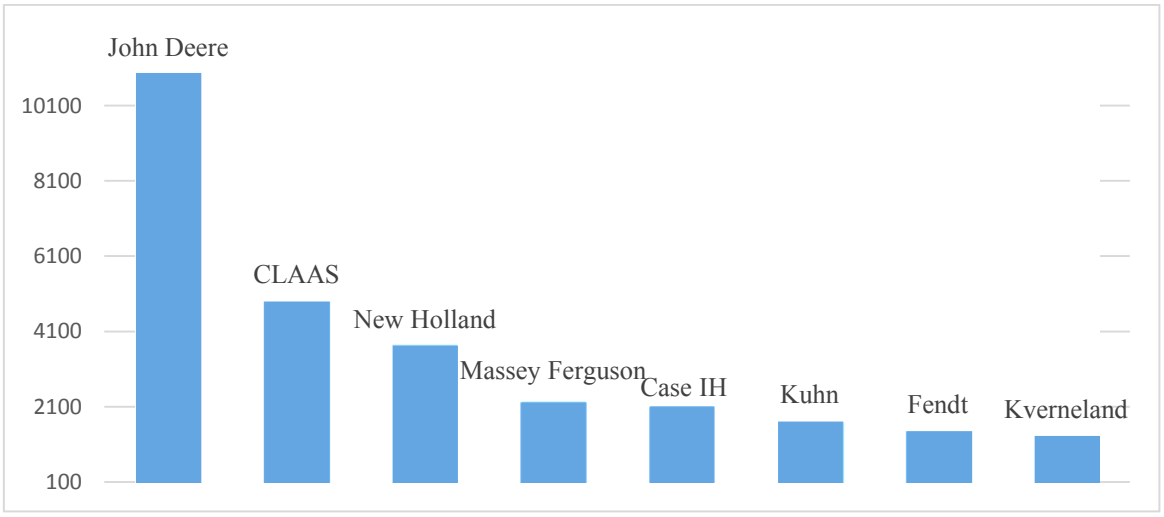

Fig. 13. The largest number of proposals under the brand of agricultural machinery and trading grounds in North America and Europe in 2016. *Source*: According www.mascus.com.ua

CONCLUSIONS

1. In high-income countries (USA, Germany, Denmark, etc.) the bulk of households (75%) are small farms with a size of 50 hectares of farmland, which create a significant number of jobs. The main area of agricultural land (48%) owned farms with an average size of 500-1,000 hectares, providing up to 75% of GDP in developed countries. In Ukraine, the share of agricultural enterprises has an area of 1,000 hectares and is bigger almost 20 more times, as an evidence of the low efficiency of land use. This is a low level of agricultural technologies and problems of agricultural enterprises' supply with modern equipment.

2. Despite of inflation in the economy in 2015 the received funds our farms are investing primarily not to bank accounts but buying modern tractors and combines to cultivate their farms and households in the region. Other farms refuse to purchase technology that formed a significant amount of pent-up demand that can provide an intensive agricultural machinery market growth in the future.

3. The main areas of efficient use of land resources is the use of modern technology that will increase productivity without expanding agricultural land, minimizing the cost of rent, administration and logistics. Diversification of production through the expansion of

business activities, focus on its own production and deep processing of agricultural products will increase the profitability of agricultural enterprises.

REFERENCES

1. **Vítor João Pereira Domingues Martinho., 2016.** Energy consumption across European Union farms: Efficiency in terms of farming output and utilized agricultural area Energy, Volume 103, Pages 543-556.
2. Barrett, C., Bellemare, M., & Hou, J. 2010. Reconsidering conventional explanations of the inverse productivity-size relationship. World Development, 38(1).
3. **V. Smolinskyy, S. Smolinska, Z. Homka., 2014.** Innovative approaches towards the analysis of the dependence of production efficiency on the parameters of agricultural enterprises land use, ECONTECHMOD. An international quarterly journal Vol. 3, №4, Pages 39-43
4. **O. Kovalyshyn, N. Kryshenyk1, N. Havryshkiv, S. Sosnowski., 2014.** Analysis of methodological approaches to evaluation of land quality in Ukraine, ECONTECHMOD. An international quarterly journal Vol. 3, №4, Pages 97-101
5. **B. Zhalezka, K. Navitskaya., 2015.** Multy-criteria fuzzy analysis of regional development, ECONTECHMOD. An international quarterly journal Vol. 4, №3, Pages 39-46.
6. **Deininger, K., Byerlee, D., Lindsay, J., Norton, A., Selod, H., & Stickler, M., 2011.** Rising global interest in farmland: Can it yield sustainable and equitable benefits? Washington, DC: World Bank.
7. **Deininger, K., & Byerlee, D. 2012.** The rise of large farms in land abundant countries: Do they have a future? World Development, 40(4), 701–714.
8. **Garner, E. & de la O Campos, A., 2014.** Identifying the ‘‘family farm”:An informal discussion of the concepts and definitions. ESA WorkingPaper 14-10. Rome: FAO.
9. Government of the Russian Federation (2006). All-Russia Census of Agriculture: Russian Federation Summary and Country-Level Data. Moscow: Statistics of Russia Information and Publishing Center. (in Russian).
10. **Hazell, P., Poulton, C., Wiggins, S., & Dorward, A., 2010.** The future of small farms: Trajectories and policy priorities. World Development, 38 (10), 1349–1361.
11. FAO (2001). Supplement to the report on the 1990 world census of agriculture. FAO statistical development series 9a. Rome: FAO.
12. FAO (2005). A system of integrated agricultural censuses and surveys. Volume 1: World programme for the census of agriculture 2010: FAO statistical development series 11. Rome: FAO.
13. FAO (2012). The State of Food and Agriculture 2012: Investing in agriculture for a better future. Rome: FAO.
14. FAO (2013). 2000 world census of agriculture methodological review (1996–2005): FAO statistical development series 14. Rome: FAO.
15. FAO. (2014a). FAOSTAT. Retrieved from <http://faostat.fao.org/site/291/default.aspx>.
16. FAO (2014b). The State of Food and Agriculture 2014: Innovation in family farming. Rome: FAO.
17. **Adamopoulos, T., & Restuccia, D., 2014.** The size distribution of farms and international productivity differences. The American Economic Review, 104(6), 1667–1697.
18. **Eastwood, R., Lipton, M., & Newell, A., 2010.** Farm size. In P. L. Pingali, & R. E. Evenson (Eds.), Handbook of agricultural economics. Elsevier: North Holland.
19. Recommendations to optimize the size of the newly established private farms based on the lease of land shares and improving lease relations / [M.V. Zubets, P.T. Sabluk, V.Y. Mesel-Veselyak and others] Ed. V.Ya.Mesel-Veselyak, M.N. Fedorov. – K .: NSC (in Ukrainian).
20. **Vlasenko T.V., 2007.** Economic evaluation of interference of the main factors forming the volume of gross agricultural output in Kharkiv region - Nauka i ekonomika Scientific-theoretical journal Khmelnitsky University of Economics. - 2007. - № 2 (6). - P. 25-35. (in Ukrainian).
21. Recommendations for the optimal size of the collective farms and their subdivisions - M.VNIESH, 1964. – 9 p. (in Russian).
22. **Sabluk P.T., 2007.** Economic mechanism of AIC in a market economic system - Economy AIC. - 2007. - № 2. - P. 3-10. (in Ukrainian).
23. **Statistical Yearbook of Ukraine, 2014** / per red.I.M. Zhuk. - K .: Nauka, 2014. - 586p.(in Ukrainian).
24. **Sabluk P.T., 2006.** The development of land relations in Ukraine - K .: NSC "IAE", 2006. - 396 p.(in Ukrainian)
25. Strategic directions of development of agriculture of Ukraine till 2020. - NSC "IAE" .- 2012. - 182 p.(in Ukrainian).
26. Mesel-Veselyak V. 2004. Forms of agricultural business (analysis of development) - K .: NSC "IAE". - 70 p.(in Ukrainian).
27. **Vlasenko T.V., Barchan K.M., 2015.** The marketing strategy of the enterprise in modern conditions - Bulletin SSS. - № 2. - P. 10-12.(in Ukrainian).
28. **Vlasovets V.M., Skoblo T.S., Moroz V.V., 2001.** Structure and distribution of components in the working layer upon reconditioning of parts by electric-arc metallization - Metal science and heat treatment. – №43 (11-12). – P. 497-500
29. **Vlasovets V.M., Skoblo T.S., 2012.** Specific Features of the Formation of Structures in 60Kh2N4GMF Precipitation-Hardening Steel. - Springer US: Materials Science - №47(5). – P.644-650.

Tractor decelometric trials by application of the ecological hydraulic oil

Zdenko Tkáč[1], Ján Kosiba[1], Juraj Jablonický[1], Vladimír Šinský[1], Taras Shchur[2]

[1]Slovak University of Agriculture
[2]Lviv National Agricultural University, St. Vladimir the Great, 1, Dublyany, Ukraine

Received July 14.2016: accepted July 19.2016

Abstract. In this article, there is resumed the accomplished impact analysis of biodegradable tractor oil HYDROS UNI application in gear - hydraulic circuit of the tractor Zetor Proxima 7441. This analysis was performed by comparative testing with standard mineral oil PP 80 on the basis of decelometric trials. Decelometric trials were carried out with measuring device XL - Meter^{TM} Pro Gamma. The measurements were executed by the 3rd and the 4th unreduced gear. The results show that the oil HYDROS UNI does not affect decelometric characteristics of the tractor Zetor Proxima 7441.

Key words: deceleration, characteristics, tractor

INTRODUCTION

Due to advantages in renewability and environmental acceptability, bio-sourced and biodegradable hydraulic fluids are increasingly used in fluid power applications [9]. In this time, the difference between a conventionally produced fluid and ecological fluid is two or three times of the price. Therefore, it is necessary to look for new solutions how to extend the technical life, which could have an effect on their increased use [5,10]. The consumption of ecological fluids in the EU is 0.12 Mt per year from total world production of 35 Mt per year [7,8]. Almost 50 % of all the sold oils in the world finish at present times as forfeits during the operation in nature [2]. Application of ecological hydraulic fluids in agricultural tractors was according to works published.[1, 4,6, 11, 12]

Decelometric trials were carried out on the tractor Zetor Proxima 7441 because this tractor has on the rear axle the wet brakes. Wet brakes are the type of brakes where the oil inflow is supplied from a common gear - hydraulic circuit [13,14]. The trials were executed with application of standard mineral oil PP 80 and after purification of tractor systems, the trials were repeated with application of biodegradable universal tractor oil HYDROS UNI [16,15]. The measurements were performed by two different gears and disposal of the front axle brakes - unreduced the 3rd gear unreduced the 4th gear.

MATERIAL AND METHODS

Measuring device XL - Meter^{TM} Pro Gamma

The measuring device XL - Meter^{TM} Pro Gamma is a universal measuring device manufactured by Invent Automotive Electronics Research & Development in Hungary. This device allows effectivity measuring of the service, engine, electric and air brakes of the vehicle. It is also able to measure the acceleration or deceleration of vehicle and the path length passed by vehicle during the measurement. In Fig. 1, there is a photo of XL - Meter^{TM} Pro Gamma location during the measurement of deceleration with the individual oil application in the gear – hydraulic circuit and wet brakes. The device location is on the windshield of the tractor.

Fig. 1. The location of XL - Meter^{TM} Pro Gamma on the windshield of the tractor Zetor Proxima 7441

The conditions of measurement

Prior to tractor measurement of deceleration, it is needed to warm the oil in the gear-hydraulic circuit at operating temperature, as close as possible to the value of 50 °C. This process is accomplished via connection of loading device OWATONA to hydraulic circuit. By force of the throttle valve and the oil flow, the oil is heated to the desired value. In Fig. 2, there can be seen the connection of loading device to hydraulic circuit.

Fig. 2. The connection of the loading unit to hydraulic circuit of the tractor Zetor Proxima 7441

Decelometric trials of tractor Zetor Proxima 7441 is necessary to execute on the flat asphalt road, long enough for needs of acceleration, stabile rate and deceleration of the tractor. Simultaneously, it is needed to carry out measurements on this area.

Measure proceeding

After the heating of the oil and location of measuring device XL - Meter™ Pro Gamma on the tractor windshield the measurement will be executed. After tractor accelerating at the speed which allows the gear, the brake pedal will be pressed and the tractor retards to a standstill. By braking, the measuring device XL - Meter™ Pro Gamma is activated and deceleration of the tractor is recorded.

Effectivity of the service brake determination

Effectivity of the service brake determination is based on the braking lane. This is specified in the Official Journal of the European Communities, Commission Directive 96/63/EC amending Council Directive 76/432/EEC on the approximation of the laws of the Member States relating to the braking devices of wheeled agricultural and forestry tractors. The effectivity of the service brake is based on the braking lane calculated by relation (1):

$$S_{max} \leq 0{,}15.v + \frac{v^2}{116} \quad (1)$$

if:

S_{max} – maximal stop distance, m,

v – maximal design speed, km*h^{-1}

On the front axle of the tractor, there are tires type Mitas RD01 340/85 R24, 13.6 R24 and on the rear axle - Mitas RD01 340/85 R34, 18.4 R34. For characteristics of tractor Zetor Proxima 7441 deceleration, it will be used the following marks:

- s_0 - stop distance, m,
- v_0 - initial speed, km*h^{-1},
- T_{br} - breaking time, s,
- MFDD - breaking deceleration, m*s^{-2}

RESULTS AND DISCUSSION

In Tab. 1 and Tab. 2, there are specified the values of stop distance, initial speed, braking time and braking deceleration for individual gears and braking modes with mineral oil PP 80 and ecological oil HYDROS UNI.

Table 1. Deceleration characteristics values with mineral oil PP 80

PARAMETER	UNIT	THE GEAR (BRAKING MODE)		
		3 (service brake)	3 (parking brake)	4 (service brake)
s_0	m	3.61	5.13	11.01
v_0	km*h^{-1}	17.75	19.44	28.55
T_{br}	s	1.41	1.7	2.6
MFDD	m*s^{-2}	3.49	3.76	3.77

Tab. 2. Deceleration characteristics values with ecological oil HYDROS UNI

PARAMETER	UNIT	THE GEAR (BRAKING MODE)		
		3 (service brake)	3 (parking brake)	4 (service brake)
s_0	m	3.57	4.96	11.49
v_0	$km*h^{-1}$	17.95	19.07	28.87
T_{br}	s	1.41	1.66	2.76
MFDD	$m*s^{-2}$	3.77	3.77	3.74

The measured value of the stop distance for tractor Zetor Proxima 7441 was compared to counted value by relationship (1). For mineral oil PP 80, the counted value for the 3rd gear was S_{max} = 5.37 m and for the 4th was S_{max} = 11.30 m. For ecological oil HYDROS UNI, the counted value for the 3rd gear was S_{max} = 5.47 m and for the 4th was S_{max} = 11.52 m. In Figures 3-5 is shown a graphical evaluation of measured data.

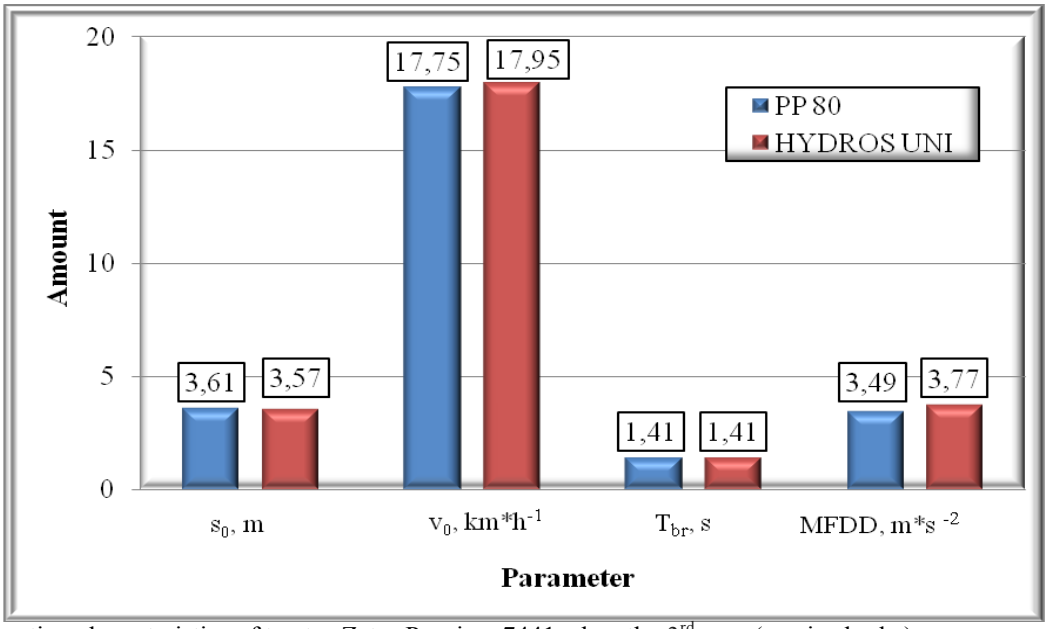

Fig. 3. Deceleration characteristics of tractor Zetor Proxima 7441 when the 3rd gear (service brake)

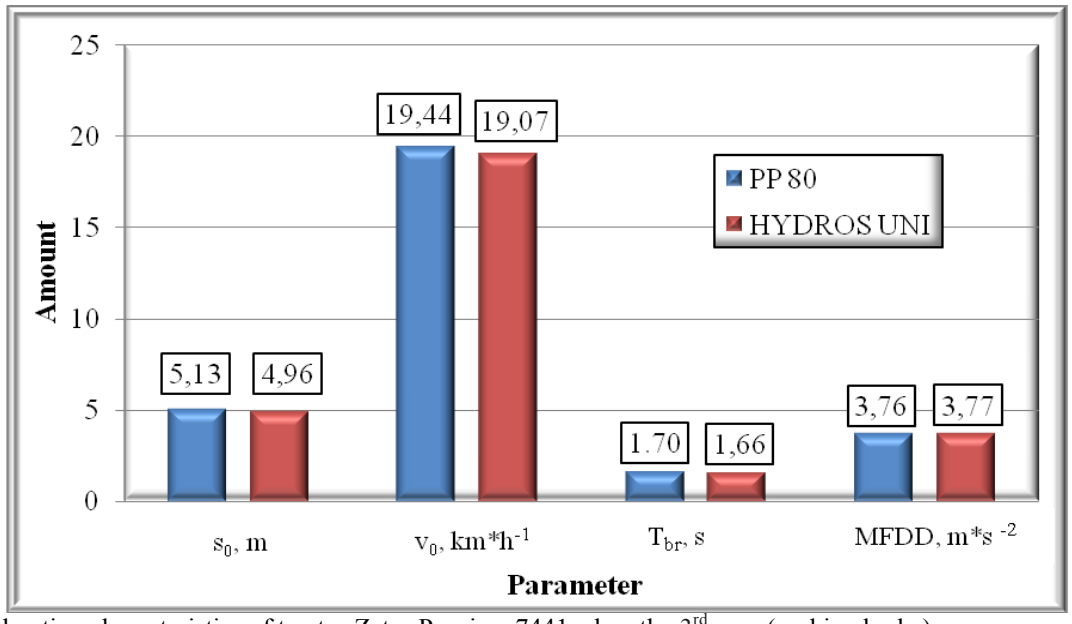

Fig. 4. Deceleration characteristics of tractor Zetor Proxima 7441 when the 3rd gear (parking brake)

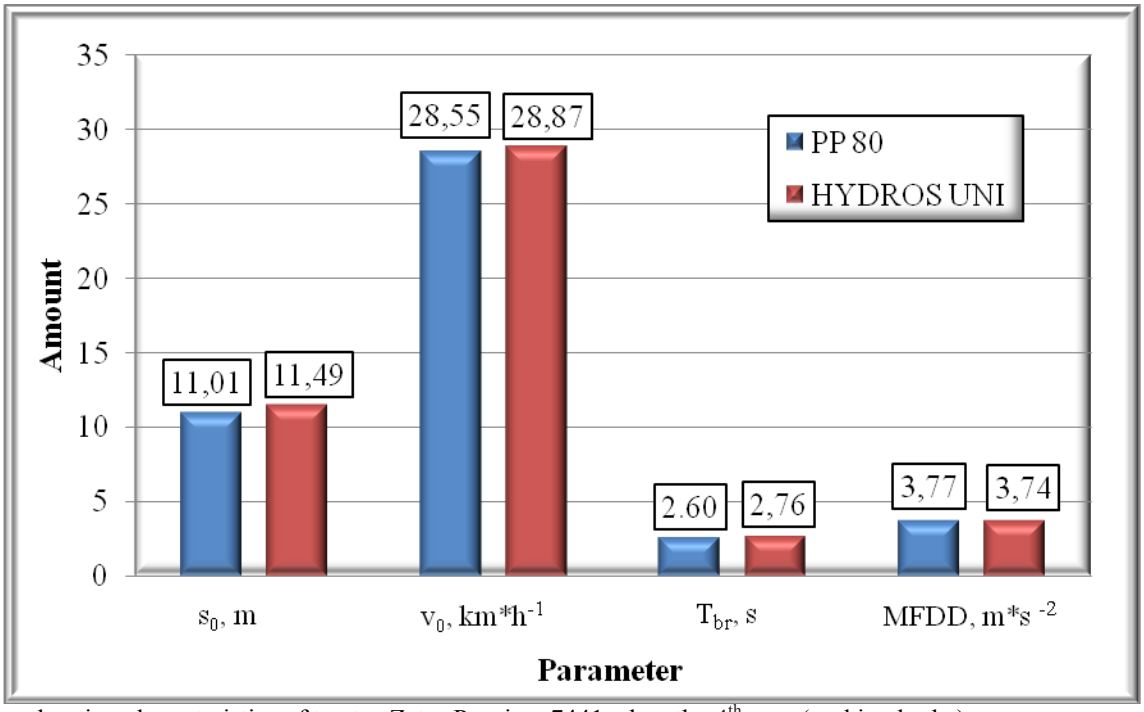

Fig. 5. Deceleration characteristics of tractor Zetor Proxima 7441 when the 4th gear (parking brake)

SUMMARY

Effectivity of the service brake determination is based on the braking lane. This is specified in the Official Journal of the European Communities, Commission Directive 96/63/EC amending Council Directive 76/432/EEC on the approximation of the laws of the Member States relating to the braking devices of wheeled agricultural and forestry tractors. Decelometric trials were carried out on the tractor Zetor Proxima 7441 because this tractor has on the rear axle the wet brakes. Wet brakes are the type of brakes where the oil inflow is supplied from a common gear - hydraulic circuit. The trials were executed with application of standard mineral oil PP 80 and after purification of tractor systems, the trials were repeated with application of biodegradable universal tractor oil HYDROS UNI. The result is that deceleration characteristics of the tractor Zetor Proxima 7441 by application of mineral oil PP 80 and accordingly by application of ecological oil HYDROS UNI are up to standard Commission Directive 96/63/EC.

ACKNOWLEDGEMENT

Supported by the Ministry of Education of the Slovak Republic, Project VEGA 1/0337/15 "Research aimed at influence of agricultural, forest and transport machinery on environment and its elimination on the basis of ecological measures application"

REFERENCES

1. **Drlička, R., Žarnovský, J., Mikuš, R., Kováč, I., Korenko, M. 2013.** Hard machining of agricultural machines parts. In *Research in agricultural engineering*. 2013, vol. 59, special iss., s. 542-548.
2. **Jakob, K., Theissen, H. 2006.** Bio-based Oils in Hydraulics – Experience from Five Years of Market Introduction in Germany. Institute for Fluid Power Drives and Controls (IFAS), RWTH Aschen University, Germany.
3. **Korenko, M., Beloev, H., Kaplík, P. 2013** *Quality control, using PPAP method : scientific monograph*. 1. vol. Ruse : Angel Kanchev University of Ruse. 139 s.
4. **Kročko, V., Žitňanský J., Drlička, R., Polák, P., Korenko, M. 2012.** Environmental impact of cutting fluids to the quality of surface finish in turning. In *MendelTech 2012*. Brno : Mendel University in Brno.
5. **Kučera, M., Rédl J. 2008.** Vplyv podmienok experimentu na tribologické vlastnosti vybraných materiálov (Effects of experimental conditions on tribologic properties of selected materials). Acta technologica agriculturae, *1*: 98-104.
6. **Majdan, R., Cvíčela, P., Bohát, M., Ivanišová, K. 2008.** The observation of hydrostatic pump deterioration during the durability test according to hydraulic fluids contamination. In *X. International conference of young scientists 2008*. Prague : Czech University of Life Sciences Prague, , s. 147-153.
7. **Majdan, R., Stančík, B., Vitázek, I., Abrahám, R., Tóth, F., Štulajter, I. 2012.** The influence of biodegradable fluids on deterioration of the hydraulic pumps elements. In *Naučni trudove : zemedelska technika i technologii, agrarni nauki i veterinarna medicina, remont i nadeždnosť : zemedelska technika i technologii, agrarnye nauki i veterinarnaja medicina, remont i nadežnosť*. Tom. 51, seria 1.1, s. 187-191.
8. **Mosolygó, E., Jánošík, Š., 2008.** Lubricants based on renewable resources. In: Interfaces'08. Sopron : Slovnaft a.s., Member of the MOL Group, 2008, pp. 111-120.
9. **Shick, D. 2008.** Compatibility testing of biodegradable hydraulic fluids [online]. Available at: http://www.msoe.edu/academics/research_centers/reu/

pdf/2008/ Compatibility% 20Testing%20of%20Biodegradable%20Hydraulic%2 0Fluids.pdf [Accessed: 03-02-2012]

10. **Tkáč, Z., Majdan, R., Tulík, J., Kosiba, J. 2012.** Study of ecological fluid properties under operational conditions of tractors. In: TEAM. Osijek-Baranja : University of Josip Juraj Strossmayer, vol. 4, no. 1, pp. 295-298.
11. **Tulík, J., Hujo, Ľ., Stančík, B., Ševčík, P. 2013.** Research of new ecological synthetic oil-based fluid. In *Journal of Central European Agriculture*. Vol. 14, no. 4, p. 1384-1393.
12. PRÍSTAVKA, Miroslav - BUJNA, Marián - KORENKO, Maroš. Reliability monitoring of grain harvester in operating conditions. In Journal of Central European Agriculture online. ISSN 1332-9049, 2013, vol. 14, no. 4, s. 1436-1443, online. Dostupné na internete: <http://jcea.agr.hr/articles/774433_RELIABILITY_MONITORING_OF_GRAIN_HARVESTER_IN_OPERATING_CONDITIONS__en.pdf>.
13. DRLIČKA, Róbert - ŽARNOVSKÝ, Jozef - MIKUŠ, Rastislav - KOVÁČ, Ivan - KORENKO, Maroš. Hard machining of agricultural machines parts. In Research in agricultural engineering. ISSN 1212-9151, 2013, vol. 59, special iss., s. 542-548.
14. KIELBASA, Pawel - KORENKO, Maroš. Vplyv pracovného odporu stroja na veľkosť preklzu hnacích kolies traktora. In Acta technologica agriculturae. ISSN 1335-2555, 2006, roč. 9, č. 2, s. 44-47.
15. FRANČÁK, Ján - MIHINA, Štefan - ANGELOVIČ, Marek - GÁLIK, Roman - KORENKO, Maroš - SIMONÍK, Ján - BOTTO, Ľubomír - JOBBÁGY, Ján - ŽITŇÁK, Miroslav. Technika v agrokomplexe. 1. vyd. Nitra : Slovenská poľnohospodárska univerzita v Nitre, 2010. 198 s. ISBN 978-80-552-0412-3.
16. KORENKO, Maroš - FRANČÁK, Ján. Vplyv technických a technologických faktorov na kvalitu sadenia zemiakov : vedecká monografia. 1. vyd. Nitra : Slovenská poľnohospodárska univerzita v Nitre, 2009. 122 s. ISBN 978-80-552-0175-7.

The improvement of mechanisms for establishing and changing boundaries of administrative and territorial units

Olexandra Kovalyshyn[1], Nadiia Kryshenyk[1]

[1]Lviv National Agrarian University; e-mail: nadya_kryshenyk@ukr.net

Received July 12.2016: accepted July 19.2016

Abstract. Modern land organization, as a complex of social-economic and ecological measures, is focused on rational organization of the territory of administrative-territorial units, which make a spatial base for territorial organization of state management and local self-governing. Thus, determination of boundaries of administrative-territorial units is very important, actual and responsible task of land organization.

Improvement of organizational and ecological mechanisms of establishment of boundaries of administrative-territorial units through the provision of these subjects with the relevant land surveying, land planning and cartographic, soil, land evaluation materials and agreed urban planning documents is still of great importance. Legislation of Ukraine determines the dependence of land use documents (land development project regarding the establishment of (changes in) the boundaries of settlements) on the town planning documentation (the general layout of a settlement, other town planning documentation), but the mechanism of its implementation is not grounded.

Key words: administrative-territorial unit, boundary, settlement, establishment, land management, land management projects.

INTRODUCTION

The main instrument of the state, which aims to provide environmentally friendly and economic viable land use, is land management. The issues of establishing boundaries of administrative - territorial units, planning and environmental constraints in land use are settled on the basis of land management decisions.

In the administrative-territorial reform, the definition of the territorial boundaries of settlements is relevant and necessary to create a holistic living environment of the local community. This distinction not only provides efficient use of land resources, but also preservation of natural landscapes and historical and cultural values.

The absence of boundaries or their unreasonable definition, not only significantly complicates the activities of local governments, but also leads to numerous violations of the land law in land management, the shortfall of local budgets revenues, causing disputes and conflicts that certainly has a negative impact on efficiency, conservation and regeneration of land within the boundaries of certain territories [1, p. 59].

ANALYSIS OF RECENT RESEARCHES AND PUBLICATIONS

The works of D. Dobriak, I. Dorosh, A. Martyn, S. Osipchuk, M. Stetsiuk, A. Tretiak, T. Yevsiukov and other scientists are devoted to the study of the problem concerning development of land management projects on establishment (change) of boundaries of settlements. The problems of legal regulation of the survey of administrative-territorial structure have been considered in the works of N. Marusenko, A. Miroshnychenko, A. Ripenko, A. Yurchenko [9, p. 395].

The diversity, complexity and importance of this issue requires further research in this area. In particular, specific mechanisms for establishing and changing boundaries of administrative-territorial units in the conditions of reforming of the administrative-territorial structure of Ukraine need to be improved.

OBJECTIVES

The objective of the study is the analysis of the current prerequisites for the establishment and change of boundaries of administrative-territorial units in Ukraine, the formation of conceptual bases of improvement of mechanisms for establishing and changing these boundaries.

THE MAIN RESULTS OF THE RESEARCH

The territorial structure of our country under the Constitution of Ukraine [4] is based on the principles of unity and integrity of the state territory, combination of centralization and decentralization in the exercise of state power, balance and socio-economic development of regions, taking into account their historical, economic, ecological, geographical and demographic peculiarities, ethnic and cultural traditions.

Ukraine's territory is divided into administrative-territorial units, which are compact parts of unitary Ukraine and is the spatial basis for organization and activity of bodies of state power and bodies of local self-government. The system of the territorial structure of Ukraine is the following: the Autonomous Republic of Crimea, regions, districts, cities, districts in cities, towns and villages.

The territory of these units is separated by a boundary. According to Article 173 of the Land Code of Ukraine, the boundary of the administrative-territorial unit is a conventionally closed line on the surface of the earth that separates the territory of a district, a village, a

settlement, a city, a district in the city from other areas [3]. But, it is rightly pointed out by A. G. Martyn, that such a definition is based on the assumption of discreteness of such a unit , and notes that the boundary of an administrative-territorial unit is a set of conditional lines, each of which separates its territory from the territory of neighboring administrative-territorial units, which are connected sequentially at the nodal points and are the same or are consistent with the boundaries of administrative-territorial units of the highest level [6].

The boundaries of administrative-territorial units are established and changed according to the land management projects on the establishment (change) of boundaries [3].

In Ukraine on January 1, 2016, there are 490 districts, 460 cities, 111 districts in cities, 885 towns, 1176 settlements, 27205 villages [2]. The boundaries of the vast majority of administrative-territorial units were formed in the period of 1991 – 1992 through the development of projects of formation of territories of village councils. Since then, there were significant changes in housing, industrial and public buildings. Large tracts of these lands are left outside the legal boundaries of villages, towns and cities. In addition, methods of development of given projects of formation of village councils territories did not provide for the inclusion of large areas of industrial use, existing at that time (commercial courtyards, farms etc) in borders of settlements.

Nowadays in Ukraine, according to the State Geocadastre [2], land management activities for establishment and change of boundaries of 16.7 thousand villages were carried out, which is 56% of the total. The lowest indexes for this type of work are in Kharkiv, Cherkasy, Lviv, and Ternopil regions. The establishment of borders in nature (on location) is only in 50 settlements with officially established and registered boundaries of settlements in Ukraine, including cities, towns and villages. 21 settlement is in Odessa region, 13 - in Rivne region, 6 - in Sumy region, 3 - in Ternopil region , 2 - in Cherkassy region and one in Kiev, Ivano-Frankivsk, Poltava, Kharkiv and Chernihiv regions. The total area of these settlements is only about 24 122 ha. However, in most districts and cities, as well as in all regions there are formally established boundaries. The question of determining the boundaries is complicated by the administrative reform, because the village councils are in the process of consolidation of territorial communities, and their number will be reduced [7].

The main reasons for the slow pace of works on establishment of boundaries are shortage of funds, imperfection of the legal and regulatory framework.

According to the Law of Ukraine "On land development", Article 46, in order to establish or change the boundaries of administrative-territorial units, projects of land management concerning their establishment (change) should be developed. This project includes: an explanatory note; tasks to do works; the decision to develop the land management project; a copy of the general layout of a settlement certified in the prescribed manner, the decision on its approval (in case of change of boundaries of a settlement); the copy of the land development plans and a feasibility study of the use and protection of lands of administrative-territorial units, and in case of its absence – a copy of the project of formation of territories of village councils; the copy of cadastral maps (plans) displaying the existing (if any) and the project boundary land within the existing (if any) and project boundaries; description of the boundaries; materials of coordination of the project; materials of the removal of boundaries in nature (on locality) with a catalog of coordinates of their turning points [8].

Let consider the improvement of mechanisms for establishing and changing boundaries of administrative-territorial units taking the village Suvorove Izmail district of Odessa region as the example. According to the Land Code of Ukraine, Article 173 [3], projects of land management on change of boundaries of settlements are developed with consideration of the General layout of settlements. Therefore, the starting materials for the development of the project is the master plan of the village Suvorove and the results of geodetic removal.

The territory of the village at the time of development of the project is 503,1670 ha. The resident population at the beginning of 2015 was 4800 people. Labor resources accounted for about 60% or 2880 people of the total population.

According to the Article 19 of the Land Code of Ukraine [3] the following categories of land purpose can be identified on the territory of the village Suvorove, Izmail district, Odessa region: agricultural lands – the crops of wheat, sunflowers; vineyards, orchards, forest shelter belts, pastures; lands under residential and public buildings – one-, two-storied manor residential development with the local area, school, gymnasium, market, shops, kindergarten, technical school; lands of recreational purpose – the stadium; lands of the water fund – the Malyi Katlabukh river, the Velykyi Katlabukh river, the eastern shore of the lake Katlabukh; lands of industrial, transport, communications, power engineering, defense and other purposes – 2 cemeteries, paved roads with a width of 4-8 m, unpaved roads with a width of 2-4 m, the factory on manufacture of asphalt, the brick factory, the feed mill, the dairy farm, the oil extraction plant. Table 1 shows the explication of lands within the village at the time of the project drafting.

Table 1. Explication of lands by categories within the village of Suvorove before the project

Land category	Area	
	ha	%
Agricultural land	72,4456	14,4
Lands under residential and public buildings	256,9170	51,0
Lands of recreational purpose	3,5920	0,7
Lands of water fund	17,4310	3,5
Land of industrial, transport, communications, power engineering, defense and other purposes	152,7820	30,4
Total	**503,1670**	**100,0**

The residential property takes a significant part - 256,9170 hectares, which is 51% of the total area. Besides, the lands of industrial, transport, communications, power engineering, defense and other

purposes occupy 30.4% of the territory of the village. Development prospects and the life of the settlement exactly depend on the industrial sector, despite the fact that this area is of seasonal operation. In this regard, the general layout provides for the expansion of boundaries of the settlement for the placing and maintenance of food industry facilities – the canning plant for storage of raw materials and finished products, with an area of 21,0206 ha.

From an environmental point of view, while developing the project, the territory of common use should be provided for landscaping (parks, squares, boulevards). Their standards are calculated in accordance with the norms [10] based on table 2.

Table 2. Area of green territories of common use

Green territories of common use within the town	Groups of towns according to the number of population, thous. people	Area of green territories , sq. m/person			
		Polesia, Subcarpathia, Transcarpathia	Forest-Steppe	Steppe	Southern Coast of Crimea
Town territories	100-1000 and more	10	11	12	15
	50-100	7	8	9	11
	To 50	8(10)	9(11)	10(12)	12(15)
	Rural settlement	12	13	14	17
Residential areas	100-1000 and more	6	6	7	8
	50-100	6	6	7	8

*Source [10].

For the village the area of green space should be 10 (12) m^2/person. The population of the village of Suvorove is 4800 people. But for the future it is planned that this figure will be 6,000 people. Therefore, the area of the projected green area will be 4.8 ha.

Lands of recreational purpose occupy only 0.7% of the territory. Therefore, two options for location of recreational areas are expected in the project: the first one - the plot of 4,8119 hectares for green areas and plantations; the second one - 4,8193 hectares for parks and recreation.

Lands, due to which the boundaries of the village are expanded, are taken from the category of agricultural lands that are unproductive and not used for their purposes (Fig 1.).

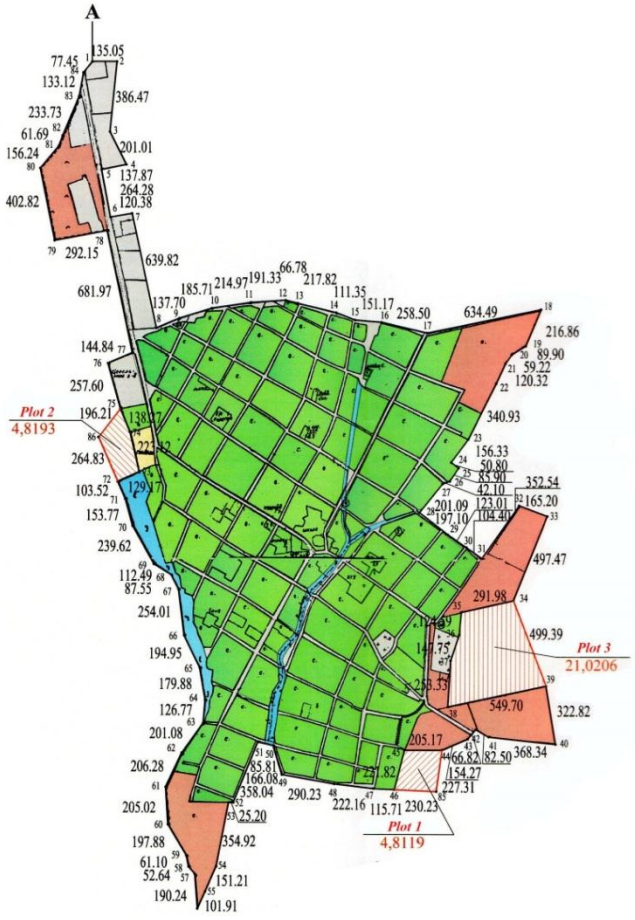

Fig.1. The fragment of the project of land management for establishment and change of boondaries of the village of Suvorove.

The strucrure of lands within the boundaries of the village of Suvorove after project decisions taking is given in table 3. Therefore, the projected area of the settlement will be 533,8188 hectares, that is, it will be increased by 6.1%. The necessity of establishing and changing the boundaries of the village of Suvorove is stipulated for its long-term development of industrial and recreational industries.

Table 3. Explication of lands by categories within the village of Suvorove according to the project

Land category	Area according to the project		Deviations between the projected and existing areas	
	ha	%	ha	%
Agricultural land	72,4456	13,6	0	0
Lands under residential and public buildings	256,9166	48,1	0	0
Lands of recreational purpose	13,2232	2,5	9,6312	1,9
Lands of water fund	17,431	3,3	0	0
Land of industrial, transport, communications, power engineering, defense and other purposes	173,8024	32,5	21,0206	4,2
Total	**533,8188**	**100,0**	**30,6518**	**6,1**

Article 186 of the Land Code of Ukraine determines that land development projects for establishment (change) of boundaries of administrative-territorial units are agreed by rural, urban, district councils and district state administrations, through which territories extension of such boundaries is planned.

The transfer in nature of the external border of the settlement from points of polygonometry of the 4th class on the locality is done with the help of the polar method. The turning points of the boundary were fixed at the location by boundary marks of Y15H type (Fig.2).

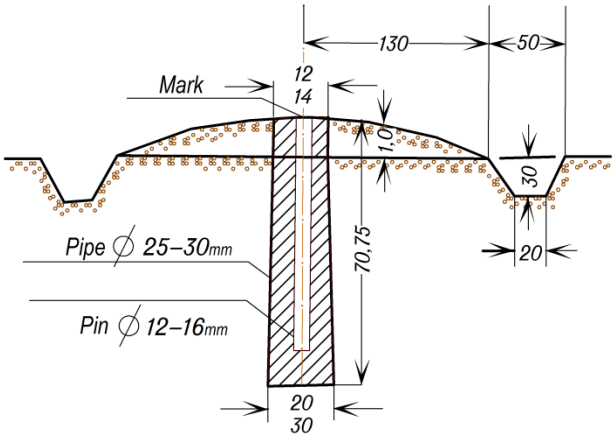

Fig.2. The center of the point of polygonometry

Analysis of the proposed activities indicates the need for improvement of certain mechanisms of the development of land management projects on the establishment of boundaries of administrative-territorial units: administrative-legal, organizational, environmental and financial-economic ones.

Legal and administrative mechanisms combine institutional, licensing, administrative control and regulatory instruments; organizing instruments – land use and planning; financial and economic instruments - instruments of economic stimulation and innovation.

Improving of legal and administrative mechanisms are implemented by:

- ✓ the improvement of normative legal and methodical bases of the establishment and change of boundaries of administrative-territorial units;
- ✓ strengthening of state supervision and control over the protection of the interests of land owners and land users with a view to preventing violations of the right of land ownership.

Improvement of organizational and environmental mechanisms are offered to be implemented through the provision of administrative-territorial entities with relevant land surveying, land planning and cartographic, soil, land evaluation materials, planning documentation, as well as through formation of the institute of restrictions in the use of lands associated with their protection, as well as of landscaped areas of public use.

Financial and economic mechanisms should be improved through the formation of investment-attractive land use of the administrative-territorial unit, development and implementation of the mechanism of economic stimulation of rational use and protection of land.

CONCLUSIONS

The formation of boundaries of administrative-territorial units in terms of reforms remains a problematic task of land management, however, it is an important prerequisite for arranging the territorial organization of our state, the normal functioning of the tax system, the implementation of the rights of territorial communities to regulate land relations on the territory, which is its spatial basis.

To ensure work on the development of land management projects in the recent period a number of normative legal documents have been amended, in particular the Law of Ukraine "On land management". However, this is not enough. It is necessary to improve administrative-legal, organizational, environmental and financial-economic mechanisms of development of land management projects regarding the establishment of boundaries of administrative-territorial units through the institutional, licensing, administrative control and regulatory, land use and planning, innovative instruments.

Improvement of organizational and ecological mechanisms of establishment of boundaries of

administrative-territorial units through the provision of these subjects with the relevant land surveying, land planning and cartographic, soil, land evaluation materials and agreed urban planning documents is still of great importance. Legislation of Ukraine determines the dependence of land use documents (land development project regarding the establishment of (changes in) the boundaries of settlements) on the town planning documentation (the general layout of a settlement, other town planning documentation), but the mechanism of its implementation is not grounded.

The formation of boundaries of administrative-territorial units will allow to lay the foundation for the administrative-territorial reform, and at the same time to optimize the system of management of territories, to regulate the relationships between authorities at different hierarchical levels, and ultimately to contribute to improving standards of living of every citizen in every urban or rural settlement.

REFERENCES

1. **Babmindra D. 2008.** Problems of establishing and changing the boundaries of the city of Zaporizhia. The Bulletin on land management. No. 1, 59-62. (in Ukrainian).
2. **Fedorovych V. 2015.** Legal support of the establishment (change) of boundaries of settlements in Ukraine: problems and solutions. Bulletin of Lviv University: legal series. Ed. 61, P. 395-401. (in Ukrainian).
3. **Kovalyshyn O. Kryshenyk N., Havryshkiv N., Sosnowski S., 2014.** Analysis of methodological approaches to evaluation of land quality in Ukraine. ECONTECHMOD. Lubin-Rzeshov, Vol. 3. No. 4, P. 97-102. (in English).
4. **Kovalyshyn A., Kryshenyk N., Len P. 2015.** Effect of engineering factors of the land plot on the efficiency of its use in the event of division. ECONTECHMOD. An interntionl quarterly journal. – Lubin – Rzesow. Vol. 4. No 4, P. 7-10. (in English).
5. **Krasnolutskyi O. Yevstiukov T. 2012.** Establishment of boundaries of settlements : modern problems and solutions. The Bulletin on land management. No. 2, P. 22-27. (in Ukrainian).
6. **Kryshenyk N., Kovalyshyn O., Soltys O. 2016.** Monitoring of land relations in Ukraine with the use of geographic information systems. VII Miedzynarodowa Konferencja Naukowa z cyklu «Innowacyjne technologie geodezyjne – zastosowanie w roznych dziedzinach gospodarki» (Kamionka, 8-10 czerwca 2016 r.), P. 55-56. (in English).
7. **Martin A. 2012.** Establishment of boundaries of administrative-territorial formations: problems and solutions. The Bulletin on land management. No. 4. P. 17-30. (in Ukrainian).
8. **Nizalov D., Ivinska K., Kubakh C. etc. 2015.** Monitoring of land relations in Ukraine 2014-2015: statistical annual. Kyiv, 95 p. (in Ukrainian).
9. On land management: the Law of Ukraine. 2003. [Electronic resource]. – Mode of access: http://zakon3.rada.gov.ua/laws/show/858-15/conv.
10. SBN 360-92** «Planning and construction of urban and rural settlements».1992. [Electronic resource]. – Mode of access : http://dbn.at.ua/load/normativy/dbn/dbn_360_92_ua/1-1-0-116. (in Ukrainian).
11. The Constitution of Ukraine. 1996. [Electronic resource]. – Mode of access: http://zakon3.rada.gov.ua/laws/show/254к/96-вр/print1472324139214840. (in Ukrainian).
12. The Land Code of Ukraine. 2001. [Electronic resource]. – Mode of access: http://zakon3.rada.gov.ua/laws/show/2768-14/print1472324139214840. (in Ukrainian).
13. The state service of Ukraine on issues of geodesy, cartography and cadastre : statistics [Electronic resource]. – Mode of access : http://land.gov.ua/info/statystyka/. (in Ukrainian).

Bulding contour line in the database of the real estate cadastre in Poland pursuant to applicable laws

M. Buśko

AGH University of Science and Technology, Poland, e-mail: mbusko@agh.edu.pl

Received July 12.2016: accepted July 19.2016

Abstract. The study analyzes the provisions of the Polish law concerning the principles of determining the digital description of building contour lines to be entered into the database of the real estate cadastre. The analyzed laws are contained in the Regulation on the register of land and buildings of 2001. The subsequent amendments to this Regulation regarding the contour of a building, made by the entry into force of the amending Regulations in 2013 and 2015, respectively, introduced significant changes. As a result of these changes in the definition of the contour of the building, some of the buildings, entered into the database of the real estate cadastre based on the previous wording of the provisions, became obsolete.

The paper also analyzes the effects of the amendments to the Regulation on the register of land and buildings. Some of them should be considered positive, as the new provisions in the Regulation clarified to some extent the earlier wordings which were unclear and gave rise to ambiguous interpretation of the record data of buildings. However, some important record data of the buildings existing in the database of the real estate cadastre, such as the digital description of the contour lines and the resulting built-up area, became outdated as a result of another part of the amended provisions, although there were no changes in the structure of the buildings.

Key words: outline of the building, built-up area, cadastre, update of the database, building contour line

INTRODUCTION

Cadastral parcel, cadastral entity and building structure, are the main objects of the database of the register of land and buildings, also known as the real estate cadastre. In Poland, the current legislative Act in the field of surveying is Geodetic and Cartographic Law [1]. Article 20.1.2) of this Act lists in general the *"information on their location, purpose, function, and general technical specifications"*, which are necessary to be captured for building structures. One of the examples of secondary legislation to Geodetic and Cartographic Law is the Regulation on the register of land and buildings of 29 March 2001 [4]. It was substantially amended and extended by the amending Regulation of 29 November 2013 [5], but shortly, there was another amendment by the amending Regulation of 6 November 2015 [6]. The issues of creating and using the database of building structures in the real estate cadastre have been the subject of numerous studies, for example [25] [28].

MATERIALS AND METHODS

This chapter will present the historical basis for entering buildings in the real estate cadastre in Poland. From the analysis of the post-war legal provisions on the register of land and buildings, it appears that the collection of the basic data about building structures was to be implemented already since the end of World War II. The legal acts which are significant for building structures, as well as their short descriptions, are summarized in Table 1.

Table 1. Legal acts concerning building structures in the real estate cadastre

Year	Title of the legal act	Remarks on building structures
1	2	3
1947	Decree on the cadastre of land and buildings	The cadastral survey was supposed to contain data on the location of the building, its function, the material used for its execution, the date of its construction and its detailed description.
1955	Decree on the register of land and buildings	It required to collect the same data about the buildings. In addition, it contained the provision that the location of the buildings is the content of the cadastral map.
1969	Decree on land records	It only required to plot the location of the buildings on the cadastral map. It did not, however, contain any provisions concerning the collection of any other data on the buildings.
1996	Regulation on the register of land and buildings	The record data of the building include its location, purpose, function and general technical specifications. The definition of the building was in accordance with the Act of 7 July 1994 - Construction Law [2].

Continuation of Table 1

1	2	3
2001	Regulation of 29 March 2001 on the register of land and buildings	14 cadastral data were introduced for the building. The definition of the building was in accordance with the Act of 29 June 1995 on official statistics [3].
2013	Regulation of 29 November 2013, amending the Regulation on the register of land and buildings	26 cadastral data were introduced for the building. There was a change in the definition of the contour of the building. The definition of the building was directly referred to the regulation on the Polish Classification of Types of Constructions [7].
2015	Regulation of 6 November 2015, amending the Regulation on the register of land and buildings	27 cadastral data were introduced for the building. There was another change in the definition of the contour of the building.

The legal acts presented in Table 1 demonstrate how often the Polish legislation regulating the cadastral records of buildings has changed. As a result of these changes and due to the lack of determination to enter the buildings in the real estate cadastre in a consistent manner, in Poland there still are many cadastral districts where the buildings are not entered into the cadastral base at all [8], [14], [24], [26].

In this study, the author will present the selected cadastral data of the building, such as the digital description of the building contour lines and the built-up area of the building which, pursuant to §63.2 of the Regulation on the register of land and buildings, should result from the digital description of the contour. The performed analyses of the Polish legislation and of the specific examples of various architectural and design solutions have demonstrated that there is still a lot of controversy regarding these attributes of the buildings. A negative consequence of such frequent amendments to the law is the loss of coherence of the meaning of the discussed cadastral data of the buildings, which were entered into the real estate cadastre subject to the previous wording of the provisions in the Regulation on the register of land and buildings.

RESULTS AND DISCUSSION

In this chapter, the author will present various buildings which, due to their architectural and design solutions, will serve as examples to illustrate defective and inconsistent provisions in the legislation. The essential definitions of the digital description of the contour of the building and the resulting value of the built-up area of the building are contained in §63 sections 1 and 2 of the Regulation on the register of land and buildings. Basing on the comparative analysis of these definitions in the subsequent amended versions of the Regulation, Table 2 summarizes structural elements of the building which formed its contour, pursuant to the individual versions of §63 of the Regulation on the register of land and buildings [4], [5], [6].

Table 2. Comparison of the elements forming the contour of the building

REGULATION ON THE REGISTER OF LAND AND BUILDINGS OF 2001 2001 – 2013	REGULATION ON THE REGISTER OF LAND AND BUILDINGS OF 2013 2013 – 2015	REGULATION ON THE REGISTER OF LAND AND BUILDINGS OF 2015 after 2015
external planes of the outer walls of the ground storey	the exterior walls of the building	the exterior walls of the building
	if the foundation wall intersects the surface - the outer edges of the foundation	if the foundation wall intersects the surface - the outer edges of the walls of the storeys which are supported on these foundation walls
if the storey is on pillars - the exterior walls of the storey supported on these pillars	if the storey is on pillars - the outer edges of the pillars	if the storey is on pillars - the exterior walls of the storey supported on these pillars if the storey is on pillars - the outer edges of the pillars if the storey is on pillars - the outer edges of the walls of the storeys which are supported on the pillars
		if the roof is on pillars - the outer edges of the roof

Table 2 demonstrates that the definition of the contour of the building has evolved with each new amendment to the Regulation on the register of land and buildings. The geometry of the same object recorded in the cadastral database in 2001, 2013 and 2015 looks quite different. It shows how difficult it is to maintain the database to be continuously compliant with the applicable laws. Further in this article, the author will present some

photos of the buildings whose contours will be used to illustrate the issues of changing the definition of the digital description of the contour of the building in the Regulation on the register of land and buildings.

The definition of the contour is relatively easy to visualize if the exterior walls of the building are the extension of the foundation walls (Fig. 1). This case is relatively easy to interpret during field surveys. However, even for such buildings, there are doubts as to the identification of the measurement point of the corner of a building, if insulation on the walls is of considerable thickness and it does not reach the surface of the ground [21]. It should be emphasized that, in accordance with the Regulation on the standards, the corner of the building as the field detail of the first-order accuracy should be determined with an error not exceeding 0.10 m relative to the nearest point of the geodetic control. In the case of thermal insulation, the thickness of its layer together with external plaster often exceeds 0.10 m, which can be a problem in determining the location of terrain details.

Since 2013, a much more controversial case is that of a building where the outer walls are not an extension of its foundation walls and the building has the so-called overhangs (Fig. 2). They can be supported by pillars, or unsupported. The fact of overhangs being supported by pillars is extremely important, as the contours of such buildings, and the resulting built-up area, will differ significantly from each other.

Fig. 1. The walls of the building as an extension of the foundation walls (Foto: M. Buśko)

Fig. 2. Buildings with overhang without pillars and overhang supported by pillars (Foto: M. Buśko)

In the case of the building on the top of Fig. 2, the contour of the building will comprise only the surface of the outline of the ground storey of the building, without the existing overhang, despite the fact that the overhang is of significant size. On the other hand, in the case of the building on the bottom of Fig. 2, the contour is determined by the foundation wall together with the outer edges of the pillars supporting the overhang of the building.

A significant change in the definition of the contour contained in the Regulation on the register of land and buildings of 2015, compared to the Regulation on the register of land and buildings of 2013 should be emphasized at this point, if applied to buildings with overhangs supported on pillars. If the contour was defined pursuant to the Regulation on the register of land and buildings of 2013, it would be determined by the outer edges of the pillars supporting the overhang of the building. If, however, the contour was to be defined as set out in the Regulation on the register of land and buildings of 2015, it would be determined by the outer edges of the storey walls in the building, which are supported on the pillars. As far as the building illustrated in Fig. 2 is concerned, this change in the definition of the contour will not change its contour in a significant way, as the outer edge of the pillars is practically the extension of the outer edge of the walls supported on these pillars. However, there are many buildings in which the pillars are situated at a greater distance from the outer edge of the overhang wall, as illustrated in Figures 3 and 4.

Fig. 3. Buildings in which the edges of the walls based on the pillars are not their extension (Foto: M. Buśko).

Fig. 4. The edges of the walls based on the pillars are not their extension (Foto: M. Buśko)

To sum up, it is worth emphasizing that according to §63 section 1b of Regulation on the register of land and buildings, in the years 2013-2015, the contour was determined by the outer edges of the pillars, and after 2015 it was defined by the outer edges of the walls supported on the pillars.

The most important change introduced in the Regulation on the register of land and buildings of 2015 is an additional entry in §63 section 1b, concerning the case of the roof of the building being supported on the pillars. In that case, the contour is defined by the outer edges of the roof. It can be presumed that the purpose of introducing such an amendment to the Regulation in 2015 was to unambiguously specify how to define the building contour lines and the resulting built-up area in the case of a specific type of a building such as an open shelter (defined so since 2013) (Fig. 5). This was due to the fact that the definition of the building was directly referred to the Regulation on the Polish Classification of Types of Constructions (Table 1).

Therefore, when the Regulation on the register of land and buildings of 2013 was in force, all the open shelters, regardless of their size and intended use, were entered into the database of the real estate cadastre. However, after the Regulation on the register of land and buildings was amended in 2015, a clarification was introduced in §78, relieving from the obligation to enter open shelters in the real estate cadastre, if their built-up area is up to 50 m² and they are located on the parcel with a residential building, or the one intended for residential construction, providing the total number of such open shelters does not exceed two per each 1,000 m² of the parcel. It should be emphasized that the effect of entering a building (including an open shelter) in the real estate cadastre is notifying the tax authorities of a change in the data of the register of land and buildings. This results in the obligation to pay a tax on the building. After the Regulation on the register of land and buildings was amended in 2015, the shelters entered into the cadastral database subject to the regulations in force between 2013 and 2015 should have been removed by the authority running the register, as this database became obsolete due to that amendment [12].

The definition of the contour of the building was broadened in the Regulation on the register of land and buildings of 2015. The contour comprised the outer edges of the roof supported on pillars. It was advantageous for the determination of the contours of open shelters. At the same time, however, as a result of this provision, some of the buildings entered into the real estate cadastre under the provisions of the Regulations on the register of land and buildings of 2001 and of 2013, automatically became obsolete with respect to two important cadastral data: digital contour of the building presented on the cadastral map and the built-up area in the descriptive data of the real estate cadastre. Fig. 6 demonstrates the examples of such buildings with the roofs supported on pillars.

Fig. 5. Shelter - a special kind of building by PKOB (Foto: M. Buśko)

Another major problem regarding the buildings whose roofs are supported on pillars concerns the determination whether the contour of the building comprises all the turn points of the roof around the building, or only those which are located directly above the pillars. If the first of the above solutions is chosen, it must be taken into account that the built-up area of the building, determined by its roof, will be much greater than the area determined by the elements of the "ground storey" of the building (even including pillars). The second solution will result in the contour of the building not keeping right angles, characteristic for the walls of the building (Fig. 7).

Fig. 6. Buildings in which the roof is based on the pillars (Foto: M. Buśko)

Fig. 7. The building with a roof based on the pillars (Foto: M. Buśko)

As to the building illustrated in Fig. 7, the analysis was performed, which regarded its presentation on the cadastral map in accordance with the requirements of the Regulation on the register of land and buildings of 2001, 2013 and 2015 (Figures 8 and 9). This will allow to visualize the changes that should be entered into the database of the real estate cadastre for the building which remained unchanged in its construction or design, necessary to be introduced only due to the amendments in the provisions of law. The building was mapped in accordance with the different versions of the Regulation, and for each version the value of the built-up area of the building components was calculated. The results are summarized in Table 4.

As it is illustrated on the Fig. 8, in the version of the Regulation of 2013, the open shelter (*"i"* function on the map) was to be drawn between the garage (*"t"* function on the map) and the residential building (*"mj2"* function on the map). This shelter must be removed from the database (go down in history), pursuant to the provisions of the Regulation of 2015, as shown in Fig. 9. Instead, the contour of the garage will be enlarged, as its roof is supported on the pillar.

The two interpretations of the provisions of the Regulation presented in Fig. 9 are due to the fact that it is impossible to unambiguously resolve whether the whole roof of the building should be measured, or only those parts which are supported on the pillars.

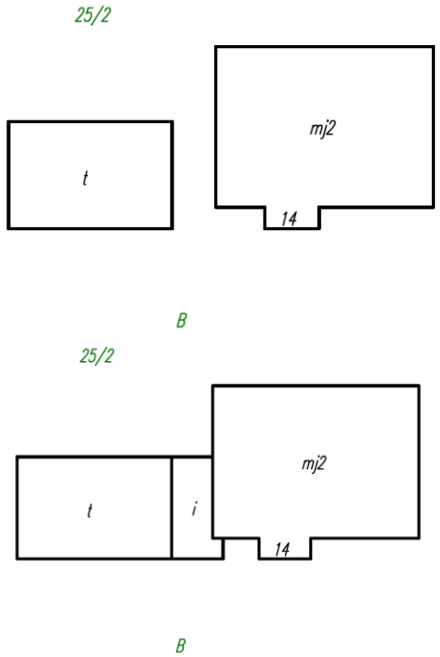

Fig. 8. Schematic contours of the building in accordance with the Regulations of 2001 (on the top of Fig. 8) and 2013 (on the bottom of Fig. 8)

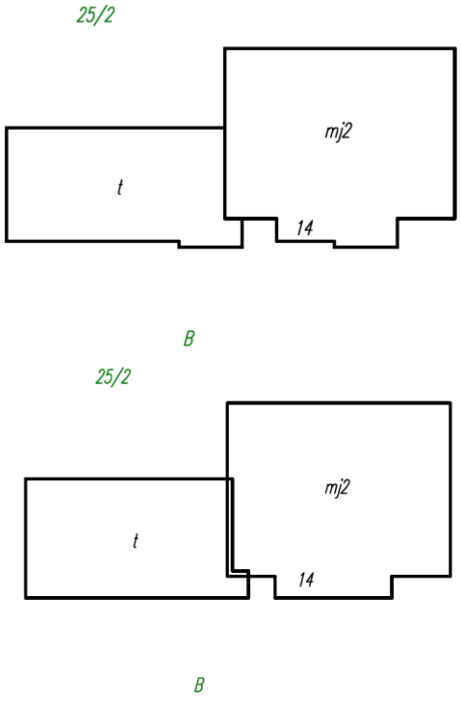

Fig. 9. Schematic contours of the building in accordance with the Regulation of 2015 – interpretation A and interpretation B

In today's legal status in Poland, the built-up area of a building is not an essential attribute in property tax assessment. Only usable floor space of a building should be taken into account for tax purposes [10]. However, in some areas of the southern Poland, due to some difficulties in determining usable space [11], it is sometimes determined as the product of the built-up area and the number of storeys of the building. This method has no legal grounds, nevertheless, it is commonly used in practice. In addition, for the owners, the value of the built-up area of the building is a very specific and clear attribute. It is expected that any changes in the value of the built-up area, despite the lack of any changes in the construction or design of the building, will result in property owners' protests, formulated as objections to the draft record of survey and property description made available for inspection. The digital description of the contour of the building and the resulting built-up area are also important factors in the currently evolving concepts of the 3D cadastre [9], [16], [18], [23], [27]. Therefore, no consistency of meaning of these data is of great significance. Updated cadastral data are also important for any digital analysis in spatial planning [13], [15], [22], and in the construction of cadastral data models (Land Administration Domain Model) in the cadastral system of spatial information [17]. The experience of Poland in the construction of the real estate cadastre may be useful also for other countries who are developing such concepts [19], [20].

Table 3. The built-up area of the elements of the building in Fig. 7

Function of the building	Built-up area [m^2]			
	Regulation of 2001	Regulation of 2013	Regulation of 2015	
			Interpretation A	Interpretation B
Residential building	310	310	324	358
Garage	150	150	196	218
Open shelter	0	50	0	0
The total built-up area	**460**	**510**	**520**	**576**

CONCLUSIONS

1. The subsequent amendments to the Regulation on the register of land and buildings of 2001, introduced in 2013 and 2015, resulted in the loss of consistency of meaning of the significant cadastral data of the buildings entered into the real estate cadastre under the previous wording of the provisions in the Regulation, such as the building contour line and the built-up area. These inconsistent amendments resulted in the loss of internal harmonization of the data contained in the database of the real estate cadastre.

2. It should be emphasized that in the revised version of the Regulation on the register of land and buildings of 2015, the wording of §63.1b was amended in such a way that the contour of the building is no longer determined by *the outer edges of the pillars*, but by *the outer edges of the walls of the storeys supported on the pillars*. This will cause a change in the building contour lines and the resulting value of the built-up area of some buildings.

3. The wording introduced in the Regulation on the register of land and buildings of 2015, which required the contour of the building whose roof is supported on pillars to be defined as *the outer edges of the roof*, is advantageous when it comes to determining the contour of open shelters, which are defined as a special type of building structures. At the same time, chaos appears with regard to ordinary buildings, whose roof is supported on pillars only in certain places.

4. During the next amendment to the Regulation on the register of land and buildings, it is advisable to introduce a separate subclause in §63.1 of the Regulation, whose wording would be as follows: *in the case of a special type of a building structure, such as an open shelter, which is subject to be entered into the database of the real estate cadastre, the building contour line is the line determined by the rectangular projection of the outer edges of the roof onto the horizontal plane.*

REFERENCES

1. The Law of 17 May 1989. Law in Geodetics and Cartography, Dz. U. 1989, No. 30, Pos. 163, as amended. d. (in Polish).
2. The Law of 7 July 1994. Construction Law, Dz. U. 1994 No. 89, Pos. 414, as amended. d. (in Polish)
3. The Law of 29 June 1995. On official statistics, Dz. U. 1995, No. 88, Pos. 439, as amended. d. (in Polish).
4. Regulation MRRiB of 29 March 2001. On the land and building, Dz. U. 2001, No. 38, Pos. 454 (in Polish).
5. Regulation of MAiC of 29 November 2013. Amending the regulation on registration of land and buildings, Dz.U. 2013 Pos. 1551 (in Polish).
6. Regulation of MAiC of 6 November 2015. Amending the regulation on registration of land and buildings, Dz. U. 2015 Pos. 2109 (in Polish).
7. Regulation of the Council of Ministers of 30 December 1999. On the Polish Classification of Types of Constructions (PKOB), Dz. U. 1999, No. 112, Pos. 1316. (in Polish)
8. **Balawejder, M., Buśko, M., Cellmer, R., Juchniewicz-Piotrowska, K., Leń, P., Mika, M., Szczepankowska, K., Wójciak, E., Wójcik-Leń, J., Źróbek, S., 2015.** The current problems of real estate management in Poland against the background of organizational and legal changes. WSI-E, Rzeszów. (in Polish)
9. **Bieda, A., Bydłosz, J., Dawid, L., Dawidowicz, A., Glanowska, M., Góźdź, K., Przewięźlikowska, A., Stupen, M., Taratula, R., Źróbek, R., 2015.** Directions of real estate cadastre development. Wyższa Szkoła Inżynieryjno-Ekonomiczna, Rzeszów. (in Polish)
10. **Bieda, A., Hanus, P., Jasińska, E., Preweda, E., 2014.** Accuracy of determination of real estate area, in International Conference "Environmental Engineering, May 22–23, 2014, Vilnius, Lithuania.
11. **Buśko, M., 2015.** Analysis of legal provisions regarding the determination of usable floor area of a building and living premises. Przegląd Geodezyjny, R. 87 nr 12, Warszawa, s. 8–12. (in Polish)
12. **Buśko, M., 2016.** Analysis of the influence of amendments to the legal provisions relating to building structures on keeping the real estate cadastral database updated. Infrastructure and Ecology of Rural Areas, ISSN 1732-5587, Nr II/1/2016, s. 395–410. (in Polish)
13. **Cagdas, V., Stubkjaer, E., 2016.** Core immovable property vocabulary for European linked land administration, SURVEY REVIEW, Volume: 47, Issue: 340 , Pages: 49-60.
14. **Dawidowicz, A., Źróbek, R., 2014.** Analysis of concepts of cadastral system technological development.Conference Proceedings. 9th International Conference "Environmental Engineering", Vilnius, Lithuania.
15. **De Smet, F., Teller, J., 2016.** Characterising the Morphology of Suburban Settlements: A Method Based on a Semi-automatic Classification of Building Clusters, LANDSCAPE RESEARCH Volume: 41, Issue: 1, Pages: 113-130.

16. **Ho, S., Rajabifard, A., Kalantari, M., 2015.** Invisible' constraints on 3D innovation in land administration: A case study on the city of Melbourne, LAND USE POLICY, Volume: 42, Pages: 412-425.
17. **Kalantari, M., Dinsmore, K., Urban-Karr, J Rajabifard, A., 2015.**A roadmap to adopt the Land Administration Domain Model in cadastral information systems, LAND USE POLICY, Volume: 49, Pages: 552-564.
18. **Karabin, M., 2013.**Koncepcja modelowego ujęcia katastru 3D w Polsce. Oficyna Wydawnicza Politechniki Warszawskiej, Warszawa (in Polish).
19. **Kovalyshyn O., Gabriel Yu., 2014.** Development of a management systems model of automatic control by using fuzzy logic.ECONTECHMOD.LubinRzeshov, Vol. 3. No. 4, 63-68. (in Polish)
20. **Kovalyshyn O. Kryshenyk N., Havryshkiv N., Sosnowski S., 2014.** Analysis of methodological approaches to evaluation of land quality in Ukraine.ECONTECHMOD.Lubin-Rzeshov, Vol. 3. No. 4, 97-102. (in Polish)
21. **Krzyżek, R., 2015.**Innovative algorithm of vector translation method for the measurements of corners of building structures using RTN GNSS technology. Geomatics and Environmental Engineering, vol. 9 no. 4, s. 73–84
22. **Kunze, C., Hecht, R., 2015.**Semantic enrichment of building data with volunteered geographic information to improve mappings of dwelling units and population, COMPUTERS ENVIRONMENT AND URBAN SYSTEMS, Volume: 53, Pages: 4-18
23. **Lee, B.M., Kim, T.J., Kwak, B.Y., Lee, Y.H., Choi, J., 2015.**Improvement of the Korean LADM country profile to build a 3D cadastre model, LAND USE POLICY, Volume: 49, Pages: 660-667
24. **Łuczyński, R., 2014**.Modernization of land and buildings registration in terms of the requirements of the modern cadastre. K. Sobolewska-Mikulska (Ed.), Real estate management and cadastre. Selected problems. Publishing House of Warsaw University of Technology, Warsaw (in Polish).
25. **Mourafetis, G., Apostolopoulos, K., Potsiou, C., Ioannidis, C., 2015.**Enhancing cadastral surveys by facilitating the participation of owners, SURVEY REVIEW, Volume: 47, Issue: 344, Pages: 316-324
26. **Siejka, M., Ślusarski, M., Mika, M., 2015.**Legal and technical aspects of modernization of land and buldingscadastreIn selected area. Reaports on Geodesy and Geoinformatics, vol. 99/2015, pp.44-53
27. **Siejka, M., Slusarski, M., Zygmunt, M., 2014.** 3D+time Cadastre, possibility of implementation in Poland, SURVEY REVIEW, Volume: 46, Issue: 335, Pages: 79-89
28. **Zupan, M., Lisec, A., Ferlan, M., Čeh, M., 2014.**DEVELOPMENT GUIDELINES IN THE FIELD OF LAND CADASTRE AND LAND ADMINISTRATION, Geodetskivestnik Vol. 58 (2014), No. 4, Pages: 710-723.

Defining quality work of a pneumatic seeding device with an extra disk

Viktoriia Abramova, Oleksii Vasylkovskyi, Kateryna Vasylkovska

Kirovograd National Technical University, e-mail: abramova_v77@mail.ru

Received July 14.2016: accepted July 19.2016

Abstract. This article is devoted to solving the problem of single-seed sugar beet sowing with a pneumatic seeding device. As a result of experimental researches the influence of sowing device parameters equipped with an additional disk for quality sowing were defined.

Key words: Seeding device, single-seed sowing, cell, seeds, extra disk, quality.

INTRODUCTION

The problem of increasing productivity and reducing the costs of crop cultivation is the main in agricultural production. Sugar beet yields are influenced by several factors, including an even distribution of seeds in a row at a given reasonable intervals. For a long time of seeding equipment history, a large number of sowing machines designs were created, each of which had the goal of improving the quality of sowing. However, the heterogeneity of seed properties and a number of other uncontrollable factors, especially in the field conditions, lead to a decrease of uniformity of seeds placing in a row, sometimes it goes far beyond the farming requirements.

Thus, improvement of devices aims at improving the quality of sowing and defines its dependence on the design parameters of the dosing element - that is an urgent task.

THE ANALYSIS OF RECENT RESEARCHES AND PUBLICATIONS

In the study of sowing process were engaged Zenin L.S., Chichkin V.P., Pogorily L.V., Zhuravlev B.I., Shmat S.I., Sviren M.O., Amosov V.V., et al. A large number of studies were devoted to the selection of the optimal number of holes, agitator and kickers design parameters and influence of suctorial forms of holes on the single filling of the sowing disk with seeds. The process of seed capturing with the suctorial disk hole is rather complex and, at an early stage it is crucial to ensure the required dosing capacity (productivity) of the device as a whole.

One of the main elements of the sowing machine, which significantly affects the quality of dosing is the seeding plate. The review of the known structures of sowing machines [1-7] showed that the diversity of the surface structures and suctorial disk holes affect the quality of seed capture.

In practice, there are various forms suctorial holes (cylindrical, conical, toroidal, etc.), but the most prevalent in domestic and foreign technology has become a cylindrical surface of the hole with the right angle edges.

We know that in the field conditions the quality of seed filling holes of suctorial disk often does not meet the agronomic requirements. At low speed of rotation of the disk, a large number of "twins" is being sown, and at high speed - increases the number of spaces that affects the density of crops.

It is known that an even distribution of seeds in a row can be achieved through the full completion of the sowing disk cells with no spaces.

The process of pneumatic sowing machine work consists of the following operations:

- seeds feeding from the bunker into the seed hopper chamber;
- capturing of one or more seeds by the suctorial disk hole;
- movement of seeds with the disk, removing the excessive seeds by the rejector unit and further movement of the seed with the disk;
- separating the seed from the disk;
- movement of the seed to the compacted furrow bottom;

The most significant factor affecting the quality performance of the exact seeding process of cultivated crops by pneumatic seeding device is to capture seeds by the suctorial disk holes and their further transportation. At the moment of capture a seed is affected by many forces including friction force of other seeds in the layer that affect the unauthorized dumping of the seed, which has been already sucked, from the hole. In order to hold it we need the suction force to be greater than the force of seeds friction.

THE MAIN RESULTS OF THE RESEARCH

An enhanced device consists of the body 1, on the drive shaft 2 of which there is the seeding plate 3 and agitator 4. Between them it is installed an additional disk 5, which has some shaped cutouts on the circuit. Thanks to the original design of the additional disk the main seed is quicklier oriented at the suctorial hole, the remaining

seeds are separated from it at a distance of the disk thickness and accept less vacuum than it is required for suction.

The aim of the series of experiments was the implementation of Box-Hunter matrix plan 2^5, as a result were defined the influence factors of dilution in a vacuum chamber *(ΔP)*, the speed of rotation of the sowing and additional disk *(V),* the thickness of the additional disk δ, radius of the extra disk basin r and size of the seed fraction z.

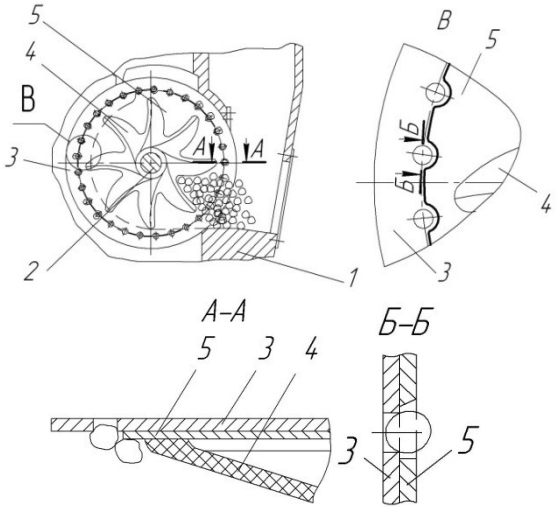

Fig. 1. An improved pneumatic seeding device:
1 - body, 2 - drive shaft, 3 - seeding plate, 4 - agitator,
5 - extra disk.

The quality of the device was estimated by coefficient of cells filling K_f, which is equal to the relation of amount of actually sown seeds for a certain period of time to the number of seed cells on the disk which passed the point of discharge at the same time.

At the same time, cell fill factor can be equal to 1 if there is a certain number of passes and the same number of doubles. To control the results of the studies we conducted digital photo and video fixation of the sowing process.

Results of the factors encoding are listed in Table 1.

Table 1. The results of the factors encoding

Factor	Natural designation	Code	Variation interval	Variation levels		
				natural		
				upper	zero	lower
The speed of rotation of the seeding and additional disk, m / s	V	x_1	0,05	0,35	0,3	0,25
The pressure in the system, kPa	P	x_2	1	3	2	1
Thickness of the additional disk, mm	δ	x_3	0,5	2	1,5	1
Radius of the additional disk basin, mm	r	x_4	0,25	2,75	2,5	2,25
Seed fraction, mm	z	x_5	0,5	5,5	5,0	4,5

Criterion of optimization Y - coefficient of cells filling K_f

The regression equation has the form

$$Y = 0{,}9709 - 0{,}1131x_1 + 0{,}4718x_2 - 0{,}1518x_3 + \\ + 0{,}0856x_4 - 0{,}2243x_5 - 0{,}0106x_1x_2 + 0{,}0306x_1x_3 - \\ - 0{,}0843x_1x_4 + 0{,}0006x_1x_5 - 0{,}0993x_2x_3 - 0{,}0268x_2x_4 + \\ + 0{,}0331x_2x_5 + 0{,}0818x_3x_4 - 0{,}0531x_3x_5 - 0{,}0281x_4x_5$$

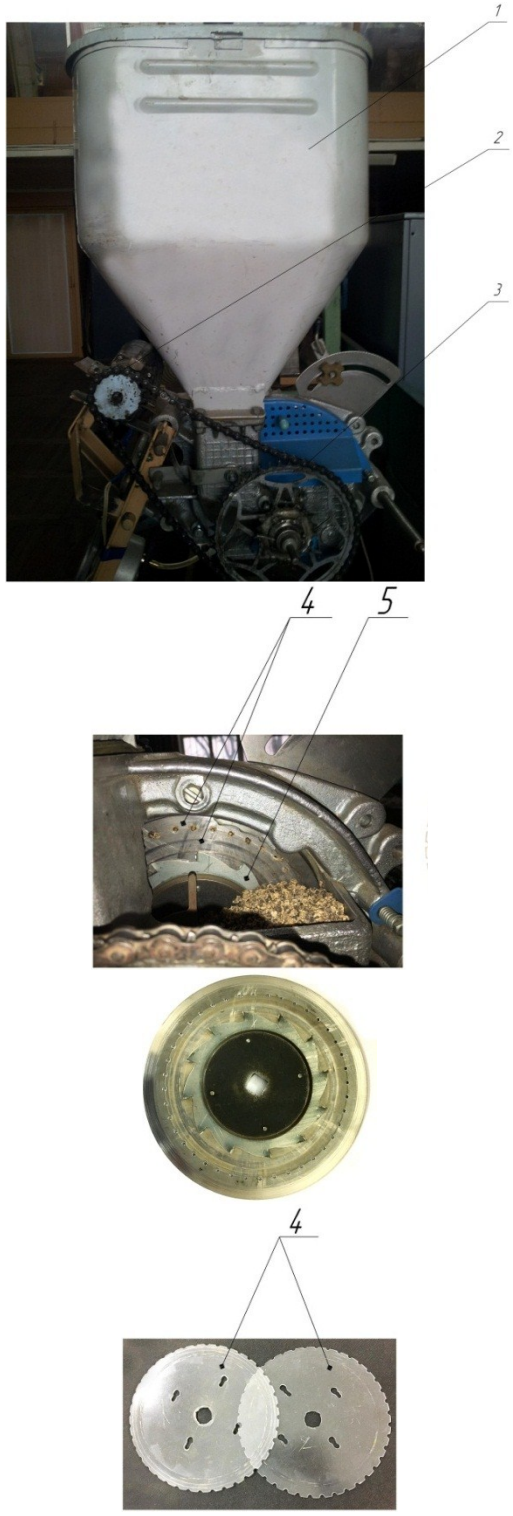

Fig. 2. General view of the experimental setup to study the process of sowing sugar beet: 1 - bunker; 2 – electric motor; 3 - chain transmission; 4 – seeding plate and extra disk; 5 – agitator

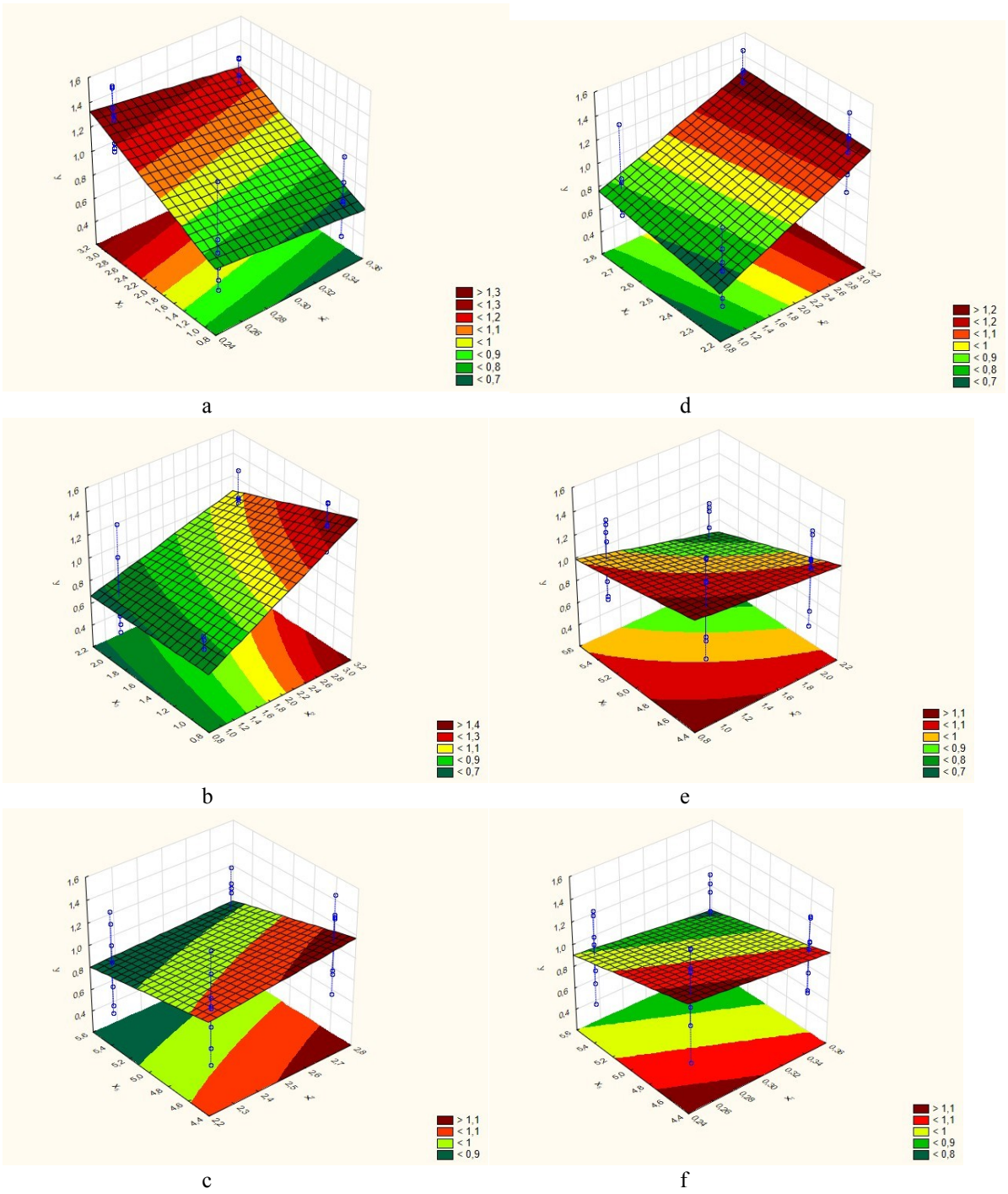

Fig. 3. Dependence of filling factor coefficient on the design parameters of the disk:
a - the dependence of K_f on ΔR system pressure and rotation speed of the sowing disc V; b - K_f dependence on the pressure in the P system and seed fraction z; c - dependence of K_f on extra disk basins radius r and seed fraction z; d - K_f dependence on the pressure in the P system and the extra disk basins radius r; e – K_f dependence on the extra disk thickness δ and seed fraction z; f - K_f dependence on disk rotation speed V and seed fraction z

Results of the experiment planning matrix realization are presented in Table 2.

For processing the experimental data the package STATISTICA 6.4 was used.

There were constructed response surfaces (Fig. 3) and line level output for cell filling coefficient of the seeding plate K_f.

After analyzing the response surface and line level output for cell filling coefficient of the seeding plate K_f, we define rational values of the investigated factors:

- circular cell speed of seeding plate $x_1 \rightarrow Vc$, should be in the range of 0.26 to 0.34 m / s.
- value of dilution in a vacuum chamber $x_2 \rightarrow \Delta P$, should be in the range of 1.7 to 2.4 kPa;

- thickness of extra disk $x_3 \rightarrow \delta$, should be in the range of 1.8 to 2.2 mm;
- radius of extra disk basin $x_4 \rightarrow r$, should be in the range of 2.2 to 2.4 mm;
- seed fraction $x_5 \rightarrow z$, should be in the range of 5 to 5.5 mm.

Table 2. Results of the experiment planning matrix realization

№ exper.	Natural factor value					Response function value Y
	x_1	x_2	x_3	x_4	x_5	
1	0,25	1	1	2,25	4,5	0,88
2	0,35	1	1	2,25	4,5	0,69
3	0,25	3	1	2,25	4,5	1,53
4	0,35	3	1	2,25	4,5	1,34
5	0,25	1	2	2,25	4,5	0,54
6	0,35	1	2	2,25	4,5	1,06
7	0,25	3	2	2,25	4,5	1,04
8	0,35	3	2	2,25	4,5	1,13
9	0,25	1	1	2,75	4,5	0,88
10	0,35	1	1	2,75	4,5	0,85
11	0,25	3	1	2,75	4,5	1,54
12	0,35	3	1	2,75	4,5	1,35
13	0,25	1	2	2,75	4,5	1,34
14	0,35	1	2	2,75	4,5	0,67
15	0,25	3	2	2,75	4,5	1,37
16	0,35	3	2	2,75	4,5	1,12
17	0,25	1	1	2,25	5,5	0,77
18	0,35	1	1	2,25	5,5	0,64
19	0,25	3	1	2,25	5,5	1,31
20	0,35	3	1	2,25	5,5	1,2
21	0,25	1	2	2,25	5,5	0,46
22	0,35	1	2	2,25	5,5	0,39
23	0,25	3	2	2,25	5,5	1,01
24	0,35	3	2	2,25	5,5	0,86
25	0,25	1	1	2,75	5,5	0,77
26	0,35	1	1	2,75	5,5	0,61
27	0,25	3	1	2,75	5,5	1,27
28	0,35	3	1	2,75	5,5	1,12
29	0,25	1	2	2,75	5,5	0,65
30	0,35	1	2	2,75	5,5	0,56
31	0,25	3	2	2,75	5,5	1,08
32	0,35	3	2	2,75	5,5	1,04

Having analyzed the Pareto card for cell filling coefficient of the seeding plate (Fig. 4) a conlusion can be made that on the quality of work of a sowing device the greatest impact has the value of dilution in a vacuum chamber x_2, thickness of extra disk x_3, and seed factions x_5 but the values of the circular cell speed x_1 and extra disk basin radius x_4 are not significant in this range.

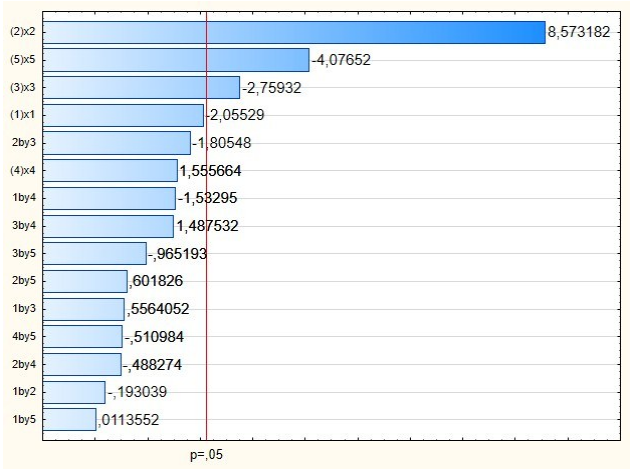

Fig. 4. Pareto map impact factors assessment of cell filling coefficient of the seeding plate

CONCLUSIONS

Thus, the use of additional seeding plate allows correctly direct a seed at the stage of capture to the center of the cell and eliminates the ability to capture "twins"; supporting the seed during transportation to the place of discharge. After a series of experimental studies, we found that even filling the cells of seeding plate significantly affect the pressure in the system, circular cell speed of seeding plate and radius of extra disk basins.

REFERENCES

1. **Sysolin P.V. 2004**. Seeding devices of seeders / Textbook. P.V.Sysolin, M.O. Sviren. - Kirovograd. – 160 p.
2. **Shmat S.I. 1984**. Row seeders / Shmat S.I., Shmat K.I. // Design and production of agricultural technology machines: Republican interdepartmental scientific and technical collection. - K .: - Vol. 11. - p. 22-24.
3. **Shmat S.I. 1989**. Increasing efficiency of pneumatic sowing machine / Shmat S.I., Sotnikov V.S. // Design and production of agricultural machines: Resp. Interdepartmental. scientific and engineering. Coll. - Vol. 19. - K .: Technique.
4. **Sviren M.O. 2012**. Scientific and technological bases of increase of efficiency of the seeding devices of seeding machines: diss. Doc. of Sciences.: spec. 05.05.11. "Machinery and mechanization of agricultural production" / Sviren M.O. - Kirovograd ,.
5. **Amosov V.V. 2007**. Justification of universal sowing device parameters for row crops: Diss. on doctor's degree, specials. 05.05.11. "Machinery and mechanization of agricultural production" [Text] / V. Amosov. - Kirovograd: KNTU.
6. **Pastukhov V.I., 2014**. Prospective directions of modernization of grain seeders / Pastukhov V.I., Bakuma M.V., Nikitin S.P., Mikhailov A.D., Abduyev M.N., Kirichenko R.V., Yashchuk D.A. Journal of Kharkov national technical University of agriculture n.a.Petro Vasilenko [text]: scientific edition, Vol. 148. Engineering. "Mechanization of agriculture" / KNTUA. - Kh: p. 77-80.

7. **Zenin L.S. 1962**. Research of pneumatic precision seed sowing machine: Author. Diss. on PhD degree. tech. Sciences [Text] / L.S. Zenin - Almaty – p.36.
8. **Zhuravlev B.I. 1961**. Research of pneumatic sowing machines for precise seeding [Text] / Zhuravlev B.I. // Tractors and agricultural machines. - №9.
9. **Chichkin V.P. 1984**. Vegetable drills and combined units [Text] / V.P. Chichkin - Chisinau: Shtiintsa - 392 p.
10. **Sydorchuk O. 2014.** Impact of meteorogical conditions on the need in adaptive perfoming of technological operations of soil tillage and crop sowing / O. Sydorchuk, P. Lub, O. Malanchuk // ECONTECHMOD: an international quarterly journal on economics in technology , new technologies and modelling processes. - Lublin; Rzeszow, - Volum 3, nomber 4, 35-39. (in English).
11. **Vasylkovska, K.V. 2014.** Justification settings of universal pneumatic sowing machine precision seeder: Dis. on Science. degree candidate. Sc. Sciences specials. 05.05.11. "Machinery and mechanization of agricultural production" / K.V. Vasylkovska. - Kirovograd, 2014. (in Ukraine).
12. **Vasylkovska, K.V. 2014.** Influence of the shape and type of seed cells drive on the quality of dispensing seeds [Text] / K.V.Vasylkovska, O.M.Vasylkovskyy // Eastern European Journal of latest technology. Vol 6, No 7 (72) (2014) - Kharkov: Technological Center, 2014, 33-36. (in Ukraine).
13. Pat. 63,895 U Ukraine, IPC A01S 04/07 (2006.01). Pneumatic seeding device / Shmat S.I. Sviren M.O., Abramov V.V., V.M. Lushnikov .; applicant patentowner, Kirovograd National Technical University. - №u201103252; appl. 21.03.2011; publ. 25.10.2011, Bull. Number 20.
14. Pat. A 58,306 Ukraine, IPC A01S 04.07. Pneumatic seeding device /
Shmat S.I., Sviren M.O., Abramova V.V., Lushnikov V. M .; applicant patentowner Kirovograd National Technical University. - № U201010953; appl. 13/09/10; publ. 11.04.11, Bull. Number 7.
15. **Abramova, V.V. 2013**. Improving the design of pneumatic sowing machine / V. Abramova, O.M. Vasylkovskyy, M.M. Shokin. // Proceedings of Lutsk National Technical University: Farm equipment LNTU, Lutsk. Vol. 24. - P. 3-9.
16. **Vasylkovskyy, O.M. 2014**. Experimental studies of pneumatic sowing device for sowing the seeds of cultivated crops / O.M. Vasylkovskyy, V.V. Abramova, K.V. Vasylkovska, D.I. Petrenko // Proceedings of Kirovograd National Technical University: Technology in agriculture, industrial engineering, automation. ed.27 - Kirovograd, KNTU, p. 161-167.
17. **Vasylkovska, K. 2015**. Determination of the optimal parameters extra seeds from seed cells disk of a pneumatic device [Text] / K.V.Vasylkovska, O.M.Vasylkovskyy // Proceedings of Kirovohrad National Technical University: Engineering in agriculture, industrial machinery, automation. Vol. 28 - Kirovograd, KNTU, 2015, 159-163. (in Ukraine).
18. **Vasylkovska, K. 2015**. Field tests with use of pneumatic seed disks with the proposed device [Text] / K.V.Vasylkovska, O.N.Vasylkovskyy S.M.Moroz // Lutsk National Technical University: Farm equipment LNTU, Lutsk. - 2015. - Vol. 30, 32-36. (in Ukraine)
19. **Borovykov V. 2003**. STATISTICA. Art data analysis on the computer now, for professionals. [Text] / V. Borovykov. - SPb.: Peter, 2003, 688.
20. **Vukolov, E. A. 2008**. Fundamentals of statistic analysis. Workshop on research of statistic methods and operations with using STATISTICA packets and EXCEL: Uchebnoeposobye. [Text] / E. A. Vukolov. - M .: Forum, 2008, 464.
21. **Pyatnytska-Pozdnyakova, I. 2003**. Basic research in higher education: Teach. guide [Text] / I.S. Pyatnytska-Pozdnyakova. - K .: Centre textbooks, 2003, 116.
22. **Haylis, G.A. 1992**. Fundamentals of design and research of agricultural machinery: Teach. guide [Text] / G.A. Haylis, DM Konovalyuk. - K .: NMKVO, 1992, 320.
23. **Researcher Manual: A manual for students of agronomic specialties [Text]** 2016 / Vasylkovskyy O., Leshchenko S., Vasylkovska K., D. Petrenko. - Kharkiv: Machulin. – p. 204.

Carrying capacity of strengthened reinforced elements on action of bending moments

Andrii Mazurak[1], Ivan Kovalyk[2]

1. Faculty of Building and Architecture of Lviv National Agrarian University, e-mail: amazurak@ukr.net
2. Faculty of Building and Architecture of Lviv National Agrarian University, e-mail:ivan_kovalyk@ukr.net

Received July 19 2015: accepted August 25 2015

*Abstract.*The article proposes methods of calculation of carrying capacity of strengthened reinforced elements on action of bending moments. Basing on the experimental research, we have carried out analysis of calculated data with the investigated results.

*Keywords:*carrying capacity, strengthening, concrete, gunned concrete, strains.

INTRODUCTION

Increase of carrying capacity of reinforced elements (RE), without a change of a constructive scheme, expects increase of a cross cut of a strengthened sample and should be made with application of such material as concrete, polymer concrete, fibre-reinforced concrete, as well as reinforcement with carbon fiber-reinforced plastic stripes and bed. Strengthening of bending reinforced structures with gunned concrete, which can be put in thin layers of a structure reinforcement, is a method, being efficient and reliable in operation [1, 2, 3, 4, 5, 6, 7, 13, 19].

To secure safety of strengthened RE and improve methods of their calculations, one needs investigation of regularities of changes of sustainability, deformation ability of materials at different degrees of stress with applied reinforcement [1, 5, 9, 11, 13, 15, 17].

THE ANALYSIS OF RECENT RESEARCHES AND PUBLICATIONS

Investigation of reinforced structures are presented in the works of Ye.M. Babych, A.Ya.Barashykov, Z.Ya. Blikharskyi, S.V. Bondarenko, O.I. Valovyi, O.B. Holyshev, V.H. Kvasha, H.A. Molodchenko, L.A. Murashko, and others [1-20]. Basing on the researches, we studied effective constructive solutions on strengthening of reinforced structures and proposed methods of calculation.

On the ground of previous researches it is described [16, 17] how concrete and gunned concrete layers of the investigated elements work jointly, secured by adhesive padding with polymer mortars and installation of pasted metal land ties [20].

OBJECTIVES

Aim of the work is to make estimation of carrying capacity of strengthened reinforced elements on action of bending moments with consideration of the reinforcement technology. Task of the research is to develop methodology and make analysis of theoretical and experimental investigation of strengthened RE considering unrelieved stress to reinforcement fulfillment.

THE MAIN RESULTS OF THE RESEARCH

The presented calculation is based on the algorithm, mentioned in normative documents on the base of a deformation model, being modified according to a certain experimental research [7,8]. The algorithm is adopted for calculation of reinforced structures by different ways (lengthening, case or hooping) and considers their joint operation.

Base of the calculation is made by formulae (1.1), presented in SBN 2.6-98 on calculation of stress strain behavior of rectangular cuts in case of eccentric extrusion and bend (fig. 1), describing equilibrium in a cut in the integral form:

$$\begin{cases} \Sigma M := \dfrac{b\cdot f_{cd}}{N_{pr}^{\,2}}\cdot\displaystyle\int_0^{y_1}\sum_{i=1}^{5}\mathrm{a}_i\cdot y^{i+1}\mathrm{d}y+\sum_{i=1}^{3}\sigma_{s_i}\cdot\mathrm{A}_{s_i}\cdot\left(x_1-z_{s_i}\right); \\ \Sigma x := \dfrac{b\cdot f_{cd}}{N_{pr}}\cdot\displaystyle\int_0^{y_1}\left(\sum_{i=1}^{5}a_i\cdot y^i\right)\mathrm{d}y+\sum_{i=1}^{3}\sigma_{s_i}\cdot A_{s_i}; \end{cases} \quad (1)$$

where $\aleph=\dfrac{1}{\rho}=\dfrac{\left(\varepsilon_{c(1)}-\varepsilon_{c(2)}\right)}{h}$ - is a bowing of bended gridline in a cut; $\varepsilon_{c(1)},\ \varepsilon_{c(2)}$ - strains of concrete of stressed and positive fiber respectively; $\gamma=\dfrac{\varepsilon_{c(1)}}{\varepsilon_{c1}}$, where ε_{c1} is a value of critical strains of concrete of stressed fiber; $x_1=\varepsilon_{c(1)}/\aleph$ - is a height of the stressed zone; $\overline{\aleph}=\aleph/\varepsilon_{c1}$ - relative bowing; z_{si} - distance of *i* rod or interlayer of reinforcement from the most stressed border of a cut.

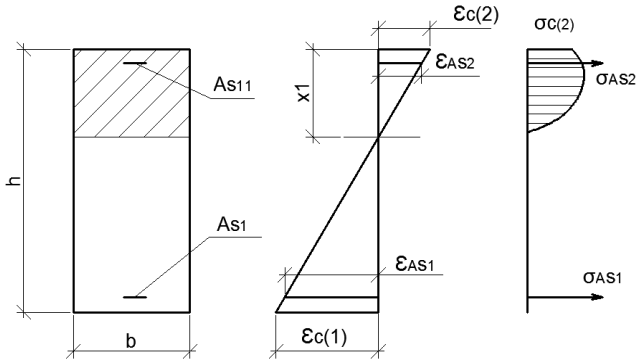

a **b** **c**

Fig. 1. Stress strain behavior of a rectangular cut: **a** – cross cut of an element; **b** – strain diagram at equilibrium; **c** – stress diagram.

A joint operation of an "old" and "new" concrete is measured by assigning of a common deflection to all elements of the cut and the deflection is calculated according to the formula:

$$f=\frac{1}{r}k_m l^2. \quad (2)$$

Because in the formula 2 all values, except bowing $\dfrac{1}{r}=\dfrac{\varepsilon_{c_{11}}-\varepsilon_{c_{12}}}{h}$, are constants, to secure an equal deflection at all stages of the beam operation, it is sufficiently that bowing growth to be the same from the moment of enforcement for all parts. This condition can be outlined in the following way:

$$\frac{\left(\varepsilon_{c_{11}}-\varepsilon_{c_{11\_0}}\right)-\left(\varepsilon_{c_{12}}-\varepsilon_{c_{12\_0}}\right)}{h}=\frac{\varepsilon_{c_{21}}-\varepsilon_{c_{22}}}{h+h_1+h_2}; \quad (3)$$

where $\varepsilon_{c_{11\_0}},\ \varepsilon_{c_{12\_0}}$ - is for strains at upper and down border of an old part of the beam at a moment of reinforcement; $\varepsilon_{c_{11}}-\varepsilon_{c_{11\_0}},\ \varepsilon_{c_{12}}-\varepsilon_{c_{12\_0}}$ - is a growth of strains at upper and down border of an old part of the beam from a moment of reinforcement respectively; $\varepsilon_{c_{21}},\ \varepsilon_{c_{22}}$ - strains at upper and down borders of a new part of the beam respectively, obtaining non-zero value from a moment of reinforcement.

In the equation 1.3 there are two unknowns: $\varepsilon_{c_{21}},\ \varepsilon_{c_{22}}$. To calculate them, one of them is assigned with a gradually growing value, and the other is calculated. The procedure is repeated until the found values satisfy an equilibrium equation (4).

Estimation of stress strain behavior of strengthened reinforced beams, having a joint operation of old and enforced parts as one of the principal criteria, can be presented in the equation (4, 5), general picture of which are demonstrated in the integral form.

$$\Sigma x=\frac{b_1\cdot f_{cd_2}}{N_{pr}}\cdot\int_0^{y_{22}}\left(\sum_{i=1}^{5}a_{20+i}\cdot y^i\right)\mathrm{d}y+\frac{b_2\cdot f_{cd_2}}{N_{pr}}\cdot\int_0^{y_{22}}\left(\sum_{i=1}^{5}a_{20+i}\cdot y^i\right)\mathrm{d}y \quad (4)$$

$$+\frac{b\cdot f_{cd_2}}{N_{pr}}\cdot\int_{y_{21}}^{y_{22}}\left(\sum_{i=1}^{5}a_{20+i}\cdot y^i\right)\mathrm{d}y+\sum_{i=1}^{3}\sigma_{s_{20+i}}\cdot A_{s_{20+i}};$$

To satisfy conditions of equilibrium we find a value of a moment *(M)*, excepted by each part of a cut:

- for a principal part of a beam

$$\mathbf{M}_1:=\frac{b\cdot f_{cd_1}}{N_{pr}^{\,2}}\cdot\int_0^{y_1}\sum_{i=1}^{5}\mathrm{a}_{1+i}\cdot y^{j+1}\mathrm{d}y+\sum_{i=1}^{3}\sigma_{s_{1+i}}\cdot\mathrm{A}_{s_{1+i}}\cdot\left(x_1-z_{s_{1+i}}\right); \quad (5)$$

- for a reinforced part of a beam

$$\mathbf{M}_2:=\frac{b_1\cdot f_{cd_2}}{N_{pr}^{\,2}}\cdot\int_0^{y_{22}}\sum_{i=1}^{5}\mathrm{a}_{20+i}\cdot y^{j+1}\mathrm{d}y+\frac{b_2\cdot f_{cd_2}}{N_{pr}^{\,2}}\cdot\int_0^{y_{22}}\sum_{i=1}^{5}\mathrm{a}_{20+i}\cdot y^{j+1}\mathrm{d}y+$$

$$+\frac{b\cdot f_{cd_2}}{N_{pr}^{\,2}}\cdot\int_{y_{21}}^{y_{22}}\sum_{i=1}^{5}\mathrm{a}_{20+i}\cdot y^{j+1}\mathrm{d}y+\sum_{i=1}^{3}\sigma_{s_{20+i}}\cdot\mathrm{A}_{s_{20+i}}\cdot\left(x_2-z_{s_{20+i}}\right); \quad (6)$$

Total value of a moment is got by addition of corresponding moments, resulted from the previous equations:

$$M = M_1 + M_2 \qquad (7)$$

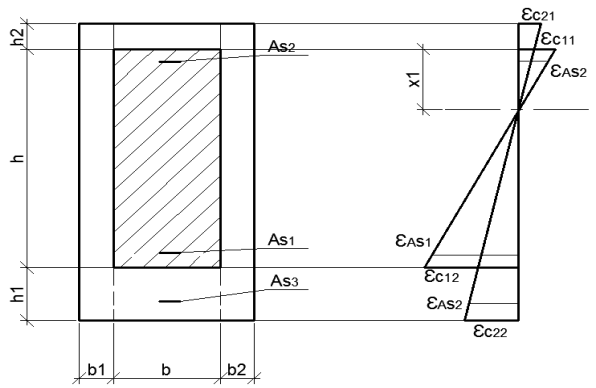

Fig.2. Scheme of stress strain behavior of a rectangular cut being reinforced

Calculation algorithm is presented at fig.3.

Series of the carried research consisted of fifteen investigated beams of projected sizes (Lxhxb) 2300x200x80(120;145). The beams under research are made reinforced (f_{cd}=23,5 MPa) by common technology, beam (B-2) without reinforcement, nine beams are reinforced by lengthening with gunned concrete technology (B-2-1…eg) and four beams are reinforced by usual concreting of input frames (B-2-2…uc). Beams are reinforced at different degrees of stress: 0,0; 0,3; 0,45; 0,6 from a critical moment, and thus got corresponding marks. In all cases of reinforcement we used adhesive padding Koster SB –Haftemulsion and metal joining land ties (Ø 8mm), projecting above the surface at 35mm. Class of the concrete of reinforcement layer for beams (B-2-1-1… eg, B-2-1-1.2…eg) - f_{cd}= 28,3 MPa, for beams (B-2-1-2… eg - f_{cd}= 23,6 MPa, and for (B-2-2-1…uc, B-2-3-1.2…uc) beams - f_{cd}= 24,1 MPa.

On the first stage of the experiment, non-reinforced beams were tested with centered stress, when loading step was equal 0;1F from a critical one. Process of beams investigation was made according to a static scheme, i.e. a beam on two supports, with a span *L*=2100 mm. When fluid behavior was achieved, the examples were relieved, their critical operation stress was taken as a control one for all beam samples being reinforced.

Next stage of the work included reinforcement of the beams under experiment (fig.4).

The main method was to apply an reinforcing layer of concrete or gunned concrete, which was put on a side surface (on one or both sides) with a previous flat reinforced frame.

Testing of the beams under experiment was made on the 440th-676th day from a date of production and on the 45th-72nd day from a date of reinforcement by application of concentrated forces in one third of their span. Experimental and calculated values of bending moments, corresponding to critical conditions and destruction, as well as their comparison are presented in the table 1.

Table 1. Strength of reinforced experimental beams

№	Beam code	Geometric sizes (reinforced) bxh, mm	Degree of stress	Value of bending moments, M, kH m		$\frac{M_u^{exper}}{M_u^{SBN}}$
				experiment, critical	calculation according to SBN [7;8]	
1	B-2	80x200		19,04	18,853	1,01
2	B-2-1-1-0,0-eg	80x200 (120x200)	0,0	30,62	29,651	1,032
3	B-2-1-1-0,3-eg	79x200 (120x200)	0,32	30,425	29,599	1,028
4	B-2-1-1-0,6-eg	80x200 (120x200)	0,62	28,84	27,274	1,057
5	B-2-1-2-0,0-eg	77x196 (120x196)	0,0	29,155	27,893	1,045
6	B-2-1-2-0,3-eg	77x196 (120x196)	0,31	28,08	26,988	1,040
7	B-2-1-2-0,6-eg	77x196 (120x196)	0,61	26,05	24,938	1,045
8	B-2-2-1-0,0-uc	79x200 (120x200)	0,0	29,86	29,304	1,019
9	B-2-2-1-0,3-uc	80x200 (120x200)	0,32	29,25	29,095	1,005
10	B-2-2-1-0,6-uc	80x200 (120x200)	0,62	24,48	27,031	0,905
11	B-2-2-1.2-0,0-uc	77x203 (148x204)	0,0	37,05	35, 26	1,051
12	B-2-2-1.2-0,45-uc	78x204 (148x204)	0,45	33,06	31,31	1.056
13	B-2-1-1.2-0,0-eg	77x203 (144x203)	0,0	34,66	33,165	1.045
14	B-2-1-1.2-0,3-eg	78x202 (145x202)	0,33	34,64	33,034	1.049
15	B-2-1-1.2-0,6-eg	78x203 (145x203)	0,63	29,75	28,20	1,055

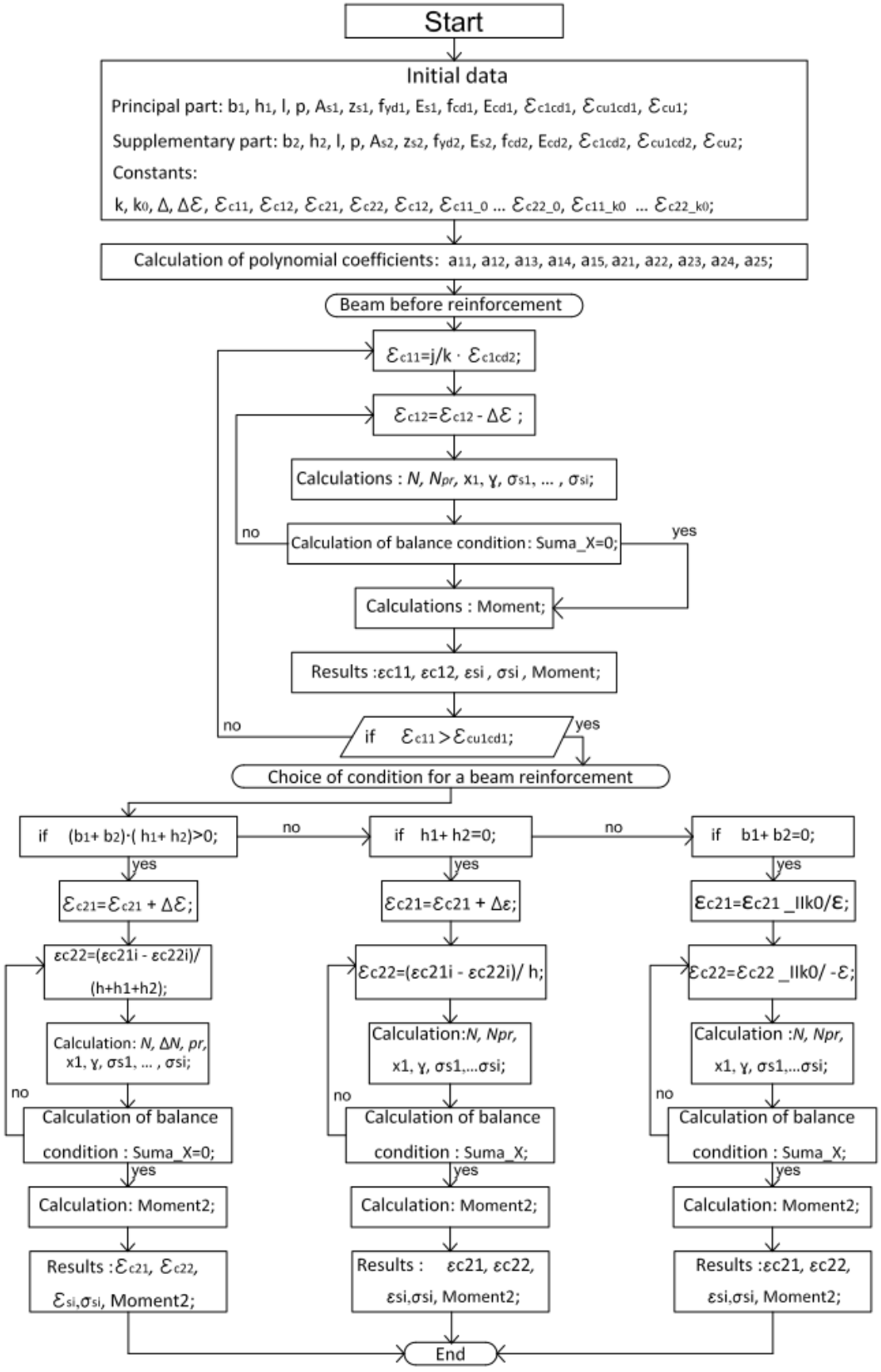

Fig. 3. Block-scheme of calculation on strengthening of reinforced beams

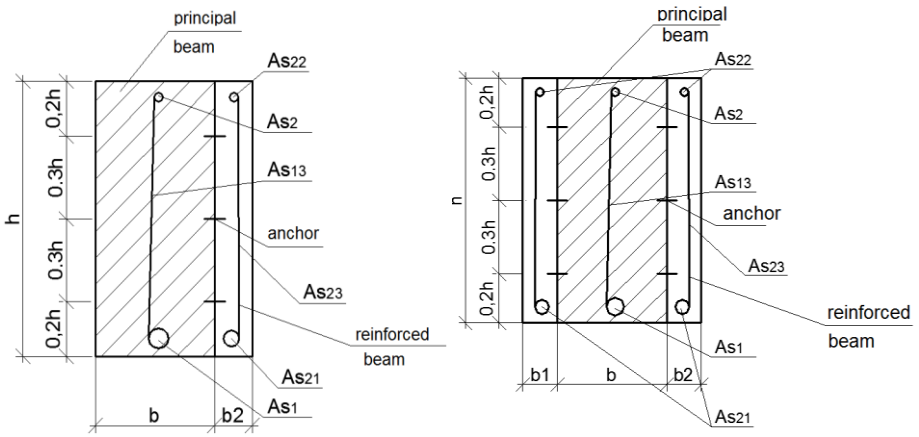

Fig. 4. Scheme of reinforcement of a side surface of experimental samples:
a) B-2-1-1, B-2-1-2, B-2-2-1; b) B-2-2-1.2, B-2-1-1.2

Having got results of experimental researches and compared them with the proposed calculation (see table 1), one can make a conclusion that theoretical and experimental values coincide, and deviation is less than 6%. It proves the fact that the suggested algorithm makes qualitative estimation of the process of RE strengthening at different degrees of stress (up to 0,62 from a critical one).

Dependence of strains on stress for beams at height of a cut has the same results as (fig 5,6), we used results of a beam B-2-1-2-0eg to be described in the article.

Diagrams of dependence of strains on stress in the beam B-2-1-2-0 eg at height of a cut are presented in (fig. 5,6), and demonstrated distribution of strains at height of a cut (h=20, for armature 170 mm). The presented graphic dependences prove that at different cuts (h=20 and h=60) theoretical and calculated values differ. Thus, for example, at operation degree of stress of 0.7 M in a cut h= 20 mm, in a principal part of the beam the difference makes 8-14% in the reinforced part 10-20%. In a cut h= 60 mm close to neutral axis, the difference in two parts of the beam makes 10-14%. Diagrams of armature strains at h= 170 mm show a deviation of values in the principal part of the beam 6-11% and in the reinforced part – 12-28%. We consider that such difference of calculated and experimental values of principal and reinforced parts of the beam is caused by late start of operation of armature in the reinforced part.

CONCLUSIONS

Analysis of the carried experimental and theoretical researches demonstrates that, according to the acting norms, methodology of calculation of carrying capacity of normal cuts of strengthened reinforced beams, made by a corresponding algorithm, gives a satisfactory result, and the deviation makes up to 6%. However, at height of a cut, value of experimental and calculated strains gives larger difference (10-20%), especially armature of reinforced parts 12-28%. Thus, in the further researches it is necessary to increase number of cuts for comparison and consider a larger range of stress degrees on reinforcement.

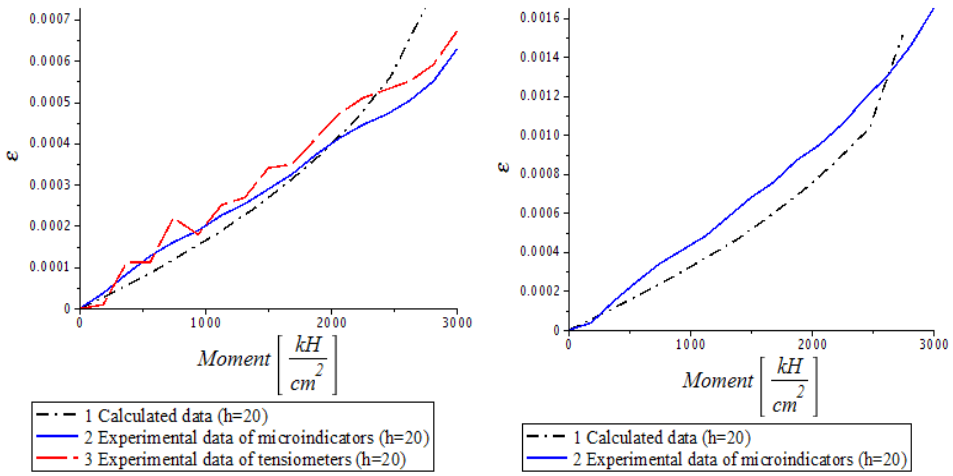

Fig. 5. Diagram of strains dependence on stress in the beam B-2-1-2-0 eg at height (h=20 mm): a) – principal part of the beam, b) reinforced part of the beam

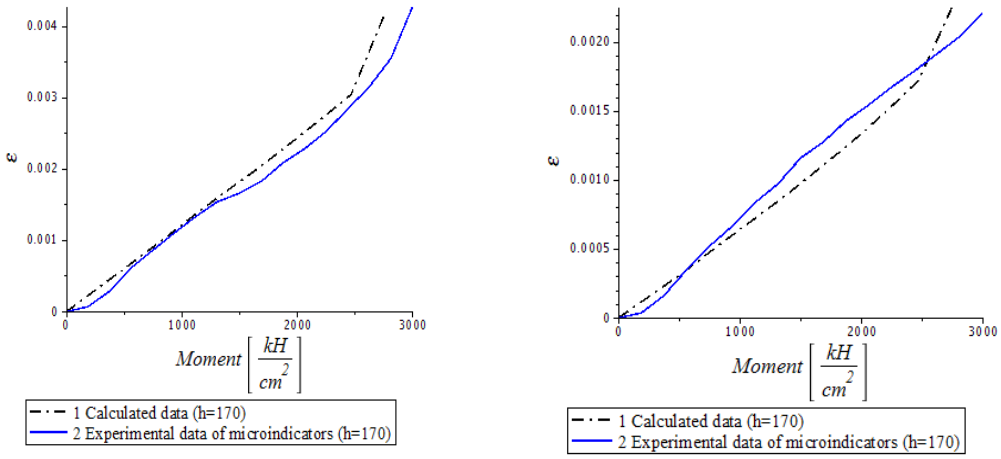

Fig. 6. Diagram of dependence of armature strains on stress in the beam B-2-1-2-0 eg at height (h=170 mm): principal part of the beam, b) – reinforced part of the beam;

REFERENCES

1. **Babich E.M., Babich V.Y., Savytskyy V.V. 2012.** Calculation of carrying capacity of cross-sectional flexural concrete elements. Sciences papers. №. 23. - P. 94-103. (in Ukrainian)
2. **Baikov V.N. 1984.** Features work pryopornyh plots beams / Concrete and zhelezobeton. -№4. P.20-22 (in Ukrainian)
3. **Bambura A.M., Barashikov A.J., Hurkivskyy O.B. 2005.** The main provisions of the calculation of concrete and reinforced concrete structures on national regulations (DBN), (in two volumes). - Volume 1. - P. 36-43. (in Ukrainian)
4. **Barabash V.M., Klymenko F.Y. 1997.** Development, research and application of a new type of band fittings periodic profile steel concrete constructions / Theory and practice of concrete. - Poltava,. – P. 37-41. (in Ukrainian)
5. **Blikharskyi Z.Y., Rymar Y.V., Dubizhanskyi D.I. 2007.** Experimental and theoretical researches of strength of reinforced beams, strengthened under stress /Theory and practice of building. – Lviv: - №600. – P. 19-22. (in Ukrainian)
6. **Boryshanskyy M.S. 1964.** Calculation of concrete structures at deysvyy poperechnыh forces / Moscow,. –P. 377. (in Russian)
7. Concrete and reinforced structure of heavy concrete. Rules of projecting: SSU B V.2.6-156:2010. – [acting since 2011-06-01]. – K.:Minregionalbuild of Ukraine, 2011. – P.116 – (National standard of Ukraine).
8. Concrete and reinforced structures. Fundamentals: SBN V.2.6-98:2009. – [acting since 2011-07-01]. – K.: Minregionalbuild of Ukraine, 2011. – P.71 – (State building norms of Ukraine).
9. **Dorofeev V.S., Bardanov V.Y., 2011**. Calculation yzhybaemыh zlementov with uchetom dyahrammы deformation of concrete: monograph. Odessa:, - P. 210. (in Ukrainian)
10. **Doroshkevych L.A., Demchyna B.G., Maksimovic S.B., 2007.** Proposals for calculating sloping sections bending strength of reinforced concrete elements / Interdepartmental nauk.- Vol. 67 - K: NIISK - P. 601-612. (in Ukrainian)
11. **Emmons P.H., Vaysburd A.M., McDonald J.E., Czarnecki L**: Durability of repair materials: current practice and challenges // International Symposium „Brittle Matrix Composites 6", Warsaw, 2000, - P.263-274.
12. Eurocode 2: Design of concrete structures. European Committee for standartization. Brussels, oct. 2001.
13. **Holyshev A.B., Tkachenko I.N. 2001.** Projecting of strengthening of reinforced structures of industrial buildings and constructions. K: Lohos,. – P. 172 . (in Ukrainian)
14. **Kashcharovski F**. / Application of spray concrete in repairing works. / F Kashcharovski, H. Kalisst // Engineering and Building, 6, 1993. – P. 222 – 224.
15. **Klimenko F.E., Bobalo T.V. 2007.** The carrier zdatnыst inclined pereгыzыv steel concrete beams. Theory and practice of construction.-Vol.6. . (in Ukrainian)
16. **Mazurak A.V., Shmyh R.A., Kovalyk I.V., Sadovyi M.V. 2013.** Calculation of strength of reinforced elements, being strengthened at different degrees of stress. Building constructions. K.: SE SRIBC, 2013. Ed. 78 v. 2. P. 499 – 504. . (in Ukrainian)
17. **Mazurak A.V., Kovalyk I.V. 2013.** Strength of a joint line while repairing or strengthening of concrete elements. Theory and practice of building. – Lviv,– Edition №755 – P. 368-375. . (in Ukrainian)
18. **Mazurak A.V. 1996.** The strength of pre-stressed steel concrete beams in the area of the transverse forces: dys.kand. tehn.nauk: 05.23.01. Lviv, - P. 199.

19. **Petsold T.N., Tur. V.V. 2003.** Concrett Constructions. Baltic State Technical University –P. 334 . (in Belorussia)
20. **Saliichuk L.V. 2011.** Experimental research and theoretical argumentation of strength and anchorage in concrete of pasted pin land ties at shift. Interdepartmental scientific-technical collector edition 74 volume 2. K.: SE SRIBC,. P. 494-506. (in Ukrainian)

Investigation of contemporary illuminants characteristics. The led lamps example

Goshko M.

Lviv National Agrarian University; e-mail: m121314@ukr.net

Received July 14.2016: accepted July 19.2016

Abstract. The problems of investigation of contemporary illuminants characteristics are considered. Particularly the LED lamps of the following trade marks were tested: «Maxus», «Electrum», «Lemaso». Photometric and electrotechnical parameters, stated by the producers, were tested.

The investigation revealed that the stated illuminants' power did not correspond to the actual experimental data, in some cases the 8% exceeding was registered (Lemaso). On the other hand, the actual power of "Maxus" and "Electrum" LED lamps was lower than stated, -22,5 % and -2,35 % accordingly.

The low power coefficient is the major drawback of LED lamps in Ukrainian market. Its actual value ranges are 0,4–0,65, whereas its minimal value for a LED lamp of 5-25 Watt power is considered to be not less than 0,8.

Key words: illuminants**,** illumination, LED lamp, luminous efficacy, power coefficient.

INTRODUCTION

The replacement of incandescent lamps (ICLs) for emitting diode (LED) lamps with light output 5-8 times higher than the LR is considered to be one of the effective ways of reducing electricity consumption for lighting. Despite the obvious benefits, proved in Latvia, the LED lamps are not yet that widespread use of which claim specialists in lighting. One reason for this is the low quality and false information about the products brought to the market Ukraine, causing distrust of consumers. These problems are not unique to Ukraine, but also for industrialized countries. So we decided to experimentally explore available to us modern electric light sources, for example LED - lamps for direct replacement of ICLs.

THE ANALYSIS OF RECENT RESEARCHES AND PUBLICATIONS

Advances in semiconductor physics, optics and optoelectronics over the last 10-15 years helped to create light sources to energy efficiency 4-10 times, and duration of combustion in 30-100 times more compared to incandescent lamps. These include solid-state light sources LED (SD). The advantages MD and forecasts for the future development of their lately published in journals lighting unusual amount of materials [1-3].

Many authors believe that today for LEDs not solved one problem - is the high cost of LEDs. Certainly, this is one of the main problems. But she is not alone. The main consumer benefits of LEDs - High luminous efficiency much higher reliability and durability of combustion compared to traditional light sources today - can not always compensate for their shortcomings.

Therefore, the problem of quality, reliability and safety of new light sources, is very important.

OBJECTIVES

Research objectives - to study the real characteristics of LED lamps which come on the market of Ukraine and conformity assessment of the declared data.

THE MAIN RESULTS OF THE RESEARCH

We researched LED lamps trademark «Maxus», «Electrum», «Lemaso» declared in accordance lighting and electrical parameters. For the study was formed three samples (sample) 3-4 LED lamps each. Complex research key features LED - bulbs produce according to method [5].

Manufacturers submitted the following characteristics of light sources:

- LED (Maxus) - 10 W, 900 lm, lifetime of 30,000 h .;
- LED (Lemaso) - 10 W, 900 lm, lifetime of 20,000 h .;
- LED (Electrum) - 10 W, 800 lm, lifetime 2000 h.

Scheme for research performance electric light sources below.

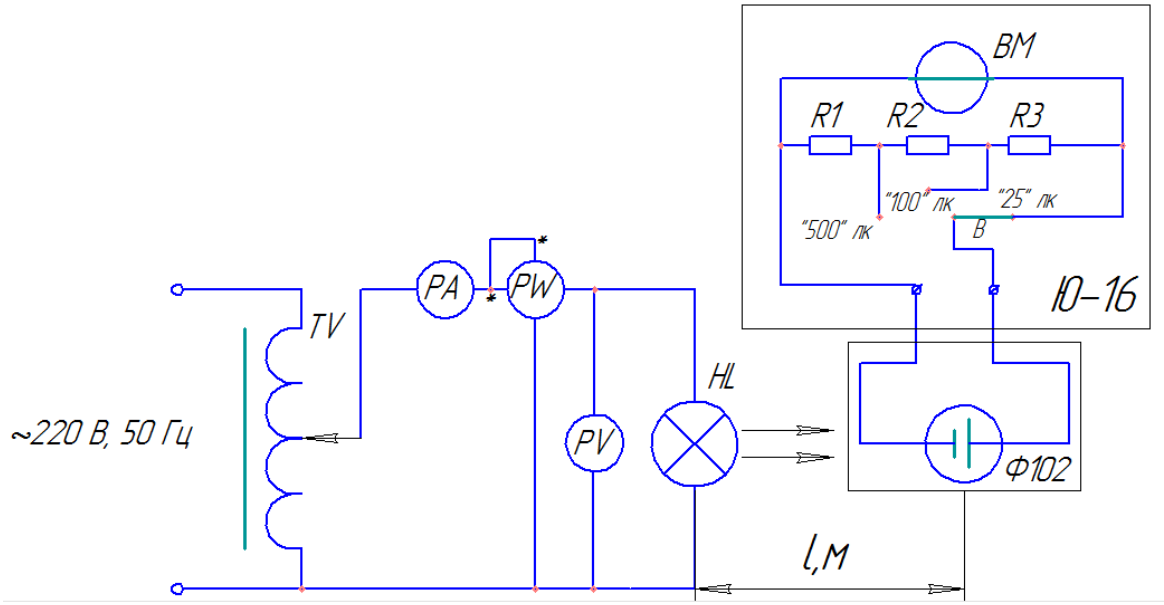

Fig. 1. The study scheme of electrical and lighting parameters of illuminants: TV - autotransformer; HL - investigated the lamp; PA, PV, PW-ammeter, voltmeter and wattmeter respectively; VM - measuring mechanism; B - switch; Ф102 - photocell; Ю -16 - luxmeter.

The value of the measurement results of light and electrical parameters LED - bulbs of various trade marks are given in Table. 2.

After some experimentation, we have indicators for active power at nominal voltage of 220 V, which are listed in the table. 1.

Table 1. Comparative characteristics of passport and measured power values CFL

Type of light source	$P_з$, W	$P_ф$, W	The difference between actual and declared capacity, %
СВД – Maxus	10	8,16	-22,5%
СВД – Lemaso	10	10,9	+8,26 %
СВД – Electrum	10	9,77	-2.35%

The results of the study indicate that among the investigated parties lamps average value of active power on all producers submitted does not meet the declared capacity of the packaging.

Table 2. The results of the LED lamps parameters measurement

lamp type	Parameter	U, B								
		160	170	180	190	200	210	220	230	240
1	2	3	4	5	6	7	8	9	10	11
Maxus, 10 W,900 lm, 30000 hor	I,A	0,06	0,066	0,0705	0,075	0,08	0,086	0,0925	-	-
	E, lx	475	525	575	615	715	825	925	-	-
	P, W	3,84	4,488	5,076	5,7	6,4	7,266	8,14	-	-
Maxus, 10 W,900 lm, 30000 hor	I,A	0,06	0,065	0,0695	0,078	0,084	0,091	0,094	-	-
	E, lx	495	575	600	670	745	860	945	-	-
	P, W	3,84	4,42	5,004	5,89	6,72	7,644	8,25	-	-
Maxus, 10 W,900 lm, 30000 hor	I,A	0,059	0,067	0,07	0,076	0,0825	0,087	0,092	-	-
	E, lx	485	535	610	655	725	790	920	-	-
	P, W	3,80	4,505	5,04	5,795	6,6	7,35	8,096	-	-
The average value E, lx		485	545	595	646,67	728,33	825	930	-	-
The average value P, W		3,82	4,471	5,04	5,795	6,573	7,42	8,162	-	-
The average value H, lx /W		126,6	121,9	118,05	111,59	110,8	111,18	113,943	-	-
Reactive power, Q		8,774	10,244	11,548	13,278	15,061	17,00	18,701		
Full power S		9,57	11,18	12,6	14,485	16,43	18,55	20,405	-	-
Power factor		0,4								

Continuation of Table 2

1	2	3	4	5	6	7	8	9	10	11
Lemaso 10 Вт,900 lm	I,A	0,039	0,0475	0,0525	0,058	0,0638	0,069	0,075	0,082	0,087
	E, lx	560	750	1010	1090	1160	1240	1330	1415	1500
	P, W	4,108	5,25	6,14	7,163	8,29	9,42	10,725	12,203	13,65
Lemaso 10 Вт,900 lm	I,A	0,04	0,046	0,0525	0,059	0,065	0,068	0,0775	0,081	0,086
	E, lx	550	760	1000	1090	1150	1225	1350	1410	1450
	P, W	4,16	5,111	6,14	7,32	8,45	9,282	11,083	12,147	13,46
Lemaso 10 W,900 lm	I,A	0,0398	0,046	0,053	0,059	0,065	0,068	0,0763	0,082	0,088
	E, lx	555	750	980	1075	1170	1200	1350	1430	1490
	P, W	4,1392	5,083	6,201	7,287	8,45	9,32	10,904	12,26	13,65
The average value E, lx		555	753,3	996,67	1085	1160	1221,67	1343,3	1418,3	1480
The average value P, W		4,136	5,147	6,162	7,256	8,396	9,34	10,904	12,203	13,585
The average value H, lx /W		134,2	146,35	161,74	149,54	138,164	130,82	123,2	116,23	108,95
Reactive power, Q		4,835	6,018	7,204	8,483	9,816	10,918	12,748	14,267	15,88
Full power S		6,363	7,92	9,48	11,16	12,92	14,37	16,78	18,77	20,9
Power factor		0,65								
Electrum 10 W, 800 lm, 20000 hor.	I,A	0,1075	0,1025	0,098	0,0935	0,089	0,085	0,0805	-	-
	E, lx	1095	1125	1155	1175	1205	1275	1360	-	-
	P, W	9,46	9,584	9,702	9,78	9,79	9,82	9,74	-	-
Electrum 10 W, 800 lm, 20000 hor.	I,A	0,105	0,1025	0,096	0,0925	0,0875	0,0835	0,08	-	-
	E, lx	1025	1095	1175	1205	1225	1275	1345	-	-
	P, W	9,24	9,584	9,653	9,67	9,625	9,64	9,68	-	-
Electrum 10 W, 800 lm, 20000 hor.	I,A	0,105	0,101	0,095	0,092	0,0863	0,0825	0,08	-	-
	E, lx	1075	1100	1150	1200	1215	1250	1375	-	-
	P, W	9,24	9,44	9,405	9,614	9,49	9,53	9,68	-	-
Electrum 10 W, 800 lm, 20000 hor.	I,A	0,11	0,105	0,1	0,094	0,088	0,084	0,0825	-	-
	E, lx	1025	1080	1125	1185	1215	1260	1325	-	-
	P, W	9,68	9,82	9,9	9,823	9,68	9,702	9,98	-	-
The average value E, lx		1055	1100	1151,25	1191,25	1215	1265	1351,25	-	-
The average value P, W		9,405	9,607	9,66	9,7185	9,65	9,67	9,78	-	-
The average value H, lx /W		112,17	114,5	119,12	122,578	125,96	130,77	138,3	-	-
Reactive power, Q		14,281	14,588	14,676	14,757	14,647	14,688	14,837		
Full power S		17,1	17,47	17,57	17,67	17,54	17,59	17,77	-	-
Power factor		0,55								

Based on this study can be stated that when the supply voltage in the range of 160-240 in luminous flux, power, light returns virtually unchanged paws Electrum only 10 W (Fig. 2 - 4), according to Table 1. These lamps power unit functions as a stabilizer power. As for the other two producers - namely brand Maxus and Lemaso, nature changes the luminous flux of light return from the supply voltage has a different relationship. This relationship is represented graphically in Figure 2.

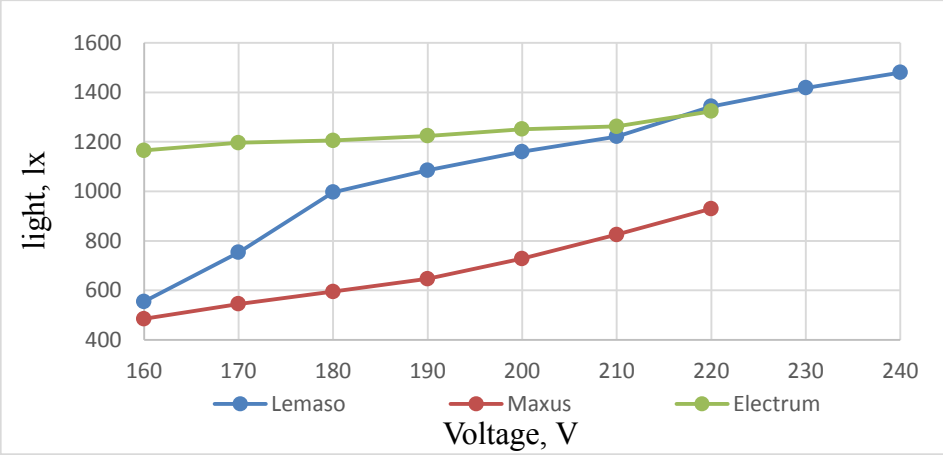

Fig. 2. Dependence of illuminants' illumination on voltage supply

The criterion is enerhoekonomichnosti luminous efficiency lamps. Cross structures investigated CFLs graphically depicted in Figure 3.

The most effective is the LED lamp company Electrum, whose luminous efficiency at the rated voltage of 220 V has a maximum value - 138.3 lux / W.

A major drawback of LED - lights coming in the market of Ukraine is the low power factor (sos φ). We have studied the power factor LED - lights manufacturers Maxus, Electrum and Lemaso ranges 0,4-0,65, although according to the Cabinet of Ministers of Ukraine on October 15, 2012 №992, the minimum allowable values of power factor LED lighting for indoor lighting devices public and industrial buildings with capacity from 5 to 25 W should be at least 0.8. Low power factor data of lighting requires more reactive power compensation lighting network, to improve technical - economic indicators for power supply and reduce energy losses.

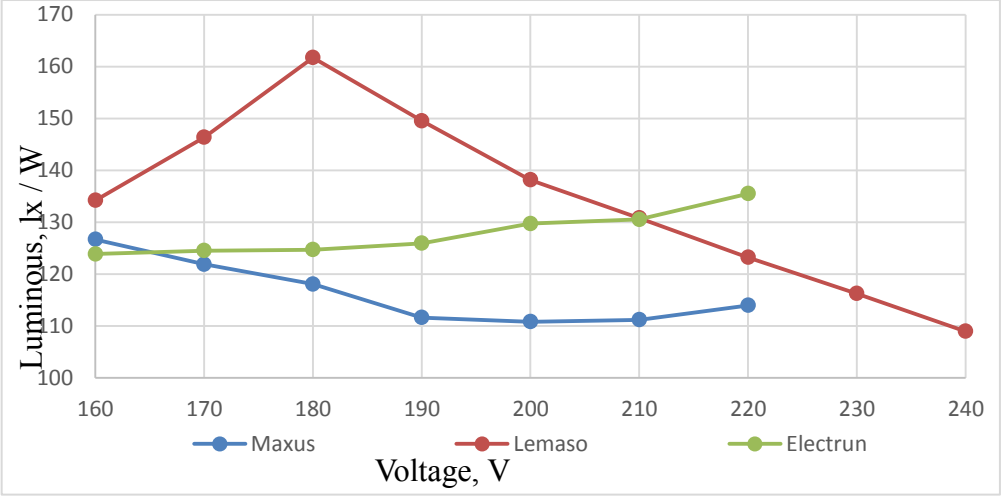

Fig. 3. The dependence of the LED lamps light output on voltage supply.

On the basis of measurements and calculations determined the dependence of active, reactive and full power from the supply voltage - Figure 4.

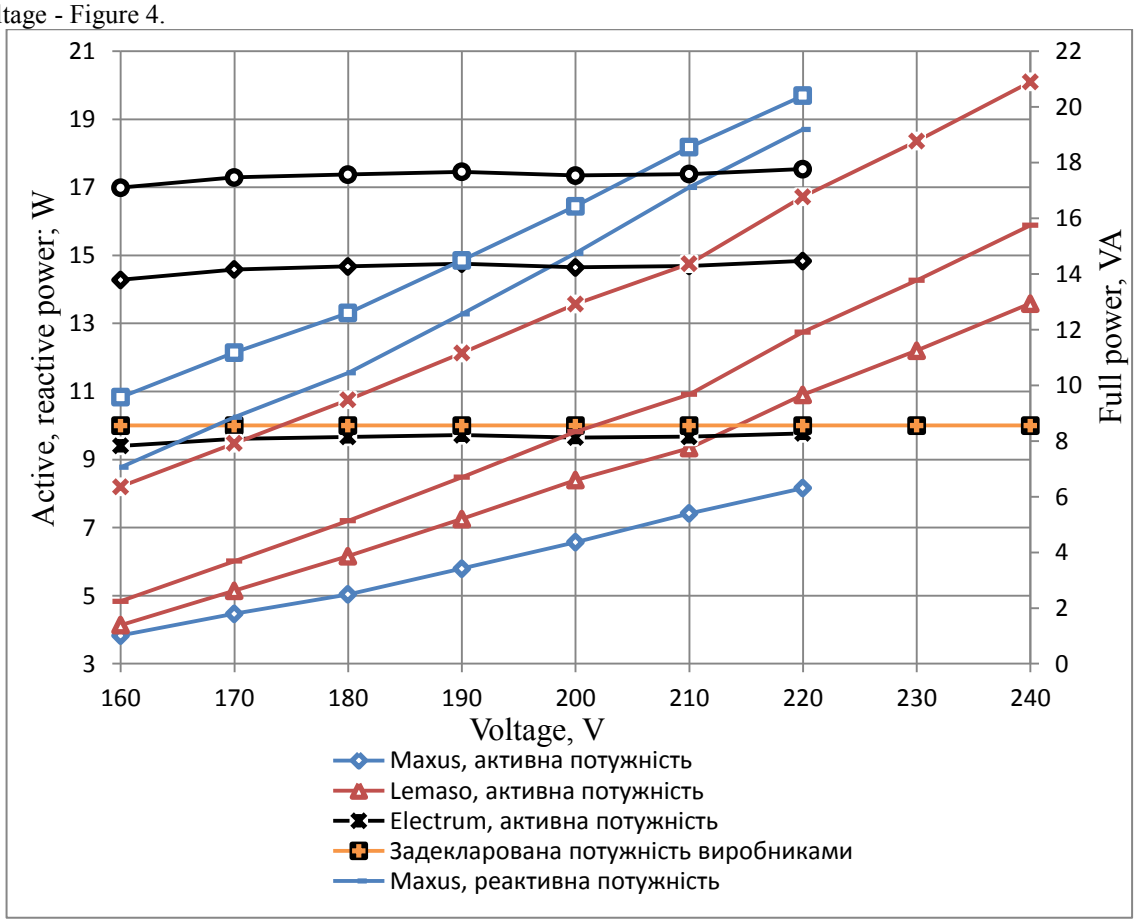

Fig. 4. Dependence of LED lamps power (active, reactive, and apparent) on voltage supply

CONCLUSIONS

LED - lights are promising light sources for special and for general lighting, but much of lamps which come on the domestic market of Ukraine does not correspond to the declared lighting, electrical parameters as we see from studies investigated the alleged power trademarks LED lamps do not meet experimentally removed the data, in some cases exceed by more than 8% - LED (Lemaso), although it should be noted that at times it was lower than declared - LED (Maxus, Electrum) respectively -22.5% and -2.35% .

In turn for light output at the rated voltage of 220 data LED lamps can rank in this spinning wheel:

1. LED (Electrum) - 135,5 lx / W;
2. LED (Lemaso) - 130,8 lx / W;
3. LED (Maxus) - 113,94 lx / W.

A major drawback of LED lamps coming to market in Ukraine is low power factor, which ranges from 0,4-0,65, while the minimum allowable values of power factor for LED lighting devices with capacity of 5 to 25 W should not be less than 0 8.

REFERENCES

1. **Alikberova L. Y., Savinkina E.V. and Davydova M.N. 2004.** *Basis of the Structure of matter.* Moscow.- 468 p.
2. **Chervinsky L.S. 2005.** *Optical technologies in livestock.* - Kyiv: Naukova Dumka.–230 p.
3. **Dambrauskas S.G., Ivanov V.V., Klopovskyy K.S., Krylov E.A., Rakhimov T.V., Saenko V.B. 2002.** *Investigation of the processes that determine the effectiveness of a wide source of VUV radiation initiated matrix microdischarges.* Moscow.-Preprint MSU.
4. **Galicia V.M., Nikitin E.E., Smirnov B.M. 1981.** *The theory of collisions of nuclear particles.* Moscow: Nauka. - 256 p.
5. **Haysak M., Hnatiuk M., Fedornyak Yu. 2011.** *Binding energy of the singlet and triplet states of negative mioniy ions.* Uzhgorod. - 240-245 p.
6. Internet resources: *http: // www.alkor.net/alkorru/FusedSilica1.html - Optical kvarts Glass.*
7. Internet resources: *https: // www.gov.uk/government/publications / – Total Energy*
8. **Kaganov I.L. 1972.** *Ion devices.* Moscow. "Energy".– 528 p.
9. **Kaptsov N.A. 1954.** *"Electronics".* Moscow. "Hostehizdat".– 470 p.
10. **Korchemnyy M., Fedoreyko V., V. Shcherban. 2001.** *Energysaving in agroindustrial complex.* Ternopil: Textbooks and manuals.– 976 p.
11. **Kovalyshyn B. 2012.** *Theoretical and experimental ground of the fuel energy efficiency rising by activating of burning reaction molecules-reagents.*- J. Econtechmod. Lublin-Lviv-Cracow, Vol. I, №1, - P.63-66.
12. **Kovalyshyn B.M. 2012.** *Justification energy efficiency fuel plants through activation molecules reaction reagents incineration*.- Pratci TDAU.- Melitopol, Vol. 12, v. 2, - P.157-164.
13. **Lopatinsky I.E., Zachek I.R., Ilchuk G.A., Romanyshyn B.M. 2005.** *Physics*.– Lviv: Poster.– 386 p.
14. **Oryr J. 1981.** Fyzyka.– Moscow: Mir.– 336 p.
15. Patent №37572 Ukraine, INC F23C 99/00 / *Method fuel efficiency installations on hydrocarbon fuels and device for its implementation* / BM Kovalyshyn (Ukraine) / Zayav.28.07.2006; publ. 10.12.2008. Bull. №23, 2008.
16. *Physical Chemistry* (editor C.S. Krasnov).– Moscow: High School, 2001, 512 p.
17. **Prakhovnik A.V., Rosen V.P., Razumovsky A.V. and et. 1999.** *Power Management: Aid train.*– Kyiv: Kyivska Not. f-ca.– 184 p.
18. **Stromberg A.G. 2001.** *Physical Chemistry.*– Moscow: High school.– 527 p.
19. **Yariv A. 1982.** *An Introduction to Theory and Applications of Quantum Mechanics.* California Institute of Technology.–185 p.
20. **Zeidel A.P., Prokofiev V.P., Rayskyy S.M., Slyty V.A., Shreyder E.Y. 1977.** *Tables of spectral lines.* Moscow: Nauka.

Optimization of linear functions on a cyclic permutation Based on the random search

Igor Grebennik, Alexey Baranov, Olga Chorna, Elena Gorbacheva
Kharkiv National University of Radioelectronics, email: igorgrebennik@gmail.com

Received July 28.2016: accepted August 30.2016

Abstract. For creating adequate mathematical models of combinatorial problems of constructing optimal cyclic routes, mathematical modeling and solving a number of planning and control tasks solutions of optimization problems on the set of cyclic permutations are required.

Review of the publications on combinatorial optimization demonstrates that the optimization problem on the cyclic permutations have not been studied sufficiently. This paper is devoted to solving optimization problem of a linear function with linear constraints on the set of cyclic permutations. For solving problems of this class using of known methods, taking into account the properties of a combinatorial set of cyclic permutations, is proposed. For this purpose we propose a method based on the ideology of random search. Heuristic method based on the strategy of the branch and bound algorithm is proposed to solve auxiliary optimization problem of a linear function without constraints on the set of cyclic permutations. Since application of the branch and bound algorithm immediately leads to an exponential growth of the complexity with increasing the dimension of the problem a number of modifications are suggested. Modifications allow reducing computational expenses for solving higher dimension problems. The effectiveness of the proposed improvements is demonstrated by computational experiments.

Key words: combinatorial optimization, linear function, cyclic permutations, random search, branch and bound algorithm, parallel computing.

INTRODUCTION

Necessity to solve a wide range of problems in a variety of scientific and applied problems caused the emergence and development of theory and methods for solving problems of linear optimization. Moreover, technology for solving linear programming problems plays a significant role in the creation of algorithms for solving mathematical programming problems of other types, such as combinatorial optimization problems [1, 2].

Mathematical models of many scientific and applied problems of design, planning, placement and control may be adequately represented on the basis of different models of combinatorial optimization [3-6]. In this case variables in these problems are considered as elements of classical combinatorial sets, such as permutations, combinations, arrangements and other [1, 2, 7-9].

Establishing additional constraints on the variables in the combinatorial optimization models leads to appearance of new classes of combinatorial optimization problems. Mathematical models of these new classes of combinatorial optimization problems could be described by subsets of classical combinatorial sets. One of such subsets is set of cyclic permutations [11-13].

There are two known groups of methods for solving combinatorial optimization problems – cutting methods and combinatorial methods [1, 2, 9, 12, 14-17]. One of the most powerful exact methods is combinatorial branch and bounds algorithm [1]. To solve combinatorial optimization problems of large dimension methods based on random search are often used [2, 18].

To improve the efficiency of the known methods of combinatorial optimization the properties of combinatorial sets, describing the admissible area of optimization problems should be used [12, 13, 20].

In this paper, for solving optimization problems on the set of cyclic permutations, an strategy based on the random search, cyclic properties of permutations and analytical solutions of systems of linear inequalities as the constraints on variables are used.

The aim of the paper is elaboration of a strategy for solving optimization problems of linear functions on the set of cyclic permutations with linear constraints.

ANALYSIS OF RECENT RESEARCH AND PUBLICATIONS

Definition 1. A linear ordering of the elements from a certain generating set $A = \{a_1, a_2, ..., a_n\}$ is called a permutation

$$\pi = \pi(a_1, a_2, ..., a_n) = (\pi(a_1), \pi(a_2), ..., \pi(a_n)) = (a_{i_1}, a_{i_2}, ..., a_{i_n}) = (p_1, p_2, ..., p_n)$$

or, if it is necessary to stress the fact that it contains n elements, n -permutation [15-17].

We denote as P_n the set of permutations generated by the elements $a_1 < a_2 < ... < a_n$.

Consider a certain permutation

$$\pi = (\pi(a_1), \pi(a_2), ..., \pi(a_n)) \in P_n$$

and its element $\pi(a_i) = a_j$, $\forall i, j \in J_n$. Then we can write down:

$$\pi(a_j) = \pi(\pi(a_i)) = \pi^2(a_i).$$

Generally this formula can be represented in the following form:

$$\pi^{k-1}(a_j) = \pi(\pi^{k-1}(a_i)) = \pi^k(a_i),$$
$$\forall i, j \in J_n,\ k \le n.$$

Thus [14], if for some $l \ge 1$ we have $\pi^l(a_i) = a_i$, $i \in J_n$ and all the elements $a_i, \pi(a_i), \pi^2(a_i), ..., \pi^{l-1}(a_i)$ are different, the sequence $(a_i, \pi(a_i), \pi^2(a_i), ..., \pi^{l-1}(a_i))$ is called an l length cycle.

Definition 2. A cyclic permutation is such a permutation π from n elements that contains a single n length cycle, i. e. $\pi^n(a_i) = a_i$, $\forall i \in J_n$ [14]. We denote such permutations as π_C.

Denote P_n^C as set of cyclic permutations without repetitions generated by n elements $a_1 < a_2 < ... < a_n$ [14-17]. Permutation set P_n and set of cyclic permutations P_n^C are Euclidean combinatorial sets, or e-sets [7, 8].

Investigate following combinatorial optimization problem: minimize the linear function with linear constraints on the set of cyclic permutations:

$$L(x) = \sum_{i=1}^{n} \alpha_i p_i \to \min; \quad (1)$$
$$Cp \le d; \quad (2)$$
$$p \in P_n^C, \quad (3)$$

where: $C = [C_{ji}]_{m \times n}$, $d \in R^n$, $\alpha_i \in R$, $p_i \ge 0$;

P_n^C — as set of cyclic permutations without repetitions generated by n real's.

Let us fulfill the enclosure mapping of the permutations set P_n and cyclic permutations P_n^C to the arithmetic Euclidian space R^n. According to [7, 8] the given mapping (which is called immersion) can be represented in the following form:

$$f : P \to R^n,\ \forall p = (p_1, p_2, ..., p_n) \in P,$$
$$x = f(\pi) = (x_1, x_2, ..., x_n) \in E \subset R^n,\ x_i = p_i,$$
$$i \in J_n.$$

As a result of the immersion f we have one-to-one correspondence between each set P_n, P_n^C and

$$E \subset R^n:\ E_n = f(P_n),\ E_n^C = f(P_n^C).$$

Formulate optimization problem equivalent to the problem (1)-(3) using immersion sets P_n, P_n^C into Euclidian space:

$$L(x) = \sum_{i=1}^{n} \alpha_i x_i \to \min; \quad (4)$$
$$Cx \le d; \quad (5)$$
$$x \in E_n^C \subset R^n, \quad (6)$$

where: $C = [C_{ji}]_{m \times n}$, $d \in R^n$, $\alpha_i \in R$, $x_i \ge 0$;

E_n^C – immerse of the cyclic permutations in Euclidean space.

OBJECTIVES

The solution of the problem (4)–(6) is the goal of this work. For reaching this goal the approach based on the random search is used. Properties of permutations immersed in Euclidean space and analytic solution of systems of linear inequalities, describing the task constraints are taken into account. Similar approach earlier was used for optimization of linear function on the set of permutations P_n with linear constraints [12].

Modification of this approach will solve problem (4)–(6) on the set of cyclic permutations. Consider a permutation polyhedron Π_n generated by a set $a_1 < a_2 < ... < a_n$, $vert\ \Pi_n = E_n$ is the set of its vertexes.

Since any cyclic permutation belongs to the set of permutations P_n,

$$\pi_C = (\pi(a_1), \pi(a_2), ..., \pi(a_n)) \in P_n$$

all cyclic permutations are vertexes of the permutation polyhedron Π_n.

Follow the work [12], build n-dimension simplex $T_n \subset R^n$ [18], inclusive polyhedron Π_n. The system of inequalities $C_1 x \le d_1$ defines simplex T_n, where C_1 – matrix of coefficients $(n+1) \times n$, $d_1 \in R^{n+1}$. Since the simplex T_n contains a polyhedron Π_n adding linear inequalities that describe simplex to the constraints (5), all feasible solutions are not changed. System of linear inequalities $W^0 x \le v^0$ combines constraints (5) with inequalities

$$C_1 x \le d_1,$$

where: $W^0 = [w_{ij}^0]$ – $(m+n+1)\times n$ -matrix, $v^0 \in R^{m+n+1}$. As a result equivalent optimization problem is constructed:

$$L(x) = \sum_{i=1}^{n} \alpha_i x_i \to \min; \quad (7)$$

$$W^0 x \le v^0; \quad (8)$$

$$x_i \ge 0; \quad (9)$$

$$x \in E_n^C \subset R^n. \quad (10)$$

Consider solution strategy for problem (7)–(10) [12]. In accordance with random search solving process contains M series with m tests in each series.

In each test solution of the system of linear inequalities is founded. According to [20], general formula of non-negative solutions of the system (8)–(9) is:

$$z = \frac{\xi_1 z^1 + \xi_2 z^2 + ... + \xi_l z^l}{\xi_1 z_{N+1}^1 + \xi_2 z_{N+1}^2 + ... + \xi_l z_{N+1}^l},$$

where: $z^1, z^2, ..., z^l$ – fundamental solutions of the following auxiliary system of linear inequalities:

$$\begin{cases} W^0 x - v^0 x_{n+1} \le 0 \\ -x_i \le 0 \end{cases}; \quad (11)$$

where: $z_{n+1}^1, z_{n+1}^2, ..., z_{n+1}^l$ – their last coordinates, $\xi_1, \xi_2, ..., \xi_l$ – arbitrary real numbers satisfying the condition:

$$\xi_1 z_{n+1}^1 + \xi_2 z_{n+1}^2 + ... + \xi_l z_{n+1}^l \ge 0.$$

Next random real numbers $\xi_1, \xi_2, ..., \xi_l$, satisfying the condition:

$$\xi_1 z_{n+1}^1 + \xi_2 z_{n+1}^2 + ... + \xi_l z_{n+1}^l \ge 0$$

will be generated. Thus will be constructed solution $z(i)$ of the system (11). The nearest to the $z(i)$ point of E_n^C could be found using:

$$x_i = \arg \min_{x \in E_n^C} \|x - z(i)\|^2. \quad (12)$$

If $x_i \in E_n^C$ isn't solution of the system (11), next test begins.

In other way we compare x_i to the previous approximations to problem (7)-(10) solution and if x_i give better value of objective function it will became a new approximation to solution of (7)-(10).

Let $\bar{x} = x_i$. We assume $\bar{x}$ current approximation to solution, and $L(\bar{x}) = \sum_{i=1}^{n} \alpha_i \bar{x}_i$ – upper bound of solution (7)–(10). Add to the system (8) linear inequality:

$$\alpha_1 x_1 + \alpha_2 x_2 + ... + \alpha_n x_n \le \bar{d}, \quad (13)$$

where: $\bar{d} = \sum_{i=1}^{n} \alpha_i \bar{x}_i$.

The result will be $W^1 x \le v^1$ – system of linear inequalities In $W^1 x \le v^1$ there will be inequality with left part, identical to (13): $\alpha_1 x_1 + \alpha_2 x_2 + ... + \alpha_n x_n \le \tilde{d}$. Compare $\tilde{d}$ и $\bar{d}$. If $\tilde{d}$ ..., replace old inequality with the new (13) one in system $W^1 x \le v^1$. It leads to reducing the area restricted with system $W^1 x \le v^1$. Let $\bar{d} = \tilde{d}$. Continue the process.

AUXILIARY PROBLEM

Optimization problem (12) is considered as auxiliary problem.

For the set of permutation solution of this problem is an absolute minimum of linear function [7]:

$$x^* = (x_1^*, x_2^*, ..., x_n^*) = \arg \min_{x \in E_n} \sum_{j=1}^{n} c_j x_j, \quad (14)$$

where: $c_j \in R^1$, $\forall j \in J_n$, $x_{m_i}^* = a_i$, $\forall i \in J_n$, and sequence $\{m_1, m_2, ..., m_n\}$ such that $c_{m_1} \ge c_{m_2} \ge ... \ge c_{m_n}$.

Since set of cyclic permutation is subset of set of permutations for each $x \in E_n^C$ problem (12) can be reduced to problem of linear function optimization.

For combinatorial set of cyclic permutations:

$$\min_{x \in E_n^C} \left(\sum_{j=1}^{n} x_j z(i)_j \right)$$

couldn't be found using simple elements ordering, so we offer to solve this problem using branch and bound algorithm [13].

Evaluation and branching rules are the main components of branch and bound algorithm [1].

In this algorithm branching rule is based on fixing various free generating elements relative the coefficient of the objective function, corresponding to a given level of the tree.

Evaluation of each node of the tree is sum of multiplication of fixed generating elements by the corresponding coefficients of the objective function and multiplication of free generating elements by the coefficients of the objective function according to (14).

The exact solution of the original problem can be obtained using this algorithm. But since solving problem (7)-(10) requires solving auxiliary problem (12) many times for each test in all series the heuristic approach based on branch and bound algorithm was proposed. This approach called up for saving computing resources.

Heuristic solving process consists of two stages. First stage – branch and bound algorithm of finding solution till a user-specified level k. Second stage – final construction of cyclic permutation by random fixing of remaining free generating elements.

Resulting heuristic solution depends on problem dimension n, user-specified level k and on coefficients of the objective function. For example, if user-specified level k almost equal to n, heuristic solution could be equal to exact solution. With decreasing k the probability of coincidence of heuristic and exact solutions decreases too.

PARALLEL COMPUTING

Described strategy for optimization of linear function with linear constraints on the set of cyclic permutations demonstrates good results with relatively small problem dimensions. But increasing n significantly increases time of solving the problem. Features of the strategy give an opportunity for parallel computing.

Solving problem (7)-(10) could be accelerated by parallel solving auxiliary problems for all random generated points in one series. In this case number of tests in one series could be equal to the number of processors.

Thus, strategy of solving problem (7)-(10) using parallel computing consists in such steps:

1) constructing simplex including permutation polyhedron;
2) forming system of constraints;
3) generating number of random points inside solution area;
4) parallel finding nearest vertexes of permutation polyhedron for each random point using branch and bound algorithm or its modification;
5) selection of the best obtained solution;
6) updating the system of constraints.

For evaluating the efficiency of parallel computing Amdahl's and Gustafson's laws are used. They allow to calculate maximum possible acceleration of the parallel computing of the program in comparison with the serial [21].

Let S be acceleration which may be obtained. An estimate for it according to Amdahl's law is:

$$S < \frac{1}{f + \frac{(1-f)}{p}},$$

where: f – the proportion of consecutive operations, p – number of processors.

Also f can be calculated as a percentage of code that couldn't be parallelized. In this case, estimation of S could be less accurate but its calculation is significantly simplified.

Analysis of proposed solutions strategy shows that in our case f is approximately 75%.

The acceleration S:

$$S < \frac{1}{0,75 + \frac{(1-0,75)}{4}} = \frac{1}{0,75 + 0,0625} = 1,23 \cdot$$

MAIN RESULTS OF THE RESEARCH

Described method of optimization of linear functions on the cyclic permutations with linear constraints implemented in software. Coefficients of the objective function and coefficients of constraints were generated randomly. Experiments were carried out in two stages. First stage was dedicated to solving of the problems with dimension of 8 and less variables. These problems were solved with proposed modification of the random search method. The results compared with exact solution obtained by exhaustive search. The coefficients of the objective function generated in the interval [10; 100].

To find the solutions 5 series were used, each series consisted of 10 experimental points. Relative error was calculated for the problems, where approximate solutions was not equal to exact solution. The results are shown in Table 1.

Table 1.

Dimension	The number of matching solutions	The number is not matched solutions	Relative error	The average time to solve, s.
3	10	0	0	0,14
4	5	5	0,077	0,269
5	3	7	0,128	0,439
6	4	6	0,072	0,734
7	3	7	0,084	1,527
8	0	10	0,134	3,402

Second stage was dedicated to solving the problems with larger dimensions. For these problems two estimates [13] for the lower estimate of minimum were calculated:

$$E_1 = \left| \frac{Est - Rnd}{Rnd} \right|,$$

$$E_2 = \left| \frac{Est - Rnd}{Est} \right|,$$

where: Est – minimum of objective function on cyclic permutations without linear constraints; Rnd – the solution by random search problem. The results are shown in Table 2.

For the problems with dimension 15 and more auxiliary problem (8) was solved heuristically. For each dimension of the problem tree level k is specified.

To solve the problems, presented in Tables 1 and 2 used 5 series, each consisted of 10 experimental points. It means that for solving each of the problems 50 auxiliary problems were solved.

Table 2.

Dimension	k	Number of tasks	Average estimate E_1	Average estimate E_2	The average time to solve, s.
15	10	10	0,256	0,255	18,19
20	15	10	0,127	0,122	225,9
25	15	3	1,716	0,44	809,17

To reduce the time and technical resources, were conducted experiments with 2 series, each consisted of 15 experimental points. The results are shown in Table 3.

Table 3.

Dimension	k	Number of tasks	Average estimate E_1	Average estimate E_2	The average time to solve, s.
25	15	7	0,1652	0,203	821,14
30	15	3	0,227	0,308	1805,86
35	15	1	0,219	0,2819	11215,516
40	20	1	0,305	0,379	33112,95

Experiments to evaluate efficiency of the parallel computing of problem (4)-(7) were conducted. The real acceleration of the parallel algorithm is the ratio of the execution time of sequential algorithm to the time of parallel algorithm execution: $S = \frac{T_1}{T_p}$, where T_1 – runtime of sequential algorithm, T_p – runtime using p processors.

To evaluate the scalability of the parallel algorithm the concept of the coefficient of efficiency of parallelization is used: $E = \frac{S}{p}$.

Table 4.

Dimension	The time to solve, T_1, s.	The time to solve $T_p = T_4$, s.	$S = \frac{T_1}{T_p}$	$E = \frac{S}{p}$
15	493,7	281,5	1,75	0,4375
20	4782,9	3297,5	1,45	0,3625
25	62559,9	31688,3	1,97	0,4925

Note, that actual acceleration obtained by using parallel computing, more than the theoretical evaluation by Amdahl's Law. This is associated with inexact rough estimate of f.

CONCLUSIONS

This paper suggests a strategy for solving a combinatorial optimization problems with linear objective function and linear constraints on the set of cyclic permutations. This strategy is based on the random search, cyclic properties of permutations and analytical solutions of systems of linear inequalities as the constraints on variables.

The solving the auxiliary problem of combinatorial optimization on the set of cyclic permutations without restriction performed using the branch and bound method. It should be noted that the use of branch and bound algorithm leads to an exponential increase in the complexity of solution with increasing dimension of the problem. Moreover, rule of branching and the rule of estimates calculating significantly depend on the complexity of solving process. The following modifications of the method are proposed to decrease the complexity:

1. heuristic method for solving the auxiliary problem;
2. modification with the parallel computing for the auxiliary problem.

These modifications allow reducing the computational expences for large-scale problems. The effectiveness of the proposed improvements is confirmed by computational experiments.

REFERENCES

1. **Sergienko I.V. 1988** Mathematical models and methods for solving discrete optimization, K.: Naukova Dumka, 472. (In Russian).
2. **Yemets O.A., Barbolina T.N. 2008** Combinatorial optimization on arrangements, K.: Naukova Dumka, 157. (In Russian).
3. **I. Alekseyev, I. Khoma, N. Shpak. 2013.** Modelling of an impact of investment maintenance on the condition of economic protectability of industrial enterprises. Econtechmod 2(2), Lublin ; Rzeszow, 3-8.
4. **Heorhiadi, N. Iwaszczuk, R. Vilhutska. 2013.** Method of morphological analysis of enterprise management organizational structure. Econtechmod 2(4), Lublin ; Rzeszow, 17-27.
5. **N. Podolchak, L. Melnyk, B. Chepil. 2014.** Improving administrative management costs using optimization modeling. Econtechmod 3(1), Lublin ; Rzeszow, 75–80.
6. **Lobozynska S. 2014.** Formation of optimal model of regulation of the banking system of Ukraine. Econtechmod 3(2), Lublin ; Rzeszow, 53-57.
7. **Stoyan, Yu., Yemets, O. 1993.** Theory and methods of Euclidean combinatorial optimization, ISDO, Kyiv. (In Ukrainian).

8. **Stoyan Y. G., Yakovlev S. V. 1986.** Mathematical models and optimization methods of geometric engineering. K.: Naukova Dumka, 268. (In Russian)
9. **Yemets O.A., Barbolina T.N. 2003** Solution of linear optimization problems on arrangements by cutting Cybernetics and Systems Analysis, №6.
10. **Valuiskaya O.A., Yakovlev S.V. 1999** On the minimization of a linear function on the tops of permutation polyhedron with given linear constraints, Options. NASU number 11, pp 103-107.
11. **Grebennik I. V. 1999** The solution of some problems of constrained optimization of linear functions on permutation polyhedron, Radioelectronics and Informatics, № 1, pp. 55–59.
12. **Grebennik I.V., Baranov A.V. 2007** Optimization of linear functions with linear constraints on combinatorial sets on the basis of a random search, Arts. intelligence, № 1, pp. 132–137.
13. **Grebennik I.V., Litvinenko A.S., Titova O.S. 2012** Optimization of a linear function on the set of cyclic permutations, Bionics Intelligence, №2(79), pp.8–12.
14. **Stanley, R. 1986.** Enumerative combinatorics, vol 1, Wadsworth, Inc. California.
15. **Bona M. 2004** Combinatorics of permutations Chapman & Hall, CRC, 337 c.
16. **Donald Knuth . 2005.** The Art of Computer Programming, Volume 4, Fascicle 2: Generating All Tuples and Permutations, Addison-Wesley, 144.
17. **Donald L.Kreher, Douglas R.Stinson. 1999.** Combinatorial Algorithms: Generation Enumeration and Search, CRC Press, 329.
18. **Rekleytis G., Reyvindran A., Regsdel K. 1986** Optimization in technology, pp. 348.
19. **Igor Grebennik, Olga Chorna 2015.** Elements transpositions and their impact on the cyclic structure of permutations. An International Quarterly Journal on Economics of Technology and Modelling Processes . — 2015. — Vol. 4, № 3. — pp. 33–38.
20. **Chernikov S.N. 1968** Linear inequalities, M .: Science, pp. 488. (In Russian).
21. **Quinn M.J. 2004** Parallel Programming in C with MPI and OpenMP, New York: NY: McGraw-Hill.

Table of contents

List of the Reviewers

1. Janusz Wojdalski
2. Andrzej Stępniewski
3. Agnieszka Sujak
4. Jaromir Mysłowski
5. Andrzej Mruk
6. Halina Pawlak
7. Jacek Skwarcz
8. Janusz Nowak
9. Małgorzata Trojanowska
10. Andrzej Baliński
11. Tadeusz Złoto
12. Rafał Longwic
13. Beata Ślaska-Grzywna
14. Mykola Medykovskyy
15. Paulo Muzyka
16. Jaroslav Kunec
17. Stepan Myagkota
18. Jaroslav Marushak
19. Volodymyr Voytov
20. Roman Kuzminskyy
21. Anton Tretyak
22. Yuriy Famulyak
23. Mykola Sviren'
24. Bohdan Hnidec'
25. Valentin O. Filatov

Editors of the "Econtechmod" magazine of the Commission of Motorization and Energetics in Agriculture would like to inform both the authors and readers that an agreement was signed with the Interdisciplinary Centre for Mathematical and Computational Modelling at the Warsaw University referred to as "ICM". Therefore, ICM is the owner and operator of the IT system needed to conduct and support a digital scientific library accessible to users via the Internet called the "ICM Internet Platform", which ensures the safety of development, storage and retrieval of published materials provided to users. ICM is obliged to put all the articles printed in the "Econtechmod" on the ICM Internet Platform. ICM develops metadata, which are then indexed in the "BazTech" database.

We are pleased to announce that the magazine "ECONTECHMOD" (ISSN 2084-5715) has undergone a positive evaluation of the IC Journals Master List 2013, the result of which is granting the ICV Index (Index Copernicus Value) 6.52 pts. The resulting score was calculated on the basis of a survey submitted by the Editorial Team as well as assessments made by the professionals from Index Copernicus. We invite you to familiarize yourself with the methodology of IC Journals Master List evaluation:

http://journals.indexcopernicus.com/masterlist.php?q=econtechmod

Impact factor of the "ECONTECHMOD" quarterly journal according to the Commission of Motorization and Energetics in Agriculture is 1,1 (September 2016).

GUIDELINES FOR AUTHORS (2016)

The journal publishes the original research papers. The papers (min. 8 pages) should not exceed 12 pages including tables and figures. Acceptance of papers for publication is based on two independent reviews commissioned by the Editor.

Authors are asked to transfer to the Publisher the copyright of their articles as well as written permissions for reproduction of figures and tables from unpublished or copyrighted materials.

Articles should be submitted electronically to the Editor and fulfill the following formal requirements:
- Clear and grammatically correct script in English,
- Format of popular Windows text editors (A4 size, 12 points Times New Roman font, single interline, left and right margin of 2,5 cm),
- Every page of the paper including the title page, text, references, tables and figures should be numbered,
- SI units should be used.

Please organize the script in the following order (without subtitles):
Title, Author(s) name (s), Affiliations, Full postal addresses, Corresponding author's e-mail
Abstract (up to 200 words), Keywords (up to 5 words), Introduction, Materials and Methods, Results, Discussion (a combined Results and Discussion section can also be appropriate), Conclusions (numbered), References, Tables, Figures and their captions

Note that the following should be observed:
An informative and concise title; Abstract without any undefined abbreviations or unspecified references; No nomenclature (all explanations placed in the text); References cited by the numbered system (max 5 items in one place); Tables and figures (without frames) placed out of the text (after References) and figures additionally prepared in the graphical file format jpg or cdr.

Make sure that the tables do not exceed the printed area of the page. Number them according to their sequence in the text. References to all the tables must be in the text. Do not use vertical lines to separate columns. Capitalize the word 'table' when used with a number, e.g. (Table1).

Number the figures according to their sequence in the text. Identify them at the bottom of line drawings by their number and the name of the author. Special attention should be paid to the lettering of figures – the size of lettering must be big enough to allow reduction (even 10 times). Begin the description of figures with a capital letter and observe the following order, e.g. Time(s), Moisture (%, vol), (%, $m^3m^{-3)}$ or (%, gg^{-1}), Thermal conductivity ($W\ m^{-1}K^{-1}$).

Type the captions to all figures on a separate sheet at the end of the manuscript.

Give all the explanations in the figure caption. Drawn text in the figures should be kept to a minimum. Capitalize and abbreviate 'figure' when it is used with a number, e.g. (Fig. 1).

Colour figures will not be printed.

Make sure that the reference list contains about 30 items. It should be numbered serially and arranged alphabetically by the name of the first author and then others, e.g.
7. Kasaja O., Azarevich G. and Bannel A.N. 2009. Econometric Analysis of Banking Financial Results in Poland. Journal of Academy of Business and Economics (JABE), Vol. IV. Nr 1, 202–210.

References cited in the text should be given in parentheses and include a number e.g. [7].

Any item in the References list that is not in English, French or German should be marked, e.g. (in Italian), (in Polish).

Leave ample space around equations. Subscripts and superscripts have to be clear. Equations should be numbered serially on the right-hand side in parentheses. Capitalize and abbreviate 'equation' when it is used with a number, e.g. Eq. (1). Spell out when it begins a sentence. Symbols for physical quantities in formulae and in the text must be in italics. Algebraic symbols are printed in upright type.

Acknowledgements will be printed after a written permission is sent (by the regular post, on paper) from persons or heads of institutions mentioned by name.